UNIVERSITAT DE BARCELONA

El receptor nuclear NOR-1 en el remodelado cardiovascular: análisis de mecanismos fisiopatológicos y validación de nuevos modelos animales de utilidad preclínica

Laia Cañes Esteve

ADVERTIMENT. La consulta d'aquesta tesi queda condicionada a l'acceptació de les següents condicions d'ús: La difusió d'aquesta tesi per mitjà del servei TDX (**www.tdx.cat**) i a través del Dipòsit Digital de la UB (**diposit.ub.edu**) ha estat autoritzada pels titulars dels drets de propietat intel·lectual únicament per a usos privats emmarcats en activitats d'investigació i docència. No s'autoritza la seva reproducció amb finalitats de lucre ni la seva difusió i posada a disposició des d'un lloc aliè al servei TDX ni al Dipòsit Digital de la UB. No s'autoritza la presentació del seu contingut en una finestra o marc aliè a TDX o al Dipòsit Digital de la UB (framing). Aquesta reserva de drets afecta tant al resum de presentació de la tesi com als seus continguts. En la utilització o cita de parts de la tesi és obligat indicar el nom de la persona autora.

ADVERTENCIA. La consulta de esta tesis queda condicionada a la aceptación de las siguientes condiciones de uso: La difusión de esta tesis por medio del servicio TDR (**www.tdx.cat**) y a través del Repositorio Digital de la UB (**diposit.ub.edu**) ha sido autorizada por los titulares de los derechos de propiedad intelectual únicamente para usos privados enmarcados en actividades de investigación y docencia. No se autoriza su reproducción con finalidades de lucro ni su difusión y puesta a disposición desde un sitio ajeno al servicio TDR o al Repositorio Digital de la UB. No se autoriza la presentación de su contenido en una ventana o marco ajeno a TDR o al Repositorio Digital de la UB (framing). Esta reserva de derechos afecta tanto al resumen de presentación de la tesis como a sus contenidos. En la utilización o cita de partes de la tesis es obligado indicar el nombre de la persona autora.

WARNING. On having consulted this thesis you're accepting the following use conditions: Spreading this thesis by the TDX (**www.tdx.cat**) service and by the UB Digital Repository (**diposit.ub.edu**) has been authorized by the titular of the intellectual property rights only for private uses placed in investigation and teaching activities. Reproduction with lucrative aims is not authorized nor its spreading and availability from a site foreign to the TDX service or to the UB Digital Repository. Introducing its content in a window or frame foreign to the TDX service or to the UB Digital Repository is not authorized (framing). Those rights affect to the presentation summary of the thesis as well as to its contents. In the using or citation of parts of the thesis it's obliged to indicate the name of the author.

El receptor nuclear NOR-1 en el remodelado cardiovascular: análisis de mecanismos fisiopatológicos y validación de nuevos modelos animales de utilidad preclínica

UNIVERSITAT DE BARCELONA

UNIVERSIDAD DE BARCELONA

Facultad de Farmacia

Programa de Doctorado en Biomedicina

Memoria presentada por

Laia Cañes Esteve

Para optar al grado de Doctor por la Universidad de Barcelona

Este trabajo ha sido realizado bajo la supervisión de los directores; Dr. José Martínez González, del Instituto de Investigaciones Biomédicas de Barcelona (IIBB-CSIC), y la Dra. Mª Cristina Rodríguez Sinovas, del Institut de Recerca d'Hospital de la Santa Creu i Sant Pau (IR), y del tutor Dr. Manuel Vázquez-Carrera, de la Facultad de Farmacia.

Los directores, El tutor,

José Martínez González **Mª Cristina Rodríguez Sinovas** **Manuel Vázquez-Carrera**

La doctoranda,

Laia Cañes Esteve

Als meus pares i germans

Als meus xiquis

ÍNDICE

ABREVIATURAS

AAA	Aneurisma de aorta abdominal
ACC	*American College of Cardiology*
ACE	Enzima convertidora de angiotensina
ADN	Ácido desoxiribonucleico
AF	*Activation function*
AHA	*American Heart Association*
AMPT	Alpha-metil-p-tirosina
AngII	Angiotensina II
ANP	Péptido natriurético auricular
AP-1	Proteína activadora 1
ApoE$^{-/-}$	Ratón deficiente en la apoliproteína E
ATP	Trifosfato de adenosina
BH_4	Tetrahidrobiopterina
BNP	Péptido natriurético de tipo B
CaMKII	Calmodulina quinasa II
CD69	*Cluster of differentation* 69
CE	Células endoteliales
CMLV	Células musculares lisas vasculares
COX2	Ciclooxigenasa 2
DBD	*DNA-binding domain*
DR	Repetición directa
EVAR	Reparación endovascular del aneursima
FDA	*Food and Drugs Administration*
GAP43	*Growth associated protein 43*
GO	*Gene ontology*
GSEA	*Gene Set Enrichment Analysis*
HDL	Lipoproteínas de alta densidad

hNOR1	NOR1 humano
HRE	*Hormone response element*
ICAM	Molécula de adhesión intercelular
IECA	Inhibidores de la enzima convertidora de angiotensina
IL	Interleuquina
ILT	*Intraluminal Thrombus*
ISO	Isoproterenol
IVST	*Interventricular septal thickness*
kDa	Kilodaltons
KO	*Knock out*
LBD	*Ligand-binding domain*
LDL	Lipoproteínas de baja densidad
LDLR	Receptor de lipoproteínas de baja densidad
LOX	Lisil oxidasa
LPS	Lipopolisacárido
LVED	*Left ventricular end-diastolic dimension*
LVEF	*Left ventricular ejection fraction*
LVFS	*Left ventricular fractional shortening*
MCP1	Proteína quimiotáctica de monocitos 1
MEC	Matriz extracelular
MHC	Cadena pesada de la miosina
MMPs	Metaloproteinasas de matriz
NBRE	*NGFIB response element*
NCX	Transportados Na^{+}/Ca^{2+}
NFAT	Factor nuclear de las células T activadas
NF-κB	*Nuclear factor kappa B*
NGFIB	*Nerve growth factor-induced clone B*

NO	Óxido nítrico
NOR-1	*Neuron-derived nuclear orphan receptor 1*
NR4A	*Nuclear receptor subfamily 4 group A*
NPY	Neuropéptido Y
NUR77	*Nur77-related factor 1*
NuRE	*Nur-Response Element*
OMS	Organización Mundial de la salud
OxCamKII	CaMKII oxidada
OxLDL	LDL oxidadas
PAH	Fenilalanina hidroxilasa
pb	Pares de bases
PDGF	Factor de crecimiento derivado de plaquetas
PLN	Fosfolamban
PPAR	*Peroxisome proliferator-activates receptors*
Ptx3	*Pentraxin-related protein* 3
PWT	*Posterior wall thickness*
ROS	Especies reactivas de oxígeno
RR	Riesgo relativo
RyR2	Receptor de rianodina tipo 2
SERCA2a	*Sarcoplasmic/endoplasmic reticulum* Ca^{2+} *ATPase 2a*
SLC6A2	*Solute carrier family 6 member 2*
SNPs	Polimorfismos de nucleótido único
TAC	*Transverse aortic constriction*
TAD	*Thoracic aortic dissection*
TGF-β	Factor de crecimiento transformante beta
TH	Tirosina hidroxilasa
Th	Linfocitos T *helpers*

TNF-α	Factor de necrosis tumoral alpha
TPAH2	Triptófano hidroxilasa
VCAM	Molécula de adhesión vascular
VEGF	Factor de crecimiento de endotelio vascular
WGA	*Wheat Germ Agglutinin*
WT	*Wild-type*

INTRODUCCIÓN

1. Las enfermedades cardiovasculares

Las enfermedades cardiovasculares son la principal causa de muerte en los países desarrollados. Según la Organización Mundial de la Salud (OMS) en 2015, causaron 17.9 millones de muertes, lo que representa el 31% de todas las muertes a nivel mundial. La distribución global de las patologías cardiovasculares es compleja y varía según las características nacionales y regionales. Aunque desde hace 2 décadas la mortalidad cardiovascular se ha visto reducida gracias a los avances en su diagnóstico y tratamiento, las enfermedades cardiovasculares continuarán encabezando la lista como primera causa de muerte. En efecto, la OMS prevé que el número de muertes por estas patologías aumentará a 23.6 millones el año 2030, y que serán el principal problema sanitario y socioeconómico de las próximas décadas (Roth *et al*., 2015).

Las enfermedades cardiovasculares abarcan un amplio abanico de desórdenes que afectan al corazón y a los vasos sanguíneos. Entre ellas destacar las enfermedades vasculares y las enfermedades del miocardio o de las cavidades cardíacas. Las enfermedades vasculares se caracterizan por un proceso activo de remodelación de la pared vascular (Gibbons & Dzau,1990). El espectro de alteraciones estructurales que pueden padecer los vasos sanguíneos es diverso y depende en parte del estímulo fisiopatológico. Las enfermedades del miocardio o de las cavidades cardíacas también abarcan patologías de origen muy diverso como anomalías auriculares y ventriculares adquiridas, algunas clases de miocarditis y la hipertrofia cardíaca, entre otras.

En este trabajo nos vamos a centrar en la hipertrofia cardíaca y el aneurisma de aorta abdominal (AAA), ambas caracterizadas por un profundo remodelado y una importante morbimortalidad.

1.1 Enfermedades del miocardio e hipertrofia cardíaca

Las enfermedades del miocardio o de las cavidades cardíacas, son patologías que afectan a la musculatura cardíaca. Entre ellas, nuestro grupo se ha centrado en el estudio de la hipertrofia cardíaca, debido a su elevada morbimortalidad asociada a un mayor riesgo de padecer insuficiencia cardíaca y/o accidente cerebrovascular.

1.1.1 Hipertrofia cardíaca

La hipertrofia cardíaca es una respuesta adaptativa del corazón a una sobrecarga de presión o de volumen. Multitud de patologías como la enfermedad isquémica, la hipertensión, el infarto de miocardio y la enfermedad valvular, conllevan una respuesta hipertrófica del miocardio. Esta hipertrofia es una respuesta compensatoria del corazón, con el objetivo de disminuir el estrés al que está sometida la pared y el consumo de oxígeno (Sandler & Dodge, 1963,

Grossman *et al*., 1975). Sin embargo, si el estrés cardíaco se prolonga en el tiempo, esta respuesta inicialmente adaptativa, desemboca en una hipertrofia cardíaca patológica que se asocia con un incremento en el riesgo de padecer insuficiencia cardíaca (Koren *et al*., 1991).

El corazón está compuesto por cardiomiocitos, fibroblastos, células endoteliales, mastocitos y células musculares lisas vasculares (CMLV), todas ellas rodeadas por la matriz extracelulas (MEC) (Bernardo *et al*., 2010). Los cardiomiocitos ventriculares representan solo un tercio del número de células totales del miocardio, pero contribuyen entre un 70-80% a la masa del corazón, por ello su crecimiento influye significativamente sobre el peso final del corazón (Nag, 1980).

A nivel celular, la hipertrofia cardíaca se caracteriza por un aumento del tamaño del cardiomiocito pero no de su número, debido a que la mayoría de cardiomiocitos son incapaces de dividirse (Soonpaa *et al*., 1996). Este aspecto presenta cierta controversia, ya que distintos estudios afirman la existencia de células progenitoras miocíticas que confieren al corazón la capacidad de replicación y reparación (Anversa *et al*., 2002, Nadal-Ginard *et al*., 2003). Otra característica de la hipertrofia cardíaca a nivel celular, es el aumento en la síntesis de proteínas y una mayor organización de los sarcómeros (Frey *et al*., 2004). Además, durante el desarrollo de la hipertrofia se producen cambios en la composición y estructura de la MEC, particularmente una mayor deposición de colágeno por parte de los cardiofibroblastos que incrementa la rigidez del corazón y dificulta la contracción normal del mismo (Baicu *et al*., 2003, Koshy *et al*., 2003).

1.1.1.1 Clasificación de la hipertrofia cardíaca

La hipertrofia cardíaca puede clasificarse como fisiológica o patológica. La hipertrofia cardíaca fisiológica incluye el crecimiento normal postnatal, el crecimiento cardíaco durante el embarazo y la hipertrofia cardíaca inducida en respuesta a ejercicio físico. En cambio, la hipertrofia cardíaca patológica ocurre como consecuencia de una sobrecarga de presión o de volumen crónico causada por la hipertensión arterial, una valvulopatía, el infarto de miocardio o una isquemia asociada con la enfermedad arterial coronaria (Bernardo *et al*., 2010). Ambos tipos de hipertrofia tienen como base un incremento del tamaño del corazón, ahora bien, la hipertrofia patológica se asocia a una pérdida de cardiomiocitos y fibrosis, produciendo disfunción cardíaca que incrementa el riesgo de padecer insuficiencia cardíaca o muerte súbita (Levy *et al*., 1990, Weber et al., 1993). Por el contrario, la hipertrofia cardíaca fisiológica se asocia a una función cardíaca normal o aumentada y es reversible si es promovida por el embarazo o el ejercicio (Scheuer *et al*., 1982, Fagard, 1997).

Ambos tipos de hipertrofia cardíaca, fisiológica y patológica se pueden clasificar como hipertrofia cardíaca concéntrica o excéntrica. Esta subdivisión depende tanto de la geometría del corazón y de la morfología de los cardiomiocitos, como del estímulo inicial (Figura 1) (Grossman *et al*., 1975).

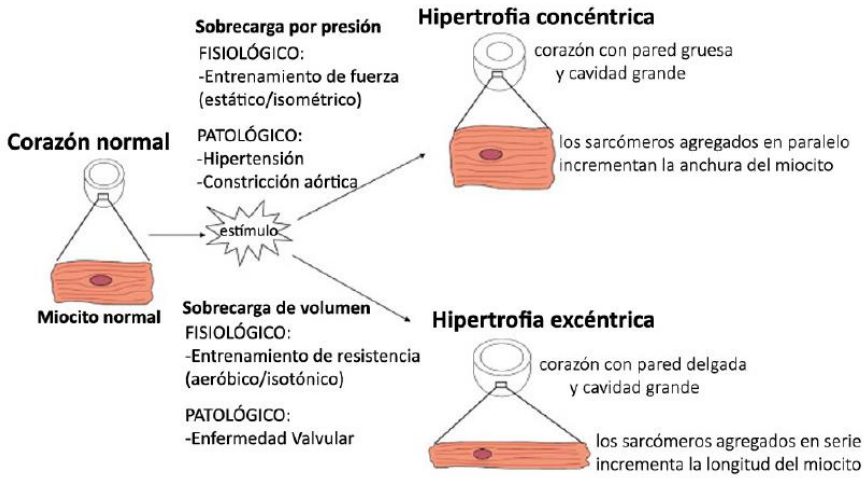

Figura 1. Resumen de las diferentes clasificaciones de hipertrofia cardíaca según el estímulo inductor. La hipertrofia puede estar ocasionada por sobrecarga de presión, bien fisiológica o patológica, que induce hipertrofia concéntrica, o bien por sobrecarga de volumen de origen fisiológico o patológico, que produce hipertrofia excéntrica. Imagen adaptada de Bernardo *et al*., (2010).

La hipertrofia concéntrica se caracteriza por un incremento del espesor de la pared ventricular y de la masa cardíaca, con una pequeña disminución o sin cambios en el volumen de la cavidad cardíaca. Los cardiomiocitos presentan un patrón determinado, ya que los sarcómeros se agregan en paralelo produciendo crecimiento en anchura del cardiomiocito. Este tipo de hipertrofia se origina en respuesta a un aumento del estrés sobre la pared en sístole, debido a una sobrecarga de presión en respuesta a un estímulo patológico, como por ejemplo la hipertensión o la estenosis aórtica. En cambio, la hipertrofia excéntrica se caracteriza por un menor incremento del espesor de la pared ventricular y un gran aumento del volumen de la cavidad ventricular y de la masa cardíaca. En este caso, los sarcómeros se disponen agregados en serie dando lugar a una célula miocítica alargada. Estímulos como la regurgitación aórtica o fístulas arteriovenosas, producen una sobrecarga de volumen con el consecuente estrés sobre la pared en diástole que da lugar a la hipertrofia excéntrica (Grossman *et al*., 1975).

Tanto la hipertrofia concéntrica como excéntrica pueden ser causadas por estímulos fisiológicos. Así, el embarazo o ejercicios aeróbicos, como natación o carreras de larga distancia, aumentan el retorno venoso al corazón, causando sobrecarga de volumen, y por tanto, una hipertrofia excéntrica (Eghbali *et al*.,

2005, Pluim *et al*., 2000). Mientras, ejercicios anaeróbicos como levantamiento de pesas, provocan generalmente una sobrecarga de presión en el miocardio, y por tanto, el desarrollo de una hipertrofia cardíaca concéntrica (Pluim *et al*., 2000).

1.1.1.2 Hipertrofia cardíaca e insuficiencia cardíaca

La comprensión de los mecanismos moleculares responsables de la hipertrofia cardíaca es de gran interés debido a la estrecha relación entre la hipertrofia cardíaca y la insuficiencia cardíaca (Levy *et al*., 1990). La hipertrofia cardíaca en su inicio es un mecanismo adaptativo en respuesta a una sobrecarga. Sin embargo, si el estrés persiste, el corazón hipertrofiado puede dilatarse, con lo que la función contráctil decae y el corazón puede fallar (Bernardo *et al*., 2010).

La insuficiencia cardíaca es un grave problema de salud en la sociedad occidental. Esta patología se diagnostica a un 10% de la población mayor de 70 años y las previsiones para las próximas décadas calculan un incremento en su prevalencia (Lloyd-Jones *et al*., 2009, Virani, *et al*., 2020). Los principales factores de riesgo de la insuficiencia cardíaca son la hipertensión, la enfermedad arterial coronaria, factores genéticos y la pérdida de miocitos debido al daño isquémico. Un estudio reciente demuestra que más de un 70% de los nuevos casos de insuficiencia cardíaca presentan un historial clínico de hipertensión y más de un 25% han padecido un infarto de miocardio (Brouwers *et al*., 2013). Además, según el estudio *Framingham*, en individuos con hipertrofia cardíaca se observa un aumento en la mortalidad de hasta 6 veces. Concretamente, un 45% de los casos de insuficiencia cardíaca se asocian con el desarrollo de la hipertrofia cardíaca (Gradman & Alfayoumi, 2006) .

1.1.1.3 Fisiopatología de la hipertrofia cardíaca

La hipertrofia cardíaca se caracteriza por alteraciones en la regulación del calcio, del metabolismo, de la expresión génica y por la muerte celular de los cardiomiocitos, además del desarrollo de inflamación, fibrosis y angiogénesis (Tham *et al*., 2015).

Regulación del metabolismo

El corazón emplea como principal fuente de energía los ácidos grasos en un 60%, mientras que el resto lo complementa con glucosa y lactato. El corazón es el órgano con un gasto de energía basal más alto (Stanley & Chandler, 2002). La hipertrofia cardíaca se asocia con una disminución de la oxidación de ácidos grasos y un aumento en la utilización de glucosa. En las fases iniciales de la hipertrofia el miocardio utiliza la glucosa para generar ATP, ya que por esta vía se requiere menos oxígeno que al utilizar ácidos grasos (Stanley *et al*., 2005). Si la hipertrofia cardíaca se prolonga en el tiempo, el metabolismo de la glucosa disminuye debido a la aparición de resistencia a la insulina, que produce una

reducción de la aportación energética y conduce al corazón a una insuficiencia cardíaca (Neubauer, 2007). El resultado global es una peor disponibilidad energética en las miofibrillas, un incremento de las disfunciones contráctiles y una pérdida de las reservas de ATP, que se ven reducidas a un 30-40% (Tham *et al*., 2015).

Cambios en la expresión génica

La hipertrofia cardíaca patológica se asocia con alteraciones en las proteínas cardíacas responsables de la contracción. En condiciones fisiológicas se expresa mayoritariamente la cadena pesada de la miosina tipo alpha (α-MHC), isoforma que facilita la contracción rápida. Sin embargo, su expresión en condiciones patológicas se ve reducida y aumenta la β-MHC, isoforma característica del desarrollo cardiaco embrionario, que cataliza la hidrólisis de ATP más lentamente y produce una contracción lenta (Bernardo *et al*., 2010). Otros estudios tanto en humanos (Arai *et al*., 1993) como en modelos animales (Iemitsu *et al*., 2001) han demostrado un aumento de la expresión de genes que se expresan normalmente durante el desarrollo fetal como el péptido natriurético auricular (ANP), el péptido natriurético de tipo B (BNP) y la α-actina. La ANP y la BNP pertenecen a una familia de hormonas que actúan sobre el sistema cardiovascular y el endocrino y que además tienen una importante actividad anti-hipertrófica sobre el cardiomiocito (Woods, 2004). Se ha observado que cuando otros mecanismos anti-hipertróficos fallan, la labor del BNP se mantiene (Rosenkranz *et al*., 2003). Por lo tanto, se considera que una elevada expresión de estos péptidos es un proceso compensatorio con gran importancia desde el punto de vista de la cardioprotección.

Fibrosis cardíaca

La hipertrofia cardíaca patológica está estrechamente asociada con la apoptosis de los miocitos. La pérdida celular se ve reemplazada por tejido conectivo en un proceso conocido como “fibrosis de reparación”, tal como sucede después de un infarto. A su vez, de forma alternativa, en las regiones no dañadas se produce la llamada “fibrosis reactiva”, que se presenta en zonas sin apoptosis de miocitos, y con deposición de fibras de colágeno de tipo I y II, (Weber, 1989).

La fibrosis se clasifica según su localización, en fibrosis intersticial producida alrededor de las células y caracterizada por una deposición generalizada de colágeno en todo el corazón; y en fibrosis perivascular, que se localiza alrededor de los vasos sanguíneos del corazón y limita el aporte de oxígeno al músculo (Brown *et al*., 2005).

A nivel cardíaco, los cardiofibroblastos son los encargados de promover el remodelado de la MEC, produciendo fibrosis. La MEC cardíaca está compuesta principalmente por fibras de colágeno de tipo I y III, constituyendo el 85% y el

10% respectivamente (Weber, 1989). En condiciones fisiológicas se mantiene un balance entre la producción y secreción de proteínas de tejido conectivo, y su degradación por proteasas específicas (Baudino *et al*., 2006). La alteración de la homeostasis de la MEC, conlleva el remodelado miocárdico y la fibrosis. En este proceso, los cardiofibroblastos se diferencian a un estado activo, los miofibroblastos. Estas células presentan mayor actividad proliferativa migratoria y contráctil respecto a los cardiofibroblastos. Además presentan una alta producción y secreción de proteínas de matriz, como la lisil oxidasa (LOX), la galectina 3, la periostina o la serpina 2 (Lu *et al*., 2012) que contribuyen a agravar el proceso fibrótico. Concretamente, estudios previos de nuestro grupo en un modelo animal transgénico, han demostrado que la sobreexpresión de la LOX altera la función diastólica durante el envejecimiento, agrava la hipertrofia cardíaca inducida por la angiotensina II (AngII) y promueve la transdiferenciación miofibroblástica (Galán *et al*., 2017, Martínez-González *et al*., 2019). La principal consecuencia de este proceso fibrótico es un aumento de la rigidez miocárdica y una reducción en la contractibilidad del corazón, que altera el rendimiento normal del miocardio (Tomasek *et al*., 2002, Baudino *et al*., 2006).

Inflamación

En los últimos años ha cobrado importancia la inflamación como característica distintiva de la hipertrofia (Yang *et al*., 2012). En el corazón hipertrofiado se ha detectado la presencia de un infiltrado inflamatorio, constituido principalmente por macrófagos y linfocitos T. También se incrementan los niveles de interleuquinas (IL-6 y IL-1β) y del factor de necrosis tumoral (TNF-α), y además se activan vías de señalización pro-inflamatorias como la vía NF-κB (del inglés *Nuclear factor kappa B*) (Erten *et al*., 2005, Kuusisto *et al*., 2012). La contribución de la inflamación a la hipertrofia no se ha caracterizado en su totalidad, pero lo más probable es que exacerbe la enfermedad (Samak *et al*., 2016). Sin embargo, existen estudios que muestran que la depleción de macrófagos agrava la hipertrofia cardíaca, por lo que es necesario profundizar en el papel de la inflamación en la hipertrofia.

Un ejemplo de la necesidad de seguir investigando la inflamación, es el caso de la función de los macrófagos en la hipertrofia y más concretamente de los dos fenotipos de macrófagos, el M1 o proinflamatorios y el M2 antiinflamatorios (Mosser & Edwards, 2008, Takeda & Manabe, 2011). El primer tipo de macrófagos promueve la inflamación del miocardio mediante la liberación de citoquinas y acelera la apoptosis, procesos que contribuyen al remodelado cardíaco, contrariamente, los macrófagos M2 estimulan rutas de reparación cardíaca y la angiogénesis (van den Akker *et al*., 2013). El estudio del proceso inflamatorio, puede desvelar puntos clave en la progresión de la patología y en la identificación de nuevas dianas terapéuticas.

Alteración homeostasis del calcio

La contracción del corazón está regulada por cambios cíclicos en la concentración de Ca^{2+} en los cardiomiocitos. Durante la excitación-contracción cardíaca, un alto potencial de Ca^{2+} entra al cardiomiocito mediante los canales de Ca^{2+} tipo L (LTCC) localizado en los túbulos T. La unión del Ca^{2+} a los receptores tipo 2 de rianodina (RyR2) situados en la membrana del retículo sarcoplásmico produce la liberación de Ca^{2+}, proceso conocido con el nombre de inducción-liberación Ca^{2+} (Bers, 2014). Esto produce un incremento de la concentración intracelular de Ca^{2+} que favorece su unión a la troponina C de los filamentos sarcoméricos. Estas interacciones entre proteínas producen la formación de puentes entre los filamentos gruesos y finos, dando lugar a la contracción (Solaro, 2010). La relajación ocurre cuando el Ca^{2+} es bombeado de nuevo al retículo sarcoplasmico mediante la ATPasa dependiente de Ca^{2+} (SERCA2a) o bien, expulsado de la células mediante el transportados Na^{+}/Ca^{2+} (NCX) (Bers, 2006). La actividad de SERCA2a es regulada por fosfolamban (PLN). Así, la desfosforilación de PLN inhibe SERCA2a (Tham *et al*., 2015).

Las alteraciones en la homeostasis del calcio pueden deberse a múltiples causas. Destacar el papel de la proteína calmodulina quinasa II dependiente de Ca^{2+} (CaMKII) clave en la regulación de los canales iónicos durante el proceso excitación-contracción del miocardio (Couchonnal & Anderson, 2008). La activación excesiva de la CaMKII en el miocardio promueve la hipertrofia (Zhang *et al*., 2003) y apoptosis de los cariomiocitos (Zhu *et al.*, 2003, Yang et al., 2006). La actividad de la CaMKII dependen de distintas modificaciones post-traducionales, entre ellas, la oxidación. Recientemente, se ha descrito que las ROS oxidan la CaMKII dando lugar a su forma oxidada (oxCaMKII) y constitutivamente activa, independientemente de los niveles de calcio (Erickson *et al*., 2008). La activación prolongada de la CaMKII tiene efectos sobre múltiples proteínas del mecanismo de excitación-contracción como el RyR2 y PLN. En general, la actividad prolongada de la CaMKII se ha asociado con hipertrofia (Kakishita *et al*., 2003), oscilaciones en el potencial de membrana de los cardiomiocitos arritmias y muerte súbita (Maier *et al*., 2003, Sag *et al*., 2009).

Todos los cambios descritos en este apartado, se caracterizan en su inicio por ser alteraciones adaptativas y reversibles, sin embargo la sobrecarga de presión o volumen prolongada en el tiempo sobre el miocardio da lugar a una hipertrofia cardíaca patológica que se asocia con un incremento en el riesgo de padecer una insuficiencia cardíaca.

1.2 Pared arterial y aneurisma de aorta abdominal

El AAA es una dilatación localizada de la aorta abdominal que se caracteriza por una degeneración progresiva de la pared arterial. Para comprender mejor esta patología primero vamos a revisar la anatomía de la arteria.

1.2.1 Anatomía de la arteria

Las arterias se clasifican según su calibre. Entre las arterias de gran calibre o elásticas se encuentran la aorta y la arteria pulmonar, que distribuyen la sangre a altas presiones. En segundo lugar, distinguimos las arterias de mediano o pequeño calibre, cuyo componente principal es el tejido muscular y por ello reciben el nombre de arterias musculares. Por último, las arteriolas que son arterias musculares con un diámetro de 100 µm o menos.

La pared arterial está constituida por tres capas bien delimitadas: la íntima, la media y la adventicia (Figura 2). La íntima es la capa más interna que está contigua a la luz del vaso y en contacto con la sangre. Está formada por una monocapa de células endoteliales (CE) en el lado luminal, y por la lámina basal de tejido fibroelástico (lámina elástica interna) sobre la que descansan las células endoteliales. Esta capa constituye una barrera de permeabilidad selectiva entre los componentes sanguíneos y el tejido vascular. A continuación, se encuentra la media que es la capa más gruesa. En las arterias musculares la capa media es principalmente muscular y las CMLV están rodeadas por fibras de colágeno y fibras elásticas. En cambio en las arterias elásticas, la media está compuesta esencialmente por láminas de elastina concéntricas y fenestradas, entre las cuales se sitúan las CMLV. Seguidamente, se encuentra una lámina elástica externa que separa la capa media de la adventicia. Esta última, contiene haces de colágeno y fibras elásticas, fibroblastos y pocas CMLV. La adventicia posee vasos linfáticos y fibras nerviosas, los primeros aportan nutrientes y oxígeno, mientras las segundas permiten la comunicación neuronal entre las arterias y el resto del organismo (Lusis, 2000).

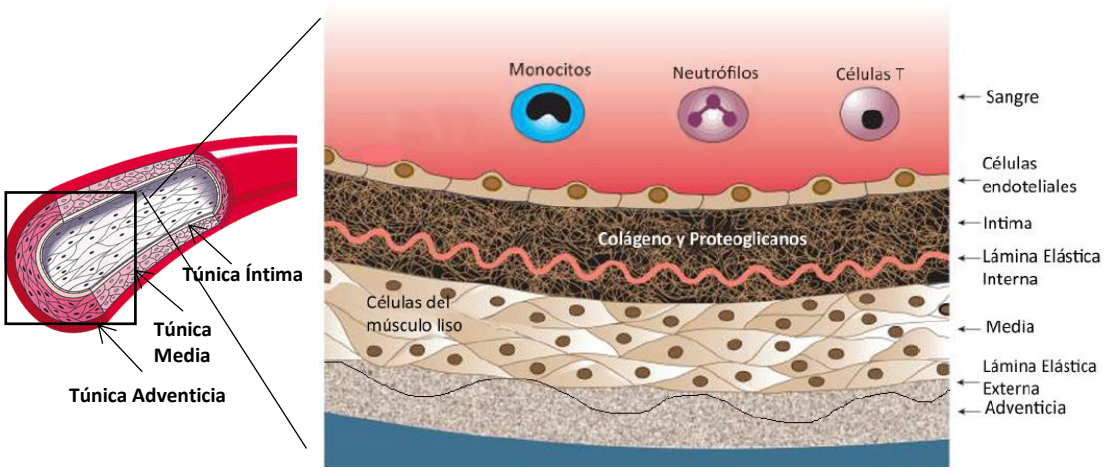

Figura 2. Representación de la anatomía de la arteria. Las arterias están formadas por la túnica íntima, media y adventicia. A la izquierda de la figura se observa un esquema de una arteria, y en la parte derecha se muestra un corte transversal. Imagen adaptada de Lusis (2000).

1.2.2 Aneurisma de aorta abdominal (AAA)

El AAA es una patología degenerativa vascular con una elevada morbilidad y mortalidad, que afecta principalmente a la población de avanzada edad. Se caracteriza por una dilatación localizada y permanente de la aorta abdominal, como consecuencia de un debilitamiento de la pared vascular. La ruptura del AAA es la consecuencia más grave de esta patología, y se asocia con una tasa de mortalidad entre el 80-90% (Weintraub, 2009). Generalmente la AAA es una patología asintomática, y su formación implica un importante proceso inflamatorio de la pared aortica, en el que se produce un aumento de la actividad proteolítica, neovascularización y apoptosis de las CMLV. Actualmente, las opciones terapéuticas son limitadas y la cirugía de reparación es la única opción para evitar el alto riesgo de ruptura del aneurisma (Nordon *et al*., 2011).

Cabe destacar, que la patología aneurismática, como muchas otras patologías cardiovasculares, se asocia con el desarrollo de aterosclerosis. La aterosclerosis es una enfermedad crónica que se inicia a temprana edad y progresa asintomáticamente. Afecta a la capa íntima de las arterias de mediano y gran calibre, caracterizándose por una inflamación y acumulación de restos celulares, tejido conectivo, lípidos y células en la pared vascular. Estos acúmulos dan lugar a la placa de ateroma o lesión aterosclerótica (Lusis, 2000, Libby *et al*., 2011). Durante el desarrollo de la enfermedad las placas de ateroma crecen, obstruyendo total o parcialmente la luz del vaso, y las placas inestables, pueden romperse y provocar trombosis que causa los episodios clínicos agudos (McGill *et al*., 2000, Lusis, 2000). Existe una gran controversia acerca de la relación entre la aterosclerosis y el AAA. Frecuentemente pacientes

con AAA presentan aterosclerosis (Cornuz *et al*., 2004, Golledge *et al*., 2006), siendo ésta un factor de riesgo independiente para el desarrollo del AAA. Sin embargo, en los últimos años se ha demostrado que el AAA no es una manifestación de la aterosclerosis, y que en su compleja etiología factores como el tabaquismo son determinantes en su formación y progresión (Golledge & Norman, 2010, Toghill *et al*., 2017) .

La aorta abdominal, región de la aorta comprendida entre el diafragma y la bifurcación aórtica, es la zona más susceptible al desarrollo de aneurismas debido a sus características anatómicas. A su vez, el AAA se puede subclasificar en aneurisma visceral, suprarrenal o infrarrenal según su localización. En el primero se ven implicadas las arterias viscerales, en el segundo se afectan las arterias renales y el último se manifiesta cuando el aneurisma se desarrolla por debajo de las arterias renales (Kuivaniemi *et al*., 2015). Generalmente, el aneurisma se manifiesta en la porción infrarrenal de la aorta, debido a que es una región sometida a importantes fuerzas hemodinámicas (Aggarwal *et al*., 2011). Considerando la definición de aneurisma como aquella dilatación superior al 50% del diámetro normal del vaso, en la zona abdominal se calificaría como patológico un diámetro superior o igual a 3 cm (Ouriel *et al*., 1992, Aggarwal *et al*., 2011).

El AAA afecta 6 veces más a los hombres que a las mujeres. La incidencia en la población masculina mayor de 65 años está entre un 5 -8%, en cambio en la población femenina en el mismo rango de edad la afectación es de un 2% (Nordon *et al*., 2011). En los últimos años, la incidencia de esta enfermedad ha aumentado debido al envejecimiento de la población, y es la responsable del 1% de las muertes de hombres mayores de 65 años, cifra que puede verse incrementada en las próximas décadas debido al aumento en la esperanza de vida de la población (Earnshaw *et al*., 2004, Torres-Fonseca *et al*., 2019).

1.2.2.1 Factores de riesgo del AAA

El AAA es una patología compleja y multifactorial en la que, como ya hemos indicado, la contribución de la aterosclerosis es motivo de controversia, y cuyos principales factores de riesgo son el tabaquismo, la edad, el sexo y la historia familiar (Nordon *et al*., 2011).

Consumo de tabaco

El tabaquismo es el factor de riesgo más importante en el AAA (Lederle *et al*., 2001). Se ha observado que el consumo de tabaco aumenta el riesgo relativo (RR) de AAA 7.6 veces (Wilmink *et al*., 1999). Los varones fumadores de más de 25 cigarrillos al día tienen un riesgo de aneurisma 15 veces superior al de varones no fumadores (Wong *et al*., 2007). No solo es importante el número de cigarrillos consumidos al día, sino también la duración del hábito tabáquico, ya que cada año de tabaquismo incrementa el RR de AAA en un 4% (Wilmink *et*

al., 1999). Una vez que cesa el consumo de cigarrillos el riesgo de padecer AAA se mantiene durante 10 años. Aún se desconocen los mecanismos por los cuales el tabaco promueve a la formación de AAA, pero se barajan distintas posibilidades como la inhibición de la síntesis de colágeno, la alteración de la expresión de metaloproteinasas de matriz (MMPs), la posible relación con el estrés oxidativo y alteraciones en la función de las células inflamatorias (Knuutinen *et al*., 2002, Jin *et al*., 2012).

Edad

La incidencia del AAA aumenta con el paso de los años, la prevalencia es del 3% en la población mayor de 50 años y sobre un 5-8% en hombres mayores de 65 años (Nordon *et al*., 2011, LeFevre & Force, 2014). Cabe destacar que las muertes por ruptura aneurismática se dan a partir de los 65 años, y desde entonces el riesgo se incrementa aproximadamente un 40% cada 5 años (Vardulaki *et al*., 2000).

Sexo

Como se ha comentado anteriormente, la incidencia en hombres es 6 veces mayor que en mujeres. Además, el aneurisma en mujeres se desarrolla aproximadamente 10 años más tarde que en hombres, lo que se ha relacionado con factores hormonales, susceptibilidad genética y la diferente exposición a factores de riesgo (Lederle *et al*., 2001). La mayoría de estudios sobre la prevalencia y los factores de riesgo para el AAA se han realizado en hombres, pocos estudios se han centrado de forma específica en el AAA en la mujer, que cuando presenta la enfermedad, suele ser más grave (Lo & Schermerhorn, 2016).

Historia familiar

Se ha llegado a considerar la influencia de un componente genético en la patología del AAA. En efecto, se ha observado un aumento de la prevalencia del aneurisma entre familiares de primer grado, siendo entre 15-19% *(Ogata et al*., 2005). Algunos estudios demuestran que la historia familiar positiva en primer grado de AAA incrementa hasta 10 veces el riesgo de padecer aneurisma, y de que se manifieste con mayor probabilidad a edades tempranas (Larsson *et al*., 2009). Concretamente, mediante el análisis genético de 233 familias con más de un individuo diagnosticado con AAA, se han identificado regiones genéticas en los cromosomas 4 y 19 (4q31 y 19p13) que se asocian con un mayor riesgo de padecer AAA (Kuivaniemi *et al*., 2003).

Otros factores de riesgo

Otros factores con menor relevancia en la enfermedad aneurismática son la hipertensión arterial y la hipercolesterolemia. Aunque la hipertensión arterial

se relaciona con un incremento del riesgo de formación del AAA y sobre todo con su ruptura, su contribución a la patología es todavía motivo de debate y el tratamiento antihipertensivo no ha demostrado eficacia limitando el desarrollo del AAA (Brady *et al*., 2004). A su vez, los estudios respecto al impacto de los niveles de lípidos sobre la formación de AAA son contradictorios (Louwrens *et al*., 1993, Forsdahl *et al*., 2009, Rizzo *et al*., 2009). Independientemente de la potencial contribución de los lípidos en la progresión del AAA, está ampliamente aceptado que los bajos niveles de las lipoproteínas de alta densidad (HDL) se asocian tanto a la presencia como a la evolución de esta patología (Golledge *et al*., 2010 A, Burillo *et al*., 2015). Estudios recientes, han identificado residuos de triptófano oxidados (Trp50 y Trp108) en la APoA1 de las HDL de pacientes con AAA. Además, estás HDL modificadas en el ambiente del trombo aneurismático son lipoproteínas no funcionales lo que empeora el pronóstico de la enfermedad. Estos resultados evidencian el importante papel del estrés oxidativo en esta patología y sugieren que el nivel de oxidación de los residuos Trp50 y Trp80 podría ser un biomarcador del AAA (Martínez-López *et al*., 2018, 2019). Por último, al contrario que ocurre en la enfermedad aterosclerótica, la diabetes mellitus se ha identificado como factor protector del desarrollo de AAA. La diabetes ejercería este papel protector a través de diferentes mecanismos: promoviendo la respuesta antiinflamatoria mediada por la activación de la vía del factor de crecimiento transformante β (TGF-β), modulando el remodelado de la MEC, entre otros efectos al incrementar la resistencia del colágeno a ser degradado, o bien reduciendo la apoptosis de las CMLV (Raffort *et al*., 2018).

1.2.2.2 La fisiopatología del AAA

El remodelado del tejido vascular propio del AAA es un proceso complejo y dinámico, que se caracteriza por la degradación proteolítica de la MEC, la apoptosis de las CMLV, la infiltración de células inflamatorias en la adventicia y el incremento del estrés oxidativo en la pared aórtica (Figura 3). Todos estos procesos están interconectados entre sí, lo que evidencia la complejidad de esta patología (Sakalihasan *et al*., 2018).

La elevada presión sanguínea en la aorta y la alteración hemodinámica del flujo sanguíneo pueden explicar la creación y desarrollo del trombo intramural (ILT, del inglés *Intraluminal Thrombus*) (Wilson *et al*., 2013) que se presenta en un 75% de los casos (Piechota-Polanczyk *et al*., 2015). El ILT está formado por una capa hemática fresca con fibras de fibrina en la zona luminal, aunque en la cara abluminal se produce una fibrinólisis activa. En lo que respecta a la estructura de la aorta, se observa una fina capa media, parcialmente degradada con escaso contenido en CMLV y falta de componentes elásticos. A su vez, se detecta una adventicia fibrosa y más gruesa, debido a la inflamación y al edema. Estudios recientes evidencian la importancia fisiopatológica del ILT en esta

enfermedad (Michel *et al*., 2011). Estos estudios indican que el grosor del trombo disminuye la biodisponibilidad de oxígeno en la pared arterial, lo que puede incrementar la reactividad de los neutrófilos y su producción de elastasa (Torres-Fonseca *et al*., 2019). Además, la continua circulación de sangre por el lumen de la aorta, produce que el ILT posea una alta capacidad proteolítica, genera un ambiente oxidativo e impide la proliferación de las células con las que entra en contacto (células endoteliales, CMLV o progenitores mesenquimales) (Sakalihasan *et al*., 2018).

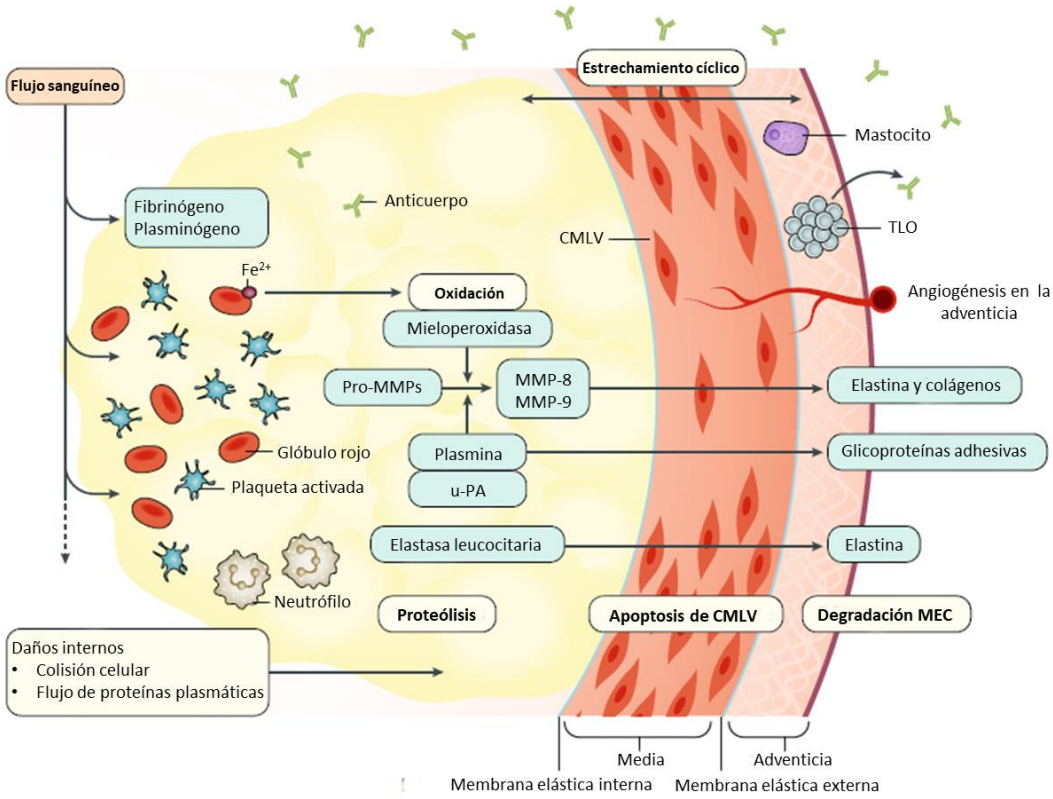

Figura 3. Representación de la progresión del aneurisma de aorta abdominal (AAA). Se indican los distintos elementos solubles del plasma y las células circulantes que interaccionan con la pared arterial. Estas interacciones promueven la formación del trombo intraluminal (ILT) que presenta actividad proteolítica y oxidativa. Ambos procesos facilitan la degradación de la matriz extracelular (MEC), la apoptosis de células musculares lisas vasculares (CMLV) y la activación de la respuesta inmune. La elastasa leucocitaria puede degradar las fibras de la MEC. La plasmina es otra proteasa de serina que degrada proteínas de adhesión produciendo la pérdida de anclaje de las CMLV y activando las pro-metaloproteinasas (Pro-MMPs: precursores inactivos de las MMPs). El plasminógeno se convierte en plasmina mediante la acción del activador de plasminogeno tipo uroquinasa (u-PA). Tanto u-PA como la elastasa leucocitaria son liberados por neutrófilos. La elastasa posee también la capacidad de degradar fibrina generando péptidos de fibrina, los cuales pueden servir como biomarcadores para la

evolución del AAA. Las MMPs son sintetizadas como precursores inactivos y se activan mediante proteólisis por la plasmina o por especies reactivas de oxígeno (ROS, *Reactive Oxigen Species*), entre otras. La adventicia del AAA esta enriquecida en mastocitos, que son células que contienen triptasa y quimasa, y promueven la formación de nuevos vasos en la adventicia (neoangiogénesis). Imagen adaptada de Sakalihasan *et al*., (2018).

Degradación de la MEC

La MEC de la pared aortica, formada por componentes fibrosos e insolubles (colágeno y elastina) sintetizados y procesados por las CMLV, soporta la carga hemodinámica de la pared aortica. La acción progresiva de las proteasas degradando la MEC se considera el mecanismo más relevante durante el desarrollo y progresión del AAA (Libby & Lee, 2000).

La degradación de la MEC se atribuye fundamentalmente a la acción de las proteasas liberadas por neutrófilos o bien a zimógenos presentes en la sangre, que atraviesan la pared (Busuttil *et al*., 1982). La degradación de elastina se asocia con una progresiva dilatación, mientras que la pérdida de colágeno favorece la ruptura del AAA (Dobrin *et al*., 1984). Dos familias de proteasas son fundamentales en la progresión del AAA: las proteasas de serina y las MMPs. Las primeras degradan la MEC directa o indirectamente, ya que promueven la proteólisis de proteínas adhesivas como la fibronectina y de componentes estructurales como la fibrilina que son más sensibles a la degradación por estas enzimas que los componentes macromoleculares. Las MMPs degradan directamente componentes estructurales de la MEC, como colágenos, elastina o proteoglicanos, entre otros sustratos. Las principales MMPs implicadas por su parte en el AAA son la MMP-2 y la MMP-9 (Sakalihasan *et al*., 1996).

En este remodelado destructivo de la MEC juegan un papel clave los leucocitos, que son los principales responsables de la producción de MMPs y de proteasas de serina (Freestone *et al*., 1995). Además, las citoquinas pro-inflamatorias liberadas en el AAA pueden regular la expresión de MMPs, de proteasas de serina y catepsinas, contribuyendo así a la formación del aneurisma (Newman *et al*., 1994). El lugar específico de la ruptura aneurismática se caracteriza por una elevada expresión de proteasas (Defawe *et al*., 2004), un importante infiltrado de leucocitos y neovascularización focal (Choke *et al*., 2006).

Apoptosis de las CMLV

La pérdida parcial de las CMLV en la patología aneurismática contribuye al debilitamiento de la pared vascular y se debe principalmente a la apoptosis promovida por la acción proteolítica y el ambiente oxidativo de la pared aórtica. Las proteasas de serina producen la pérdida de anclaje de las CMLV a la MEC,

lo que causa su muerte (Jean-Baptiste, 2003, Wang *et al*., 2015). En paralelo, el intenso estrés oxidativo también provoca la apoptosis de las CMLV. En este proceso participan, entre otros, los ceroides (polímeros compuestos de lípidos y proteínas oxidadas), marcadores de estrés oxidativo, altamente tóxicos para CMLV, están presentes en la pared de la AAA (Michel *et al*., 2014, Wang *et al*., 2015).

El infiltrado inflamatorio, principalmente macrófagos y linfocitos T, producen mediadores citotóxicos como las citoquinas, la perforina y el ligando de Fas que promueven la agregación de CMLV y su consiguiente muerte (Henderson *et al*., 1999). También se ha descrito que los macrófagos infiltrados en la pared del aneurisma expresan altos niveles de ciclooxigenasa 2 (COX-2), que regula la síntesis de la prostaglandina E que inhibe la proliferación de CMLV (Walton *et al*., 1999).

Estrés oxidativo

El estrés oxidativo se produce en los tejidos cuando la generación de especies reactivas de oxígeno (ROS, *Reactive Oxigen Species*) supera la capacidad de las defensas antioxidantes. Este desequilibrio provoca la producción de proteínas oxidadas, peróxidos y daño al DNA que promueven apoptosis (Sakalihasan *et al*., 2005). Esta respuesta está íntimamente relacionada con la inflamación vascular. Las células inflamatorias pueden generar ROS y mediadores como el TNF-α, la proteína quimiotáctica de monocitos (MCP1) o el factor de crecimiento derivado de plaquetas (PDGF), los cuales a su vez pueden aumentar la producción de ROS por las CMLV (Satriano *et al*., 1993, Marumo *et al*., 1997).

En estudios recientes, se ha observado que en muestras procedentes de pacientes con AAA hay una mayor actividad de enzimas pro-oxidantes como la NADPH oxidasa, la mieloperoxidasa, la lipoxigenasa y la leucotrieno hidrolasa (Houard *et al*., 2009). En cambio, se ha descrito una disminución de las enzimas antioxidantes como la superóxido dismutasa, la glutatión peroxidasa y la glutatión reductasa, en comparación con aortas sanas (Hunter *et al*., 1991, Dubick *et al*., 1999). En concordancia, en un modelo experimental de AAA, la suplementación de catalasa inhibió la formación de aneurismas (Grigoryants *et al*., 2005). Nuestro grupo ha descrito elevados niveles circulantes del oxiesterol 7-cetocolesterol en el suero de pacientes con AAA respecto a muestras de donantes sanos. Además, los niveles del 7-cetocolesterol correlacionan con la expresión de marcadores de estrés oxidativo y estrés de retículo (Navas-Madroñal *et al*., 2019). Por último, otros estudios ponen de manifiesto que diferentes tipos celulares (fibroblastos, células endoteliales y linfocitos activados T y B) liberan tiorredoxina en respuesta a un ambiente oxidativo (Rubartelli *et al*., 1992), y se ha observado que los niveles de tiorredoxina son elevados en el ILT (Martinez-Pinna *et al*., 2010). Además, los

niveles circulantes de tiorredoxina correlacionan con el tamaño del AAA y su crecimiento. Todo ello, destaca la importancia del estrés oxidativo en esta patología, y la posible utilidad de estos enzimas como biomarcadores (Michel *et al*., 2011).

La inflamación en el AAA

La inflamación es otra de las características fisiopatológicas del AAA, que como ya hemos comentado, contribuye de forma decisiva al desarrollo de la enfermedad. La pared arterial aneurismática presenta un importante infiltrado inflamatorio, constituido fundamentalmente por linfocitos T y B, neutrófilos y macrófagos (Dale *et al*., 2015, Raffort *et al*., 2017). El mecanismo que desencadena esta respuesta inflamatoria es desconocido, lo más probable es que los propios péptidos derivados de la degradación de la MEC actúen como agentes quimiotácticos para las células inflamatorias como los macrófagos. Además, el incremento de los niveles de IL-8, MCP1 y RANTES favorecería el reclutamiento de leucocitos (Torres-Fonseca *et al*., 2019).

Como se ha indicado anteriormente, las células inflamatorias son las principales productoras de MMPs. De igual manera, las MMPs pueden modular la respuesta inflamatoria a través de la regulación de la biodisponibilidad de citoquinas de forma directa o indirecta (Parks *et al*., 2004). Así, las MMP-2 y MMP-9 son encargadas de potenciar, inactivar o antagonizar la actividad de las citoquinas mediante su procesamiento proteolítico (Hellenthal *et al*., 2009).

1.2.2.3 Diagnóstico y manejo clínico

El AAA es una enfermedad asintomática por lo que el diagnóstico de esta enfermedad suele ser casual, cuando los pacientes son sometidos a pruebas de imagen (ultrasonografía, tomografía axial computarizada o resonancia magnética) realizadas en el contexto de otra patología. Esta situación ha llevado a algunos países a instaurar programas de detección precoz de la enfermedad. Estos programas someten a los grupos de mayor riesgo de la población a revisiones periódicas mediante ecografía, estrategia que ha permitido disminuir la incidencia de ruptura del AAA en hombres de forma eficaz y coste-efectiva (Lindholt *et al*., 2010).

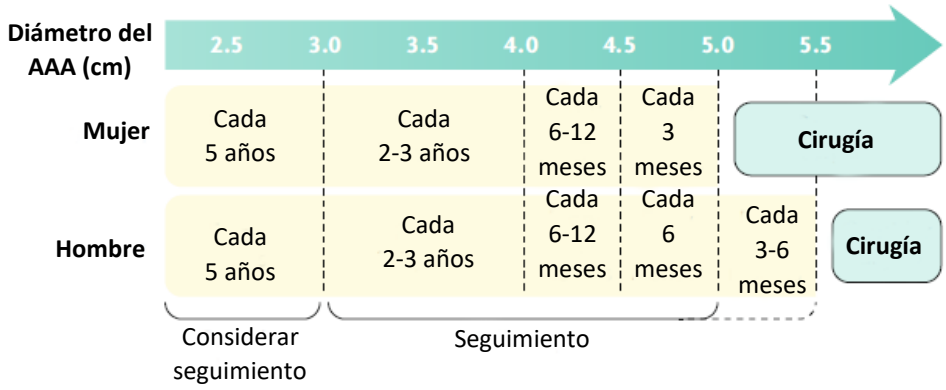

Figura 4. Protocolo de vigilancia de pacientes con AAA. Se muestra el programa de seguimiento de los pacientes con AAA hasta la cirugía. La intervención quirúrgica puede realizarse antes de lo previsto por este protocolo, si el paciente presenta un rápido crecimiento del aneurisma (AAA con un crecimiento superior o igual a 10 mm por año). Si el paciente no puede ser intervenido debido al elevado riesgo de la intervención (por presencia de co-morbilidades, edad muy avanzada, etc.) el límite se puede incrementar hasta diámetros superiores a 6 cm. Imagen adaptada de Sakalihasan *et al*., (2018).

El protocolo a seguir en el manejo del AAA es conservador cuando el diámetro se mantiene entre 3-5 cm (Figura 4). Se realiza un seguimiento periódico con pruebas de imagen, además de un exhaustivo control de los factores de riesgo y un tratamiento farmacológico que suele incluir terapia antiagregante y estatinas, aunque en la actualidad no existe ningún tratamiento efectivo que limite la progresión o evite la ruptura del AAA. En situaciones en las que el riesgo de ruptura es mayor que el riesgo de la propia intervención quirúrgica, la mejor opción es la cirugía. La decisión se toma cuando el diámetro vascular supera los 5-5,5 cm, si bien puede adelantarse ante la presencia de síntomas (como dolor abdominal) o una elevada tasa de crecimiento del AAA (superior a 1 cm/año) (Sakalihasan *et al*., 2018). Existen dos tipos de intervenciones quirúrgicas, la cirugía intravascular o la cirugía abierta. La elección dependerá de las características del paciente, del riesgo quirúrgico, de la morfología, de la localización, del diámetro aórtico y de la tasa de crecimiento del AAA (Rutherford 2006). La cirugía abierta consiste en una reparación profiláctica, mediante una laparotomía en la zona abdominal y el reemplazo de la zona aneurismática dañada por un injerto aórtico (Steuer *et al*., 2015). Tras 30 días post-intervención, la mortalidad asociada a esta cirugía es de un 4% a un 12%. Por otro lado, en la década de los 90, se empezó a utilizar un método endovascular para la reparación del AAA (EVAR *Endovascular Aneurysm Repair*). Esta intervención consiste en introducir a través de la arteria femoral, un catéter con una prótesis en su interior que se sitúa en la zona del aneurisma. Cuando está localizado correctamente, la prótesis se libera mediante la retirada del catéter y se expande adaptándose al diámetro del vaso. Este

método permite que el flujo sanguíneo circule por el interior de la prótesis sin impactar sobre la región aneurismática. Desde que la FDA (*Food and Drug Administration*) aprobó el uso de la EVAR en 1999, su utilización se ha visto incrementada ya que reduce la pérdida de sangre de la cirugía abierta y la mortalidad perioperativa (Kuivaniemi *et al*., 2015). Con este método menos invasivo, a los 30 días de la intervención la mortalidad disminuye dos tercios en comparación a la cirugía abierta, si bien existe un mayor riesgo de complicaciones postquirúrgicas como las provocadas por el desplazamiento de la prótesis (Parodi *et al*., 1991).

1.2.2.4 Tratamiento farmacológico del AAA

En la actualidad, la única estrategia para evitar la ruptura del aneurisma sigue siendo la intervención quirúrgica. Además, un adecuado control de los factores de riesgo puede ser una herramienta ventajosa para hacer frente a la progresión del AAA. Hoy en día, existen ciertos fármacos empleados para el tratamiento de otras patologías, que han tenido resultados beneficiosos en su uso contra el AAA, si bien ninguno de ellos ha logrado frenar la evolución de la enfermedad.

Antihipertensivos

Los betabloqueantes han sido los fármacos más estudiados en esta enfermedad. Entre ellos, el bisoprolol ha demostrado una disminución en la mortalidad por causa cardíaca después de la cirugía por AAA. No está verificado el mismo efecto para todos los betabloqueantes, pero las guías médicas de ACC/AHA (*American College of Cardiology / American Heart Association*) recomiendan el uso de los mismos durante el periodo perioperatorio (Hirsch *et al*., 2006).

También se utilizan con frecuencia inhibidores de la enzima convertidora de angiotensina (IECA), debido a que la activación del sistema renina-angiotensina se ha visto implicado en la progresión del AAA (Zhang *et al*., 2018). En trabajos con alrededor de 10.000 pacientes, se ha asociado la administración de IECA con una reducción en la mortalidad en pacientes que aún no se habían sometido a la intervención quirúrgica, en comparación con los pacientes no tratados con estos inhibidores (Kristensen *et al*., 2015). Ahora bien, otras publicaciones muestran resultados contradictorios, un aumento en la tasa de crecimiento y una mayor mortalidad perioperatoria en pacientes tratados con IECA (Railton *et al.*, 2010, Sweeting *et al*., 2010).

Por último, el uso de antagonistas del calcio en el AAA es controvertido. Determinados estudios muestran resultados beneficiosos como es el caso del nifedipino que ralentizaría la progresión del AAA a través de la inhibición de la vía dependiente de NF-κB y MMP-9 (Tomita *et al*., 2008). En cambio, otros fármacos de esta familia no han dado resultados beneficiosos y se han asociado con un aumento en la rigidez aortica (Yokokura *et al*., 2007).

Tratamiento antiagregante

Como se ha comentado anteriormente el ILT presenta un papel esencial en la progresión y riesgo de ruptura del AAA (Mosorin *et al*., 2001). Estudios en modelos animales sometidos a daño vascular y tratados con aspirina, han demostrado una significativa reducción del tamaño del trombo, que se asocia con una progresión más lenta y una reducción en el número de rupturas del AAA (Owens *et al*., 2015). Estos efectos pueden ser debidos en parte al efecto antioxidante de la aspirina mediante la reducción de la peroxidación lipídica en células endoteliales. A pesar de que estos estudios experimentales con terapia antiagregante sugieren un efecto positivo retrasando el crecimiento del aneurisma (Owens *et al*., 2015), los estudios observacionales muestran una gran discrepancia en sus resultados (Wemmelund *et al*., 2017). En cualquier caso, y pese a la controversia, se recomienda que los pacientes con AAA sean tratados con dosis bajas de aspirina (Hirsch *et al*., 2006).

Además de la aspirina, otros fármacos antiagregantes como el cilostazol presentarían un efecto beneficioso sobre la patología aneurismática. Un estudio reciente, ha demostrado que el cilostazol atenúa la formación del AAA inducida por AngII en el modelo de ratón deficiente en la apoliproteína E ($ApoE^{-/-}$). Este resultado se debe a su efecto antiinflamatorio a través de la inhibición de la fosfodiesterasa III en la pared aortica (Umebayashi *et al*., 2018).

Estatinas

Pese a ser un tema controvertido, un estudio reciente en el que se realiza una minuciosa revisión de todos los estudios observacionales en pacientes con AAA tratados con estatinas publicados entre 2004 y 2018 (Salata *et al*., 2018), demuestra una firme asociación entre el uso de estatinas y la mejora de esta patología. Concretamente, se observa una reducción en el crecimiento del aneurisma y en el riesgo de ruptura, así como una disminución en la mortalidad perioperatoria. Además, la alta prevalencia de factores de riesgo cardiovasculares en pacientes con AAA, junto a su bajo coste y su relativa seguridad, hacen que las estatinas se prescriban rutinariamente con el objetivo de reducir la morbimortalidad cardiovascular concomitante (Salata *et al*., 2018).

El mecanismo exacto por el que las estatinas atenuarían el crecimiento del AAA se desconoce. Sin embargo, se ha descrito que las estatinas, a parte de su capacidad para disminuir el nivel de lípidos, pueden modular la inflamación directamente mejorando determinadas funciones de las células endoteliales, las CMLV, las plaquetas y las células inmunitarias. En células endoteliales y CMLV las estatinas mejoran la disponibilidad de óxido nítrico (NO), lo que produce efectos vasodilatadores, antioxidantes y antiinflamatorios, beneficiosos para el control del AAA (Liberale *et al*., 2020). Uno de los mecanismos antiinflamatorios es la disminución de la expresión de MMPs en

el ILT (Nagashima *et al*., 2002, Schweitzer *et al*., 2009, Yoshimura *et al*., 2015), lo que estabiliza el aneurisma y se asocia con una reducción de su diámetro, así como con un menor número de rupturas de las fibras elásticas de la pared vascular (Salata *et al*., 2018). También, se ha demostrado la capacidad protectora de las estatinas frente a la producción de ROS, siendo este un factor clave en la disminución del riesgo de ruptura del aneurisma. Particularmente, la simvastatina disminuye la formación de radicales libres y de moléculas pro-inflamatorias como el TNF-α en la pared del aneurisma (Piechota-Polanczyk *et al*., 2012).

Inhibidores de las MMPs: Doxiciclina

La doxiciclina, es un antibiótico que inhibe la actividad de las MMPs, y ha mostrado resultados excelentes en modelos experimentales, en los que previene el desarrollo de AAA (Curci *et al*., 1998, Prall *et al*., 2002). De hecho, existen multitud de estudios en diferentes modelos animales de aneurisma, entre ellos, el modelo de la elastasa en rata (Sho *et al*., 2004) y ratón (Bartoli *et al*., 2006), el modelo múrido de infusión de AngII (Turner *et al*., 2008) o la infusión de AngII combinada con dieta de alto contenido en grasa en ratones (Manning *et al*., 2003), en los cuales se observa una mejoría de la patología tras el tratamiento con doxiciclina. Principalmente, se describe una inhibición y/o reducción de la dilatación de la aorta en el grupo tratado respecto al grupo control (Dodd & Spence, 2011).

Los ensayos clínicos en humanos con doxiciclina describen una reducción de la actividad MMPs y la disminución del contenido de neutrófilos en la pared vascular (Curci *et al*., 2000, Abdul-Hussien *et al*., 2009). A pesar de ello, en la mayoría de estudios clínicos la doxiciclina no ha mostrado claramente su eficacia, ya que no se han obtenido efectos beneficiosos en lo referente al tamaño y la progresión del aneurisma (Newby, 2012). Por lo tanto, a pesar de los hallazgos obtenidos en modelos animales, los estudios en humanos son insuficientes y presentan algunas deficiencias que habría que solventar en futuros ensayos. Concretamente, estos ensayos han incluido un bajo número de pacientes, con una corta exposición a la doxiciclina, usada a una única dosis, independientemente del peso del paciente y sin que se realizara un ajuste adecuado de las varaibles de confución (por ejemplo, diabetes, consumo de tabaco,etc.) (Dodd & Spence, 2011). Por último, cabe destacar que la tolerancia a la doxiciclina sólo se ha analizado en el estudio más largo que comprendía 6 meses de tratamiento (Baxter *et al*., 2002), por lo que la seguridad a largo término no ha sido estudiada. Este punto es de gran importancia, ya que no hay que olvidar que la doxiciclina es un antibiótico y su uso prolongado podría causar problemas de resistencia.

En lo que concierne al tratamiento del AAA las guías clínicas recomiendan el uso de estatinas y antiagregantes. Tanto el uso de estatinas como el

tratamiento con bajas dosis de aspirina se prescribe una vez diagnosticado el paciente, y se suele seguir en el periodo perioperativo durante un tiempo indefinido. También se recomienda dejar el hábito tabáquico, seguir una dieta saludable y realizar ejercicio físico (Moll *et al*., 2011). Sin embargo, en la actualidad no se dispone de herramientas farmacológicas que limiten el crecimiento del AAA, promuevan su regresión o prevengan su ruptura. Por ello, es fundamental la identificación de nuevas dianas farmacológicas y de nuevos biomarcadores con función diagnóstica, pronóstica y terapéutica.

2. Los receptores nucleares

Los receptores nucleares son factores de transcripción que tienen la capacidad de unirse a elementos de respuesta específicos presentes en los promotores de sus genes dianas y de regular la expresión en respuesta a señales intra- y extra-celulares. Actualmente en humanos la familia de receptores nucleares está compuesta por 48 miembros (Mazaira *et al*., 2018).

Los receptores nucleares ejercen multitud de funciones en condiciones fisiológicas, entre las que se incluyen la regulación de la proliferación celular, la respuesta inmunitaria, el metabolismo, el desarrollo y la reproducción (Kadmiel & Cidlowski, 2013, Hoffmann & Partridge, 2015). Debido precisamente al gran número de procesos biológicos controlados por los receptores nucleares su alteración juega un papel fundamental en un sinnúmero de procesos patológicos como el cáncer, la diabetes, patologías neuronales, enfermedades cardiovasculares y el síndrome metabólico, entre otros (Oyekan, 2011, Kadmiel & Cidlowski, 2013, Ranhotra, 2013). A pesar de ser una familia ampliamente estudiada históricamente, estos factores siguen despertando gran interés en la investigación biomédica y representan dianas terapéuticas con un alto potencial para el desarrollo de agonistas/antagonistas selectivos con utilidad clínica (Mazaira *et al*., 2018).

2.1 Clasificación de los receptores nucleares

La activación de receptores clásicos o receptores nucleares hormonales se produce cuando el receptor que está inactivo en el citoplasma se une a un ligando, normalmente una molécula lipofílica que puede atravesar las membranas celulares (Mangelsdorf *et al*., 1995). Se les denomina clásicos porque la mayoría de sus ligandos son hormonales, como por ejemplo las hormonas esteroideas, los retinoides, las hormonas tiroideas y la vitamina D3. Otros ligandos provienen del metabolismo lipídico, como los ácidos grasos, los leucotrienos, las prostaglandinas y otros derivados del colesterol como los ácidos biliares (Aranda & Pascual, 2001).

Los llamados receptores huérfanos, se caracterizan por tener un ligando desconocido, bien porque aún no se ha identificado, bien porque

verdaderamente no lo requieren para su activación. Es un grupo muy heterogéneo y presenta diferencias relevantes en los dominios funcionales, lo que da lugar a una gran diversidad en el mecanismo de acción y en sus funciones biológicas (Benoit *et al*., 2006). Existe la teoría de que ancestralmente los receptores nucleares eran activos constitutivamente, como ocurre con los receptores huérfanos, y que la capacidad de respuesta frente a ligandos se ha adquirido durante la evolución (Laudet, 1997).

La organización estructural de los receptores nucleares está conservada evolutivamente. Mediante análisis filogenéticos se ha definido un ancestro común (Escriva *et al*., 2004), y según la homología entre las secuencias, se pueden diferenciar 6 familias o clases (Tabla 1), y un grupo misceláneo, formado por los receptores DAX1 y 2DBD-NR (Laudet, 1997, Aranda & Pascual, 2001). Las familias son las siguientes:

- **FAMILIA I:** Receptores similares a los receptores de hormonas tiroideas.
- **FAMILIA II:** Receptores similares a los receptores X retinoides.
- **FAMILIA III:** Receptores similares a los receptores de estrógenos.
- **FAMILIA IV:** Receptores correspondientes a los factores de crecimiento nervioso IB.
- **FAMILIA V:** Receptores correspondientes a factores esteroidogénicos.
- **FAMILIA VI:** Receptores correspondientes a los factores nucleares de células germinales.

Tabla 1. Clasificación de las seis familias de receptores nucleares humanos descritos. Se indican los ligando correspondientes según criterios filogenéticos. Tabla adaptada de Holzer *et al*., (2017).

Familia	Grupo	Símbolo	Abreviatura	Ligando
I	A	NR1A1	TRα	Hormona tiroidea
		NR1A2	TRβ	
	B	NR1B1	RARα	Vitamina A y compuestos relacionados
		NR1B2	RARβ	
		NR1B3	RARγ	
	C	NR1C1	PPARα	Ácidos grasos y prostaglandinas
		NR1C2	PPARβ/δ	
		NR1C3	PPARγ	
	D	NR1D1	Rev-ErbAα	Hemo
		NR1D2	Rev-ErbAβ	
	F	NR1F1	RORα	Melatonina, colesterol, ácido transretinoico
		NR1F2	RORβ	
		NR1F3	RORγ	
	H	NR1H3	LXRα	Oxiesterol
		NR1H2	LXRβ	
		NR1H4	FXRγ	
	I	NR1I1	VDR	Vitamina D
		NR1I2	PXR	Xenobióticos
		NR1I3	CAR	Androstano
II	A	NR2A1	HNF4α	Ácidos grasos
		NR2A2	HNF4β	
	B	NR2B1	RXRα	Retinoides
		NR2B2	RXRβ	
		NR2B3	RXRγ	
	C	NR2C1	TR2	No identificado
		NR2C2	TR4	
	E	NR2E1	TLX	No identificado
		NR2E2	PNR	
	F	NR2F1	COUP-TFI	No identificado
		NR2F1	COUP-TFII	
		NR2F6	EAR-2	
III	A	NR3A1	ERα	Estrógenos
		NR3A2	ERβ	
	B	NR3B1	ERRα	Dietilestilbestrol
		NR3B2	ERRβ	
		NR3B3	ERRγ	
	C	NR3C1	GR	Cortisol
		NR3C2	MR	Aldosterona
		NR3C3	PR	Progesterona
		NR3C4	AR	Testoosterona
IV	A	NR4A1	NUR77	No identificado
		NR4A2	NURR1	
		NR4A3	NOR-1	
V	A	NR5A1	SF1	Fosfolípidos
		NR5A2	LRH-1	No identificado
VI	A	NR6A1	GCNF	No identificado

2.2 Estructura de los receptores nucleares

Los receptores nucleares poseen una organización estructural común, que consta de cinco regiones funcionales diferentes (Figura 5). A pesar, de compartir una estructura común, existen diferencias entre estas regiones, que no alteran su función primaria pero sí definen la especificidad de cada receptor (Aranda & Pascual, 2001). Las distintas regiones que forman la estructura del receptor nuclear son las siguientes:

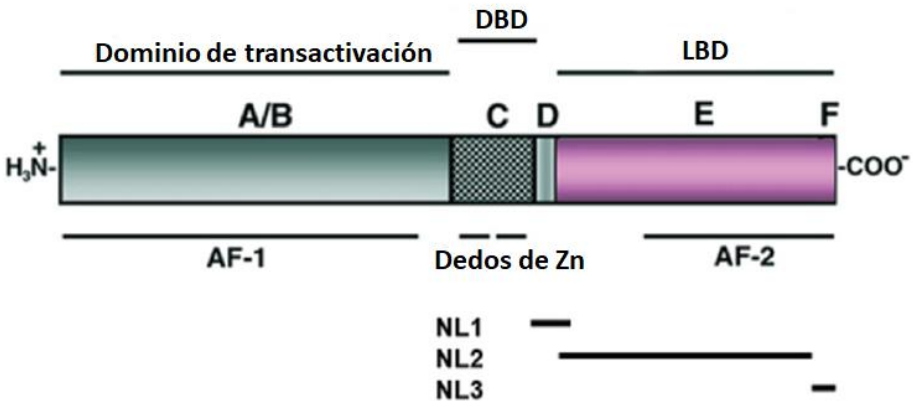

Figura 5. Esquema representativo de la estructura general de los receptores nucleares. El dominio de unión a DNA (DBD) o región C consiste en dos motivos de tipo dedos de zinc, que a veces incluyen el dominio bisagra o región D. La señal de localización nuclear (NL1) se sitúa normalmente en el extremo C-terminal de esta región. El dominio de unión al ligando (LBD) o región E/F une el correspondiente ligando. Las zonas AF-1 y AF-2 suelen unirse a moléculas co-reguladoras, con la salvedad de que la unión a AF-1 es ligando independiente, mientras que AF-2 es una región ligando dependiente. Imagen adaptada de Mazaira *et al*., (2018).

Región A/B

Esta región está situada en el extremo N-terminal, y es la región más variable en tamaño y secuencia (de 50 a más de 500 aminoácidos). Esta región contiene el dominio de transactivación AF-1 (*Activation Function 1*), y su acción es independiente de la unión de ligando (Wärnmark *et al*., 2003). La actividad del receptor puede modularse a través de la fosforilación de esta región que también puede interactuar con cofactores y otros factores de transcripción. El proceso de empalme alternativo de esta región da lugar a distintas isoformas del receptor específicas del tipo celular.

Región C

Esta región constituye el dominio de unión al ADN (DBD; del inglés *DNA-binding domain*), es la región más conservada entre las diferentes familias de

receptores nucleares. Su principal función es el reconocimiento y la unión del receptor a las secuencias específicas denominadas elementos de respuesta a hormonas (HRE; del inglés hormone response element), que están presentes en regiones reguladoras de los genes diana. El dominio DBD está compuesto por dos “dedos de zinc” de entre 60 y 70 aminoácidos y una extensión C-terminal de una longitud de unos 25 aminoácidos (Glass & Ogawa, 2006).

Región D

Esta región está poco conservada entre las diferentes familias de receptores nucleares. Representa una unión flexible, por ello recibe el nombre de bisagra, lo que permite cambios conformacionales entre las regiones DBD y la E. Además, esta región se caracteriza por poseer señales de localización nuclear y permite la interacción del receptor nuclear con los corepresores (Chen & Evans, 1995, Hörlein *et al*., 1995).

Región E

Esta región es la más larga del receptor y comprende el dominio de unión al ligando (LBD; del inglés *ligand-binding domain*). Este dominio funcional está moderadamente conservado entre familias, y no solo interviene en la unión al ligando, sino también en otros procesos como la dimerización entre receptores, y la actividad transcripcional dependiente de ligando, entre otras (Aranda & Pascual, 2001).

A pesar de las diferencias en la secuencia del dominio LBD entre los distintos receptores, a nivel estructural, este dominio está altamente conservado (Moras & Gronemeyer, 1998). La interacción con el ligando tiene lugar en una cavidad hidrofóbica denominada "bolsillo de unión al ligando”. Generalmente, la unión del ligando produce un cambio conformacional que permite la unión de coactivadores a la región conservada AF-2 y produce la activación del receptor.

Región F

Es una región muy variable, que solo está presente en determinados receptores nucleares. Se le atribuye un papel de regulación negativa de la transcripción, inhibiendo la capacidad de transactivación del receptor nuclear (Sladek *et al*., 1999). Aun así, su estructura y función sigue estando en estudio.

2.3 Mecanismos de acción

Los receptores nucleares son factores de transcripción que regulan la expresión génica mediante el reconocimiento y su posterior unión a las secuencias HRE, situadas en zonas reguladoras de los genes diana. En la mayoría de casos los

HRE se localizan en la región promotora del gen diana, aunque también se pueden localizar en regiones reguladoras alejadas del inicio de transcripción.

En general, los HRE están compuestos por dos secuencias hexámeras, separadas por no más de 5 pares de bases, y se organizan en forma de palíndromos, palíndromos invertidos o repeticiones directas. Esta organización estructural permite la unión de los receptores nucleares en forma de dímeros. Sin embargo, existen determinados receptores nucleares huérfanos que son capaces de unirse con afinidad como monómeros a una única secuencia hexámera, que suele estar precedida por una región rica en A/T (Aranda & Pascual, 2001).

La unión del receptor nuclear al ADN puede dar lugar tanto a la activación como a la represión del gen diana, ya que se han identificado elementos de respuesta negativa presentes en zonas reguladoras de diversos genes. Esta secuencia es muy diferente a la secuencia de los elementos activadores clásicos. A pesar de la existencia de elementos de respuesta negativos, la acción inhibidora de los receptores nucleares se suele llevar a término mediante otros mecanismos.

La unión del receptor nuclear a la secuencia HRE del gen diana es solo el primer paso del proceso de regulación transcripcional, que requiere de la intervención de múltiples factores (factores de transcripción basales y proteínas que interaccionen para estabilizar la unión al ADN) para iniciar el complejo proceso de transcripción. De hecho, los propios receptores nucleares pueden reclutar otras moléculas co-reguladoras o co-represoras de la transcripción (Glass & Rosenfeld 2000, Aranda & Pascual 2001).

2.4 La familia NR4A

La familia NR4A está formada por los receptores huérfanos NR4A1 (Nur77, TR3, NGFI-B, DHR38), NR4A2 (Nurr1, NOT) y NR4A3 (NOR-1, TEC, MINOR, CHN). El receptor NGFI-B (*Nerve Growth Factor I-B*; Nur77) fue el primer miembro en clonarse, se identificó en fibroblastos estimulados con agentes mitógenos (Hazel *et al*., 1988) y en neuronas estimuladas con el factor de crecimiento nervioso (Milbrandt, 1988). Posteriormente, se identificó el receptor NURR1 (*Nur77-Related factor 1*). Fue caracterizado en neuronas dopaminérgicas como un factor de transcripción específico del cerebro (Law *et al*., 1992). Por último, se describió a NOR-1 (*Neuron-derived nuclear Orphan Receptor*), que se identificó por primera vez en neuronas en cultivo y en linfocitos T activados (Hedvat & Irving, 1995, Ohkura *et al*., 1996 A). Todos ellos se expresan en tejidos con elevada actividad metabólica como son el cerebro, el corazón, el músculo esquelético, el tejido adiposo, los riñones y el hígado (Maxwell & Muscat, 2006).

Los tres miembros presentan la estructura típica de los receptores nucleares con una elevada homología en la región DBD (el 94% de los residuos son idénticos), una homología moderada en la región LBD, y una baja homología en el dominio N-terminal. La familia NR4A se caracteriza por una rápida expresión en respuesta a un elevado número de estímulos, hecho que hace que se clasifiquen como genes de respuesta temprana. Entre los estímulos capaces de inducir su expresión se encuentran las hormonas (Fahrner *et al.*, 1990), los factores de crecimiento (Martínez-González & Badimon, 2005), las citoquinas pro-inflamatorias (Pei *et al*., 2005), las lipoproteínas (Rius *et al.*, 2004), los factores físicos (Bandoh *et al*., 1998) y la despolarización de la membrana plasmática (Katagiri *et al*., 1997). La respuesta a esta gran variedad de estímulos y su amplia distribución en los diferentes tejidos y tipos celulares sitúan a los miembros de esta familia en el control de múltiples procesos biológicos tales como el desarrollo embrionario y el desarrollo de neuronas dopaminérgicas (Maxwell & Muscat, 2006) y además participan en el control de procesos celulares como la supervivencia/apoptosis (Li *et al*., 2000, Alonso *et al*., 2016) y la inflamación (Calvayrac *et al*., 2015). Esta complejidad explica, la relación de los receptores NR4A con diversas enfermedades como la diabetes (Fu *et al*., 2007, Lappas, 2014), patologías cardiovasculares (Qing *et al*., 2014), el cáncer (Delgado *et al*., 2016, Ji *et al*., 2017) y el Parkinson (Decressac *et al*., 2013).

2.4.1 Unión al ADN

Una vez inducida su expresión los receptores de la familia NR4A se pueden unir al ADN en forma de monómeros o de dímeros. Como monómeros se unen a una secuencia específica conocida como elemento NBRE (*NGFI-B Response Element*), compuesta por una secuencia consenso octámera (5'-AAAGGTCA-3') (Wilson *et al*., 1991). En forma de homodímeros los NR4A reconocen y se unen al elemento NuRE (*Nur-Response Element*) formado por dos octámeros invertidos parecidos al NBRE (5'-TG(G/A)(C/T)ATTTn6AAAT(G/A)(C/T)CA-3') y separados por un número limitado de nucleótidos (Philips *et al*., 1997). El receptor NOR-1 presenta una menor afinidad por este último tipo de elemento, y por tanto, posee menor capacidad de activar la transcripción (Maira *et al*., 1999). Además, los receptores Nur77 y Nurr1 se pueden unir como heterodímeros con el 9-cis RAR a una secuencia imperfecta de tipo repetición directa (DR) separada por cinco nucleótidos (GGTTCACCGAAAGGTCA) (DR-5) (Perlmann & Jansson, 1995, Zetterström *et al*., 1996).

2.4.2 Estructura genética y proteica de NOR-1

La elevada similitud de secuencia entre los tres miembros de la familia NR4A sugiere que estos receptores derivan de un gen ancestral común (Maruyama *et*

al., 1998). En humanos, el gen que codifica para NOR-1 se localiza en el cromosoma 9 y está compuesto por 8 exones, con una estructura exón-intrón muy parecida a la del resto de receptores nucleares *(*Ohkura *et al*., 1996 B).

Los tres miembros de la familia presentan la estructura típica de receptores nucleares, aunque poseen algunas particularidades. La mayor diferencia se encuentra en a la zona LBD; como se ha comentado anteriormente es una región esencial para el reclutamiento de pequeñas moléculas lipofílicas (ligando). Los receptores NR4A presentan una atípica región LBD. Diferentes estudios mediante cristalografía de rayos X revelan que el dominio LBD en Nurr1 contiene grandes residuos hidrofóbicos en el lugar del bolsillo de unión al ligando impidiendo la formación del mismo y la posible entrada de ligandos (Wang *et al*., 2003). Estudios similares realizados en DHR38, el ortólogo de NOR-1 en Drosophila, revelan la ausencia del sitio clásico de unión a ligando (Baker *et al*., 2003). Teniendo en cuenta estos estudios, la posibilidad de que la familia de NR4A este regulada a través de ligando es limitada, y por ello se definen como factores de transcripción independientes de ligando (Wang *et al*., 2003, Codina *et al*., 2004).

El mecanismo más general de activación de esta familia de receptores es mediante el incremento de su expresión. También se activan en respuesta a modificaciones post-traduccionales como la fosforilación (Li & Lau, 1997) o la sumoilación (Arredondo *et al*., 2013). A pesar de ello, estudios posteriores han identificado la citosporona B (Csn-B) como una molécula capaz de unirse con gran afinidad a la región LBD de Nur77 e inducir su actividad transcripcional (Zhan *et al*., 2008). Sería el primer ligando que se vincularía a esta familia. Otros estudios sugieren que algunos ácidos grasos podrían interaccionar con la zona LBD de Nur77 (Vinayavekhin & Saghatelian, 2011).

2.4.3 Papel de los receptores NR4A a nivel cardiovascular

Los receptores NR4A son fuertemente activados por estímulos pro-aterogénicos en diferentes tipos celulares como CMLV, células endoteliales y macrófagos (Martínez-González & Badimon, 2005). Sin embargo, actualmente existe cierta controversia sobre el papel fisiopatológico de esta familia, ya que mientras Nur77 y Nurr1 muestran un papel protector, NOR-1 promovería el desarrollo de la lesión arteriosclerótica (Martínez-González & Badimon, 2005, Ranhotra 2014). A continuación se detallan las evidencias experimentales para entender mejor la relación de la familia NR4A, y más concretamente del receptor NOR-1, con las enfermedades cardiovasculares.

Los receptores NR4A en la proliferación y la migración

La proliferación y la migración de CMLV tienen un papel muy importante en el remodelado cardiovascular, concretamente en el desarrollo de la arteriosclerosis. También, la proliferación de las células endoteliales es clave

en procesos como la reparación del endotelio y la formación de nuevos vasos sanguíneos. El receptor NOR-1 ha estado vinculado con dichos procesos pero con resultados contradictorios, ya que se le atribuye tanto, funciones pro-proliferativas como anti-proliferativas (Martínez-González & Badimon, 2005).

Las investigaciones de nuestro grupo en células vasculares en cultivo sugieren un papel pro-proliferativo a NOR-1. Así, se demostró por primera vez mediante el bloqueo de la expresión de NOR-1 con oligonucleótidos anti-sentido o con ARN de interferencia. Estas estrategias redujeron la proliferación celular inducida por diferentes mitógenos como el suero y las lipoproteínas de baja densidad (LDL) en CMLV (Martínez-González *et al*., 2003, Rius *et al*., 2004), o por el factor de crecimiento de endotelio vascular (VEGF) y la trombina en células endoteliales (Rius *et al*., 2006, Martorell *et al*., 2007), con una disminución drástica de la síntesis de ADN y una alteración del ciclo celular. Además la inhibición de NOR-1 también limitó la migración celular inducida por estos estímulos en células vasculares. En estudios posteriores se han identificado algunos de los genes diana de NOR-1 responsables de estas respuestas, como la vitronectina (VTN), una glicoproteína implicada en la adhesión, la migración y la proliferación celular (Martí-Pàmies *et al*., 2017) que presenta un elemento de tipo NBRE en su región promotora. La expresión de NOR-1 se incrementa también en respuesta al factor de crecimiento PDGF de tipo BB, lo que refuerza el papel pro-proliferativo de este receptor en CMLV (Nomiyama *et al*., 2006, Martorell *et al*., 2007, Thakar *et al*., 2009, Gizard *et al*., 2011, Li *et al*., 2013).

Análogamente, los estudios *in vivo*, desarrollados por nuestro grupo sugieren la contribución de este receptor nuclear al desarrollo de aterosclerosis. Así, observamos que la expresión de NOR-1 en CMLV aumentaba en un modelo porcino de lesión intravascular por angioplastia en arterias coronarias (Martínez-González *et al*., 2003). Estudios posteriores, en un ratón transgénico que sobreexpresa NOR-1 específicamente en CML desarrollado en nuestro laboratorio, mostraron que la transgénesis de NOR-1 iba asociada a un aumento de la formación de neoíntima inducida por la ligadura de la arteria carótida. Las CMLV de estos animales transgénicos también muestran una mayor actividad mitogénica (Rodríguez-Calvo *et al*., 2013). En concordancia con nuestros resultados, investigaciones de otros grupos mostraron cómo la deficiencia de NOR-1 en ratón iba acompañada de una menor formación de neoíntima inducida por daño vascular y una disminución de la proliferación (Nomiyama *et al*., 2009).

Pese a que los datos anteriormente mencionados atribuyen un papel pro-aterogénico a NOR-1, existen resultados controvertidos. En un ratón que sobreexpresa un dominante negativo que suprime la acción de los tres miembros de la familia NR4A, se detectó un incremento en la formación de neoíntima inducida por ligadura de carótida, así como un aumento de la

actividad mitogénica de las CMLV procedentes de estos animales (Arkenbout *et al*., 2002). Cabe destacar que en este último caso el bloqueo simultáneo de los tres receptores de la famíla NR4A, complica el análisis de los resultados ya que, en determinados escenarios Nur77 presenta una función pro-proliferativa (Zeng *et al*., 2006, Wang *et al*., 2010, 2011), mientras en otros estudios a Nur77 y Nurr1 se les atribuye un efecto anti-proliferativo en células vasculares (Arkenbout *et al*., 2002, Bonta *et al*., 2010, Huo *et al*., 2014, Liu *et al*., 2014) .

Para comprender los mecanismos por los que los receptores NR4A modulan la proliferación y la migración, hay que tener en cuenta que estos receptores regulan la expresión de proteínas implicadas en el ciclo celular. NOR-induce la expresión de ciclinas como la D1 y D2, que activan la entrada al ciclo celular (Nomiyama *et al*., 2006, 2009). También se ha descrito que NOR-1 regula la proteína SKP2 (proteína quinasa 2 asociada a la fase S) en CMLV a través de un elemento NBRE presente en su promotor, lo que tiene como consecuencia un aumento de la proliferación (Gizard *et al*., 2011).

En resumen, estos resultados revelan la gran complejidad del sistema para mantener el equilibrio entre la actividad proliferativa y la quiescencia.

Los receptores NR4A en la supervivencia celular y la apoptosis

El proceso de muerte celular puede estar regulado por diversas vías, en particular se ha demostrado la participación del receptor Nur77 en la activación de la apoptosis de linfocitos T y B (Liu *et al*., 1994, Woronicz *et al*., 1994), así como en macrófagos (Kim *et al*., 2003 A). También, se ha observado que en un ratón transgénico que sobreexpresa NOR-1 y Nur77 en células T en desarrollo, se produce una apoptosis masiva de linfocitos inmaduros (Woronicz *et al*., 1994, Cheng *et al*., 1997) .

A nivel vascular, son pocos los estudios que relacionan el papel de NOR-1 con el proceso apoptótico. Nuestro grupo ha demostrado que NOR-1 es un factor implicado en la supervivencia de las células endoteliales sometidas a hipoxia (Martorell *et al*., 2009). Este efecto anti-apoptótico podría estar relacionado con la capacidad de NOR-1 para inducir la expresión de la proteína inhibidora de la apoptosis (cIAP2), que contiene un elemento NBRE en su promotor (Martorell *et al*., 2009, Alonso *et al*., 2016).

Los receptores NR4A y la inflamación

Históricamente, la familia de receptores NR4A se ha descrito como factores proinflamatorios (Pei *et al*., 2005), ya que se ha observado una expresión aberrante en tejidos sinoviales inflamados, en cáncer colorrectal y en lesiones ateroscleróticas, entre otros. Además, hay un incremento de su expresión frente a un amplio abanico de estímulos proinflamatorios como el lipopolisacárido (LPS), citoquinas y lípidos oxidados (Murphy *et al*., 2001, Pei *et al*., 2005,

Holla *et al*., 2006, Aherne *et al*., 2009). Sin embargo, recientes estudios sugieren que los miembros de la familia NR4A pueden actuar como represores en respuestas inflamatorias específicas del tipo celular. Estímulos inflamatorios como el LPS, el TNFα o las LDL oxidadas (oxLDL) inducen la expresión de NOR-1, y también de Nurr1 y Nur77, en macrófagos y monocitos (Pei *et a*l., 2005, Barish *et al*., 2005, Bonta *et al*., 2006). La sobreexpresión de los receptores NR4A en estas células tiene consecuencias antiinflamatorias entre las que destacan una disminución en la captación de oxLDL mediante la inhibición de la expresión de algunos receptores *scavengers*, la disminución de la expresión de citoquinas pro-inflamatorias (como la IL1β, IL6, IL8 y MCP1) y de enzimas como la cicloxigenasa 2 (COX2) (Bonta *et al*., 2006, Shao *et al*., 2010). Los estudios *in vivo* ratifican este papel antiinflamatorio ya que los macrófagos procedentes de ratones deficientes para Nur77 presentan una mayor producción de citoquinas inflamatorias (Hamers *et al*., 2012, Hanna *et al*., 2012). Recientemente, hemos demostrado que el receptor CD69 (*Cluster of Differentation* 69) actúa como receptor de oxLDL en linfocitos T humanos y que la unión de oxLDL a CD69 incrementa la expresión de los receptores NR4A y desencadena respuestas antiinflamatorias (Tsilingiri *et al*., 2019). De hecho, en ratón, la deficiencia de CD69 en el compartimento linfoide, favorece el desarrollo de aterosclerosis, y se asocia a una baja expresión de Nur77 y NOR-1 en leucocitos de sangre periférica y nódulos linfáticos para-aórticos. Cabe destacar que en pacientes con aterosclerosis subclínica, la expresión de Nur77 y CD69 disminuye en leucocitos de sangre periférica lo que concuerda con la hipótesis de que los receptores NR4A desempeñan una función antiinflamatoria y antiaterogénica en estas células (Tsilingiri *et al*., 2019).

Estudios *in vivo* realizados por nuestro grupo en un ratón transgénico que sobreexpresa NOR-1 en CMLV demuestran que la sobreexpresión de NOR-1 va asociada a una menor inducción de citoquinas inflamatorias (IL6, IL8, IL1β, CCL20 y MCP1) en respuesta al LPS y TNFα (Calvayrac *et al*., 2015). El efecto antiinflamatorio de NOR-1 en CMLV se debe a la capacidad de este receptor nuclear de limitar la activación de la ruta de NF-κB. Análogamente, otros autores han demostrado cómo Nurr1 tiene la capacidad de inhibir la expresión de TNFα, IL1β y MCP1 en CMLV (Bonta *et al*., 2010).

En cuanto al impacto de los receptores NR4A sobre la funcionalidad de las células endoteliales las investigaciones se han centrado en el papel antiinflamatorio de Nur77, que impide la activación de NF-κB, y previene la activación endotelial inducida por la IL1β y el TNFα, hecho que tiene como consecuencia una reducción de la expresión de moléculas de adhesión intercelulares y vasculares (ICAM-1 y VCAM-1), y por consiguiente un menor reclutamiento de monocitos (Gruber *et al*., 2003, Bei e*t al*., 2009). Por el contrario, se han descrito efectos pro-inflamatorios de NOR-1 en células endoteliales. Así, la sobreexpresión de NOR-1 en HUVEC induce la expresión

de las moléculas de adhesión ICAM-1 y VCAM-1, mientras la inhibición de este receptor reduce la adhesión endotelial de monocitos *in vitro* e *in vivo* (Zhao *et al*., 2010). En estudios en células endoteliales, nuestro grupo, ha descrito que miR-17 y miR20 regulan NOR-1 y de ese modo atenúan la expresión del factor de crecimiento del endotelio vascular (VEGF) (Sambri *et al*., 2015).

Los receptores NR4A en el miocardio

Los receptores NR4A presentan una elevada expresión en corazón por lo que en los últimos años ha aumentado el interés del papel de estos receptores en la fisiopatología de enfermedades cardíacas (Medzikovic *et al*., 2019).

Nur77 es el miembro de esta familia más ampliamente estudiado en el corazón (Myers *et al*., 2009, Medzikovic *et al*., 2015). Distintos modelos animales muestran una rápida inducción de la expresión de Nur77 promovida por diferentes estímulos patológicos como la estimulación de la vía β–adrenérgica mediante isoproterenol (ISO) (Myers *et al*., 2009), la infusión de AngII (Wang *et al*., 2013), la coartación aórtica (TAC; del inglés *transverse aortic constriction*) (Cheng *et al*., 2011), el daño por isquemia/reperfusión y el infarto de miocardio (Zheng *et al*., 2014).

Nur77 se ha definido como un factor de transcripción protector frente al desarrollo de diferentes patologías cardíacas. Dos grupos de investigación independientes han demostrado que Nur77 protege frente al remodelado cardíaco inducido por una estimulación β adrenérgica crónica. Por un lado, el silenciamiento de Nur77 en cardiomiocitos neonatales de rata promueve la hipertrofia inducida por ISO (Medzikovic *et al*., 2015, Yan *et al*., 2015). Del mismo modo, en el modelo de ratón deficiente (KO; del inglés *knock out*) en Nur77 se observa una reducción en la supervivencia de los cardiomiocitos, un aumento de la hipertrofia y una mayor fibrosis cardíaca tras la infusión crónica de ISO (Medzikovic *et al*., 2015). También se ha demostrado que Nur77 regula la hipertrofia de los cardiomiocitos de forma paracrina a través del neuropéptido Y (NPY) (Medzikovic *et al*., 2018). Por último, frente al daño por isquémia/reperfusión el ratón KO para Nur77 presenta menor disfunción contráctil que los controles (Zhou *et al*., 2018).

A pesar del gran número de evidencias que avalan el papel protector de Nur77 a nivel cardíaco, la sobreexpresión de este receptor nuclear en el miocardio mediante un sistema adenoviral inhibe la respuesta hipertrófica desencadenada por el ISO (Yan *et al*., 2015). Una respuesta similar ocurre en el ratón deficiente Nur77; se observa una atenuación de la hipertrofia cardíaca, de la fibrosis y de la apoptosis, además de mejorar la función del ventrículo izquierdo tras la infusión crónica de AngII (Wang *et al*., 2013).

En comparación con Nur77, se sabe mucho menos del papel funcional de los receptores Nurr1 y NOR-1 en la función cardíaca y el remodelado. La

expresión de Nurr1 se induce en corazones de ratones (Myers *et al*., 2009) y en cardiomiocitos neonatales de rata tras la estimulación con ISO (Medzikovic *et al*., 2015), sin embargo, las implicaciones funcionales de este receptor en la hipertrofia cardíaca y el infarto de miocardio todavía no se han caracterizado en profundidad. En cuanto a NOR-1, éste se expresa en el corazón sano humano murino y porcino (Ohkura *et al*., 1996 B, Martínez-González *et al*., 2003, Myers *et al*., 2009). Se ha descrito que su expresión disminuye en los apéndices atriales de pacientes con fibrilación auricular debida a una disfunción de la válvula mitral o con enfermedad arterial coronaria, respecto a pacientes control (Kharlap *et al*., 2006). En relación a la hipertrofia cardíaca la expresión de NOR-1 está incrementada en corazones de ratón y en cardiomiocitos neonatales de rata expuestos a ISO (Myers *et al*., 2009, Feng *et al*., 2015, Medzikovic *et al*., 2015). En este modelo celular, el silenciamiento de NOR-1 atenúa la hipertrofia mientras, la sobreexpresión de NOR-1 la promueve. Asimismo, *in vivo* se ha observado que la sobreexpresión de NOR-1 potencia la hipertrofia cardíaca inducida por ISO a través de la regulación de la actividad enzimática de PARP-1 (*Poly ADP-Ribose Polymerases*) (Feng *et al*., 2015).

Los receptores NR4A y el AAA

El receptor NOR-1 es el único miembro de esta familia que ha sido estudiado en el contexto del AAA (Neels *et al.*, 2020). Las investigaciones de nuestro grupo han detectado una mayor expresión de NOR-1 en muestras aneurismáticas humanas, específicamente en las CMLV, que la observada en aortas de donantes sanos (Alonso *et al*., 2016). A pesar del efecto antiinflamatorio de NOR-1 en macrófagos, experimentos de transplante de médula ósea deficiente en NOR-1 realizados en ratón KO para el receptor de LDL (LDLR) mostraron que la deficiencia de NOR-1 en células hematopoyéticas no alteró la progresión ni la ruptura del AAA inducido por la infusión de AngII (Qing *et al*., 2017). Debido a la escasez de estudios en este ámbito, el papel de la familia de NR4A en la patología aneurismática es desconocido.

3. Tirosina hidroxilasa

La enzima tirosina hidroxilasa (TH; EC 1.14.16.2) es uno de los primeros genes identificado como gen diana de la familia de los receptores NR4A (Liu *et al*., 1997, Sakurada *et al*., 1999), y ha sido objeto de múltiples investigaciones debido a su importancia como enzima limitante en la síntesis de catecolaminas. La TH cataliza la hidroxilación de la tirosina a L-DOPA (Molinoff & Axelrod, 1971). Los productos de esta vía son las catecolaminas (dopamina, epinefrina y norepinefrina), hormonas y neurotransmisores relevantes en el sistema nervioso central y periférico. Las catecolaminas intervienen en procesos centrales como la memoria en el cerebro (Arnsten, 1997), pero también

modulan la respuesta frente a estrés en tejidos y órganos periféricos. Entre otras respuestas, destacar el aumento de la presión sanguínea y del pulso cardíaco, vasodilatación en músculo esquelético, corazón y cerebro (Tank & Wong, 2015).

3.1 Estructura y distribución de la TH

La TH también denominada tirosina 3-monooxigenasa, pertenece a la familia de enzimas hidroxilasas de aminoácido aromáticos. Esta familia está compuesta por tres miembros, la TH, la fenilalanina hidroxilasa y la triptófano hidroxilasa. Esta familia realiza la hidroxilación de anillos aromáticos presentes en los aminoácidos. Para llevar a cabo la reacción utilizan oxígeno molecular (O_2), tetrahidrobiopterina (BH_4) como coenzima y un grupo hemo (Fe^{2+}) como cofactor. El átomo de hierro se mantiene en el sitio activo del enzima mediante dos residuos de histidinas y un residuo de glutamato.

La estructura de la TH consta de un dominio amino terminal regulador (R) de tamaño variable de 100 a 150 residuos de aminoácidos, seguido de un dominio catalítico (C) de unos 330 residuos, y un dominio en espiral en el carboxilo terminal de aproximadamente 20 aminoácidos (Daubner *et al*., 2011).

La TH se ha localizado en el cerebro en células dopaminérgicas, adrenérgicas y noradrenérgicas, también en el intestino, el sistema nervioso simpático y en la médula adrenal. Asimismo, se ha identificado la expresión de TH en linfocitos T, y su implicación en el proceso de diferenciación a linfocitos T *helpers* (Th1, Th2 y Th17) (Zhao *et al.,* 2013, Huang *et al.,* 2016, Wang *et al*., 2016). Estudios recientes, han descrito la expresión de la TH en las células endoteliales y las CMLV en condiciones de hipoxia (Pfeil *et al*., 2014). Generalmente, se encuentra en el citoplasma en forma de homotetrámero (aprox. 240 kDa) (Haycock *et al*., 1985). La TH está codificada por un único gen en humanos, pero presenta 4 isoformas producidas por al empalme alternativo. (Haycock, 2002).

3.2 Función de la TH

Como se ha comentado la TH cataliza el paso limitante en la síntesis de catecolaminas (Figura 6). Para ello, requiere L-tirosina como sustrato, BH_4, O_2 y Fe^{2+}. Esta reacción da lugar a la síntesis de DOPA y a la producción de dihidrobiopterina y agua como subproductos.

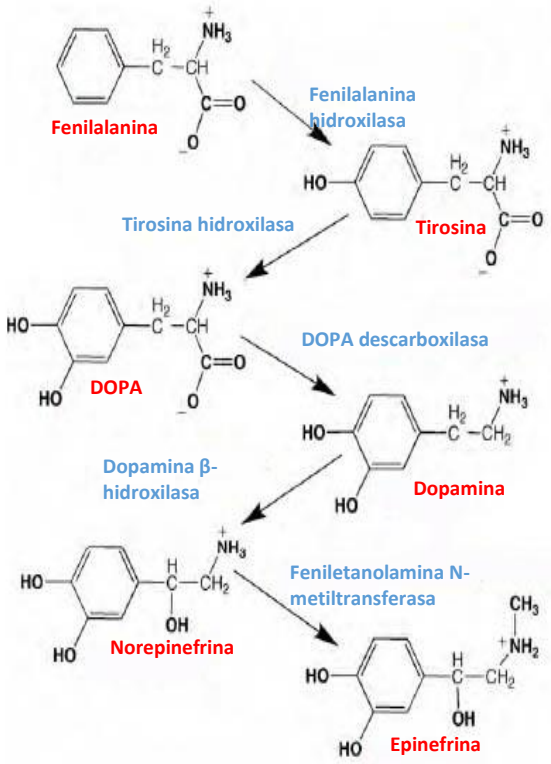

Figura 6. Ruta de síntesis de catecolaminas. La fenilalanina hidroxilasa (PAH) convierte la fenilalanina en tirosina. A su vez, la tirosina hidroxilasa (TH) hidroxila la tirosina para dar lugar a DOPA. La DOPA se convierte en dopamina a través de la enzima DOPA descarboxilasa (DDC). La enzima dopamina β-hidroxilasa (DBH) hidroxila la dopamina que se transforma en norepinefrina, la cual es metilada a epinefrina mediante la enzima feniletanolamina N-metiltransferasa. La TH es la enzima limitante de esta vía. Adaptada de Daubner *et al*., (2010).

Las catecolaminas son importantes neurotransmisores en el sistema nervioso central y periférico, pero también tienen un papel fundamental como neurohormonas circulantes, secretadas por la medula adrenal y los nervios simpáticos. En situaciones de lucha-huida, estas neurohormonas son rápidamente liberadas en los órganos viscerales, los vasos sanguíneos, los músculos lisos y glándulas. Los efectos que producen pueden afectar al corazón, los pulmones, el cerebro, y a nivel vascular se produce un aumento de la presión sanguínea. Concretamente, se produce la vasoconstricción en los vasos sanguíneos pertenecientes a órganos viscerales (riñón, tracto gastrointestinal y piel), y así se puede redistribuir la sangre hacia los músculos esqueléticos. A pesar, de que las catecolaminas son necesarias a corto plazo para la supervivencia del organismo, elevados niveles circulantes de catecolaminas se han relacionado con patologías como la hipertensión y la

hipertrofia cardíaca (Tank & Wong, 2015). Al ser el enzima limitante de la vía las alteraciones en la actividad de la TH tienen efectos directos en los procesos regulados por las catecolaminas. Por ello, el estudio de la regulación de la TH es de gran interés en la investigación biomédica.

3.3 Regulación de la TH

La regulación de la TH es compleja y engloba dos grandes aspectos, la regulación a medio-largo plazo del gen (a nivel transcripcional, la estabilidad del mensajero de RNA y el procesamiento alternativo del RNA) y la regulación directa a corto plazo de la actividad (y que incluye la inhibición por retroalimentación, la regulación alostérica, la fosforilación del enzima y modificaciones post-traduccionales).

En esta introducción nos vamos a centrar exclusivamente en los mecanismos de regulación a largo plazo, y más concretamente en la regulación transcripcional del enzima.

3.3.1 Regulación a medio-largo plazo

La expresión de la TH es altamente dependiente de tejido y de tipo celular. El estudio de la regulación de la actividad transcripcional de este enzima se ve dificultado por la baja homología entre el promotor humano de la TH y los promotores de ratón y rata. Se identifican solo cinco regiones con elevada homología. Específicamente, la homología entre el promotor humano y de ratón es del 46.6%, y entre el promotor humano y de rata es sólo del 30% (Kessler *et al.*, 2003). A pesar de la baja homología, resaltar dos regiones (CR1: -2367 pb a -2303 pb y CR2: -101 pb a +23 pb) muy conservadas evolutivamente en las tres especies, lo que sugiere que son zonas clave implicadas en la expresión de la TH durante el desarrollo (Kim *et al*., 2003 B). El análisis de secuencias ha demostrado que esas regiones conservadas contienen sitios consenso de unión para Nurr1 (Zetterström *et al*., 1997, Witta *et al*., 2000, Kim *et al*., 2003 B) y Ptx3 (*Pentraxin-related protein* 3) (Lebel *et al*., 2001), que tienen un papel importante durante la neurogénesis dopaminérgica en el mesencéfalo. Concretamente, se ha identificado un elemento NBRE (GGTTAAA) conservado para las tres especies. También se ha descrito en dichas regiones elementos CRE y la caja TATA necesarios para la transcripción basal (Kim *et al*., 2003 B).

A pesar de los esfuerzos en investigación durante las dos últimas décadas, los mecanismos de control de la expresión de la TH específicos de tipo celular siguen en estudio. De hecho dependiendo del tipo celular y de la especie, Nurr1 puede actuar como activador o represor de la actividad de la TH. Desde los años 90 utilizando estrategias de ganancia de función se ha demostrado que Nurr1 regula directa e indirectamente la expresión de la TH (Wagner *et al*., 1999, Chung *et al*., 2002). Posteriormente, en estudios realizados con el promotor de

rata de la TH, se observó una clara regulación de la TH por Nurr1 en líneas celulares como HeLa, 293T, C6 y SL2, entre otras (Kim *et al*., 2003 C). También se ha observado, que en células progenitoras neurales en rata Nurr1 activa la expresión de la TH de forma independiente del receptor RXR (Sakurada *et al*., 1999). En cambio, en células progenitoras neurales humanas la expresión de la TH no depende de Nurr1, a diferencia de los sistemas de rata y ratón (Jin *et al*., 2006). Actualmente, la hipótesis más aceptada sugiere que la regulación transcripcional de la TH esta mediada por grupos de factores diferentes en cada tipo celular, y está sujeta a variación entre especies.

3.4 Catecolaminas y patología cardiovascular

La TH ha sido ampliamente estudiada en las patologías neuronales, ya que alteraciones en la síntesis o en la secreción de catecolaminas se han relacionado con enfermedades como el Parkinson, la depresión, la esquizofrenia y la adicción (Tank & Wong, 2015). Sin embargo, la TH se ha vinculado con patologías cardiovasculares como la hipertensión, la disección aortica torácica (TAD) e incluso el infarto de miocardio.

Estudios genéticos han asociado diversas variantes comunes, concretamente polimorfismos de nucleótido único (SNPs) en el promotor de la TH con una predisposición a padecer hipertensión (Rao *et al*., 2010) . También, un estudio reciente, ha demostrado una elevada actividad del sistema nervioso simpático en la aorta de pacientes con TAD, respecto a muestras control. Concretamente, en el grupo de muestras pertenecientes a pacientes con disección de la aorta torácica (TAD; del inglés *thoracic aortic dissection*) se detectó mayor concentración de norepinefrina en el plasma, y una mayor expresión de TH y de GAP43 (*Growth Associated Protein 43*) en las fibras nerviosas de la aorta (Zhipeng *et al*., 2014).

Por último, se ha observado un nivel elevado de norepinefrina en el plasma de pacientes con infarto de miocardio. Esto sugiere una relación entre la desregulación de la vía de síntesis de las catecolaminas, señalando a la TH como enzima clave al ser el enzima limitante, y el infarto de miocardio (Kaye *et al*., 1995, Scrogin *et al*., 2013).

En resumen, la investigación de la participación de la TH en patologías cardiovasculares es bastante reciente y escasa, pese a las evidencias, por lo que se requiere seguir investigando para establecer su papel de forma clara.

HIPÓTESIS Y OBJETIVOS

Las enfermedades cardiovasculares son una de las principales causas de mortalidad a nivel mundial. Entre las enfermedades con mayor morbimortalidad encontramos el AAA y la hipertrofia cardíaca, ambas caracterizadas por un proceso de remodelado en respuesta a un daño. En este proceso se altera profundamente la expresión génica y los factores de transcripción juegan un papel clave (Martínez-González *et al*., 2001). La identificación de los factores de transcripción implicados y la determinación del papel que desempeñan resulta imprescindible para entender las bases fisiopatológicas en la evolución de las enfermedades.

En la actualidad no se dispone de fármacos que limiten la progresión o promuevan la regresión de los AAA. Además, por la naturaleza de esta patología no es posible analizar muestras de tejido humano cuando el aneurisma se encuentra en desarrollo (Torres-Fonseca *et al*., 2019). Tampoco se dispone de tratamientos farmacológicos que reviertan la hipertrofia cardíaca, y los tratamientos actuales sólo retrasan su progresión (Samak *et al*., 2016). Por tanto, es importante disponer de modelos animales adecuados en los que estudiar los mecanismos fisiopatológicos de estas enfermedades y realizar estudios preclínicos.

En nuestro grupo se ha descrito que la expresión de NOR-1 aumenta de forma muy importante en AAA humanos (Alonso *et al*., 2016), si bien actualmente, se desconoce el papel de NOR-1 en el aneurisma de aorta. Recientemente, hemos observado que un modelo de ratón que sobreexpresa este receptor en la pared vascular (TgNOR1^{CMLV}) presenta predisposición a desarrollar aneurismas inducidos por sobrecarga de presión. Alrededor del 60% de los animales TgNOR1^{CMLV} infundidos con AngII desarrollan aneurisma. En los aneurismas de estos animales se observa un aumento de la expresión de elementos que clásicamente están implicados en la enfermedad humana como MMP-2, citoquinas y quimioquinas. Estos resultados indican que nuestro modelo animal recoge aspectos relevantes de esta enfermedad y podría ser útil para estudiar los mecanismos celulares y moleculares del AAA y como modelo pre-clínico para el análisis de nuevas estrategias terapéuticas.

En cuanto a la relación de NOR-1 y la hipertrofia cardíaca, no existen estudios en modelos específicos que analicen su papel en este proceso ni en la supervivencia/apoptosis de los cardiomiocitos. Sin embargo, la expresión de NOR-1 es inducida por agonistas β-adrenérgicos que promueven este proceso patológico (Myers *et al*., 2009). En estudios preliminares, observamos que la sobrecarga de presión (infusión AngII) en un modelo animal que expresa el receptor NOR-1 humano en el miocardio (TgNOR-1), agravaba la hipertrofia. La implicación de NOR-1 en procesos celulares relacionados con la hipertrofia como la supervivencia/apoptosis, la inflamación y el estrés oxidativo, también sugieren que, como factor de transcripción, podría desempeñar un papel

importante en la coordinación de la expresión de genes relevantes en este proceso.

De acuerdo con los antecedentes expuestos, y con los resultados preliminares, nuestra hipótesis de trabajo es que el receptor nuclear NOR-1 juega un papel relevante en el remodelado cardiovascular asociado a enfermedades cardiovasculares como el AAA y la hipertrofia cardíaca, y que modelos animales modificados genéticamente para este receptor pueden ser útiles en el estudio de los mecanismos celulares y moleculares de estas enfermedades y en el análisis preclínico de potenciales terapias. En este contexto, hemos propuestos los siguientes objetivos:

1) Analizar los mecanismos celulares y moleculares que implican a NOR-1 en la hipertrofia cardíaca e identificar y caracterizar genes diana de NOR-1 a nivel del miocardio.
2) Analizar los mecanismos celulares y moleculares que implican a NOR-1 en el AAA e identificar y caracterizar genes diana de NOR-1 a nivel de la pared vascular.
3) Determinar la utilidad de ratones transgénicos para NOR-1 como nuevos modelos animales en estudios preclínicos de fármacos útiles en el tratamiento de patologías cardiovasculares.

RESULTADOS

MINISTERIO
DE CIENCIA E
INNOVACION

CSIC
CONSEJO SUPERIOR DE INVESTIGACIONES CIENTÍFICAS
IibB
INSTITUTO DE INVESTIGACIONES BIOMÉDICAS
DE BARCELONA

A quien corresponda:

Por la presente los Dres. José Martínez González y Mª Cristina Rodríguez Sinovas, directores de la tesis doctoral presentada por Laia Cañes Esteve informan sobre el factor de impacto y la participación de la doctoranda en las siguientes publicaciones:

1. **Cañes L***, Martí-Pàmies I*, Ballester-Servera C, Herraiz-Martínez A, Alonso J, Galán M, Nistal JF, Muniesa P, Osada J, Hove-Madsen L, Rodríguez C, Martínez-González J. Neuron-derived orphan receptor-1 modulates cardiac gene expression and exacerbates angiotensin II-induced cardiac hypertrophy. *Clin Sci (Lond)*. 2020;134:359-377. doi: 10.1042/CS20191014. ***Contribuyeron igualmente**
   Factor de impacto: 5,223; 1er cuartil (24/138, *Medicine, Research & Experimental*).

   La participación de Laia Cañes en este estudio consistió en:

   - Puesta a punto del aislamiento de cardiomiocitos y desarrollo de los estudios de caracterización de los cardiomiocitos y cardiofibroblastos de los ratones TgNOR-1; resultados correspondientes a: *Figure 2* y *Figure 3*.
   - Realización de nuevos estudios *in vivo* con el objetivo de incrementar la n y reevaluación de los datos ecocardiográficos que conforman la *Table 1*.
   - Valoración de fibrosis e inflamación cardiaca; resultados incluidos en: *Figure 5*.
   - Ampliación del número de muestras, reevaluación de los niveles de expresión génica y realización de los estudios de *Western blot*: *Figure 6*.
   - Cuantificación de los niveles de mRNA de *Col3a1*, *Ctgf*, *Pai1*, *Lox* y *Loxl2*: *Figure 7B-F*.
   - Clonaje del promotor de *Loxl2* y análisis de actividad transcripcional: *Figure 8C* y *D*.
   - Análisis de función cardiaca en ratones WT y TgNOR-1 de 4 y 12 meses de edad: *Supplementary Table S1*.
   - Aislamiento de esplenocitos para el análisis por TLA: *Figure S1*.
   - Análisis de expresión correspondientes a la *Figure S4*.
   - Estudios para responder los requerimientos de los revisores del manuscrito incluidos en el Anexo de este artículo: Figuras A1-A3 y Tabla A1.

2. **Cañes L***, Martí-Pàmies I*, Ballester-Servera C, Alonso J, Serrano E, Briones AM, Rodríguez C, Martínez-González J. High neuron derived orphan receptor-1 (NOR-1) expression strengthens the vascular wall response to angiotensin II leading to aneurysm formation in mice. *Hypertension*. 2020;77 (*In press*). doi:10.1161/HYPERTENSIONAHA.120.16078. ***Contribuyeron igualmente.**
   Factor de impacto: 7,713; 1er decil (4/65, *Peripheral Vascular Disease*).

   La participación de Laia Cañes en este estudio consistió en:

   - Realización de nuevos estudios *in vivo* para la generación de las muestras necesarias para los análisis cuantitativos incluidos en: *Figure* 2, *Figure*3A, y *Figure S2*.
   - Evaluación de la función renal y hepática; resultados incluidos en: *Figure* S3
   - Análisis de actividad MMP por zimografía incluido en: *Figure* 3C.
   - Desarrollo de un nuevo estudio *in vivo* con doxiciclina para incrementar el número de animales y realizar los análisis cuantitativos que figuran en: *Figures* 4 y 5, *Figures S5, S6* y *Supplemental Table S2*.

ROSELLÓN 161, 6ª PLANTA
08036 BARCELONA
TEL.: 93 363 83 00
FAX: 93 363 83 01

MINISTERIO
DE CIENCIA E
INNOVACION

CSIC
CONSEJO SUPERIOR DE INVESTIGACIONES CIENTÍFICAS
IibB
INSTITUTO DE INVESTIGACIONES BIOMÉDICAS
DE BARCELONA

- Realización de los análisis de GSEA de los estudios de microarray y validación de los resultados: *Table* 1, *Supplemental Tables S4* y *S5* y *Figure S7.*
- Caracterización por inmunohistoquímica y *Western blot* de la expresión vascular de MMP-12 en el modelo TgNOR-1^{VSMC}: *Figure* S8.
- Estudios para responder los requerimientos de los revisores del manuscrito incluidos en el Anexo de este artículo: Figuras A1 y A2B.

La Dra Ingrid Martí Pàmies incluyó parte de los resultados que figuran en estos artículos en su tesis doctoral titulada: "NOR-1 en el remodelado cardiovascular: Identificación de genes diana i caracterització d'animals transgènics per a NOR-1 com a models en patologies cardiovasculars.

3. **Cañes L**, Alonso J, Ballester-Servera C, Varona S, Rodríguez C, Martínez-González J. Targeting tyrosine hydroxylase for abdominal aortic aneurysm: impact on inflammation, oxidative stress and vascular remodeling. 2021 (manuscrito en revisión).

Firmado:

Dr José Martínez González

Dra Mª Cristina Rodríguez Sinovas

Barcelona 18 de Diciembre de 2020

ROSELLÓN 161, 6ª PLANTA
08036 BARCELONA
TEL.: 93 363 83 00
FAX: 93 363 83 01

PUBLICACIÓN 1

Neuron-derived orphan receptor-1 modulates cardiac gene expression and exacerbates angiotensin II-induced cardiac hypertrophy

Laia Cañes†, Ingrid Martí-Pàmies†, Carme Ballester-Servera, Adela Herraiz-Martínez, Judith Alonso, María Galán, J Francisco Nistal, Pedro Muniesa, Jesús Osada, Leif Hove-Madsen, Cristina Rodríguez,* and José Martínez-González*

† Both first authors contributed equally to this work.

*These authors contributed equally to this work.

***Clinical Science*, Volume 134, Issue 3, 14 February 2020, Pages 359-377**

Introducción y objetivos: La hipertrofia cardíaca se manifiesta inicialmente como un mecanismo compensatorio en respuesta a una sobrecarga de presión o volumen. Sin embargo, el estrés sobre el miocardio prolongado en el tiempo da lugar a alteraciones en la función ventricular y representa un factor de riesgo crítico para el desarrollo de insuficiencia cardíaca. La hipertrofia cardíaca se define como un incremento en la masa del corazón, y se caracteriza por un aumento en el tamaño de los cardiomiocitos y un mayor número de cardiofibroblastos que promueven fibrosis y en consecuencia un incremento de la rigidez del miocardio. Se produce, además, un aumento en la síntesis proteica y la reactivación de genes que se expresan normalmente durante el desarrollo fetal como los péptidos natriuréticos (BNP y ANP) o la cadena pesada de la miosina (MYH7). En la actualidad, los mecanismos que promueven los cambios transcripcionales durante el desarrollo de la hipertrofia cardíaca en respuesta a sobrecarga de presión no están completamente dilucidados.

El receptor NOR-1 es un factor de transcripción que se expresa en el músculo esquelético y el corazón. Se ha observado que en respuesta a estímulos prohipertróficos como el agonista β-adrenérgico isoproterenol se produce un aumento de la expresión de NOR-1 en cardiomiocitos neonatales de rata, los cuales aumentan de tamaño y expresan marcadores característicos de la hipertrofia. Sin embargo, se desconoce el papel de NOR-1 *in vivo* en el proceso de hipertrofia por sobrecarga de presión. Por lo tanto, nuestro objetivo es estudiar las consecuencias de la sobreexpresión de NOR-1 sobre la función y la hipertrofia cardíaca en respuesta a la sobrecarga de presión inducida por AngII en un modelo de ratón transgénico con una fuerte expresión del NOR-1 humano en el corazón (TgNOR1).

Resultados: Nuestro grupo ha desarrollado un ratón transgénico (TgNOR-1) en el que el transgén humano de NOR-1 se encuentra bajo el control del promotor CAG, que dirige la expresión preferentemente al miocardio. En estos animales, la expresión del transgén en los cardiomiocitos es mayor que en los cardiofibroblastos. Los cardiomiocitos transgénicos aislados se caracterizan por una mayor área celular y un incremento de la longitud de acortamiento tras una estimulación eléctrica. También, observamos un aumento de la expresión de *Myh7*, mientras que el nivel de mRNA de *Myh6* permanece estable. Esto da lugar a un incremento significativo de la ratio *Myh7/Myh6*. A su vez, los cardiofibroblastos transgénicos en cultivo exhiben mayor actividad migratoria, mayor expresión de marcadores de la transición fenotípica a miofibroblastos (*Acta1* y *Sm22α*) y sinterizaron más colágeno que los cardiofibroblastos control (WT, del inglés *wild-type*).

Para determinar los efectos de la sobreexpresión de NOR-1 en la función cardíaca y el remodelado ventricular, se realizaron análisis ecocardiográficos en ratones control y TgNOR-1 de 4 y 12 meses de edad. No se observaron diferencias en ningún parámetro ecocardiográfico entre los animales TgNOR-

1 y WT de 4 meses. Sin embargo, se detectó un incremento significativo en la masa del ventrículo izquierdo en los ratones transgénicos de 12 meses con respecto a ratones control de la misma edad. Esta diferencia se asoció a un incremento del grosor de la pared ventricular (PWT; del inglés *posterior wall thickness*) en los animales transgénicos, pero no se observaron alteraciones en otros parámetros como el diámetro interno del ventrículo izquierdo (LVEDd; del inglés *left ventrivular end-diastolic dimension*) en ninguno de los grupos. Tampoco se encontraron diferencias en la fracción de eyección del ventrículo izquierdo (LVEF; del inglés *left ventricular ejection fraction*) o en la fracción de acortamiento del ventrículo izquierdo (LVFS; del inglés *left ventricular fractional shortening*), como parámetros indicadores de función sistólica.

Para analizar con mayor profundidad el papel de NOR-1 en la hipertrofia cardíaca, ratones WT y TgNOR-1 se sometieron a infusión de AngII durante 28 días. En los ratones transgénicos los análisis ecocardiográficos mostraron una mayor masa del ventrículo izquierdo asociado a un incremento del PWT y del grosor del septo intraventricular (IVST; del inglés *intraventricular septum thickness*). También, se observó un incremento en la función sistólica en los ratones TgNOR-1 tratados con AngII, tal y como demostró el aumento de la fracción de eyección y de acortamiento. Tras la infusión de AngII los ratones TgNOR-1, presentaban una hipertrofia concéntrica más grave que los ratones WT.

Los estudios inmunohistoquímicos revelaron que en respuesta a AngII el infiltrado de macrófagos en el miocardio de los ratones TgNOR-1 era mayor que en los ratones control. Mediante la tinción de aglutinina de germen de trigo (WGA; del inglés *Wheat Germ Agglutinin*), que permite teñir la membrana plasmática para cuantificar el área de la célula, se observó que la infusión de AngII incrementó el área de los cardiomiocitos transgénicos en mayor medida que en los animales WT. Además, los ratones transgénicos infundidos con solución salina presentaron un área ligeramente superior que la de los animales WT, lo que concuerda con lo observado en cardiomiocitos aislados.

Respecto a la fibrosis cardíaca, la sobreexpresión de NOR-1 agravó la fibrosis intersticial y perivascular inducida por AngII, con un aumento en la deposición de colágeno, un mayor entrecruzamiento de las fibras de colágeno y un incremento en los niveles de mRNA de marcadores pro-fibróticos (*Col1a1*, *Col3a1*, *Ctgf*, *Pai-1*, *Lox* y *Loxl2)*. Destacar que en condiciones basales (infusión con solución salina) la expresión de *Loxl2* en el miocardio de los ratones transgénicos era mayor que en los WT.

Asimismo, la transgénesis de NOR-1 potenció el aumento de la expresión de marcadores de hipertrofia cardíaca (*Bnp*, *Anp* y *Myh7*) inducidos por la infusión de AngII. Concretamente, del mismo modo que ocurría en cardiomiocitos aislados de ratones TgNOR-1, los corazones de animales

transgénicos infundidos con solución salina presentaban mayor expresión de *Myh7* que los animales WT.

Como se ha mencionado, en condiciones basales en los animales transgénicos para NOR-1 se observó una mayor expresión de *Myh7*, implicado en la disfunción cardíaca, y de *Loxl2*, relacionado con remodelado de la MEC. Mediante análisis *in silico* se identificaron elementos reguladores NBRE en el promotor de ambos genes. Para verificar si NOR-1 regula su expresión, se clonó el promotor proximal de los genes humanos *MYH7* y *LOXL2 e*n el vector reportero pGL3. Los ensayos de actividad transcripcional en CMLV co-transfectadas con dichas construcciones y un vector de expresión de NOR-1 (pCMV5/hNOR-1) mostraron un incremento de la actividad transcripcional de ambos genes en respuesta a NOR-1.

Conclusiones: Nuestro estudio muestra por primera vez la contribución de NOR-1 a la hipertrofia cardíaca asociada a la edad, y en mayor medida a la hipertrofia por sobrecarga de presión, a través de la regulación transcripcional de genes como *Loxl2* y *Myh7* clave en el desarrollo de la hipertrofia cardíaca hipertensiva.

Clinical Science (2020) **134** 359–377
https://doi.org/10.1042/CS20191014

Research Article

Neuron-derived orphan receptor-1 modulates cardiac gene expression and exacerbates angiotensin II-induced cardiac hypertrophy

Laia Cañes[1,2,3,*], Ingrid Martí-Pàmies[1,2,3,*], Carme Ballester-Servera[1,3], Adela Herraiz-Martínez[1,3], Judith Alonso[1,2,3], María Galán[2,3,4], J. Francisco Nistal[2,5], Pedro Muniesa[6,7], Jesús Osada[7,8], Leif Hove-Madsen[1,2,3], Cristina Rodríguez[2,3,4,*] and José Martínez-González[1,2,3,*]

[1]Instituto de Investigaciones Biomédicas de Barcelona (IIBB-CSIC), Barcelona, Spain; [2]CIBER de Enfermedades Cardiovasculares, Instituto de Salud Carlos III, Madrid, Spain; [3]Instituto de Investigación Biomédica Sant Pau (IIB-Sant Pau), Barcelona, Spain; [4]Institut de Recerca Hospital de la Santa Creu i Sant Pau-Programa ICCC, Barcelona, Spain; [5]Hospital Universitario Marqués de Valdecilla, IDIVAL, Universidad de Cantabria, Santander, Spain; [6]Facultad de Veterinaria, Universidad de Zaragoza, Spain; [7]CIBER de Fisiopatología de la Obesidad y Nutrición, Instituto de Salud Carlos III, Madrid, Spain; [8]Facultad de Veterinaria, Instituto de Investigación Sanitaria de Aragón-Universidad de Zaragoza, Spain

Correspondence: Cristina Rodríguez (crodriguezs@csic-iccc.org) or José Martínez-González (jose.martinez@iibb.csic.es)

Hypertensive cardiac hypertrophy (HCH) is a common cause of heart failure (HF), a major public health problem worldwide. However, the molecular bases of HCH have not been completely elucidated. Neuron-derived orphan receptor-1 (NOR-1) is a nuclear receptor whose role in cardiac remodelling is poorly understood. The aim of the present study was to generate a transgenic mouse over-expressing NOR-1 in the heart (TgNOR-1) and assess the impact of this gain-of-function on HCH. The CAG promoter-driven transgenesis led to viable animals that over-expressed NOR-1 in the heart, mainly in cardiomyocytes and also in cardiofibroblasts. Cardiomyocytes from TgNOR-1 exhibited an enhanced cell surface area and myosin heavy chain 7 (*Myh7*)/*Myh6* expression ratio, and increased cell shortening elicited by electric field stimulation. TgNOR-1 cardiofibroblasts expressed higher levels of myofibroblast markers than wild-type (WT) cells (α 1 skeletal muscle actin (*Acta1*), transgelin (*Sm22α*)) and were more prone to synthesise collagen and migrate. TgNOR-1 mice experienced an age-associated remodelling of the left ventricle (LV). Angiotensin II (AngII) induced the cardiac expression of NOR-1, and NOR-1 transgenesis exacerbated AngII-induced cardiac hypertrophy and fibrosis. This effect was associated with the up-regulation of hypertrophic (brain natriuretic peptide (*Bnp*), *Acta1* and *Myh7*) and fibrotic markers (collagen type I α 1 chain (*Col1a1*), *Pai-1* and lysyl oxidase-like 2 (*Loxl2*)). NOR-1 transgenesis up-regulated two key genes involved in cardiac hypertrophy (*Myh7*, encoding for β-myosin heavy chain (β-MHC)) and fibrosis (*Loxl2*, encoding for the extracellular matrix (ECM) modifying enzyme, *Loxl2*). Interestigly, in transient transfection assays, NOR-1 drove the transcription of *Myh7* and *Loxl2* promoters. Our findings suggest that NOR-1 is involved in the transcriptional programme leading to HCH.

[*]These authors contributed equally to this work.

Received: 01 October 2019
Revised: 21 January 2020
Accepted: 27 January 2020

Accepted Manuscript online: 27 January 2020
Version of Record published: 04 February 2020

Introduction

Cardiac hypertrophy is a compensatory response of the heart to neurohormonal stress and haemodynamic overload (e.g. hypertension and valvular diseases) whose prolongation in time leads to congestive heart failure (HF) [1,2], the leading cause of hospitalisation in the elderly and one of the major public health problems worldwide. Cardiac hypertrophy is defined as an increase in heart mass, characterised by an increase in protein synthesis, cell size and reactivation of the foetal gene programme [1]. Nowadays, the

© 2020 The Author(s). Published by Portland Press Limited on behalf of the Biochemical Society

Downloaded from http://portlandpress.com/clinsci/article-pdf/134/3/359/867300/cs-2019-1014.pdf by Universitat de Barcelona user on 09 November 2020

PORTLAND PRESS

Clinical Science (2020) **134** 359–377
https://doi.org/10.1042/CS20191014

mechanisms underlying the changes in the transcriptional programme leading to hypertensive cardiac hypertrophy (HCH) are not completely understood.

Neuron-derived orphan receptor-1 (NOR-1) is a transcription factor belonging to the Nuclear receptor subfamily 4 group A (NR4A) [3]. NOR-1 (NR4A3) as well as Nur77 (NR4A1) and Nurr1 (NR4A2) seem to be constitutively active (ligand-independent) nuclear receptors whose transcriptional activity depends on their expression levels. These receptors play a key role in an array of tissues and have been associated with a variety of high-incidence human pathologies including coronary artery disease (CAD), diabetes, obesity and cancer [3–6]. We and others implicated NOR-1 in vascular remodelling and CAD [7–10]. In vascular tissues, NOR-1 is expressed at low levels, but it is quickly induced by growth factors and cytokines, acting as an immediate-early gene involved in vascular hyperplasia [7,8,11,12] by regulating genes required for cell spreading, migration and proliferation [8,13,14]. NOR-1 is also expressed in the heart and skeletal muscle (at high levels compared with other organs) [7,15]. In skeletal muscle, it has been associated with the modulation of genes involved in specific aspects of lipid, carbohydrate and energy homoeostasis [16,17], as well as in myotube differentiation and hypertrophy [16,18]. Concerning the heart, the most studied member of the NR4A family (Nur77) has been linked to cardiac hypertrophy, although conflicting results have been reported [19,20]. Much less is known about the role of NOR-1 in cardiac function and remodelling. NOR-1 seems to participate in cardiomyocyte hypertrophy *in vitro* [21]; however, neither studies in angiotensin II (AngII)-induced cardiac overload models nor in NOR-1 genetically modified animals have been performed so far.

In the present study, we have generated a mouse model that over-expresses NOR-1 in the heart and assessed the effect of a gain-of-function of this receptor on AngII-induced cardiac hypertrophy. Our results involve the nuclear receptor NOR-1 in the regulation of key genes implicated in cardiac function and remodelling.

Materials and methods

Generation of an expression plasmid for human NOR-1

An expression plasmid was generated by cloning a full-length human *NOR-1* cDNA (GenBank Accession No. D78579; position 513–2872), excised by digestion with *EcoR*I from a pBlueScript-NOR-1 construct (kindly provided by Dr. N. Ohkura, Growth Factor Division, National Cancer Center Research Institute, Tokyo, Japan) [22], into the *EcoR*I site of pCAGGS vector. The resulting construct (pCAGGS/hNOR-1) (Figure 1A) was verified by sequence analysis and validated as an NOR-1 expression plasmid by assessing NOR-1 mRNA and protein levels in cells transfected with pCAGGS/hNOR-1.

Generation of transgenic mice

The expression cassette (4629 bp) was recovered by double digestion with *Sal*I and *Hind*III (Figure 1A), purified by QIAquick™ Gel Extraction Kit (Qiagen; Hilden, Germany), and used for pronuclear injection of zygotes as previously described [23]. All procedures were carried out in the Transgenesis Unit of the Aragon Health Science Institute under the Project Licenses PI29/08 and PI30/08 approved by the in-house Ethics Committee for Animal Experiments from the University of Zaragoza. Embryos were obtained from B6D2F1/J mice mated to B6D2F1/J males (Charles River, Wilmington, MA, U.S.A.). Four- to six-week-old females were superovulated by an intraperitoneal (i.p.) injection of pregnant mare's serum gonadotropin (5 IU), followed 48 h later by an i.p. injection of human chorionic gonadotropin (7.5 IU). After mating, fertilized eggs were harvested at 20 h post-hCG. After removing cumulus cells with hyaluronidase, zygotes were thoroughly washed, selected for good morphology and collected. Fertilized eggs (one-celled embryos) were cultured in EmbryoMax™ KSOM medium (MR-020P; Millipore, Burlington, MA, U.S.A.) at 37°C in an atmosphere of 5% CO_2, 90% relative humidity. One-celled embryos were microinjected into the pronucleus in an M-2 medium (M7167; Sigma–Aldrich, St. Louis, MO, U.S.A.) and transferred into the reproductive tract of pseudopregnant recipients (Crl:CD-1) to complete their development. Offspring (3 weeks after birth) were screened by PCR analysis of genomic DNA that was extracted from mouse tail biopsies by using the DNeasy Blood and Tissue kit (Qiagen). PCR was performed by using specific primers selected to amplify a 456-bp fragment (forward: 5′-TTCGGCTTCTGGCGTGTGAC-3′, reverse: 5′-GGTTCATGATCTCCGTGGTG-3′). PCR was performed in a volume of 25 µl containing genomic DNA (100 ng), 1× MyTaq™ Reaction Buffer (Bioline, London, U.K.), 0.4 µM of each primer and 1.25 U of MyTaq™ polymerase. PCR was run in a thermocycler (GeneAmp® PCR System 9700, Applied Biosystems, Foster City, CA, U.S.A.) programmed for 30 cycles: denaturation (94°C for 1 min), annealing (54°C for 45 s) and polymerisation (72°C for 1 min). PCR products were resolved by electrophoresis on a 1% agarose gel containing ethidium bromide, and were visualised under UV light. Images were captured using the Bio-Rad Gel

© 2020 The Author(s). Published by Portland Press Limited on behalf of the Biochemical Society

Downloaded from http://portlandpress.com/clinsci/article-pdf/134/3/359/867300/cs-2019-1014.pdf by Universitat de Barcelona user on 09 November 2020

Clinical Science (2020) **134** 359–377
https://doi.org/10.1042/CS20191014

PORTLAND PRESS

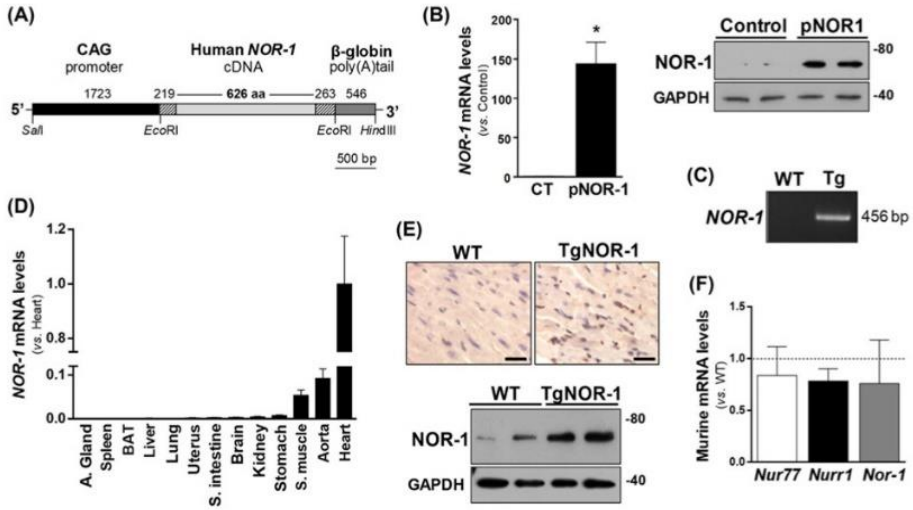

Figure 1. Generation of transgenic mice over-expressing NOR-1 in the heart mice

(**A**) Transgene structure. The CAG promoter (in black) was fused 5′ of the human *NOR-1* cDNA (shaded fragments: UTRs. Light grey: coding region), and the β-globin polyadenylation site (dark grey) was fused at 3′ to the cDNA. The *SalI–Hin*dIII fragment was microinjected into mouse zygotes. (**B**) Cells were transfected with the pCAGGS/hNOR-1 construct (pNOR-1) or the empty vector (Control; CT) and human *NOR-1* mRNA and NOR-1 protein levels were analysed by real-time PCR (left panel) and Western blot (right panel), respectively. Human *NOR-1* mRNA levels were undetectable in cells transfected with the empty vector, but an arbitrary value of 1 was assigned for comparative purposes. Results are the mean ± SEM (n=4). *P<0.01 *vs*. CT cells. GAPDH was used as loading control in Western blot assays, in which protein size was estimated by the indicated position of molecular weight markers (in kDa). (**C**) Offspring was screened by PCR of genomic DNA from mouse tail. The Ethidium Bromide-stained agarose gel shows the amplification of a 456-bp fragment only in TgNOR-1 mice. (**D**) Human *NOR-1* mRNA levels were analysed by real-time PCR in several mouse organs. For comparative purposes, an arbitrary value of 1 was attributed to human *NOR-1* mRNA levels in the heart (that displays the highest expression). Data are mean ± SEM (n=4). Abbreviations: A. Gland, adrenal gland; BAT, brown adipose tissue; S. Intestine, small intestine; S muscle, skeletal muscle (quadriceps femoris muscle). (**E**) Myocardial NOR-1 expression was analysed by immunohistochemistry (upper panel) and Western blot (lower panel). GAPDH was used as loading control in Western blot assays. Scale bars: 25 μm. (**F**) Endogenous expression of mouse *Nr4a* receptors in hearts from WT and TgNOR-1 mice analysed by real-time PCR. Data relative to levels in WT animals (indicated by a dotted line and normalized to 1) are expressed as mean ± SEM (WT, n=13; TgNOR-1, n=10). Abbreviations: GAPDH, glyceraldehyde-3-phosphate dehydrogenase; TgNOR-1, transgenic mouse over-expressing NOR-1 in the heart; WT, wild-type.

Doc 1000 Multi-Analyst 1.1 (Bio-Rad, Hercules, CA, U.S.A.). A stable transgenic mouse line was established by back-crossing the transgene-carrying founder with C57BL/6J mice up to the tenth generation to guarantee the 99.9% of purity in this genetic background.

Transgene integration site sequencing

The identification of the transgene insertion site was performed by Cergentis B.V. (Utrecht, The Netherlands) using the Targeted Locus Amplification (TLA) technology [24]. Briefly, splenocytes were isolated from transgenic mice by spleen homogenisation and purification through a 40-μm mesh filter. After red blood cells lysis, splenocytes were cryopreserved until TLA processing. Three sets of primers targeting the transgene sequence were used to perform TLA analysis (Set 1 Fw: 5′-CAGCTCGGAATACACCACGG-3, Rv: 5′-GTTTCTAGAGGTACCACGCGT-3′; Set 2 Fw: 5′-TTGGTTTAGAGTTTGGCAAC-3′, Rv: CCAACACACTATTGCAATGA-3′ and Set 3 Fw: 5′-GTCAAT GACGGTAAATGGC-3′, Rv: 5′-TTATGTAACGCGGAACTCC-3′). PCR products were purified, amplicons were library-prepped using the Illumina NexteraXT protocol, and sequenced on an Illumina Miniseq sequencer.

© 2020 The Author(s). Published by Portland Press Limited on behalf of the Biochemical Society

Downloaded from http://portlandpress.com/clinsci/article-pdf/134/3/359/867300/cs-2019-1014.pdf by Universitat de Barcelona user on 09 November 2020

PORTLAND PRESS

Clinical Science (2020) **134** 359–377
https://doi.org/10.1042/CS20191014

Animal handling

Animals were bred in the Animal Experimentation Unit (Institut de Recerca de l'Hospital de la Santa Creu i Sant Pau, Barcelona, Spain). Animal handling and disposal were performed in accordance with the principles and guidelines established by the Spanish Policy for Animal Protection RD53/2013 and the European Union Directive 2010/63/UE. All procedures were approved by the local ethical committee (Law 5/June 21, 1995; Generalitat de Catalunya).

In a first study, the impact of NOR1 transgenesis on cardiac function was determined by echocardiography in 4-month-old male wild-type (WT) and transgenic mouse overexpressing NOR-1 in the heart (TgNOR-1) mice at baseline and after 8 months (when animals were 12 months old; n=11). In a second experimental approach, 3-month-old male WT and TgNOR-1 mice were randomly divided into AngII or saline-infused animals (n=13–14). AngII [1000 ng/kg body weight (BW)/min; Sigma–Aldrich] was infused in WT and TgNOR-1 mice via osmotic minipumps (model 1004, Alzet; Durect Corporation, Cupertino, CA, U.S.A.) for 28 days as described [25]. WT and TgNOR-1 mice infused with saline were used as controls [25]. For the implantation of osmotic minipumps, mice were anaesthetised with isofluorane inhalation (2%). Anaesthetic depth was confirmed by loss of blink reflex and/or lack of response to tail pinch. The procedure took approximately 15 min/mouse. Recovery after surgical procedures was carried out using aseptic techniques in a dedicated approved surgical area. Antibiotics (penicillin, 450000 u/kg, intramuscular) and analgesics (buprenorphine, 0.05 mg/kg, subcutaneous) were given immediately after surgery to prevent infection and discomfort. The animals were kept warm in a heating pad until awake after surgery, and observed carefully by the investigators throughout the post-surgery period. Systolic blood pressure was non-invasively measured in conscious mice prior to and following AngII infusion using the tail-cuff plethysmography method, as described [25,26].

Echocardiographic data were recorded at baseline and after 2 and 4 weeks of AngII infusion. At the end of the experimental procedures, mice were killed via isofluorane overdose and cardiac hypertrophy was calculated as the heart weight (HW) to BW ratio (HW/BW) [27] and as the HW-tibia length ratio (HW/TL) [28].

Basic measurements of cardiac function by echocardiography (M-mode and Doppler)

Anaesthetized mice (2% isofluorane inhalation) were subjected to a transthoracic echocardiography, using a Vevo 2100 ultrasound with a 30 MHz transducer (VisualSonics, Toronto, ON, Canada). Two-dimensional and M-mode images were obtained in parasternal long-axis and short-axis views, respectively. The following parameters were recorded: heart rate (HR), end-diastolic interventricular septum thickness (IVSTd), left ventricle (LV) end-diastolic dimension (LVEDd), LV end-systolic dimension (LVESd), end-diastolic LV posterior wall thickness (PWTd) and LV anterior wall thickness (AWTd). LV mass, LV ejection fraction (LVEF) and LV fractional shortening (LVFS) were determined. LV mass was calculated from the M-mode measurements in diastole using the corrected cube formula (also known as Troy formula or Devereux and Reichek formula) as follows:

$$\text{LV mass (M - mode)} = 1.053 \times \left[(\text{LVED} + \text{PW} + \text{IVST})^3 - \text{LVED}\right]$$

$$\text{Corrected LV mass (M - Mode)} = \text{LV mass (M - Mode)} \times 0.8$$

LV stroke volume, cardiac output (CO), LVED relative radius and relative posterior wall thickness (rPWT) were calculated:

$$\text{LV stroke volume } (\mu\text{l}) = \text{LV end-diastolic volume} - \text{LV end-systolic volume}$$

$$\text{CO (ml/min)} = \frac{(\text{LV stroke volume} \times \text{HR})}{1000}$$

$$\text{LVED relative radius} = \frac{(\text{LVEDd}/2)}{\text{PWTd}}$$

$$\text{rPWT} = \frac{(2 \times \text{PWTd})}{\text{LVEDd}}$$

© 2020 The Author(s). Published by Portland Press Limited on behalf of the Biochemical Society

Downloaded from http://portlandpress.com/clinsci/article-pdf/134/3/359/867300/cs-2019-1014.pdf by Universitat de Barcelona user on 09 November 2020

Clinical Science (2020) **134** 359–377
https://doi.org/10.1042/CS20191014

PORTLAND PRESS

Isolation of cardiomyocytes and measurement of cell size and cell shortening

Ventricular cardiomyocytes were isolated from mouse hearts by enzymatic digestion as described [29]. Briefly, mouse hearts were perfused at a constant flow rate of 3 ml/min on a Langendorf perfusion system. The heart was first perfused for 5 min with nominally calcium-free Tyrode's solution containing (in mM): NaCl 88, sucrose 78, KCl 5.4, $MgCl_2$ 1, HEPES 10, Na-pyruvate 5 and glucose 10 plus 2 mg/ml fatty acid-free BSA. The heart was digested for 8 min with nominally calcium-free Tyrode's solution containing collagenase (0.4 mg/ml, type II; Worthington, Lakewood, NJ, U.S.A.). Subsequently, atria were removed and myocytes released in calcium-free Tyrode's solution by gentle agitation. To increase cardiomyocyte yield, remaining ventricular tissue was subjected to additional digestion for 5 min in fresh collagenase-containing solution with gentle agitation. This process was repeated three times and cardiomyocytes were pooled in calcium-free Tyrode's solution and the extracellular calcium concentration was increased stepwise from 0.2 to 0.4, and 0.8 mM. Only calcium-tolerant, quiescent, rod-shaped cardiomyocytes showing clear cross-striations were used. The cross-sectional area was measured from the transmission images using Leica LASAF software (Leica, Wetzlar, Germany) or a custom-made program [30]. Cardiomyocyte contractile function was estimated by measuring cell shortening along the longitudinal cell axis using a custom-made program as previously described [31]. Cell shortening was expressed as fractional shortening (dl/L) by normalising the maximal change in cell length during cell shortening (dL) to the cell length at rest (L).

Isolation of cardiofibroblasts and assessment of migratory activity

Cardiofibroblasts were isolated from a pool of two hearts of adult mice as described [27]. Cells were used between passages 2 and 4. Cardiofibroblast migratory activity was determined in wound healing assays. Cells were grown until confluence on 12-well plates and then serum-starved for 48 h. Next, the monolayer was wounded by scraping with a P200 pipette tip. After washing, 20% FCS medium was added, and the extent of healing was determined after 16 h. Four different fields were visualized, photographed and quantified (ImageJ software).

Analysis of mRNA levels

Total RNA was isolated using TRIsure™ reagent (Bioline) and reverse transcribed into cDNA using the High Capacity cDNA Reverse Transcription Kit (Applied Biosystems). Quantification of mRNA levels was performed by real-time PCR using the ABI PRISM 7900HT sequence detection system (Applied Biosystems). Specific primers and probes (provided by Applied Biosystems or Integrated DNA Technologies Inc, Coralville, IA, U.S.A.) were used for the quantification of mRNA levels for: human *NOR-1* (Hs00175077_m1), and mouse *Nor-1* (Mm00450074_m1), *Nurr1* (Mm00443056_m1), *Nur77* (Mm00439358_m1), brain natriuretic peptide (*Bnp*; Mm.PT.58.8584045.g), α 1 skeletal muscle actin (*Acta1*; Mm.PT.58.7312945), myosin heavy chain 7 (*Myh7*; Mm.PT.58.17465550.g), transgelin (*Sm22*α) (Mm.PT.58.5329269), plasminogen activator inhibitor-1 (*Pai-1*; Mm00435858_m1), collagen type I α 1 chain (*Col1a1*; Mm.PT.58.7562513), *Col1a3* (Mm00802300_m1), lysyl oxidase (*Lox*; Mm99495386_m1), lysyl oxidase-like 2 (*Loxl2*) (Mm00804740_m1) and connective tissue growth factor (*Ctgf*; Mm01192933_g1). TATA-binding protein (*Tbp*; Mm00446973_m1) and glyceraldehyde-3-phosphate dehydrogenase (*Gapdh;* Mm.PT.58.39a.1) expression were used as reference genes. Similar results were obtained after normalisation with both housekeeping genes.

Generation of promoter constructs and luciferase reporter assays

The human *MYH7* promoter (positions −1791 to +39 relative to the Transcription Start Site [TSS]) was amplified by PCR from genomic DNA. The primers used were: 5′- TTAAGAGCTCCCCTCATCGCCAATCCTTGA-3′ (forward; *Sac*I site is underlined) and 5′- TTAACTCGAGGGGGCTGTATATATGGGGCA-3′ (reverse; *Xho*I site is underlined). The PCR product was cloned into the pGL3 vector (Promega, Madison, WI, U.S.A.) (pGL3/pMYH7-1830). Similarly, a 1810-bp fragment of the human *LOXL2* promoter (positions −1688 to +122 relative to the TSS) was amplified by PCR from genomic DNA using the following primers: 5′-TATACTCGAGTTCAAAGGTCCTGGGGTGTG-3′ (forward; *XhoI* site is underlined) and 5′-TATAAAGCTTGCGCGTTTACTCTTTTCCCC-3′ (reverse; *HindIII* site is underlined). The PCR product was cloned into the pGL3 vector (Promega) (pGL3/pLOXL2-1810). These constructs were used in transient transfection assays performed in 12-well plates using 0.5 μg of the luciferase reporter plasmid together with pCMV5/NOR-1 expression vector or the pCMV5 vector (0.05 μg), 0.5 μl PLUS™ Reagent and 1.25 μl of Lipofectamine™ LTX Reagent (Invitrogen) per well. The pRL-SV40 (25 ng) was included as an internal control (Promega). Firefly and *Renilla* luciferase activities were measured using the Dual-Luciferase™ Reporter Assay System (Promega) and a luminometer (Orion I; Berthold Detection Systems, Pforzheim, Germany). Results were expressed as the ratio of firefly to *Renilla* activity.

© 2020 The Author(s). Published by Portland Press Limited on behalf of the Biochemical Society

Downloaded from http://portlandpress.com/clinsci/article-pdf/134/3/359/867300/cs-2019-1014.pdf by Universitat de Barcelona user on 09 November 2020

PORTLAND PRESS

Clinical Science (2020) **134** 359–377
https://doi.org/10.1042/CS20191014

Immunoblotting

Whole-cell extracts and tissue lysates were separated on SDS/polyacrylamide gels, transferred to polyvinylidene diflouride membranes (Immobilon, Merck Millipore; IPVH00010). Blots were incubated with antibodies directed against NOR-1 (H00008013-M06, 1:1000; Abnova, Taipei City, Taiwan), GAPDH (MAB374, 1:20000; Merck Millipore), SM22α (sc-18513, 1:1000; Santa Cruz Biotechnology, Dallas, TX, U.S.A.), ACTA1 (ab52218, 1:2000; Abcam, Cambridge, U.K.), BNP (sc-67455, 1:1000; Santa Cruz Biotechnology) or β-myosin heavy chain (β-MHC) (MAB90961, 1:2000; R&D Systems, Minneapolis, MN, U.S.A.). Bound antibodies were detected after incubation with appropriate HRP–conjugated secondary antibodies (Dako Products, Agilent, Santa Clara, CA, U.S.A.) and using the SuperSignal West Dura Extended Duration Substrate (Thermo Fisher Scientific, Waltham, MA, U.S.A.). The size of detected proteins was estimated using protein molecular-mass standards (Hyperpage Prestained Protein Marker; Bioline, Paris, France). Equal loading of protein in each lane was verified by Ponceau staining and by GAPDH signal.

Histological, immunohistochemical and immunocytochemical analyses

Mouse tissues were fixed in 4% paraformaldehyde/0.1 M PBS (pH 7.4) for 24 h and embedded in paraffin. Tissue sections (5 μm) were deparaffinised in xylene and rehydrated in graded ethanol solutions. Slides were then rinsed in distilled water and treated with 3% hydrogen peroxide in methanol for 30 min to remove endogenous peroxidase activity. Sections were then blocked with 10% normal serum and incubated overnight at 4°C with an anti-human NOR-1 (H00008013-M06, 1:50; Abnova) or with an anti-Mac-3 (sc-19991, 1:150; Santa Cruz Biotechnology) antibody. After washing, samples were incubated for 1 h with a biotinylated secondary antibody (Vector Laboratories, Burlingame, CA, U.S.A.). After rinsing three times in PBS, standard Vectastain (ABC) avidin–biotin peroxidase complex (Vector Laboratories) was applied, and the slides were incubated for 30 min. Colour was developed using 3,3′-diaminobenzidine (DAB) and sections were counterstained with Haematoxylin before dehydration, clearing and mounting. Negative controls in which the primary antibody was omitted were included to test for non-specific binding.

Cardiac fibrosis was determined by Picrosirius Red staining (Sigma–Aldrich). Images were captured at low magnification and the percentage of fibrosis was determined as the ratio between collagen area and the total area of the heart section [27]. Collagen cross-link was visualised under polarized light microscopy and refringence was quantified using ImageJ software [27]. Cardiomyocyte cross-sectional area was analyzed in sections stained with FITC-conjugated wheat germ agglutinin (WGA). Cross-sectional area was calculated as an average of at least 30–40 cells per section taken from different fields of the LV using ImageJ software. Collagen I deposition and structure in cultured cardiofibroblasts was visualised by confocal immunocytochemistry as previously described [32]. Cardiofibroblasts from WT and TgNOR-1 mice were plated on to 35-mm diameter μ-dishes (Ibidi, Martinsried, Germany). Six days after plating, cells were fixed with 4% paraformaldehyde, and nonpermeabilised cardiofibroblasts were incubated overnight with a rabbit antibody against collagen Iα1 (NB600-408, 1:150; Novus Biologicals, Cambridge, U.K.). Dishes were washed and incubated for 1 h with a fluorescence–conjugated secondary antibody (Goat Anti-Rabbit Alexa Fluor 488; Thermo Fisher Scientific). Samples were washed and mounted with ProLong Gold Antifade Reagent with DAPI (Thermo Fisher Scientific). Fluorescence images were acquired with a Leica DMIRE2 Confocal Microscope using Leica Confocal Software (Leica). Quantitative analysis of the extent of collagen deposition was performed using ImageJ software.

Statistical analyses

Results are shown as mean ± standard deviation (SD) or mean ± standard error of the mean (SEM). Significant differences were analysed using the Student's *t* test (two-tailed) or two-way ANOVA and the Tukey's test. When normality failed, the Mann–Whitney rank sum test was applied. Data were analysed with the GraphPad Prism version 6.01. Differences were considered significant at $P<0.05$.

Results

Generation of a transgenic mouse model that overexpresses NOR-1 in the heart

We generated a transgenic mouse that overexpresses NOR-1 mainly in the heart. The full-length human *NOR-1* cDNA was cloned into the *Eco*RI site of the pCAGGS vector (Figure 1A). This construct was able to efficiently drive NOR-1 expression (both mRNA and protein) (Figure 1B). Transgenic animals on a C57BL/6J background were generated by conventional methods. F1 transgenic mice (TgNOR-1) grew to adulthood normally and were phenotypically indistinguishable from their WT littermates. The transgene was stably transmitted to subsequent generations (Figure 1C)

© 2020 The Author(s). Published by Portland Press Limited on behalf of the Biochemical Society

Downloaded from http://portlandpress.com/clinsci/article-pdf/134/3/359/867300/cs-2019-1014.pdf by Universitat de Barcelona user on 09 November 2020

Clinical Science (2020) **134** 359–377
https://doi.org/10.1042/CS20191014

following the expected Mendelian distribution, which suggested that NOR-1 transgenesis did not compromise embryo development. TgNOR-1 mice were viable and fertile, without phenotypic differences with WT littermates. TLA analysis evidenced that the transgene integration site lies within chromosome 7, specifically in the area Chr7:33723172 corresponding to a non-coding region (Supplementary Figure S1). Although the exact copy number cannot be determined by TLA at least four copies of the transgene, three of them inserted in tandem were found. Quantitative analysis of transgene expression evidenced a strong expression in heart, medium expression in aorta and skeletal muscle (approximately 9 and 5% of that observed in the heart, respectively), and lower expression in other tissues (Figure 1D and Supplementary Figure S2A). NOR-1 overexpression was confirmed by immunohistochemistry and Western blot (Figure 1E and Supplementary Figure S2A–C). It should be noted that NOR-1 transgenesis did not affect the endogenous expression of *Nr4a* receptors (Figure 1F and Supplementary Figure S2D).

Effect of NOR-1 over-expression on cardiac cells

Cardiomyocytes from TgNOR-1 mice exhibited higher expression of the transgene than cardiofibroblasts (Figure 2A). Accordingly, NOR-1 protein levels were significantly increased in TgNOR-1 cardiomyocytes (Figure 2B). Cell surface area of TgNOR-1 cardiomyocytes was greater than that of WT (Figure 2C). As shown in Figure 2D, in transgenic cells *Myh7* expression was up-regulated, while *Myh6* mRNA levels remained unchanged, yielding a significant increase in the *Myh7*/*Myh6* expression ratio relative to WT cells (approximately two-fold) (Figure 2D). Further, cardiomyocytes from TgNOR-1 mice showed an increased fractional cell shortening elicited by electric field stimulation (Figure 2E).

TgNOR-1 cardiofibroblasts in culture also showed increased NOR-1 protein levels (Figure 3A) and an enhanced expression of *Acta1* and *Sm22α*, markers of the phenotypic switch of fibroblasts to myofibroblasts, as well as *Col1a1* and *Pai-1* (Figure 3B). In agreement, higher protein levels of ACTA1, SM22α (Figure 3C) and collagen (Figure 3D) were detected in TgNOR-1 cardiofibroblasts. In wound healing assays, transgenic cells exhibited an increased ability to migrate and invade the denuded area than cells from WT animals (Figure 3E).

Effects of NOR-1 over-expression on cardiac function and ventricular remodelling

As a first approach to determine the impact of NOR-1 overexpression on cardiac function and ventricular remodelling, LV geometry and function were assessed by echocardiography in 4- and 12 month old mice (Supplementary Table S1). No differences in chamber dimensions, wall thicknesses or systolic function parameters were found between TgNOR-1 and WT mice in young animals (4 months old). However, a significant increase in LV mass was observed in 12-month-old-TgNOR-1 mice as compared with age-matched WT animals (44 and 28% mass gains in either genotype during the observation period). These differences were due to increased wall thickening in transgenic animals, and not to greater chamber dilation, as reflected by the similar time-course in concentricity parameters LVEDd relative radius and rPWT in the two genotypes. No significant differences were detected at any age in LVEF or LVFS, as indicators of the LV systolic function.

NOR-1 transgenesis aggravates AngII-induced cardiac hypertrophy

To clarify the role of this nuclear receptor in cardiac hypertrophy, TgNOR-1 and WT mice were subjected to chronic infusion of AngII. AngII increased blood pressure to a similar level in WT and TgNOR-1 mice (Figure 4A). No differences in echocardiographic data were detected between saline-infused groups (Table 1). AngII-infused WT mice developed a concentric hypertrophy geometric pattern, with a wall thickening-based moderate increase in LV mass after 14 or 28 days of treatment, increased sphericity and no change of systolic function parameters such as LVEF and LVFS (Table 1). In TgNOR-1 mice, AngII triggered a more robust increase in LV mass, driven by a greater thickening of interventricular septum (IVS) and LV posterior wall (PW), with statistical significant differences after 4 weeks of treatment (Table 1). This augmented LV hypertrophy was accompanied by a more concentric geometric pattern and an increased systolic function, as evidenced by the enhanced LVFS and LVEF (Table 1). Figure 4B shows representative frame images of M-mode recordings of the short-axis view from hearts of AngII-infused animals. These data suggest that TgNOR-1 mice exhibited a more exacerbated concentric remodelling in response to AngII than WT mice did. Consistently, the enhanced HW/BW (and the HW/TL) induced by Ang II was more prominent in TgNOR-1 mice as an indication of a greater hypertrophic response (Figure 4C,D). In fact, AngII infusion evoked a higher increase in cardiomyocyte cross-sectional area in TgNOR-1 mice as compared with non-transgenic littermates (Figure 4E). Cardiomyocyte cross-sectional areas from saline-infused TgNOR-1 mice were slightly greater than those from WT animals, in agreement with the differential cell size observed in isolated cardiomyocytes. Other parameters such as the HR were unaffected by NOR-1 over-expression.

© 2020 The Author(s). Published by Portland Press Limited on behalf of the Biochemical Society

Downloaded from http://portlandpress.com/clinsci/article-pdf/134/3/359/867300/cs-2019-1014.pdf by Universitat de Barcelona user on 09 November 2020

PORTLAND PRESS

Clinical Science (2020) **134** 359–377
https://doi.org/10.1042/CS20191014

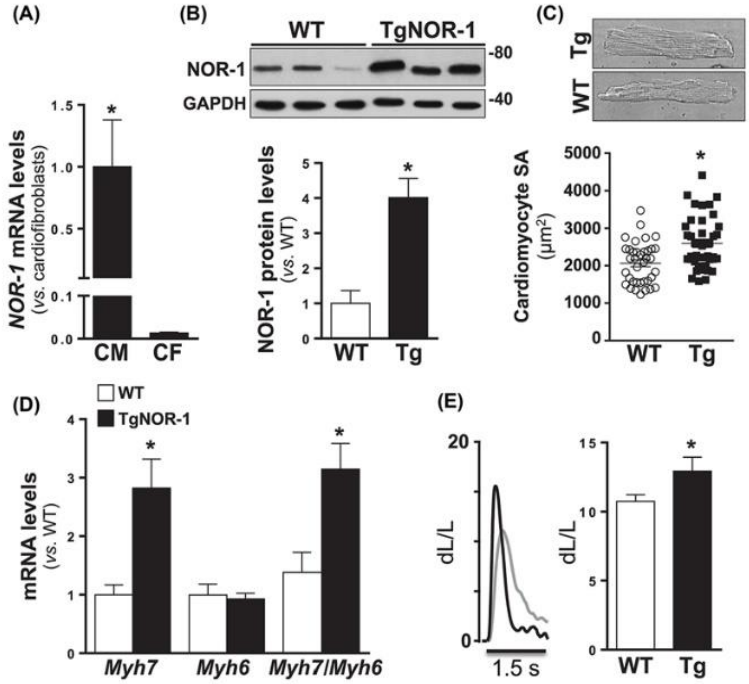

Figure 2. Characterisation of cardiomyocytes from TgNOR-1 mice

(**A**) Relative expression of the transgene (human *NOR-1*) in cardiomyocytes (CM) and cardiofibroblasts (CF) from TgNOR-1 mice analysed by real-time PCR. For comparative purposes, an arbitrary value of 1 was assigned to cardiomyoctytes the cells that displayed the highest expression of the transgene. Results are expressed as mean ± SEM (CM, n=10; CF, n=12); *P<0.01 *vs.* cardiofibroblasts. (**B**) NOR-1 protein levels in cardiomyocytes isolated from TgNOR-1 (Tg; black bars) and WT (white bars) mice. Representative Western blot images are shown. Protein size was estimated by the indicated position of molecular weight markers (in kDa). GAPDH was analysed as a loading control. The lower panel shows the quantitative analysis of Western blots. Results are expressed as mean ± SEM (WT, n=4; TgNOR-1, n=5). *P<0.05 *vs.* WT. (**C**) Average myocyte surface area (SA) in TgNOR-1 (Tg) and WT cardiomyocytes. Representative transmission images of a cardiomyocyte from a TgNOR-1 and a WT mouse are shown (upper panel). Results are expressed as mean ± SEM (WT, n=38; TgNOR-1, n=41). *P<0.001 *vs.* WT cells. (**D**) mRNA levels of *Myh7* and *Myh6*, and *Myh7*/*Myh6* expression ratio assessed by real-time PCR in cardiomyocytes from TgNOR-1 (black bars) and WT mice (white bars). Results are expressed as mean ± SEM (n=8). *P<0.05 *vs.* WT. (**E**) Representative images showing the degree of cell shortening for TgNOR-1 (black) and WT (gray) cardiomyocytes in response to electric field stimulation. Bar graph corresponds to maximal shortening (dL) normalised to the resting cell length (L). L was not significantly different between WT and TgNOR-1 cells (WT: 121.1 ± 20.1 *vs.* TgNOR-1: 121.9 ± 9.9 μm). Results are expressed as mean ± SEM (WT, n=19; TgNOR-1, n=11). *P<0.05 vs. WT cells.

NOR-1 transgenesis enhances cardiac fibrosis, collagen cross-linking and inflammation induced by AngII

Both interstitial and perivascular cardiac fibrosis were significantly increased by AngII in TgNOR-1 and WT mice. NOR-1 overexpression exacerbated this response increasing collagen deposition (Figure 5A and Supplementary Figure S3A), collagen cross-linking (Figure 5B) and the infiltration of monocytes/macrophages (Figure 5C and Supplementary Figure S3B).

© 2020 The Author(s). Published by Portland Press Limited on behalf of the Biochemical Society

Downloaded from http://portlandpress.com/clinsci/article-pdf/134/3/359/867300/cs-2019-1014.pdf by Universitat de Barcelona user on 09 November 2020

Clinical Science (2020) **134** 359–377
https://doi.org/10.1042/CS20191014

PORTLAND PRESS

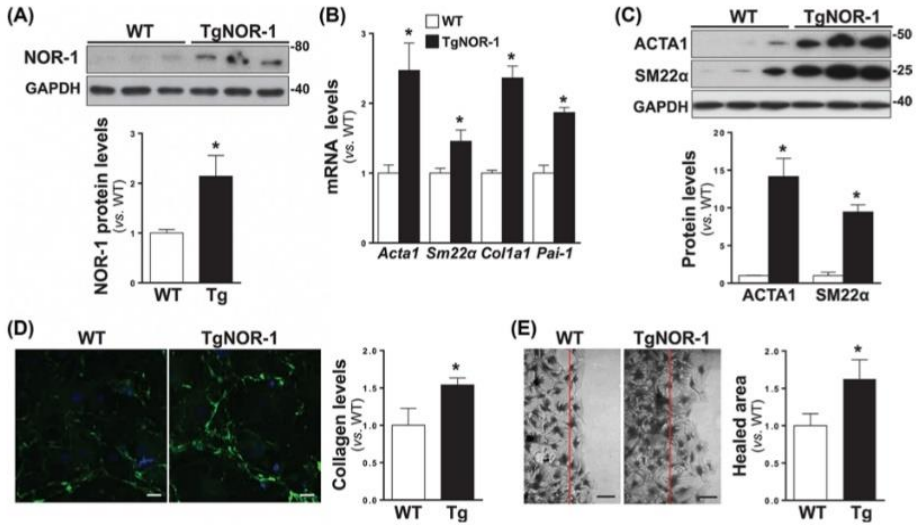

Figure 3. Characterisation of cardiofibroblasts from TgNOR-1 mice

(**A**) NOR-1 protein levels were evaluated by Western blot in cell lysates from both WT (white bars) and TgNOR-1 (Tg; black bars) mice. Levels of GAPDH are shown as a loading control. Protein size was estimated by the indicated position of molecular weight markers (in kDa). Data are expressed as mean ± SEM (n=4). *P<0.05 *vs.* WT cells. (**B**) *Acta1*, *Sm22α*, *Col1a1* and *Pai-1* mRNA levels were analysed by real-time PCR in these cells. Results are expressed as mean ± SEM (n=6). *P<0.05 *vs.* WT cells. (**C**) Protein levels of ACTA1 and SM22α assessed by Western blot in WT and transgenic cardiofibroblasts. (Top panel) Representative Western blot images. Levels of GAPDH are shown as a loading control. The lower panel shows the quantitative analysis of Western blots. Data are expressed as mean ± SEM (n=4). *P<0.05 *vs.* WT cells. (**D**) Collagen type-I (in green) was analysed by confocal immunohistochemistry. Representative confocal images of collagen type-I deposition (in green) by WT and TgNOR-1 cardiofibroblasts are shown (left panel). Nuclei were stained with DAPI (blue). Bar graph showing quantitative analysis using ImageJ software (rigth panel). Results are expressed as mean ± SEM (n=7). *P<0.05 *vs.* WT cells. Scale bars: 50 μm. (**E**) Healed area in wound-healing assays performed in FCS-induced WT and TgNOR-1 cardiofibroblasts. (Left panel) Representative images. The red line marks the position of the original wound border. (Right panel) Bar graph showing the quantitative analysis using ImageJ software. Results are expressed as mean ± SEM (WT, n=5; TgNOR-1, n=6). *P<0.05 *vs.* WT cells. Bar: 200 μm.

NOR-1 modulates the cardiac expression of *Myh7* and *Loxl2*

AngII infusion induced the expression of *Nor-1* in the heart (Supplementary Figure S4A). In cardiofibroblasts in culture, however, AngII did not modulate *Nor-1* expression (Supplementary Figure S5). AngII also up-regulated cardiac hypertrophy markers (*Bnp*, *Acta1* and *Myh7*) (Figure 6A–D) and, interestingly, NOR-1 transgenesis potentiates the induction of the hypertrophy markers triggered by AngII. Consistent with the enhanced *Myh7* expression detected in cardiomyocytes isolated from TgNOR-1, in the heart of saline-treated animals *Myh7* expression was higher in TgNOR-1 mice than in WT animals (Figure 6C).

In agreement with the exacerbated fibrotic response observed in TgNOR-1 mice, NOR-1 transgenesis enhanced the up-regulation of cardiac fibrosis markers (*Col1a1*, *Col3a1*, *Ctgf*, *Pai-1*, *Lox* and *Loxl2*) (Figure 7A–F). Noteworthy, in the heart of saline-infused animals the expression of *Loxl2*, a gene encoding for extracellular matrix (ECM) modifying enzyme critical in cardiac remodelling [33], was higher in TgNOR-1 mice than in WT animals (Figure 7F).

Thus, NOR-1 seems to regulate two genes encoding for key proteins involved in cardiac function/hypertrophy (*Myh7*) and ECM remodelling/fibrosis (*Loxl2*). By *in silico* analysis we identified putative regulatory elements in the promoter region of *MYH7* and *LOXL2* that could explain their responsiveness to NOR-1 (Figure 8A,C). We generated reporter constructs containing the proximal promoter region of *MYH7* (pMYH7-1830) and *LOXL2* (pLOXL2-1810). Cotransfection assays with a NOR-1 expression plasmid confirmed that NOR-1 drives the transcriptional activity of both *MYH7* and *LOXL2* promoters (Figure 8B,D).

© 2020 The Author(s). Published by Portland Press Limited on behalf of the Biochemical Society

Downloaded from http://portlandpress.com/clinsci/article-pdf/134/3/359/867300/cs-2019-1014.pdf by Universitat de Barcelona user on 09 November 2020

PORTLAND PRESS

Clinical Science (2020) **134** 359–377
https://doi.org/10.1042/CS20191014

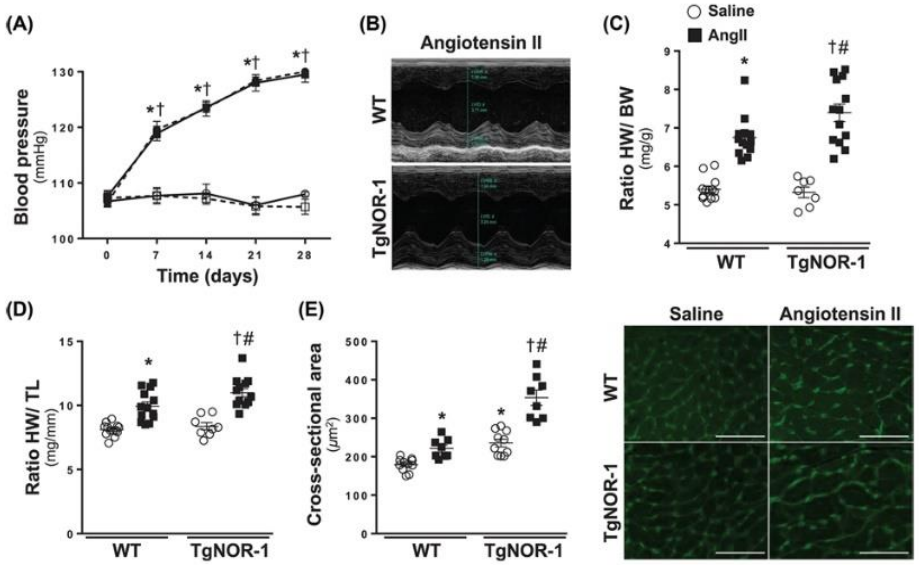

Figure 4. NOR-1 transgenesis increases AngII-induced cardiac hypertrophy

WT (squares) and TgNOR-1 (circles) mice were infused with AngII (1000 ng/kg/min; filled symbols/columns) or saline solution for 28 days (open symbols/columns). (**A**) Blood pressure was assessed once a week in each experimental group. Data are mean ± SEM (WT saline: n=5; WT AngII: n=9; Tg saline: n=7; Tg AngII: n=10). *P<0.0001 *vs*. Saline-infused WT mice; †P<0.05 *vs*. Saline-infused TgNOR-1 animals. (**B**) Representative frames images of M-mode recordings of the short-axis view from hearts of AngII-infused animals. (**C**) HW/BW ratio for each group of mice. (**D**) HW/TL ratio. (C,D) Data are mean ± SEM (WT saline, n=13; WT AngII, n=13; Tg saline, n=8; Tg AngII, n=13). *P<0.05 *vs*. Saline-infused WT mice; †P<0.05 *vs*. Saline-infused TgNOR-1 animals; #P<0.05 *vs*. AngII-infused WT mice. (**E**) WGA staining and cardiomyocyte cross-sectional area determined in these animals. The histogram shows the quantification by the ImageJ software (left panel) (WT saline, n=11; WT AngII, n=8; Tg saline, n=10; Tg AngII, n=8). Representative images are shown (right panel, bars, 50 μm). (C–E) Data are mean ± SEM. *P<0.05 *vs*. Saline-infused WT mice; †P<0.05 *vs*. Saline-infused TgNOR-1 animals; #P<0.05 *vs*. AngII-infused WT mice.

Discussion

Hypertension is a highly prevalent disorder and a major public health problem [34]. Sustained hypertension is associated with HCH, a process resulting from cardiomyocyte hypertrophy, inflammation and fibrosis, which triggers structural and functional changes in the heart ultimately leading to HF. Chronic elevation of circulating AngII, the main effector peptide of the renin–angiotensin system, is a critical factor in the pathogenesis of HCH; however, the underlying mechanisms are not completely understood. In this work, we show that NOR-1, a nuclear receptor whose cardiac expression is up-regulated by AngII, regulates key genes involved in cardiac function and remodelling modulating ventricular hypertrophy in response to pressure overload.

The TgNOR-1 mouse model was generated by using the CAG promoter (human cytomegalovirus [*CMV*] immediate early promoter enhancer with chicken β-actin/rabbit β-globin hybrid promoter) to drive transgene expression. This promoter contains critical response elements that govern cardiac expression and has previously been successfully used to achieve the expression of the transgene preferably into the heart [27,35]. Using this strategy, we generated a construct that was validated *in vitro* in transient transfections, and was subsequently used to generate a transgenic mouse by standard procedures. NOR-1 over-expression had no effect on embryonic development or viability, and TgNOR-1 mice did not show obvious phenotypic differences compared with their WT littermates. By both RNA and protein analyses we confirmed the anticipated pattern of CAG-directed transgene expression in TgNOR-1 mice: mainly in cardiovascular tissues, in particular in the heart. Therefore, the CAG promoter-driven transgenesis

© 2020 The Author(s). Published by Portland Press Limited on behalf of the Biochemical Society

Downloaded from http://portlandpress.com/clinsci/article-pdf/134/3/359/867300/cs-2019-1014.pdf by Universitat de Barcelona user on 09 November 2020

Clinical Science (2020) **134** 359–377
https://doi.org/10.1042/CS20191014

Table 1 Echocardiographic LV parameters of TgNOR-1 and WT mice after Ang II or saline infusion

	WT			TgNOR-1		
	Saline	Ang II (2 weeks)	Ang II (4 weeks)	Saline	Ang II (2 weeks)	Ang II (4 weeks)
n	14	14	14	13	13	13
BW (g)	25.73 ± 0.42	25.46 ± 0.59	25.28 ± 0.74	25.89 ± 0.31	25.85 ± 0.34	25.08 ± 0.38
LVEDd (mm)	3.58 ± 0.10	3.54 ± 0.09	3.56 ± 0.09	3.61 ± 0.09	3.45 ± 0.08	3.40 ± 0.08
LVESd (mm)	2.36 ± 0.12	2.31 ± 0.12	2.38 ± 0.10	2.37 ± 0.14	2.06 ± 0.11	1.98 ± 0.09
IVSTd (mm)	0.92 ± 0.02	1.01 ± 0.03	1.08 ± 0.04*	0.86 ± 0.02	1.01 ± 0.02†	1.21 ± 0.04†,‡,§
AWTd (mm)	0.90 ± 0.02	1.07 ± 0.03*	1.10 ± 0.03*	0.91 ± 0.02	1.11 ± 0.02†	1.16 ± 0.03†
PWTd (mm)	0.87 ± 0.02	1.02 ± 0.02*	1.07 ± 0.02*	0.84 ± 0.02	1.11 ± 0.03†	1.23 ± 0.03†,‡,§
LVED relative radius	2.09 ± 0.08	1.75 ± 0.07*	1.67 ± 0.04*	2.14 ± 0.08	1.56 ± 0.05†	1.39 ± 0.05†,‡
rPWT	0.49 ± 0.02	0.58 ± 0.02*	0.60 ± 0.02*	0.48 ± 0.02	0.65 ± 0.02†	0.73 ± 0.03†,‡
LVFS (%)	34.46 ± 1.84	35.24 ± 2.11	33.22 ± 1.49	36.35 ± 2.61	40.64 ± 2.24	41.89 ± 1.47‡
LVEF (%)	63.80 ± 2.61	64.72 ± 2.62	62.29 ± 2.12	65.69 ± 3.29	71.39 ± 2.58	73.09 ± 1.68‡
LV mass (mg)	91.07 ± 3.70	110.80 ± 3.99*	120.50 ± 5.00*	89.83 ± 3.03	118.10 ± 5.26†	137.90 ± 3.91†,‡,§
LV stroke volume (μl)	33.77 ± 1.58	33.76 ± 1.66	33.84 ± 1.74	35.64 ± 1.02	35.13 ± 1.87	34.99 ± 1.67
HR (bpm)	364 ± 6	354 ± 9	365 ± 14	357 ± 6	365 ± 12	353 ± 8
CO (ml/min)	12.75 ± 0.69	12.39 ± 0.66	12.51 ± 0.81	12.70 ± 0.37	12.81 ± 0.81	12.31 ± 0.56

Results are expressed as mean ± SEM.
$P<0.05$: * vs. WT Saline.
† *vs.* TgNOR-1 Saline.
‡ *vs.* Ang II-infused WT mice at the same time.
§ *vs.* AngII-infused TgNOR-1 mice for 2 weeks. These parameters were estimated using the Vevo 2100 ultrasound equipment (VisualSonics).

of NOR-1 led to viable animals which were born at the expected frequency and exhibited a tissue-expression pattern of human *NOR-1* compatible with that described for this promoter.

As a first approach to assess the functional consequences of NOR-1 transgenesis in the heart we analysed the impact of NOR-1 overexpression in cardiomyocytes and cardiofibroblasts. In cardiomyocytes, the expression of the transgene was approximately 100-fold higher than in cardiofibroblasts, in agreement with previous results showing that CAG is a robust promoter driving gene expression into these cells [35]. Interestingly, analysis of the cell area in longitudinal cross-sections of isolated myocytes revealed that the area of cells from TgNOR-1 mice was significantly larger than that of WT myocytes. Transgenic cells also exhibited increased *Myh7* expression, and elevation of the *Myh7*/*Myh6* expression ratio. *MYH7* encodes β-MHC the main contractile protein of the sarcomere which forms the thick filament, and in humans represent more than 90% of ventricular myosin [36]. β-MHC is a mechanoenzyme that converts the energy from ATP hydrolysis into mechanical force which drives muscle contractibility, and relative to α-MHC (encoded by *MYH6*) has increased energy efficiency in generating contractile force [37]. Alterations in β-MHC have been associated with disturbed cell contractility [38]. Therefore, we assessed whether the contractile function could be altered in TgNOR-1 cardiomyocytes. For this purpose, we measured cardiomyocyte shortening in response to electric field stimulation. Indeed, NOR-1 overexpression increased fractional cell shortening (an index of contractility). Concerning cardiofibroblasts, NOR-1 transgenesis potentiated the expression of markers of the phenotypic switch of fibroblasts to myofibroblasts, as well as that of collagen and PAI-1, a serine protease inhibitor (Serpin) implicated in wound healing and tissue remodelling [39]. TgNOR-1 cardiofibroblasts were more active than controls invading the denuded area in a wound-healing migration assay, confirming and expanding previous studies showing that NOR-1 modulates cell migration [7,11,12]. Therefore, NOR-1 overexpression exerts effects on cardiac cells potentially related to cardiac hypertrophy.

To evaluate the effect of a gain-of-function of NOR-1 on cardiac function *in vivo*, first, we comparatively analysed the impact of age on echocardiographic parameters in transgenic *versus* WT animals. Neither systolic function nor structural parameters were different between TgNOR-1 and WT young mice. However, a significant increase in LV mass was observed in 12 months old-TgNOR-1 mice compared with age-matched WT animals. Thus, NOR-1 transgenesis seemed to predispose to hypertrophy. The cardiac expression of *Nor-1* but not *Nurr1* or *Nur77* was induced by AngII in both WT and TgNOR-1 mice. This is in agreement with previous data showing that NOR-1 expression is up-regulated in the heart of mice infused with AngII [40], and in cell cultures treated with pro-hypertrophic stimuli [21,41,42]. However, we were unable to detect an up-regulation of NOR-1 by AngII in cardiofibroblasts in culture, suggesting that a more complex interplay among pathways and mediators operating *in vivo* is required for

© 2020 The Author(s). Published by Portland Press Limited on behalf of the Biochemical Society

Downloaded from http://portlandpress.com/clinsci/article-pdf/134/3/359/867300/cs-2019-1014.pdf by Universitat de Barcelona user on 09 November 2020

PORTLAND PRESS

Clinical Science (2020) **134** 359–377
https://doi.org/10.1042/CS20191014

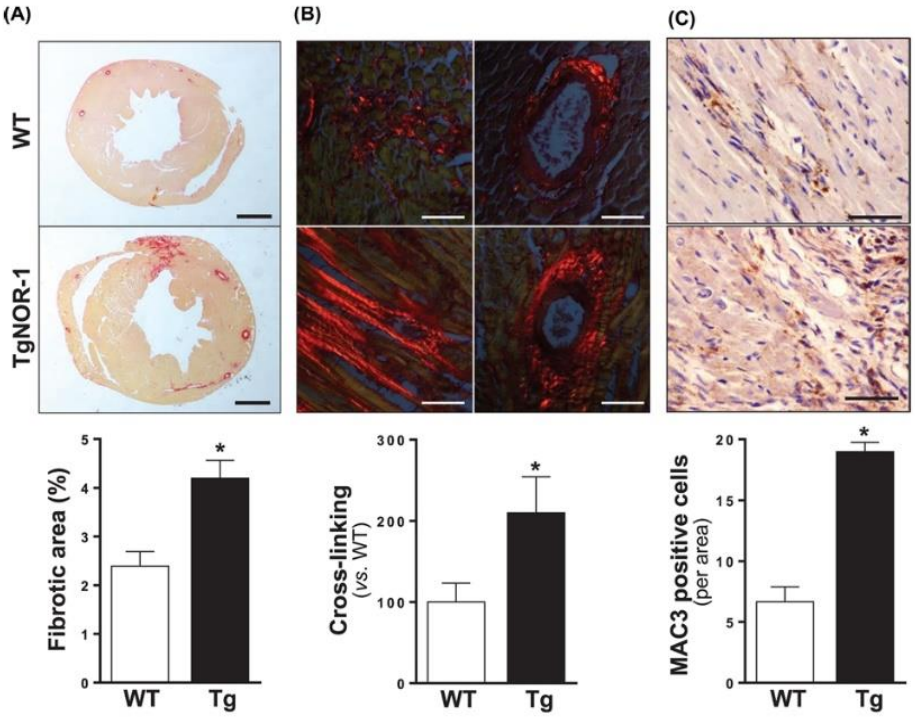

Figure 5. NOR-1 transgenesis increases AngII-induced cardiac fibrosis, collagen cross-linking and inflammation

WT and TgNOR-1 (Tg) mice were infused with AngII (1000 ng/kg BW/min) for 28 days. (**A**) Cardiac fibrosis assessed by Picrosirius Red staining captured under bright field. (Top panel) Representative images from AngII-infused WT and TgNOR-1 mice. (Bottom panel) Bar graph showing the quantitative analysis. Data are mean ± SEM (WT, n=9; TgNOR-1, n=7). *P<0.01 *vs*. WT mice. Bar: 1 mm. (**B**) Cardiac collagen cross-linking analysed by Picrosirius Red staining visualized under polarized light. (Top panel) Representative images from AngII-infused WT and TgNOR-1 mice. Scale bar: 50 μm. (Bottom panel) Bar graph showing the quantitative analysis. Data are mean ± SEM (n=7). *P<0.05 *vs*. Ang II-infused WT mice. (**C**) MAC3 immunostaining in heart sections. (Top panel) Representative images from AngII-infused WT and TgNOR-1 mice are shown. Scale bar: 50 μm. (Bottom panel) The histogram shows the quantification of MAC-3-positive cells *per* area of heart section. Data are mean ± SEM (n=4). *P<0.05 *vs*. AngII-infused WT mice.

the up-regulation of this nuclear receptor observed in the heart of AngII treated animals. Thus, NOR-1 could be involved in the cardiac hypertrophic effects of AngII. This was confirmed in mice infused with AngII to provoke pressure overload. TgNOR-1 mice were more prone to develop AngII-induced cardiac hypertrophy and fibrosis than WT animals. The early cardiac response to AngII-induced pressure overload varies from no change [43,44] to enhanced ventricular performance indicative of a compensatory reaction [45]. In our study, AngII did not affect cardiac performance in WT animals, which exhibit mild hypertrophy and fibrosis, but the exacerbated cardiac remodeling observed in TgNOR-1 was associated with a compensatory increase in LVEF and LVFS. Since AngII infusion similarly increased blood pressure in transgenic and WT mice, these differential effects seem to be independent of haemodynamic changes. Rather they were associated with a greater up-regulation of cardiac hypertrophy (*Bnp*, *Acta1* and *Myh7*) and fibrosis markers (*Col1a1*, *Col3a1*, *Ctgf*, *Pai-1* and *Loxl2*) in AngII-infused TgNOR-1 mice. More strikingly, between saline-infused groups, a significant up-regulation of two of these key genes involved in cardiac function and remodelling (*Myh7* and *Loxl2*) was observed in TgNOR-1 animals.

© 2020 The Author(s). Published by Portland Press Limited on behalf of the Biochemical Society

Downloaded from http://portlandpress.com/clinsci/article-pdf/134/3/359/867300/cs-2019-1014.pdf by Universitat de Barcelona user on 09 November 2020

Clinical Science (2020) **134** 359–377
https://doi.org/10.1042/CS20191014

PORTLAND PRESS

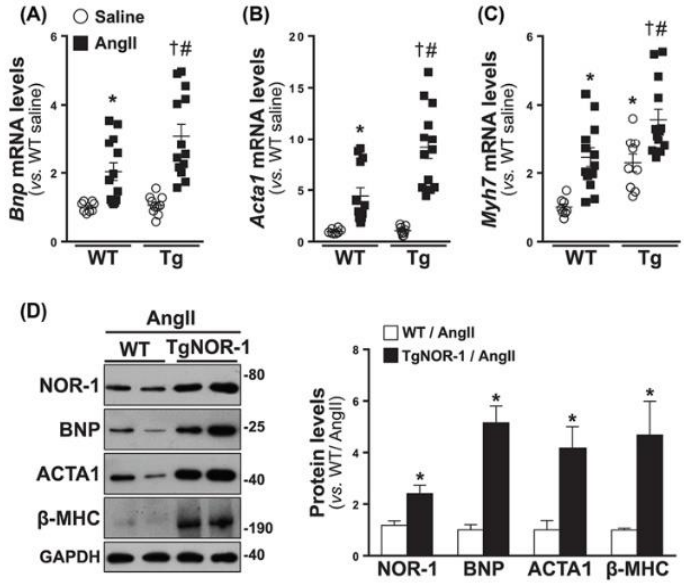

Figure 6. NOR-1 transgenesis potentiates the AngII-mediated induction of hypertrophic markers

TgNOR-1 (Tg) and WT mice were infused with AngII (1000 ng/kg/min; black bars) or saline solution for 28 days (white bars). Cardiac mRNA levels of *Bnp* (**A**), *Acta1* (**B**) and *Myh7* (**C**) were analysed by real-time PCR. Results are expressed as mean ± SEM (WT saline, n=8; WT AngII, n=13; Tg saline, n=9; Tg AngII, n=13). *P<0.05 *vs*. Saline-infused WT mice; †P<0.05 *vs*. Saline-infused TgNOR-1 animals; #P<0.05 *vs*. AngII-infused WT mice. (**D**) Protein levels were evaluated in heart lysates from AngII-infused mice. (Left panel) Representative Western blot images. Levels of GAPDH are shown as a loading control. Protein size was estimated by the indicated position of molecular weight markers (in kDa). (Right panel) Bar graph showing the quantitative analysis of Western blots from WT (white bars) and TgNOR-1 (black bars) mice infused with Ang II. Data are expressed as mean ± SEM (n=4). *P<0.05 *vs*. AngII-infused WT mice.

MYH7 was the first gene associated with familial hypertrophic cardiomyopathy, and mutations in *MYH7* account for approximately 40% of this pathology, which is the most common inherited cardiovascular disease [46]. In experimental models, the cardiac expression of *Myh7* is up-regulated by hypertrophic stimuli including AngII [47]. We observed that NOR-1 transgenesis enhanced *Myh7* expression in AngII-treated animals and, more significantly, that saline-infused TgNOR-1 mice exhibited higher expression levels of *Myh7* than WT animals, suggesting a direct regulation of *Myh7* by NOR-1. This was confirmed in transient co-transfection assays in which NOR-1 was able to drive the transcriptional activity of human *MYH7* promoter. The regulation of *MYH7* by NOR-1 is also supported by data from human vascular smooth muscle cells (VSMCs) lentivirally transduced to overexpress NOR-1. VSMC subjected to sustained over-expression of supraphysiological levels of NOR-1 experienced hypertrophy and up-regulated the expression of genes encoding for proteins typically expressed in skeletal muscle, including *MYH7* [18]. Given the central role played by β-MHC in cardiac function and hypertrophy, the modulation of *MYH7* by NOR-1 may contribute to explain why TgNOR-1 mice are more likely to develop both spontaneous and AngII-induced cardiac hypertrophy.

The up-regulation of *Loxl2* in TgNOR-1 mice is consistent with the higher collagen cross-linking observed in these animals infused with AngII. Collagen cross-linking determines ventricular stiffness and function in the pressure overloaded heart [48,49], and an excess of collagen cross-link is associated with poor prognosis in patients with hypertensive HF [50]. The oxidative deamination of the ε-amino group in certain lysine and hydroxylysine residues of collagens by members of the LOX family is critical for collagen cross-linking [51]. Increased levels of these enzymes, in particular of the two major isoforms (LOX and LOXL2), have been reported in myocardial fibrosis of HF

© 2020 The Author(s). Published by Portland Press Limited on behalf of the Biochemical Society

Downloaded from http://portlandpress.com/clinsci/article-pdf/134/3/359/867300/cs-2019-1014.pdf by Universitat de Barcelona user on 09 November 2020

PORTLAND PRESS

Clinical Science (2020) **134** 359–377
https://doi.org/10.1042/CS20191014

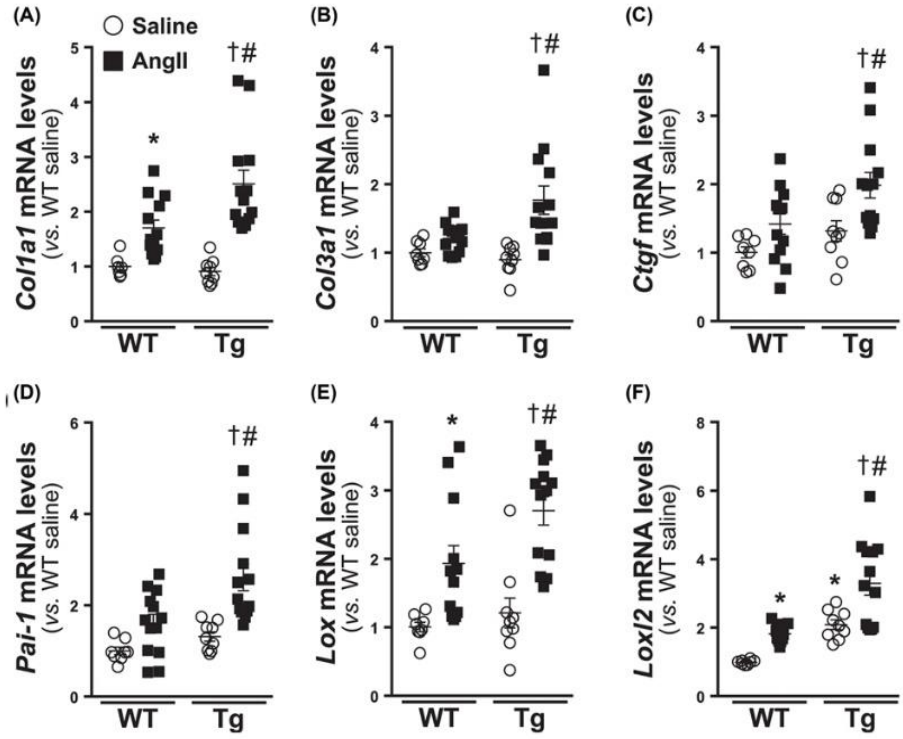

Figure 7. NOR-1 transgenesis potentiates the AngII-mediated induction of fibrosis markers

TgNOR-1 (Tg) and WT mice were infused with AngII (1000 ng/kg/min; black bars) or saline solution (white bars) for 28 days. *Col1a1* (**A**), *Col3a1* (**B**), *Ctgf* (**C**), *Pai-1* (**D**), *Lox* (**E**) and *Loxl2* (**F**) cardiac mRNA levels assessed by real-time PCR. Results are expressed as mean ± SEM (WT saline, n=8; WT AngII, n=13; Tg saline, n=9; Tg AngII, n=13). $^{*}P<0.05$ *vs*. Saline-infused WT mice; $^{\dagger}P<0.05$ *vs*. Saline-infused TgNOR-1 animals; $^{\#}P<0.05$ *vs*. AngII-infused WT mice.

patients [48,49,52] and in models of cardiac injury [33,53]. LOX and LOXL2 are up-regulated in cardiac hypertrophy following myocardial infarction [53,54], and their inhibition ameliorates cardiovascular remodelling and improves cardiac function [28,33]. Thus, LOXL2 has been proposed as a target for the treatment of cardiac fibrosis and HF [33]. Despite this critical role of LOXL2 in cardiac remodelling, little information on its transcriptional regulation is available. *LOXL2* promoter contains Smad, Sp1 and SMYD3 binding elements [55,56]. However, specific studies analysing the factors involved in the up-regulation of LOXL2 in cardiac hypertrophy are still missing. Our results implicating NOR-1 in the regulation of *LOXL2* in the heart expand the knowledge on the regulation of human *LOXL2* promoter, and help to explain previous results showing up-regulation of this receptor in processes associated with cardiac fibrosis such as post-infarction hypertrophy [57].

The TgNOR-1 mouse model has allowed us to explore the contribution of the nuclear receptor NOR-1 to the hypertrophic response triggered by pressure overload induced by Ang infusion. Our approach evidence effects on cardiac remodeling and a slight increase in EF and FS as would be expected in an initial adaptive phase to the cardiac stress caused by pressure overload. This can be considered a limitation of the study. Subsequent studies should further assess the impact of NOR-1 overexpression on systolic and dyastolic functions in long-term experiments.

In conclusion, we have generated a mouse model that overexpresses human NOR-1 mainly in the heart. NOR-1 overexpression increased cardiomyocyte size and contractile function, as well as cardiofibroblast synthetic and migratory activities. NOR-1 transgenesis exacerbated AngII-induced LV hypertrophy through the regulation of key genes

© 2020 The Author(s). Published by Portland Press Limited on behalf of the Biochemical Society

Downloaded from http://portlandpress.com/clinsci/article-pdf/134/3/359/867300/cs-2019-1014.pdf by Universitat de Barcelona user on 09 November 2020

Clinical Science (2020) **134** 359–377
https://doi.org/10.1042/CS20191014

PORTLAND PRESS

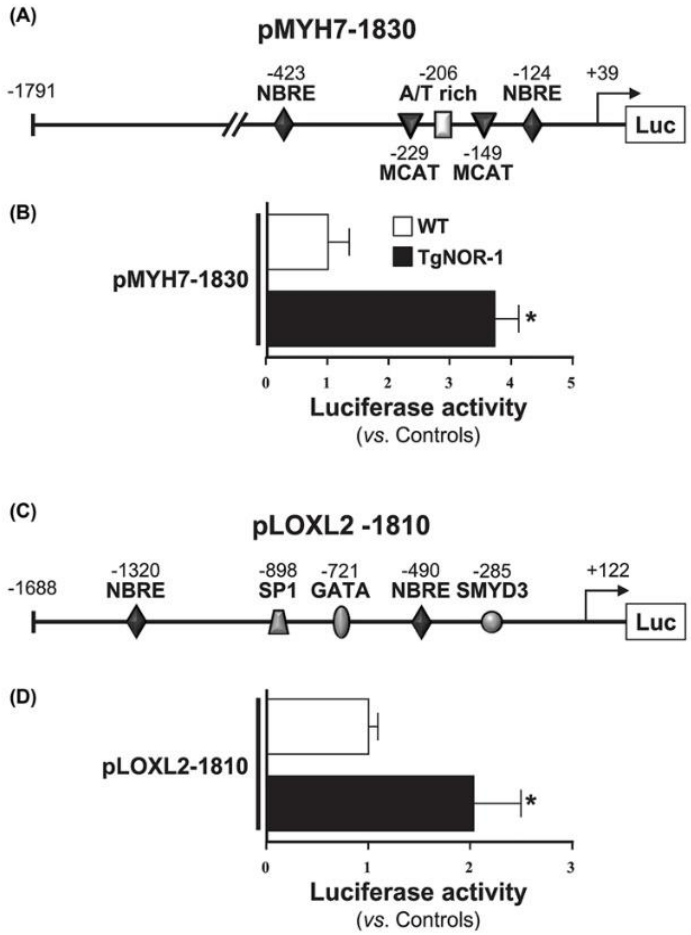

Figure 8. Modulation of MYH7 and LOXL2 transcriptional activities by NOR-1

(**A**) Scheme depicting the structure of the human *MYH7* proximal promoter cloned into the pGL3 luciferase reporter vector (pMYH7-1830). The putative NBRE sites located at −423 and −124 bp are highlighted, and regulatory elements previously characterized are also depicted. (**B**) Luciferase activity (normalized by *Renilla*) evaluated in cells co-transfected with pMYH7-1830 and a NOR-1 expression vector (pCMV5/NOR-1; black bars) or the corresponding empty plasmid (pCMV5; white bars). Values are mean ± SD (n=6). *P<0·05 *vs.* cells co-transfected with pCMV5 pCMV5. (**C**) Scheme depicting the structure of the human *LOXL2* proximal promoter cloned into the pGL3 luciferase reporter vector (pLOXL-1810). The putative NBRE sites located at −1320 and −490 bp are highlighted, and regulatory elements previously characterized are also depicted. (**D**) Luciferase activity (normalized by *Renilla*) evaluated in cells co-transfected with pLOXL2-1810 and pCMV5/NOR-1 (black bars) or pCMV5 (white bars). Values are mean ± SD (n=6). *P<0.05 *vs.* cells co-transfected with pCMV5.

involved in cardiac function and remodelling such as *Myh7* and *Loxl2*. Therefore, the nuclear receptor NOR-1 is involved in the transcriptional programme leading to HCH, and TgNOR-1 mouse could be a useful tool for further studies on the molecular bases of this human pathology.

© 2020 The Author(s). Published by Portland Press Limited on behalf of the Biochemical Society

Downloaded from http://portlandpress.com/clinsci/article-pdf/134/3/359/867300/cs-2019-1014.pdf by Universitat de Barcelona user on 09 November 2020

PORTLAND PRESS

Clinical Science (2020) **134** 359–377
https://doi.org/10.1042/CS20191014

Clinical perspectives

- HCH is a process resulting from cardiomyocyte hypertrophy, inflammation and fibrosis which triggers structural and functional changes in the heart ultimately leading to HF. The molecular mechanisms underlying HCH are not completely understood, and the prevalence of HF is increasing worldwide, while effective treatments remain elusive. Thus, there is great interest in disease models instrumental in developing new therapies.
- Our findings demonstrate that the nuclear receptor NOR-1 is a relevant transcription factor in the gene programme which governs the pathological myocardial remodeling in HCH. We have established a translational mouse model that over-express NOR-1 in the heart which exhibits an age-associated remodeling of the LV and an increased responsiveness to AngII-induced pressure overload, associated with enhanced cardiomyocyte hypertrophy, inflammation and fibrosis.
- This model could be useful to investigate the intricate networks of genes and pathways underlying HCH and its transition to HF, in order to develop therapies to target pathological remodelling of the heart with the intent to prevent, arrest or reverse the otherwise inexorable progression of this disease.

Downloaded from http://portlandpress.com/clinsci/article-pdf/134/3/359/867300/cs-2019-1014.pdf by Universitat de Barcelona user on 09 November 2020

Competing Interests

The authors declare that there are no competing interests associated with the manuscript.

Funding

This work was supported by the Sociedad Española de Cardiología (SEC; Proyecto de Investigación Básica SEC-2018); the Spanish Ministerio de Ciencia, Innovación y Universidades (MICIU) and Instituto de Salud Carlos III (ISCIII) [grant numbers RTI2018-094727-B-100, SAF2015-64767-R, SAF2017-88019-C3-1R, PI18/0919, PI17/01837, PI18/00543]; the Fundació La Marató TV3 [grant number 20152330]; the Agencia de Gestio d'Ajuts Universitaris i de Recerca (AGAUR; program of Support to Research Groups) [grant number 2017-SGR-00333]; the study was co-founded by Fondo Europeo de Desarrollo Regional (FEDER), a way to make Europe; the FI fellowship (AGAUR) [grant number 2017FI_B_00175 (to L.C.)]; and the Miguel de Servet Program (ISCIII) [grant number CP15/00126 (to M.G.)].

Author Contribution

J.M.-G. and C.R. designed and supervised the study, interpreted the data, and wrote the manuscript. L.C. and I.M.-P. performed experiments and analysed and interpreted the data. C.B.-S., A.H.-M., J.A. and L.H.-M. performed specific experiments and analysed and interpreted the data. M.G. analysed and interpreted specific data. J.F.N. participated in the analysis and interpretation of echocardiographic data. P.M. and J.O. participated in transgenic mice generation and all authors were involved in writing the paper and gave their final approval to the submitted version.

Acknowledgements

We thank Silvia Aguiló for her technical assistance.

Abbreviations

ACTA1/*Acta1*, α 1 skeletal muscle actin; AngII, angiotensin II; BNP/*Bnp*, brain natriuretic peptide; BW, body weight; CAD, coronary artery disease; Col1a1, collagen type I α 1 chain; *Ctgf*, connective tissue growth factor; ECM, extracellular matrix; GAPDH, glyceraldehyde-3-phosphate dehydrogenase; HCH, hypertensive cardiac hypertrophy; HF, heart failure; HR, heart rate; HW, heart weight; HW/BW, HW to BW ratio; HW/TL, HW-tibia length ratio; i.p., intraperitoneal; Lox, lysyl oxidase; *Loxl2*, lysyl oxidase-like 2; LV, left ventricle; LVEDd, LV end-diastolic dimension; LVEF, LV ejection fraction; LVFS, LV fractional shortening; Myh7, myosin heavy chain 7; NOR-1, neuron-derived orphan receptor-1; NR4A, nuclear receptor subfamily 4 group A; *Pai-1*, plasminogen activator inhibitor-1; rPWT, relative posterior wall thickness; *SM22*α, transgelin; Tbp, TATA-binding protein; TgNOR-1, transgenic mouse overexpressing NOR-1 in the heart; TLA, targeted locus amplification; TSS, transcription start site; VSMC, vascular smooth muscle cell; WT, wild-type; β-MHC, β-myosin heavy chain.

© 2020 The Author(s). Published by Portland Press Limited on behalf of the Biochemical Society

Clinical Science (2020) **134** 359–377
https://doi.org/10.1042/CS20191014

References

1 Heineke, J. and Molkentin, J.D. (2006) Regulation of cardiac hypertrophy by intracellular signalling pathways. *Nat. Rev. Mol. Cell. Biol.* **7**, 589–600, https://doi.org/10.1038/nrm1983

2 Barry, S.P. and Townsend, P.A. (2010) What causes a broken heart–molecular insights into heart failure. *Int. Rev. Cell. Mol. Biol.* **284**, 113–179, https://doi.org/10.1016/S1937-6448(10)84003-1

3 Martínez-González, J. and Badimon, L. (2005) The NR4A subfamily of nuclear receptors: new early genes regulated by growth factors in vascular cells. *Cardiovasc. Res.* **65**, 609–618, https://doi.org/10.1016/j.cardiores.2004.10.002

4 Pei, L., Waki, H., Vaitheesvaran, B., Wilpitz, D.C., Kurland, I.J. and Tontonoz, P. (2006) NR4A orphan nuclear receptors are transcriptional regulators of hepatic glucose metabolism. *Nat. Med.* **12**, 1048–1055, https://doi.org/10.1038/nm1471

5 Mohan, H.M., Aherne, C.M., Rogers, A.C., Baird, A.W., Winter, D.C. and Murphy, E.P. (2012) Molecular pathways: the role of NR4A orphan nuclear receptors in cancer. *Clin. Cancer Res.* **18**, 3223–3228, https://doi.org/10.1158/1078-0432.CCR-11-2953

6 Sekiya, T., Kashiwagi, I., Yoshida, R., Fukaya, T., Morita, R., Kimura, A. et al. (2013) Nr4a receptors are essential for thymic regulatory T cell development and immune homeostasis. *Nat. Immunol.* **14**, 230–237, https://doi.org/10.1038/ni.2520

7 Martínez-González, J., Rius, J., Castelló, A., Cases-Langhoff, C. and Badimon, L. (2003) Neuron-derived orphan receptor-1 (NOR-1) modulates vascular smooth muscle cell proliferation. *Circ. Res.* **92**, 96–103, https://doi.org/10.1161/01.RES.0000050921.53008.47

8 Nomiyama, T., Zhao, Y., Gizard, F., Findeisen, H.M., Heywood, E.B., Jones, K.L. et al. (2009) Deficiency of the NR4A neuron-derived orphan receptor-1 attenuates neointima formation after vascular injury. *Circulation* **119**, 577–586, https://doi.org/10.1161/CIRCULATIONAHA.108.822056

9 Zhao, Y., Howatt, D.A., Gizard, F., Nomiyama, T., Findeisen, H.M., Heywood, E.B. et al. (2010) Deficiency of the NR4A orphan nuclear receptor NOR1 decreases monocyte adhesion and atherosclerosis. *Circ. Res.* **107**, 501–511, https://doi.org/10.1161/CIRCRESAHA.110.222083

10 Rodríguez-Calvo, R., Guadall, A., Calvayrac, O., Navarro, M.A., Alonso, J., Ferrán, B. et al. (2013) Over-expression of neuron-derived orphan receptor-1 (NOR-1) exacerbates neointimal hyperplasia after vascular injury. *Hum. Mol. Genet.* **22**, 1949–1959, https://doi.org/10.1093/hmg/ddt042

11 Rius, J., Martínez-González, J., Crespo, J. and Badimon, L. (2006) NOR-1 is involved in VEGF-induced endothelial cell growth. *Atherosclerosis* **184**, 276–282, https://doi.org/10.1016/j.atherosclerosis.2005.04.008

12 Martorell, L., Martínez-González, J., Crespo, J., Calvayrac, O. and Badimon, L. (2007) Neuron-derived orphan receptor-1 (NOR-1) is induced by thrombin and mediates vascular endothelial cell growth. *J. Thromb. Haemost.* **5**, 1766–1773, https://doi.org/10.1111/j.1538-7836.2007.02627.x

13 Rodríguez-Calvo, R., Ferrán, B., Alonso, J., Martí-Pàmies, I., Aguiló, S., Calvayrac, O. et al. (2015) NR4A receptors upregulate the antiproteinase alpha-2 macroglobulin (A2M) and modulate MMP-2 and MMP-9 in vascular smooth muscle cells. *Thromb. Haemost.* **113**, 1323–1334, https://doi.org/10.1160/TH14-07-0645

14 Martí-Pàmies, I., Cañes, L., Alonso, J., Rodríguez, C. and Martínez-González, J. (2017) The nuclear receptor NOR-1/NR4A3 regulates the multifunctional glycoprotein vitronectin in vascular smooth muscle cells. *FASEB. J.* **31**, 4588–4599, https://doi.org/10.1096/fj.201700136RR

15 Myers, S.A., Eriksson, N., Burow, R., Wang, S.C. and Muscat, G.E. (2009) Beta-adrenergic signaling regulates NR4A nuclear receptor and metabolic gene expression in multiple tissues. *Mol. Cell. Endocrinol.* **309**, 101–108, https://doi.org/10.1016/j.mce.2009.05.006

16 Pearen, M.A., Ryall, J.G., Maxwell, M.A., Ohkura, N., Lynch, G.S. and Muscat, G.E. (2006) The orphan nuclear receptor, NOR-1, is a target of beta-adrenergic signaling in skeletal muscle. *Endocrinology* **147**, 5217–5227, https://doi.org/10.1210/en.2006-0447

17 Pearen, M.A., Goode, J.M., Fitzsimmons, R.L., Eriksson, N.A., Thomas, G.P., Cowin, G.J. et al. (2013) Transgenic muscle-specific Nor-1 expression regulates multiple pathways that effect adiposity, metabolism, and endurance. *Mol. Endocrinol.* **27**, 1897–1917, https://doi.org/10.1210/me.2013-1205

18 Ferrán, B., Martí-Pàmies, I., Alonso, J., Rodríguez-Calvo, R., Aguiló, S., Vidal, F. et al. (2016) The nuclear receptor NOR-1 regulates the small muscle protein, X-linked (SMPX) and myotube differentiation. *Sci. Rep.* **6**, 25944, https://doi.org/10.1038/srep25944

19 Wang, R.H., He, J.P., Su, M.L., Luo, J., Xu, M., Du, X.D. et al. (2013) The orphan receptor TR3 participates in angiotensin II-induced cardiac hypertrophy by controlling mTOR signalling. *EMBO Mol. Med.* **5**, 137–148, https://doi.org/10.1002/emmm.201201369

20 Medzikovic, L., de Vries, C.J.M. and de Waard, V. (2019) NR4A nuclear receptors in cardiac remodeling and neurohormonal regulation. *Trends Cardiovasc. Med.* **29**, 429–437, https://doi.org/10.1016/j.tcm.2018.11.015

21 Feng, X.J., Gao, H., Gao, S., Li, Z., Li, H., Lu, J. et al. (2015) The orphan receptor NOR1 participates in isoprenaline-induced cardiac hypertrophy by regulating PARP-1. *Br. J. Pharmacol.* **172**, 2852–2863, https://doi.org/10.1111/bph.13091

22 Ohkura, N., Ito, M., Tsukada, T., Sasaki, K., Yamaguchi, K. and Miki, K. (1996) Structure, mapping and expression of a human NOR-1 gene, the third member of the Nur77/NGFI-B family. *Biochim. Biophys. Acta* **1308**, 205–214, https://doi.org/10.1016/0167-4781(96)00101-7

23 Nagy, A., Gertsenstein, M., Vintersten, K. and Behringer, R. (2003) *Manipulating the Mouse Embryo: A Laboratory Manual*, Cold Spring Harbor Laboratory Press, New York

24 de Vree, P.J., de Wit, E., Yilmaz, M., van de Heijning, M., Klous, P., Verstegen, M.J. et al. (2014) Targeted sequencing by proximity ligation for comprehensive variant detection and local haplotyping. *Nat. Biotechnol.* **32**, 1019–1025, https://doi.org/10.1038/nbt.2959

25 Galán, M., Varona, S., Orriols, M., Rodríguez, J.A., Aguiló, S., Dilmé, J. et al. (2016) Induction of histone deacetylases (HDACs) in human abdominal aortic aneurysm: therapeutic potential of HDAC inhibitors. *Dis. Model Mech.* **9**, 541–552, https://doi.org/10.1242/dmm.024513

26 Orriols, M., Varona, S., Martí-Pàmies, I., Galán, M., Guadall, A., Escudero, J.R. et al. (2016) Down-regulation of Fibulin-5 is associated with aortic dilation: role of inflammation and epigenetics. *Cardiovasc. Res.* **110**, 431–442, https://doi.org/10.1093/cvr/cvw082

27 Galán, M., Varona, S., Guadall, A., Orriols, M., Navas, M., Aguiló, S. et al. (2017) Lysyl oxidase over-expression accelerates cardiac remodeling and aggravates angiotensin II-induced hypertrophy. *FASEB J.* **31**, 3787–3799, https://doi.org/10.1096/fj.201601157RR

© 2020 The Author(s). Published by Portland Press Limited on behalf of the Biochemical Society

Downloaded from http://portlandpress.com/clinsci/article-pdf/134/3/359/867300/cs-2019-1014.pdf by Universitat de Barcelona user on 09 November 2020

PORTLAND PRESS

Clinical Science (2020) **134** 359–377
https://doi.org/10.1042/CS20191014

28 Martínez-Martínez, E., Rodríguez, C., Galán, M., Miana, M., Jurado-López, R., Bartolomé, M.V. et al. (2016) The lysyl oxidase inhibitor (β-aminopropionitrile) reduces leptin profibrotic effects and ameliorates cardiovascular remodeling in diet-induced obesity in rats. *J. Mol. Cell. Cardiol.* **92**, 96–104, https://doi.org/10.1016/j.yjmcc.2016.01.012
29 Lozano-Velasco, E., Hernández-Torres, F., Daimi, H., Serra, S.A., Herraiz, A., Hove-Madsen, L. et al. (2016) Pitx2 impairs calcium handling in a dose-dependent manner by modulating Wnt signalling. *Cardiovasc. Res.* **109**, 55–66, https://doi.org/10.1093/cvr/cw207
30 Herraiz-Martínez, A., Llach, A., Tarifa, C., Gandía, J., Jiménez-Sabado, V., Lozano-Velasco, E. et al. (2019) The 4q25 variant rs13143308T links risk of atrial fibrillation to defective calcium homoeostasis. *Cardiovasc. Res.* **115**, 578–589, https://doi.org/10.1093/cvr/cvy215
31 Soliman, H., Nyamandi, V., Garcia-Patino, M., Zhang, P.C., Lin, E., Jia, Z.P. et al. (2019) ROCK2 promotes ryanodine receptor phosphorylation and arrhythmic calcium release in diabetic cardiomyocytes. *Int. J. Cardiol.* **281**, 90–98, https://doi.org/10.1016/j.ijcard.2019.01.075
32 Jover, E., Silvente, A., Marín, F., Martínez-González, J., Orriols, M., Martínez, C.M. et al. (2018) Inhibition of enzymes involved in collagen cross-linking reduces vascular smooth muscle cell calcification. *FASEB J.* **32**, 4459–4469, https://doi.org/10.1096/fj.201700653R
33 Yang, J., Savvatis, K., Kang, J.S., Fan, P., Zhong, H., Schwartz, K. et al. (2016) Targeting LOXL2 for cardiac interstitial fibrosis and heart failure treatment. *Nat. Commun.* **7**, 13710, https://doi.org/10.1038/ncomms13710
34 Lawes, C.M., Vander Hoorn, S., Rodgers, A and International Society of Hypertension (2008) Global burden of blood-pressure-related disease, 2001. *Lancet* **371**, 1513–1518, https://doi.org/10.1016/S0140-6736(08)60655-8
35 Orban, T.I., Apati, A., Nemeth, A., Varga, N., Krizsik, V., Schamberger, A. et al. (2009) Applying a "double-feature" promoter to identify cardiomyocytes differentiated from human embryonic stem cells following transposon-based gene delivery. *Stem Cells* **27**, 1077–1087, https://doi.org/10.1002/stem.45
36 Miyata, S., Minobe, W., Bristow, M.R. and Leinwand, L.A. (2000) Myosin heavy chain isoform expression in the failing and nonfailing human heart. *Circ. Res.* **86**, 386–390, https://doi.org/10.1161/01.RES.86.4.386
37 Sugiura, S., Kobayakawa, N., Fujita, H., Yamashita, H., Momomura, S., Chaen, S. et al. (1998) Comparison of unitary displacements and forces between 2 cardiac myosin isoforms by the optical trap technique: molecular basis for cardiac adaptation. *Circ. Res.* **82**, 1029–1034, https://doi.org/10.1161/01.RES.82.10.1029
38 Spudich, J.A., Aksel, T., Bartholomew, S.R., Nag, S., Kawana, M., Yu, E.C. et al. (2016) Effects of hypertrophic and dilated cardiomyopathy mutations on power output by human β-cardiac myosin. *J. Exp. Biol.* **219**, 161–167, https://doi.org/10.1242/jeb.125930
39 Ghosh, A.K. and Vaughan, D.E. (2012) PAI-1 in tissue fibrosis. *J. Cell. Physiol.* **227**, 493–507, https://doi.org/10.1002/jcp.22783
40 Sawaki, D., Hou, L., Tomida, S., Sun, J., Zhan, H., Aizawa, K. et al. (2015) Modulation of cardiac fibrosis by Krüppel-like factor 6 through transcriptional control of thrombospondin 4 in cardiomyocytes. *Cardiovasc. Res.* **107**, 420–430, https://doi.org/10.1093/cvr/cvv155
41 Amirak, E., Fuller, S.J., Sugden, P.H. and Clerk, A. (2013) p90 ribosomal S6 kinases play a significant role in early gene regulation in the cardiomyocyte response to G(q)-protein-coupled receptor stimuli, endothelin-1 and α(1)-adrenergic receptor agonists. *Biochem. J.* **450**, 351–363, https://doi.org/10.1042/BJ20121371
42 Das, S., Zhang, E., Senapati, P., Amaram, V., Reddy, M.A., Stapleton, K. et al. (2018) A novel angiotensin II-induced long noncoding RNA Giver regulates oxidative stress, inflammation, and proliferation in vascular smooth muscle cells. *Circ. Res.* **123**, 1298–1312, https://doi.org/10.1161/CIRCRESAHA.118.313207
43 Tsuruda, T., Sekita-Hatakeyama, Y., Hao, Y., Sakamoto, S., Kurogi, S., Nakamura, M. et al. (2016) Angiotensin II stimulation of cardiac hypertrophy and functional decompensation in osteoprotegerin-deficient mice. *Hypertension* **67**, 848–856, https://doi.org/10.1161/HYPERTENSIONAHA.115.06689
44 Murdoch, C.E., Chaubey, S., Zeng, L., Yu, B., Ivetic, A., Walker, S.J. et al. (2014) Endothelial NADPH oxidase-2 promotes interstitial cardiac fibrosis and diastolic dysfunction through proinflammatory effects and endothelial-mesenchymal transition. *J. Am. Coll. Cardiol.* **63**, 2734–2741, https://doi.org/10.1016/j.jacc.2014.02.572
45 Frank, D., Kuhn, C., van Eickels, M., Gehring, D., Hanselmann, C., Lippl, S. et al. (2007) Calsarcin-1 protects against angiotensin-II induced cardiac hypertrophy. *Circulation* **116**, 2587–2596, https://doi.org/10.1161/CIRCULATIONAHA.107.711317
46 Sabater-Molina, M., Pérez-Sánchez, I., Hernández Del Rincón, J.P. and Gimeno, J.R. (2018) Genetics of hypertrophic cardiomyopathy: a review of current state. *Clin. Genet.* **93**, 3–14, https://doi.org/10.1111/cge.13027
47 Martín-Sánchez, P., Luengo, A., Griera, M., Orea, M.J., López-Olañeta, M., Chiloeches, A. et al. (2018) H-ras deletion protects against angiotensin II-induced arterial hypertension and cardiac remodeling through protein kinase G-Iβ pathway activation. *FASEB J.* **32**, 920–934, https://doi.org/10.1096/fj.201700134RRRR
48 Kasner, M., Westermann, D., Lopez, B., Gaub, R., Escher, F., Kühl, U. et al. (2011) Diastolic tissue Doppler indexes correlate with the degree of collagen expression and cross-linking in heart failure and normal ejection fraction. *J. Am. Coll. Cardiol.* **57**, 977–985, https://doi.org/10.1016/j.jacc.2010.10.024
49 López, B., Querejeta, R., González, A., Larman, M. and Díez, J. (2012) Collagen cross-linking but not collagen amount associates with elevated filling pressures in hypertensive patients with stage C heart failure: potential role of lysyl oxidase. *Hypertension* **60**, 677–683, https://doi.org/10.1161/HYPERTENSIONAHA.112.196113
50 Ravassa, S., López, B., Querejeta, R., Echegaray, K., San José, G., Moreno, M.U. et al. (2017) Phenotyping of myocardial fibrosis in hypertensive patients with heart failure. Influence on clinical outcome. *J. Hypertens.* **35**, 853–861, https://doi.org/10.1097/HJH.0000000000001258
51 Rodríguez, C., Rodríguez-Sinovas, A. and Martínez-González, J. (2008) Lysyl oxidase as a potential therapeutic target. *Drug News Perspect.* **21**, 218–224, https://doi.org/10.1358/dnp.2008.21.4.1213351
52 López, B., Querejeta, R, González, A., Beaumont, J., Larman, M. and Díez, J. (2009) Impact of treatment on myocardial lysyl oxidase expression and collagen cross-linking in patients with heart failure. *Hypertension* **53**, 236–242, https://doi.org/10.1161/HYPERTENSIONAHA.108.125278
53 González-Santamaría, J., Villalba, M., Busnadiego, O., López-Olañeta, M.M., Sandoval, P., Snabel, J. et al. (2016) Matrix cross-linking lysyl oxidases are induced in response to myocardial infarction and promote cardiac dysfunction. *Cardiovasc. Res.* **109**, 67–78, https://doi.org/10.1093/cvr/cvv214

© 2020 The Author(s). Published by Portland Press Limited on behalf of the Biochemical Society

Downloaded from http://portlandpress.com/clinsci/article-pdf/134/3/359/867300/cs-2019-1014.pdf by Universitat de Barcelona user on 09 November 2020

Clinical Science (2020) **134** 359–377
https://doi.org/10.1042/CS20191014

54 Stefanon, I., Valero-Muñoz, M., Fernandes, A.A., Ribeiro, Jr, R.F., Rodríguez, C., Miana, M. et al. (2013) Left and right ventricle late remodeling following myocardial infarction in rats. *PLoS ONE* **8**, e64986, https://doi.org/10.1371/journal.pone.0064986

55 Zhu, Y., Zhu, M.X., Zhang, X.D., Xu, X.E., Wu, Z.Y., Liao, L.D. et al. (2016) SMYD3 stimulates EZR and LOXL2 transcription to enhance proliferation, migration, and invasion in esophageal squamous cell carcinoma. *Hum. Pathol.* **52**, 153–163, https://doi.org/10.1016/j.humpath.2016.01.012

56 Kim, I.K., Lee, Y.S., Kim, H.S., Dong, S.M., Park, J.S. and Yoon, D.S. (2019) Specific protein 1(SP1) regulates the epithelial-mesenchymal transition via lysyl oxidase-like 2 (LOXL2) in pancreatic ductal adenocarcinoma. *Sci. Rep.* **9**, 5933, https://doi.org/10.1038/s41598-019-42501-6

57 Louhelainen, M., Merasto, S., Finckenberg, P., Vahtola, E., Kaheinen, P., Levijoki, J. et al. (2010) Effects of the calcium sensitizer OR-1896, a metabolite of levosimendan, on post-infarct heart failure and cardiac remodeling in diabetic Goto-Kakizaki rats. *Br. J. Pharmacol.* **160**, 142–152, https://doi.org/10.1111/j.1476-5381.2010.00680.x

Downloaded from http://portlandpress.com/clinsci/article-pdf/134/3/359/867300/cs-2019-1014.pdf by Universitat de Barcelona user on 09 November 2020

© 2020 The Author(s). Published by Portland Press Limited on behalf of the Biochemical Society

SUPLEMENTARY INFORMATION

Neuron-derived orphan receptor-1 modulates cardiac gene expression and exacerbates angiotensin II-induced cardiac hypertrophy

Laia Cañes[†], Ingrid Martí-Pàmies[†], Carme Ballester-Servera, Adela Herraiz-Martínez, Judith Alonso, María Galán, J Francisco Nistal, Pedro Muniesa, Jesús Osada, Leif Hove-Madsen, Cristina Rodríguez,* and José Martínez-González

[†] Both first authors contributed equally to this work.

*These authors contributed equally to this work.

Supplementary material

Neuron-derived orphan receptor-1 overexpression modulates cardiac remodelling and angiotensin II-induced cardiac hypertrophy

Laia Cañes[1,2,3,†], Ingrid Martí-Pàmies[1,2,3,†], Carme Ballester-Servera[1,3], Adela Herraiz-Martínez[1,3], Judith Alonso[1,2,3], María Galán[2,3,4], J Francisco Nistal[2,5], Pedro Muniesa[6,7], Jesús Osada[7,8], Leif Hove-Madsen[1,2,3], Cristina Rodríguez[2,3,4,*] and José Martínez-González[1,2,3,*]

[1]Instituto de Investigaciones Biomédicas de Barcelona (IIBB-CSIC), Barcelona, Spain.
[2]CIBER de Enfermedades Cardiovasculares, Instituto de Salud Carlos III, Madrid, Spain.
[3]Instituto de Investigación Biomédica Sant Pau (IIB-Sant Pau), Barcelona, Spain.
[4]Institut de Recerca Hospital de la Santa Creu i Sant Pau-Programa ICCC, Barcelona, Spain.
[5]Hospital Universitario Marqués de Valdecilla, IDIVAL, Universidad de Cantabria, Santander, Spain
[6]Facultad de Veterinaria, Universidad de Zaragoza, Spain.
[7]CIBER de Fisiopatología de la Obesidad y Nutrición, Instituto de Salud Carlos III, Madrid, Spain.
[8]Facultad de Veterinaria, Instituto de Investigación Sanitaria de Aragón-Universidad de Zaragoza, Spain.

[†] Both first authors contributed equally to this work.

[*]These authors contributed equally to this work. Correspondence should be addressed to C.R. Institut de Recerca Hospital de la Santa Creu i Sant Pau, C/Antoni Mª Claret, 08025 Barcelona, Spain (email: crodriguezs@csic-iccc.org) or J.M.-G. Instituto de Investigaciones Biomédicas de Barcelona (IIBB-CSIC), Rosselló, 161, 08036 Barcelona, Spain (email: jose.martinez@iibb.csic.es)

Supplementary Table S1. Echocardiographic LV parameters of 4- and 12-mo-old TgNOR-1 and WT mice

	WT 4 mo	WT 12 mo	TgNOR-1 4 mo	TgNOR-1 12 mo
n	11	11	11	11
BW (g)	30.50±0.87	41.21±1.15*	28.53±0.61	38.51±1.58*
LVEDd (mm)	3.67±0.07	3.78±0.08	3.59±0.09	3.93±0.06*
LVESd (mm)	2.53±0.83	2.63±0.12	2.40±0.14	2.68±0.08
IVSTd (mm)	0.86±0.03	1.02±0.05*	0.86±0.03	1.09±0.05*
AWTd (mm)	0.88±0.01	1.02±0.03*	0.89±0.03	1.03±0.04*
PWTd (mm)	0.84±0.03	0.86±0.04	0.84±0.02	0.97±0.02*†
LVED relative radius	2.23±0.08	2.21±0.15	2.20±0.12	2.06±0.09
rPWT	0.45±0.02	0.48±0.04	0.48±0.03	0.50±0.03
LVFS (%)	31.25±1.35	29.06±2.03	35.01±2.78	31.63±1.04
LVEF (%)	59.52±1.98	55.92±3.20	64.07±3.81	60.99±1.32
LV mass (mg)	87.81±2.24	112.0±2.57*	85.24±2.49	122.90±3.54*†
LV stroke volume (µL)	33.86±1.29	36.48±2.36	33.92±1.59	39.46±1.19
HR (bpm)	348±6	378±12	343±10	364±11
CO (mL/min)	12.51±0.82	11.75±1.47	11.69±0.71	14.16±0.64

AWTd: end-diastolic LV anterior wall thickness; BW: body weight; CO: cardiac output; HR: heart rate; IVSTd: LV end-diastolic interventricular septal thickness; LVEDd: LV end-diastolic dimension; LVEF: LV ejection fraction; LVESd: LV end-systolic dimension; LVFS: LV fractional shortening; Mo: month; PWTd: end-diastolic posterior wall thickness; rPWT: relative posterior wall thickness. Results are expressed as mean±SEM. $p < 0.05$: * *vs.* 4-mo-old (WT or TgNOR-1) mice; † *vs.* 12-mo-old WT mice.

Figure S1. Analysis by TLA of the transgene integration site in TgNOR-1 mice. (**A**) TLA sequence coverage across the mouse genome using a specific pair of primers for the transgene. The different chromosomes and the chromosomal position are indicated. Encircled in red is the region containing the transgene integration site. (**B**) TLA sequence coverage across the transgene integration locus on chromosome 7. Sequence coverage (in grey) generated with three different primer pairs is depicted.

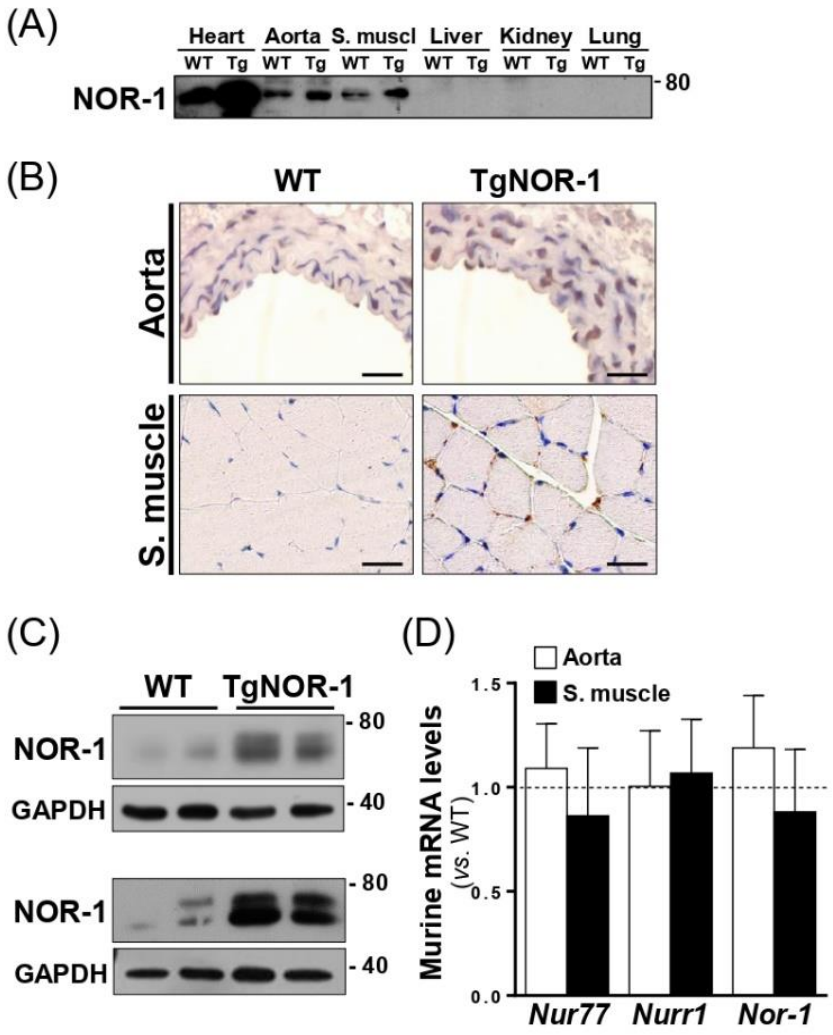

Figure S2. Overexpression of NOR-1 in TgNOR-1 mice. NOR-1 expression was analysed by Western blot (**A**) in different tissues from wild-type (WT) and TgNOR-1 mice. Immunohistochemistry (**B**) and Western blot (**C**) analysis for NOR-1 in aorta (upper panels) and skeletal muscle (S. muscle [quadriceps femoris muscle]; lower panels) from WT and TgNOR-1 mice were specifically assessed Scale bar: 25 µm. (**D**) Endogenous expression of *Nr4a* receptors (mouse receptors) in aorta (white bars) and skeletal muscle (S. muscle; black bars) from WT and TgNOR-1 mice. Data relative to levels in WT mice (indicated by a dotted line and normalized to 1) are expressed as mean±SEM (Aorta: n=10 (WT and TgNOR-1); Skeletal muscle: WT, n=11 and TgNOR-1, n=10).

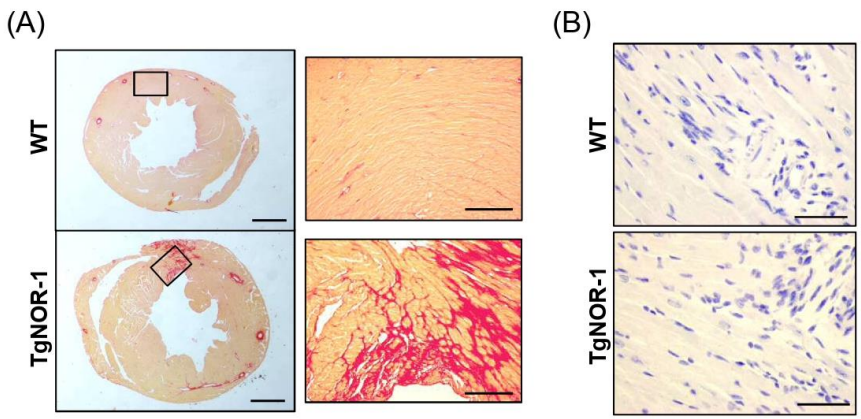

Figure S3. NOR-1 transgenesis exacerbates Angiotensin II-induced myocardial fibrosis. WT and TgNOR-1 (Tg) mice were infused with AngII (1000 ng/kg body weight/min) for 28 days. (**A**) Representative images of cardiac fibrosis assessed by picrosirius red stainning captured under brightfield (left panel; Scale bars: 1 mm). The indicated areas are shown at high magnification (right panel; Scale bars: 200 μm). (**B**) Negative controls corresponding to immunohistochemical analysis shown in Figure 5C, in which the primary antibody was omitted (Scale bars: 50 μm).

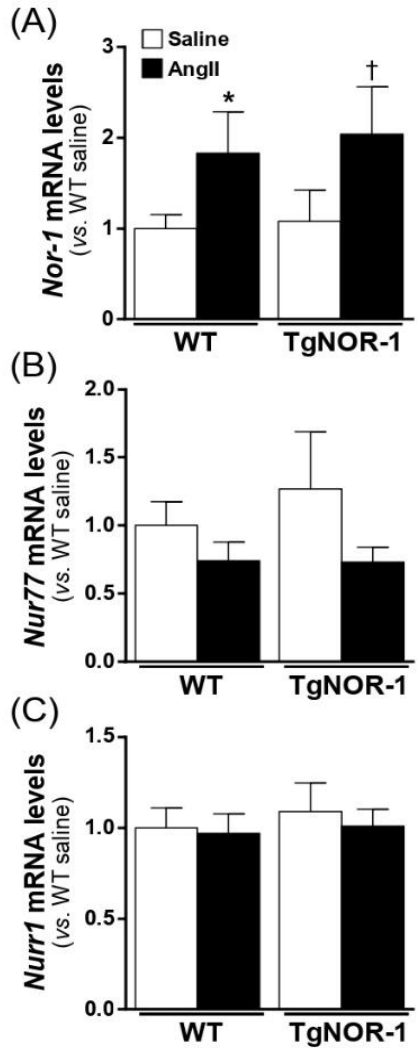

Figure S4. Angiotensin II infusion up-regulated the expression of mouse *Nor1*. WT and TgNOR-1 mice were infused with saline (white bars) or angiotensin II (AngII; black bars) for 4 weeks and the endogenous expression of *Nr4a* receptors was analyzed by real-time PCR: (**A**) mouse *Nor-1*, (**B**) mouse *Nur77* and (**C**) mouse *Nurr1*. Data (relative to levels in saline-infused WT animals) are expressed as mean±SEM (WT saline, n= 6; WT AngII, n= 8; Tg saline, n= 9; Tg AngII, n= 8). *P< 0.05 vs. Saline-infused WT mice, and †P< 0.05 vs. Saline-infused TgNOR-1.

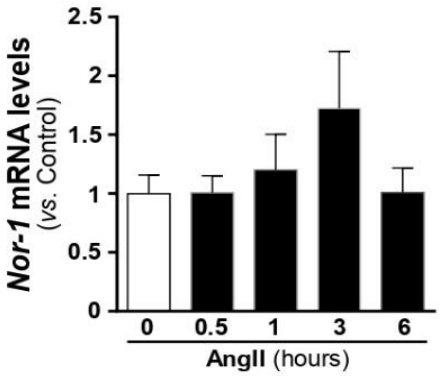

Figure S5. Angiotensin II does not modify *Nor-1* mRNA levels in cardiofibroblasts in culture. Cardiofibroblasts from wild-type mice were incubated during the indicated times with AngII (5 x 10^{-7} M) and *Nor-1* mRNA levels were analyzed by real-time PCR. Data are expressed as mean±SEM (n= 6).

ANEXO-1

Resultados: Figura A1, A2, A3 y Tabla A1.

El análisis comparativo de los niveles de proteína mostró que NOR-1 se expresa principalmente en miocardio, y que la transgénesis induce un marcado incremento de su expresión en este tejido (Figura A1). También se detectó expresión de NOR-1 en la aorta y el músculo esquelético de los animales control (WT) y la transgénesis también aumentó su expresión. Los niveles de NOR-1 en tejidos no musculares como el hígado, riñón y pulmón fueron indetectables en nuestras condiciones experimentales.

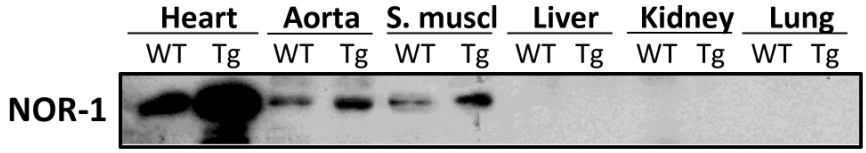

Figura A1. Niveles de proteína NOR-1 en diferentes tejidos de ratones *wild-type* (WT) y TgNOR-1. Se realizó un análisis por *Western blot* a partir de lisados de proteínas de cada tejido. La carga proteica fue de 10 µg por carril. (*S. muscl*: *skeletal muscle*).

El análisis de la expresión génica en el miocardio de ratones control (WT) y ratones transgénicos para NOR-1 (TgNOR-1), evidenció que estos últimos presentan un ligero incremento en la expresión de genes implicados en la homeostasis del calcio como *Serca2a* y *Casq2* (*Calsequestrin 2*) con respecto a los controles (WT) (Figura A2). Asimismo, la transgénesis de NOR-1 aumentó el estrés oxidativo en el miocardio, lo que se evidenció por el aumento de la tinción con DHE. Este fenómeno se asoció con un mayor nivel de oxidación de la CaMKII (*Calcium/calmodulin-dependent protein kinase II*) en el miocardio de ratones TgNOR-1 con respecto a los WT (Figura A3).

También hemos analizado la respuesta de los animales transgénicos a la hipertrofia inducida por el agonista β-adrenérgico isoproterenol. Los análisis ecocardiográficos mostraron que en los ratones TgNOR-1 la infusión con isoproterenol aumentó significativamente el PWT, el rPWT y el IVST respecto a ratones control infundidos con ISO (Tabla A1). Este aumento, sin embargo, no se reflejó en la masa del ventrículo izquierdo, que solo aumentó respecto a los ratones infundidos con solución salina. Análogamente, en los parámetros cardíacos indicativos de la función sistólica como la LVFS y LVEF sólo se observaron diferencias respecto a los animales control, pero no en los animales WT y TgNOR-1, probablemente porque el estímulo hipertrófico de isoproterenol es tan potente que no permite apreciar modulación por la transgénesis de NOR-1 (algo que si se observó en la infusión con AngII).

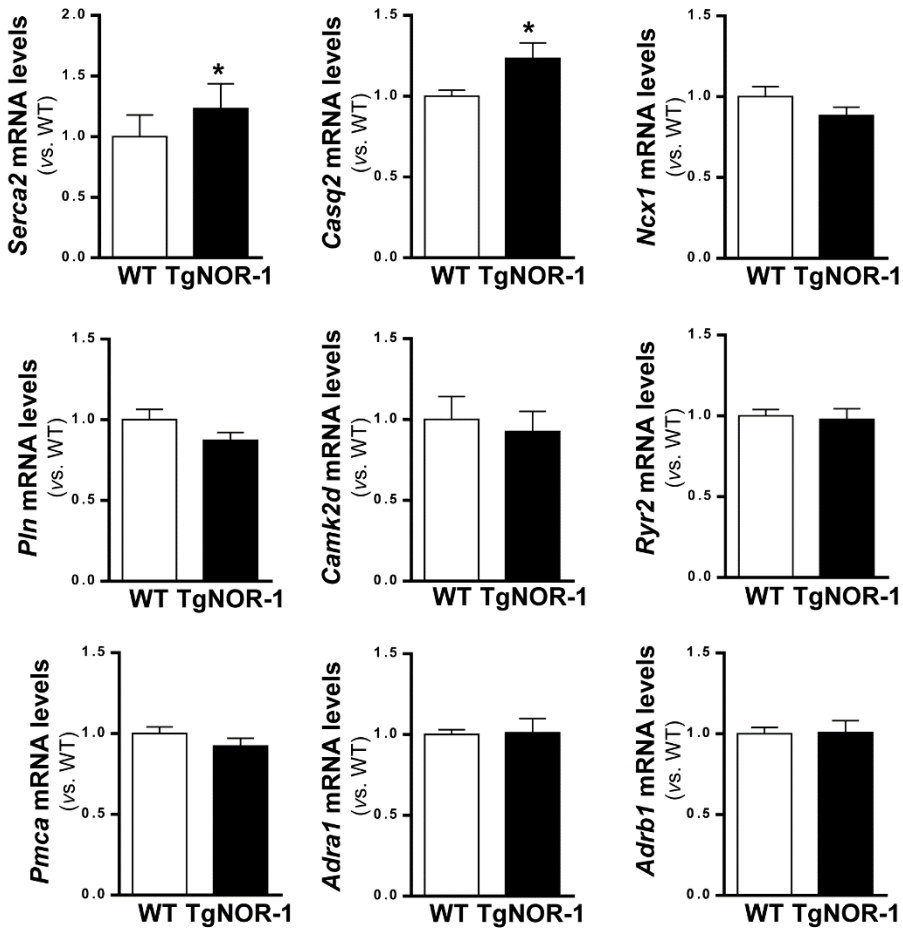

Figura A2. Expresión de genes implicados en la homeostasis del calcio en ratones *wild-type* (WT) y TgNOR-1. Los niveles de RNA mensajero de *Serca2a*, *Casq2*, *Ncx1*, *Pln*, *Camk2d*, *Ryr1*, *Pmca1*, *Adra1* y *Adrab1* se analizaron mediante PCR a tiempo real en corazones de ratones WT y TgNOR-1. Los valores se expresan como media ± SEM (WT, n=16 y TgNOR-1, n= 11). *P<0.05: *, *vs.* WT. Mann-Whitney. *Serca2* (*Sarco/endoplasmic reticulum* Ca^{2+} *ATPase*), *Casq2* (*Calsequestrin 2*), *Ncx1* (*Sodium/Calcium exchanger protein*), *Pln* (*Phospholamban*), *Camk2d* (*Calcium/calmodulin-dependent protein kinase II delta*), *Ryr2* (*Ryanodine receptor 2*), *Pmca1* Ca^{2+} (*Transporting, plasma membrane 1*), *Adra1* (*Adrenergic receptor alpha 1*) y *Adrb1* (*Adrenergic receptor beta 1*).

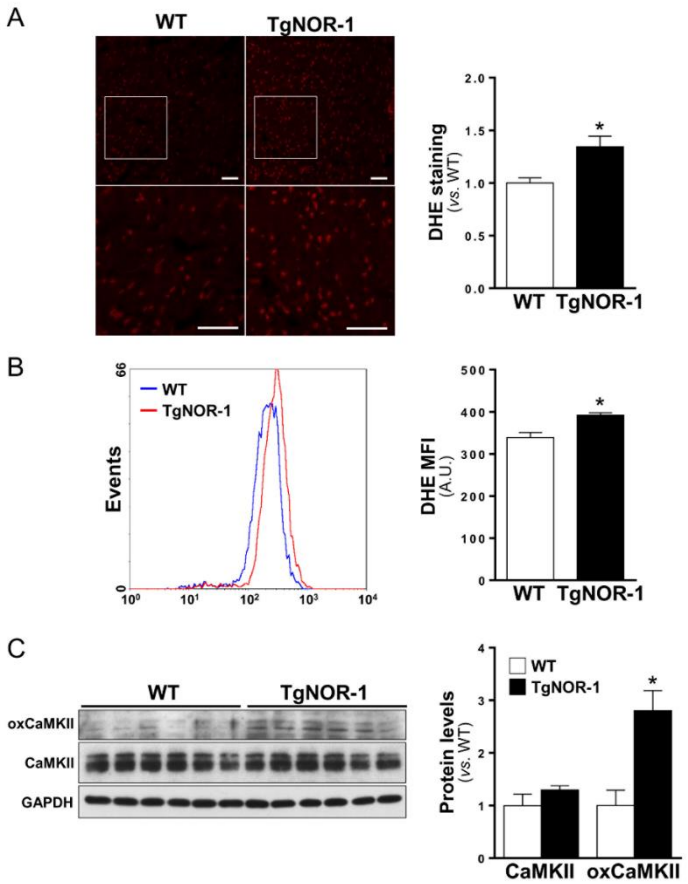

Figura A3. La transgénesis de NOR-1 exacerba el estrés oxidativo en el miocardio. A). El estrés oxidativo se analizó mediante la tinción de dihidroetidio (DHE) (en rojo) en secciones transversales de miocardios de los ratones *wild-type* (WT) y TgNOR-1. Imágenes representativas de microscopia de confocal para la tinción de DHE (Paneles superiores, barra de 50 µm). Las imágenes inferiores muestran un zoom de la imagen superior (Barra 150 µm). El gráfico muestra la cuantificación de la tinción DHE mediante el *software* ImageJ. Los valores se expresan como media ± SEM (n= 8). **P*<0.001; *, *vs.* ratones WT. **B)** El estrés oxidativo se analizó también en cardiofibroblastos de animales WT y TgNOR-1 en cultivo marcados con DHE mediante citometría de flujo. El gráfico muestra la intensisdad media de fluorescencia para el DHE. Los valores se expresan como media ± SEM (n= 6). *P<0.01; *, *vs.* Ratones WT. **C)** Los niveles de proteína de CaMKII y de su forma oxidada CaMKII (oxCaMKII) fueron analizados mediante *Western blot* en extractos de proteínas de corazones de ratones WT y TgNOR-1. Se muestra imagen representativa. El tamaño de las proteínas se estimó mediante la posición del marcador de peso molecular (en kDa). Los niveles de gliceraldheído-3-fosfato deshidrogenasa (GAPDH) se muestran como controles de carga. El gráfico muestra la cuantificación proteica mediante el *software*

ImageLab 6 de la CaMKII y su forma oxidada, ambas normalizadas por la GAPDH. Los valores se expresan como media ± SEM (n= 6). *P<0.01; *, *vs.* Ratones WT.Mann-Whitney (A). Two-way ANOVA (B).

Tabla A1. Parámetros ecocardiográficos del ventrículo izquierdo de animales *wild-type* (WT) y TgNOR-1 tras la infusión con solución salina o isoproterenol (ISO).

	WT			**TgNOR-1**		
	Saline	ISO (1 weeks)	ISO (2 weeks)	Saline	ISO (1 weeks)	ISO (2 weeks)
n	8	8	8	10	9	10
BW (g)	29.3±0.2	30.0±0.4	30.8±0.3	30.6±0.5	30.6±0.5	31.4±0.6
LVEDd (mm)	3.69±0.06	3.69±0.18	3.90±0.11	3.98±0.1	3.76±0.18	1.30±0.07†
LVESd (mm)	2.81±0.1	2.27±0.21	2.61±0.11	3.02±0.12	2.39±0.21†	2.28±0.29†
IVSTd (mm)	0.89±0.03	1.20±0.03*	1.13±0.04*	0.93±0.04	1.41±0.07*,†,‡	1.33±0.07*,†,‡
AWTd (mm)	0.94±0.03	1.28±0.05*	1.16±0.03*	0.94±0.04	1.42±0.08*,†	1.30±0.07*,†,§
PWTd (mm)	0.84±0.03	1.14±0.08*	1.08±0.04*	0.81±0.03	1.06±0.06*,†	1.31±0.11*,†,‡,§
LVED relative radius	2.22±0.06	1.69±0.18*	1.83±0.11	2.49±0.10	1.84±0.16†	1.47±0.17*,†
rPWT	0.45±0.01	0.64±0.07*	0.56±0.03	0.41±0.02	0.58±0.06†	0.78±0.10*,†,‡,§
LVFS (%)	23.88±2.31	39.28±3.65*	33.05±1.54	24.22±1.47	37.39±2.88*,†	38.31±4.85*,†
LVEF (%)	47.89±3.83	69.31±4.33*	62.04±2.24*	48.48±2.50	67.26±3.62*,†	66.52±6.01*,†
LV mass (mg)	95.54±4.63	149.8±6.34*	144.8±7.21*	105.3±4.75	159.1±7.75*,†	167.1±12.87*,†
LV stroke volume (µL)	27.75±2.65	39.96±4.13*	40.86±2.54*	33.24±1.89	36.11±4.71	33.57±2.70
HR (bpm)	349±8	552±18*	502±11*	354±11	563±20*,†	534±12*,†
CO (mL/min)	9.70±1.00	21.96±2.39*	20.56±1.52*	11.71±0.66	20.10±2.53*,†	17.81±1.31*,†

Se implantaron minibombas osmóticas subcutáneamente (modelo 2002, Alzet) para la liberación de ISO (15 mg/kg/day, 14 días) en los animales transgénicos de NOR1 y en los controles. Para estudiar la evolución de la hipertrofia cardíaca se monitorizaron los animales a 7 y 14 días mediante ecografía *Doppler* transtorácica usando un equipo de ultrasonidos acoplado a un transductor de 30 MHz (*Vevo2100 Imaging systems*) y *software* de análisis específico. Los valores se expresan como media ± SEM. *P*<0.05: *, *vs.* ratones WT infundidos con solución salina (Saline). †, *vs.* ratones TgNOR-1 infundidos con solución salina. ‡, *vs.* ratones WT infundidos con ISO al mismo tiempo. §, vs. ratones TgNOR1 infundidos con ISO a 1 semana. Two-way ANOVA. LV: *left ventricle*; BW: *body weight;* HR: heart rate; CO: *cardiac output*; AWTd: *end-diastolic LV anterior wall thickness*; IVSTd*: LV end-diastolic interventricular septal thickness*; LVEDd: *LV end-diastolic dimension*; LVEF: *LV ejection fraction*; LVESd: *LV end-systolic dimension*; LVFS: *LV fractional shortening*; PWTd: *end- diastolic posterior wall thickness*; rPWT: *relative posterior wall thickness*.

PUBLICACIÓN 2

High neuron derived orphan receptor-1 (NOR-1) expression strengthens the vascular wall response to angiotensin II leading to aneurysm formation in mice

Laia Cañes†, Ingrid Martí-Pàmies†, Carme Ballester-Servera, Judith Alonso, Elena Serrano, Cristina Rodríguez,* and José Martínez-González*

† Both first authors contributed equally to this work.

*These authors contributed equally to this work.

***Hypertension*, Volume 77, February 2021. *In press*.**

Introducción y objetivos: El AAA es una enfermedad cardiovascular degenerativa caracterizada por una dilatación gradual e irreversible de la aorta abdominal. La ruptura del AAA es la consecuencia más grave de esta patología, y se asocia con una tasa de mortalidad entre el 80-90% (Weintraub, 2009). En la actualidad, el único tratamiento eficaz es la intervención quirúrgica de los AAA que presentan un alto riesgo de ruptura, aquellos con diámetros superiores a 5 y 5.5 cm en mujeres y hombres respectivamente. Desgraciadamente, hasta el momento las estrategias farmacológicas para limitar el desarrollo o promover la regresión del AAA, analizados, como las estatinas, antihipertensivos y antiagregantes plaquetarios, no han demostrado su efectividad en estudios clínicos.

El AAA es un proceso multifactorial que se caracteriza por la apoptosis de las CMLV, la destrucción de la MEC y la inflamación crónica (Dale *et al*., 2015). A pesar del avance considerable en el estudio del desarrollo de esta patología, tan solo se conocen parcialmente los mecanismos moleculares responsables del inicio y progresión del AAA (Zhang *et al*., 2016). El receptor NOR-1 es un factor de transcripción que se ha relacionado con procesos inflamatorios (Nomiyama *et al*., 2009, Zhao *et al*., 2010, Rodríguez-Calvo *et al*., 2013), el estrés oxidativo (Alonso *et al*., 2018) y el remodelado celular y extracelular (Martínez-González *et al*., 2003, Alonso *et al*., 2016, Martí-Pàmies *et al*., 2017). Cabe destacar que se ha observado una mayor expresión de NOR-1 en AAA humanos (Alonso *et al*., 2016). Sin embargo, actualmente se desconoce si este receptor contribuye activamente al desarrollo del aneurisma. Por ello, nuestro objetivo es establecer las consecuencias de la sobreexpresión de NOR-1 en la pared vascular sobre el desarrollo del AAA inducido por AngII. Los estudios se desarrollaron en dos modelos de ratones transgénicos (TgNOR1 y TgNOR-1^{CMLV}) con una fuerte expresión de NOR-1 en la aorta.

Resultados: Nuestros estudios en el modelo de ratón que sobrexpresa NOR-1 humano (hNOR-1) preferentemente a nivel cardiovascular (TgNOR-1), revelaron un incremento gradual en el diámetro de la aorta en respuesta a la infusión de AngII durante 4 semanas. Concretamente un 50% de los animales transgénicos desarrollaron AAA frente al 10% de animales WT. Con el objetivo de estudiar con más detalle la implicación de NOR-1 en el AAA, nuestro grupo ha desarrollado un ratón transgénico en el que el transgen humano de NOR-1 se encuentra bajo el control del promotor mínimo del gen SM22α, que dirige la expresión específicamente a células musculares (TgNOR-1^{CMLV}). Los dos modelos trangénicos presentan una expresión aórtica similar del transgen humano. Al infundir AngII durante 4 semanas los animales TgNOR-1^{CMLV} mostraron un mayor incremento del diámetro que los TgNOR-1, aunque ambos modelos presentaron una incidencia y gravedad del AAA similar. El aumento de presión arterial en respuesta a AngII fue comparable en ambos modelos.

Los análisis de expresión por PCR a tiempo real revelaron un mayor incremento del nivel de mRNA de marcadores inflamatorios (EMR-1) y mediadores proinflamatorios (MCP-1 y CXCL2) en ambos modelos transgénicos tras la infusión de AngII respecto al detectado en ratones control. Asimismo, en los análisis inmunohistoquímicos los ratones transgénicos infundidos con AngII mostraron un mayor infiltrado de macrófagos. La transgénesis de NOR-1 agravó el remodelado destructivo de la pared vascular inducido por la AngII. De hecho, en la tinción de orceína se observó un mayor número de roturas de las fibras elásticas en las aortas de los ratones transgénicos de NOR-1 respecto a los animales WT. Estos resultados indican que la sobreexpresión de NOR-1 promueve la formación de AAA en respuesta a AngII. Puesto que ambos modelos presentan una susceptibilidad al AAA similar, los siguientes estudios se realizaron exclusivamente en el modelo TgNOR-1^{CMLV}.

La degradación de la MEC inducida por la infusión de AngII en los ratones TgNOR-1^{CMLV} se asoció con un mayor incremento en la expresión de MMP-2 que el detectado en los ratones WT, y con un mayor aumento de la actividad gelatinasa evaluada mediante zimografía. También, la transgénesis de NOR-1 promovió una mayor producción de ROS en respuesta a AngII que en los animales control.

La doxiciclina, es un inhibidor de metaloproteinasas, que previene la formación del aneurisma en modelos experimentales. En este contexto estudiamos qué efecto tendría la doxiciclina sobre el desarrollo del AAA inducido por AngII en los ratones TgNOR-1^{CMLV}. La doxiciclina atenuó el desarrollo del AAA en estos animales, un efecto significativo a los 14 días de infusión de AngII y administración simultánea de doxiciclina. Además, redujo la incidencia y gravedad del aneurisma a niveles similares a los de los ratones control. Este fármaco previno el remodelado inducido por la AngII en los ratones TgNOR-1^{CMLV} y preservó la integridad de las fibras elásticas. Asimismo, en los ratones tratados con doxiciclina se observó una menor inducción de la expresión de la MMP-2 y de marcadores inflamatorios (EMR-1, MCP-1, IL6, IL1β y CXCL2). Los estudios inmunohistoquímicos para macrófagos (MAC3), linfocitos (CD3) y neutrófilos (ELANE) revelaron que la doxiciclina atenuó la acumulación de células inflamatorias en la pared aortica y disminuyó la expresión vascular de MCP-1 en respuesta a la AngII en los ratones TgNOR-1^{CMLV}. Estos resultados indican que la doxiciclina es capaz de inhibir el proceso aneurismático inducido por la AngII en el modelo de ratón TgNOR-1^{CMLV}.

Por último, el análisis de expresión génica a gran escala mediante *microarray* y el posterior análisis de vías de transducción de señales y procesos biológicos regulados diferencialmente (GSEA, *Gene Set Enrichment Analysis*) revelaron que la transgénesis de NOR-1 regula genes y procesos biológicos,

alguno de ellos previamente vinculados al desarrollo de la patología humana y a la formación de aneurismas en modelos animales. Entre ellos los implicados en inflamación, ciclo celular y citoesqueleto, pero también procesos biológicos relacionados con la diferenciación de la célula muscular y la activación del sistema nervioso simpático.

Conclusiones: Nuestro estudio demuestra por primera vez la contribución de NOR-1 al desarrollo del AAA, y determina la utilidad del modelo animal TgNOR-1^{CMLV} para futuros estudios pre-clínicos de nuevos fármacos para tratar esta enfermedad.

LWW | December9,20202:39AM | 4 Color Fig(s): F1-5 | Art:HYP16078

Journal Article

Hypertension

ORIGINAL ARTICLE

High NOR-1 (Neuron-Derived Orphan Receptor 1) Expression Strengthens the Vascular Wall Response to Angiotensin II Leading to Aneurysm Formation in Mice

Laia Cañes,* Ingrid Martí-Pàmies,* Carme Ballester-Servera, Judith Alonso, Elena Serrano, Ana M. Briones, Cristina Rodríguez,† José Martínez-González†

ABSTRACT: No drug therapy has shown to limit abdominal aortic aneurysm (AAA) growth or rupture, and the understanding of the disease biology is incomplete; whereby, one challenge of vascular medicine is the development of good animal models and therapies for this life-threatening condition. The nuclear receptor NOR-1 (neuron-derived orphan receptor 1) controls biological processes involved in AAA; however, whether it plays a role in this pathology is unknown. Through a gain-of-function approach we assessed the impact of NOR-1 expression on the vascular response to Ang II (angiotensin II). We used 2 mouse models that overexpress human NOR-1 in the vasculature, one of them specifically in vascular smooth muscle cells. NOR-1 transgenesis amplifies the response to Ang II, enhancing vascular inflammation (production of proinflammatory cytokines, chemokines, and reactive oxygen species), increasing MMP (matrix metalloproteinase) activity and disturbing elastin integrity, thereby broking the resistance of C57BL/6 mice to Ang II-induced AAA. Genes encoding for proteins critically involved in AAA formation (*Il-6*, *Il-1β*, *Cxcl2*, *Mcp-1*, and *Mmp2*) were upregulated in aneurysmal tissues. Both animal models show a similar incidence and severity of AAA, suggesting that high expression of NOR-1 in vascular smooth muscle cell is a sufficient condition to strengthen the response to Ang II. These alterations, including AAA formation, were prevented by the MMP inhibitor doxycycline. Microarray analysis identified gene sets that could explain the susceptibility of transgenic animals to Ang II-induced aneurysms, including those related with extracellular matrix remodeling, inflammatory/immune response, sympathetic activity, and vascular smooth muscle cell differentiation. These results involve NOR-1 in AAA and validate mice overexpressing this receptor as useful experimental models. **(*Hypertension*. 2020;77:00-00. DOI: 10.1161/HYPERTENSIONAHA.120.16078.)** • **Data Supplement**

Key Words: cytokines ■ dilation ■ doxycycline ■ elastin ■ prevalence

Abdominal aortic aneurysm (AAA) is a common and life-threatening condition whose prevalence in men aged 65 to 80 years ranges from 4% to 8%.[1] AAA consists of a localized and permanent dilatation of the abdominal aorta that exceeds the normal diameter by 50% (or >3 cm). Aneurysms tend to expand with time and the risk of rupture increases as aortic diameter grows. Aortic rupture accounts for 1% to 2% of all deaths. AAAs cause >16 000 deaths and 33 000 repairing procedures to prevent future aneurysm ruptures each year in the United States.[2] Despite the high morbidity and mortality associated with this pathology, there is no medical treatment to slow down aneurysm expansion or prevent rupture. Therefore, a better understanding of the cellular and

Correspondence to: Cristina Rodríguez, IRHSCSP, C/Antoni Mª Claret, 08025 Barcelona, Spain, Email crodriguezs@csic-iccc.org or José Martínez-González, IIBB, Rosselló, 161, 08036 Barcelona, Spain, Email jose.martinez@iibb.csic.es
*These authors contributed equally to this work.
†These authors contributed equally to this work.
The Data Supplement is available with this article at https://www.ahajournals.org/doi/suppl/10.1161/HYPERTENSIONAHA.120.16078.
For Sources of Funding and Disclosures, see page XXX.
© 2020 American Heart Association, Inc.
Hypertension is available at www.ahajournals.org/journal/hyp

<zjs;Original Article> • <zjss;10012,10014,10041,10054> • <zdoi;10.1161/HYPERTENSIONAHA.120.16078>

LWW	December9,20202:39AM	4 Color Fig(s): F1-5	Art:HYP16078

ORIGINAL ARTICLE

Novelty and Significance

What Is New?

- We have previously demonstrated that the nuclear receptor NOR-1 (neuron-derived orphan receptor 1) plays a pivotal role in vascular remodeling and function, while being upregulated in human abdominal aortic aneurysm; however, the contribution of NOR-1 to this disease was not previously addressed.
- We assessed the susceptibility of 2 transgenic mouse models overexpressing NOR-1 in the vascular wall to Ang II (angiotensin II)-induced aneurysms.

What Is Relevant?

- Our study evidences the critical contribution of NOR-1 to the pathophysiology of abdominal aortic aneurysm.
- NOR-1 exacerbates Ang II-induced inflammation, MMP (matrix metalloproteinase) activity, elastin disruption, and reactive oxygen species production and thoroughly alters vascular gene expression.
- NOR-1 transgenic mice recapitulate key aspects of human abdominal aortic aneurysm and have been validated as novel preclinical models for this disease.

Summary

Our study confirms NOR-1 as a relevant transcription factor in vascular biology whose upregulation positively contributes to aneurysm formation and shows the potential usefulness of mice overexpressing this nuclear receptor either as new animal models to deepen the investigation of pathological mechanisms of the disease, or as tools to address pharmacological preclinical studies.

Nonstandard Abbreviation and Acronyms

AAA	abdominal aortic aneurysm
Ang II	angiotensin II
DEG	differential expressed gene
hNOR-1	human NOR-1
LDLR$^{-/-}$	low-density lipoprotein receptor-deficient
NOR-1	neuron-derived orphan receptor 1
NR4A	nuclear receptor subfamily 4 group A
N-TA(3)CT	Non-Invasive Treatment of Abdominal Aortic Aneurysm Clinical Trial
VSMC	vascular smooth muscle cells
WT	wild type

molecular processes involved in the onset, and progression of aneurysms is required for the development and implementation of effective therapies.

The destructive remodeling of connective tissue in AAA involves several interrelated mechanisms including excessive inflammation, characterized by elevated production of proinflammatory cytokines, chemokines, and reactive oxygen species; local upregulation of matrix-degrading proteinases; progressive destruction of structural matrix proteins, particularly elastin, and compensatory collagen deposition; and depletion of medial vascular smooth muscle cells (VSMC). Studies of human aortic tissues and experimental approaches in animal models have allowed to elucidate these mechanisms.[3] New animal models that recapitulate key aspects of the disease could be instrumental to further progress in the understanding of AAA pathophysiology and as preclinical models for screening therapeutic agents.

NOR-1 (neuron-derived orphan receptor 1) is a transcription factor belonging to the NR4A (nuclear receptor subfamily 4 group A).[4] NOR-1 (NR4A3) as well as Nur77 (NR4A1) and Nurr1 (NR4A2) seem to be constitutively active nuclear receptors whose transcriptional activity depends mainly on their expression levels. These receptors play a key role in an array of tissues and have been associated with a variety of high-incidence human pathologies including coronary artery disease, diabetes, obesity, and cancer.[4–7] In vascular tissues, NOR-1 is expressed at low levels, but it is induced by multiple cues and modulates genes involved in inflammation, oxidative stress, and cellular and extracellular matrix remodeling.[8–13] Although these mechanisms operate in AAA, and NOR-1 is upregulated in human AAA,[14] no studies have assessed whether vascular NOR-1 plays an active role in this pathology. In this study, we use 2 transgenic mouse models that overexpress NOR-1 in the vascular wall to assess the effect of a gain-of-function of this receptor on Ang II (angiotensin II)-induced AAA. Our results involve NOR-1 in the development of AAA and show the usefulness of mice overexpressing this nuclear receptor as new experimental models of aneurysmal disease.

MATERIALS AND METHODS

A detailed Methods section is provided in the Data Supplement. The data that support the findings of this study are available from the corresponding author upon reasonable request.

Animal Handling

Two mouse models that overexpress the hNOR-1 (human NOR-1) cDNA in the vascular wall (TgNOR-1 and TgNOR-1^{VSMC}) in a C57BL/6J genetic background were used.[11,15] Ang II (1000 ng/kg body weight/min; Sigma-Aldrich) or saline solution were

LWW	December9,20202:39AM	4 Color Fig(s): F1-5	Art:HYP16078

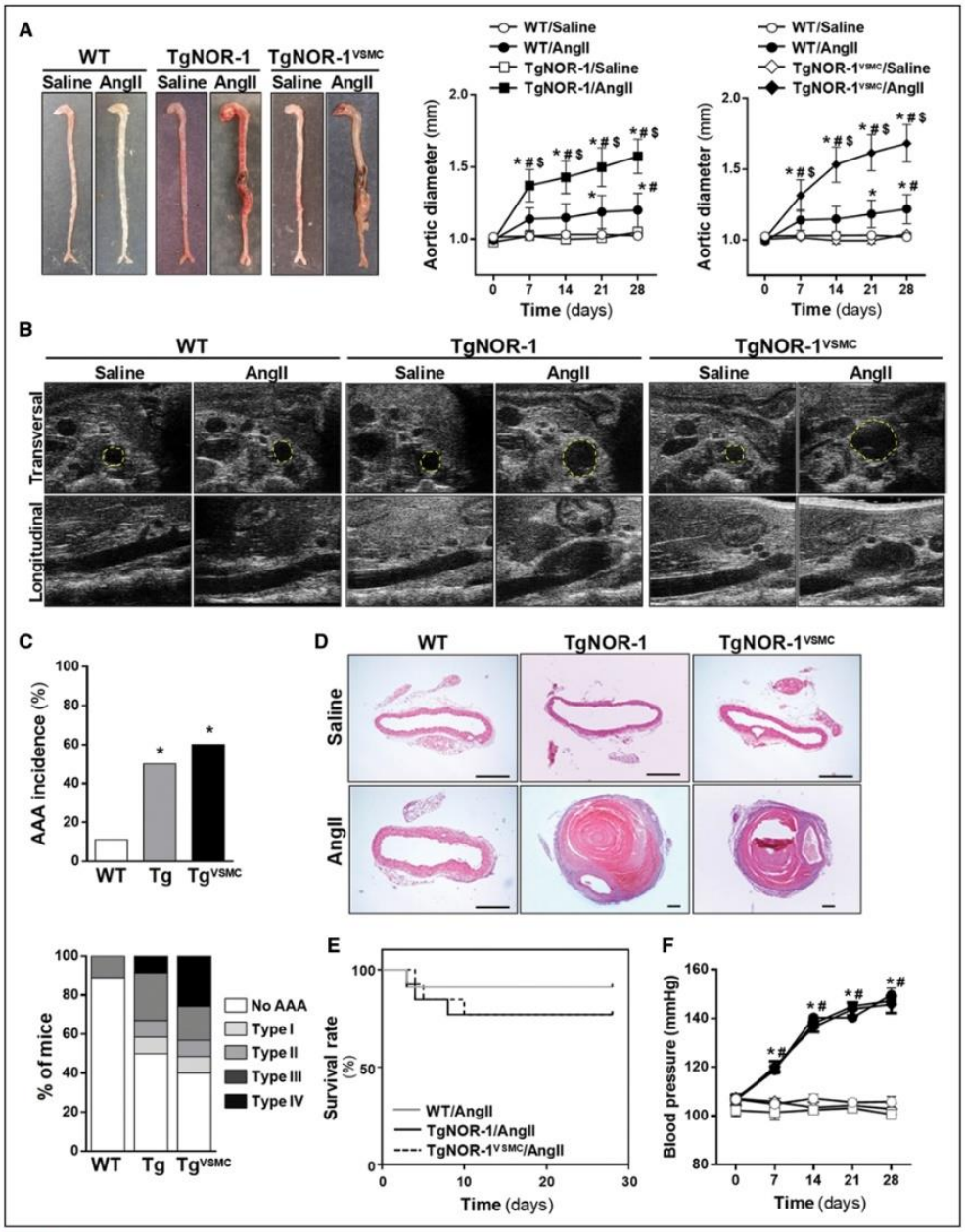

Figure 1. NOR-1 (neuron-derived orphan receptor 1) transgenesis promotes Ang II (angiotensin II)-induced abdominal aortic aneurysm (AAA) formation.

Wild-type (WT), TgNOR-1 (Tg) and TgNOR-1^{VSMC} (Tg^{VSMC}) mice were infused with Ang II (1000 ng/kg per minute; filled symbols) or saline solution (open symbols) for 28 days. **A**, **Left**, macroscopic characteristics of excised aortas. **Middle** and **right**, assessment of abdominal aortic diameter by ultrasonography. Data are mean±SEM (n=10). $P<0.05$; *versus t=0 for each experimental condition; (*Continued*)

LWW | December9,20202:39AM | 4 Color Fig(s): F1-5 | Art:HYP16078

infused to transgenic or wild-type (WT) mice via osmotic minipumps (model 1004, Alzet; Durect Corporation) for 28 days.[16]

Microarray Gene Expression Analysis

Differential gene expression analysis was performed in aorta from Ang II–infused TgNOR-1^{VSMC} and WT mice using microarrays according to the Two-Color Microarray-Based expression Analysis v. 6.5 protocol (Agilent Technologies) using 4 SurePrint G3 mouse Gene Expression Microarrays (Agilent Technologies, Design ID 028005, Catalog No. G4852A). Data was handled and processed using the R package EMA and the Bioconductor packages Limma, marray and pcaMethods in R.[17] Background correction was performed using the normexp method (offset=10).[18] Gene Set Enrichment Analysis was performed using Gene Set Enrichment Analysis Desktop v4.0.3 software (Broad Institute). The Benjamini-Hochberg False Discovery Rate *q* value ≤0.05 was used to define significantly enriched gene sets. Probes and primers used to validate selected differential expressed genes (DEGs) are shown in Table S1 in the Data Supplement.

Statistical Analysis

Results are shown as mean±SEM. Significant differences were analyzed using 1-way ANOVA, 2-way ANOVA or 2-way ANOVA with repeated measures and the Tukey tests. When normality failed, the Kruskal-Wallis and Dunn test was applied. Differences in AAA incidence were analyzed by the χ^2 test. Data were analyzed with the GraphPad Prism version 6.01. Differences were considered significant at $P<0.05$.

RESULTS

Overexpression of NOR-1 Predisposes to Aortic Aneurysm

We assessed the impact of Ang II infusion on AAA formation in a transgenic mouse model that overexpresses hNOR-1 in vascular tissues (TgNOR-1).[15] Four weeks after Ang II infusion, a notable aortic bulging was evident in TgNOR-1 mice (Figure 1A left panel). Echocardiography revealed that Ang II progressively increased the diameter of the abdominal aorta from week 1 to 4. This increase was significantly larger in TgNOR-1 mice than in WT animals (Figure 1A [left graph] and Figure 1B [left and middle panels]). Approximately 50% of TgNOR-1 mice developed aneurysms (diameter >1.5 mm) compared with only 10% in the WT group (Figure 1C, upper graph). NOR-1 transgenesis provoked the formation of severe aneurysms (Figure 1C, lower graph) with intramural hematomas (left panel in Figure 1A and middle panels in Figure 1D).

To gain more insight into the cellular elements responsible for the enhanced susceptibility to AAA of NOR-1 transgenic mice, Ang II was infused in a mouse model that specifically overexpresses hNOR-1 in SMC (TgNOR-1^{VSMC})[11] and shows similar aortic hNOR-1 expression levels than TgNOR-1 (Figure S1). TgNOR-1^{VSMC} challenged with Ang II experienced a marked and progressive enlargement of suprarenal abdominal aorta diameter, comparable to that found in TgNOR-1 mice (right panels in Figure 1A, 1B, and 1D). The aneurysms were heterogeneous in shape and showed dilated lumen and increased outer aortic area (Figure S2A). In the most severe forms, NOR-1 transgenesis provoked the formation of large size aneurysms with an important adventitial remodeling and intramural hematomas (Figure S2B). Occasionally, the organized thrombus was partially exposed to the lumen at the points where the aorta breaks down, and a false channel into the hematoma was sometimes observed (Figure S2B). Both NOR-1 transgenic mouse models show a similar incidence (60% versus 50% in TgNOR-1^{VSMC} and TgNOR-1, respectively) and severity of AAA (Figure 1C). Ang II infusion led to an early death of around 20% of transgenic mice and 10% of WT animals without significant differences between them (Figure 1E). Deaths were mainly due to abdominal aortic rupture (exceptionally, one animal died due to rupture of the aortic arch). A comparable increase in blood pressure in response to Ang II was detected in all experimental groups (Figure 1F). Further, NOR-1 transgenesis did not significantly affect body weight neither in Ang II– nor in saline-infused mice (Table S2). The organ expression pattern of hNOR-1 in transgenic mice was similar to that previously described[11,15] and was not affected by Ang II (data not shown). Finally, Ang II did not affect plasma levels of aspartate and alanine transaminases, which also remained unaltered in transgenic mice (Figure S3A and S3B). Likewise, circulating creatinine and blood urea nitrogen levels in transgenic mice were similar to those detected in WT animals (Figure S3C and S3D). Ang II similarly induced a slight increase in blood urea nitrogen in WT and transgenic mice.

Enhanced Vascular Degeneration and Inflammation in NOR-1 Transgenic Mice in Response to Ang II

Orcein staining showed that Ang II infusion elicited higher disruption of elastin fibers in NOR-1 transgenic

Figure 1 Continued. #versus the same type of animal infused with saline solution at the same time; $versus Ang II–infused WT mice at the same time. **B**, Representative ultrasound images at the end of the experimental procedure. Aortic diameter is traced with a yellow line. Transverse and longitudinal images are shown. **C**, Incidence (**upper**) and severity (**lower**; based on Manning scale)[19] of AAA in Ang II–infused groups. $P<0.05$; *versus Ang II–infused WT mice (n=10). **D**, Hematoxylin-eosin staining of abdominal aortic sections (bars: 250 µm). **E**, Graph showing the survival rate from Ang II–infused groups (Ang II–infused WT, n=11; Ang II–infused TgNOR-1, n=13; Ang II–infused TgNOR-1^{VSMC}, n=13). There were no deaths in saline-infused groups (not shown). **F**, Blood pressure levels in all experimental groups. Data are mean±SEM (n=6) $P<0.05$; *versus t=0 for each experimental condition; #versus the same type of animal infused with saline solution at the same time. Symbols as indicated in **B**. Two-way ANOVA with repeated measures (**A** and **F**) and χ^2 (**C**).

LWW | December9,20202:39AM | 4 Color Fig(s): F1-5 | Art:HYP16078

animals than in WT mice, yielding a disordered arrangement of ruptured fibers (Figure 2A). Similarly, the trend for greater aortic expression of inflammatory cell markers (EMR-1) and proinflammatory mediators (MCP-1 and CXCL2) observed in Ang II–infused control mice reached statistical significance in both transgenic groups (Figure 2B through 2D). Consequently, NOR-1 transgenic mice showed an exacerbated macrophage infiltration within adventitia and media associated with a stronger aortic staining for MCP-1 (Figure S4). Collectively, these data support that vascular NOR-1 overexpression fosters AAA formation in response to Ang II. Because both TgNOR-1 and TgNOR-1^{VSMC} mice comparably develop Ang II–induced aneurysms, further studies were focused on TgNOR-1^{VSMC}.

Exacerbated Vascular Oxidative Stress and MMP Activity in TgNOR-1^{VSMC} Mice

Vascular DHE staining revealed that NOR-1 transgenesis enhanced the production of reactive oxygen species induced by Ang II (Figure 3A). Further, the increase of aortic MMP2 expression evoked by Ang II in WT animals was exacerbated in TgNOR-1^{VSMC} mice (Figure 3B), and accordingly, in situ zymography evidenced that MMP activity was significantly increased (Figure 3C).

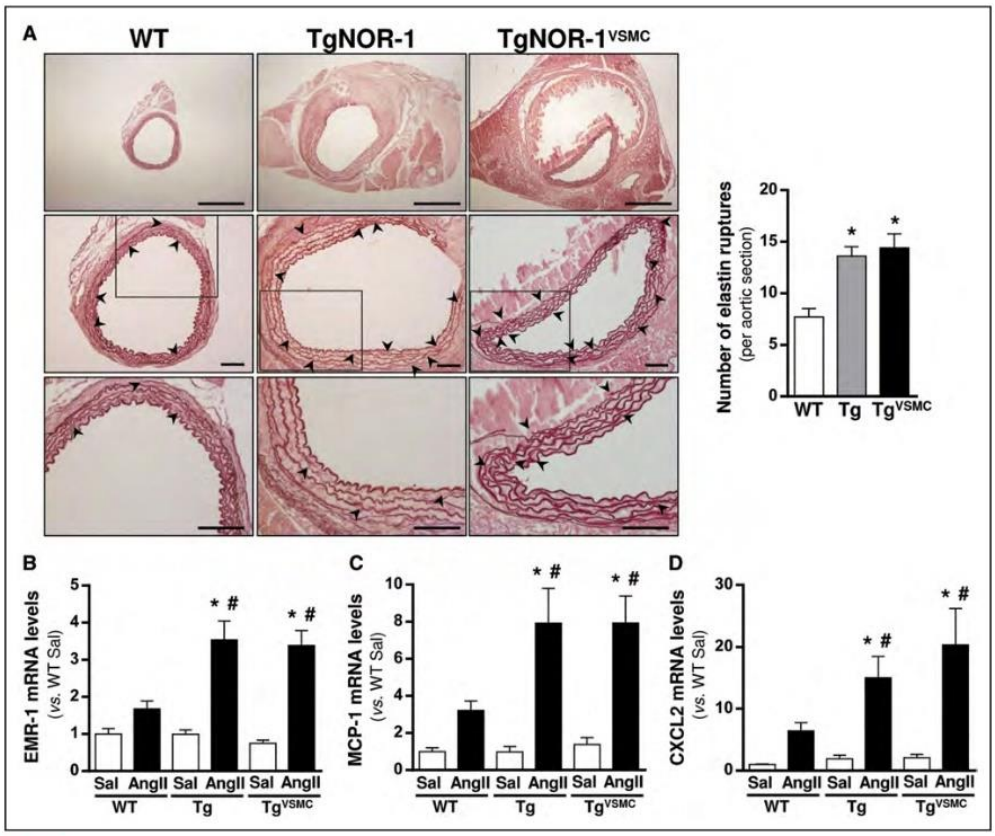

Figure 2. NOR-1 (neuron-derived orphan receptor 1) transgenesis exacerbates the Ang II (angiotensin II)-mediated disruption of elastin integrity and increases the expression of inflammatory mediators.
Wild-type (WT), TgNOR-1 (Tg), and TgNOR-1^{VSMC} (Tg^{VSMC}) mice were infused with Ang II (1000 ng/kg per minute) or saline solution for 28 days. **A**, Orcein staining of abdominal aortas from Ang II–infused mice. Arrows mark elastin fiber ruptures. The indicated areas are magnified in **lower** (bars: 500 μm [**upper**] and 100 μm [**middle** and **lower**]). The number of ruptures in elastin fibers per aortic section for each group is quantified. Data are mean±SEM (n=10). *P<0.001 versus Ang II–infused WT mice. **B**–**D**, mRNA levels of EMR-1 (**B**), MCP-1 (**C**), and CXCL2 (**D**) analyzed by real-time polymerase chain reaction in abdominal aortas from each experimental group. Data, normalized to GADPH expression, are expressed as mean±SEM (saline-infused mice, n=7; Ang II–infused mice, n=10). P<0.05; *versus the same type of animal infused with saline solution; #versus Ang II–infused WT mice. One-way ANOVA (**A**) and 2-way ANOVA (**B**–**D**).

LWW | December9,20202:39AM | 4 Color Fig(s): F1-5 | Art:HYP16078

ORIGINAL ARTICLE

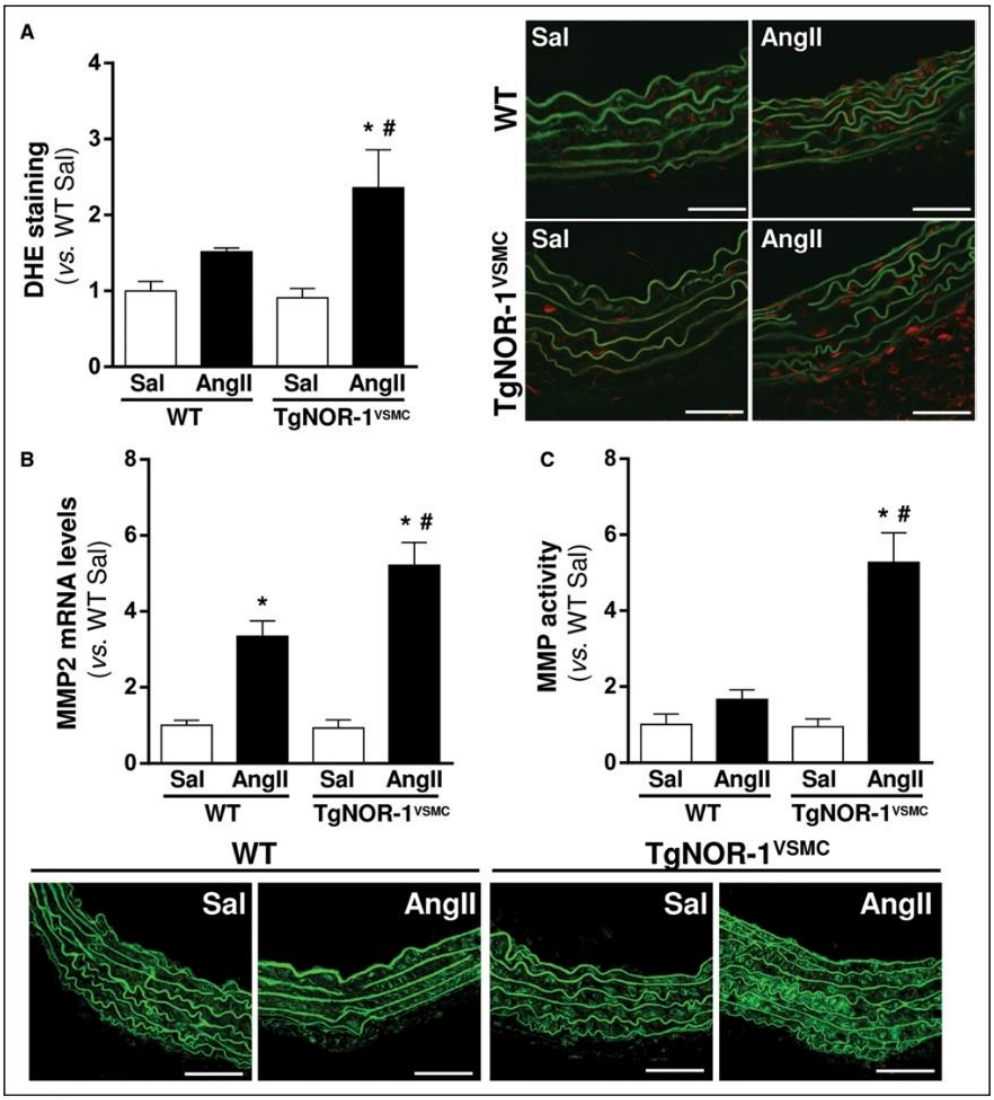

Figure 3. TgNOR-1VSMC mice exhibit enhanced oxidative stress and MMP (matrix metalloproteinase) expression and activity in abdominal aorta after Ang II (angiotensin II)-challenge.
Wild-type (WT) and TgNOR-1^{VSMC} mice were infused with Ang II (1000 ng/kg per minute) or saline solution (Sal) for 28 days. **A**, Vascular superoxide anion production visualized by DHE staining in aortic sections from each group. Representative images are shown. Data are represented as mean±SEM (n=6). Bars: 50 µm. **B**, MMP2 mRNA levels assessed by real-time polymerase chain reaction in abdominal aortas from each experimental group. Data, normalized to GADPH expression, are expressed as mean±SEM (saline-infused mice, n=7; Ang II-infused mice, n=10). **C**, Aortic MMP activity per aortic section analyzed by in situ zymography. Representative images are shown in the lower panel. Bars: 50 µm. Data are expressed as mean±SEM (saline-infused mice, n=6; Ang II-infused animals, n=8). $P<0.05$; *versus Saline-infused mice; #versus Ang II-infused WT animals. Two-way ANOVA (**A**–**C**).

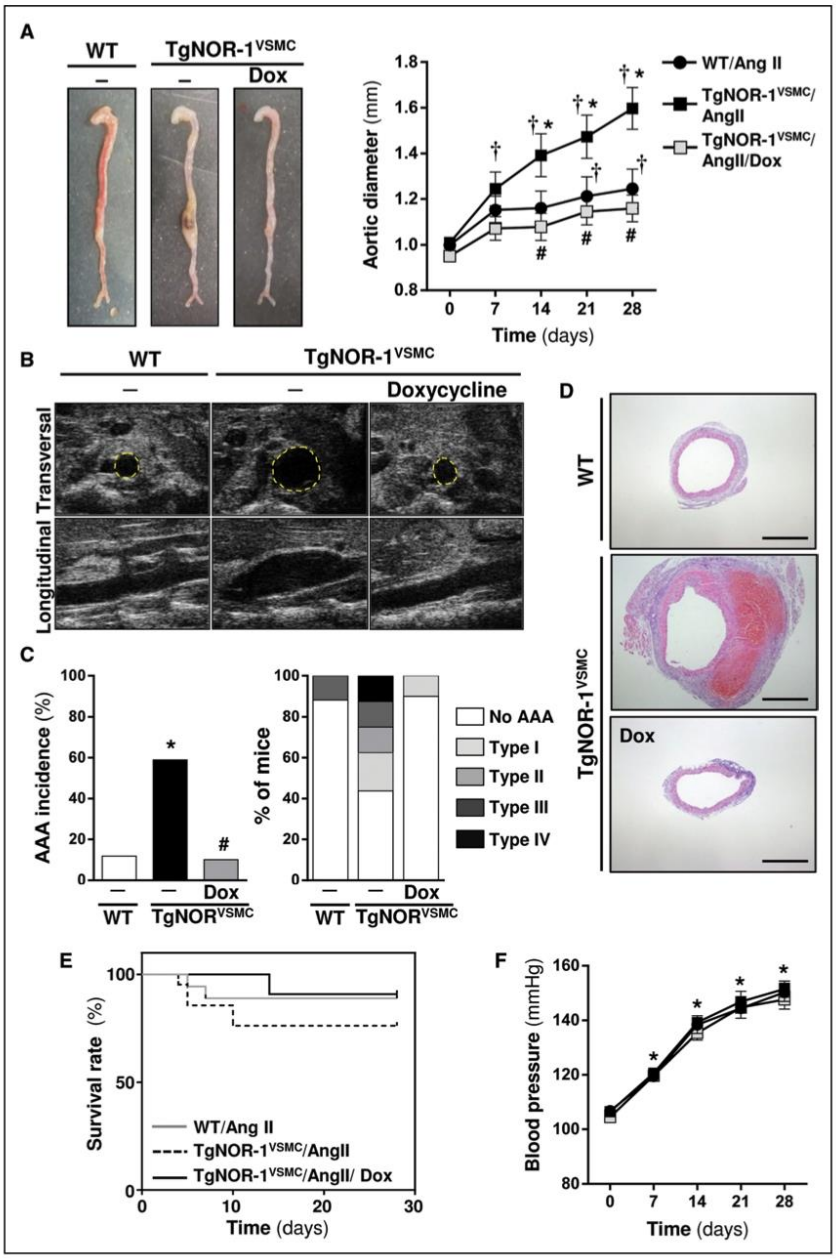

Figure 4. Doxycycline prevents aneurysm formation in Ang II (angiotensin II)-infused TgNOR-1VSMC mice.
Wild-type (WT) and TgNOR-1^{VSMC} mice were infused with Ang II (1000 ng/kg per minute for 28 days). TgNOR-1^{VSMC} mice were treated or not with Doxycycline (Dox; 30 mg/kg body weight/d). **A**, Representative images of excised aortas from animals challenged with Ang II (**left**). The graph on **right** shows the assessment of abdominal aortic diameter by ultrasonography. Data are mean±SEM (Ang II-infused WT mice, n=17; Ang II-infused TgNOR-1^{VSMC} mice, n=16; challenged TgNOR-1^{VSMC} mice treated with Doxycycline, n=10). (*Continued*)

LWW | December9,20202:39AM | 4 Color Fig(s): F1-5 | Art:HYP16078

ORIGINAL ARTICLE

Doxycycline Prevents Ang II-Induced AAA Formation in TgNOR-1^{VSMC} Mice

Data described above prompt us to assess whether doxycycline, a metalloproteinase inhibitor that prevents AAA formation,[19] could exert a similar effect in our model. As shown in Figure 4A and 4B, this drug blunted the increase in aortic diameter induced by Ang II in NOR-1 transgenic mice. The attenuation of aneurysm expansion produced by doxycycline was already observed after 14 days of Ang II infusion, and no further dilation was detected from that moment on (graph in Figure 4A). Doxycycline reduced the incidence and severity of AAA to a level comparable to that of WT mice (Figure 4C) and prevented the structural wall alterations observed in Ang II-infused TgNOR-1^{VSMC} mice (Figure 4D). Further, a trend towards a delay in fatal episodes and an improvement in survival rates was observed in doxycycline-treated TgNOR-1^{VSMC} mice (Figure 4E), while this drug did not affect blood pressure levels (Figure 4F).

The amelioration of vascular remodeling induced by doxycycline was associated with a preserved integrity of elastin fibers (Figure 5A). Accordingly, this drug counteracted the enhanced MMP activity (Figure 5B) and the increased expression of MMP2, inflammatory cell markers, and proinflammatory mediators (EMR-1, MCP-1, IL6, IL1β, and CXCXL2) triggered by Ang II in transgenic animals (Figure 5C). Consequently, immunostaining for macrophages (MAC3), lymphocytes (CD3), and neutrophils (ELANE) revealed that doxycycline significantly attenuated the accumulation of inflammatory cells in the aortic wall of challenged TgNOR-1^{VSMC} mice, while ameliorated aortic MCP-1 staining (Figure S5). Neither hNOR-1 mRNA levels nor endogenous NOR-1 expression in mouse aorta were altered by doxycycline (Figure S6). Therefore, doxycycline blunted aneurysm formation in the Ang II-infused TgNOR-1^{VSMC} mouse.

Vascular NOR-1 Overexpression Strikingly Alters Aortic Gene Expression

Whole transcriptome gene expression was evaluated in aorta from Ang II-treated TgNOR-1^{VSMC} mice and compared with that of WT challenged animals. Microarray expression profiling revealed that NOR-1 transgenesis profoundly alters vascular gene expression in response to Ang II infusion, leading to 968 up- and 544 down-regulated genes (adjusted $P<0.05$) as compared with WT animals (Table S3). Gene Set Enrichment Analysis analysis linked the higher aortic aneurysm susceptibility of TgNOR-1^{VSMC} mice to the regulation of several pathways and biological processes, some of them previously reported to underlie the development of aneurysmal diseases in animal models and humans (Table S4). Differential expression of representative genes from selected pathways (Table S5 and Figure S7) was validated by real-time polymerase chain reaction. All selected genes were confirmed to be differentially expressed (Table). The upregulation of MMP12 was further confirmed by immunohistochemistry and immunoblot assays (Figure S8).

DISCUSSION

We and others have involved NOR-1 in inflammation and immunomodulation,[10,20] ECM remodeling,[12] oxidative stress[13] and cell survival/apoptosis.[14] While these processes are hallmarks of AAA and NOR-1 is upregulated in human AAA,[14] it remains currently unknown whether NOR-1 contributes to AAA pathogenesis. Therefore, we analyzed whether a gain-of-function of this receptor in the vasculature affect Ang II-induced AAA formation. Our results involve NOR-1 in the development of AAA and show the usefulness of NOR-1 transgenic mice as new animal models to investigate aneurysmal mechanisms and test drugs in preclinical studies.

One of the most commonly used methods to induce AAA in animal models is the subcutaneous infusion of Ang II into hyperlipidemic mice,[21] a model that recapitulates some of the main features of the human pathology, including marked inflammation. Based on the dual pro-inflammatory[10,22] and anti-inflammatory functions played by NOR-1 in monocytes/macrophages,[23,24] Qing et al[25] hypothesized that this nuclear receptor might be involved in AAA formation. However, deletion of NOR-1 in hematopoietic stem cells from LDLR$^{-/-}$ (low-density lipoprotein receptor-deficient) mice reduced inflammation, but not AAA induced by Ang II infusion combined with a diet enriched in saturated fat. These results suggested that macrophage NOR-1 function would play a minor role in AAA, at least in this model. Nevertheless, NOR-1 is expressed in all cell types of the vascular wall, is induced by multiple cues potentially associated with AAA pathogenesis,[4,6] and, in fact, is upregulated in human AAA.[14]

Figure 4 Continued. $P<0.05$; †versus t=0 for each experimental condition; *versus Ang II-infused WT mice; #versus Ang II-infused TgNOR-1^{VSMC} mice. **B**, Representative images of the ultrasonographic analysis in Ang II-challenged mice at 28 days. Transversal and longitudinal images are shown, and the aortic diameter is traced with a yellow line. **C**, Incidence (on **left**) and severity (**right** graph; based on Manning scale)[19] of abdominal aortic aneurysm (AAA) in challenged mice. $P<0.05$; *versus Ang II-infused WT mice; #versus Ang II-infused TgNOR-1^{VSMC} mice (n as indicated in **A**). **D**, Representative hematoxylin-eosin staining of abdominal aortic sections from Ang II-infused mice (bars: 500 μm). **E**, Graph showing the survival rate of each experimental group. (Ang II-infused WT, n=19; Ang II-infused TgNOR-1^{VSMC}, n=21; Ang II-infused TgNOR-1^{VSMC} with doxycycline n=11). **F**, Blood pressure levels in all experimental groups. Symbols as indicated in **B**. Data are mean±SEM (Ang II-infused WT, n=8; Ang II-infused TgNOR-1^{VSMC}, n=10; Ang II-infused TgNOR-1^{VSMC} with doxycycline, n=9). $P<0.05$; *versus t=0 for each experimental condition. Two-way ANOVA with repeated measures (**A** and **F**) and χ^2 (**C**).

LWW	December9,20202:39AM	4 Color Fig(s): F1-5	Art:HYP16078

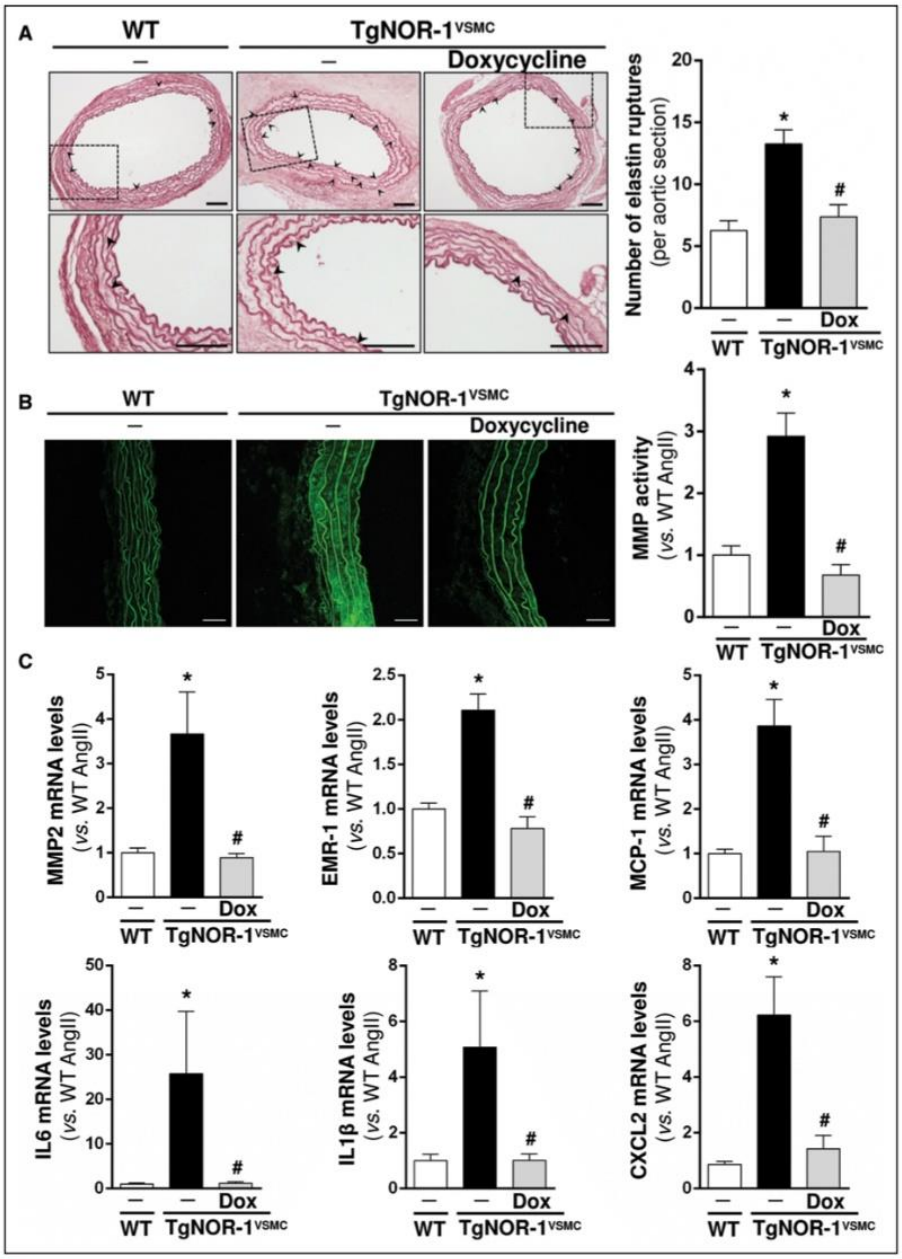

Figure 5. Doxycycline preserves elastin integrity and prevents the increased expression of inflammatory markers induced by Ang II (angiotensin II) in TgNOR-1VSMC mice.
Wild-type (WT) and TgNOR-1^{VSMC} mice were infused with Ang II (1000 ng/kg per minute) for 28 days. TgNOR-1^{VSMC} mice were treated or not with Doxycycline (Dox; 30 mg/kg body weight/d). **A**, Orcein staining of abdominal aortas from Ang II–infused mice. Arrowheads mark elastin fibers ruptures. The indicated areas are magnified in **lower**. Quantification of the number of ruptures in elastin fibers per (*Continued*)

LWW | December9,20202:39AM | 4 Color Fig(s): F1-5 | Art:HYP16078

Thus, a possible role for this nuclear receptor in AAA cannot be excluded. Hence, we sought to investigate whether NOR-1 transgenesis could modulate the susceptibility to experimentally induced AAA in normocholesterolemic C57BL/6 mice, a mouse strain considered resistant to Ang II-induced aneurysms. First, in a transgenic mouse that overexpresses NOR-1 in vascular tissues (TgNOR-1),[15] we observed that NOR-1 transgenesis promotes the formation of Ang II-driven AAA triggering severe aneurysmal forms that were not detected in challenged C57BL/6J mice. TgNOR-1 mice overexpress this receptor in all cell types of the vascular wall,[15] and to a lesser extent, in bone marrow-derived cells (data not shown). To gain more insight into the cell type responsible for the proaneurysmal effect of NOR-1 overexpression, we replicated the same experimental approach in TgNOR-1^{VSMC}, a mouse model that overexpresses NOR-1 driven by the SM22α promoter, which specifically targets SMC.[11] TgNOR-1^{VSMC} mice exhibit high expression of hNOR-1 in aortic VSMC, while the transgene was undetectable in other vascular cells such as adventitial fibroblasts (data not shown). Similar AAA incidence and severity was observed in both NOR-1 transgenic models, which developed aneurysms with the typical features observed in Ang II-infused hyperlipidemic mouse models: suprarenal location, upregulation of proinflammatory and proteolytic markers, profuse elastin fragmentation, reactive oxygen species production, and intramural hematoma. Therefore, dysregulation of NOR-1 expression in medial VSMC was enough to exacerbate the response triggered by Ang II in the vascular wall, thereby potentiating the infiltration of inflammatory cells, and favoring aortic dilatation and AAA formation. Our model seems to recapitulate key aspects of human pathology, but like other murine models of Ang II-induced aneurysm, it differs from human pathology, since in patients AAA are located in the suprarenal aorta and are commonly associated with a nonocclusive intraluminal thrombus. This prompted us to assess whether Ang II-infused TgNOR-1^{VSMC} mouse could be useful as a new animal model to test potential therapies against AAA. For this purpose, we used doxycycline, a MMP inhibitor which prevents the formation of experimental AAA in animal models,[19] and reduced vascular inflammation in clinical trials.[26] Doxycycline blunted aneurysm formation in TgNOR-1^{VSMC} mouse, preserved the integrity of elastin fibers and abolished the inflammatory response induced by Ang II. These results validate our single-gene transgenic mouse overexpressing NOR-1 specifically in VSMC on a normolipemic background as a new preclinical animal model for future translational research. It should be noted, however, that despite the effectiveness of doxycycline in animal models of AAA, no trial has so far shown a similar benefit in patients. The N-TA(3)CT (Non-Invasive Treatment of Abdominal Aortic Aneurysm Clinical Trial) has recently concluded that doxycycline does not reduce the growth of small AAA.[27] While these findings may be discouraging, the authors noticed that the AAA growth rate found in this study was lower than that previously reported, suggesting that the follow-up of 2 years could be too short to evidence the response to doxycycline. Further, doxycycline reduced C-reactive levels suggesting an anti-inflammatory effect. Therefore, the potential benefit of MMP inhibition on AAA stabilization in humans could not be excluded and further research is warranted.

In the aneurysmal aortic wall of our transgenic animal model, we made evident the upregulation of chemokines, cytokines, and proteolytic enzymes (IL-6, IL-1β, CXCL2, MCP-1, and MMP2) recognized as critically involved in AAA formation. Further, we were interested in identifying gene sets and pathways whose exacerbated response to Ang II could contribute to explain the increased susceptibility to AAA observed in NOR-1 transgenic animals. A whole transcriptome analysis comparing the aortic gene expression profile from WT and TgNOR-1^{VSMC} mice, both treated with Ang II, found about 1500 genes differentially regulated. Because both groups were exposed to Ang II, the magnitude of the differences was moderated. However, part of these genes match with those most differentially regulated in aneurysms from ApoE$^{-/-}$ mice exposed to Ang II[28] (101 out of the 300 and 22 out of the 290 genes nonredundantly upregulated or downregulated, respectively). Therefore, an important number of genes were not commonly regulated. Gene Set Enrichment Analysis identified gene sets significantly enriched in Ang II-treated TgNOR-1^{VSMC} mice corresponding to biological processes related with inflammation, cell cycle, and sympathetic activation and GO cellular components associated to extracellular matrix remodeling among others. In turn, down-regulated DEGs were mainly involved in GO biological processes related with muscle contraction and actin cytoskeleton. Consistently, similar functional annotations were uncovered by Reactome analysis.

Differential expression of specific genes, selected based on their classification into GO processes, their fold-change values, and their potential contribution to aneurysmal disease, was validated by real-time polymerase chain reaction. They include upregulated DEGs

Figure 5 Continued. aortic section for each group. Data are mean±SEM (n=8). $P<0.001$; *versus Ang II-infused WT mice; # versus Ang II-infused TgNOR-1^{VSMC} mice (bars: 100 μm). **B**, MMP (matrix metalloproteinase) activity per aortic section assessed by in situ zymography. Data are mean±SEM (untreated Ang II-infused mice, n=8; Ang II-infused mice treated with doxycycline, n=9). $P<0.001$; *versus Ang II-infused WT mice; #versus Ang II-infused TgNOR-1^{VSMC} mice (bars: 50 μm). **C**, mRNA levels of MMP2, EMR-1, MCP-1, IL6, IL1β, and CXCL2 analyzed by real-time polymerase chain reaction in abdominal aortas from Ang II-treated mice. Data, normalized to GADPH expression, are expressed as mean±SEM (Ang II-infused WT or TgNOR-1^{VSMC} mice, n=15; Ang II-infused TgNOR-1^{VSMC} mice treated with doxycyline, n=10). $P<0.05$; *versus Ang II-infused WT mice; #versus Ang II-infused TgNOR-1^{VSMC} mice. One-way ANOVA or Kruskal–Wallis test.

LWW | December9,20202:39AM | 4 Color Fig(s): F1-5 | Art:HYP16078

Table. Differentially Expressed Genes in Aorta From Ang II-Infused TgNOR-1^{VSMC} Mice Compared With WT Challenged Mice

Gene	Gene name	Mean FC (array)	Mean FC qPCR	*P value	Category
Mmp12	Matrix metallopeptidase 12	↑2.59	↑5.80	<0.05	GO_REGULATION_OF_IMMUNE_ SYSTEM _PROCESS
Ccnb1	cyclin B1	↑2.42	↑5.80	<0.0001	GO_MITOTIC_CELL_ CYCLE GO_CELLULAR_ RESPONSE_TO_DNA_ DAMAGE_STIMULUS
Adam8	ADAM metallopeptidase domain 8	↑3.13	↑5.69	≤0.05	GO_REGULATION_OF_ IMMUNE_ SYSTEM_ PROCESS GO_MYELOID_LEUKOCYTE_ MIGRATION
Col10a1	Collagen type X alpha 1 chain	↑17.32	↑5.43	<0.001	GO_COLLAGEN_ TRIMER
Cthrc1	Collagen triple helix repeat containing 1	↑4.77	↑4.75	<0.0001	GO_COLLAGEN_ TRIMER
Cdc20	Cell-division cycle protein 20	↑2.02	↑3.88	<0.0001	GO_MITOTIC_CELL_ CYCLE GO_SYNAPTIC_ SIGNALING
Scg2	Secretogranin II	↑7.42	↑3.75	<0.01	GO_MYELOID_LEUKOCYTE_ MIGRATION
Npy	Neuropeptide Y	↑7.07	↑3.72	<0.001	GO_SYNAPTIC_ SIGNALING
Syt4	Synaptotagmin IV	↑5.62	↑3.67	<0.01	GO_SYNAPTIC_ SIGNALING
Kif20a	Kinesin family member 20A	↑2.17	↑2.80	<0.01	GO_MITOTIC_CELL_ CYCLE
Uhrf1	Ubiquitin-like, containing PHD and RING finger domains, 1	↑2.24	↑2.742	<0.05	GO_CELLULAR_ RESPONSE_TO_DNA_ DAMAGE_ STIMULUS
Dync1i1	Dynein cytoplasmic 1 intermediate chain 1	↑7.12	↑2.66	0.01	GO_ANTIGEN_ PROCESSING_AND_ PRESENTATION
Cd5l	CD5 molecule like	↑4.86	↑2.47	<0.05	GO_REGULATION_OF_ IMMUNE_ SYSTEM_ PROCESS
Loxl2	lysyl oxidase-like 2	↑1.90	↑2.45	<0.01	GO_COLLAGEN_FIBRIL_ ORGANIZATION
Cd300c2	CD300C molecule 2	↑2.74	↑2.24	<0.01	GO_REGULATION_OF_ IMMUNE_ SYSTEM_ PROCESS
Sh2d1b1	SH2 domain containing 1B1	↑2.09	↑2.07	<0.02	GO_REGULATION_OF_ IMMUNE_ SYSTEM_ PROCESS
Myh11	Myosin, heavy polypeptide 11, smooth muscle	↓2.98	↓2.36	<0.02	GO_MUSCLE_STRUCTURE_ DEVELOPMENT GO_ACTIN_ CYTOSKELETON
Acta2	Actin alpha 2, smooth muscle	↓2.56	↓1.78	≤0.05	GO_ACTIN_ CYTOSKELETON
Itga8	Integrin alpha 8	↓3.23	↓1.76	≤0.05	GO_MUSCLE_STRUCTURE_ DEVELOPMENT

Ang II indicates angiotensin II; FC, fold change; NOR-1, neuron-derived orphan receptor-1; qPCR, quantitative polymerase chain reaction; and WT, wild type.
*P value for qPCR data.

representing biological processes such as extracellular matrix remodeling (*Col10a1*, *Cthrc1*, *Mmp12*, and *Loxl2*), immune response (*Cd5l*, *Adam8*, *Dync1i1*, *Cd300c2*, *Sh2d1b*, and *Scg2*), sympathetic activity (*Scg2*, *Npy*, and *Syt4*) and cell cycle and response to DNA damage (*Uhrf1*, *Ccnb1*, *Kif20a*, and *Cdc20*), and down-regulated DEGs, implicated in muscle cell function and actin cytoskeleton organization (*Acta2*, *Myh11*, and *Itga8*). All selected genes were confirmed as being differentially expressed. In particular, COL10A1, MMP12, and CTHRC1 have been reported to be upregulated in AAA and other aneurysm types both in human[29,30] and in experimental models.[28,31–34] Meanwhile, LOXL2, an ECM modifying enzyme regulated by NOR-1,[15] has been found to be a susceptibility gene to intracranial aneurysms[35] and is upregulated in aneurysms from ApoE$^{-/-}$ mice exposed to Ang II.[28] Among genes involved in the immune response upregulated in Ang II-challenged TgNOR-1^{VSMC} mice, it has been reported that CD5L positively correlates with human aneurysm growth,[36] upregulation of CD300C (orthologue of *Cd300c2*), and DYNC1I1 has been observed in aneurysms from humans[30] and experimental models,[33] respectively, while high expression levels of ADAM8 have been associated to both human[30,37] and experimental aneurysms.[28,33] In turn, SCG2, which is involved in transendothelial migration of inflammatory/immune cells and considered a marker of sympathetic activity, has been associated with hypertension and found upregulated in different forms of human aneurysms.[32,33] SCG2 is co-stored in chromaffin granules with NPY, a sympathetic neurotransmitter also expressed in VSMC,[39] and involved in pathological conditions characterized by sympathetic hyperactivity such as hypertension and vascular remodeling.[40] Concurrently, SYT4, a vesicular calcium-binding protein expressed in neurons and VSMC,[39] is considered a mediator of aneurysm progression in ascending aorta.[41] DEGs related to cell cycle and response to DNA damage were also induced in TgNOR-1^{VSMC}. UHRF1, which orchestrates SMC plasticity in arterial disease, was reported to be induced both in human and experimental AAA.[42] CDC20, CCNB1, and KIF20A have been associated with human atherosclerosis and aortic dissections[43,44]; and the latter 2 genes are strongly upregulated in Ang II-induced experimental aortic aneurysms[28] and in the ascending aorta of a model of Marfan syndrome.[45]

Interestingly, previous whole genome-expression profiling analysis identified NOR-1, as well as Nurr1 and Nur77, among the most upregulated genes at the rupture site of human aneurysms.[46] Accordingly, enriched

LWW | December9,20202:39AM | 4 Color Fig(s): F1-5 | Art:HYP16078

gene sets in TgNOR-1^{VSMC} aneurysmal aorta comprises genes identified by bioinformatics analysis as top hub genes crucial in the protein-protein interaction network in human aortic dissection (CDC20, CCNB1, KIF20A, CDK1, PBK, RACGAP, TOP2A, CCNB2, MAD2L1, and AURKA).[43,44] Finally, we confirmed the downregulation of the 3 selected VSMC-expressed genes (ACTA2, MYH11, and ITGA8), which have previously been documented in human aneurysmal disease and associated to inherited predisposition to aneurysms.[47] Thus, Ang II promotes the formation of aneurysm in TgNOR-1^{VSMC} through the modulation of pathways and specific genes which recapitulate critical mechanisms involved in aneurysm pathology. However, a number of genes regulated in NOR-1 transgenic mice were not similarly regulated in Ang II-infused ApoE$^{-/-}$ mice, the murine model most studied and experimentally closer to ours.[28,31] In particular, our model, but not the apoE-deficient mouse, reproduces the upregulation reported in human aneurysms of *Cd5l*, that has been associated to aneurysm growth,[36] and other genes encoding for proteins involved in the inflammatory/immune response such as *Cd300c2* (orthologue of *CD300C*),[30] *Sh2d1b1* (orthologue of *SH2D1B*),[38] and *Scg2*[32,34], as well as the downregulation of genes involved in the regulation of actin cytoskeleton.[48] Interestingly, it should be emphasized that the ApoE$^{-/-}$ mouse model did not reproduce the upregulation of NOR-1 reported in human AAA,[14,46] which could explain that certain genes, directly or indirectly regulated by NOR-1, were not modulated in the same way in that model.

Therefore, using 2 animal models generated by our group, we show that the upregulation of NOR-1 in vascular tissues amplifies the expression of an array of genes induced by Ang II, thereby exacerbating the ability of this peptide hormone to promote aneurysm formation. These animals could be new experimental and preclinical models. Further studies should determine the structural genes that make NOR-1 a key facilitator of the aneurysmal process.

PERSPECTIVES

No drug therapy has been convincingly shown to limit AAA growth or rupture, and the underlying molecular mechanisms involved in this disease are not completely understood. Our study points out NOR-1 as a relevant transcription factor in vascular biology whose upregulation positively contributes to aneurysm formation and shows the potential usefulness of mice overexpressing this nuclear receptor both as new animal models to deepen the investigation of pathological mechanisms of the disease and as tools to address pharmacological preclinical studies. Because NOR-1 transgenesis leads to modulation of multiple genes and biological processes associated with aneurysmal disease, further studies will clarify whether the role played by NOR-1 on aortic aneurysm lies on the vascular activity of a limited number of structural genes early and directly regulated by NOR-1 rather than small changes in multiple genes either directly or indirectly regulated by this transcription factor.

ARTICLE INFORMATION

Received August 4, 2020; accepted November 30, 2020.

Affiliations

From the Instituto de Investigaciones Biomédicas de Barcelona (IIBB-CSIC), Spain (L.C., I.M.-P., C.B.-S., J.A., J.M.-G.); CIBER de Enfermedades Cardiovasculares, ISCIII, Madrid, Spain (L.C., I.M.-P., J.A., A.M.B., C.R., J.M.-G.); Instituto de Investigación Biomédica Sant Pau, Barcelona, Spain (L.C., I.M.-P., C.B.-S., J.A., E.S., C.R., J.M.-G.); Institut de Recerca Hospital de la Santa Creu i Sant Pau (IRHSCSP), Barcelona, Spain (E.S., C.R.); and Facultad de Medicina, Universidad Autónoma de Madrid, Instituto de Investigación Hospital La Paz, Spain (A.M.B.).

Acknowledgments

We thank Silvia Aguiló for her technical assistance.

Sources of Funding

This work was supported by the Spanish MINECO-ISCIII [RTI2018-094727-B-100, PI18/0919], and AGAUR (2017-SGR-00333), and Sociedad Española de Arteriosclerosis (SEA-2019). The study was co-founded by Fondo Europeo de Desarrollo Regional (FEDER), a way to make Europe. L. Cañes and C. Ballester-Servera were supported by a FI (AGAUR) and a FPU fellowship (MINECO), respectively.

Disclosures

None.

REFERENCES

1. Nordon IM, Hinchliffe RJ, Loftus IM, Thompson MM. Pathophysiology and epidemiology of abdominal aortic aneurysms. *Nat Rev Cardiol*. 2011;8:92–102. doi: 10.1038/nrcardio.2010.180
2. Mozaffarian D, Benjamin EJ, Go AS, Arnett DK, Blaha MJ, Cushman M, de Ferranti S, Després JP, Fullerton HJ, Howard VJ, et al; American Heart Association Statistics Committee and Stroke Statistics Subcommittee. Heart disease and stroke statistics–2015 update: a report from the American Heart Association. *Circulation*. 2015;131:e29–322. doi: 10.1161/CIR.0000000000000152
3. Golledge J. Abdominal aortic aneurysm: update on pathogenesis and medical treatments. *Nat Rev Cardiol*. 2019;16:225–242. doi: 10.1038/s41569-018-0114-9
4. Martínez-González J, Badimon L. The NR4A subfamily of nuclear receptors: new early genes regulated by growth factors in vascular cells. *Cardiovasc Res*. 2005;65:609–618. doi: 10.1016/j.cardiores.2004.10.002
5. Pei L, Waki H, Vaitheesvaran B, Wilpitz DC, Kurland IJ, Tontonoz P. NR4A orphan nuclear receptors are transcriptional regulators of hepatic glucose metabolism. *Nat Med*. 2006;12:1048–1055. doi: 10.1038/nm1471
6. Zhao Y, Bruemmer D. NR4A orphan nuclear receptors: transcriptional regulators of gene expression in metabolism and vascular biology. *Arterioscler Thromb Vasc Biol*. 2010;30:1535–1541. doi: 10.1161/ATVBAHA.109.191163
7. Mohan HM, Aherne CM, Rogers AC, Baird AW, Winter DC, Murphy EP. Molecular pathways: the role of NR4A orphan nuclear receptors in cancer. *Clin Cancer Res*. 2012;18:3223–3228. doi: 10.1158/1078-0432.CCR-11-2953
8. Martínez-González J, Rius J, Castelló A, Cases-Langhoff C, Badimon L. Neuron-derived orphan receptor-1 (NOR-1) modulates vascular smooth muscle cell proliferation. *Circ Res*. 2003;92:96–103. doi: 10.1161/01.es.0000050921.53008.47
9. Nomiyama T, Zhao Y, Gizard F, Findeisen HM, Heywood EB, Jones KL, Conneely OM, Bruemmer D. Deficiency of the NR4A neuron-derived orphan receptor-1 attenuates neointima formation after vascular injury. *Circulation*. 2009;119:577–586. doi: 10.1161/CIRCULATIONAHA.108.822056

10. Zhao Y, Howatt DA, Gizard F, Nomiyama T, Findeisen HM, Heywood EB, Jones KL, Conneely OM, Daugherty A, Bruemmer D. Deficiency of the NR4A orphan nuclear receptor NOR1 decreases monocyte adhesion and atherosclerosis. *Circ Res*. 2010;107:501–511. doi: 10.1161/CIRCRESAHA.110.222083
11. Rodríguez-Calvo R, Guadall A, Calvayrac O, Navarro MA, Alonso J, Ferrán B, de Diego A, Muniesa P, Osada J, Rodríguez C, et al. Over-expression of neuron-derived orphan receptor-1 (NOR-1) exacerbates neointimal hyperplasia after vascular injury. *Hum Mol Genet*. 2013;22:1949–1959. doi: 10.1093/hmg/ddt042
12. Martí-Pàmies I, Cañes L, Alonso J, Rodríguez C, Martínez-González J. The nuclear receptor NOR-1/NR4A3 regulates the multifunctional glycoprotein vitronectin in human vascular smooth muscle cells. *FASEB J*. 2017;31:4588–4599. doi: 10.1096/fj.201700136RR
13. Alonso J, Cañes L, García-Redondo AB, de Frutos PG, Rodríguez C, Martínez-González J. The nuclear receptor NOR-1 modulates redox homeostasis in human vascular smooth muscle cells. *J Mol Cell Cardiol*. 2018;122:23–33. doi: 10.1016/j.yjmcc.2018.08.002
14. Alonso J, Galán M, Martí-Pàmies I, Romero JM, Camacho M, Rodríguez C, Martínez-González J. NOR-1/NR4A3 regulates the cellular inhibitor of apoptosis 2 (cIAP2) in vascular cells: role in the survival response to hypoxic stress. *Sci Rep*. 2016;6:34056. doi: 10.1038/srep34056
15. Cañes L, Martí-Pàmies I, Ballester-Servera C, Herraiz-Martínez A, Alonso J, Galán M, Nistal JF, Muniesa P, Osada J, Hove-Madsen L, et al. Neuron-derived orphan receptor-1 modulates cardiac gene expression and exacerbates angiotensin II-induced cardiac hypertrophy. *Clin Sci (Lond)*. 2020;134:359–377. doi: 10.1042/CS20191014
16. Galán M, Varona S, Orriols M, Rodríguez JA, Aguiló S, Dilmé J, Camacho M, Martínez-González J, Rodriguez C. Induction of histone deacetylases (HDACs) in human abdominal aortic aneurysm: therapeutic potential of HDAC inhibitors. *Dis Model Mech*. 2016;9:541–552. doi: 10.1242/dmm.024513
17. Huber W, Carey VJ, Gentleman R, Anders S, Carlson M, Carvalho BS, Bravo HC, Davis S, Gatto L, Girke T, et al. Orchestrating high-throughput genomic analysis with Bioconductor. *Nat Methods*. 2015;12:115–121. doi: 10.1038/nmeth.3252
18. Ritchie ME, Silver J, Oshlack A, Holmes M, Diyagama D, Holloway A, Smyth GK. A comparison of background correction methods for two-colour microarrays. *Bioinformatics*. 2007;23:2700–2707. doi: 10.1093/bioinformatics/btm412
19. Manning MW, Cassis LA, Daugherty A. Differential effects of doxycycline, a broad-spectrum matrix metalloproteinase inhibitor, on angiotensin II-induced atherosclerosis and abdominal aortic aneurysms. *Arterioscler Thromb Vasc Biol*. 2003;23:483–488. doi: 10.1161/01.ATV.0000058404.92759.32
20. Tsilingiri K, de la Fuente H, Relaño M, Sánchez-Díaz R, Rodríguez C, Crespo J, Sánchez-Cabo F, Dopazo A, Alonso-Lebrero JL, Vara A, et al. Oxidized low-density lipoprotein receptor in lymphocytes prevents atherosclerosis and predicts subclinical disease. *Circulation*. 2019;139:243–255. doi: 10.1161/CIRCULATIONAHA.118.034326
21. Daugherty A, Manning MW, Cassis LA. Angiotensin II promotes atherosclerotic lesions and aneurysms in apolipoprotein E-deficient mice. *J Clin Invest*. 2000;105:1605–1612. doi: 10.1172/JCI7818
22. Pei L, Castrillo A, Tontonoz P. Regulation of macrophage inflammatory gene expression by the orphan nuclear receptor Nur77. *Mol Endocrinol*. 2006;20:786–794. doi: 10.1210/me.2005-0331
23. Qing H, Liu Y, Zhao Y, Aono J, Jones KL, Heywood EB, Howatt D, Binkley CM, Daugherty A, Liang Y, et al. Deficiency of the NR4A orphan nuclear receptor NOR1 in hematopoietic stem cells accelerates atherosclerosis. *Stem Cells*. 2014;32:2419–2429. doi: 10.1002/stem.1747
24. De Paoli F, Eeckhoute J, Copin C, Vanhoutte J, Duhem C, Derudas B, Dubois-Chevalier J, Colin S, Zawadzki C, Jude B, et al. The neuron-derived orphan receptor 1 (NOR1) is induced upon human alternative macrophage polarization and stimulates the expression of markers of the M2 phenotype. *Atherosclerosis*. 2015;241:18–26. doi: 10.1016/j.atherosclerosis.2015.04.798
25. Qing H, Jones KL, Heywood EB, Lu H, Daugherty A, Bruemmer D. Deletion of the NR4A nuclear receptor NOR1 in hematopoietic stem cells reduces inflammation but not abdominal aortic aneurysm formation. *BMC Cardiovasc Disord*. 2017;17:271. doi: 10.1186/s12872-017-0701-4
26. Lindeman JH, Abdul-Hussien H, van Bockel JH, Wolterbeek R, Kleemann R. Clinical trial of doxycycline for matrix metalloproteinase-9 inhibition in patients with an abdominal aneurysm: doxycycline selectively depletes aortic wall neutrophils and cytotoxic T cells. *Circulation*. 2009;119:2209–2216. doi: 10.1161/CIRCULATIONAHA.108.806505
27. Baxter BT, Matsumura J, Curci JA, McBride R, Larson L, Blackwelder W, Lam D, Wijesinha M, Terrin M; N-TA3CT Investigators. Effect of doxycycline on aneurysm growth among patients with small infrarenal abdominal aortic aneurysms: a randomized clinical trial. *JAMA*. 2020;323:2029–2038. doi: 10.1001/jama.2020.5230
28. Spin JM, Hsu M, Azuma J, Tedesco MM, Deng A, Dyer JS, Maegdefessel L, Dalman RL, Tsao PS. Transcriptional profiling and network analysis of the murine angiotensin II-induced abdominal aortic aneurysm. *Physiol Genomics*. 2011;43:993–1003. doi: 10.1152/physiolgenomics.00044.2011
29. Courtois A, Nusgens BV, Hustinx R, Namur G, Gomez P, Kuivaniemi H, Defraigne JO, Colige AC, Sakalihasan N. Gene expression study in positron emission tomography-positive abdominal aortic aneurysms identifies CCL18 as a potential biomarker for rupture risk. *Mol Med*. 2015;20:697–706. doi: 10.2119/molmed.2014.00065
30. Kleinloog R, Verweij BH, van der Vlies P, Deelen P, Swertz MA, de Muynck L, Van Damme P, Giuliani F, Regli L, van der Zwan A, et al. RNA sequencing analysis of intracranial aneurysm walls reveals involvement of lysosomes and immunoglobulins in rupture. *Stroke*. 2016;47:1286–1293. doi: 10.1161/STROKEAHA.116.012541
31. Rush C, Nyara M, Moxon JV, Trollope A, Cullen B, Golledge J. Whole genome expression analysis within the angiotensin II-apolipoprotein E deficient mouse model of abdominal aortic aneurysm. *BMC Genomics*. 2009;10:298. doi: 10.1186/1471-2164-10-298
32. Shi C, Awad IA, Jafari N, Lin S, Du P, Hage ZA, Shenkar R, Getch CC, Bredel M, Batjer HH, et al. Genomics of human intracranial aneurysm wall. *Stroke*. 2009;40:1252–1261. doi: 10.1161/STROKEAHA.108.532036
33. Holcomb M, Ding YH, Dai D, McDonald RJ, McDonald JS, Kallmes DF, Kadirvel R. RNA-sequencing analysis of messenger RNA/MicroRNA in a rabbit aneurysm model identifies pathways and genes of interest. *AJNR Am J Neuroradiol*. 2015;36:1710–1715. doi: 10.3174/ajnr.A4390
34. Sulkava M, Raitoharju E, Mennander A, Levula M, Seppälä I, Lyytikäinen LP, Järvinen O, Illig T, Klopp N, Mononen N, et al. Differentially expressed genes and canonical pathways in the ascending thoracic aortic aneurysm - the Tampere Vascular Study. *Sci Rep*. 2017;7:12127. doi: 10.1038/s41598-017-12421-4
35. Akagawa H, Narita A, Yamada H, Tajima A, Krischek B, Kasuya H, Hori T, Kubota M, Saeki N, Hata A, et al. Systematic screening of lysyl oxidase-like (LOXL) family genes demonstrates that LOXL2 is a susceptibility gene to intracranial aneurysms. *Hum Genet*. 2007;121:377–387. doi: 10.1007/s00439-007-0333-3
36. Behr Andersen C, Lindholt JS, Urbonavicius S, Halekoh U, Jensen PS, Stubbe J, Rasmussen LM, Beck HC. Abdominal aortic aneurysms growth is associated with high concentrations of plasma proteins in the intraluminal thrombus and diseased arterial tissue. *Arterioscler Thromb Vasc Biol*. 2018;38:2254–2267. doi: 10.1161/ATVBAHA.117.310126
37. Levula M, Paavonen T, Valo T, Pelto-Huikko M, Laaksonen R, Kahonen M, Huovila A, Lehtimaki T, Tarkka M, Mennander AA. A disintegrin and metalloprotease -8 and -15 and susceptibility for ascending aortic dissection. *Scand J Clin Lab Invest*. 2011;71:515–522. doi: 10.3109/00365513.2011.591939
38. Hinterseher I, Schworer CM, Lillvis JH, Stahl E, Erdman R, Gatalica Z, Tromp G, Kuivaniemi H. Immunohistochemical analysis of the natural killer cell cytotoxicity pathway in human abdominal aortic aneurysms. *Int J Mol Sci*. 2015;16:11196–11212. doi: 10.3390/ijms160511196
39. Barnes RH 2nd, Akama T, Öhman MK, Woo MS, Bahr J, Weiss SJ, Eitzman DT, Chun TH. Membrane-tethered metalloproteinase expressed by vascular smooth muscle cells limits the progression of proliferative atherosclerotic lesions. *J Am Heart Assoc*. 2017;6:e003693.
40. Tan CMJ, Green P, Tapoulal N, Lewandowski AJ, Leeson P, Herring N. The role of neuropeptide Y in cardiovascular health and disease. *Front Physiol*. 2018;9:1281. doi: 10.3389/fphys.2018.01281
41. Tobin SW, Alibhai FJ, Lee MM, Yeganeh A, Wu J, Li SH, Guo J, Tsang K, Tumiati L, Rocha R, et al. Novel mediators of aneurysm progression in bicuspid aortic valve disease. *J Mol Cell Cardiol*. 2019;132:71–83. doi: 10.1016/j.yjmcc.2019.04.022
42. Elia L, Kunderfranco P, Carullo P, Vacchiano M, Farina FM, Hall IF, Mantero S, Panico C, Papait R, Condorelli G, et al. UHRF1 epigenetically orchestrates smooth muscle cell plasticity in arterial disease. *J Clin Invest*. 2018;128:2473–2486. doi: 10.1172/JCI96121
43. Jiang T, Si L. Identification of the molecular mechanisms associated with acute type A aortic dissection through bioinformatics methods. *Braz J Med Biol Res*. 2019;52:e8950. doi: 10.1590/1414-431X20198950

LWW | December9,20202:39AM | 4 Color Fig(s): F1-5 | Art:HYP16078

44. Schwill S, Seppelt P, Grünhagen J, Ott CE, Jugold M, Ruhparwar A, Robinson PN, Karck M, Kallenbach K. The fibrillin-1 hypomorphic mgR/mgR murine model of Marfan syndrome shows severe elastolysis in all segments of the aorta. *J Vasc Surg*. 2013;57:1628–36, 1636.e1. doi: 10.1016/j.jvs.2012.10.007
45. Wang W, Liu Q, Wang Y, Piao H, Li B, Zhu Z, Li D, Wang T, Xu R, Liu K. Verification of hub genes in the expression profile of aortic dissection. *PLoS One*. 2019;14:e0224922. doi: 10.1371/journal.pone.0224922
46. Choke E, Cockerill GW, Laing K, Dawson J, Wilson WR, Loftus IM, Thompson MM. Whole genome-expression profiling reveals a role for immune and inflammatory response in abdominal aortic aneurysm rupture. *Eur J Vasc Endovasc Surg*. 2009;37:305–310. doi: 10.1016/j.ejvs.2008.11.017
47. Armstrong PJ, Johanning JM, Calton WC Jr, Delatore JR, Franklin DP, Han DC, Carey DJ, Elmore JR. Differential gene expression in human abdominal aorta: aneurysmal versus occlusive disease. *J Vasc Surg*. 2002;35:346–355. doi: 10.1067/mva.2002.121071
48. Modrego J, López-Farré AJ, Martínez-López I, Muela M, Macaya C, Serrano J, Moñux G. Expression of cytoskeleton and energetic metabolism-related proteins at human abdominal aortic aneurysm sites. *J Vasc Surg*. 2012;55:1124–1133. doi: 10.1016/j.jvs.2011.10.033

SUPLEMENTARY INFORMATION

High neuron derived orphan receptor-1 (NOR-1) expression strengthens the vascular wall response to angiotensin II leading to aneurysm formation in mice

Laia Cañes[†], Ingrid Martí-Pàmies[†], Carme Ballester-Servera, Judith Alonso, Elena Serrano, Cristina Rodríguez,* and José Martínez-González*

[†] Both first authors contributed equally to this work.

*These authors contributed equally to this work.

On-line Data Supplement

High neuron derived orphan receptor-1 (NOR-1) expression strengthens the vascular wall response to angiotensin II leading to aneurysm formation in mice

Laia Cañes[1,2,3†], Ingrid Martí-Pàmies[1,2,3†], Carme Ballester-Servera[1,3], Judith Alonso[1,2,3], Elena Serrano[3,4], Ana M Briones[2,5], Cristina Rodríguez[2,3,4,*] and José Martínez-González[1,2,3,*]

[1]Instituto de Investigaciones Biomédicas de Barcelona (IIBB-CSIC), Barcelona, Spain.
[2]CIBER de Enfermedades Cardiovasculares, ISCIII, Madrid, Spain.
[3]Instituto de Investigación Biomédica Sant Pau, Barcelona, Spain.
[4]Institut de Recerca Hospital de la Santa Creu i Sant Pau (IRHSCSP), Barcelona, Spain.
[5]Universidad Autónoma de Madrid, Instituto de Investigación Hospital La Paz, Madrid, Spain.

Short title: NOR-1 predisposes to aortic aneurysm.

Address for correspondence:

José Martínez-González.
Instituto de Investigaciones Biomédicas de Barcelona (IIBB-CSIC).
C/Rosselló, 161,
08036 Barcelona, Spain
Tel: +34935565896. Email: jose.martinez@iibb.csic.es or
Cristina Rodríguez
Institut de Recerca Hospital de la Santa Creu i Sant Pau (IRHSCSP).
C/Antoni Mª Claret,
08025 Barcelona, Spain
Tel: +34935565897. Email: crodriguezs@csic-iccc.org

Methods

Animal Handling

Two animal models that over-express the human NOR-1 cDNA in the vascular wall (TgNOR-1 and TgNOR-1^{VSMC}) were used.[1,2]. Transgenic mice and control littermates (wild-type; WT) on a C57BL/6J genetic background were bred in the Animal Experimentation Unit (Institut de Recerca de l'Hospital de la Santa Creu i Sant Pau, Barcelona, Spain). Animal handling and disposal were performed in accordance with the principles and guidelines established by the Spanish Policy for Animal Protection RD53/2013 and the European Union Directive 2010/63/UE. All procedures were approved by the local ethical committee (Law 5/June 21, 1995; Generalitat de Catalunya).

Due to the sexual dimorphism characterizing AAA, with higher prevalence in males both in humans and animal models, the studies were exclusively performed in male mice. Three-mo-old male transgenic (TgNOR-1 and TgNOR-1^{VSMC}) and WT mice were randomly divided, by an operator unaware of the nature of the experiments, into AngII or saline-infused animals. AngII [1000 ng/kg body weight (BW)/min; Sigma-Aldrich, St Louis, MO, USA] was infused via osmotic minipumps (model 1004, Alzet; Durect Corporation, Cupertino, CA, USA) for 28 days.[3] WT and transgenic mice infused with saline were used as controls. Animals were fed with a standard chow diet throughout the experimental procedure.. For the implantation of osmotic minipumps, mice were anaesthetised by isofluorane inhalation (1.5%). Anaesthetic depth was confirmed by loss of blink reflex and/or lack of response to tail pinch. The procedure takes about 15 min/mouse. Antibiotics (penicillin, 450,000 u/kg, intramuscular) and analgesics (buprenorphine, 0.05 mg/kg, subcutaneous) were given immediately after surgery to prevent infection and discomfort. Recovery after surgical procedures was carried out using aseptic techniques in a dedicated approved surgical area. The animals were kept warm in a heating pad until awake after surgery, and observed carefully by the investigators throughout the post-surgery period.

In specific studies TgNOR-1^{VSMC} mice were treated with doxycycline (Sigma-Aldrich; 30 mg/kg/day) 24 h before the implantation of AngII osmotic minipumps. Doxycycline was orally administered in the drinking water throughout the 28 days experimental period. A group of AngII-challenged WT animals was also included.

Non-invasive measurement of systolic blood pressure

Systolic blood pressure (SBP) was non-invasively measured in conscious mice using the tail-cuff plethysmography method (CODA® tail-cuff blood pressure system; Kent Scientific Corporation; Torrington, CT, USA). Mice were trained for tail-cuff measurements over a period of 1 week. Blood pressure measurements were performed at the same time (between 9 a.m. and 11 a.m.) in order to avoid the influence of the circadian cycle.[3]

Basic measurements of ultrasound recording for abdominal aortas

Mice were anaesthetised with 1.5% isofluorane inhalation as indicated above and were lightly secured in the supine position to a warming platform. After shaving the precordium, an abdominal echography was performed to record abdominal aorta diameter using a Vevo 2100 ultrasound with a 30 MHz transducer (VisualSonics, Toronto, ON, Canada).[3] Abdominal aortas with external diameters $\geq$1.5 mm were considered as aneurysms. All primary measurements were made from images captured on cine loops of 100 frames at the time of the study using the software provided by the echography machine.

Echocardiographic data was recorded at baseline and weekly throughout the experimental period. At the end of the experimental procedures (28 days), mice were anaesthetised with ketamine (150 mg/kg) and medetomidine (1 mg/kg) and sacrificed by thoracotomy. Then aortas were excised and processed for further analysis. The bottom segment of the abdominal aorta, including 2/3 of the aneurysmal region and the rest of the abdominal aorta until the iliac bifurcation, was snap frozen in liquid nitrogen for mRNA isolation. The upper segment of the aneurysm was formalin-fixed and paraffin-embedded for histological and immunohistochemical analysis. Dihydroethidium (DHE) staining and zymography were performed in frozen and OCT-embedded aorta segments immediately adjacent to the aneurysm. The severity of the aneurysm was based on a 4-point grading scale previously described in detail: type 0, no aneurysm; type I, dilated lumen in the suprarenal region of the aorta with no thrombus; type II, remodelled tissue in the suprarenal region that frequently contained thrombus; type III, a pronounced bulbous form of type II that contained thrombus, and type IV, a form in which there are multiple AAAs containing thrombus.[4] All measurements were performed by an experienced and blinded operator.

Analysis of mRNA levels

Total RNA was isolated using the TriPure Isolation Reagent (Sigma-Aldrich) and reverse transcribed into cDNA using the High Capacity cDNA Reverse Transcription Kit (Applied Biosystems, Foster City, CA, USA). Quantification of mRNA levels was performed by real-time PCR using the ABI PRISM 7900HT sequence detection system (Applied Biosystems). Specific primers and probes (provided by Applied Biosystems or Integrated DNA Technologies Inc, Coralville, IA, USA.) were used for the quantification of mouse mRNA levels for NOR-1 (Mm00450074_m1), IL6 (Mm00446191_m1), IL-1β (Mm00434228_m1), MCP-1 (Mm00441242_m1), MMP-2 (MmPT.58.9606100), EMR-1 (MmPT.56a.11087779) and CXCL2 (Mm00436450_m1). GAPDH (Mm.PT.58.39a.1) expression was used as a reference gene. Other primers and probes employed for validation of microarray results are shown in Table S1.

In situ detection of vascular O_2^- production

The oxidative fluorescent dye DHE (Sigma-Aldrich) was used to evaluate the *in situ* production of O_2^-. DHE staining and zymography should be performed in frozen sections embedded in OCT, these analysis were performed in the thoracic aorta segment immediately adjacent to the aneurysm Arterial segments were placed in phosphate-buffered saline (PBS) containing 30% sucrose for 20–50 min, transferred to a cryomold-containing Tissue Tek OCT embedding medium (Sakura Finetek Europe B.V., Alphen aan Den Rijn, The Netherlands), and frozen in liquid nitrogen. Arterial sections were equilibrated for 30 min at 37°C in Krebs-HEPES buffer (in mM: 130 NaCl, 5.6 KCl, 2 $CaCl_2$, 0.24 $MgCl_2$, 8.3 HEPES, 11 glucose, pH = 7.4). DHE (2 μM) was topically applied onto each section, cover-slipped and incubated for 30 min in a light-protected humidified chamber at 37°C. Fluorescence was visualized with a fluorescent laser scanning confocal microscope (Leica TCS SP2 equipped with a krypton/argon laser, x10 and × 40 objectives; Leica Microsistemas S.L.U., L'Hospitalet de Llobregat, Spain). Fluorescence was detected with a 568 nm long-pass filter by using the same imaging settings for all experimental conditions. The mean fluorescence densities in the target region were quantified using ImageJ software. To minimize laser fluctuations from one day to another, data were expressed as % of signal in control arteries.

Immunoblotting

Tissue lysates were separated on SDS-polyacrylamide gels and transferred to polyvinylidene diflouride membranes (Immobilon, Merck-Millipore; IPVH00010). Blots were incubated with an antibody directed against MMP12 (sc-390863, Santa Cruz Biotechnology, Dallas, TX, USA) and β-actin (A5441, Sigma-Aldrich). Bound antibodies were detected after incubation with appropriate HRP-conjugated secondary antibodies (Dako Products, Agilent, Santa Clara, CA, USA) and using the SuperSignal West Dura Extended Duration Substrate (Thermo Fisher Scientific, Waltham, MA, USA). The size of detected proteins was estimated using protein molecular-mass standards (Fermentas, Thermo Fisher Scientific). Equal loading of protein in each lane was verified by Ponceau staining and by β-actin signal.

Histological, immunohistochemical and immunocytochemical analysis

Tissues were fixed in 4% paraformaldehyde/0.1 M PBS (pH 7.4) for 24 hours and embedded in paraffin. Tissue sections (5-µm) were deparaffinised in xylene and rehydrated in graded ethanol solutions. Slides were then rinsed in distilled water and treated with 3% hydrogen peroxide in methanol for 30 min to remove endogenous peroxidase activity. Sections were then blocked with 10% normal serum and incubated overnight at 4° C with antibodies against MMP-12 (sc-390863, Santa Cruz Biotechnology), MAC-3 (sc-19991, Santa Cruz Biotechnology, Dallas, TX, USA), CD3 (A0452, Dako, Agilent Technologies Co., Hamburg, Germany), MCP-1 (sc-1785, 1:100, Santa Cruz Biotechnology Inc.) or ELANE (M0752, Dako). After washing, samples were incubated for 1 h with a biotinylated secondary antibody (Vector Laboratories, Burlingame, CA, USA). After rinsing three times in PBS, standard Vectastain (ABC) avidin-biotin peroxidase complex (Vector Laboratories) was applied, and the slides were incubated for 30 min. Colour was developed using 3,3'-diaminobenzidine (DAB) and sections were counterstained with haematoxylin before dehydration, clearing, and mounting. Negative controls in which the primary antibody was omitted were included to test for non-specific binding. The histological characterization of aortic samples was performed by haematoxylin-eosin staining. A blinded operator carried out the quantitative morphological assessment of luminal and outer abdominal aortic areas performed by image analysis on haematoxylin-eosin stained sections using ImageJ software. To assess elastic fibre integrity, arterial sections were stained with orcein using a commercial kit (Casa Álvarez, Madrid, Spain).

***In situ* Zymography**

Gelatinolytic activity was assessed in OCT-embedded unfixed frozen tissue sections (8 µm) using Quenched Fluorogenic DQ™ gelatin (D-12054, Thermo Fisher Scientific, Waltham, Massachusetts, MA, USA) as a fluorogenic substrate. Briefly, DQ-gelatin was dissolved in water at 1mg/mL and then diluted 1:10 in 1% (w/v) low gelling temperature agarose (A9414, Sigma-Aldrich). The mixture was applied onto each section and cover-slipped. Samples were incubated at 4° C for 30 min, to allow gelatin gelling, and then maintained at room temperature for 24 h protected from light. FITC fluorescence was visualized using a Leica TCS SP5 confocal microscopy (excitation wavelength: 495 nm; emission wavelength: 515 nm) and the Leica LAS AF Lite software (Leica Microsistemas S.L.U). The fluorescence intensity of each section, excluding elastin fiber autofluorescence, was determined using Image J software. Negative controls in which samples were pre-incubated with 20 mM EDTA before the addition of the labelled substrate were included.

Microarrays

2. Rodríguez-Calvo R, Guadall A, Calvayrac O, Navarro MA, Alonso J, Ferrán B, de Diego A, Muniesa P, Osada J, Rodríguez C, Martínez-González J. Over-expression of neuron-derived orphan receptor-1 (NOR-1) exacerbates neointimal hyperplasia after vascular injury. *Hum Mol Genet* 2013;22:1949-1959.
3. Galán M, Varona S, Orriols M, Rodríguez JA, Aguiló S, Dilmé J, Camacho M, Martínez-González J, Rodriguez C. Induction of histone deacetylases (HDACs) in human abdominal aortic aneurysm: therapeutic potential of HDAC inhibitors. *Dis Model Mech*. 2016;9:541-552.
4. Manning MW, Cassis LA, Daugherty A. Differential effects of doxycycline, a broad-spectrum matrix metalloproteinase inhibitor, on angiotensin II-induced atherosclerosis and abdominal aortic aneurysms. *Arterioscler Thromb Vasc Biol*. 2003;23:483-488.
5. Huber W, Carey VJ, Gentleman R, Anders S, Carlson M, Carvalho BS, Bravo HC, Davis S, Gatto L, Girke T, Gottardo R, Hahne F, Hansen KD, Irizarry RA, Lawrence M, Love MI, MacDonald J, Obenchain V, Oleś AK, Pagès H, Reyes A, Shannon P, SmythGK, Tenenbaum D, Waldron L, Morgan M. Orchestrating high-throughput genomic analysis with Bioconductor. *Nat Methods*. 2015;12:115-121.
6. Ritchie ME, Silver J, Oshlack A, Holmes M, Diyagama D, Holloway A, Smyth GK. A comparison of background correction methods for two-colour microarrays. *Bioinformatics*. 2007;23:2700-2707.

Table S1. TaqMan Gene Expression Assays-on-Demand or oligonucleotides for real-time PCR with SYBR-Green used for the validation of microarray data.

Target gene	Oligonucleotides or Taqman Gene Expression Assays
Acta2	F: 5'-TGACTCACAACGTGCCTATC-3' R: 5'-GCTCGGCAGTAGTCACGAA-3'
Adam8	F: 5'-GCCCCAAAGATACCAAATCAGTTTA-3' R: 5- GGTGCAAAGGTTGGCTTGAC-3'
Ccnb1	F: 5'-TTGTGTGCCCAAGAAGATGC-3' R: 5'-ACGTCAACCTCTCCGACTTT-3'
Cd300c2	F: 5'-GGCTCCTTGGGGTTCGATAA-3' R:5'- GCAGGGAGCAGGAATTGTGT-3'
Cd5l	F: 5'-GGAGGTGATCTGCACAGACTT-3' R: 5'-AGCCCACAGCCTGATGTAAC-3'
Cdc20	Mm00650983_g1
Col10a	F: 5'-AACAGGTATGCCCGTGTCTG-3' R: 5'-TCATCAAATGGGATGGGGGC-3'
Cthrc1	F: 5'-GTGTTCGTGGAGTTCGCTGA-3' R: 5'-AAGCGAGCCACTGAACAGAA-3'
Dync1i1	F: 5'-CAGCGTGAGACAGCACATC-3' R: 5'-GTCAGACATGTTTGCTTCCTGA-3'
Itg8	F: 5'- ACACGTTCCTCAAGAGAAAGAA-3' R: 5'- TAACCGACGTCTTAACCGCT -3'
Kif20a	Mm00436226_m1
Loxl2	Mm00804740_m1
Mmp12	F: 5'-AGTCGGAGGGAACAGGTTGA-3' R: 5'-ATCTTGACAAGTACCATTCAGCAA-3'
Myh11	F: 5'-CAGGAGGTAGAAGGTGCTGTC-3' R: 5'-TTTGCTTCAGCGACTTGGTG-3'
Npy	Mm01410146_m1
Scg2	F: 5'-CAGCGGCAGAGAGGAGC-3' R: 5'-AGCCATGTCTTAAAGATTTCCTCTG-3'
Sh2d1b1	F: 5'-TGTGCCTCTGTGTCTCGTTT-3' R: 5'-TCCCTCTTTGGCATAGGTTG-3'
Syt4	F: 5'- GGGGTGAACTTCTGGTCTCTC -3' R: 5'- CACTTTGACGTAGGGATCTGAAA -3'
Uhrf1	F: 5'-TGTGGACGTGCGTGACAATA-3' R: 5'- CTCCATGCTCTGGATAGTCATCA-3'

F: Forward primer; R: Reverse primer

Table S2. Body weight of WT and NOR-1 transgenic mice subjected to AngII or saline infusion in the presence or in the absence of doxycycline

		0 DAYS	7 DAYS	14 DAYS	21 DAYS	28 DAYS
1	**WT/Sal** (n=10)	25.2 ± 0.6	25.8 ± 0.6	26,1 ± 0.7	26.5 ± 0.6	26.5 ± 0.6
2	**WT/AngII** (n=10)	26.3 ± 0.6	25.9 ± 0.6	26.4 ± 0.6	26.7 ± 0.6	27.2 ± 0.6
3	**TgNOR-1/Sal** (n=10)	25.6 ± 1.1	26.0 ± 1.1	26.5 ± 0.9	26.9 ± 0.9	26.7 ± 0.9
4	**TgNOR-1/AngII** (n=10)	25.8 ± 0.4	25.2 ± 0.5	26.1 ± 0.6	26.7 ± 0.5	26.1 ± 0.4
5	**TgNOR-1^{VSMC}/Sal** (n=10)	25.2 ± 0.9	25.5 ± 0.7	26.3 ± 0.9	26.8 ±1.2	26.9 ± 1.1
6	**TgNOR-1^{VSMC}/ AngII** (n=10)	24.3 ± 0.9	23.5 ± 0.5	24.2 ± 0.5	24.4 ± 0.6	24.9 ± 0.8
7	**WT/AngII** (n=17)	24.6 ± 0.7	24.6 ± 0.7	24.5 ± 0.6	24.9 ± 0.6	25.2 ± 0.7
8	**TgNOR-1^{VSMC}/AngII** (n=16)	24.2 ± 0.6	25.9 ± 0.5	26.0 ± 0.4	26.4 ± 0.4*	26.9 ± 0.5*
9	**TgNOR-1^{VSMC}/AngII/Dox** (n=10)	24.5 ± 0.2	24.4 ± 0.3	24.8 ± 0.4	25.4 ± 0.4	25.8 ± 0.3

Body weight (g) is expressed as mean±SEM. * $p<0.05$ *vs.* t=0. Two-way ANOVA with repeated measures. Numbers in left colum indicate the experimental group. Dox: doxycycline. Animals were grouped according to the experimental approach (1 to 6 and 7 to 9).

Table S3. Differentially expressed genes (DEGs) between TgNOR-1^{VSMC} and WT mice after AngII infusion

ProbeName	SystematicName	EnsemblID	gene_id	GeneSymbol	GeneName	FC	logFC	P.Value	adj.P.Val
A_55_P2089520	NM_009925	ENSMUST00000105511	12813	*Col10a1*	collagen, type X, alpha 1	17,3260136	4,11486785	3,87E-06	0,03291643
A_51_P339934	NM_010910	ENSMUST00000022639	18039	*Nefl*	neurofilament, light polypeptide	13,3567752	3,73949983	1,11E-04	0,03291643
A_55_P2034870	NM_001024147	ENSMUST00000031124	545758	*Slc10a4l*	solute carrier family 10 (sodium/bile acid cotransporter family), me	12,905585	3,68992363	3,03E-04	0,03315398
A_55_P2058957	NM_001252341	ENSMUST00000064054	20979	*Syt1*	synaptotagmin I	12,7440043	3,67174675	4,84E-04	0,03469594
A_55_P2162988	NM_178915	ENSMUST00000066791	104885	*Tmem179*	transmembrane protein 179	12,4869072	3,64234428	8,81E-05	0,03291643
A_55_P1956567	NM_023852	ENSMUST00000167824	67295	*Rab3c*	RAB3C, member RAS oncogene family	9,83670425	3,29817503	3,23E-04	0,03315398
A_51_P237668	NM_009749	ENSMUST00000049130	12069	*Bex2*	brain expressed X-linked 2	8,66531931	3,11525291	5,58E-05	0,03291643
A_55_P1953861	NM_198627	ENSMUST00000109523	277432	*Vstm2l*	V-set and transmembrane domain containing 2-like	8,53030172	3,09259677	2,41E-04	0,03291643
A_52_P98614	NM_009209	ENSMUST00000072939	20538	*Slc6a2*	solute carrier family 6 (neurotransmitter transporter, noradrenalin	8,09293199	3,01666247	2,01E-04	0,03291643
A_51_P191669	NM_007694	ENSMUST00000028826	12653	*Chgb*	chromogranin B	7,99863067	2,99975304	5,66E-04	0,03481832
A_51_P163953	NM_008741	ENSMUST00000020537	18197	*Nsg2*	neuron specific gene family member 2	7,98977913	2,99815562	4,28E-04	0,03393479
A_55_P2072233	NM_028325	ENSMUST00000115256	72693	*Zcchc12*	zinc finger, CCHC domain containing 12	7,48093457	2,90321851	1,34E-04	0,03291643
A_55_P1992490	NM_009129	ENSMUST00000049972	20254	*Scg2*	secretogranin II	7,42230729	2,89186773	7,01E-04	0,03558895
A_51_P140690	NM_009133	ENSMUST00000103045	20262	*Stmn3*	stathmin-like 3	7,3668767	2,8810531	3,15E-05	0,03291643
A_51_P277275	NM_009065	ENSMUST00000153060	19762	*Rit2*	Ras-like without CAAX 2	7,34376825	2,87652053	1,63E-04	0,03291643
A_55_P2110497	NM_001190448	ENSMUST00000109659	13195	*Ddc*	dopa decarboxylase	7,27178547	2,86230964	1,12E-04	0,03291643
A_55_P2000284	NM_008887	ENSMUST00000008090	11859	*Phox2a*	paired-like homeobox 2a	7,25464569	2,85890516	1,85E-04	0,03291643
A_55_P2100375	NM_007729	ENSMUST00000092155	12814	*Col11a1*	collagen, type XI, alpha 1	7,16451654	2,84086936	1,85E-04	0,03291643
A_55_P2090429	NM_010063	ENSMUST00000115555	13426	*Dync1i1*	dynein cytoplasmic 1 intermediate chain 1	7,12091029	2,83206168	2,88E-05	0,03291643
A_51_P305003	NM_001033124	ENSMUST00000029712	18211	*Ntrk1*	neurotrophic tyrosine kinase, receptor, type 1	7,11232597	2,83032145	8,25E-05	0,03291643
A_55_P2041828	NM_023279	ENSMUST00000071134	22152	*Tubb3*	tubulin, beta 3 class III	7,09658845	2,82712564	3,11E-04	0,03315398
A_51_P454873	NM_023456	ENSMUST00000031843	109648	*Npy*	neuropeptide Y	7,07450101	2,82262839	3,69E-04	0,03369759
A_52_P236448	NM_033217	ENSMUST00000000122	18053	*Ngfr*	nerve growth factor receptor (TNFR superfamily, member 16)	7,06709176	2,82111664	3,95E-04	0,03373901
A_55_P2090025	NM_001252292	ENSMUST00000163949	17294	*Mest*	mesoderm specific transcript	7,04011347	2,81559868	1,52E-03	0,04214302
A_55_P2081785	NM_173774	ENSMUST00000037827	242773	*Slc45a1*	solute carrier family 45, member 1	6,99066053	2,80542878	8,55E-05	0,03291643
A_55_P1968895	NM_013639	ENSMUST00000047104	19132	*Prph*	peripherin	6,87651385	2,78167735	4,25E-05	0,03291643
A_55_P2055127	NM_172861	ENSMUST00000091259	241919	*Slc7a14*	solute carrier family 7 (cationic amino acid transporter, y+ system)	6,86373321	2,77899348	1,85E-04	0,03291643
A_52_P562676	NM_013873	ENSMUST00000082365	29859	*Sult4a1*	sulfotransferase family 4A, member 1	6,81041387	2,76774247	1,28E-04	0,03291643
A_55_P2164659	NM_009392	ENSMUST00000089641	21909	*Tlx2*	T cell leukemia, homeobox 2	6,80229832	2,76602228	1,22E-04	0,03291643
A_51_P290074	NM_021272	ENSMUST00000020024	12140	*Fabp7*	fatty acid binding protein 7, brain	6,71434572	2,74724682	2,72E-04	0,03315398
A_55_P2125311	NM_023537	ENSMUST00000003502	69908	*Rab3b*	RAB3B, member RAS oncogene family	6,46409302	2,69244796	7,60E-05	0,03291643
A_52_P465980	NM_007756	ENSMUST00000046892	12889	*Cplx1*	complexin 1	6,42567126	2,68384717	1,14E-04	0,03291643
A_55_P1974243	NM_138942	ENSMUSP00000000910	13166	*Dbh*	dopamine beta hydroxylase	6,26395003	2,6470727	8,21E-05	0,03291643
A_55_P2275249	NM_009377	ENSMUST00000000219	21823	*Th*	tyrosine hydroxylase	6,13547812	2,61717577	2,53E-05	0,03291643
A_55_P2090330	NM_021452	ENSMUST00000068233	58802	*Kcnmb4*	potassium large conductance calcium-activated channel, subfamily	6,07129222	2,60200361	3,47E-04	0,03319727
A_55_P2040549	NM_008888	ENSMUST00000012664	18935	*Phox2b*	paired-like homeobox 2b	5,96292675	2,57602062	4,03E-04	0,03373901
A_55_P2000943	NM_020610	ENSMUST00000033331	78593	*Nrip3*	nuclear receptor interacting protein 3	5,82266982	2,54168081	2,72E-04	0,03315398
A_55_P2081323	NM_019690	ENSMUST00000180362	14683	*Gnas*	GNAS (guanine nucleotide binding protein, alpha stimulating) com	5,80494201	2,53728165	6,57E-05	0,03291643
A_55_P1979848	NM_175235	ENSMUST00000121266	76183	*Celf6*	CUGBP, Elav-like family member 6	5,71918724	2,51581014	3,01E-04	0,03315398
A_52_P628915	NM_009308	ENSMUST00000025110	20983	*Syt4*	synaptotagmin IV	5,62104782	2,49083909	3,37E-04	0,03315398
A_55_P2096867	NM_008083	ENSMUST00000125187	14432	*Gap43*	growth associated protein 43	5,60562737	2,48687585	6,09E-05	0,03291643
A_55_P2053181	NM_010904	ENSMUST00000093369	380684	*Nefh*	neurofilament, heavy polypeptide	5,45959692	2,44879444	1,00E-04	0,03291643
A_55_P2111322	AY170578		16142	*Iglv1*	immunoglobulin lambda variable 1	5,37138903	2,42529521	9,41E-05	0,03291643
A_52_P101399	NM_177735	ENSMUST00000061446	243339	*Tmem130*	transmembrane protein 130	5,3612857	2,42257902	3,72E-04	0,03370264
A_55_P1968858	NM_012061	ENSMUST00000177814	27062	*Cadps*	Ca2+-dependent secretion activator	5,29018748	2,40331885	1,68E-04	0,03291643
A_51_P423518	NM_175007	ENSMUST00000003345	218038	*Amph*	amphiphysin	5,28001111	2,40054096	7,94E-04	0,03629498
A_51_P145220	NM_008691	ENSMUST00000022638	18040	*Nefm*	neurofilament, medium polypeptide	5,05736688	2,33838644	2,58E-04	0,03291643
A_55_P2143946	NM_172523	ENSMUST00000026084	214084	*Slc18a2*	solute carrier family 18 (vesicular monoamine), member 2	4,99285556	2,31986517	3,44E-04	0,03315398
A_55_P2105135	NM_001177731	ENSMUST00000179313	244958	*Mrap2*	melanocortin 2 receptor accessory protein 2	4,97929001	2,31594005	1,28E-04	0,03291643
A_55_P2291054	NM_001177883	ENSMUST00000107124	15569	*Elavl2*	ELAV like RNA binding protein 1	4,92621428	2,30047938	9,79E-04	0,03761298
A_51_P358316	NM_007693	ENSMUST00000021610	12652	*Chga*	chromogranin A	4,87046164	2,28405852	2,31E-03	0,04795298
A_51_P205779	NM_009690	ENSMUST00000015998	11801	*Cd5l*	CD5 antigen-like	4,862883	2,28181188	1,78E-03	0,04399008

A_51_P438841	NM_009819	ENSMUST00000159626	12386	*Ctnna2*	catenin (cadherin associated protein), alpha 2	4,79599159	2,26182913	1,19E-03	0,03904427
A_52_P453785	NM_026778	ENSMUST00000067072	68588	*Cthrc1*	collagen triple helix repeat containing 1	4,77274874	2,25482039	1,48E-04	0,03291643
A_55_P2007500	NM_001013749	ENSMUST00000180252	210573	*Tmem151b*	transmembrane protein 151B	4,71029351	2,23581696	8,14E-04	0,03629498
A_51_P334876	NM_007384	ENSMUST00000021045	11418	*Asic2*	acid-sensing (proton-gated) ion channel 2	4,55166993	2,18639594	4,20E-05	0,03291643
A_55_P2031021	NM_009052	ENSMUST00000113118	19716	*Bex1*	brain expressed gene 1	4,51216757	2,17382065	7,42E-05	0,03291643
A_51_P107020	NM_001039000	ENSMUST00000099172	16572	*Kif5a*	kinesin family member 5A	4,48608183	2,16545594	6,34E-04	0,03546117
A_55_P1960351	NM_001159647	ENSMUST00000068378	12805	*Cntn1*	contactin 1	4,4734987	2,1614036	6,36E-04	0,03546117
A_51_P448478	NM_173403	ENSMUST00000031127	231290	*Slc10a4*	solute carrier family 10 (sodium/bile acid cotransporter family), me	4,47172864	2,16083264	8,88E-05	0,03291643
A_55_P2038422	NM_001033877	ENSMUST00000098382	233332	*Adamts17*	a disintegrin-like and metallopeptidase (reprolysin type) with throı	4,42473844	2,14559217	8,17E-05	0,03291643
A_51_P461779	NM_172994	ENSMUST00000031003	269643	*Ppp2r2c*	protein phosphatase 2, regulatory subunit B, gamma	4,40378425	2,13874379	4,16E-04	0,03386016
A_55_P2058330	NM_020287	ENSMUST00000051857	56856	*Insm2*	insulinoma-associated 2	4,37758974	2,13013675	1,29E-03	0,03982756
A_55_P2085060	NM_001039385	ENSMUST00000041543	381677	*Vgf*	VGF nerve growth factor inducible	4,372054	2,12831122	1,08E-04	0,03291643
A_51_P282594	NM_026805	ENSMUST00000058472	68666	*Svop*	SV2 related protein	4,36218317	2,12505035	1,57E-04	0,03291643
A_55_P1963965	NM_198959	ENSMUST00000030562	230777	*Hcrtr1*	hypocretin (orexin) receptor 1	4,30180932	2,10494358	8,32E-05	0,03291643
A_55_P2117425	NM_016908	ENSMUST00000065957	53420	*Syt5*	synaptotagmin V	4,27302026	2,09525616	4,21E-04	0,03391783
A_51_P392303	NM_010733	ENSMUST00000043884	16981	*Lrrn3*	leucine rich repeat protein 3, neuronal	4,26385257	2,09215756	3,11E-04	0,03315398
A_55_P2181341	NM_001277925	ENSMUST00000027463	13599	*Ece1*	endothelin converting enzyme-like 1	4,23378466	2,08194789	2,60E-05	0,03291643
A_51_P516870	NM_008409	ENSMUST00000033591	16431	*Itm2a*	integral membrane protein 2A	4,22739523	2,079769	1,17E-04	0,03291643
A_51_P346491	NM_001111015	ENSMUST00000009538	20965	*Syn2*	synapsin II	4,20943936	2,0736281	2,02E-03	0,0464094
A_51_P360396	NM_001025305	ENSMUST00000064976	21419	*Tfap2b*	transcription factor AP-2 beta	4,14990216	2,05307732	3,44E-04	0,03315398
A_52_P90805	NM_028973	ENSMUST00000064606	74488	*Lrrc15*	leucine rich repeat containing 15	4,12064147	2,04286894	3,17E-04	0,03315398
A_52_P627068	NM_170593	ENSMUST00000037547	214240	*Disp2*	dispatched RND transporter family member 2	4,10068056	2,03586336	1,79E-04	0,03291643
A_51_P448784	NM_009513	ENSMUST00000057866	22360	*Nrsn1*	neurensin 1	4,05423606	2,01943009	9,54E-04	0,0372285
A_55_P1981929	NM_009162	ENSMUST00000024005	20394	*Scg5*	secretogranin V	4,0281899	2,0101317	2,52E-04	0,03291643
A_55_P2068673	NM_025285	ENSMUST00000029002	20257	*Stmn2*	stathmin-like 2	4,01236237	2,00445191	2,86E-04	0,03315398
A_51_P307168	NM_026993	ENSMUST00000029845	69219	*Ddah1*	dimethylarginine dimethylaminohydrolase 1	3,98228931	1,99359804	1,36E-04	0,03291643
A_55_P2048119	NM_146257	ENSMUST00000058418	243328	*Slc29a4*	solute carrier family 29 (nucleoside transporters), member 4	3,96659125	1,98789974	1,79E-04	0,03291643
A_55_P2020607	NM_001286743	ENSMUST00000045896	23969	*Pacsin1*	protein kinase C and casein kinase substrate in neurons 1	3,94255136	1,97912955	1,27E-03	0,03970879
A_55_P2121185	NM_011010	ENSMUST00000098281	18378	*Omp*	olfactory marker protein	3,93262019	1,97549086	8,24E-04	0,03629498
A_51_P389988	NM_016917	ENSMUST00000027137	53945	*Slc40a1*	solute carrier family 40 (iron-regulated transporter), member 1	3,93235048	1,97539191	1,71E-03	0,04357357
A_52_P400425	NM_178656	ENSMUST00000123434	193003	*Pirt*	phosphoinositide-interacting regulator of transient receptor poten	3,88219005	1,95687074	5,79E-04	0,03507191
A_55_P2248806	XM_006540361	ENSMUST00000038163	71691	*Pnmal1*	PNMA-like 1	3,85912975	1,94827555	1,59E-03	0,04266154
A_51_P259029	NM_025869	ENSMUST00000170204	66959	*Dusp26*	dual specificity phosphatase 26 (putative)	3,7655988	1,9128793	4,94E-04	0,03476444
A_55_P2167486	NM_009049	ENSMUST00000039534	19711	*Resp18*	regulated endocrine-specific protein 18	3,74573841	1,90525015	3,43E-04	0,03315398
A_51_P220278	NM_028392	ENSMUST00000025377	72930	*Ppp2r2b*	protein phosphatase 2, regulatory subunit B, beta	3,70241643	1,88846717	1,55E-03	0,04234259
A_55_P2017600	NM_001136058	ENSMUST00000114158	12933	*Crmp1*	collapsin response mediator protein 1	3,68339152	1,88103476	2,56E-04	0,03291643
A_55_P2177658	NM_019945	ENSMUST00000153000	56527	*Mast1*	microtubule associated serine/threonine kinase 1	3,68159426	1,88033064	9,99E-04	0,03807877
A_55_P1993840	NM_175432	ENSMUST00000119026	208213	*Tmem132c*	transmembrane protein 132C	3,67761848	1,87877182	1,44E-04	0,03291643
A_51_P419117	NM_134050	ENSMUST00000021459	104886	*Rab15*	RAB15, member RAS oncogene family	3,66935834	1,8755278	4,81E-04	0,03469594
A_55_P2003541	NM_176930	ENSMUST00000020939	319504	*Nrcam*	neuronal cell adhesion molecule	3,65047718	1,86808506	1,01E-03	0,03808028
A_51_P391291	NM_010316	ENSMUST00000096259	14704	*Gng3*	guanine nucleotide binding protein (G protein), gamma 3	3,62078693	1,85630328	2,43E-04	0,03291643
A_55_P1971010	NM_010373	ENSMUST00000089549	14942	*Gzme*	granzyme E	3,6042405	1,84969528	2,22E-03	0,04740503
A_51_P307741	NM_009827	ENSMUST00000031093	12425	*Cckar*	cholecystokinin A receptor	3,5753678	1,83809166	7,96E-06	0,03291643
A_55_P1999532	NM_007740	ENSMUST00000054588	12839	*Col9a1*	collagen, type IX, alpha 1	3,57052657	1,83613685	8,30E-04	0,03629498
A_51_P108183	NM_022322	ENSMUST00000033602	64103	*Tnmd*	tenomodulin	3,54361741	1,82522285	5,42E-04	0,03476444
A_55_P2026530	NM_177814	ENSMUST00000090302	238988	*Erc2*	ELKS/RAB6-interacting/CAST family member 2	3,52806101	1,81887551	8,17E-04	0,03629498
A_55_P2096035	NM_001252347	ENSMUST00000107102	51799	*Rundc3a*	RUN domain containing 3A	3,4670421	1,79370536	3,15E-04	0,03315398
A_51_P486681	NM_021492	ENSMUST00000082090	11775	*Ap3b2*	adaptor-related protein complex 3, beta 2 subunit	3,44538132	1,78466366	4,29E-04	0,03393479
A_52_P596595	NM_175498	ENSMUST00000089236	239157	*Pnma2*	paraneoplastic antigen MA2	3,40420965	1,76731989	5,87E-04	0,03507191
A_55_P1982186	NM_172718	ENSMUST00000057209	52850	*Sgsm1*	small G protein signaling modulator 1	3,40052851	1,76575899	1,10E-03	0,03829864
A_55_P2143251	ENSMUST00000071(	ENSMUST00000071093	242662	*Rims3*	regulating synaptic membrane exocytosis 3	3,39447766	1,76318959	3,21E-04	0,03315398
A_55_P1961968	NM_009538	ENSMUST00000121646	22634	*Plagl1*	pleiomorphic adenoma gene-like 1	3,36975162	1,75264226	5,17E-04	0,03476444
A_55_P2086240	NM_001003824	ENSMUST00000149964	16536	*Kcnq2*	potassium voltage-gated channel, subfamily Q, member 2	3,36188258	1,74926933	1,06E-03	0,03818548
A_52_P265937	NM_019754	ENSMUST00000096057	56370	*Tagln3*	transgelin 3	3,36180791	1,74923729	1,76E-03	0,04380084
A_55_P2164629	NM_008973	ENSMUST00000101534	19242	*Ptn*	pleiotrophin	3,34740225	1,74304193	5,59E-04	0,03476444

A_52_P370392	NM_021921	ENSMUST00000023291	60597	*Mapk8ip2*	mitogen-activated protein kinase 8 interacting protein 2	3,28327672	1,71513635	3,61E-04	0,03369759
A_55_P1971599	NM_007529	ENSMUST00000090971	12032	*Bcan*	brevican	3,27730617	1,71251046	6,14E-04	0,0352913
A_55_P2105472	NM_019409	ENSMUST00000164465	18377	*Omg*	oligodendrocyte myelin glycoprotein	3,26670423	1,70783584	1,35E-03	0,04041885
A_55_P2062469	NM_001290308	ENSMUST00000071750	12816	*Col12a1*	collagen, type XII, alpha 1	3,24717151	1,69918359	8,20E-05	0,03291643
A_52_P500979	NM_013628	ENSMUST00000022075	18548	*Pcsk1*	proprotein convertase subtilisin/kexin type 1	3,23180891	1,6923419	2,19E-04	0,03291643
A_55_P2162910	NM_153457	ENSMUST00000021497	104001	*Rtn1*	reticulon 1	3,22670911	1,69006352	3,12E-04	0,03315398
A_52_P239320	NM_207708	ENSMUST00000009727	20972	*Syngr1*	synaptogyrin 1	3,21804934	1,68618645	1,47E-03	0,04166534
A_55_P1992572	NM_001146292	ENSMUST00000115816	108013	*Celf4*	CUGBP, Elav-like family member 4	3,202273	1,67909631	1,71E-03	0,04366843
A_51_P142813	NM_025711	ENSMUST00000021820	66695	*Aspn*	asporin	3,19865509	1,67746543	1,25E-04	0,03291643
A_51_P417251	NM_134022	ENSMUST00000238695	103712	*6330403K07Rik*	RIKEN cDNA 6330403K07 gene	3,17191737	1,66535519	1,65E-04	0,03291643
A_51_P462391	NM_010267	ENSMUST00000026879	14545	*Gdap1*	ganglioside-induced differentiation-associated-protein 1	3,16350616	1,6615244	8,11E-04	0,03629498
A_55_P2107432	NM_153054	ENSMUST00000037478	110877	*Slc18a1*	solute carrier family 18 (vesicular monoamine), member 1	3,15140673	1,65599596	1,25E-05	0,03291643
A_52_P365660	NM_178725	ENSMUST00000162807	241568	*Lrrc4c*	leucine rich repeat containing 4C	3,14789452	1,6543872	7,89E-04	0,03629498
A_55_P2033376	NM_001163145	ENSMUST00000080751	72301	*Shisal1*	shisa like 1	3,13285424	1,64747765	0,00030995	0,03315398
A_55_P2025765	NM_007403	ENSMUST00000128332	11501	*Adam8*	a disintegrin and metallopeptidase domain 8	3,12624943	1,64443289	0,00148434	0,04180691
A_55_P2043627	NM_001081120	ENSMUST00000055257	69627	*Fam89a*	family with sequence similarity 89, member A	3,11013632	1,63697782	0,00062123	0,03546117
A_52_P496202	NM_013892	ENSMUST00000041096	30052	*Pcsk1n*	proprotein convertase subtilisin/kexin type 1 inhibitor	3,10193113	1,63316665	0,00025288	0,03291643
A_55_P1997831	NM_028146	ENSMUST00000074879	72185	*Dbndd1*	dysbindin (dystrobrevin binding protein 1) domain containing 1	3,09501117	1,62994461	0,00020466	0,03291643
A_51_P249286	NM_011267	ENSMUST00000027748	19734	*Rgs16*	regulator of G-protein signaling 16	3,09442394	1,62967086	0,0002538	0,03291643
A_55_P2070992	NM_009657	ENSMUST00000017534	11676	*Aldoc*	aldolase C, fructose-bisphosphate	3,08245984	1,6240821	0,00064577	0,03555961
A_55_P2109326	NM_001290010	ENSMUST00000150983	11423	*Ache*	acetylcholinesterase	3,06701402	1,61683476	1,25E-04	0,03291643
A_52_P671132	NM_152915	ENSMUST00000049126	227325	*Dner*	delta/notch-like EGF-related receptor	3,05720788	1,61221466	3,48E-05	0,03291643
A_55_P2171206	NM_013592	ENSMUST00000103103	17183	*Matn4*	matrilin 4	3,05472143	1,61104082	0,00053741	0,03476444
A_55_P2126192	NM_010195	ENSMUST00000020350	14160	*Lgr5*	leucine rich repeat containing G protein coupled receptor 5	3,0415289	1,60479671	1,82E-03	0,04447998
A_52_P292792	NM_007739	ENSMUST00000089332	12837	*Col8a1*	collagen, type VIII, alpha 1	3,01848024	1,59382236	0,00040971	0,03379356
A_55_P1958165	NM_001276398	ENSMUST00000056035	109225	*Ms4a7*	membrane-spanning 4-domains, subfamily A, member 7	3,00153938	1,5857026	0,00073439	0,03593548
A_51_P144957	NM_146140	ENSMUST00000058994	229801	*Tram1l1*	translocation associated membrane protein 1-like 1	2,99935947	1,58465444	9,40E-05	0,03291643
A_55_P2146214	NM_001035510	ENSMUST00000113067	66995	*Zcchc18*	zinc finger, CCHC domain containing 18	2,98416861	1,57732905	5,78E-04	0,03507191
A_55_P2127433	NM_026571	ENSMUST00000080780	328789	*Lhfpl5*	lipoma HMGIC fusion partner-like 5	2,97659645	1,57366364	0,00028917	0,03315398
A_55_P2025690	NM_022025	ENSMUST00000095712	63993	*Slc5a7*	solute carrier family 5 (choline transporter), member 7	2,97328537	1,57205794	1,22E-03	0,03916734
A_52_P121342	NM_020252	ENSMUST00000160844	18189	*Nrxn1*	neurexin I	2,96363442	1,5673675	0,0006857	0,03558895
A_55_P2176792	NM_017400	ENSMUST00000032874	20408	*Sh3gl3*	SH3-domain GRB2-like 3	2,94386057	1,55770934	0,00072882	0,03593548
A_51_P143951	NM_007495	ENSMUST00000046110	11899	*Astn1*	astrotactin 1	2,93587211	1,55378913	0,00173442	0,04380084
A_55_P1984815	NM_198214	ENSMUST00000028951	241727	*Snph*	syntaphilin	2,9242289	1,54805624	0,00048225	0,03469594
A_51_P295237	NM_172784	ENSMUST00000019931	237253	*Lrp11*	low density lipoprotein receptor-related protein 11	2,90283602	1,53746308	5,97E-04	0,03507191
A_51_P106591	NM_172434	ENSMUST00000029784	78784	*Celf3*	CUGBP, Elav-like family member 3	2,90054795	1,53632547	0,00067014	0,03555961
A_66_P138406	NM_027218	ENSMUST00000077228	69810	*Clec4b1*	C-type lectin domain family 4, member b1	2,88020786	1,52617293	0,00021841	0,03291643
A_55_P2160910	NM_028224	ENSMUST00000023750	72393	*Faim2*	Fas apoptotic inhibitory molecule 2	2,87843082	1,52528254	0,00127259	0,03970879
A_55_P2008437	NM_009877	ENSMUST00000060501	12578	*Cdkn2a*	cyclin-dependent kinase inhibitor 2A	2,8678428	1,51996594	0,00123475	0,0393138
A_55_P2179587	NM_080437	ENSMUST00000024238	107934	*Celsr3*	cadherin, EGF LAG seven-pass G-type receptor 3	2,86526271	1,51866742	0,00151147	0,04191356
A_51_P417720	NM_176922	ENSMUST00000034774	319480	*Itga11*	integrin alpha 11	2,86525431	1,51866319	0,00018983	0,03291643
A_55_P1960631	NM_199473	ENSMUST00000070132	329941	*Col8a2*	collagen, type VIII, alpha 2	2,86110315	1,51657151	0,0001468	0,03291643
A_51_P220343	NM_018865	ENSMUST00000005255	22402	*Ccn4*	cellular communication network factor 4	2,85741524	1,5147107	1,26E-04	0,03291643
A_51_P515532	NM_029881	ENSMUST00000066049	77220	*Tmem200a*	transmembrane protein 200A	2,85465473	1,51331626	0,00010912	0,03291643
A_55_P2060991	NM_181681	ENSMUST00000166057	216152	*Plppr3*	phospholipid phosphatase related 3	2,85025022	1,51108858	0,00024748	0,03291643
A_51_P389885	NM_011461	ENSMUST00000133724	20728	*Spic*	Spi-C transcription factor (Spi-1/PU.1 related)	2,84578817	1,50882827	0,00107019	0,03823006
A_55_P1983773	NM_001012273	ENSMUST00000081387	11799	*Birc5*	baculoviral IAP repeat-containing 5	2,83610924	1,5039131	0,00026638	0,03315398
A_55_P2182835	NM_148944	ENSMUST00000034854	108015	*Chrnb4*	cholinergic receptor, nicotinic, beta polypeptide 4	2,79733375	1,48405239	0,00121214	0,03911544
A_51_P108226	NM_183249	ENSMUST00000070832	66107	*Wfdc21*	WAP four-disulfide core domain 21	2,79175262	1,48117111	0,00162902	0,04294518
A_51_P408649	NM_145463	ENSMUST00000053949	219134	*Shisa2*	shisa family member 2	2,79162006	1,4811026	0,00013345	0,03291643
A_55_P1964965	NM_001033458	ENSMUST00000142510	381633	*Gm1673*	predicted gene 1673	2,77078033	1,47029234	7,73E-05	0,03291643
A_55_P2132873	NM_144891	ENSMUST00000018087	228858	*Gdap1l1*	ganglioside-induced differentiation-associated protein 1-like 1	2,75911396	1,46420505	0,00059087	0,03507191
A_55_P2034864	NM_023716	ENSMUST00000075774	73710	*Tubb2b*	tubulin, beta 2B class IIB	2,75080112	1,45985184	0,00156398	0,04242288
A_55_P1978216	NM_134158	ENSMUST00000141188	140497	*Cd300c2*	CD300C molecule 2	2,73888362	1,45358796	1,66E-03	0,04318211
A_52_P297093	NM_010770	ENSMUST00000020899	17182	*Matn3*	matrilin 3	2,72647486	1,44703685	2,37E-03	0,0482972

A_55_P1998066	NM_153776	ENSMUST00000058491	69195	*Tmem121*	transmembrane protein 121	2,71625658	1,44161976	0,00010199	0,03291643
A_55_P2154480	NM_001162934	ENSMUST00000099452	381418	*Ctxn2*	cortexin 2	2,70903327	1,43777811	1,02E-04	0,03291643
A_51_P241995	NM_016919	ENSMUST00000004201	53867	*Col5a3*	collagen, type V, alpha 3	2,69887101	1,43235602	0,00039424	0,03373901
A_55_P1961720	NM_175462	ENSMUST00000037580	227632	*Kcnt1*	potassium channel, subfamily T, member 1	2,69067993	1,42797078	0,00172105	0,04371333
A_51_P283016	NM_009200	ENSMUST00000005490	20513	*Slc1a6*	solute carrier family 1 (high affinity aspartate/glutamate transport	2,68960456	1,42739408	4,08E-05	0,03291643
A_51_P172085	NM_008113	ENSMUST00000025019	14570	*Arhgdig*	Rho GDP dissociation inhibitor (GDI) gamma	2,68293071	1,4238098	2,82E-05	0,03291643
A_55_P1988413	NM_011993	ENSMUST00000121184	26757	*Dpysl4*	dihydropyrimidinase-like 4	2,67057933	1,41715274	0,00022476	0,03291643
A_55_P1962937	NM_001272078	ENSMUST00000113237	83433	*Trem2*	triggering receptor expressed on myeloid cells 2	2,6606866	1,41179859	0,00125579	0,03955441
A_51_P161248	NM_009130	ENSMUST00000034699	20255	*Scg3*	secretogranin III	2,65257657	1,40739439	0,00141251	0,041007
A_55_P2066593	NM_011012	ENSMUST00000184795	18389	*Oprl1*	opioid receptor-like 1	2,63732543	1,3990756	0,00090184	0,03680238
A_52_P517247	NM_001033354	ENSMUST00000129815	243621	*Iqsec3*	IQ motif and Sec7 domain 3	2,61472349	1,38665839	0,00203138	0,04641055
A_55_P2072816	NM_177751	ENSMUST00000026750	245684	*Cnksr2*	connector enhancer of kinase suppressor of Ras 2	2,60558063	1,3816049	0,00127219	0,03970879
A_55_P2024803	NM_008605	ENSMUST00000127722	17381	*Mmp12*	matrix metallopeptidase 12	2,5872608	1,37142549	1,46E-05	0,03291643
A_55_P2119772	NM_018732	ENSMUST00000100069	20269	*Scn3a*	sodium channel, voltage-gated, type III, alpha	2,56316572	1,35792676	0,00111229	0,03830608
A_55_P2181356	NM_009866	ENSMUST00000075190	12552	*Cdh11*	cadherin 11	2,54574877	1,34809005	0,00032469	0,03315398
A_51_P290576	NM_152804	ENSMUST00000022212	20620	*Plk2*	polo-like kinase 2	2,54399864	1,3470979	1,39E-05	0,03291643
A_52_P645862	NM_177322	ENSMUST00000066412	11607	*Agtr1a*	angiotensin II receptor, type 1a	2,53119729	1,33981996	0,00039579	0,03373901
A_51_P472217	NM_001081085	ENSMUST00000129214	72080	*Sapcd2*	suppressor APC domain containing 2	2,52105517	1,33402769	0,00010209	0,03291643
A_55_P1978371	NM_001081376	ENSMUST00000030775	269610	*Chd5*	chromodomain helicase DNA binding protein 5	2,5123608	1,32904367	0,00197131	0,04607464
A_55_P2103706	XM_006544821		434175	*Ccnb1-ps*	cyclin B1, pseudogene	2,5100385	1,32770949	0,00019079	0,03291643
A_55_P2074736	NM_008923	ENSMUST00000026973	19085	*Prkar1b*	protein kinase, cAMP dependent regulatory, type I beta	2,50244133	1,32333625	0,00217505	0,04740503
A_55_P2012478	NM_028326	ENSMUST00000064814	72701	*Zfp618*	zinc finger protein 618	2,50220517	1,32320009	3,75E-05	0,03291643
A_55_P2011436	AK030082	ENSMUST00000120560	100039888	*Gm11223*	predicted gene 11223	2,50104037	1,32252834	0,00011561	0,03291643
A_55_P2076891	NM_001145192	ENSMUST00000169935	320722	*Akain1*	A kinase (PRKA) anchor inhibitor 1	2,49476185	1,3189021	0,0008377	0,03629498
A_51_P253803	NM_001081117	ENSMUST00000033310	17345	*Mki67*	antigen identified by monoclonal antibody Ki 67	2,48898547	1,31555781	0,00013168	0,03291643
A_51_P215038	NM_182991	ENSMUST00000045286	67937	*Tmem59l*	transmembrane protein 59-like	2,47962157	1,31011996	0,00087131	0,03654939
A_51_P477121	NM_021451	ENSMUST00000025399	58801	*Pmaip1*	phorbol-12-myristate-13-acetate-induced protein 1	2,47466478	1,30723311	0,00130452	0,04002069
A_51_P164014	NM_173762	ENSMUST00000062893	229841	*Cenpe*	centromere protein E	2,4717487	1,30553207	0,00042187	0,03391783
A_55_P2026139	NM_001013773	ENSMUST00000110929	381680	*Nxpe5*	neurexophilin and PC-esterase domain family, member 5	2,47029886	1,30468559	0,00054504	0,03476444
A_55_P2027083	NM_001039484	ENSMUST00000056136	16513	*Kcnj10*	potassium inwardly-rectifying channel, subfamily J, member 10	2,4668052	1,3026438	0,00123635	0,0393138
A_55_P2118520	NM_007742	ENSMUST00000001547	12842	*Col1a1*	collagen, type I, alpha 1	2,46106941	1,29928535	0,00010268	0,03291643
A_55_P2129348	NM_153510	ENSMUST00000058897	231805	*Pilra*	paired immunoglobin-like type 2 receptor alpha	2,46042056	1,29890493	9,67E-06	0,03291643
A_52_P130787	NM_013568	ENSMUST00000040751	16494	*Kcna6*	potassium voltage-gated channel, shaker-related, subfamily, meml	2,45906649	1,29811075	0,00066642	0,03555961
A_55_P2143499	NM_171824	ENSMUST00000052580	209966	*Pgbd5*	piggyBac transposable element derived 5	2,45664762	1,29669093	0,00197932	0,04608319
A_55_P1985433	NM_178591	ENSMUST00000073884	211323	*Nrg1*	neuregulin 1	2,4532419	1,29468949	0,00020777	0,03291643
A_66_P114461	NM_177328	ENSMUST00000172951	108073	*Grm7*	glutamate receptor, metabotropic 7	2,45220897	1,29408193	0,00254312	0,04970107
A_55_P2078433	NM_026656	ENSMUST00000011152	68279	*Mcoln2*	mucolipin 2	2,45186198	1,29387777	0,00013583	0,03291643
A_52_P628067	NM_013538	ENSMUST00000134637	14793	*Cdca3*	cell division cycle associated 3	2,44648702	1,29071163	0,00016928	0,03291643
A_66_P131398	NM_013846	ENSMUST00000021918	26564	*Ror2*	receptor tyrosine kinase-like orphan receptor 2	2,43400888	1,28333443	0,00111253	0,03830608
A_51_P204402	NM_011369	ENSMUST00000022945	20419	*Shcbp1*	Shc SH2-domain binding protein 1	2,43257793	1,28248602	0,00070233	0,03558895
A_55_P2068663	NM_019641	ENSMUST00000030636	16765	*Stmn1*	stathmin 1	2,42595839	1,27855481	0,00024474	0,03291643
A_55_P2065671	NM_172301	ENSMUST00000147790	268697	*Ccnb1*	cyclin B1	2,42122998	1,27574012	0,00037136	0,03370264
A_52_P599317	NM_001077202	ENSMUST00000088172	50786	*Hs6st2*	heparan sulfate 6-O-sulfotransferase 2	2,40585378	1,26654896	0,00038506	0,03373901
A_51_P422685	NM_177086	ENSMUST00000042352	320158	*Zmat4*	zinc finger, matrin type 4	2,40503335	1,2660569	0,00179907	0,04428159
A_55_P1957459	NM_001291894	ENSMUST00000105481	14728	*Lilrb4a*	leukocyte immunoglobulin-like receptor, subfamily B, member 4	2,40111754	1,26370603	0,00119218	0,03904427
A_51_P363187	NM_008176	ENSMUST00000031327	14825	*Cxcl1*	chemokine (C-X-C motif) ligand 1	2,39950325	1,26273576	8,18E-05	0,03291643
A_55_P2237129	ENSMUST000000442	ENSMUST00000044278	26938	*St6galnac5*	ST6 (alpha-N-acetyl-neuraminyl-2,3-beta-galactosyl-1,3)-N-acetylg	2,39795691	1,26180573	0,0020361	0,04649107
A_52_P304056	NM_001163637	ENSMUST00000082254	76217	*Jakmip2*	janus kinase and microtubule interacting protein 2	2,39390912	1,25936838	0,0017808	0,04399008
A_55_P1962771	NM_001252460	ENSMUST00000093166	76884	*Cyfip2*	cytoplasmic FMR1 interacting protein 2	2,39119864	1,25773398	0,00097139	0,03751707
A_51_P264656	NM_144518	ENSMUST00000056521	67254	*Bmerb1*	bMERB domain containing 1	2,39010871	1,25707624	0,00050256	0,03476444
A_55_P2052281	NM_176834	ENSMUST00000114355	68846	*Rnf208*	ring finger protein 208	2,3814259	1,25182566	0,0008568	0,03629498
A_52_P26299	NM_178675	ENSMUST00000105473	215085	*Slc35f1*	solute carrier family 35, member F1	2,37046216	1,24516836	0,00026043	0,03302481
A_51_P374726	NM_008987	ENSMUST00000029421	19288	*Ptx3*	pentraxin related gene	2,36730382	1,24324487	0,00015606	0,03291643
A_51_P270949	NM_020034	ENSMUST00000080511	56702	*Hist1h1b*	histone cluster 1, H1b	2,36591755	1,2423998	0,0011832	0,03904427
A_51_P513530	NM_017407	ENSMUST00000045026	54141	*Spag5*	sperm associated antigen 5	2,35824526	1,23771377	0,00013974	0,03291643

A_55_P2101367	NM_029741	ENSMUST00000003961	76787	*Ppfia3*	protein tyrosine phosphatase, receptor type, f polypeptide (PTPRF	2,35503049	1,23574574	0,00014106	0,03291643
A_55_P2041708	NM_008087	ENSMUST00000051912	14453	*Gas2*	growth arrest specific 2	2,34496666	1,22956741	0,00040684	0,03376519
A_51_P510891	NM_007423	ENSMUST00000042755	11576	*Afp*	alpha fetoprotein	2,33678159	1,2245229	0,00058164	0,03507191
A_55_P2039699	NM_009921	ENSMUST00000112022	12796	*Camp*	cathelicidin antimicrobial peptide	2,33497021	1,22340415	0,00061207	0,0352913
A_51_P497768	NM_001081089	ENSMUST00000062211	215456	*Gpat2*	glycerol-3-phosphate acyltransferase 2, mitochondrial	2,32995986	1,2203051	0,00209877	0,04685046
A_52_P228551	NM_201367	ENSMUST00000039160	381413	*Gpr176*	G protein-coupled receptor 176	2,32761576	1,21885292	0,00055021	0,03476444
A_51_P481920	NM_009828	ENSMUST00000029270	12428	*Ccna2*	cyclin A2	2,32686047	1,2183847	0,00052555	0,03476444
A_51_P139320	NM_025273	ENSMUST00000020298	13180	*Pcbd1*	pterin 4 alpha carbinolamine dehydratase/dimerization cofactor of	2,30800469	1,20664615	0,00242116	0,04872435
A_55_P2137527	NM_029283	ENSMUST00000060581	75429	*Fam183b*	family with sequence similarity 183, member B	2,30595481	1,20536424	0,00247449	0,04921934
A_51_P497171	NM_008534	ENSMUST00000143463	17085	*Ly9*	lymphocyte antigen 9	2,30401877	1,20415247	0,00067082	0,03555961
A_55_P1995537	NM_010824	ENSMUST00000020779	17523	*Mpo*	myeloperoxidase	2,29108484	1,19603089	0,00115355	0,03884838
A_55_P1974687	NM_177597	ENSMUST00000155819	211147	*March11*	membrane-associated ring finger (C3HC4) 11	2,29062857	1,19574354	0,00106393	0,03818548
A_51_P284686	NM_001040106	ENSMUST00000089519	269774	*Aak1*	AP2 associated kinase 1	2,28734226	1,19367226	0,00085576	0,03629498
A_55_P2139077	NM_001039485	ENSMUST00000046860	667742	*Piezo2*	piezo-type mechanosensitive ion channel component 2	2,27580873	1,18637931	9,46E-05	0,03291643
A_51_P357647	NM_028333	ENSMUST00000027885	72713	*Angptl1*	angiopoietin-like 1	2,27413883	1,18532033	0,00038254	0,03373901
A_66_P132576	NM_001253355	ENSMUST00000058738	319415	*Hs3st5*	heparan sulfate (glucosamine) 3-O-sulfotransferase 5	2,27171921	1,18378453	0,00065172	0,03555961
A_55_P2173982	NM_009104	ENSMUST00000020980	20135	*Rrm2*	ribonucleotide reductase M2	2,26856401	1,18177937	0,0003696	0,03369759
A_52_P69194	NM_177572	ENSMUST00000049994	194237	*Rimkla*	ribosomal modification protein rimK-like family member A	2,25874169	1,17551929	0,00075241	0,03604365
A_55_P1954393	NM_144796	ENSMUST00000085724	96935	*Susd4*	sushi domain containing 4	2,25835714	1,17527365	0,00013083	0,03291643
A_51_P179258	NM_001161665	ENSMUST00000161017	269152	*Kif26b*	kinesin family member 26B	2,25808494	1,17509976	0,00037628	0,03373901
A_55_P2115225	NM_007986	ENSMUST00000102732	14089	*Fap*	fibroblast activation protein	2,25507372	1,1731746	0,0003139	0,03315398
A_51_P380005	NM_015736	ENSMUST00000028378	14425	*Galnt3*	polypeptide N-acetylgalactosaminyltransferase 3	2,25139963	1,17082217	0,00039415	0,03373901
A_55_P2097206	NM_009793	ENSMUST00000042868	12326	*Camk4*	calcium/calmodulin-dependent protein kinase IV	2,24509249	1,16677488	0,00016859	0,03291643
A_55_P2000833	NM_001013368	ENSMUST00000058745	108961	*E2f8*	E2F transcription factor 8	2,2445008	1,16639461	0,00020039	0,03291643
A_51_P282144	NM_011780	ENSMUST00000087374	23792	*Adam23*	a disintegrin and metallopeptidase domain 23	2,24328657	1,16561393	0,00010432	0,03291643
A_55_P1990309	NM_010488	ENSMUST00000106597	15572	*Elavl4*	ELAV like RNA binding protein 4	2,24269963	1,16523641	0,00163674	0,04295205
A_55_P2007630	NM_144926	ENSMUST00000134471	233878	*Sez6l2*	seizure related 6 homolog like 2	2,24161505	1,16453854	0,00013212	0,03291643
A_55_P2063336	NM_134041	ENSMUST00000049271	104732	*Tedc1*	tubulin epsilon and delta complex 1	2,24147088	1,16444576	5,26E-05	0,03291643
A_55_P2035286	NM_010931	ENSMUST00000001258	18140	*Uhrf1*	ubiquitin-like, containing PHD and RING finger domains, 1	2,24004222	1,16352592	0,00052342	0,03476444
A_55_P1960097	NM_013813	ENSMUST00000112680	13823	*Epb41l3*	erythrocyte membrane protein band 4.1 like 3	2,23705804	1,16160269	0,00043027	0,03393479
A_51_P125135	NM_026410	ENSMUST00000025704	67849	*Cdca5*	cell division cycle associated 5	2,23696284	1,16154129	0,00069569	0,03558895
A_52_P263518	NM_010315	ENSMUST00000160013	14702	*Gng2*	guanine nucleotide binding protein (G protein), gamma 2	2,22913236	1,15648228	0,00073431	0,03593548
A_52_P326657	NM_182783	ENSMUST00000052835	230766	*Fam167b*	family with sequence similarity 167, member B	2,22869822	1,15620128	0,00185769	0,04494434
A_51_P293862	NM_013530	ENSMUST00000129251	14695	*Gnb3*	guanine nucleotide binding protein (G protein), beta 3	2,22413956	1,15324732	0,00121109	0,03911544
A_55_P2148931	NM_001167925	ENSMUST00000118510	225583	*Minar2*	membrane integral NOTCH2 associated receptor 2	2,22261314	1,15225686	0,00256747	0,04980172
A_51_P492830	NM_021886	ENSMUST00000075550	26886	*Cenph*	centromere protein H	2,22116265	1,15131504	0,00012761	0,03291643
A_51_P141012	NM_199065	ENSMUST00000100322	76965	*Slitrk1*	SLIT and NTRK-like family, member 1	2,21407174	1,14670197	0,00100948	0,03808028
A_51_P246653	NM_020008	ENSMUST00000112076	56644	*Clec7a*	C-type lectin domain family 7, member a	2,21244879	1,14564406	0,0003185	0,03315398
A_51_P250797	NM_010298	ENSMUST00000029654	14658	*Glrb*	glycine receptor, beta subunit	2,20712197	1,14216636	0,0025018	0,04938663
A_55_P2017636	NM_011580	ENSMUST00000039559	21825	*Thbs1*	thrombospondin 1	2,20644945	1,1417267	0,00146707	0,04166534
A_51_P358894	NM_028417	ENSMUST00000008088	73032	*Ttc9b*	tetratricopeptide repeat domain 9B	2,2020495	1,1388469	0,00088251	0,03654939
A_55_P2048588	NM_007659	ENSMUST00000119827	12534	*Cdk1*	cyclin-dependent kinase 1	2,19700902	1,13554079	0,00137922	0,04068336
A_55_P1965154	NM_001199123	ENSMUST00000112320	66442	*Spc25*	SPC25, NDC80 kinetochore complex component, homolog (S. cere	2,19552646	1,13456692	0,00060081	0,03507191
A_55_P2032659	NM_145711	ENSMUST00000039987	252838	*Tox*	thymocyte selection-associated high mobility group box	2,19385209	1,13346626	0,00047271	0,03469594
A_55_P2056654	NM_145588	ENSMUST00000032915	110033	*Kif22*	kinesin family member 22	2,19261988	1,13265572	0,00014906	0,03291643
A_55_P1980426	NM_001291128	ENSMUST00000153739	18111	*Nnat*	neuronatin	2,19180609	1,13212017	0,00087381	0,03654939
A_55_P2041653	NR_037697	ENSMUST00000136948	76505	*1500009C09Rik*	RIKEN cDNA 1500009C09 gene	2,19168994	1,13204371	0,00096613	0,03742542
A_55_P2020497	NM_178739	ENSMUST00000060481	245404	*Dcaf12l1*	DDB1 and CUL4 associated factor 12-like 1	2,18018253	1,12444893	0,00136023	0,04045235
A_55_P2004867	NM_011111	ENSMUST00000064916	18788	*Serpinb2*	serine (or cysteine) peptidase inhibitor, clade B, member 2	2,1794281	1,12394961	2,42E-06	0,03291643
A_51_P452153	NM_027222	ENSMUST00000025211	69816	*Mzb1*	marginal zone B and B1 cell-specific protein 1	2,17480725	1,12088755	0,00086095	0,03635301
A_51_P242930	NM_020044	ENSMUST00000036362	56743	*Lat2*	linker for activation of T cells family, member 2	2,17439196	1,12061203	0,00051261	0,03476444
A_51_P133137	NM_009004	ENSMUST00000166044	19348	*Kif20a*	kinesin family member 20A	2,17149169	1,11868643	0,00046696	0,03462675
A_55_P2124751	NM_028266	ENSMUST00000135675	107581	*Col16a1*	collagen, type XVI, alpha 1	2,16743594	1,11598935	0,00135984	0,04045235
A_51_P480073	NM_007689	ENSMUST00000040418	12643	*Chad*	chondroadherin	2,16606944	1,11507949	0,0004144	0,03386016
A_55_P2063736	NM_001291892	ENSMUST00000102894	14727	*Lilr4b*	leukocyte immunoglobulin-like receptor, subfamily B, member 4B	2,16450294	1,11403576	0,00252963	0,04968765

A_55_P1988228	NM_009791	ENSMUST00000053364	12316	*Aspm*	abnormal spindle microtubule assembly	2,16371025	1,11350732	0,00020882	0,03291643
A_55_P2054445	NM_013489	ENSMUST00000042302	12523	*Cd84*	CD84 antigen	2,15683416	1,10891525	0,00179571	0,04424604
A_51_P239984	NM_012012	ENSMUST00000039725	26909	*Exo1*	exonuclease 1	2,15613865	1,10844995	0,00028584	0,03315398
A_51_P105709	NM_027182	ENSMUST00000022053	69716	*Trip13*	thyroid hormone receptor interactor 13	2,15565307	1,10812501	0,00042576	0,03393479
A_55_P1991016	NM_027395	ENSMUST00000058845	70350	*Basp1*	brain abundant, membrane attached signal protein 1	2,15135858	1,10524801	0,00074016	0,03604365
A_55_P1955437	NM_026066	ENSMUST00000037814	67272	*Cmtm5*	CKLF-like MARVEL transmembrane domain containing 5	2,14960815	1,10407369	0,00029192	0,03315398
A_52_P196105	NM_175274	ENSMUST00000042661	78339	*Ttyh3*	tweety family member 3	2,14763474	1,10274865	0,00040532	0,03373901
A_55_P2009375	NM_008795	ENSMUST00000027697	18557	*Cdk18*	cyclin-dependent kinase 18	2,14217944	1,09907934	0,0003016	0,03315398
A_51_P491987	NM_019955	ENSMUST00000168716	56532	*Ripk3*	receptor-interacting serine-threonine kinase 3	2,14174841	1,09878902	0,00089403	0,03656038
A_51_P258281	NM_010253	ENSMUST00000025842	14419	*Gal*	galanin and GMAP prepropeptide	2,13953678	1,09729848	0,00063196	0,03546117
A_55_P2152771	NM_172589	ENSMUST00000118195	218454	*Lhfpl2*	lipoma HMGIC fusion partner-like 2	2,13530204	1,09444016	0,00037842	0,03373901
A_51_P404463	NM_024283	ENSMUST00000027217	78896	*Ecrg4*	ECRG4 augurin precursor	2,13444695	1,0938623	0,00180914	0,04440825
A_55_P2049282	NM_011837	ENSMUST00000065417	23934	*Ly6h*	lymphocyte antigen 6 complex, locus H	2,1340562	1,09359817	0,00151823	0,04206839
A_51_P202633	NM_015766	ENSMUST00000003274	50498	*Ebi3*	Epstein-Barr virus induced gene 3	2,13159493	1,09193331	0,00023639	0,03291643
A_55_P2046744	NM_001166273	ENSMUST00000035058	29873	*Cspg5*	chondroitin sulfate proteoglycan 5	2,1315657	1,09191352	0,00034209	0,03315398
A_51_P501773	NM_175434	ENSMUST00000108759	210027	*Slc35f3*	solute carrier family 35, member F3	2,13054748	1,0912242	0,00211142	0,04699813
A_55_P1989474	NM_145129	ENSMUST00000034851	110834	*Chrna3*	cholinergic receptor, nicotinic, alpha polypeptide 3	2,12600108	1,08814233	0,00115292	0,03884838
A_51_P270355	NM_019978	ENSMUST00000054237	13175	*Dclk1*	doublecortin-like kinase 1	2,12554617	1,0878336	0,00255922	0,0497393
A_55_P2182975	NM_153400	ENSMUST00000058016	231602	*P2rx2*	purinergic receptor P2X, ligand-gated ion channel, 2	2,12452046	1,08713724	0,00147549	0,04171535
A_51_P344566	NM_011121	ENSMUST00000033154	18817	*Plk1*	polo-like kinase 1	2,12326474	1,08628427	0,00123747	0,0393138
A_55_P2181738	NM_013590	ENSMUST00000092162	17110	*Lyz1*	lysozyme 1	2,12098775	1,08473629	0,00010725	0,03291643
A_66_P133404	NM_026515	ENSMUST00000045802	68026	*Pclaf*	PCNA clamp associated factor	2,1173327	1,08224798	0,00024832	0,03291643
A_55_P2030938	NM_025863	ENSMUST00000107802	66949	*Trim59*	tripartite motif-containing 59	2,11541964	1,08094388	0,00211063	0,04699813
A_55_P2144386	NM_010130	ENSMUST00000086763	13733	*Adgre1*	EGF-like module containing, mucin-like, hormone receptor-like sec	2,11493751	1,08061504	0,00035958	0,03369759
A_55_P1967010	NM_012014	ENSMUST00000099506	26913	*Gprin1*	G protein-regulated inducer of neurite outgrowth 1	2,10976439	1,07708189	0,00239207	0,04851956
A_55_P2183438	NM_001111023	ENSMUST00000168195	12394	*Runx1*	runt related transcription factor 1	2,10959211	1,07696408	0,00153744	0,04228489
A_52_P139650	NM_025581	ENSMUST00000040188	66468	*Ska1*	spindle and kinetochore associated complex subunit 1	2,10912597	1,07664526	0,00012495	0,03291643
A_52_P472302	NM_022004	ENSMUST00000085939	59095	*Fxyd6*	FXYD domain-containing ion transport regulator 6	2,10536085	1,07406752	0,00059866	0,03507191
A_55_P2000133	NM_007664	ENSMUST00000025166	12558	*Cdh2*	cadherin 2	2,10490289	1,07375367	0,00043763	0,03393479
A_55_P1980636	NM_011497	ENSMUST00000028997	20878	*Aurka*	aurora kinase A	2,0979545	1,06898339	0,00034966	0,03328289
A_55_P1995205	NM_011623	ENSMUST00000154332	21973	*Top2a*	topoisomerase (DNA) II alpha	2,09659461	1,06804793	0,00043592	0,03393479
A_51_P421303	NM_026769	ENSMUST00000166758	68566	*Caly*	calcyon neuron-specific vesicular protein	2,09647767	1,06796747	0,00221043	0,04740503
A_52_P22763	NM_001039934	ENSMUST00000114018	17756	*Map2*	microtubule-associated protein 2	2,09573806	1,06745841	0,00105663	0,03814748
A_52_P59206	NM_028623	ENSMUST00000025764	73720	*Cst6*	cystatin E/M	2,09514552	1,06705045	0,00025788	0,03291643
A_55_P2003753	NM_001099631	ENSMUST00000105823	230863	*Sh2d5*	SH2 domain containing 5	2,09456305	1,06664931	0,00147191	0,04167499
A_55_P2085771	NM_175561	ENSMUST00000047239	270109	*Pcnx2*	pecanex homolog 2	2,092939	1,06553027	0,00075937	0,03611065
A_51_P274259	NM_001081277	ENSMUST00000045262	229949	*Ak5*	adenylate kinase 5	2,09154413	1,06456843	0,00127242	0,03970879
A_51_P496540	NM_012009	ENSMUST00000179976	26904	*Sh2d1b1*	SH2 domain protein 1B1	2,08748758	1,06176762	0,00086282	0,03639109
A_55_P1967291	NM_144818	ENSMUST00000110387	215387	*Ncaph*	non-SMC condensin I complex, subunit H	2,08633727	1,06097239	0,00013858	0,03291643
A_55_P1987291	NM_029425	ENSMUST00000039564	75769	*Plppr5*	phospholipid phosphatase related 5	2,08562282	1,06047827	0,00029879	0,03315398
A_51_P155142	NM_026560	ENSMUST00000084296	52276	*Cdca8*	cell division cycle associated 8	2,08228719	1,05816906	0,00047114	0,03469594
A_51_P174215	NM_027790	ENSMUST00000022820	71412	*Dhrs2*	dehydrogenase/reductase member 2	2,08163133	1,05771458	0,00197374	0,04607464
A_52_P348031	NM_021889	ENSMUST00000130414	60510	*Syt9*	synaptotagmin IX	2,07782314	1,05507286	0,00154419	0,04228695
A_55_P2196027	XM_006527616	ENSMUST00000072451	236727	*Slc9a7*	solute carrier family 9 (sodium/hydrogen exchanger), member 7	2,07776176	1,05503024	0,00108466	0,03828376
A_55_P2000027	NM_183284	ENSMUST00000065216	69982	*Spink2*	serine peptidase inhibitor, Kazal type 2	2,07471789	1,05291518	0,0014168	0,04101694
A_51_P241068	NM_020265	ENSMUST00000029665	56811	*Dkk2*	dickkopf WNT signaling pathway inhibitor 2	2,06964034	1,04938008	0,00054582	0,03476444
A_51_P457528	NM_007630	ENSMUST00000034742	12442	*Ccnb2*	cyclin B2	2,06678932	1,04739133	0,001991	0,04619284
A_55_P1985623	NM_029600	ENSMUST00000021231	76408	*Abcc3*	ATP-binding cassette, sub-family C (CFTR/MRP), member 3	2,06314398	1,0448445	0,00052767	0,03476444
A_55_P2111985	NM_178738	ENSMUST00000036426	244954	*Prss35*	protease, serine 35	2,06311065	1,0448212	0,00220164	0,04740503
A_55_P2031949	NM_177235	ENSMUST00000062289	320705	*Bend6*	BEN domain containing 6	2,05963766	1,04239056	0,00018334	0,03291643
A_55_P2035946	NM_001002927	ENSMUST00000070375	18619	*Penk*	preproenkephalin	2,05893871	1,04190089	0,00014062	0,03291643
A_51_P367310	NM_028083	ENSMUST00000128316	110749	*Chaf1b*	chromatin assembly factor 1, subunit B (p60)	2,05684598	1,04043376	0,00076834	0,03619952
A_52_P330214	NM_016925	ENSMUST00000035495	14087	*Fanca*	Fanconi anemia, complementation group A	2,05014074	1,03572296	0,00121397	0,03911544
A_51_P123405	NM_009772	ENSMUST00000028858	12235	*Bub1*	BUB1, mitotic checkpoint serine/threonine kinase	2,04331822	1,0309139	0,00035672	0,03369759
A_51_P153423	NM_001081416	ENSMUST00000097425	68655	*Fndc1*	fibronectin type III domain containing 1	2,04086774	1,02918269	0,00042046	0,03391783

A_51_P366061	NM_007984	ENSMUST00000031565	14086	*Fscn1*	fascin actin-bundling protein 1	2,03958148	1,02827315	0,00204656	0,04655586
A_52_P424784	NM_022319	ENSMUST00000035027	64085	*Clstn2*	calsyntenin 2	2,03750418	1,02680302	0,00019459	0,03291643
A_52_P138806	NM_198618	ENSMUST00000106094	242667	*Dlgap3*	DLG associated protein 3	2,03736843	1,0267069	0,00141707	0,04101694
A_51_P451151	NM_026785	ENSMUST00000088248	68612	*Ube2c*	ubiquitin-conjugating enzyme E2C	2,03526253	1,0252149	0,0007039	0,03558895
A_51_P160673	NM_021487	ENSMUST00000134825	66240	*Kcne1l*	potassium voltage-gated channel, Isk-related family, member 1-like	2,03372282	1,02412306	0,00035247	0,03339594
A_55_P1976278	NM_008855	ENSMUST00000143692	18751	*Prkcb*	protein kinase C, beta	2,03287738	1,0235232	0,00049639	0,03476444
A_51_P155843	NM_001162884	ENSMUST00000039419	242050	*Igsf10*	immunoglobulin superfamily, member 10	2,03187752	1,02281344	0,00019199	0,03291643
A_66_P100853	NM_001177544	ENSMUST00000081342	665433	*Hist1h2ao*	histone cluster 1, H2ao	2,03097633	1,02217343	0,00063801	0,03546117
A_52_P463518	NM_021325	ENSMUST00000057488	57781	*Cd200r1*	CD200 receptor 1	2,02854925	1,02044833	0,00047499	0,03469594
A_55_P2237432	NM_001290708	ENSMUST00000101616	93761	*Smarca1*	SWI/SNF related, matrix associated, actin dependent regulator of c	2,02774765	1,01987812	0,00016147	0,03291643
A_55_P2047809	NM_175692	ENSMUST00000138307	319317	*Snhg11*	small nucleolar RNA host gene 11	2,02580817	1,01849756	0,00164297	0,04301439
A_55_P1984886	NM_011827	ENSMUST00000075062	23900	*Hcst*	hematopoietic cell signal transducer	2,02388366	1,01712636	0,00154923	0,04232468
A_51_P481398	NM_010615	ENSMUST00000012587	16551	*Kif11*	kinesin family member 11	2,02285784	1,01639494	0,00039574	0,03373901
A_55_P2109717	NM_183046	ENSMUST00000087341	240641	*Kif20b*	kinesin family member 20B	2,02156783	1,01547461	0,00020703	0,03291643
A_55_P1996946	NM_023223	ENSMUST00000006565	107995	*Cdc20*	cell division cycle 20	2,01657979	1,01191049	0,00079629	0,03629498
A_52_P186033	NM_009259	ENSMUST00000049931	20737	*Spn*	sialophorin	2,01528035	1,01098055	0,00077947	0,03629498
A_55_P2028655	NM_175090	ENSMUST00000084526	20529	*Slc31a1*	solute carrier family 31, member 1	2,0150604	1,01082308	0,00044027	0,03393479
A_55_P2020331	NM_144817	ENSMUST00000016323	215303	*Camk1g*	calcium/calmodulin-dependent protein kinase I gamma	2,0149473	1,01074211	1,43E-03	0,0413313
A_55_P1954196	NM_153155	ENSMUST00000061545	227580	*C1ql3*	C1q-like 3	2,01140995	1,00820715	0,00074676	0,03604365
A_55_P2073338	NM_013680	ENSMUST00000081893	20964	*Syn1*	synapsin I	2,01056782	1,007603	0,0011302	0,03857573
A_55_P1983708	NM_011832	ENSMUST00000029711	23920	*Insrr*	insulin receptor-related receptor	2,01020087	1,00733967	0,00154588	0,04229276
A_55_P2017373	NM_146100	ENSMUST00000037636	226180	*Ina*	internexin neuronal intermediate filament protein, alpha	2,00815752	1,00587244	0,00218321	0,04740503
A_51_P260683	NM_015811	ENSMUST00000167812	50778	*Rgs1*	regulator of G-protein signaling 1	2,00758324	1,00545981	0,00183513	0,04462436
A_55_P1958394	NM_001291227	ENSMUST00000170109	20563	*Slit2*	slit guidance ligand 2	2,00677155	1,00487639	0,00030073	0,03315398
A_55_P2029420	NM_183287	ENSMUST00000093336	70458	*2610318N02Rik*	RIKEN cDNA 2610318N02 gene	2,00431002	1,00310568	6,05E-05	0,03291643
A_66_P129564	NM_022414	ENSMUST00000021420	64242	*Ngb*	neuroglobin	1,9983842	0,99883397	0,00045764	0,03432803
A_51_P369862	NM_178772	ENSMUST00000046515	320024	*Nceh1*	neutral cholesterol ester hydrolase 1	1,99427466	0,99586412	0,00111251	0,03830608
A_65_P11853	NM_172964	ENSMUST00000024840	268970	*Arhgap28*	Rho GTPase activating protein 28	1,99261766	0,99466491	1,01E-05	0,03291643
A_66_P110435	NM_175510	ENSMUST00000061620	329178	*Unc80*	unc-80, NALCN activator	1,99118102	0,99362438	1,91E-03	0,04552521
A_55_P2160815	NM_010425	ENSMUST00000087285	15221	*Foxd3*	forkhead box D3	1,99088458	0,99340958	3,93E-05	0,03291643
A_55_P2212603	NM_001291166	ENSMUST00000032732	11784	*Apba2*	amyloid beta (A4) precursor protein-binding, family A, member 2	1,98904275	0,99207428	0,00022105	0,03291643
A_52_P151320	NM_025566	ENSMUST00000077788	66443	*Tnfaip8l1*	tumor necrosis factor, alpha-induced protein 8-like 1	1,98865895	0,99179588	0,00070828	0,03571784
A_55_P2158011	NM_026412	ENSMUST00000177103	51944	*Knstrn*	kinetochore-localized astrin/SPAG5 binding	1,98834529	0,99156831	4,16E-05	0,03291643
A_51_P515605	NM_009930	ENSMUST00000087883	12825	*Col3a1*	collagen, type III, alpha 1	1,98227283	0,98715554	0,00021772	0,03291643
A_55_P2013336	NM_010790	ENSMUST00000045607	17279	*Melk*	maternal embryonic leucine zipper kinase	1,98183671	0,9868381	2,88E-04	0,03315398
A_55_P2122871	NM_172855	ENSMUST00000144671	241391	*Galnt5*	polypeptide N-acetylgalactosaminyltransferase 5	1,97955227	0,98517416	0,00016212	0,03291643
A_55_P1960074	NM_008776	ENSMUST00000005583	18476	*Pafah1b3*	platelet-activating factor acetylhydrolase, isoform 1b, subunit 3	1,97768577	0,98381322	5,99E-05	0,03291643
A_55_P2037439	NM_001172092	ENSMUST00000106041	76131	*Depdc1a*	DEP domain containing 1a	1,97759543	0,98374731	2,80E-05	0,03291643
A_55_P2089804	NM_146065	ENSMUST00000108828	223922	*Atf7*	activating transcription factor 7	1,97744533	0,98363781	0,00140078	0,04084925
A_52_P199614	NM_001146022	ENSMUST00000061753	545030	*Wdfy4*	WD repeat and FYVE domain containing 4	1,97394956	0,98108513	0,00117155	0,03904427
A_55_P2013913	NM_008779	ENSMUST00000032159	18488	*Cntn3*	contactin 3	1,96916792	0,97758614	0,00048014	0,03469594
A_55_P2001553	NM_001290315	ENSMUST00000077696	56741	*Igdcc4*	immunoglobulin superfamily, DCC subclass, member 4	1,96872021	0,97725809	2,47E-03	0,04921934
A_51_P324838	NM_025276	ENSMUST00000037007	14027	*Evpl*	envoplakin	1,96863966	0,97719907	0,00096856	0,03748194
A_51_P515120	NM_178870	ENSMUST00000058652	15478	*Hs3st3a1*	heparan sulfate (glucosamine) 3-O-sulfotransferase 3A1	1,96716133	0,97611528	0,00100156	0,03807877
A_55_P2158121	NM_025312	ENSMUST00000041407	66042	*Sostdc1*	sclerostin domain containing 1	1,96071884	0,97138267	0,00155746	0,04238381
A_55_P2013184	NM_177236	ENSMUST00000088429	320707	*Atp2b3*	ATPase, Ca++ transporting, plasma membrane 3	1,95987254	0,97075983	0,00019352	0,03291643
A_55_P2084631	NM_178184	ENSMUST00000091751	319170	*Hist1h2an*	histone cluster 1, H2an	1,9589011	0,97004456	0,00045497	0,03426432
A_55_P1967105	NM_001290714	ENSMUST00000106017	230775	*Adgrb2*	adhesion G protein-coupled receptor B2	1,95751039	0,96901996	0,00036804	0,03369759
A_55_P1967538	NM_015755	ENSMUST00000065856	26559	*Hunk*	hormonally upregulated Neu-associated kinase	1,95653175	0,96829852	0,00037924	0,03373901
A_55_P1997400	NM_144852	ENSMUST00000116648	224022	*Slc7a4*	solute carrier family 7 (cationic amino acid transporter, y+ system)	1,95588121	0,96781875	0,00121674	0,03911544
A_55_P1971897	NM_010784	ENSMUST00000028672	17242	*Mdk*	midkine	1,95492709	0,9671148	0,00241537	0,04866626
A_51_P315666	NM_008695	ENSMUST00000022340	18074	*Nid2*	nidogen 2	1,95463679	0,96690055	0,0013713	0,04050525
A_55_P2017681	NM_001173550	ENSMUST00000168818	12273	*C5ar1*	complement component 5a receptor 1	1,95024281	0,96365376	0,00037732	0,03373901
A_55_P2121608	ENSMUST000000672	ENSMUST00000067230	20677	*Sox4*	SRY (sex determining region Y)-box 4	1,94918354	0,96286995	0,00065694	0,03555961
A_55_P2249556	AK042310	ENSMUST00000195842	98754	*A630081D01Rik*	RIKEN cDNA A630081D01 gene	1,94865452	0,96247834	0,00205514	0,04655586

A_52_P30989	NM_028222	ENSMUST00000067426	72391	*Cdkn3*	cyclin-dependent kinase inhibitor 3	1,94738645	0,96153921	8,71E-05	0,03291643
A_55_P2127702	NM_001253809	ENSMUST00000023756	26934	*Racgap1*	Rac GTPase-activating protein 1	1,94689769	0,96117707	0,00135293	0,04041885
A_51_P400543	NM_019467	ENSMUST00000172679	11629	*Aif1*	allograft inflammatory factor 1	1,94641277	0,96081769	0,00214465	0,0473211
A_52_P56397	NM_001081099	ENSMUST00000105866	69885	*Aunip*	aurora kinase A and ninein interacting protein	1,945214	0,95992888	0,00037974	0,03373901
A_55_P2060922	NM_153131	ENSMUST00000109994	107448	*Unc5a*	unc-5 netrin receptor A	1,94513184	0,95986795	1,84E-03	0,044633
A_55_P2109613	NM_013464	ENSMUST00000116436	11622	*Ahr*	aryl-hydrocarbon receptor	1,94468811	0,95953879	0,00100257	0,03807877
A_55_P2019784	NM_028880	ENSMUST00000161677	74342	*Lrrtm1*	leucine rich repeat transmembrane neuronal 1	1,94390867	0,95896044	0,00188114	0,04514203
A_55_P1988384	NM_007515	ENSMUST00000113710	11989	*Slc7a3*	solute carrier family 7 (cationic amino acid transporter, y+ system)	1,94324815	0,95847014	0,00248737	0,04932867
A_52_P308413	NM_001163616	ENSMUST00000039191	69069	*Tmem273*	transmembrane protein 273	1,94285721	0,95817987	9,34E-04	0,03698032
A_55_P2076048	NM_023284	ENSMUST00000028000	66977	*Nuf2*	NUF2, NDC80 kinetochore complex component	1,9416778	0,95730382	8,91E-04	0,03656038
A_55_P2013823	NM_016922	ENSMUST00000078757	53897	*Gal3st1*	galactose-3-O-sulfotransferase 1	1,93985791	0,95595098	3,32E-04	0,03315398
A_55_P2104894	NM_007737	ENSMUST00000086430	12832	*Col5a2*	collagen, type V, alpha 2	1,9382409	0,95474789	0,00034236	0,03315398
A_51_P487999	NM_028232	ENSMUST00000024736	72415	*Sgol1*	shugoshin 1	1,93809706	0,95464082	0,00128138	0,03979485
A_51_P414637	NM_015734	ENSMUST00000028280	12831	*Col5a1*	collagen, type V, alpha 1	1,93771327	0,9543551	0,00054379	0,03476444
A_55_P2126615	XM_006513678		260315	*Nav3*	neuron navigator 3	1,93737051	0,95409989	0,00075416	0,03604365
A_55_P2148624	NM_175470	ENSMUST00000116284	229714	*Gpr61*	G protein-coupled receptor 61	1,93736869	0,95409853	0,00093252	0,03698032
A_51_P408071	NM_001042421	ENSMUST00000031366	208628	*Kntc1*	kinetochore associated 1	1,93563878	0,95280975	0,00028669	0,03315398
A_52_P162298	NM_026940	ENSMUST00000142576	69101	*Ydjc*	YdjC homolog (bacterial)	1,93386209	0,95148491	0,00081358	0,03629498
A_51_P254805	NM_008446	ENSMUST00000048962	16571	*Kif4*	kinesin family member 4	1,93199189	0,95008904	2,02E-04	0,03291643
A_55_P2085984	NM_010512	ENSMUST00000122386	16000	*Igf1*	insulin-like growth factor 1	1,93111556	0,9494345	0,00184624	0,04478246
A_55_P2058942	NM_026316	ENSMUST00000051803	67689	*Aldh3b1*	aldehyde dehydrogenase 3 family, member B1	1,92982544	0,94847035	7,70E-05	0,03291643
A_55_P2115955	NM_198193	ENSMUST00000065527	379043	*Raet1e*	retinoic acid early transcript 1E	1,92908478	0,94791655	0,00084882	0,03629498
A_52_P162099	NM_001004140	ENSMUST00000046916	80986	*Ckap2*	cytoskeleton associated protein 2	1,92824165	0,94728586	1,94E-03	0,04568444
A_55_P1955726	NM_013643	ENSMUST00000102626	19259	*Ptpn5*	protein tyrosine phosphatase, non-receptor type 5	1,9262438	0,94579032	1,65E-03	0,04303926
A_52_P502577	NM_010101	ENSMUST00000087978	13610	*S1pr3*	sphingosine-1-phosphate receptor 3	1,92537734	0,94514122	0,00067043	0,03555961
A_51_P490509	NM_009773	ENSMUST00000038341	12236	*Bub1b*	BUB1B, mitotic checkpoint serine/threonine kinase	1,92317557	0,94349048	1,19E-03	0,03904427
A_52_P399584	NM_181589	ENSMUST00000052708	70466	*Ckap2l*	cytoskeleton associated protein 2-like	1,91420674	0,93674665	0,00018686	0,03291643
A_55_P2059357	NM_008663	ENSMUST00000107128	17921	*Myo7a*	myosin VIIA	1,90704559	0,93133933	0,00191193	0,04552509
A_51_P222337	NM_172815	ENSMUST00000063492	239405	*Rspo2*	R-spondin 2	1,90527367	0,92999824	5,91E-05	0,03291643
A_51_P151732	NM_019645	ENSMUST00000027667	18772	*Pkp1*	plakophilin 1	1,90475873	0,92960827	0,00151156	0,04191356
A_52_P498208	NM_178183	ENSMUST00000074752	319169	*Hist1h2ak*	histone cluster 1, H2ak	1,90463536	0,92951482	2,54E-04	0,03291643
A_66_P109183	NM_001109914	ENSMUST00000167323	381823	*Apold1*	apolipoprotein L domain containing 1	1,90422339	0,92920273	5,49E-06	0,03291643
A_66_P112305	NM_053214	ENSMUST00000173372	17916	*Myo1f*	myosin IF	1,90346769	0,92863008	2,22E-03	0,04740503
A_51_P275949	NM_033325	ENSMUST00000022660	94352	*Loxl2*	lysyl oxidase-like 2	1,9025354	0,9279233	0,00024649	0,03291643
A_55_P2017759	NM_001033711	ENSMUST00000170799	14017	*Evi2a*	ecotropic viral integration site 2a	1,90127804	0,92696952	0,00112348	0,03853569
A_55_P1974407	NM_011074	ENSMUST00000115452	18647	*Cdk14*	cyclin-dependent kinase 14	1,90045308	0,9263434	1,27E-03	0,03970879
A_55_P2227335	NM_011212	ENSMUST00000073961	19267	*Ptpre*	protein tyrosine phosphatase, receptor type, E	1,89678631	0,92355715	0,00041519	0,03386016
A_51_P352968	NM_008538	ENSMUST00000092584	17118	*Marcks*	myristoylated alanine rich protein kinase C substrate	1,89452877	0,92183905	0,0016072	0,04275477
A_51_P214985	NM_145492	ENSMUST00000025288	225207	*Zfp521*	zinc finger protein 521	1,89449814	0,92181572	6,14E-04	0,0352913
A_51_P401668	NM_010686	ENSMUST00000151698	16792	*Laptm5*	lysosomal-associated protein transmembrane 5	1,89269852	0,92044463	0,00249935	0,04938663
A_51_P229676	NM_011636	ENSMUST00000093801	22038	*Plscr1*	phospholipid scramblase 1	1,89072953	0,918943	0,00039115	0,03373901
A_55_P2039324	NM_007634	ENSMUST00000115390	12449	*Ccnf*	cyclin F	1,88957729	0,91806353	1,26E-03	0,03964697
A_55_P2067362	ENSMUST00000034373	ENSMUST00000034373	319446	*Dpep2*	dipeptidase 2	1,88804076	0,91688991	2,03E-03	0,0464094
A_55_P1979998	NM_027283	ENSMUST00000102877	69987	*Spaca9*	sperm acrosome associated 9	1,88274843	0,91284024	0,00200211	0,0463625
A_55_P2110245	NM_001163359	ENSMUST00000171938	60530	*Fignl1*	fidgetin-like 1	1,88233994	0,9125272	7,12E-05	0,03291643
A_55_P2023235	NM_007999	ENSMUST00000142241	14156	*Fen1*	flap structure specific endonuclease 1	1,87996233	0,91070375	6,68E-04	0,03555961
A_55_P2056473	NM_026282	ENSMUST00000098942	67629	*Spc24*	SPC24, NDC80 kinetochore complex component, homolog (S. cere	1,87959089	0,91041868	0,00088785	0,0365513
A_55_P2152364	AK159059	ENSMUST00000097320	100038355	*Runx2os1*	runt related transcription factor 2, opposite strand 1	1,87886352	0,90986028	0,00125156	0,03954206
A_55_P2062543	NM_001195298	ENSMUST00000114361	100502766	*Kifc1*	kinesin family member C1	1,8748268	0,90675732	0,00112008	0,03848696
A_55_P2166833	XM_006527509		383435	*Ms4a14*	membrane-spanning 4-domains, subfamily A, member 14	1,87478463	0,90672487	0,00166168	0,04319932
A_52_P196568	NR_003633	ENSMUST00000146701	17263	*Meg3*	maternally expressed 3	1,87306711	0,90540259	0,00228748	0,04777578
A_55_P2108784	NM_153800	ENSMUST00000111956	239027	*Arhgap22*	Rho GTPase activating protein 22	1,87029999	0,90326969	0,00013432	0,03291643
A_51_P499551	NM_133983	ENSMUST00000165365	102657	*Cd276*	CD276 antigen	1,86783541	0,90136733	5,62E-04	0,03481832
A_55_P1976127	NM_007900	ENSMUST00000184113	13605	*Ect2*	ect2 oncogene	1,86588345	0,89985887	8,49E-05	0,03291643
A_55_P2033490	XM_006521692		107522	*Ece2*	endothelin converting enzyme 2	1,86543056	0,89950865	2,24E-03	0,04747585

A_55_P2004370	NM_009802	ENSMUST00000030817	12353	*Car6*	carbonic anhydrase 6	1,86392089	0,89834063	5,91E-04	0,03507191
A_55_P2007273	NM_011132	ENSMUST00000141506	18973	*Pole*	polymerase (DNA directed), epsilon	1,86234274	0,89711861	0,00011099	0,03291643
A_55_P2095019	ENSMUST00000000441	ENSMUST00000044155	72828	*Ubash3b*	ubiquitin associated and SH3 domain containing, B	1,85576258	0,89201215	5,21E-04	0,03476444
A_51_P254986	NM_011353	ENSMUST00000142155	20365	*Serf1*	small EDRK-rich factor 1	1,8531938	0,89001376	0,00025	0,03291643
A_55_P2099961	NM_178186	ENSMUST00000091741	319167	*Hist1h2ag*	histone cluster 1, H2ag	1,84843057	0,88630085	0,00115624	0,0388719
A_52_P529570	NM_198654	ENSMUST00000078259	381318	*Nsl1*	NSL1, MIS12 kinetochore complex component	1,84813969	0,8860738	0,00014805	0,03291643
A_51_P148105	NM_011234	ENSMUST00000152327	19361	*Rad51*	RAD51 homolog	1,84766815	0,88570566	6,27E-04	0,03546117
A_52_P93910	NM_001077403	ENSMUST00000075144	18187	*Nrp2*	neuropilin 2	1,84547974	0,8839959	0,00072376	0,03593548
A_51_P366207	NM_008671	ENSMUST00000121720	17954	*Nap1l2*	nucleosome assembly protein 1-like 2	1,84543226	0,88395878	1,36E-03	0,0404341
A_52_P371135	NM_177000	ENSMUST00000164078	319772	*C130050O18Rik*	RIKEN cDNA C130050O18 gene	1,84439697	0,8831492	7,49E-04	0,03604365
A_51_P108020	NM_001029929	ENSMUST00000136029	574428	*Zmynd15*	zinc finger, MYND-type containing 15	1,84431351	0,88308392	0,00257775	0,04986609
A_51_P185939	NM_029771	ENSMUST00000066211	76854	*Gper1*	G protein-coupled estrogen receptor 1	1,8434943	0,88244296	0,00029086	0,03315398
A_55_P2025790	NM_145946	ENSMUST00000036865	208836	*Fanci*	Fanconi anemia, complementation group I	1,84132259	0,8807424	0,00014562	0,03291643
A_51_P191649	NM_023294	ENSMUST00000024851	67052	*Ndc80*	NDC80 kinetochore complex component	1,84118026	0,88063088	4,38E-05	0,03291643
A_55_P2098880	NM_134189	ENSMUST00000066987	171212	*Galnt10*	polypeptide N-acetylgalactosaminyltransferase 10	1,84020227	0,87986435	9,26E-04	0,0369201
A_51_P321150	NM_017372	ENSMUST00000092163	17105	*Lyz2*	lysozyme 2	1,83596621	0,8765395	2,44E-03	0,04893861
A_51_P161086	NM_008908	ENSMUST00000025419	19038	*Ppic*	peptidylprolyl isomerase C	1,83317855	0,87434731	0,00027932	0,03315398
A_55_P2171493	NM_153544	ENSMUST00000133930	217216	*Hrob*	homologous recombination factor with OB-fold	1,83158678	0,87309406	0,00085617	0,03629498
A_52_P572178	NM_001081051	ENSMUST00000141572	210108	*D130043K22Rik*	RIKEN cDNA D130043K22 gene	1,83010521	0,87192659	0,001599	0,04267063
A_51_P289107	NM_133849	ENSMUST00000056480	99296	*Hrh3*	histamine receptor H3	1,82953097	0,87147384	0,00195903	0,04592118
A_55_P2098200	NM_011627	ENSMUST00000006559	21983	*Tpbg*	trophoblast glycoprotein	1,82872307	0,87083662	0,00034845	0,03324921
A_55_P2135331	NM_001163394	ENSMUST00000021689	14026	*Evl*	Ena-vasodilator stimulated phosphoprotein	1,82677617	0,86929988	2,21E-03	0,04740503
A_51_P369200	NM_028109	ENSMUST00000028969	72119	*Tpx2*	TPX2, microtubule-associated	1,82551019	0,86829972	0,00177933	0,04399008
A_55_P1993503	NM_007413	ENSMUST00000018644	11541	*Adora2b*	adenosine A2b receptor	1,82398902	0,86709704	1,20E-03	0,03904427
A_51_P130095	NM_001077189	ENSMUST00000159969	14130	*Fcgr2b*	Fc receptor, IgG, low affinity IIb	1,8239022	0,86702837	0,00226014	0,0475368
A_55_P2076777	NM_001109973	ENSMUST00000035375	17240	*Mdfi*	MyoD family inhibitor	1,82312521	0,86641365	2,09E-03	0,04671098
A_55_P2031836	NM_145066	ENSMUST00000115492	64450	*Gpr85*	G protein-coupled receptor 85	1,81965231	0,86366282	0,00254379	0,04970107
A_65_P03197	NM_001199556	ENSMUST00000119722	244810	*AW551984*	expressed sequence AW551984	1,81907682	0,86320647	0,00018705	0,03291643
A_51_P133612	NM_026014	ENSMUST00000006760	67177	*Cdt1*	chromatin licensing and DNA replication factor 1	1,81884835	0,86302526	1,91E-03	0,04550393
A_51_P119429	NM_153505	ENSMUST00000047405	105855	*Nckap1l*	NCK associated protein 1 like	1,81875286	0,86294952	0,00107325	0,03823006
A_51_P182303	NM_007743	ENSMUST00000031668	12843	*Col1a2*	collagen, type I, alpha 2	1,81724232	0,86175081	8,15E-05	0,03291643
A_51_P259603	NM_007407	ENSMUST00000070756	11517	*Adcyap1r1*	adenylate cyclase activating polypeptide 1 receptor 1	1,81716186	0,86168693	0,00150364	0,04189237
A_55_P1959393	NM_144881	ENSMUST00000044190	226861	*Hhat*	hedgehog acyltransferase	1,81689114	0,86147198	9,35E-04	0,03698032
A_55_P2069306	NM_011206	ENSMUST00000027302	19253	*Ptpn18*	protein tyrosine phosphatase, non-receptor type 18	1,8152923	0,86020187	1,00E-03	0,03807877
A_52_P56751	NM_008879	ENSMUST00000131802	18826	*Lcp1*	lymphocyte cytosolic protein 1	1,81394977	0,8591345	0,0022596	0,0475368
A_51_P164203	NM_019731	ENSMUST00000025007	56520	*Nme4*	NME/NM23 nucleoside diphosphate kinase 4	1,81312082	0,85847506	0,0017048	0,04357357
A_55_P2056493	ENSMUST00000153298	ENSMUST00000153298	21877	*Tk1*	thymidine kinase 1	1,81142168	0,85712243	0,00108008	0,03826064
A_55_P1953489	NM_001033550	ENSMUST00000112707	433926	*Lrrc8b*	leucine rich repeat containing 8 family, member B	1,80995417	0,85595317	8,33E-05	0,03291643
A_55_P1970763	NM_001024932	ENSMUST00000164886	545812	*Pilrb2*	paired immunoglobin-like type 2 receptor beta 2	1,80891497	0,8551246	0,0010034	0,03807877
A_55_P1972575	NM_021436	ENSMUST00000030032	230157	*Tmeff1*	transmembrane protein with EGF-like and two follistatin-like doma	1,80722301	0,85377455	1,59E-03	0,04260286
A_51_P408946	NM_007633	ENSMUST00000108023	12447	*Ccne1*	cyclin E1	1,80273394	0,85018649	1,83E-03	0,04449278
A_52_P151393	NM_198860	ENSMUST00000051129	192734	*Lrrc75b*	leucine rich repeat containing 75B	1,80188188	0,84950444	4,40E-04	0,03393479
A_55_P1972948	NM_176954	ENSMUST00000118763	319586	*Celf5*	CUGBP, Elav-like family member 5	1,80144265	0,84915273	2,23E-04	0,03291643
A_55_P2053561	NM_001126318	ENSMUST00000102522	242711	*Cela3a*	chymotrypsin-like elastase family, member 3A	1,80036318	0,84828797	0,00258597	0,04989265
A_52_P156190	NM_010332	ENSMUST00000034029	13617	*Ednra*	endothelin receptor type A	1,79661307	0,84527973	2,49E-03	0,04932867
A_52_P49042	NM_001033258	ENSMUST00000019999	215821	*Arfgef3*	ARFGEF family member 3	1,79566682	0,84451969	1,69E-03	0,04345841
A_51_P324287	NM_024245	ENSMUST00000034815	71819	*Kif23*	kinesin family member 23	1,79462004	0,84367842	0,00149983	0,04189237
A_52_P101303	NM_019664	ENSMUST00000113854	16516	*Kcnj15*	potassium inwardly-rectifying channel, subfamily J, member 15	1,79445315	0,84354426	8,92E-04	0,03656038
A_51_P240453	NM_133851	ENSMUST00000068225	108907	*Nusap1*	nucleolar and spindle associated protein 1	1,79317785	0,84251858	8,00E-04	0,03629498
A_52_P320261	NM_001024698	ENSMUST00000096066	232680	*Cpa2*	carboxypeptidase A2, pancreatic	1,79316251	0,84250624	5,13E-04	0,03476444
A_55_P2005838	NM_029835	ENSMUST00000035977	77011	*Ticrr*	TOPBP1-interacting checkpoint and replication regulator	1,79124537	0,84096298	0,00189582	0,04525218
A_66_P101600	NM_008482	ENSMUST00000002979	16777	*Lamb1*	laminin B1	1,78854532	0,83878668	1,68E-03	0,04345841
A_66_P106525	NR_033140		381524	*Mexis*	macrophage expressed LXRa(NR1H3)-dependent amplifier of Abca	1,7883242	0,8386083	7,84E-04	0,03629498
A_55_P2160296	NM_001038612	ENSMUST00000102879	56177	*Olfm1*	olfactomedin 1	1,7882608	0,83855716	3,84E-04	0,03373901
A_52_P52849	NM_018867	ENSMUST00000033149	55987	*Cpxm2*	carboxypeptidase X 2 (M14 family)	1,78622076	0,8369104	0,000236	0,03291643

A_66_P111090	NM_001012322	ENSMUST00000072886	319229	*Sctr*	secretin receptor	1,78588746	0,83664117	2,15E-03	0,0473211
A_52_P227391	NM_010620	ENSMUST00000040717	209737	*Kif15*	kinesin family member 15	1,78543707	0,83627729	0,00054331	0,03476444
A_52_P432969	NM_001105245	ENSMUST00000149154	279653	*Pcdh19*	protocadherin 19	1,78470336	0,8356843	1,65E-04	0,03291643
A_55_P1965694	NM_008073	ENSMUST00000109292	14406	*Gabrg2*	gamma-aminobutyric acid (GABA) A receptor, subunit gamma 2	1,78374988	0,83491334	0,00123054	0,03926729
A_51_P186476	NM_013612	ENSMUST00000131511	18173	*Slc11a1*	solute carrier family 11 (proton-coupled divalent metal ion transpc	1,78186747	0,83339004	1,19E-03	0,03904427
A_55_P2109479	NM_001001180	ENSMUST00000106052	407812	*Zfp941*	zinc finger protein 941	1,78064542	0,83240026	0,00235409	0,0482972
A_55_P2050439	NM_144553	ENSMUST00000179465	218977	*Dlgap5*	DLG associated protein 5	1,78048119	0,8322672	0,00020516	0,03291643
A_51_P337523	NM_153534	ENSMUST00000022013	210044	*Adcy2*	adenylate cyclase 2	1,77947935	0,83145519	0,00125909	0,03962623
A_55_P2140651	NM_170597	ENSMUST00000053355	263764	*Creg2*	cellular repressor of E1A-stimulated genes 2	1,77903053	0,83109127	0,00219188	0,04740503
A_52_P354744	NM_011401	ENSMUST00000168704	20527	*Slc2a3*	solute carrier family 2 (facilitated glucose transporter), member 3	1,77813442	0,83036439	0,00231173	0,04795298
A_55_P2002757	NM_008528	ENSMUST00000054769	17060	*Blnk*	B cell linker	1,7768255	0,829302	0,00240139	0,04852362
A_51_P228171	NM_025495	ENSMUST00000021818	66336	*Cenpp*	centromere protein P	1,77622859	0,82881726	0,00036504	0,03369759
A_55_P1957413	NM_019391	ENSMUST00000149521	16985	*Lsp1*	lymphocyte specific 1	1,77559601	0,82830337	0,00041679	0,03387501
A_52_P588881	NM_001033484	ENSMUST00000071812	404710	*Iqgap3*	IQ motif containing GTPase activating protein 3	1,77529104	0,82805556	0,00205888	0,04655586
A_55_P1958210	NM_173447	ENSMUST00000035129	270190	*Ephb1*	Eph receptor B1	1,77422568	0,82718953	0,00132792	0,04018556
A_52_P637172	NM_029011	ENSMUST00000076505	74580	*Pyroxd2*	pyridine nucleotide-disulphide oxidoreductase domain 2	1,77202847	0,82540178	0,00232555	0,04798501
A_52_P153291	NM_145700	ENSMUST00000076147	252837	*Ackr4*	atypical chemokine receptor 4	1,771627	0,82507489	0,00150417	0,04189237
A_52_P102248	NM_175366	ENSMUST00000082237	108797	*Mex3b*	mex3 RNA binding family member B	1,76853288	0,82255304	0,00207365	0,0465836
A_55_P2153431	NM_009058	ENSMUST00000028170	19730	*Ralgds*	ral guanine nucleotide dissociation stimulator	1,76747519	0,82168996	0,00010107	0,03291643
A_52_P104824	NM_019670	ENSMUST00000168889	56419	*Diaph3*	diaphanous related formin 3	1,76484323	0,81954003	0,00074274	0,03604365
A_52_P167382	NM_021793	ENSMUST00000025010	60455	*Tmem8*	transmembrane protein 8	1,76469548	0,81941925	0,0014347	0,04134299
A_51_P140710	NM_011337	ENSMUST00000001008	20302	*Ccl3*	chemokine (C-C motif) ligand 3	1,7643673	0,81915093	0,00104156	0,03812918
A_51_P114462	NM_011332	ENSMUST00000034232	20295	*Ccl17*	chemokine (C-C motif) ligand 17	1,76380824	0,81869372	0,0001128	0,03291643
A_52_P344138	NM_008071	ENSMUST00000039697	14402	*Gabrb3*	gamma-aminobutyric acid (GABA) A receptor, subunit beta 3	1,76053975	0,8160178	0,00079023	0,03629498
A_52_P190647	NM_016662	ENSMUST00000146181	17121	*Mxd3*	Max dimerization protein 3	1,7595197	0,81518167	0,00133473	0,04022942
A_52_P251366	NM_146208	ENSMUST00000047768	234258	*Neil3*	nei like 3 (E. coli)	1,75795153	0,81389529	0,00028795	0,03315398
A_55_P2064984	NM_145924	ENSMUST00000101251	102920	*Cenpi*	centromere protein I	1,75761892	0,8136223	0,00120115	0,03908156
A_55_P1984976	NM_001271757	ENSMUST00000178696	22419	*Wnt5b*	wingless-type MMTV integration site family, member 5B	1,75647678	0,8126845	0,00027696	0,03315398
A_55_P1985768	NM_053273	ENSMUST00000045779	117160	*Ttyh2*	tweety family member 2	1,75383277	0,81051119	0,00090323	0,0368081
A_51_P219444	NM_013880	ENSMUST00000043938	224860	*Plcl2*	phospholipase C-like 2	1,75222094	0,8091847	0,00238342	0,04851956
A_52_P409731	NM_020270	ENSMUST00000046587	56807	*Scamp5*	secretory carrier membrane protein 5	1,74847756	0,80609928	0,00029626	0,03315398
A_55_P2004801	NM_001040435	ENSMUST00000114426	21335	*Tacc3*	transforming, acidic coiled-coil containing protein 3	1,74485136	0,80310414	0,00147457	0,04171535
A_55_P2163729	NM_001013778	ENSMUST00000051118	383103	*Tvp23a*	trans-golgi network vesicle protein 23A	1,7439865	0,80238888	0,00012292	0,03291643
A_55_P1983523	NM_145437	ENSMUST00000045075	217305	*Cd300ld*	CD300 molecule-like family member d	1,74377447	0,80221346	0,00019617	0,03291643
A_52_P549166	NM_173451	ENSMUST00000093976	271970	*Arsj*	arylsulfatase J	1,74174319	0,80053193	0,00139817	0,04083433
A_51_P452203	NM_144879	ENSMUST00000047409	226841	*Vash2*	vasohibin 2	1,73939237	0,79858341	0,00074781	0,03604365
A_55_P2001608	NM_172781	ENSMUST00000113370	237010	*Klhl4*	kelch-like 4	1,73683622	0,79646172	0,00104269	0,03812918
A_55_P2012960	NM_024198	ENSMUST00000030332	67305	*Gpx7*	glutathione peroxidase 7	1,73666396	0,79631863	0,00051535	0,03476444
A_52_P547612	NM_178715	ENSMUST00000042975	238257	*Tmem30b*	transmembrane protein 30B	1,73650113	0,79618335	0,00030594	0,03315398
A_55_P2179309	NM_001122596	ENSMUST00000067249	213438	*P2ry10b*	purinergic receptor P2Y, G-protein coupled 10B	1,73635097	0,79605859	0,00151091	0,04191356
A_52_P284889	NM_008860	ENSMUST00000103178	18762	*Prkcz*	protein kinase C, zeta	1,73633331	0,79604392	0,000958	0,03725879
A_55_P1973770	NM_029770	ENSMUST00000077925	107449	*Unc5b*	unc-5 netrin receptor B	1,73355332	0,79373221	0,00018986	0,03291643
A_55_P2079167	NM_010065	ENSMUST00000113352	13429	*Dnm1*	dynamin 1	1,73252347	0,7928749	0,00032145	0,03315398
A_55_P2418745	AK084380		106251	*D230034L24Rik*	RIKEN cDNA D230034L24 gene	1,72791123	0,7890291	0,0011977	0,03905162
A_51_P438821	NM_023258	ENSMUST00000033056	66824	*Pycard*	PYD and CARD domain containing	1,72687033	0,78815975	0,00215338	0,04733954
A_55_P2141084	NM_011858	ENSMUST00000107162	23966	*Tenm4*	teneurin transmembrane protein 4	1,72652422	0,78787057	0,00032488	0,03315398
A_55_P2054342	NR_038009	ENSMUST00000150749	69941	*2810408I11Rik*	RIKEN cDNA 2810408I11 gene	1,72352946	0,78536596	0,00114148	0,03867628
A_55_P2015670	NM_008397	ENSMUST00000112101	16403	*Itga6*	integrin alpha 6	1,72338145	0,78524206	0,00074506	0,03604365
A_52_P330395	NM_134082	ENSMUST00000026635	223254	*Farp1*	FERM, RhoGEF (Arhgef) and pleckstrin domain protein 1 (chondroc	1,72298076	0,78490659	0,00013756	0,03291643
A_55_P2232057	NR_045719	ENSMUST00000227886	105976	*AU022793*	expressed sequence AU022793	1,72131311	0,78350955	0,00024301	0,03291643
A_55_P2077083	NM_023438	ENSMUST00000092852	270893	*Tmem132e*	transmembrane protein 132E	1,7197356	0,78218678	0,00091051	0,03681936
A_52_P31641	NM_183311	ENSMUST00000108409	330485	*Tmem145*	transmembrane protein 145	1,71802123	0,78074787	0,00157539	0,04243679
A_51_P254045	NM_011634	ENSMUST00000049348	22036	*Traip*	TRAF-interacting protein	1,7121459	0,77580564	0,00029818	0,03315398
A_51_P321886	NM_024217	ENSMUST00000034343	68119	*Cmtm3*	CKLF-like MARVEL transmembrane domain containing 3	1,71188961	0,77558968	0,002391	0,04851956
A_55_P2101757	NM_183089	ENSMUST00000023059	72107	*Dscc1*	DNA replication and sister chromatid cohesion 1	1,71126609	0,7750641	0,00101239	0,03808028

A_55_P2030269	NM_001164669	ENSMUST00000064948	330355	*Dnah6*	dynein, axonemal, heavy chain 6	1,70894139	0,77310292	0,00042149	0,03391783
A_55_P2008181	NM_008369	ENSMUST00000090591	16188	*Il3ra*	interleukin 3 receptor, alpha chain	1,70873217	0,77292628	0,00083875	0,03629498
A_51_P285779	NM_028386	ENSMUST00000031291	72898	*Asphd2*	aspartate beta-hydroxylase domain containing 2	1,7084271	0,77266868	0,00168433	0,04345841
A_55_P2018116	NM_001101479	ENSMUST00000166505	241989	*Pabpc4l*	poly(A) binding protein, cytoplasmic 4-like	1,70763324	0,77199815	0,00107649	0,03823783
A_66_P116683	NR_045629		328594	*D630010B17Rik*	RIKEN cDNA D630010B17 gene	1,70643527	0,77098569	0,00193124	0,04564964
A_52_P515880	NM_012038	ENSMUST00000072299	26950	*Vsnl1*	visinin-like 1	1,70538584	0,77009818	0,00098086	0,03765882
A_55_P2124586	NM_001081642	ENSMUST00000114530	434794	*Xlr4a*	X-linked lymphocyte-regulated 4A	1,70399545	0,76892148	0,00080882	0,03629498
A_55_P2104988	NM_001289791	ENSMUST00000023758	11419	*Asic1*	acid-sensing (proton-gated) ion channel 1	1,70067444	0,76610699	0,00013989	0,03291643
A_55_P2129925	NM_008652	ENSMUST00000018005	17865	*Mybl2*	myeloblastosis oncogene-like 2	1,70048267	0,7659443	0,00182961	0,0445458
A_51_P230098	NM_023209	ENSMUST00000022612	52033	*Pbk*	PDZ binding kinase	1,69774015	0,76361566	0,00012876	0,03291643
A_51_P182257	NM_001039494	ENSMUST00000057716	67077	*Catsperz*	cation channel sperm associated auxiliary subunit zeta	1,69763964	0,76353025	0,00119045	0,03904427
A_55_P2084656	NM_175659	ENSMUST00000091742	319168	*Hist1h2ah*	histone cluster 1, H2ah	1,69541708	0,76164023	0,00056382	0,03481832
A_55_P2079669	NM_007532	ENSMUST00000111742	12035	*Bcat1*	branched chain aminotransferase 1, cytosolic	1,69502212	0,7613041	0,00104472	0,03812918
A_51_P424878	NM_025582	ENSMUST00000030935	66469	*Prxl2b*	peroxiredoxin like 2B	1,69342336	0,75994269	0,00011921	0,03291643
A_52_P368057	NM_011990	ENSMUST00000029297	26570	*Slc7a11*	solute carrier family 7 (cationic amino acid transporter, y+ system)	1,69284152	0,75944692	0,0012217	0,03914579
A_66_P105046	NM_008360	ENSMUST00000059081	16173	*Il18*	interleukin 18	1,69247039	0,7591306	0,00220237	0,04740503
A_55_P1975155	NM_001161767	ENSMUST00000052069	207839	*Galnt6*	polypeptide N-acetylgalactosaminyltransferase 6	1,69211692	0,75882926	0,0003132	0,03315398
A_55_P1968245	NM_010240	ENSMUST00000094434	14325	*Ftl1*	ferritin light chain 1	1,69183488	0,75858877	0,00069748	0,03558895
A_55_P2114118	NM_207675	ENSMUST00000085909	54725	*Cadm1*	cell adhesion molecule 1	1,69133052	0,75815862	0,0014913	0,04187212
A_51_P395373	NM_021464	ENSMUST00000109441	19281	*Ptprt*	protein tyrosine phosphatase, receptor type, T	1,69027934	0,75726169	0,00233241	0,04805255
A_55_P1954486	NM_001285454	ENSMUST00000106989	17762	*Mapt*	microtubule-associated protein tau	1,68862237	0,75584673	0,00161484	0,04282509
A_55_P2027386	NM_153394	ENSMUST00000061274	239845	*Gpr156*	G protein-coupled receptor 156	1,68677233	0,75426526	0,00231612	0,04796206
A_55_P2010622	NM_033354	ENSMUST00000086130	89867	*Sec16b*	SEC16 homolog B (S. cerevisiae)	1,68652196	0,75405111	0,00014608	0,03291643
A_51_P100174	NM_008613	ENSMUST00000034746	17427	*Mns1*	meiosis-specific nuclear structural protein 1	1,6853478	0,75304635	0,00184914	0,04479702
A_55_P2075191	NR_002874	ENSMUST00000125401	594843	*Has2os*	hyaluronan synthase 2, opposite strand	1,68390737	0,75181278	0,00011777	0,03291643
A_55_P1999992	NM_172693	ENSMUST00000107744	230145	*Galnt12*	polypeptide N-acetylgalactosaminyltransferase 12	1,68144418	0,74970088	0,00066663	0,03555961
A_55_P1991688	NM_009013	ENSMUST00000112221	19362	*Rad51ap1*	RAD51 associated protein 1	1,68072644	0,74908493	0,0020852	0,04671098
A_55_P2046101	NM_021365	ENSMUST00000124904	27083	*Xlr4b*	X-linked lymphocyte-regulated 4B	1,67944971	0,74798859	0,00191545	0,04552521
A_55_P1972172	NM_007583	ENSMUST00000019290	12300	*Cacng2*	calcium channel, voltage-dependent, gamma subunit 2	1,67892495	0,74753774	0,00066121	0,03555961
A_51_P501018	NM_010892	ENSMUST00000027931	18005	*Nek2*	NIMA (never in mitosis gene a)-related expressed kinase 2	1,67668362	0,74561049	0,00017916	0,03291643
A_55_P2023818	NM_021476	ENSMUST00000113480	58861	*Cysltr1*	cysteinyl leukotriene receptor 1	1,67581915	0,74486646	0,0017596	0,04380084
A_66_P116998	NM_001002272	ENSMUST00000087253	56191	*Tro*	trophinin	1,6748393	0,74402268	0,00120382	0,03908748
A_55_P1958487	NM_028799	ENSMUST00000028721	74176	*Tgm5*	transglutaminase 5	1,6733772	0,74276268	2,14E-05	0,03291643
A_55_P2141699	NM_001033135	ENSMUST00000062525	67702	*Rnf149*	ring finger protein 149	1,67315032	0,74256707	0,00172244	0,04371333
A_66_P136228	NM_030690	ENSMUST00000090339	75646	*Rai14*	retinoic acid induced 14	1,67308651	0,74251204	0,0016896	0,04345841
A_52_P305995	NM_019496	ENSMUST00000041317	56068	*Ammecr1*	Alport syndrome, mental retardation, midface hypoplasia and ellip	1,67198892	0,74156529	0,00014929	0,03291643
A_52_P442710	NM_172399	ENSMUST00000054351	68169	*Ndnf*	neuron-derived neurotrophic factor	1,67138147	0,74104105	0,00075554	0,03604663
A_66_P125209	NM_001290662	ENSMUST00000065896	73804	*Kif2c*	kinesin family member 2C	1,67007585	0,73991363	0,00088333	0,03654939
A_52_P658437	NM_001014976	ENSMUST00000064924	105988	*Espl1*	extra spindle pole bodies 1, separase	1,66993549	0,73979237	0,00139323	0,04080226
A_51_P466229	NM_026840	ENSMUST00000034004	68797	*Pdgfrl*	platelet-derived growth factor receptor-like	1,66932099	0,73926139	0,00072259	0,03593548
A_51_P128463	NM_001099296	ENSMUST00000060050	72690	*Grrp1*	glycine/arginine rich protein 1	1,66805286	0,73816501	0,00206883	0,0465836
A_51_P305628	NM_015803	ENSMUST00000080368	50769	*Atp8a2*	ATPase, aminophospholipid transporter-like, class I, type 8A, mem	1,66594172	0,73633794	0,00182175	0,04447998
A_52_P623511	AK080592		100042510	*Gm3877*	predicted gene 3877	1,66251288	0,73336551	0,00152584	0,04215919
A_55_P2092750	NM_139305	ENSMUST00000030183	230099	*Car9*	carbonic anhydrase 9	1,66178746	0,73273588	0,00032379	0,03315398
A_52_P663600	NM_011035	ENSMUST00000033040	18479	*Pak1*	p21 (RAC1) activated kinase 1	1,66096474	0,73202145	0,00227061	0,04759365
A_55_P2001250	NM_153107	ENSMUST00000038676	242939	*Cpz*	carboxypeptidase Z	1,65730202	0,72883654	0,00214608	0,0473211
A_55_P2121701	XR_374811		414123	*Mir670hg*	MIR670 host gene (non-protein coding)	1,65707676	0,72864043	0,00183454	0,04462436
A_51_P214306	NM_145462	ENSMUST00000022784	219072	*Haus4*	HAUS augmin-like complex, subunit 4	1,6563302	0,72799031	0,00105686	0,03814748
A_52_P214630	NM_011448	ENSMUST00000000579	20682	*Sox9*	SRY (sex determining region Y)-box 9	1,65436115	0,72627421	0,00011608	0,03291643
A_66_P124052	NM_016778	ENSMUST00000027499	51800	*Bok*	BCL2-related ovarian killer protein	1,65422548	0,7261559	0,00116513	0,03904427
A_52_P384718	NM_009865	ENSMUST00000176146	320873	*Cdh10*	cadherin 10	1,65371914	0,72571424	0,00155128	0,04232468
A_55_P2044922	NM_175669	ENSMUST00000053659	319200	*Gpr82*	G protein-coupled receptor 82	1,65329787	0,72534667	0,00188425	0,04514203
A_55_P2036883	NM_175666	ENSMUST00000177113	319189	*Hist2h2bb*	histone cluster 2, H2bb	1,65264742	0,72477897	0,00019863	0,03291643
A_55_P2017362	NM_207203	ENSMUST00000168386	73072	*Prr36*	proline rich 36	1,6524509	0,7246074	0,00027067	0,03315398
A_55_P2041397	NM_007971	ENSMUST00000081721	14056	*Ezh2*	enhancer of zeste 2 polycomb repressive complex 2 subunit	1,65055554	0,72295169	0,00125547	0,03955441

A_51_P198775	NM_201364	ENSMUST00000045876	381306	*BC055324*	cDNA sequence BC055324	1,64864667	0,72128224	0,00096102	0,03733895
A_51_P190111	NM_008566	ENSMUST00000164309	17218	*Mcm5*	minichromosome maintenance complex component 5	1,64670542	0,71958249	0,00206763	0,0465836
A_52_P622850	NM_010419	ENSMUST00000049621	15208	*Hes5*	hes family bHLH transcription factor 5	1,64660515	0,71949464	0,00043763	0,03393479
A_55_P1978201	NM_016692	ENSMUST00000025562	16319	*Incenp*	inner centromere protein	1,64624392	0,71917811	0,00114011	0,03866356
A_55_P1969311	NM_172768	ENSMUST00000118159	235283	*Gramd1b*	GRAM domain containing 1B	1,64483336	0,71794143	0,00159959	0,04267063
A_55_P2003033	NM_177161	ENSMUST00000139790	320452	*P4ha3*	procollagen-proline, 2-oxoglutarate 4-dioxygenase (proline 4-hydr	1,643641	0,71689522	0,00214511	0,0473211
A_51_P130079	NM_008511	ENSMUST00000135984	16970	*Lrmp*	lymphoid-restricted membrane protein	1,64337641	0,71666296	0,00108984	0,03828376
A_55_P2074591	NM_001110218	ENSMUST00000067918	319468	*Ppm1h*	protein phosphatase 1H (PP2C domain containing)	1,63829822	0,712198	0,00224849	0,04750753
A_51_P156857	NM_134133	ENSMUST00000042710	106878	*Smim3*	small integral membrane protein 3	1,63741507	0,71142008	0,00122054	0,03914579
A_52_P526396	NM_178628	ENSMUST00000021466	73991	*Atl1*	atlastin GTPase 1	1,63689172	0,71095889	0,00215979	0,04739734
A_55_P2306336	XR_380814		100504412	*Kcnmb4os2*	potassium large conductance calcium-activated channel, subfamily	1,63532732	0,70957942	0,00161161	0,04279788
A_51_P488991	NM_178644	ENSMUST00000034512	102644	*Oaf*	out at first homolog	1,63498312	0,70927574	0,00047745	0,03469594
A_55_P2156583	NM_009871	ENSMUST00000053413	12569	*Cdk5r1*	cyclin-dependent kinase 5, regulatory subunit 1 (p35)	1,63443811	0,70879475	0,00221572	0,04740503
A_55_P1965101	NM_001081643	ENSMUST00000138149	574437	*Xlr3b*	X-linked lymphocyte-regulated 3B	1,63415085	0,70854116	0,00056613	0,03481832
A_51_P403834	NM_011522	ENSMUST00000007236	20974	*Syngr3*	synaptogyrin 3	1,63407671	0,70847571	0,00229119	0,04779939
A_51_P507942	NM_029097	ENSMUST00000151517	74772	*Atp13a2*	ATPase type 13A2	1,63096802	0,70572849	0,00073475	0,03593548
A_52_P408757	NM_010188	ENSMUST00000164044	14131	*Fcgr3*	Fc receptor, IgG, low affinity III	1,63086955	0,70564138	0,00186263	0,04498682
A_51_P207751	NM_008189	ENSMUST00000059348	14913	*Guca1a*	guanylate cyclase activator 1a (retina)	1,62978472	0,70468141	0,00107523	0,03823006
A_51_P441426	NM_019932	ENSMUST00000031320	56744	*Pf4*	platelet factor 4	1,62963905	0,70455246	0,00195403	0,04589987
A_55_P2046812	NM_009242	ENSMUST00000018737	20692	*Sparc*	secreted acidic cysteine rich glycoprotein	1,62889929	0,70389741	0,00074292	0,03604365
A_51_P309589	NR_024720	ENSMUST00000182402	77022	*2700099C18Rik*	RIKEN cDNA 2700099C18 gene	1,62728697	0,70246869	0,00073346	0,03593548
A_65_P09285	NM_181075	ENSMUST00000100850	330173	*2610524H06Rik*	RIKEN cDNA 2610524H06 gene	1,62642228	0,70170188	5,93E-05	0,03291643
A_66_P121459	NM_007681	ENSMUST00000134372	12615	*Cenpa*	centromere protein A	1,62421349	0,69974128	0,00215666	0,0473821
A_55_P2084413	NM_178005	ENSMUST00000091636	107065	*Lrrtm2*	leucine rich repeat transmembrane neuronal 2	1,6238211	0,6993927	0,00038806	0,03373901
A_55_P1952414	NM_001113214	ENSMUST00000028128	18286	*Odf2*	outer dense fiber of sperm tails 2	1,62252853	0,69824385	0,00165165	0,04305746
A_55_P2094721	NM_009234	ENSMUST00000079063	20666	*Sox11*	SRY (sex determining region Y)-box 11	1,62097449	0,69686138	0,00014475	0,03291643
A_51_P459661	NM_021460	ENSMUST00000049572	16889	*Lipa*	lysosomal acid lipase A	1,6205691	0,69650053	0,00106269	0,03818548
A_55_P1966194	NM_019549	ENSMUST00000020321	56193	*Plek*	pleckstrin	1,61985389	0,69586369	0,00094117	0,03703145
A_55_P1954990	NM_001001445	ENSMUST00000102526	193034	*Trpv1*	transient receptor potential cation channel, subfamily V, member	1,61984265	0,69585367	6,00E-05	0,03291643
A_51_P128987	NM_008012	ENSMUST00000038406	14187	*Akr1b8*	aldo-keto reductase family 1, member B8	1,61893988	0,69504941	0,00067934	0,03558895
A_55_P2064676	AK171905		237436	*Gas2l3*	growth arrest-specific 2 like 3	1,61803251	0,6942406	0,00010118	0,03291643
A_55_P1992839	NM_025853	ENSMUST00000103130	66934	*Dsn1*	DSN1 homolog, MIS12 kinetochore complex component	1,61787282	0,69409821	0,00102866	0,03812918
A_52_P594410	NM_010827	ENSMUST00000027062	17681	*Msc*	musculin	1,61770195	0,69394583	0,00056234	0,03481832
A_55_P2364738	NM_001163608	ENSMUST00000107565	72324	*Plxdc1*	plexin domain containing 1	1,61769224	0,69393717	0,00030533	0,03315398
A_52_P566396	NM_175136	ENSMUST00000046941	68867	*Rnf122*	ring finger protein 122	1,61514277	0,6916617	0,00169701	0,0434933
A_51_P317031	NM_025779	ENSMUST00000122961	66815	*Mcub*	mitochondrial calcium uniporter dominant negative beta subunit	1,61409671	0,69072703	0,00128923	0,03982756
A_51_P413539	NM_021606	ENSMUST00000112902	59126	*Nek6*	NIMA (never in mitosis gene a)-related expressed kinase 6	1,61401131	0,69065069	0,00058549	0,03507191
A_52_P299832	NM_018797	ENSMUST00000099337	54712	*Plxnc1*	plexin C1	1,61223249	0,6890598	0,00254453	0,04970107
A_51_P328652	NM_133348	ENSMUST00000030779	70025	*Acot7*	acyl-CoA thioesterase 7	1,6118926	0,68875562	0,00055846	0,03476444
A_55_P1969002	NM_198052	ENSMUST00000079719	21386	*Tbx3*	T-box 3	1,60987063	0,68694476	0,00129413	0,03982756
A_55_P2144556	NM_001172160	ENSMUST00000110057	71436	*Flrt3*	fibronectin leucine rich transmembrane protein 3	1,60981968	0,6868991	0,00127599	0,03970879
A_55_P2082929	NM_010389	ENSMUST00000095342	15002	*H2-Ob*	histocompatibility 2, O region beta locus	1,60824818	0,68549006	0,00171535	0,04370748
A_51_P314285	NM_026436	ENSMUST00000010451	67893	*Tmem86a*	transmembrane protein 86A	1,60648233	0,68390511	0,00174582	0,04380084
A_51_P444437	NM_025968	ENSMUST00000030069	67103	*Ptgr1*	prostaglandin reductase 1	1,60608666	0,68354974	1,00E-04	0,03291643
A_52_P282838	NM_001005370	ENSMUST00000049999	278240	*Spin2c*	spindlin family, member 2C	1,60583704	0,68332549	0,00112167	0,03850773
A_55_P2073694	NM_001033248	ENSMUST00000010673	212539	*Gm266*	predicted gene 266	1,60232095	0,68016315	0,00055252	0,03476444
A_55_P1987151	NM_011860	ENSMUST00000015866	23968	*Nlrp5*	NLR family, pyrin domain containing 5	1,59971544	0,6778153	0,00017994	0,03291643
A_55_P1977473	NM_023118	ENSMUST00000110664	13132	*Dab2*	disabled 2, mitogen-responsive phosphoprotein	1,59811482	0,67637106	0,00022491	0,03291643
A_65_P10673	NM_172614	ENSMUST00000149110	224090	*Tmem44*	transmembrane protein 44	1,59699862	0,67536306	0,00110705	0,03830608
A_51_P277006	NM_175140	ENSMUST00000154629	68947	*Chst8*	carbohydrate sulfotransferase 8	1,59694277	0,67531261	0,00013496	0,03291643
A_51_P347240	NM_001081406	ENSMUST00000110621	69706	*Lrr1*	leucine rich repeat protein 1	1,5963391	0,67476714	0,00253727	0,04970107
A_55_P1994927	NM_144538	ENSMUST00000121418	74760	*Rab3il1*	RAB3A interacting protein (rabin3)-like 1	1,59073343	0,6696921	0,0007601	0,03611065
A_51_P359800	NM_009131	ENSMUST00000004587	20256	*Clec11a*	C-type lectin domain family 11, member a	1,59005985	0,66908107	0,00070059	0,03558895
A_51_P314907	NM_013726	ENSMUST00000171808	27214	*Dbf4*	DBF4 zinc finger	1,58785661	0,66708063	0,00055214	0,03476444
A_51_P351363	NR_000040	ENSMUST00000219550	22172	*Tyms-ps*	thymidylate synthase, pseudogene	1,58666393	0,66599659	0,00150267	0,04189237

A_66_P125392	NM_001080944	ENSMUST00000040149	241633	*Atp8b4*	ATPase, class I, type 8B, member 4	1,58469514	0,66420532	0,00207206	0,0465836
A_52_P148514	NM_152803	ENSMUST00000045617	15442	*Hpse*	heparanase	1,58430285	0,66384814	0,00115468	0,03885309
A_55_P1995055	NM_001030296	ENSMUST00000046533	432763	*Prr7*	proline rich 7 (synaptic)	1,58395959	0,66353553	0,00144493	0,04149019
A_52_P368384	NM_028712	ENSMUST00000049064	74012	*Rap2b*	RAP2B, member of RAS oncogene family	1,58358345	0,6631929	0,000275	0,03315398
A_52_P1026777	NM_001033141	ENSMUST00000097618	68545	*Ecscr*	endothelial cell surface expressed chemotaxis and apoptosis regul	1,58344484	0,66306661	0,00012345	0,03291643
A_55_P2406852	NM_025681	ENSMUST00000115576	66643	*Lix1*	limb and CNS expressed 1	1,58295993	0,66262473	0,00174837	0,04380084
A_52_P381303	NM_178856	ENSMUST00000126094	272551	*Gins2*	GINS complex subunit 2 (Psf2 homolog)	1,58155677	0,66134534	0,00135381	0,04041885
A_51_P218774	NM_026418	ENSMUST00000033133	67865	*Rgs10*	regulator of G-protein signalling 10	1,58105163	0,66088448	0,00093565	0,03698032
A_51_P228295	NM_001001880	ENSMUST00000111435	68481	*Mpzl1*	myelin protein zero-like 1	1,5803229	0,66021937	0,00053928	0,03476444
A_51_P282523	NM_054044	ENSMUST00000033876	78560	*Adgra2*	G protein-coupled receptor 124	1,57978203	0,65972551	0,00076092	0,03611065
A_55_P2066543	NM_178751	ENSMUST00000041048	269717	*Orai2*	ORAI calcium release-activated calcium modulator 2	1,57909978	0,65910234	0,0017872	0,04408364
A_52_P536494	NM_008709	ENSMUST00000043396	18109	*Mycn*	v-myc myelocytomatosis viral related oncogene, neuroblastoma d	1,57899611	0,65900762	0,00013359	0,03291643
A_51_P208680	NM_145409	ENSMUST00000168914	214901	*Chtf18*	CTF18, chromosome transmission fidelity factor 18	1,57817109	0,65825362	0,00143713	0,04138233
A_55_P2075469	NM_080640	ENSMUST00000226440	118452	*Baalc*	brain and acute leukemia, cytoplasmic	1,57777603	0,65789243	0,00221888	0,04740503
A_51_P196973	NM_013733	ENSMUST00000002914	27221	*Chaf1a*	chromatin assembly factor 1, subunit A (p150)	1,57750785	0,65764719	0,00204286	0,04655586
A_51_P473272	NM_019656	ENSMUST00000087557	56496	*Tspan6*	tetraspanin 6	1,57675532	0,6569588	0,00019997	0,03291643
A_51_P503896	ENSMUST000000261	ENSMUST00000026133	209027	*Pycr1*	pyrroline-5-carboxylate reductase 1	1,57635218	0,65658989	0,00078124	0,03629498
A_51_P256246	NM_025359	ENSMUST00000020896	66109	*Tspan13*	tetraspanin 13	1,57579126	0,65607644	0,0014947	0,04188934
A_55_P2108255	NM_011175	ENSMUST00000021607	19141	*Lgmn*	legumain	1,57340468	0,65388978	0,00118792	0,03904427
A_55_P2068260	NM_145073	ENSMUST00000080859	97908	*Hist1h3g*	histone cluster 1, H3g	1,57291981	0,65344513	0,00171547	0,04370748
A_55_P2083121	NM_001164567	ENSMUST00000074734	22351	*Vill*	villin-like	1,57241342	0,65298058	0,00160149	0,04267063
A_55_P2084666	NM_175661	ENSMUST00000073261	319173	*Hist1h2af*	histone cluster 1, H2af	1,57166621	0,65229485	0,00080912	0,03629498
A_52_P539310	NM_001160326	ENSMUST00000064517	72661	*Serp2*	stress-associated endoplasmic reticulum protein family member 2	1,57018639	0,65093582	0,00220808	0,04740503
A_52_P655285	NM_172867	ENSMUST00000098070	242466	*Zfp462*	zinc finger protein 462	1,56873743	0,6496039	0,00128735	0,03982756
A_51_P241769	NM_011270	ENSMUST00000030627	19746	*Rhd*	Rh blood group, D antigen	1,5678248	0,64876435	0,00132681	0,04018556
A_55_P2028788	NM_001166503	ENSMUST00000042657	69806	*Slc39a11*	solute carrier family 39 (metal ion transporter), member 11	1,56757614	0,64853552	0,00126176	0,03964697
A_51_P138923	NM_013788	ENSMUST00000094339	27412	*Peg12*	paternally expressed 12	1,5626804	0,64402275	0,00064628	0,03555961
A_55_P2091928	NM_009017	ENSMUST00000065527	19369	*Raet1b*	retinoic acid early transcript beta	1,56265239	0,64399689	0,00207117	0,0465836
A_51_P324934	AK088142	ENSMUST00000053266	17215	*Mcm3*	minichromosome maintenance deficient 3 (S. cerevisiae)	1,56259536	0,64394423	0,00059393	0,03507191
A_51_P202074	NM_146171	ENSMUST00000043848	68298	*Ncapd2*	non-SMC condensin I complex, subunit D2	1,56099603	0,64246687	0,00197525	0,04607464
A_51_P158210	NM_008564	ENSMUST00000058011	17216	*Mcm2*	minichromosome maintenance deficient 2 mitotin (S. cerevisiae)	1,55999177	0,64153842	0,00101848	0,03812555
A_51_P519791	NM_198605	ENSMUST00000022536	219114	*Ska3*	spindle and kinetochore associated complex subunit 3	1,55920366	0,64080938	0,00239594	0,04851956
A_51_P416509	NM_030609	ENSMUST00000055770	80838	*Hist1h1a*	histone cluster 1, H1a	1,55770085	0,6394182	0,00062587	0,03546117
A_66_P129188	NM_175662	ENSMUST00000090782	319176	*Hist2h2ac*	histone cluster 2, H2ac	1,5542601	0,63622795	0,00091468	0,03681936
A_51_P305437	NM_009037	ENSMUST00000127019	19672	*Rcn1*	reticulocalbin 1	1,55424369	0,63621273	0,001391	0,04077792
A_55_P2317665	NM_007891	ENSMUST00000000894	13555	*E2f1*	E2F transcription factor 1	1,55340025	0,63542961	0,00022871	0,03291643
A_55_P2047106	NM_153793	ENSMUST00000070709	225392	*Rell2*	RELT-like 2	1,55247283	0,63456802	0,00155139	0,04232468
A_52_P231075	NM_030707	ENSMUST00000090986	80891	*Fcrls*	Fc receptor-like S, scavenger receptor	1,55155696	0,63371666	0,00056594	0,03481832
A_55_P2105658	NM_028528	ENSMUST00000028984	73388	*Bpifa3*	BPI fold containing family A, member 3	1,55041357	0,6326531	0,00113219	0,03857573
A_55_P2419296	AK003491		76286			1,55036804	0,63261074	0,00036699	0,03369759
A_51_P303749	NM_178683	ENSMUST00000051594	218581	*Depdc1b*	DEP domain containing 1B	1,55027456	0,63252375	0,00031039	0,03315398
A_55_P2152165	XM_006541351		102640292			1,54981488	0,6320959	0,00147048	0,04166534
A_55_P2116664	NM_133255	ENSMUST00000064495	170833	*Hook2*	hook microtubule tethering protein 2	1,54946315	0,63176844	0,00198532	0,04609624
A_51_P207988	NM_008965	ENSMUST00000047379	19219	*Ptger4*	prostaglandin E receptor 4 (subtype EP4)	1,54916295	0,6314889	0,00113257	0,03857573
A_55_P2133255	NM_019499	ENSMUST00000116605	56150	*Mad2l1*	MAD2 mitotic arrest deficient-like 1	1,54773694	0,63016029	0,00175419	0,04380084
A_55_P1985410	NM_178256	ENSMUST00000112334	194590	*Reps2*	RALBP1 associated Eps domain containing protein 2	1,54717061	0,6296323	0,00220963	0,04740503
A_55_P1985239	NM_178617	ENSMUST00000108273	69352	*Necab1*	N-terminal EF-hand calcium binding protein 1	1,5459695	0,62851186	0,00060076	0,03507191
A_55_P2096797	NM_001040696	ENSMUST00000108515	637515	*Nlrp1b*	NLR family, pyrin domain containing 1B	1,54564553	0,6282095	0,00040061	0,03373901
A_55_P2069659	NM_030728	ENSMUST00000145171	80982	*Cemip*	cell migration inducing protein, hyaluronan binding	1,54499733	0,62760434	0,00176363	0,04382991
A_51_P217463	NM_009140	ENSMUST00000075433	20310	*Cxcl2*	chemokine (C-X-C motif) ligand 2	1,54440146	0,62704782	0,0003341	0,03315398
A_51_P337089	NM_027014	ENSMUST00000028948	69270	*Gins1*	GINS complex subunit 1 (Psf1 homolog)	1,54416131	0,62682347	0,00180235	0,04429746
A_51_P126626	NM_145459	ENSMUST00000043409	218820	*Zfp503*	zinc finger protein 503	1,54394012	0,6266168	0,00223183	0,04740503
A_55_P2098210	NM_172741	ENSMUST00000085592	233103	*Garre1*	granule associated Rac and RHOG effector 1	1,54355977	0,62626135	0,00017949	0,03291643
A_66_P111430	NR_030738	ENSMUSG00000086841	69221	*2410006H16Rik*	RIKEN cDNA 2410006H16 gene	1,54327137	0,62599177	0,00197323	0,04607464
A_51_P493671	NM_001081327	ENSMUST00000084628	195646	*Hs3st2*	heparan sulfate (glucosamine) 3-O-sulfotransferase 2	1,54312663	0,62585646	0,00163481	0,04294518

A_55_P1989573	NM_028223	ENSMUST00000120327	72392	*Tmem175*	transmembrane protein 175	1,54242291	0,62519839	0,00058387	0,03507191
A_55_P1976734	NM_001174047	ENSMUST00000085092	56808	*Cacna2d2*	calcium channel, voltage-dependent, alpha 2/delta subunit 2	1,54208128	0,6248788	0,00182081	0,04447998
A_52_P106259	NM_207655	ENSMUST00000020329	13649	*Egfr*	epidermal growth factor receptor	1,54092724	0,62379874	0,00097513	0,03754991
A_55_P2065529	NM_011973	ENSMUST00000021701	26448	*Mok*	MOK protein kinase	1,54084373	0,62372056	0,00023571	0,03291643
A_55_P1971244	NM_001098789	ENSMUST00000035735	407790	*Ndufa4l2*	Ndufa4, mitochondrial complex associated like 2	1,53653109	0,61967696	0,00139007	0,04077792
A_51_P235123	NM_008690	ENSMUST00000024742	18037	*Nfkbie*	nuclear factor of kappa light polypeptide gene enhancer in B cells i	1,53319524	0,61654143	0,00181286	0,04444355
A_55_P1972927	NM_013508	ENSMUST00000129827	13713	*Elk3*	ELK3, member of ETS oncogene family	1,53112896	0,6145958	0,00021784	0,03291643
A_66_P102853	NM_178793	ENSMUST00000151343	320924	*Ccbe1*	collagen and calcium binding EGF domains 1	1,52730309	0,61098639	0,00088188	0,03654939
A_51_P251205	NM_028627	ENSMUST00000096029	73728	*Psd*	pleckstrin and Sec7 domain containing	1,52630494	0,61004323	0,00090387	0,0368081
A_51_P323878	NM_030205	ENSMUST00000038552	78885	*Coro7*	coronin 7	1,5261696	0,60991529	0,00014199	0,03291643
A_55_P2170034	NM_016846	ENSMUST00000027760	19731	*Rgl1*	ral guanine nucleotide dissociation stimulator,-like 1	1,52595886	0,60971607	0,00068788	0,03558895
A_52_P155805	NR_027924	ENSMUST00000128571	68355	*2010204K13Rik*	RIKEN cDNA 2010204K13 gene	1,52587446	0,60963627	0,000885	0,03654939
A_51_P202596	NM_172628	ENSMUST00000051720	225608	*Sh3tc2*	SH3 domain and tetratricopeptide repeats 2	1,52549508	0,60927752	0,00012318	0,03291643
A_55_P1994997	NM_181416	ENSMUST00000110947	228482	*Arhgap11a*	Rho GTPase activating protein 11A	1,52408148	0,60794003	0,00138151	0,04068336
A_55_P1975690	NM_031397	ENSMUST00000131445	83675	*Bicc1*	BicC family RNA binding protein 1	1,52300969	0,60692512	0,00019594	0,03291643
A_51_P223709	NM_080850	ENSMUST00000133886	269224	*Pask*	PAS domain containing serine/threonine kinase	1,51802821	0,6021986	0,00044233	0,03394989
A_51_P305547	NM_011415	ENSMUST00000023356	20583	*Snai2*	snail homolog 2 (Drosophila)	1,51800708	0,60217852	0,00149629	0,04188934
A_55_P2002122	NM_173402	ENSMUST00000030984	71729	*Rgs12*	regulator of G-protein signaling 12	1,51721289	0,60142353	0,00186351	0,04498682
A_51_P516728	NM_010404	ENSMUST00000138603	15114	*Hap1*	huntingtin-associated protein 1	1,51667601	0,60091294	0,00141096	0,041007
A_55_P2092310	AK195427		236539	*Phgdh*	3-phosphoglycerate dehydrogenase	1,51537251	0,59967248	8,35E-05	0,03291643
A_55_P2045571	NM_007400	ENSMUST00000067680	11489	*Adam12*	a disintegrin and metallopeptidase domain 12 (meltrin alpha)	1,51522413	0,59953121	0,00140075	0,04084925
A_65_P05152	NM_201518	ENSMUST00000057324	399558	*Flrt2*	fibronectin leucine rich transmembrane protein 2	1,51236692	0,5968082	0,00109267	0,03828376
A_55_P2037513	NM_011116	ENSMUST00000117611	18807	*Pld3*	phospholipase D family, member 3	1,51104451	0,59554616	0,00226247	0,0475368
A_55_P2157195	XR_380278		102637112	*Gm34006*	uncharacterized LOC102637112	1,51078627	0,59529958	0,00046042	0,03433826
A_55_P1973995	NR_076393	ENSMUST00000180647	627427	*Gm6756*	predicted gene 6756	1,51039586	0,59492672	0,00021106	0,03291643
A_51_P451106	NM_009765	ENSMUST00000044620	12190	*Brca2*	breast cancer 2	1,50970776	0,5942693	0,00055688	0,03476444
A_55_P2048751	NM_008937	ENSMUST00000175916	19130	*Prox1*	prospero homeobox 1	1,50943946	0,5940129	0,00084153	0,03629498
A_51_P215530	XM_006517759	ENSMUST00000224011	71816	*Rnf180*	ring finger protein 180	1,5083501	0,59297132	0,00060301	0,0350957
A_55_P1954061	NM_001205234	ENSMUST00000077182	18190	*Nrxn2*	neurexin II	1,50804096	0,59267561	0,00088574	0,03654939
A_55_P2124641	ENSMUST00000141413	ENSMUST00000141333	232313	*Gxylt2*	glucoside xylosyltransferase 2	1,50803436	0,5926693	0,00111285	0,03830608
A_51_P115817	NM_023884	ENSMUST00000063199	78255	*Ralgps2*	Ral GEF with PH domain and SH3 binding motif 2	1,50669239	0,59138491	0,00249118	0,04932867
A_55_P2022604	NM_001289489	ENSMUST00000072646	74190	*Exoc3l4*	exocyst complex component 3-like 4	1,50496076	0,58972587	0,00080713	0,03629498
A_55_P2048928	NM_001161458	ENSMUST00000052209	12400	*Cbfb*	core binding factor beta	1,5024578	0,58732447	0,0022252	0,04740503
A_51_P429212	NM_028749	ENSMUST00000041874	74091	*Npl*	N-acetylneuraminate pyruvate lyase	1,50222379	0,58709975	0,00179943	0,04428159
A_51_P167763	NM_146037	ENSMUST00000049788	217826	*Kcnk13*	potassium channel, subfamily K, member 13	1,50207209	0,58695405	0,00173164	0,04380084
A_52_P361081	NM_001112744	ENSMUST00000144145	230972	*Arhgef16*	Rho guanine nucleotide exchange factor (GEF) 16	1,501763	0,58665715	0,00099532	0,03807877
A_55_P1965050	NM_025415	ENSMUST00000075853	66197	*Cks2*	CDC28 protein kinase regulatory subunit 2	1,50171664	0,58661261	0,00200344	0,0463625
A_55_P2131438	NM_178212	ENSMUST00000091708	319192	*Hist2h2aa2*	histone cluster 2, H2aa2	1,50140772	0,5863158	0,00074296	0,03604365
A_55_P2020577	NM_008788	ENSMUST00000146589	18542	*Pcolce*	procollagen C-endopeptidase enhancer protein	1,49981079	0,58478051	0,00072605	0,03593548
A_51_P196925	NM_009142	ENSMUST00000034230	20312	*Cx3cl1*	chemokine (C-X3-C motif) ligand 1	1,49956221	0,58454138	0,00059299	0,03507191
A_51_P230439	NM_008905	ENSMUST00000040056	19024	*Ppfibp2*	PTPRF interacting protein, binding protein 2 (liprin beta 2)	1,49914248	0,58413751	0,00109201	0,03828376
A_55_P2078695	NM_001199632	ENSMUST00000051358	320118	*Fbxl13*	F-box and leucine-rich repeat protein 13	1,49723637	0,582302	0,00015225	0,03291643
A_66_P107038	NM_028243	ENSMUST00000076052	72461	*Prcp*	prolylcarboxypeptidase (angiotensinase C)	1,49619027	0,58129366	0,00069042	0,03558895
A_55_P1962516	NM_182807	ENSMUST00000050756	268354	*Tafa2*	TAFA chemokine like family member 2	1,49300762	0,57822152	0,00122612	0,03919053
A_55_P2010704	NM_001037279	ENSMUST00000154179	72657	*Selenoh*	selenoprotein H	1,49289486	0,57811257	0,00229471	0,04782329
A_55_P2425761	AK083074	ENSMUST00000201865	320715	*C530043K16Rik*	RIKEN cDNA C530043K16 gene	1,4926576	0,57788327	0,00068333	0,03558895
A_52_P276955	NM_010140	ENSMUST00000064405	13837	*Epha3*	Eph receptor A3	1,49265681	0,5778825	0,00112778	0,03857573
A_52_P574653	NM_007544	ENSMUST00000004560	12122	*Bid*	BH3 interacting domain death agonist	1,49257317	0,57780166	0,00225379	0,04753096
A_55_P1992079	NM_011213	ENSMUST00000124758	19268	*Ptprf*	protein tyrosine phosphatase, receptor type, F	1,49231968	0,57755662	0,00238782	0,04851956
A_55_P2114133	NM_178888	ENSMUST00000049618	99326	*Gaml3*	GTPase activating RANGAP domain-like 3	1,49152329	0,5767865	0,00202334	0,0464094
A_51_P246066	NM_029612	ENSMUST00000027830	98365	*Slamf9*	SLAM family member 9	1,49066391	0,57595502	0,00159582	0,04267063
A_55_P2131238	NM_153392	ENSMUST00000064129	230603	*Ttc39a*	tetratricopeptide repeat domain 39A	1,4904867	0,57578351	0,00136712	0,04050525
A_51_P488554	NM_026543	ENSMUST00000020647	68067	*Mrnip*	MRN complex interacting protein	1,4898912	0,57520698	0,00021159	0,03291643
A_65_P19149	NM_029447	ENSMUST00000109315	75805	*Nln*	neurolysin (metallopeptidase M3 family)	1,48927193	0,5746072	0,00064288	0,03555961
A_55_P1978895	NM_177578	ENSMUST00000170945	195564	*Skint3*	selection and upkeep of intraepithelial T cells 3	1,48906495	0,57440668	0,00073076	0,03593548

A_52_P168449	NM_011161	ENSMUST00000088823	19094	*Mapk11*	mitogen-activated protein kinase 11	1,48872702	0,57407924	0,0024261	0,04873607
A_52_P502771	NM_001039556	ENSMUST00000070755	623474	*Rad54b*	RAD54 homolog B (S. cerevisiae)	1,48706001	0,57246287	0,00230815	0,04792459
A_55_P2297300	NR_040324	ENSMUST00000206959	319783	*A730056A06Rik*	RIKEN cDNA A730056A06 gene	1,48554563	0,57099292	0,000942	0,03703145
A_51_P115666	NM_134087	ENSMUST00000170153	105732	*Fam83h*	family with sequence similarity 83, member H	1,48424056	0,56972494	0,00058214	0,03507191
A_55_P1966987	NM_010717	ENSMUST00000015137	16885	*Limk1*	LIM-domain containing, protein kinase	1,48413428	0,56962163	0,00235999	0,0482972
A_55_P1963150	NM_011804	ENSMUST00000140769	433375	*Creg1*	cellular repressor of E1A-stimulated genes 1	1,48249481	0,56802706	0,0013131	0,04015729
A_51_P123134	NM_146235	ENSMUST00000056904	236930	*Ercc6l*	excision repair cross-complementing rodent repair deficiency com	1,4824818	0,56801439	0,00128249	0,03979485
A_51_P270519	NM_027263	ENSMUST00000132672	69928	*Cenps*	centromere protein S	1,48227524	0,56781336	0,00091644	0,03681936
A_52_P650387	NM_001045530	ENSMUST00000050574	380694	*Ccnjl*	cyclin J-like	1,48132063	0,56688395	0,00091457	0,03681936
A_55_P2005585	NM_032000	ENSMUST00000077935	83925	*Trps1*	transcriptional repressor GATA binding 1	1,48122583	0,56679161	0,00068582	0,03558895
A_55_P1976729	AK163925		100042497	*Gm3871*	predicted gene 3871	1,48023872	0,56582986	0,00069503	0,03558895
A_55_P1969032	NM_011268	ENSMUST00000103062	19739	*Rgs9*	regulator of G-protein signaling 9	1,47917068	0,56478853	0,00102208	0,03812918
A_51_P355852	NM_008856	ENSMUST00000021527	18755	*Prkch*	protein kinase C, eta	1,47605139	0,56174295	0,00050316	0,03476444
A_55_P1982916	NM_172449	ENSMUST00000039627	207777	*Tspoap1*	TSPO associated protein 1	1,47574624	0,56144466	0,00088911	0,0365513
A_66_P129622	NM_001102613	ENSMUST00000073325	232970	*Phldb3*	pleckstrin homology-like domain, family B, member 3	1,4751914	0,56090215	0,00052296	0,03476444
A_55_P2040743	NM_026507	ENSMUST00000122091	68014	*Zwilch*	zwilch kinetochore protein	1,47410272	0,55983705	0,00055143	0,03476444
A_55_P2005946	NM_026915	ENSMUST00000077706	69032	*Lyzl4*	lysozyme-like 4	1,47349868	0,55924577	0,00036775	0,03369759
A_55_P1979833	NM_007709	ENSMUST00000101336	12705	*Cited1*	Cbp/p300-interacting transactivator with Glu/Asp-rich carboxy-ter	1,47219138	0,55796523	0,00122152	0,03914579
A_51_P207622	NM_021355	ENSMUST00000048183	14264	*Fmod*	fibromodulin	1,47059812	0,55640305	0,00254782	0,04970107
A_52_P476075	NM_175554	ENSMUST00000048391	269582	*Clspn*	claspin	1,46984424	0,55566328	0,00024164	0,03291643
A_55_P1981704	NM_172914	ENSMUST00000041569	244608	*Ccdc113*	coiled-coil domain containing 113	1,46652125	0,55239798	0,00074918	0,03604365
A_55_P2182452	NM_177371	ENSMUST00000062246	326623	*Tnfsf15*	tumor necrosis factor (ligand) superfamily, member 15	1,46651592	0,55239273	0,00035257	0,03339594
A_65_P15875	NM_133913	ENSMUST00000121863	100910	*Chpf2*	chondroitin polymerizing factor 2	1,46557193	0,55146378	0,00080269	0,03629498
A_55_P2175180	AK033636		100039704	*Gm2379*	predicted gene 2379	1,46146738	0,54741763	0,00086372	0,03639109
A_55_P2218334	AK034586		319791	*9430011C21Rik*	RIKEN cDNA 9430011C21 gene	1,46127999	0,54723264	0,00106422	0,03818548
A_55_P2140348	BC103785		16061	*Igh-VJ558*	immunoglobulin heavy chain (J558 family)	1,45795264	0,54394386	0,00221348	0,04740503
A_55_P2006153	NM_001101656	ENSMUST00000100240	100043123	*Cd300ld4*	CD300 molecule like family member D4	1,45625316	0,54226118	0,00114931	0,03878076
A_55_P2085412	NM_172756	ENSMUST00000119976	234396	*Ankle1*	ankyrin repeat and LEM domain containing 1	1,45602753	0,54203764	0,00084523	0,03629498
A_51_P269792	NM_009014	ENSMUST00000079533	19363	*Rad51b*	RAD51 homolog B	1,45535775	0,54137384	0,00042342	0,03391783
A_55_P2077263	NM_021790	ENSMUST00000022227	60411	*Cenpk*	centromere protein K	1,45495736	0,54097687	0,00075781	0,03611043
A_51_P116601	NM_172447	ENSMUST00000148347	207686	*Cfap69*	cilia and flagella associated protein 69	1,45475087	0,54077211	0,00192373	0,04561071
A_55_P2167025	NM_008990	ENSMUST00000075447	19294	*Nectin2*	nectin cell adhesion molecule 2	1,45450149	0,54052478	0,00157352	0,04242288
A_55_P1987439	NM_133779	ENSMUST00000103101	78928	*Pigt*	phosphatidylinositol glycan anchor biosynthesis, class T	1,45438521	0,54040943	0,00075078	0,03604365
A_55_P1969341	NM_178309	ENSMUST00000149748	237911	*Brip1*	BRCA1 interacting protein C-terminal helicase 1	1,45408386	0,54011047	0,00011625	0,03291643
A_55_P2238406	NR_028126		70720	*6330407A03Rik*	RIKEN cDNA 6330407A03 gene	1,45318366	0,53921705	0,00214431	0,0473211
A_55_P1984908	NM_172590	ENSMUST00000046437	218460	*Wdr41*	WD repeat domain 41	1,45255602	0,53859381	0,00020397	0,03291643
A_51_P410451	NM_028006	ENSMUST00000019991	71924	*Tube1*	tubulin, epsilon 1	1,45209562	0,53813645	0,00128634	0,03982756
A_52_P65237	NM_145356	ENSMUST00000058997	207259	*Zbtb7c*	zinc finger and BTB domain containing 7C	1,45140417	0,53744932	0,00218198	0,04740503
A_51_P169714	NM_001024539	ENSMUST00000020564	216148	*Shc2*	SHC (Src homology 2 domain containing) transforming protein 2	1,45043501	0,53648565	0,00057348	0,03507191
A_52_P203560	NM_175284	ENSMUST00000117102	93897	*Fzd10*	frizzled class receptor 10	1,44998176	0,53603476	0,00012153	0,03291643
A_55_P2074688	NM_013553	ENSMUST00000100164	15423	*Hoxc4*	homeobox C4	1,44966299	0,53571755	0,0016227	0,04294518
A_55_P2071834	NM_001081242	ENSMUST00000040025	70549	*Tln2*	talin 2	1,44782321	0,53388545	0,00218904	0,04740503
A_55_P1959425	NM_030696	ENSMUST00000100130	80879	*Slc16a3*	solute carrier family 16 (monocarboxylic acid transporters), memb	1,44691952	0,53298468	0,00043109	0,03393479
A_51_P279712	NM_145923	ENSMUST00000087327	100532	*Rell1*	RELT-like 1	1,44442149	0,53049179	0,00145171	0,04157492
A_55_P1988048	NM_001163522	ENSMUST00000122064	59308	*Emcn*	endomucin	1,44354313	0,52961422	0,00084446	0,03629498
A_55_P2048096	NM_001290453	ENSMUST00000182293	109889	*Mzf1*	myeloid zinc finger 1	1,44349798	0,52956909	0,00064984	0,03555961
A_55_P2075274	NM_175543	ENSMUST00000017783	268451	*Rab11fip4*	RAB11 family interacting protein 4 (class II)	1,44262904	0,52870037	0,00063676	0,03546117
A_51_P448545	NM_028145	ENSMUST00000037359	72184	*Klhl35*	kelch-like 35	1,44074216	0,52681217	0,00232223	0,04798501
A_52_P451644	NM_010882	ENSMUST00000038775	17984	*Ndn*	necdin	1,44059472	0,52666452	6,06E-05	0,03291643
A_66_P119421	NM_011034	ENSMUST00000135573	18477	*Prdx1*	peroxiredoxin 1	1,43963424	0,52570232	0,00065603	0,03555961
A_55_P2072005	ENSMUST000001311	ENSMUST00000131108	13032	*Ctsc*	cathepsin C	1,43786085	0,52392407	0,00050014	0,03476444
A_52_P284958	NM_173784	ENSMUST00000051053	327900	*Ubtd2*	ubiquitin domain containing 2	1,43659896	0,52265737	0,00100452	0,03807877
A_55_P2095360	NM_011576	ENSMUST00000028487	21788	*Tfpi*	tissue factor pathway inhibitor	1,4364864	0,52254433	0,00121475	0,03911544
A_55_P1992715	ENSMUST000001358	ENSMUST00000135887	16009	*Igfbp3*	insulin-like growth factor binding protein 3	1,4363899	0,52244742	0,00174833	0,04380084
A_52_P407692	NM_177688	ENSMUST00000074556	232440	*H2afj*	H2A histone family, member J	1,43609516	0,52215135	0,00147655	0,04171535

A_55_P2009567	NM_144904	ENSMUST00000102883	230257	*Ptbp3*	polypyrimidine tract binding protein 3	1,43604248	0,52209843	0,00150649	0,04189237
A_51_P471791	NM_145838	ENSMUST00000003509	241230	*St8sia6*	ST8 alpha-N-acetyl-neuraminide alpha-2,8-sialyltransferase 6	1,43534893	0,52140149	0,00252599	0,04964134
A_51_P157270	NM_001177503	ENSMUST00000140770	217682	*Plekhd1*	pleckstrin homology domain containing, family D (with coiled-coil	1,43411485	0,52016057	0,00169532	0,0434933
A_55_P2083059	XM_006526775	ENSMUST00000069298	192236	*Hps1*	HPS1, biogenesis of lysosomal organelles complex 3 subunit 1	1,43358801	0,51963047	0,00109531	0,03828637
A_51_P302139	NM_025979	ENSMUST00000028119	67121	*Mastl*	microtubule associated serine/threonine kinase-like	1,43307758	0,51911672	0,00254946	0,04970107
A_51_P230987	NM_025951	ENSMUST00000031081	67073	*Pi4k2b*	phosphatidylinositol 4-kinase type 2 beta	1,43280174	0,51883899	0,00066886	0,03555961
A_55_P2037962	NM_153417	ENSMUST00000040489	225997	*Trpm6*	transient receptor potential cation channel, subfamily M, member	1,43258755	0,51862331	0,00117676	0,03904427
A_55_P2037717	NM_001042760	ENSMUST00000052348	18400	*Slc22a18*	solute carrier family 22 (organic cation transporter), member 18	1,43206225	0,5180942	0,00154189	0,04228695
A_51_P441983	NM_008396	ENSMUST00000056117	16398	*Itga2*	integrin alpha 2	1,43084884	0,51687127	0,00255227	0,04970258
A_52_P504268	NM_020026	ENSMUST00000061826	26879	*B3galnt1*	UDP-GalNAc:betaGlcNAc beta 1,3-galactosaminyltransferase, poly	1,42989169	0,51590587	0,0016939	0,0434933
A_55_P2324976	NR_029464	ENSMUST00000221669	77675	*5033406O09Rik*	RIKEN cDNA 5033406O09 gene	1,42932452	0,51533351	0,00015278	0,03291643
A_52_P509710	NM_025635	ENSMUST00000160337	52696	*Zwint*	ZW10 interactor	1,42813931	0,51413671	0,00022144	0,03291643
A_52_P556099	NM_001042653	ENSMUST00000123818	70645	*Oip5*	Opa interacting protein 5	1,42726446	0,51325268	0,00062499	0,03546117
A_51_P424959	NM_007528	ENSMUST00000000326	12029	*Bcl6b*	B cell CLL/lymphoma 6, member B	1,42677226	0,51275508	0,00209012	0,04671098
A_55_P2124736	NM_181277	ENSMUST00000110217	12818	*Col14a1*	collagen, type XIV, alpha 1	1,42624337	0,51222018	0,0022131	0,04740503
A_51_P176365	NM_175035	ENSMUST00000055558	317757	*Gimap5*	GTPase, IMAP family member 5	1,42598036	0,51195411	0,00258207	0,04989265
A_55_P2163428	NM_008021	ENSMUST00000112148	14235	*Foxm1*	forkhead box M1	1,42508713	0,51105013	0,00048151	0,03469594
A_51_P414548	NM_007611	ENSMUST00000026062	12369	*Casp7*	caspase 7	1,42335171	0,5092922	0,00110298	0,03830608
A_51_P345792	NM_029186	ENSMUST00000086969	75146	*Mfsd13a*	major facilitator superfamily domain containing 13a	1,42275465	0,50868689	0,00221981	0,04740503
A_52_P393607	NM_021286	ENSMUST00000000646	20370	*Sez6*	seizure related gene 6	1,42254172	0,50847096	0,00095786	0,03725879
A_55_P1994862	NM_001081215	ENSMUST00000093485	234311	*Ddx60*	DExD/H box helicase 60	1,41804029	0,50389852	0,00154272	0,04228695
A_55_P2008634	NM_053135	ENSMUST00000051126	93881	*Pcdhb10*	protocadherin beta 10	1,41548857	0,5013001	0,00057476	0,03507191
A_52_P88773	NM_152800	ENSMUST00000149720	30933	*Tor2a*	torsin family 2, member A	1,40990318	0,49559609	0,00189013	0,04519944
A_52_P671769	NM_176837	ENSMUST00000142284	73910	*Arhgap18*	Rho GTPase activating protein 18	1,4095812	0,49526659	0,00166224	0,04319932
A_52_P853177	NM_011923	ENSMUST00000004208	26360	*Angptl2*	angiopoietin-like 2	1,40913164	0,49480639	0,00175706	0,04380084
A_55_P2147101	NM_013757	ENSMUST00000113297	27359	*Sytl4*	synaptotagmin-like 4	1,40891236	0,49458187	0,00039646	0,03373901
A_55_P2143042	NR_033590	ENSMUST00000209921	666422	*Gm8096*	predicted gene 8096	1,40852878	0,49418905	0,00084002	0,03629498
A_51_P205326	NM_177743	ENSMUST00000043011	245050	*Gask1a*	golgi associated kinase 1A	1,4079261	0,49357161	0,00205208	0,04655586
A_55_P2383897	XR_377571		77209	*8030453O22Rik*	RIKEN cDNA 8030453O22 gene	1,40627268	0,49187636	0,00200973	0,0463625
A_52_P127465	NM_023249	ENSMUST00000115729	106369	*Ypel1*	yippee like 1	1,40516247	0,49073695	0,00019137	0,03291643
A_55_P2100968	NM_001160386	ENSMUST00000069293	227058	*Dnah7b*	dynein, axonemal, heavy chain 7B	1,40498245	0,49055211	0,00227677	0,04762875
A_55_P2016376	NM_030174	ENSMUST00000125209	78771	*Mctp1*	multiple C2 domains, transmembrane 1	1,40372411	0,48925941	0,000702	0,03558895
A_55_P2019690	NM_001081349	ENSMUST00000121114	72401	*Slc43a1*	solute carrier family 43, member 1	1,401881	0,48736389	0,00183812	0,044633
A_66_P124969	NM_029982	ENSMUST00000173620	77798	*A930009A15Rik*	RIKEN cDNA A930009A15 gene	1,40050645	0,48594863	0,00146813	0,04166534
A_55_P1970676	NM_013709	ENSMUST00000128814	24057	*Sh3yl1*	Sh3 domain YSC-like 1	1,39924183	0,48464533	0,00185496	0,04491004
A_51_P375201	NM_013807	ENSMUST00000147730	12795	*Plk3*	polo-like kinase 3	1,39778337	0,48314079	0,00042336	0,03391783
A_51_P300936	NM_001081223	ENSMUST00000047322	225182	*Rbbp8*	retinoblastoma binding protein 8, endonuclease	1,39595968	0,48125727	0,00106248	0,03818548
A_55_P2078830	BC080727		434166	*Gm5589*	predicted gene 5589	1,3955417	0,48082523	0,00048346	0,03469594
A_51_P502082	NM_009103	ENSMUST00000033283	20133	*Rrm1*	ribonucleotide reductase M1	1,39545918	0,48073993	0,00159354	0,04267063
A_55_P2094964	XM_006504239		100503799	*Gm7931*	predicted pseudogene 7931	1,39540452	0,48068341	0,00240411	0,04852362
A_55_P2078073	NM_145384	ENSMUST00000172747	212555	*Pqlc2*	PQ loop repeat containing 2	1,39509374	0,48036206	0,00057748	0,03507191
A_55_P2064333	NM_010680	ENSMUST00000092070	16774	*Lama3*	laminin, alpha 3	1,39342836	0,47863884	0,00195671	0,04591716
A_51_P296608	NM_007836	ENSMUST00000043098	13197	*Gadd45a*	growth arrest and DNA-damage-inducible 45 alpha	1,39170383	0,47685222	0,00216265	0,04740503
A_51_P267239	NM_019980	ENSMUST00000023143	56722	*Litaf*	LPS-induced TN factor	1,38752338	0,47251208	0,00156037	0,04239131
A_55_P1994290	NR_045889	ENSMUST00000227835	100038614	*Gm10791*	predicted gene 10791	1,38730532	0,47228533	0,00254747	0,04970107
A_52_P497021	NM_182927	ENSMUST00000048923	101809	*Spred3*	sprouty-related, EVH1 domain containing 3	1,38367702	0,46850722	0,00078194	0,03629498
A_55_P2073313	NM_001081017	ENSMUST00000085079	217843	*Unc79*	unc-79 homolog	1,38282955	0,46762334	0,0023129	0,04795298
A_51_P201581	NM_173184	ENSMUST00000061923	212108	*Rln3*	relaxin 3	1,38193669	0,46669153	0,00136276	0,04046247
A_55_P1994939	NM_008252	ENSMUST00000067925	97165	*Hmgb2*	high mobility group box 2	1,38186505	0,46661673	0,00221872	0,04740503
A_52_P609109	NM_145823	ENSMUST00000103064	71795	*Pitpnc1*	phosphatidylinositol transfer protein, cytoplasmic 1	1,38150715	0,46624303	0,00160168	0,04267063
A_52_P265578	NM_001013607	ENSMUST00000021179	327956	*Vmo1*	vitelline membrane outer layer 1 homolog (chicken)	1,38134366	0,46607229	0,00088153	0,03654939
A_51_P220317	NM_146040	ENSMUST00000021592	217946	*Cdca7l*	cell division cycle associated 7 like	1,37992408	0,4645889	0,00072157	0,03593548
A_51_P461108	NM_148958	ENSMUST00000182199	74486	*Osbpl10*	oxysterol binding protein-like 10	1,37824766	0,46283515	0,00116887	0,03904427
A_51_P195034	NM_028039	ENSMUST00000022613	71988	*Esco2*	establishment of sister chromatid cohesion N-acetyltransferase 2	1,37784366	0,4624122	0,00126981	0,03970879
A_52_P65077	NM_029281	ENSMUST00000084141	75424	*Zfp820*	zinc finger protein 820	1,37606767	0,46055142	0,00071599	0,03592056

A_52_P139788	AK020115	ENSMUST00000107178	77739	*Adamtsl1*	ADAMTS-like 1	1,31037538	0,38998015	0,00163366	0,04294518
A_52_P505192	NM_010947	ENSMUST00000024931	18209	*Ntn3*	netrin 3	1,3101269	0,38970656	0,00251144	0,04943016
A_51_P487718	NM_010093	ENSMUST00000102948	13557	*E2f3*	E2F transcription factor 3	1,30740131	0,38670205	0,00089335	0,03656038
A_52_P231292	NM_010008	ENSMUST00000030303	13110	*Cyp2j6*	cytochrome P450, family 2, subfamily j, polypeptide 6	1,30535744	0,38444491	0,00054914	0,03476444
A_51_P320105	NM_026796	ENSMUST00000027897	226830	*Smyd2*	SET and MYND domain containing 2	1,30405979	0,38301002	0,00169644	0,0434933
A_55_P2021841	NM_007590	ENSMUST00000019514	12315	*Calm3*	calmodulin 3	1,30395203	0,3828908	0,00134743	0,04041344
A_55_P2183433	NM_029494	ENSMUST00000107180	75985	*Rab30*	RAB30, member RAS oncogene family	1,30234659	0,38111344	0,0014967	0,04188934
A_51_P242201	NM_025972	ENSMUST00000159345	67111	*Naaa*	N-acylethanolamine acid amidase	1,3016499	0,38034146	0,00213518	0,04731067
A_52_P654043	NM_144898	ENSMUST00000147828	229524	*Msto1*	misato 1, mitochondrial distribution and morphology regulator	1,30136446	0,38002506	0,00111187	0,03830608
A_51_P272283	NM_181588	ENSMUST00000070918	69574	*Cmbl*	carboxymethylenebutenolidase-like (Pseudomonas)	1,30081609	0,37941701	0,00200953	0,0463625
A_55_P2022895	NM_134251	ENSMUST00000121925	171286	*Slc12a8*	solute carrier family 12 (potassium/chloride transporters), membe	1,29783968	0,37611218	0,00152889	0,04218368
A_52_P574697	NM_011317	ENSMUST00000066257	20218	*Khdrbs1*	KH domain containing, RNA binding, signal transduction associatec	1,29717084	0,3753685	0,00246268	0,04914129
A_51_P208145	NM_021882	ENSMUST00000054125	20431	*Pmel*	premelanosome protein	1,29669225	0,37483612	0,00258523	0,04989265
A_55_P2115507	NM_152922	ENSMUST00000097345	81701	*Egfl8*	EGF-like domain 8	1,29618623	0,37427301	0,0022085	0,04740503
A_55_P2080870	NM_133978	ENSMUST00000035009	102545	*Cmtm7*	CKLF-like MARVEL transmembrane domain containing 7	1,29607436	0,37414849	0,00234642	0,04825583
A_51_P101137	NM_146025	ENSMUST00000055947	217125	*Samd14*	sterile alpha motif domain containing 14	1,29446401	0,37235486	0,00218679	0,04740503
A_52_P649296	NM_010937	ENSMUST00000029445	18176	*Nras*	neuroblastoma ras oncogene	1,29423736	0,37210223	0,00162476	0,04294518
A_51_P208121	NM_182782	ENSMUST00000206019	207952	*Klhl25*	kelch-like 25	1,29123575	0,36875243	0,00097672	0,03757388
A_55_P1960311	NM_027109	ENSMUST00000075821	69537	*Dnase1l1*	deoxyribonuclease 1-like 1	1,29008053	0,36746113	0,00194802	0,04589615
A_66_P122362	NM_145954	ENSMUST00000007977	69748	*Aldh16a1*	aldehyde dehydrogenase 16 family, member A1	1,28965714	0,36698757	0,00167079	0,04333476
A_52_P488612	NM_027060	ENSMUST00000168787	224671	*Btbd9*	BTB (POZ) domain containing 9	1,28962245	0,36694877	0,00214258	0,0473211
A_51_P405227	NM_026012	ENSMUST00000035069	67169	*Nradd*	neurotrophin receptor associated death domain	1,28223242	0,35865779	0,00233052	0,04805255
A_52_P681310	NM_011113	ENSMUST00000002284	18793	*Plaur*	plasminogen activator, urokinase receptor	1,28188583	0,35826778	0,00145546	0,04160232
A_51_P229925	NM_021715	ENSMUST00000044138	60322	*Chst7*	carbohydrate (N-acetylglucosamino) sulfotransferase 7	1,28091026	0,3571694	0,00241637	0,04866626
A_51_P392244	NM_029878	ENSMUST00000155666	108903	*Tbcd*	tubulin-specific chaperone d	1,27929585	0,35534994	0,00226162	0,0475368
A_52_P48546	NM_026259	ENSMUST00000096386	67588	*Rnf41*	ring finger protein 41	1,27830904	0,35423666	0,00246045	0,04914129
A_55_P2096370	ENSMUST000001819	ENSMUST00000181994	74055	*Plce1*	phospholipase C, epsilon 1	1,27567678	0,35126284	0,00219269	0,04740503
A_55_P2128869	NM_026439	ENSMUST00000061050	67896	*Ccdc80*	coiled-coil domain containing 80	1,27270635	0,34789959	0,00256031	0,0497393
A_55_P2145617	NM_028770	ENSMUST00000077196	74127	*Krt80*	keratin 80	1,27236752	0,34751545	0,00226883	0,04759365
A_55_P2004427	NM_133694	ENSMUST00000177667	68431	*Fbxl15*	F-box and leucine-rich repeat protein 15	1,27149627	0,34652723	0,00168721	0,04345841
A_52_P147666	NM_023214	ENSMUST00000067485	66500	*Slc30a7*	solute carrier family 30 (zinc transporter), member 7	1,26862098	0,3432611	0,00213158	0,04728457
A_55_P2181888	NM_001290706	ENSMUST00000106064	66260	*Tmem54*	transmembrane protein 54	1,26792293	0,34246706	0,00200602	0,0463625
A_55_P1958480	XM_006518205		100041262	*Gm3239*	predicted gene 3239	1,26580624	0,34005658	0,00139068	0,04077792
A_52_P189984	NM_172528	ENSMUST00000183734	214345	*Lrrc1*	leucine rich repeat containing 1	1,25986426	0,3332683	0,00245374	0,04908868
A_55_P2101088	NM_146198	ENSMUST00000033035	233836	*Slc5a11*	solute carrier family 5 (sodium/glucose cotransporter), member 11	1,24219142	0,3128875	0,00247887	0,04923726
A_51_P479434	NM_027009	ENSMUST00000140067	69263	*Rfc3*	replication factor C (activator 1) 3	1,2341947	0,30357	0,00248866	0,04932867
A_55_P1954998	NM_009343	ENSMUST00000073724	21652	*Phf1*	PHD finger protein 1	-1,24004337	-0,31039058	0,00204626	0,04655586
A_65_P15689	NM_008650	ENSMUST00000169611	17850	*Mut*	methylmalonyl-Coenzyme A mutase	-1,25609995	-0,32895127	0,00210121	0,04687799
A_55_P2196442	NR_040614	ENSMUST00000123377	75166	*4930533B01Rik*	RIKEN cDNA 4930533B01 gene	-1,25628938	-0,32916882	0,00243972	0,0489381
A_55_P2175615	NM_144901	ENSMUST00000029446	229663	*Csde1*	cold shock domain containing E1, RNA binding	-1,25718228	-0,33019385	0,00157799	0,0424553
A_55_P1966438	NM_008183	ENSMUST00000012348	14863	*Gstm2*	glutathione S-transferase, mu 2	-1,26021043	-0,33366465	0,00239184	0,04851956
A_51_P135654	NM_010124	ENSMUST00000020288	13688	*Eif4ebp2*	eukaryotic translation initiation factor 4E binding protein 2	-1,26398039	-0,33797408	0,00220032	0,04740503
A_55_P2124097	NR_023357		629557	*Gm6981*	predicted pseudogene 6981	-1,26657012	-0,34092695	0,00181618	0,04447998
A_55_P2125791	XR_375774		100042237	*Gm3740*	predicted gene 3740	-1,26793133	-0,34247662	0,00227121	0,04759365
A_52_P278154	NM_027236	ENSMUST00000025759	69860	*Eif1ad*	eukaryotic translation initiation factor 1A domain containing	-1,26845696	-0,34307457	0,00227143	0,04759365
A_55_P2037425	NM_008084	ENSMUST00000118875	14433	*Gapdh*	glyceraldehyde-3-phosphate dehydrogenase	-1,26924888	-0,34397498	0,00182407	0,04447998
A_51_P464981	NM_025735	ENSMUST00000154596	66734	*Map1lc3a*	microtubule-associated protein 1 light chain 3 alpha	-1,26925939	-0,34398693	0,00094604	0,03704536
A_52_P1068723	NM_001081371	ENSMUST00000041772	240283	*Dmxl1*	Dmx-like 1	-1,27256305	-0,34773714	0,00218893	0,04740503
A_51_P333111	NM_009676	ENSMUST00000001027	11761	*Aox1*	aldehyde oxidase 1	-1,27317131	-0,34842656	0,00259435	0,04997561
A_52_P78373	NM_011366	ENSMUST00000022682	20410	*Sorbs3*	sorbin and SH3 domain containing 3	-1,28079298	-0,35703731	0,00072617	0,03593548
A_52_P347942	NM_146472	ENSMUST00000060434	258464	*Olfr1384*	olfactory receptor 1384	-1,28181771	-0,35819111	0,00188133	0,04514203
A_52_P592909	NM_026384	ENSMUST00000033001	67800	*Dgat2*	diacylglycerol O-acyltransferase 2	-1,28412515	-0,36078581	0,00206865	0,0465836
A_55_P1956223	NM_001271496	ENSMUST00000025760	12660	*Chka*	choline kinase alpha	-1,29008614	-0,3674674	0,00223344	0,04740503
A_55_P2001589	NM_178741	ENSMUST00000131843	246293	*Klhl8*	kelch-like 8	-1,29285903	-0,37056498	0,002284	0,04775425
A_51_P148675	NM_010017	ENSMUST00000171412	13138	*Dag1*	dystroglycan 1	-1,29326072	-0,37101315	0,00126847	0,03970879

A_55_P2137001	NM_001044380	ENSMUST00000021685	214305	*Hhipl1*	hedgehog interacting protein-like 1	1,37585477	0,4603282	0,00081051	0,03629498
A_52_P141687	NM_134438	ENSMUST00000027682	171469	*Gpr37l1*	G protein-coupled receptor 37-like 1	1,37362141	0,45798443	0,00253498	0,04970107
A_52_P610808	NM_001001333	ENSMUST00000124925	238023	*Hexdc*	hexosaminidase (glycosyl hydrolase family 20, catalytic domain) cc	1,37083624	0,45505624	0,00205093	0,04655586
A_51_P101006	NM_001033874	ENSMUST00000074156	68870	*Ak8*	adenylate kinase 8	1,37024818	0,45443722	0,0023623	0,0482972
A_55_P2181655	NM_001083587	ENSMUST00000020695	319939	*Tns3*	tensin 3	1,37024112	0,45442979	0,00066598	0,03555961
A_55_P2066299	NM_031999	ENSMUST00000021738	83924	*Gpr137b*	G protein-coupled receptor 137B	1,36994769	0,45412081	0,00099066	0,03799738
A_52_P144297	NM_198617	ENSMUST00000099194	241732	*Tspyl3*	TSPY-like 3	1,36930162	0,45344026	0,00085864	0,03629498
A_55_P2275817	XR_385827		320021	*C430042M11Rik*	RIKEN cDNA C430042M11 gene	1,3688352	0,45294876	0,00223393	0,04740503
A_51_P366161	NM_010822	ENSMUST00000142964	268395	*Mpg*	N-methylpurine-DNA glycosylase	1,36801003	0,45207881	0,00100753	0,03808028
A_51_P351970	NM_008234	ENSMUST00000025965	15201	*Hells*	helicase, lymphoid specific	1,3670094	0,45102316	0,00154401	0,04228695
A_55_P2005470	NM_029568	ENSMUST00000126308	76293	*Mfap4*	microfibrillar-associated protein 4	1,36585035	0,44979942	0,00137038	0,04050525
A_51_P137111	NM_016681	ENSMUST00000066160	50883	*Chek2*	checkpoint kinase 2	1,36400078	0,44784447	0,00130615	0,04002652
A_55_P2331804	NR_102381	ENSMUST00000223443	104932	*AU015791*	expressed sequence AU015791	1,36299642	0,44678178	0,00155792	0,04238381
A_55_P2051199	NR_046046	ENSMUST00000126679	672763	*Gm13710*	predicted gene 13710	1,36277549	0,44654791	0,00162769	0,04294518
A_51_P453519	NM_023740	ENSMUST00000026154	74168	*Zdhhc16*	zinc finger, DHHC domain containing 16	1,3627202	0,44648937	0,00128285	0,03979485
A_52_P529195	NM_053129	ENSMUST00000056712	93875	*Pcdhb4*	protocadherin beta 4	1,35970262	0,44329116	0,00256213	0,04974876
A_66_P121285	NM_173396	ENSMUST00000081335	228839	*Tgif2*	TGFB-induced factor homeobox 2	1,35915898	0,44271422	0,00178799	0,04408364
A_55_P2056120	NM_001093775	ENSMUST00000049784	17933	*Myt1l*	myelin transcription factor 1-like	1,35739029	0,4408356	0,00191871	0,04554709
A_55_P2012799	NM_133641	ENSMUST00000065512	20166	*Rtkn*	rhotekin	1,35563185	0,43896544	0,00182235	0,04447998
A_51_P234847	NM_027035	ENSMUST00000022007	69315	*1700001L19Rik*	RIKEN cDNA 1700001L19 gene	1,35359708	0,43679836	0,00078935	0,03629498
A_51_P371051	NM_028608	ENSMUST00000162508	73690	*Glipr1*	GLI pathogenesis-related 1 (glioma)	1,35312189	0,4362918	0,0017751	0,04399008
A_55_P2007001	NM_023465	ENSMUST00000105692	67087	*Ctnnbip1*	catenin beta interacting protein 1	1,35286692	0,43601993	0,00229606	0,04782329
A_55_P1952269	NM_145828	ENSMUST00000116349	217119	*Xylt2*	xylosyltransferase II	1,35155124	0,43461621	0,0010163	0,03808028
A_55_P1984837	ENSMUST000001508	ENSMUST00000150841	69920	*Polr2i*	polymerase (RNA) II (DNA directed) polypeptide I	1,35141774	0,4344737	0,00165236	0,04305746
A_55_P2094474	NR_110572	ENSMUST00000127150	433424	*Zeb2os*	zinc finger E-box binding homeobox 2, opposite strand	1,35052213	0,43351728	0,00202806	0,0464094
A_52_P235347	NM_020013	ENSMUST00000033099	56636	*Fgf21*	fibroblast growth factor 21	1,3497818	0,43272621	0,00256866	0,04980172
A_55_P1990235	NM_021328	ENSMUST00000022680	57784	*Bin3*	bridging integrator 3	1,34965803	0,43259391	0,00171524	0,04370748
A_55_P2002642	NM_181816	ENSMUST00000115593	234964	*Deup1*	deuterosome assembly protein 1	1,34941288	0,43233184	0,00188415	0,04514203
A_51_P386562	NM_010095	ENSMUST00000022637	13592	*Ebf2*	early B cell factor 2	1,34909693	0,43199401	0,00047878	0,03469594
A_51_P430423	NM_007398	ENSMUST00000017841	11486	*Ada*	adenosine deaminase	1,34696563	0,42971304	0,00189251	0,04522863
A_55_P2102533	NM_025799	ENSMUST00000121465	66848	*Fuca2*	fucosidase, alpha-L- 2, plasma	1,34637113	0,42907615	0,00043865	0,03393479
A_55_P2109057	NM_177354	ENSMUST00000021681	238328	*Vash1*	vasohibin 1	1,34334443	0,42582926	0,00177556	0,04399008
A_66_P131406	AK084985		791367	*Gm10099*	predicted gene 10099	1,34057984	0,42285714	0,00104074	0,03812918
A_51_P378934	NM_025977	ENSMUST00000170304	67119	*Ccdc159*	coiled-coil domain containing 159	1,33882464	0,42096701	0,002589	0,04992201
A_55_P2044439	NM_008595	ENSMUST00000018313	17305	*Mfng*	MFNG O-fucosylpeptide 3-beta-N-acetylglucosaminyltransferase	1,3371583	0,41917026	0,00083028	0,03629498
A_51_P148060	NM_011197	ENSMUST00000102694	19221	*Ptgfrn*	prostaglandin F2 receptor negative regulator	1,33705149	0,41905502	0,00110769	0,03830608
A_55_P2036337	NM_010508	ENSMUST00000023689	15975	*Ifnar1*	interferon (alpha and beta) receptor 1	1,33596932	0,41788688	0,00202894	0,0464094
A_51_P310649	NM_009713	ENSMUST00000023292	11883	*Arsa*	arylsulfatase A	1,33590472	0,41781711	0,00061366	0,0352913
A_55_P2042743	NM_008132	ENSMUST00000067625	14659	*Glrp1*	glutamine repeat protein 1	1,33314667	0,41483551	0,00138072	0,04068336
A_52_P644114	NM_028481	ENSMUST00000047677	73254	*Ccdc18*	coiled-coil domain containing 18	1,32851841	0,40981821	0,00063352	0,03546117
A_52_P127362	NM_029478	ENSMUST00000018315	75909	*Vmp1*	vacuole membrane protein 1	1,32785336	0,40909583	0,00116543	0,03904427
A_55_P2045549	NM_172920	ENSMUST00000115277	244745	*Dpy19l1*	dpy-19-like 1 (C. elegans)	1,32727646	0,4084689	0,00177509	0,04399008
A_66_P107231	NM_001164311	ENSMUST00000026190	67573	*Loxl4*	lysyl oxidase-like 4	1,32686438	0,40802092	0,00203087	0,04641055
A_51_P501897	NM_001042502	ENSMUST00000042587	18741	*Pitx2*	paired-like homeodomain transcription factor 2	1,32558523	0,40662943	0,00067196	0,03555961
A_55_P2086094	NM_028662	ENSMUST00000041353	73836	*Slc35b2*	solute carrier family 35, member B2	1,3241746	0,40509336	0,00247152	0,04921934
A_66_P115034	NM_026279	ENSMUST00000139876	67621	*Bend5*	BEN domain containing 5	1,3212619	0,40191646	0,0012755	0,03970879
A_55_P2044627	NM_029145	ENSMUST00000022424	75019	*Rnase10*	ribonuclease, RNase A family, 10 (non-active)	1,31985911	0,40038393	0,00124278	0,0394317
A_51_P374869	NM_013850	ENSMUST00000171637	27403	*Abca7*	ATP-binding cassette, sub-family A (ABC1), member 7	1,3165741	0,39678872	0,00163147	0,04294518
A_55_P2048518	NM_009569	ENSMUST00000054052	22761	*Zfpm1*	zinc finger protein, multitype 1	1,31573996	0,39587438	0,0012884	0,03982756
A_55_P2048478	NM_172907	ENSMUST00000120990	244198	*Olfml1*	olfactomedin-like 1	1,31571891	0,39585131	0,00103437	0,03812918
A_55_P2173702	NM_026598	ENSMUST00000022494	68177	*Ebpl*	emopamil binding protein-like	1,31568257	0,39581146	0,00176704	0,04387286
A_52_P235278	NM_153556	ENSMUST00000027267	227099	*Pms1*	PMS1 homolog 1, mismatch repair system component	1,31396509	0,39392694	0,00231409	0,04795298
A_55_P1959218	NM_001137547	ENSMUST00000095755	635253	*Usp51*	ubiquitin specific protease 51	1,31226112	0,39205482	0,00239476	0,04851956
A_52_P117576	NM_009810	ENSMUST00000093517	12367	*Casp3*	caspase 3	1,31211546	0,39189468	0,00149567	0,04188934
A_55_P1991500	NM_175360	ENSMUST00000182873	108689	*Stn1*	STN1, CST complex subunit	1,3104773	0,39009236	0,00132807	0,04018556

A_55_P1957954	NM_009105	ENSMUST00000028059	20163	*Rsu1*	Ras suppressor protein 1	-1,29401495	-0,37185428	0,00157327	0,04242288
A_55_P2043287	NM_010347	ENSMUST00000002518	14797	*Tle5*	TLE family member 5, transcriptional modulator	-1,29837789	-0,37671034	0,00223429	0,04740503
A_55_P2015520	NM_133942	ENSMUST00000048180	101476	*Plekha1*	pleckstrin homology domain containing, family A (phosphoinositid	-1,299851	-0,37834626	0,00215079	0,04733317
A_55_P1986567	NM_001205034	ENSMUST00000178581	100503388	*Gm19668*	predicted gene, 19668	-1,30125461	-0,37990328	0,00108658	0,03828376
A_55_P2177911	NM_010704	ENSMUST00000151733	16847	*Lepr*	leptin receptor	-1,30277018	-0,3815826	0,00161396	0,04282509
A_52_P400677	NM_134067	ENSMUST00000038690	105351	*AW209491*	expressed sequence AW209491	-1,30366283	-0,38257079	0,0025862	0,04989265
A_51_P443872	NM_148673	ENSMUST00000020681	193116	*Slu7*	SLU7 splicing factor homolog (S. cerevisiae)	-1,30484507	-0,38387852	0,0025169	0,04951257
A_55_P2180854	NM_203492	ENSMUST00000058092	381974	*Mrgprg*	MAS-related GPR, member G	-1,30748182	-0,38679089	0,00250512	0,04938663
A_55_P2026400	NM_009795	ENSMUST00000001845	12336	*Capns1*	calpain, small subunit 1	-1,30836475	-0,3877648	0,00122115	0,03914579
A_55_P1959648	NM_008305	ENSMUST00000155648	15530	*Hspg2*	perlecan (heparan sulfate proteoglycan 2)	-1,30845067	-0,38785954	0,00130677	0,04002652
A_65_P13547	NM_010593	ENSMUST00000107403	16480	*Jup*	junction plakoglobin	-1,30846962	-0,38788042	0,00186462	0,04498682
A_55_P1990919	NM_013759	ENSMUST00000115262	27361	*Msrb1*	methionine sulfoxide reductase B1	-1,31044031	-0,39005164	0,00224395	0,04748532
A_51_P519648	NM_153396	ENSMUST00000077159	194401	*Mical3*	microtubule associated monooxygenase, calponin and LIM domain	-1,31449115	-0,39450443	0,00107517	0,03823006
A_51_P179131	NM_009499	ENSMUST00000032561	22323	*Vasp*	vasodilator-stimulated phosphoprotein	-1,315503	-0,39561454	0,00152862	0,04218368
A_52_P217240	NM_028292	ENSMUST00000032963	72590	*Ppme1*	protein phosphatase methylesterase 1	-1,32048637	-0,40106941	0,00195924	0,04592118
A_51_P441387	NM_177645	ENSMUST00000068168	68691	*Kansl1l*	KAT8 regulatory NSL complex subunit 1-like	-1,32082865	-0,40144332	0,0016657	0,04326043
A_55_P2021014	NM_207278	ENSMUST00000062623	403175	*Tigd4*	tigger transposable element derived 4	-1,32096118	-0,40158807	0,00208653	0,04671098
A_55_P2008996	AK164250		100125977	*Gm10034*	predicted gene 10034	-1,32351842	-0,40437827	0,00257051	0,04980172
A_55_P2177944	ENSMUST000000984	ENSMUST00000098453	66320	*Tmem208*	transmembrane protein 208	-1,32692745	-0,4080895	0,00140652	0,04092507
A_51_P167513	NM_027203	ENSMUST00000019878	69757	*Leng1*	leukocyte receptor cluster (LRC) member 1	-1,32699508	-0,40816302	0,00246224	0,04914129
A_55_P2053943	NM_146534	ENSMUST00000055298	258527	*Olfr1368*	olfactory receptor 1368	-1,32946248	-0,41084306	0,00193048	0,04564964
A_55_P2033250	NM_010191	ENSMUST00000054963	14137	*Fdft1*	farnesyl diphosphate farnesyl transferase 1	-1,33168171	-0,4132493	0,00087657	0,03654939
A_55_P2247789	NR_046011	ENSMUST00000205370	78108	*Particl*	promoter of Mat2a antisense radiation induced circulating long no	-1,3330729	-0,41475567	0,00206939	0,0465836
A_52_P88793	NM_198619	ENSMUST00000105718	242747	*Zfp933*	zinc finger protein 933	-1,33553593	-0,41741879	0,00207203	0,0465836
A_55_P2319370	NM_031256	ENSMUST00000111920	83435	*Plekha3*	pleckstrin homology domain-containing, family A (phosphoinositid	-1,3362609	-0,41820172	0,00214781	0,0473211
A_55_P1998561	NR_045392		100039043	*Gm10731*	predicted gene 10731	-1,33749891	-0,41953772	0,00107947	0,03826064
A_55_P2107362	NM_008122	ENSMUST00000107075	14615	*Gjc1*	gap junction protein, gamma 1	-1,33776561	-0,41982536	0,00221292	0,04740503
A_52_P662098	NM_019671	ENSMUST00000091853	56349	*Net1*	neuroepithelial cell transforming gene 1	-1,33907595	-0,42123779	0,0024435	0,04895927
A_55_P1992781	XM_006509527		102636193	*Gm33328*	predicted gene, 33328	-1,3454881	-0,42812963	0,0017423	0,04380084
A_66_P126640	NM_007592	ENSMUST00000066674	12319	*Car8*	carbonic anhydrase 8	-1,34772257	-0,43052355	0,00257097	0,04980172
A_55_P2116647	NM_001080774	ENSMUST00000151174	17913	*Myo1c*	myosin IC	-1,34993023	-0,43288484	0,0006775	0,03555961
A_52_P407022	NM_177411	ENSMUST00000000727	19344	*Rab5b*	RAB5B, member RAS oncogene family	-1,35026085	-0,43323814	0,00204763	0,04655586
A_55_P2072543	NM_009188	ENSMUST00000004494	20467	*Sin3b*	transcriptional regulator, SIN3B (yeast)	-1,35347785	-0,43667128	0,00061643	0,0352913
A_51_P262721	NR_038126	ENSMUST00000143813	66838	*0610009L18Rik*	RIKEN cDNA 0610009L18 gene	-1,35360445	-0,43680622	0,00198237	0,04609624
A_55_P2094602	NM_001033439	ENSMUST00000088970	380916	*Lrch1*	leucine-rich repeats and calponin homology (CH) domain containin	-1,35388095	-0,43710089	0,00142027	0,04104857
A_55_P1957835	NM_001290826	ENSMUST00000079754	208922	*Cpeb3*	cytoplasmic polyadenylation element binding protein 3	-1,35389009	-0,43711063	0,00237493	0,04844509
A_55_P2449750	NM_001100116	ENSMUST00000177768	100101807	*Fam177a2v*	family with sequence similarity 177 member A2	-1,35404837	-0,43727927	0,00153799	0,04228489
A_55_P2043762	NM_026366	ENSMUST00000054442	67768	*N6amt1*	N-6 adenine-specific DNA methyltransferase 1 (putative)	-1,35894753	-0,44248976	0,00114955	0,03878076
A_66_P136801	NR_002864	ENSMUST00000202826	353342	*Peg13*	paternally expressed 13	-1,35948318	-0,44305831	0,0015474	0,04230471
A_51_P312846	NM_023605	ENSMUST00000001402	71538	*Fbxo9*	f-box protein 9	-1,36080269	-0,4444579	0,00239144	0,04851956
A_66_P108770	NM_024188	ENSMUST00000110690	67041	*Oxct1*	3-oxoacid CoA transferase 1	-1,36114437	-0,4448201	0,0023583	0,0482972
A_51_P454691	NM_175128	ENSMUST00000054471	68281	*4930430F08Rik*	RIKEN cDNA 4930430F08 gene	-1,36478106	-0,44866953	0,00193382	0,04565538
A_55_P2110738	NM_013917	ENSMUST00000020685	30939	*Pttg1*	pituitary tumor-transforming gene 1	-1,36508882	-0,44899483	0,00201209	0,0463625
A_51_P506045	NM_176073	ENSMUST00000042167	54381	*Cpq*	carboxypeptidase Q	-1,36625292	-0,45022457	0,00240016	0,04852362
A_55_P2137476	NM_008622	ENSMUST00000114631	17527	*Mpv17*	MpV17 mitochondrial inner membrane protein	-1,36675364	-0,45075322	0,00162393	0,04294518
A_66_P120507	NM_152813	ENSMUST00000103077	72469	*Plcd3*	phospholipase C, delta 3	-1,36729234	-0,45132174	0,00243406	0,04887083
A_55_P2367117	NM_019640	ENSMUST00000086635	56305	*Pitpnb*	phosphatidylinositol transfer protein, beta	-1,36946635	-0,45361381	0,00026777	0,03315398
A_51_P192162	NM_172493	ENSMUST00000167619	54004	*Diaph2*	diaphanous homolog 2 (Drosophila)	-1,37047155	-0,45467238	0,00082506	0,03629498
A_55_P2051696	NM_008783	ENSMUST00000072863	18514	*Pbx1*	pre B cell leukemia homeobox 1	-1,37067029	-0,45488157	0,00032232	0,03315398
A_66_P101646	ENSMUST000000824	ENSMUST00000082402	17708	*COX1*	cytochrome c oxidase subunit I	-1,3736232	-0,45798631	0,00047126	0,03469594
A_52_P257426	NM_133191	ENSMUST00000140025	98845	*Eps8l2*	EPS8-like 2	-1,37404946	-0,45843393	0,00174732	0,04380084
A_55_P2050628	NM_201640	ENSMUST00000030480	666168	*Cyp4a31*	cytochrome P450, family 4, subfamily a, polypeptide 31	-1,3755332	-0,45999096	0,00134309	0,04031445
A_52_P239292	NM_133818	ENSMUST00000010434	98404	*AI597479*	expressed sequence AI597479	-1,37576688	-0,46023603	0,00131818	0,04018556
A_55_P2091350	ENSMUST000000840	ENSMUST00000084013	17720	*ND4L*	NADH dehydrogenase subunit 4L	-1,37994606	-0,46461188	0,00067424	0,03555961
A_66_P135179	ENSMUST000001083	ENSMUST00000108344	11652	*Akt2*	thymoma viral proto-oncogene 2	-1,38224676	-0,46701519	0,00075455	0,03604365

A_51_P269634	NM_011748	ENSMUST00000207873	243906	*Zfp14*	zinc finger protein 14	-1,43854758	-0,52461294	0,00025429	0,03291643
A_55_P1954555	XR_383945		102637894	*Gm34590*	predicted gene, 34590	-1,43982636	-0,52589484	0,00071284	0,03585477
A_51_P320022	NM_009728	ENSMUST00000168747	11982	*Atp10a*	ATPase, class V, type 10A	-1,44567634	-0,53174459	0,00162923	0,04294518
A_52_P321318	ENSMUST000000824	ENSMUST00000082408	17705	*ATP6*	ATP synthase F0 subunit 6	-1,44582571	-0,53189366	0,00052578	0,03476444
A_55_P1954365	NM_001267622	ENSMUST00000040111	209683	*Ttc28*	tetratricopeptide repeat domain 28	-1,44593059	-0,5319983	0,00105246	0,03814748
A_51_P166023	NM_146001	ENSMUST00000060311	215114	*Hip1*	huntingtin interacting protein 1	-1,44700415	-0,53306906	0,00134149	0,04029753
A_52_P339742	NM_029787	ENSMUST00000162834	109754	*Cyb5r3*	cytochrome b5 reductase 3	-1,45066144	-0,53671086	0,00067774	0,03555961
A_55_P2005025	NM_020007	ENSMUST00000099087	56758	*Mbnl1*	muscleblind like splicing factor 1	-1,45076548	-0,53681432	0,00193241	0,04564964
A_52_P169181	NM_177047	ENSMUST00000182974	319974	*Auts2*	autism susceptibility candidate 2	-1,45365538	-0,53968529	0,00060046	0,03507191
A_55_P2172747	NM_001285920	ENSMUST00000030884	170731	*Mfn2*	mitofusin 2	-1,45443138	-0,54045523	0,00162767	0,04294518
A_55_P2016691	XR_373459		73346	*1700039I01Rik*	RIKEN cDNA 1700039I01 gene	-1,45467882	-0,54070065	0,00139393	0,04080226
A_55_P2228122	BC024137		234757	*BC024137*	cDNA sequence BC024137	-1,45625675	-0,54226474	0,00133953	0,04028731
A_55_P2105271	NM_001114088	ENSMUST00000046246	67399	*Pdlim7*	PDZ and LIM domain 7	-1,45658167	-0,5425866	0,00242176	0,04872435
A_51_P245525	ENSMUST000000824	ENSMUST00000082414	17719	*ND4*	NADH dehydrogenase subunit 4	-1,45694968	-0,54295105	0,00046649	0,03462675
A_51_P520936	NM_013867	ENSMUST00000029766	29815	*Bcar3*	breast cancer anti-estrogen resistance 3	-1,45704437	-0,54304481	0,00083343	0,03629498
A_52_P686091	NM_011078	ENSMUST00000035540	18676	*Phf2*	PHD finger protein 2	-1,45726577	-0,54326401	0,00012089	0,03291643
A_52_P516034	NM_011200	ENSMUST00000027232	19243	*Ptp4a1*	protein tyrosine phosphatase 4a1	-1,45736854	-0,54336576	0,00062741	0,03546117
A_55_P2074536	NM_011151	ENSMUST00000112304	19043	*Ppm1b*	protein phosphatase 1B, magnesium dependent, beta isoform	-1,45761109	-0,54360585	0,0004049	0,03373901
A_55_P2055975	NM_178795	ENSMUST00000110626	327655	*Ppip5k1*	diphosphoinositol pentakisphosphate kinase 1	-1,46015438	-0,54612091	0,00113083	0,03857573
A_55_P2065231	NM_010359	ENSMUST00000004136	14864	*Gstm3*	glutathione S-transferase, mu 3	-1,46060425	-0,54656533	0,00081127	0,03629498
A_55_P1956087	NM_001081387	ENSMUST00000179693	664799	*Ctcfl*	CCCTC-binding factor (zinc finger protein)-like	-1,46091363	-0,54687088	0,00109351	0,03828376
A_51_P319879	NM_007382	ENSMUST00000072697	11364	*Acadm*	acyl-Coenzyme A dehydrogenase, medium chain	-1,46153932	-0,54748864	0,00083931	0,03629498
A_51_P315595	ENSMUST000000824	ENSMUST00000082421	17711	*CYTB*	cytochrome b	-1,46903875	-0,55487245	0,00043727	0,03393479
A_51_P463860	NM_172581	ENSMUST00000021659	217705	*Fam161b*	family with sequence similarity 161, member B	-1,47046632	-0,55627374	0,00144514	0,04149019
A_52_P407280	NM_001285435	ENSMUST00000137576	66548	*Adamtsl5*	ADAMTS-like 5	-1,47076781	-0,55656951	0,00248183	0,04924582
A_55_P2099650	NM_053195	ENSMUST00000110007	94249	*Slc24a3*	solute carrier family 24 (sodium/potassium/calcium exchanger), m	-1,47096682	-0,55676471	0,00065367	0,03555961
A_52_P590661	NM_007908	ENSMUST00000047875	13631	*Eef2k*	eukaryotic elongation factor-2 kinase	-1,47114897	-0,55694334	0,0017335	0,04380084
A_55_P2137937	NM_052992	ENSMUST00000039909	56188	*Fxyd1*	FXYD domain-containing ion transport regulator 1	-1,47124001	-0,55703262	0,00079734	0,03629498
A_52_P60303	NM_001033455	ENSMUST00000047207	381580	*Ccdc27*	coiled-coil domain containing 27	-1,47223176	-0,5580048	0,00015086	0,03291643
A_55_P2030627	NM_001081227	ENSMUST00000136521	381310	*Stum*	mechanosensory transduction mediator	-1,47241383	-0,55818321	0,00228891	0,04777999
A_51_P314186	NM_001079686	ENSMUST00000095899	64009	*Syne1*	spectrin repeat containing, nuclear envelope 1	-1,47383504	-0,55957506	0,00220301	0,04740503
A_52_P650180	NM_145469	ENSMUST00000040791	223473	*Nipal2*	NIPA-like domain containing 2	-1,47561496	-0,56131632	0,00104592	0,03812918
A_51_P357085	NM_011722	ENSMUST00000131839	22428	*Dctn6*	dynactin 6	-1,4757318	-0,56143055	0,00181194	0,04444355
A_51_P440047	NM_173752	ENSMUST00000047028	216551	*Lgalsl*	lectin, galactoside binding-like	-1,47602942	-0,56172148	0,00216362	0,04740503
A_51_P271984	NM_144936	ENSMUST00000048050	235135	*Tmem45b*	transmembrane protein 45b	-1,47813302	-0,56377611	0,00185868	0,04494434
A_55_P1974612	NM_001112731	ENSMUST00000120004	112415	*Zfp607b*	zinc finger protein 607B	-1,47933215	-0,56494601	0,00083543	0,03629498
A_55_P1988970	NM_001286981	ENSMUST00000110089	59030	*Mkks*	McKusick-Kaufman syndrome	-1,48159271	-0,5671489	0,00195269	0,04589987
A_55_P1965772	NM_001163337	ENSMUST00000163326	53313	*Atp2a3*	ATPase, Ca++ transporting, ubiquitous	-1,48160246	-0,56715839	0,00225099	0,04752342
A_51_P366138	NM_008587	ENSMUST00000140221	17289	*Mertk*	c-mer proto-oncogene tyrosine kinase	-1,4831385	-0,56865333	0,00104652	0,03812918
A_66_P115580	AK076360		73265	*1700038P13Rik*	RIKEN cDNA 1700038P13 gene	-1,48394361	-0,56943627	0,00214493	0,0473211
A_52_P667477	NM_148925	ENSMUST00000084715	17281	*Fyco1*	FYVE and coiled-coil domain containing 1	-1,48526837	-0,57072363	0,0010425	0,03812918
A_52_P451574	NM_011273	ENSMUST00000027741	19775	*Xpr1*	xenotropic and polytropic retrovirus receptor 1	-1,48581525	-0,57125474	0,00238551	0,04851956
A_52_P451378	NM_023053	ENSMUST00000024906	65960	*Twsg1*	twisted gastrulation homolog 1 (Drosophila)	-1,48755116	-0,57293928	0,00076868	0,03619952
A_55_P2149931	NM_178407	ENSMUST00000076623	212285	*Arap2*	ArfGAP with RhoGAP domain, ankyrin repeat and PH domain 2	-1,48761939	-0,57300546	0,00097391	0,03753982
A_55_P2030560	NM_001085549	ENSMUST00000094894	666048	*Trabd2b*	TraB domain containing 2B	-1,48786652	-0,5732451	0,00140653	0,04092507
A_51_P437478	NM_152814	ENSMUST00000088785	72556	*Zfp566*	zinc finger protein 566	-1,48971184	-0,5750333	0,00043397	0,03393479
A_55_P2103206	NM_008748	ENSMUST00000039926	18218	*Dusp8*	dual specificity phosphatase 8	-1,49051518	-0,57581107	0,00195026	0,04589615
A_55_P1977583	NM_013469	ENSMUST00000133547	11744	*Anxa11*	annexin A11	-1,49314107	-0,57835047	0,00078248	0,03629498
A_52_P581435	NM_008810	ENSMUST00000033662	18597	*Pdha1*	pyruvate dehydrogenase E1 alpha 1	-1,49606635	-0,58117416	0,00101612	0,03808028
A_55_P2033500	NM_175641	ENSMUST00000108369	108075	*Ltbp4*	latent transforming growth factor beta binding protein 4	-1,49622064	-0,58132294	0,00050383	0,03476444
A_55_P2050192	ENSMUST000000824	ENSMUST00000082418	17721	*ND5*	NADH dehydrogenase subunit 5	-1,4979084	-0,5829494	0,00077021	0,03619952
A_51_P443403	NM_022316	ENSMUST00000021564	64075	*Smoc1*	SPARC related modular calcium binding 1	-1,49795179	-0,58299119	0,00174713	0,04380084
A_51_P389004	NM_011891	ENSMUST00000077221	24052	*Sgcd*	sarcoglycan, delta (dystrophin-associated glycoprotein)	-1,49906502	-0,58406296	0,00236526	0,0482972
A_51_P191520	NM_019990	ENSMUST00000172630	56018	*Stard10*	START domain containing 10	-1,49979664	-0,5847669	0,00121119	0,03911544
A_51_P281380	NM_019571	ENSMUST00000142890	56224	*Tspan5*	tetraspanin 5	-1,50161562	-0,58651556	0,0007118	0,03584877

A_55_P2114427	NM_009952	ENSMUST00000049932	12912	*Creb1*	cAMP responsive element binding protein 1	-1,38310795	-0,46791376	0,00257698	0,04986609
A_55_P2026738	NM_009062	ENSMUST00000027991	19736	*Rgs4*	regulator of G-protein signaling 4	-1,38507082	-0,46995974	0,00131919	0,04018556
A_55_P2065389	NM_001276361	ENSMUST00000114167	227634	*Camsap1*	calmodulin regulated spectrin-associated protein 1	-1,38622876	-0,47116536	0,00215822	0,04738956
A_55_P2088131	NM_001008427	ENSMUST00000107992	434179	*Zfp975*	zinc finger protein 975	-1,386896	-0,4718596	0,00229962	0,04782329
A_55_P1999349	NM_027722	ENSMUST00000020217	71207	*Nudt4*	nudix (nucleoside diphosphate linked moiety X)-type motif 4	-1,38809645	-0,47310781	0,00092596	0,0369201
A_55_P2052016	NM_030209	ENSMUST00000132583	78892	*Crispld2*	cysteine-rich secretory protein LCCL domain containing 2	-1,38842052	-0,47344459	0,00224901	0,04750753
A_55_P1967133	NM_177741	ENSMUST00000070481	244416	*Ppp1r3b*	protein phosphatase 1, regulatory (inhibitor) subunit 3B	-1,38893558	-0,47397969	0,00113137	0,03857573
A_52_P229044	NM_011394	ENSMUST00000067786	20516	*Slc20a2*	solute carrier family 20, member 2	-1,39043966	-0,47554114	0,00169007	0,04345841
A_55_P2155016	NM_001286663	ENSMUST00000114779	381760	*Ssbp1*	single-stranded DNA binding protein 1	-1,3909892	-0,47611122	0,0021694	0,04740503
A_55_P2060111	ENSMUST000000824	ENSMUST00000082407	17706	*ATP8*	ATP synthase F0 subunit 8	-1,39229194	-0,47746175	0,0008399	0,03629498
A_51_P117618	NM_023154	ENSMUST00000077191	66071	*Ethe1*	ethylmalonic encephalopathy 1	-1,39306323	-0,47826074	0,0010091	0,03808028
A_52_P436447	NM_028048	ENSMUST00000102606	71998	*Slc25a35*	solute carrier family 25, member 35	-1,39382867	-0,47905323	0,00190718	0,04548743
A_51_P217382	NM_153103	ENSMUST00000094499	16562	*Kif1c*	kinesin family member 1C	-1,39463341	-0,47988595	0,00077134	0,03619952
A_55_P2011031	NM_025876	ENSMUST00000148289	66971	*Cdk5rap1*	CDK5 regulatory subunit associated protein 1	-1,39497696	-0,4802413	0,00180094	0,04429087
A_55_P1964408	NM_001289782	ENSMUST00000034562	12955	*Cryab*	crystallin, alpha B	-1,39500787	-0,48027326	0,00070153	0,03558895
A_51_P457331	NM_016710	ENSMUST00000033597	50887	*Hmgn5*	high-mobility group nucleosome binding domain 5	-1,39530823	-0,48058386	0,00178036	0,04399008
A_66_P121312	NM_001011529	ENSMUST00000099767	259145	*Olfr1251*	olfactory receptor 1251	-1,39538969	-0,48066807	0,00132324	0,04018556
A_55_P2425235	AK051059		328530			-1,39552594	-0,48080894	0,0001937	0,03291643
A_55_P1991600	NM_001102455	ENSMUST00000072634	11804	*Aplp2*	amyloid beta (A4) precursor-like protein 2	-1,39581569	-0,48110845	0,00073259	0,03593548
A_55_P2361647	NR_030700		320965	*4831440E17Rik*	RIKEN cDNA 4831440E17 gene	-1,39843342	-0,48381157	0,00212823	0,04723723
A_52_P89567	NM_007483	ENSMUST00000067384	11852	*Rhob*	ras homolog gene family, member B	-1,39852181	-0,48390275	0,00067645	0,03555961
A_55_P1976978	NM_001081065	ENSMUST00000131496	69020	*Zfp707*	zinc finger protein 707	-1,40018899	-0,48562157	0,00146291	0,04166534
A_55_P1958537	NM_001043355	ENSMUST00000107100	17760	*Map6*	microtubule-associated protein 6	-1,40064228	-0,48608854	0,00053205	0,03476444
A_55_P2179106	NM_001081086	ENSMUST00000040915	228005	*Ppig*	peptidyl-prolyl isomerase G (cyclophilin G)	-1,4012981	-0,48676389	0,00202823	0,0464094
A_51_P250058	NM_010137	ENSMUST00000024954	13819	*Epas1*	endothelial PAS domain protein 1	-1,40187294	-0,48735559	0,00216791	0,04740503
A_55_P2100025	NM_001290436	ENSMUST00000120809	232878	*Zscan22*	zinc finger and SCAN domain containing 22	-1,4037873	-0,48932435	0,00028898	0,03315398
A_55_P2032258	NM_016861	ENSMUST00000068439	54132	*Pdlim1*	PDZ and LIM domain 1 (elfin)	-1,40462486	-0,49018487	0,00124547	0,039485
A_55_P2139473	NM_001161724	ENSMUST00000138150	16202	*Ilk*	integrin linked kinase	-1,40527432	-0,49085178	0,00253478	0,04970107
A_55_P2044847	NM_175340	ENSMUST00000052747	105193	*Nhlrc1*	NHL repeat containing 1	-1,4055423	-0,49112688	0,00144844	0,0415238
A_55_P2157048	NM_027326	ENSMUST00000078090	70122	*Mllt3*	myeloid/lymphoid or mixed-lineage leukemia; translocated to, 3	-1,40702255	-0,49264545	0,00045242	0,03423628
A_51_P184969	NM_021430	ENSMUST00000062153	75695	*Rilpl1*	Rab interacting lysosomal protein-like 1	-1,40974066	-0,49542979	0,00023139	0,03291643
A_52_P168338	NM_026126	ENSMUST00000033541	67391	*Fundc2*	FUN14 domain containing 2	-1,41109695	-0,49681711	0,00120208	0,03908156
A_55_P2064567	NM_001286040	ENSMUST00000025058	224650	*Anks1*	ankyrin repeat and SAM domain containing 1	-1,4114642	-0,49719253	0,00119364	0,03904427
A_52_P307749	NM_028756	ENSMUST00000023344	74102	*Slc35a5*	solute carrier family 35, member A5	-1,41238069	-0,498129	0,00066912	0,03555961
A_51_P481693	NM_015774	ENSMUST00000022378	50527	*Ero1a*	endoplasmic reticulum oxidoreductase 1 alpha	-1,41313636	-0,49890069	0,00224519	0,04748532
A_52_P109010	NM_010434	ENSMUST00000028600	15259	*Hipk3*	homeodomain interacting protein kinase 3	-1,41334523	-0,49911391	0,00078564	0,03629498
A_66_P113487	NM_011862	ENSMUST00000056177	23970	*Pacsin2*	protein kinase C and casein kinase substrate in neurons 2	-1,41407047	-0,49985401	0,0008287	0,03629498
A_55_P2041961	NM_007553	ENSMUST00000028836	12156	*Bmp2*	bone morphogenetic protein 2	-1,41482053	-0,50061906	0,00050419	0,03476444
A_55_P2026753	NM_175446	ENSMUST00000064659	215693	*Zmat1*	zinc finger, matrin type 1	-1,41488432	-0,5006841	0,0023002	0,04782329
A_52_P202029	NM_172406	ENSMUST00000027186	70827	*Trak2*	trafficking protein, kinesin binding 2	-1,41604363	-0,50186572	0,0022303	0,04740503
A_55_P2302290	AK054025		328243			-1,41762844	-0,50347946	0,00103219	0,03812918
A_52_P200359	NM_080633	ENSMUST00000023116	11429	*Aco2*	aconitase 2, mitochondrial	-1,42245859	-0,50838665	0,00192626	0,04564291
A_55_P2044967	XM_006540384		72723	*Zfp74*	zinc finger protein 74	-1,42315657	-0,50909439	0,000443	0,03394989
A_55_P1961913	NM_011224	ENSMUST00000113483	19309	*Pygm*	muscle glycogen phosphorylase	-1,42515639	-0,51112024	0,00054867	0,03476444
A_55_P2076106	NR_110776		320604	*Ccdc169*	coiled-coil domain containing 169	-1,42552792	-0,5114963	0,00186506	0,04498682
A_55_P1966332	NM_207229	ENSMUST00000184142	211623	*Plac9a*	placenta specific 9a	-1,42720347	-0,51319103	0,00247572	0,04921934
A_51_P363905	NM_025877	ENSMUST00000040280	66972	*Slc25a23*	solute carrier family 25 (mitochondrial carrier; phosphate carrier),	-1,42825378	-0,51425234	0,00172233	0,04371333
A_55_P2289819	NM_053094	ENSMUST00000032234	93671	*Cd163*	CD163 antigen	-1,42935313	-0,51536238	0,0011823	0,03904427
A_55_P1952182	NM_001104573	ENSMUST00000092491	210876	*Vmn2r111*	vomeronasal 2, receptor 111	-1,42970729	-0,51571981	0,00233283	0,04805255
A_51_P464308	NM_013531	ENSMUST00000184130	14696	*Gnb4*	guanine nucleotide binding protein (G protein), beta 4	-1,42991023	-0,51592458	0,00136892	0,04050525
A_52_P57622	NM_198636	ENSMUST00000165067	380660	*Acss3*	acyl-CoA synthetase short-chain family member 3	-1,43373167	-0,51977504	0,00249192	0,04932867
A_55_P2033720	NM_001011861	ENSMUST00000081743	100502887	*Olfr331*	olfactory receptor 331	-1,43409586	-0,52014147	0,00157206	0,04242288
A_55_P1986552	NM_023061	ENSMUST00000098852	84004	*Mcam*	melanoma cell adhesion molecule	-1,43443514	-0,52048274	0,00234274	0,0482313
A_66_P105175	NM_009738	ENSMUST00000029367	12038	*Bche*	butyrylcholinesterase	-1,43540093	-0,52145376	0,00118504	0,03904427
A_51_P487298	NM_139307	ENSMUST00000038770	246154	*Vasn*	vasorin	-1,43644821	-0,52250598	0,00109138	0,03828376

A_66_P130241	NM_153150	ENSMUST00000003622	13358	*Slc25a1*	solute carrier family 25 (mitochondrial carrier, citrate transporter),	-1,50191769	-0,58680575	0,00109279	0,03828376
A_66_P108188	NM_007608	ENSMUST00000057653	12352	*Car5a*	carbonic anhydrase 5a, mitochondrial	-1,50270364	-0,58756051	0,00095272	0,03720193
A_52_P655803	NM_144807	ENSMUST00000073783	212862	*Chpt1*	choline phosphotransferase 1	-1,5033317	-0,58816337	0,00081872	0,03629498
A_52_P17098	NM_001161620	ENSMUST00000115869	75739	*Mpp7*	membrane protein, palmitoylated 7 (MAGUK p55 subfamily memb	-1,50411537	-0,58891523	0,00020718	0,03291643
A_51_P398260	NM_182839	ENSMUST00000022057	72948	*Tppp*	tubulin polymerization promoting protein	-1,50551646	-0,59025848	0,00239572	0,04851956
A_52_P266320	NM_001081956	ENSMUST00000051906	338351	*Akap17b*	A kinase (PRKA) anchor protein 17B	-1,50816563	-0,59279487	0,00117358	0,03904427
A_51_P127681	NM_013885	ENSMUST00000037099	29876	*Clic4*	chloride intracellular channel 4 (mitochondrial)	-1,51243005	-0,59686842	0,00081234	0,03629498
A_65_P02177	NM_026764	ENSMUST00000106670	14865	*Gstm4*	glutathione S-transferase, mu 4	-1,5134092	-0,59780212	0,00068329	0,03558895
A_55_P1969530	NM_011980	ENSMUST00000062181	26465	*Zfp146*	zinc finger protein 146	-1,51470801	-0,59903971	4,88E-05	0,03291643
A_51_P425962	NM_010158	ENSMUST00000022954	13992	*Khdrbs3*	KH domain containing, RNA binding, signal transduction associatec	-1,51840444	-0,60255612	0,00236423	0,0482972
A_51_P464387	NM_030704	ENSMUST00000133335	80888	*Hspb8*	heat shock protein 8	-1,51933931	-0,6034441	0,00032847	0,03315398
A_55_P2168722	NM_001161765	ENSMUST00000107050	14263	*Fmo5*	flavin containing monooxygenase 5	-1,52502398	-0,60883192	0,00034706	0,03319727
A_51_P176352	NM_013864	ENSMUST00000004673	29811	*Ndrg2*	N-myc downstream regulated gene 2	-1,52538515	-0,60917356	0,00026615	0,03315398
A_66_P101724	NM_001243857	ENSMUST00000039064	629059	*Fam124a*	family with sequence similarity 124, member A	-1,52618329	-0,60992824	0,00120887	0,03911544
A_55_P2077458	ENSMUST000001078	ENSMUST00000107887	67468	*Mmd*	monocyte to macrophage differentiation-associated	-1,52644655	-0,61017707	0,00255195	0,04970258
A_55_P2078670	NM_144855	ENSMUST00000078509	12411	*Cbs*	cystathionine beta-synthase	-1,52644872	-0,61017912	0,0011006	0,03830608
A_55_P2052699	NM_183312	ENSMUST00000051389	233335	*Synm*	synemin, intermediate filament protein	-1,52810378	-0,61174253	0,00113888	0,03866356
A_55_P1960366	NM_001033478	ENSMUST00000131166	384198	*Fam47e*	family with sequence similarity 47, member E	-1,5297737	-0,61331825	0,00148406	0,04180691
A_66_P117730	NM_013500	ENSMUST00000022108	12950	*Hapln1*	hyaluronan and proteoglycan link protein 1	-1,53190409	-0,61532597	0,00247671	0,04921934
A_55_P2016667	NM_026672	ENSMUST00000004137	68312	*Gstm7*	glutathione S-transferase, mu 7	-1,53538641	-0,61860178	0,00016889	0,03291643
A_52_P532559	NM_009380	ENSMUST00000022303	21834	*Thrb*	thyroid hormone receptor beta	-1,53547427	-0,61868434	0,00061471	0,0352913
A_51_P479645	NM_177647	ENSMUST00000036350	227526	*Cdnf*	cerebral dopamine neurotrophic factor	-1,53658423	-0,61972685	0,00040513	0,03373901
A_66_P100159	NM_007688	ENSMUST00000078124	12632	*Cfl2*	cofilin 2, muscle	-1,53702937	-0,62014473	0,00083793	0,03629498
A_51_P394788	NM_021895	ENSMUST00000068045	60595	*Actn4*	actinin alpha 4	-1,53824261	-0,62128306	0,00188109	0,04514203
A_51_P439612	NM_020266	ENSMUST00000187058	56812	*Dnajb2*	DnaJ heat shock protein family (Hsp40) member B2	-1,53995534	-0,62288851	0,00075336	0,03604365
A_55_P2054042	NR_033551	ENSMUST00000139017	100037262	*Gm12359*	predicted gene 12359	-1,54157652	-0,62440651	0,00230707	0,04792459
A_52_P1831	NM_009560	ENSMUST00000108336	22718	*Zfp60*	zinc finger protein 60	-1,5422136	-0,6250026	0,00013138	0,03291643
A_52_P631356	NM_177025	ENSMUST00000132979	319876	*Cobll1*	Cobl-like 1	-1,54334271	-0,62605846	0,00044997	0,03415709
A_55_P2007155	NM_134072	ENSMUST00000118717	105387	*Akr1c14*	aldo-keto reductase family 1, member C14	-1,54379517	-0,62648135	0,00152097	0,04211434
A_55_P2000127	NM_001289550	ENSMUST00000070656	21804	*Tgfb1i1*	transforming growth factor beta 1 induced transcript 1	-1,54500737	-0,62761372	0,00175971	0,04380084
A_51_P100289	NM_020493	ENSMUST00000015749	20807	*Srf*	serum response factor	-1,54546874	-0,62804447	0,00172644	0,04375782
A_55_P1962901	NM_011859	ENSMUST00000057021	23967	*Osr1*	odd-skipped related transcription factor 1	-1,54884547	-0,63119321	0,00156035	0,04239131
A_51_P362538	NM_001166064	ENSMUST00000039517	214804	*Syde2*	synapse defective 1, Rho GTPase, homolog 2 (C. elegans)	-1,55015159	-0,6324093	0,00050957	0,03476444
A_66_P100561	NM_016787	ENSMUST00000085393	12175	*Bnip2*	BCL2/adenovirus E1B interacting protein 2	-1,55170105	-0,63385064	0,00203865	0,04652213
A_52_P522754	NM_026932	ENSMUST00000030501	69072	*Ebna1bp2*	EBNA1 binding protein 2	-1,55397577	-0,63596401	0,00109598	0,03828637
A_55_P1967761	NM_008592	ENSMUST00000062292	17300	*Foxc1*	forkhead box C1	-1,56193692	-0,64333619	0,00052579	0,03476444
A_52_P30451	NM_016854	ENSMUST00000087321	53412	*Ppp1r3c*	protein phosphatase 1, regulatory (inhibitor) subunit 3C	-1,56227563	-0,64364901	0,00031235	0,03315398
A_51_P400040	NM_145441	ENSMUST00000142867	217379	*Ubxn2a*	UBX domain protein 2A	-1,56243573	-0,64379685	0,00065932	0,03555961
A_65_P12104	NM_198967	ENSMUST00000060095	387314	*Tmtc1*	transmembrane and tetratricopeptide repeat containing 1	-1,56275212	-0,64408896	0,00165046	0,04305746
A_55_P2183208	NM_001045532	ENSMUST00000099658	666317	*Prl2c1*	Prolactin family 2, subfamily c, member 1	-1,56495934	-0,64612517	0,00081574	0,03629498
A_55_P2011887	NM_010617	ENSMUST00000056978	16553	*Kif13a*	kinesin family member 13A	-1,56584494	-0,64694136	0,00113545	0,03860618
A_51_P342716	NM_172707	ENSMUST00000015100	19046	*Ppp1cb*	protein phosphatase 1, catalytic subunit, beta isoform	-1,56772795	-0,64867523	0,0017594	0,04380084
A_55_P2162573	NM_181728	ENSMUST00000120781	109979	*Art3*	ADP-ribosyltransferase 3	-1,56814076	-0,64905507	0,00129516	0,03982756
A_55_P2030524	NM_013703	ENSMUST00000164509	22359	*Vldlr*	very low density lipoprotein receptor	-1,5682079	-0,64911683	0,00061617	0,0352913
A_55_P2373872	AK049951	ENSMUST00000183194	791088	*Tmem147os*	transmembrane protein 147, opposite strand	-1,56851799	-0,64940208	0,00065677	0,03555961
A_51_P338397	NM_026145	ENSMUST00000134532	330171	*Kctd10*	potassium channel tetramerisation domain containing 10	-1,56960057	-0,65039747	0,00160232	0,04267063
A_55_P1992954	NM_022563	ENSMUST00000027985	18214	*Ddr2*	discoidin domain receptor family, member 2	-1,57161994	-0,65225237	0,00048576	0,0346996
A_52_P447196	NM_053185	ENSMUST00000101205	94216	*Col4a6*	collagen, type IV, alpha 6	-1,57205624	-0,65265283	0,00198345	0,04609624
A_55_P1988699	NM_001110843	ENSMUST00000101581	12293	*Cacna2d1*	calcium channel, voltage-dependent, alpha2/delta subunit 1	-1,57542847	-0,65574425	0,00014716	0,03291643
A_52_P68477	NM_172763	ENSMUST00000072465	235047	*Zfp809*	zinc finger protein 809	-1,57606839	-0,65633014	0,00173602	0,04380084
A_51_P291078	NM_172710	ENSMUST00000031090	231238	*Sel1l3*	sel-1 suppressor of lin-12-like 3 (C. elegans)	-1,57705243	-0,65723062	0,00085503	0,03629498
A_51_P350666	NM_033602	ENSMUST00000073150	93834	*Peli2*	pellino 2	-1,57764423	-0,6577719	0,00070263	0,03558895
A_55_P2028320	NM_139128	ENSMUST00000021190	216961	*Coro6*	coronin 6	-1,57767543	-0,65780043	0,0011084	0,03830608
A_55_P2178678	NM_033321	ENSMUST00000006104	94045	*P2rx5*	purinergic receptor P2X, ligand-gated ion channel, 5	-1,57928015	-0,65926712	0,00212356	0,0471604
A_51_P158120	NM_178640	ENSMUST00000099747	97884	*B3galnt2*	UDP-GalNAc:betaGlcNAc beta 1,3-galactosaminyltransferase, polyı	-1,58018969	-0,66009775	0,00210243	0,04687843

A_55_P2150555	NM_029508	ENSMUST00000225920	76073	*Pcgf5*	polycomb group ring finger 5	-1,58141121	-0,66121255	0,00111805	0,03845114
A_52_P541175	NM_183195	ENSMUST00000184186	277010	*Marveld1*	MARVEL (membrane-associating) domain containing 1	-1,5826953	-0,66238354	0,00118598	0,03904427
A_55_P2132853	NM_028096	ENSMUST00000162875	72097	*Cracdl*	capping protein inhibiting regulator of actin like	-1,58273451	-0,66241928	0,00022761	0,03291643
A_52_P360330	NM_008634	ENSMUST00000064762	17755	*Map1b*	microtubule-associated protein 1B	-1,58372384	-0,66332079	0,0022223	0,04740503
A_55_P2038747	NM_178642	ENSMUST00000121758	101772	*Ano1*	anoctamin 1, calcium activated chloride channel	-1,58418424	-0,66374013	0,0014705	0,04166534
A_66_P111285	NM_001024606	ENSMUST00000059588	382051	*Pdp2*	pyruvate dehyrogenase phosphatase catalytic subunit 2	-1,58591319	-0,6653138	0,00174976	0,04380084
A_55_P2179027	NM_010276	ENSMUST00000108304	14579	*Gem*	GTP binding protein (gene overexpressed in skeletal muscle)	-1,58795028	-0,66716574	0,00236447	0,0482972
A_66_P100349	NM_028731	ENSMUST00000100986	52635	*Esyt2*	extended synaptotagmin-like protein 2	-1,5905886	-0,66956073	0,00079429	0,03629498
A_66_P107482	NM_001145452	ENSMUST00000068175	381112	*Arhgef33*	Rho guanine nucleotide exchange factor (GEF) 33	-1,59126167	-0,67017109	0,00207161	0,0465836
A_51_P142153	NM_001040397	ENSMUST00000159414	78749	*Filip1l*	filamin A interacting protein 1-like	-1,59567468	-0,67416655	0,00195479	0,04589987
A_52_P429364	NM_177471	ENSMUST00000055040	52570	*Ccdc69*	coiled-coil domain containing 69	-1,59664573	-0,67504424	0,00046964	0,03469594
A_55_P1970636	NM_133952	ENSMUST00000107368	101869	*Unc45a*	unc-45 myosin chaperone A	-1,5973114	-0,6756456	0,00048234	0,03469594
A_51_P520639	NM_177822	ENSMUST00000047098	328783	*Mslnl*	mesothelin-like	-1,5995912	-0,67770325	0,00048801	0,03476444
A_55_P2191675	AK018197		70745	*6330418B08Rik*	RIKEN cDNA 6330418B08 gene	-1,59962911	-0,67773744	0,00072753	0,03593548
A_55_P2062058	NM_026797	ENSMUST00000109349	52840	*Dbndd2*	dysbindin (dystrobrevin binding protein 1) domain containing 2	-1,60021933	-0,67826966	0,0010776	0,03824255
A_52_P532313	NM_001085497	ENSMUST00000047655	194744	*Slc25a43*	solute carrier family 25, member 43	-1,60139097	-0,67932558	0,00052318	0,03476444
A_55_P1966114	NM_001252188	ENSMUST00000179936	13855	*Epn2*	epsin 2	-1,6022233	-0,68007523	0,00051964	0,03476444
A_52_P635182	NM_009101	ENSMUST00000044111	20130	*Rras*	related RAS viral (r-ras) oncogene	-1,60580434	-0,68329612	0,00025945	0,03300913
A_55_P2055638	NM_146120	ENSMUST00000028239	227753	*Gsn*	gelsolin	-1,60702802	-0,68439509	0,00028103	0,03315398
A_51_P176972	NM_178114	ENSMUST00000053106	105827	*Amigo2*	adhesion molecule with Ig like domain 2	-1,60748045	-0,68480119	0,0001212	0,03291643
A_55_P1985265	NM_001167949	ENSMUST00000048953	381290	*Atp2b4*	ATPase, Ca++ transporting, plasma membrane 4	-1,60911449	-0,68626698	0,00174859	0,04380084
A_52_P417859	NM_025757	ENSMUST00000070681	66771	*Gid4*	GID complex subunit 4, VID24 homolog (S. cerevisiae)	-1,61411006	-0,69073895	0,00148517	0,04180691
A_55_P1957213	AK019465		77570	*3930401B19Rik*	RIKEN cDNA 3930401B19 gene	-1,61591091	-0,69234766	0,00071875	0,03593548
A_51_P181865	NM_028053	ENSMUST00000030127	52076	*Tmem38b*	transmembrane protein 38B	-1,61719962	-0,69349777	0,00232491	0,04798501
A_55_P2126473	NM_001099298	ENSMUST00000028377	110876	*Scn2a*	sodium channel, voltage-gated, type II, alpha 1	-1,61929833	-0,6953688	0,00168373	0,04345841
A_52_P281702	NM_010518	ENSMUST00000027377	16011	*Igfbp5*	insulin-like growth factor binding protein 5	-1,62177169	-0,69757074	0,0005366	0,03476444
A_55_P2052563	NM_010495	ENSMUST00000109824	15901	*Id1*	inhibitor of DNA binding 1	-1,62197618	-0,69775263	0,00157128	0,04242288
A_55_P2011912	NM_001012324	ENSMUST00000051504	407800	*Ecm2*	extracellular matrix protein 2, female organ and adipocyte specific	-1,62497525	-0,70041774	0,00121445	0,03911544
A_55_P2004797	NM_001004468	ENSMUST00000084513	57752	*Tacc2*	transforming, acidic coiled-coil containing protein 2	-1,62536471	-0,70076348	0,00093319	0,03698032
A_51_P227345	NM_007876	ENSMUST00000019422	13479	*Dpep1*	dipeptidase 1	-1,62775078	-0,70287983	0,00192339	0,04561071
A_55_P2141851	NM_145629	ENSMUST00000033547	102866	*Pls3*	plastin 3 (T-isoform)	-1,62839052	-0,70344672	0,00149178	0,04187212
A_51_P288916	NM_177368	ENSMUST00000061506	278279	*Tmtc2*	transmembrane and tetratricopeptide repeat containing 2	-1,62869735	-0,70371854	0,0022861	0,0477725
A_55_P2176145	NM_001161822	ENSMUST00000117676	56533	*Rgs17*	regulator of G-protein signaling 17	-1,63382778	-0,70825592	0,00133342	0,04022942
A_55_P2177488	NM_178214	ENSMUST00000090781	319190	*Hist2h2be*	histone cluster 2, H2be	-1,63540217	-0,70964546	0,00044797	0,03412929
A_55_P2162945	ENSMUST000001464	ENSMUST00000146428	27045	*Nit1*	nitrilase 1	-1,63656434	-0,71067032	0,00073113	0,03593548
A_55_P2154173	XR_140431		433297	*Gm5526*	predicted pseudogene 5526	-1,63674389	-0,71082859	0,00164249	0,04301439
A_51_P183051	NM_133995	ENSMUST00000039925	103149	*Upb1*	ureidopropionase, beta	-1,63765203	-0,71162884	0,0006253	0,03546117
A_55_P2052824	NM_001033042	ENSMUST00000022064	432779	*Lrrc14b*	leucine rich repeat containing 14B	-1,63988041	-0,71359061	0,00085325	0,03629498
A_51_P268094	NM_009255	ENSMUST00000027467	20720	*Serpine2*	serine (or cysteine) peptidase inhibitor, clade E, member 2	-1,64057061	-0,71419768	0,00216629	0,04740503
A_51_P156800	NM_028308	ENSMUST00000084418	101513	*Mob2*	MOB kinase activator 2	-1,6417251	-0,71521258	0,00085271	0,03629498
A_55_P2084703	NM_133360	ENSMUST00000020843	107476	*Acaca*	acetyl-Coenzyme A carboxylase alpha	-1,64505521	-0,718136	0,0008675	0,03647161
A_65_P03874	NM_175272	ENSMUST00000064395	78286	*Nav2*	neuron navigator 2	-1,64640454	-0,71931886	0,00039446	0,03373901
A_55_P1966432	NM_010358	ENSMUST00000153314	14862	*Gstm1*	glutathione S-transferase, mu 1	-1,64679804	-0,71966364	0,00015948	0,03291643
A_52_P418489	NM_023476	ENSMUST00000105998	94242	*Tinagl1*	tubulointerstitial nephritis antigen-like 1	-1,64839878	-0,7210653	0,00058698	0,03507191
A_55_P2025514	NM_054088	ENSMUST00000045289	116939	*Pnpla3*	patatin-like phospholipase domain containing 3	-1,65156256	-0,72383162	0,00207628	0,04661566
A_52_P64687	NM_025451	ENSMUST00000050918	66259	*Camk2n1*	calcium/calmodulin-dependent protein kinase II inhibitor 1	-1,6528039	-0,72491557	0,0003691	0,03369759
A_55_P2186180	NM_026209	ENSMUST00000059666	67509	*Saysd1*	SAYSVFN motif domain containing 1	-1,65301178	-0,72509701	0,00026895	0,03315398
A_51_P155196	NM_178890	ENSMUST00000076212	99382	*Abtb2*	ankyrin repeat and BTB (POZ) domain containing 2	-1,65306117	-0,72514011	0,00033359	0,03315398
A_55_P2018666	NM_009381	ENSMUST00000043077	21835	*Thrsp*	thyroid hormone responsive	-1,65900166	-0,73031533	0,00183776	0,044633
A_51_P431996	NM_175494	ENSMUST00000059817	238673	*Zfp367*	zinc finger protein 367	-1,66005429	-0,73123042	0,00223692	0,04740678
A_55_P2014224	NM_009154	ENSMUST00000067458	20356	*Sema5a*	sema domain, seven thrombospondin repeats (type 1 and type 1-li	-1,66197428	-0,73289805	0,00129297	0,03982756
A_55_P2065824	NM_001284428	ENSMUST00000075118	29856	*Smtn*	smoothelin	-1,66536765	-0,73584071	0,00167476	0,04338482
A_55_P1982902	NM_001029978	ENSMUST00000113100	594844	*Tceal3*	transcription elongation factor A (SII)-like 3	-1,66740843	-0,73760754	0,00245187	0,04908868
A_52_P306351	NM_001177850	ENSMUST00000084915	65973	*Asph*	aspartate-beta-hydroxylase	-1,66840605	-0,73847045	0,00032892	0,03315398
A_55_P2064841	NM_001081268	ENSMUST00000121394	330657	*Prss53*	protease, serine 53	-1,6705159	-0,74029372	0,00103407	0,03812918

A_51_P267494	NM_026514	ENSMUST00000068958	260409	*Cdc42ep3*	CDC42 effector protein (Rho GTPase binding) 3	-1,76892217	-0,82287057	0,00049127	0,03476444
A_51_P451075	NM_009722	ENSMUST00000177974	11938	*Atp2a2*	ATPase, Ca++ transporting, cardiac muscle, slow twitch 2	-1,76893786	-0,82288337	0,0006954	0,03558895
A_55_P1985273	NM_144799	ENSMUST00000032376	30937	*Lmcd1*	LIM and cysteine-rich domains 1	-1,76903103	-0,82295935	0,00223694	0,04740678
A_55_P1975235	NM_009753	ENSMUST00000111513	12121	*Bicd1*	BICD cargo adaptor 1	-1,76940685	-0,82326581	0,00187351	0,04513469
A_51_P257951	NM_020509	ENSMUST00000023329	57262	*Retnla*	resistin like alpha	-1,77966618	-0,83160665	0,00258534	0,04989265
A_51_P300337	NM_007792	ENSMUST00000020403	13008	*Csrp2*	cysteine and glycine-rich protein 2	-1,78192117	-0,83343351	0,0017387	0,04380084
A_55_P2024406	NM_178728	ENSMUST00000060899	242864	*Napepld*	N-acyl phosphatidylethanolamine phospholipase D	-1,78690486	-0,83746282	0,00061735	0,03529254
A_55_P2039284	NM_013560	ENSMUST00000005077	15507	*Hspb1*	heat shock protein 1	-1,78922707	-0,83933649	0,00076225	0,03611065
A_51_P325862	NM_013751	ENSMUST00000089824	27281	*Hrasls*	HRAS-like suppressor	-1,79067385	-0,84050259	0,0007823	0,03629498
A_55_P1987156	NM_001288618	ENSMUST00000003568	12922	*Crhr2*	corticotropin releasing hormone receptor 2	-1,79731372	-0,84584225	0,00100409	0,03807877
A_55_P1998995	NM_001085371	ENSMUST00000113590	11790	*Speg*	SPEG complex locus	-1,80499131	-0,85199189	0,00131446	0,04016748
A_52_P399095	NM_177793	ENSMUST00000058747	327747	*Mettl24*	methyltransferase like 24	-1,80573146	-0,85258336	0,00053782	0,03476444
A_51_P423880	NM_025891	ENSMUST00000030791	66993	*Smarcd3*	SWI/SNF related, matrix associated, actin dependent regulator of c	-1,80590499	-0,85272199	0,00091454	0,03681936
A_55_P2124791	NM_001109991	ENSMUST00000072755	12822	*Col18a1*	collagen, type XVIII, alpha 1	-1,8074646	-0,85396739	0,00201361	0,0463625
A_51_P114826	NM_019707	ENSMUST00000117160	12554	*Cdh13*	cadherin 13	-1,80848918	-0,85478497	0,00127587	0,03970879
A_52_P137378	NM_178143	ENSMUST00000030243	108079	*Prkaa2*	protein kinase, AMP-activated, alpha 2 catalytic subunit	-1,80910014	-0,85527227	9,23E-05	0,03291643
A_55_P1961873	NM_011785	ENSMUST00000111159	23797	*Akt3*	thymoma viral proto-oncogene 3	-1,80931963	-0,8554473	0,00107255	0,03823006
A_52_P240542	NM_010496	ENSMUST00000020974	15902	*Id2*	inhibitor of DNA binding 2	-1,81028874	-0,85621983	0,00088368	0,03654939
A_52_P220879	NM_009373	ENSMUST00000103122	21817	*Tgm2*	transglutaminase 2, C polypeptide	-1,8130879	-0,85844887	0,00076727	0,03619952
A_55_P2343648	BX512981	ENSMUST00000231167	73600	*1700120C14Rik*	RIKEN cDNA 1700120C14 gene	-1,81458963	-0,85964332	0,00125235	0,03954206
A_55_P2234704	AK040933		103767	*Sgcd*	sarcoglycan, delta (dystrophin-associated glycoprotein)	-1,8191307	-0,8632492	0,00045009	0,03415709
A_55_P2139809	NM_001290414	ENSMUST00000033473	14168	*Fgf13*	fibroblast growth factor 13	-1,82397955	-0,86708955	0,00114319	0,03870044
A_52_P682382	NM_009127	ENSMUST00000041331	20249	*Scd1*	stearoyl-Coenzyme A desaturase 1	-1,82490263	-0,86781949	0,00027244	0,03315398
A_51_P255304	NM_007617	ENSMUST00000075477	12391	*Cav3*	caveolin 3	-1,82564132	-0,86840335	0,00129783	0,03987819
A_51_P483544	NM_013930	ENSMUST00000031707	30956	*Aass*	aminoadipate-semialdehyde synthase	-1,82981747	-0,87169974	0,00070082	0,03558895
A_55_P2072801	NM_029806	ENSMUST00000032683	76942	*Lypd5*	Ly6/Plaur domain containing 5	-1,83144427	-0,8729818	0,00031281	0,03315398
A_51_P127297	NM_008288	ENSMUST00000016338	15483	*Hsd11b1*	hydroxysteroid 11-beta dehydrogenase 1	-1,83260633	-0,87389691	0,00049229	0,03476444
A_55_P2128734	NM_146131	ENSMUST00000038942	229534	*Pbxip1*	pre B cell leukemia transcription factor interacting protein 1	-1,8341706	-0,87512783	0,00040291	0,03373901
A_55_P2332194	XR_401002		100038411	*Gm15998*	predicted gene 15998	-1,83440288	-0,87531052	0,00079488	0,03629498
A_55_P2049429	NM_172992	ENSMUST00000118174	68770	*Phtf2*	putative homeodomain transcription factor 2	-1,83542065	-0,87611074	0,0003944	0,03373901
A_55_P1988795	NM_019811	ENSMUST00000133654	60525	*Acss2*	acyl-CoA synthetase short-chain family member 2	-1,83653077	-0,87698307	0,00071926	0,03593548
A_55_P2096257	NM_010860	ENSMUST00000164181	17904	*Myl6*	myosin, light polypeptide 6, alkali, smooth muscle and non-muscle	-1,84237351	-0,88156557	0,00119375	0,03904427
A_66_P100165	NM_009250	ENSMUST00000161776	20713	*Serpini1*	serine (or cysteine) peptidase inhibitor, clade I, member 1	-1,84237475	-0,88156654	0,00223442	0,04740503
A_55_P2159480	NM_172682	ENSMUST00000118408	229488	*Fam160a1*	family with sequence similarity 160, member A1	-1,84772526	-0,88575026	3,86E-05	0,03291643
A_66_P124659	NM_145515	ENSMUST00000027929	226778	*Mark1*	MAP/microtubule affinity-regulating kinase 1	-1,84798586	-0,88595372	0,00218527	0,04740503
A_55_P2016842	NM_001198933	ENSMUST00000034989	17436	*Me1*	malic enzyme 1, NADP(+)-dependent, cytosolic	-1,84880904	-0,88659622	0,00025303	0,03291643
A_52_P590781	NM_024244	ENSMUST00000105436	71721	*Fam13c*	family with sequence similarity 13, member C	-1,85313293	-0,88996637	0,00030018	0,03315398
A_51_P182693	NM_008727	ENSMUST00000142243	18160	*Npr1*	natriuretic peptide receptor 1	-1,85884919	-0,89440973	7,70E-06	0,03291643
A_51_P223036	NM_027968	ENSMUST00000129456	71865	*Fbxo30*	F-box protein 30	-1,86245627	-0,89720656	0,00055895	0,03476444
A_55_P2146384	NM_001081243	ENSMUST00000172740	70598	*Filip1*	filamin A interacting protein 1	-1,86486962	-0,89907477	0,00014956	0,03291643
A_51_P135517	NM_007728	ENSMUST00000164782	12810	*Coch*	cochlin	-1,86596069	-0,89991859	0,00218288	0,04740503
A_55_P1975215	NM_153553	ENSMUST00000056129	225872	*Npas4*	neuronal PAS domain protein 4	-1,86785913	-0,90138565	0,00220194	0,04740503
A_55_P2001518	NM_023898	ENSMUST00000057650	78600	*Pde6h*	phosphodiesterase 6H, cGMP-specific, cone, gamma	-1,86792583	-0,90143717	0,00083354	0,03629498
A_55_P1972039	NM_001285833	ENSMUST00000032781	50490	*Nox4*	NADPH oxidase 4	-1,87013731	-0,9031442	0,00016382	0,03291643
A_55_P2422685	NR_040463		100504561	*9230112J17Rik*	RIKEN cDNA 9230112J17 gene	-1,87109526	-0,90388301	0,00084672	0,03629498
A_51_P346445	NM_013868	ENSMUST00000102486	29818	*Hspb7*	heat shock protein family, member 7 (cardiovascular)	-1,87261361	-0,90505325	0,00157621	0,04243679
A_51_P298107	NM_028813	ENSMUST00000024880	74199	*Vit*	vitrin	-1,87522506	-0,90706376	0,00088227	0,03654939
A_55_P2168667	NM_028030	ENSMUST00000169003	71973	*Rbpms2*	RNA binding protein with multiple splicing 2	-1,87933432	-0,91022174	0,00051357	0,03476444
A_55_P2340221	ENSMUST00000141414	ENSMUST00000141419	329251	*Ppp1r12b*	protein phosphatase 1, regulatory (inhibitor) subunit 12B	-1,88437331	-0,9140848	0,00013799	0,03291643
A_52_P1124229	AK083203	ENSMUST00000136217	100042178	*Prdm16os*	Prdm16 opposite strand transcript	-1,88600456	-0,91533316	0,00057642	0,03507191
A_55_P1970755	NM_024124	ENSMUST00000110819	79221	*Hdac9*	histone deacetylase 9	-1,88602634	-0,91534982	0,00068562	0,03558895
A_55_P2131016	NM_009123	ENSMUST00000054562	20231	*Nkx1-2*	NK1 homeobox 2	-1,88651639	-0,91572464	0,00204745	0,04655586
A_52_P179068	NM_017469	ENSMUST00000029635	54195	*Gucy1b3*	guanylate cyclase 1, soluble, beta 3	-1,88717088	-0,91622506	0,00134012	0,04028731
A_52_P201558	NM_029879	ENSMUST00000063551	52882	*Rgs7bp*	regulator of G-protein signalling 7 binding protein	-1,88999634	-0,91838344	0,0003397	0,03315398
A_51_P508770	NM_011846	ENSMUST00000031390	23948	*Mmp17*	matrix metallopeptidase 17	-1,89694155	-0,92367522	0,00175605	0,04380084

A_51_P340699	NM_026864	ENSMUST00000031646	68895	*Rasl11a*	RAS-like, family 11, member A	-1,67189527	-0,74148447	0,00060926	0,03524409
A_55_P2134616	AK129475	ENSMUST00000199659	329650	*Med12l*	mediator complex subunit 12-like	-1,67351789	-0,74288397	0,00022679	0,03291643
A_55_P2077741	NM_177074	ENSMUST00000112420	320106	*Slc38a11*	solute carrier family 38, member 11	-1,67390718	-0,74321953	0,0024232	0,04872811
A_51_P153013	NR_027800	ENSMUST00000123544	24082	*Map2k3os*	mitogen-activated protein kinase kinase 3, opposite strand	-1,67478901	-0,74397935	0,0012353	0,0393138
A_52_P222624	NM_024441	ENSMUST00000042790	69253	*Hspb2*	heat shock protein 2	-1,67592459	-0,74495723	0,00104933	0,03814335
A_51_P266546	NM_173181	ENSMUST00000051064	67306	*Zc2hc1a*	zinc finger, C2HC-type containing 1A	-1,67847696	-0,74715274	0,00117913	0,03904427
A_52_P34378	NM_001038624	ENSMUST00000055993	320360	*Ric3*	resistance to inhibitors of cholinesterase 3 homolog (C. elegans)	-1,6795378	-0,74806427	0,00249541	0,04934456
A_51_P160824	NM_139001	ENSMUST00000035661	121021	*Cspg4*	chondroitin sulfate proteoglycan 4	-1,68100783	-0,74932644	0,00208588	0,04671098
A_55_P2091651	NM_177033	ENSMUST00000109681	319922	*Vwc2*	von Willebrand factor C domain containing 2	-1,68177747	-0,74998683	0,00255518	0,04971302
A_55_P2028942	NM_010875	ENSMUST00000114476	17967	*Ncam1*	neural cell adhesion molecule 1	-1,682047	-0,75021802	0,00032403	0,03315398
A_52_P196632	NM_028974	ENSMUST00000068307	74492	*Kbtbd13*	kelch repeat and BTB (POZ) domain containing 13	-1,68410605	-0,75198299	0,00023577	0,03291643
A_55_P1967736	NM_027280	ENSMUST00000034086	93960	*Nkd1*	naked cuticle 1	-1,68875934	-0,75596375	0,00074318	0,03604365
A_52_P256914	NM_010000	ENSMUST00000082214	13094	*Cyp2b9*	cytochrome P450, family 2, subfamily b, polypeptide 9	-1,69257613	-0,75922072	0,00118122	0,03904427
A_52_P333289	NM_033615	ENSMUST00000134742	110751	*Adam33*	a disintegrin and metallopeptidase domain 33	-1,69488566	-0,76118795	0,00097041	0,03751641
A_51_P347862	NM_134156	ENSMUST00000167327	109711	*Actn1*	actinin, alpha 1	-1,69734159	-0,76327694	6,57E-05	0,03291643
A_51_P183561	NM_145473	ENSMUST00000152678	105859	*Csdc2*	cold shock domain containing C2, RNA binding	-1,69739761	-0,76332455	0,00063528	0,03546117
A_52_P100252	NM_007988	ENSMUST00000055655	14104	*Fasn*	fatty acid synthase	-1,69989993	-0,76544982	0,00238193	0,04851956
A_55_P1958532	NM_021877	ENSMUST00000022691	15460	*Hr*	lysine demethylase and nuclear receptor corepressor	-1,70099259	-0,76637685	0,00245516	0,04909184
A_55_P2150757	NM_008504	ENSMUST00000151213	16904	*Gzmm*	granzyme M (lymphocyte met-ase 1)	-1,70111779	-0,76648304	0,00055829	0,03476444
A_55_P2146520	NM_134148	ENSMUST00000167055	107239	*Carns1*	carnosine synthase 1	-1,70226051	-0,76745184	0,00141634	0,04101694
A_55_P2021119	NM_001205345	ENSMUST00000162392	223697	*Sun2*	Sad1 and UNC84 domain containing 2	-1,70558004	-0,77026246	0,00072174	0,03593548
A_52_P364140	NM_010577	ENSMUST00000023128	16402	*Itga5*	integrin alpha 5 (fibronectin receptor alpha)	-1,7067057	-0,77121431	0,00212043	0,04711792
A_55_P2198983	AI606402		73880	*4930415C11Rik*	RIKEN cDNA 4930415C11 gene	-1,70696846	-0,7714364	0,00037225	0,03370264
A_55_P1963863	NM_001081116	ENSMUST00000107032	207212	*Arhgef17*	Rho guanine nucleotide exchange factor (GEF) 17	-1,70772069	-0,77207203	0,00120963	0,03911544
A_55_P1961320	NM_207176	ENSMUST00000115467	21753	*Tes*	testis derived transcript	-1,70841439	-0,77265796	0,00254917	0,04970107
A_66_P121288	NM_025355	ENSMUST00000033783	66104	*Tceal6*	transcription elongation factor A (SII)-like 6	-1,71056944	-0,77447667	0,00121645	0,03911544
A_55_P2105843	XM_006525709	ENSMUST00000097530	17190	*Mbd1*	methyl-CpG binding domain protein 1	-1,7114029	-0,77517944	0,00104599	0,03812918
A_55_P2394490	XM_006513411		20503	*Slc16a7*	solute carrier family 16 (monocarboxylic acid transporters), memb	-1,71376229	-0,77716702	0,00163405	0,04294518
A_55_P2106033	NM_028901	ENSMUST00000182189	74376	*Myo18b*	myosin XVIIIb	-1,71583475	-0,77891062	0,00259031	0,04992246
A_66_P136095	NM_001164376	ENSMUST00000075099	216033	*Ctnna3*	catenin (cadherin associated protein), alpha 3	-1,71783968	-0,7805954	0,00095142	0,03718864
A_52_P105537	NM_010930	ENSMUST00000050027	18133	*Nov*	nephroblastoma overexpressed gene	-1,71908862	-0,78164392	0,00136361	0,04046247
A_66_P130813	NM_001037221	ENSMUST00000137543	74480	*Samd4*	sterile alpha motif domain containing 4	-1,72023634	-0,78260679	0,00119647	0,03904427
A_55_P2220937	NM_027715	ENSMUST00000052168	71198	*Otud1*	OTU domain containing 1	-1,72063455	-0,78294071	0,00021171	0,03291643
A_55_P2025954	NM_001199296	ENSMUST00000165111	104112	*Acly*	ATP citrate lyase	-1,72236722	-0,78439277	0,00104862	0,03814335
A_55_P2129658	NM_008542	ENSMUST00000041029	17130	*Smad6*	SMAD family member 6	-1,72253036	-0,78452941	0,00245309	0,04908868
A_52_P552665	NM_008057	ENSMUST00000114246	14369	*Fzd7*	frizzled class receptor 7	-1,72308734	-0,78499583	0,00087765	0,03654939
A_55_P1957918	NM_001135192	ENSMUST00000064595	211914	*Asap2*	ArfGAP with SH3 domain, ankyrin repeat and PH domain 2	-1,73024224	-0,79097403	0,00235385	0,0482972
A_55_P2157966	NM_032393	ENSMUST00000094639	17754	*Map1a*	microtubule-associated protein 1 A	-1,73189153	-0,79234857	0,00059515	0,03507191
A_52_P920129	NM_010305	ENSMUST00000074694	14677	*Gnai1*	guanine nucleotide binding protein (G protein), alpha inhibiting 1	-1,73282437	-0,79312543	0,00029752	0,03315398
A_51_P315391	NM_138628	ENSMUST00000037964	378431	*Txlnb*	taxilin beta	-1,73483503	-0,79479848	0,00214006	0,0473211
A_55_P2012729	NM_013569	ENSMUST00000036092	16511	*Kcnh2*	potassium voltage-gated channel, subfamily H (eag-related), meml	-1,74028003	-0,79931947	0,00242496	0,04873607
A_55_P2087414	NM_011348	ENSMUST00000073957	20349	*Sema3e*	sema domain, immunoglobulin domain (Ig), short basic domain, se	-1,74096064	-0,79988358	0,00170437	0,04357357
A_52_P449871	NM_031166	ENSMUST00000021810	15904	*Id4*	inhibitor of DNA binding 4	-1,74184029	-0,80061235	0,00201712	0,04639816
A_51_P355427	NM_080639	ENSMUST00000032462	110595	*Timp4*	tissue inhibitor of metalloproteinase 4	-1,74710523	-0,8049665	0,00164546	0,04303025
A_55_P2002723	NM_001127363	ENSMUST00000026550	212111	*Inpp5a*	inositol polyphosphate-5-phosphatase A	-1,75197354	-0,80898099	0,00029183	0,03315398
A_52_P609868	NM_178759	ENSMUST00000068877	276891	*Timd4*	T cell immunoglobulin and mucin domain containing 4	-1,75292458	-0,80976392	0,00160906	0,04275919
A_55_P2019954	NM_013460	ENSMUST00000103184	11550	*Adra1d*	adrenergic receptor, alpha 1d	-1,75385182	-0,81052687	0,00227435	0,04760355
A_55_P2043612	NM_001033281	ENSMUST00000091900	225518	*Prdm6*	PR domain containing 6	-1,75530795	-0,81172416	0,00138708	0,04077792
A_52_P616580	NM_001033409	ENSMUST00000044828	329252	*Lgr6*	leucine-rich repeat-containing G protein-coupled receptor 6	-1,75744898	-0,81348281	0,00216651	0,04740503
A_51_P452768	NM_022434	ENSMUST00000054174	64385	*Cyp4f14*	cytochrome P450, family 4, subfamily f, polypeptide 14	-1,75818464	-0,81408659	0,00054882	0,03476444
A_55_P2408778	NR_027907		102623		expressed sequence AI414108	-1,75939278	-0,8150776	0,0012301	0,03926729
A_51_P196726	NM_010582	ENSMUST00000042290	16425	*Itih2*	inter-alpha trypsin inhibitor, heavy chain 2	-1,76364276	-0,81855836	0,00060088	0,03507191
A_55_P2071811	NM_028153	ENSMUST00000148246	72205	*Eml2*	echinoderm microtubule associated protein like 2	-1,76602743	-0,82050775	0,00116495	0,03904427
A_52_P227	NR_040383	ENSMUST00000147689	75116	*4930520O04Rik*	RIKEN cDNA 4930520O04 gene	-1,76773273	-0,82190016	0,00023206	0,03291643
A_55_P2099594	NM_024450	ENSMUST00000026220	30049	*Scd3*	stearoyl-coenzyme A desaturase 3	-1,76784809	-0,82199431	0,00167495	0,04338482

A_51_P307082	NM_013904	ENSMUST00000019924	15214	*Hey2*	hairy/enhancer-of-split related with YRPW motif 2	-2,15044093	-1,10463251	0,0005527	0,03476444
A_51_P466685	NM_175206	ENSMUST00000056890	74165	*Fbxl22*	F-box and leucine-rich repeat protein 22	-2,15105147	-1,10504204	0,00066923	0,03555961
A_55_P2055031	NM_182808	ENSMUST00000122120	320265	*Tafa1*	TAFA chemokine like family member 1	-2,15123121	-1,10516259	0,00055266	0,03476444
A_51_P333518	NM_172966	ENSMUST00000074679	269016	*Sh3rf2*	SH3 domain containing ring finger 2	-2,15341971	-1,10662954	0,00014445	0,03291643
A_52_P172014	NM_016894	ENSMUST00000097648	51801	*Ramp1*	receptor (calcitonin) activity modifying protein 1	-2,16515349	-1,1144693	0,00050983	0,03476444
A_51_P451052	NM_175013	ENSMUST00000047666	226041	*Pgm5*	phosphoglucomutase 5	-2,17460081	-1,12075059	0,00177673	0,04399008
A_55_P1983754	NM_025557	ENSMUST00000111332	66425	*Pcp4l1*	Purkinje cell protein 4-like 1	-2,17517562	-1,12113188	0,00093074	0,03697411
A_51_P425798	NM_029920	ENSMUST00000085554	77521	*Mtus2*	microtubule associated tumor suppressor candidate 2	-2,17552958	-1,12136663	0,00053299	0,03476444
A_51_P283300	NM_023116	ENSMUST00000114723	12296	*Cacnb2*	calcium channel, voltage-dependent, beta 2 subunit	-2,17600534	-1,1216821	0,00032864	0,03315398
A_51_P105927	NM_001033158	ENSMUST00000085453	70784	*Rasl12*	RAS-like, family 12	-2,17995417	-1,1242978	0,00087417	0,03654939
A_52_P380301	NM_009472	ENSMUST00000106236	22253	*Unc5c*	unc-5 netrin receptor C	-2,18534913	-1,12786378	0,00036215	0,03369759
A_55_P2414619	XM_006520017	ENSMUST00000036439	12563	*Cdh6*	cadherin 6	-2,19739528	-1,13579441	0,00071583	0,03592056
A_55_P2107667	NM_010135	ENSMUST00000078719	13800	*Enah*	ENAH actin regulator	-2,20186473	-1,13872584	0,00158097	0,04250601
A_52_P419373	NM_175413	ENSMUST00000029573	109245	*Lrrc39*	leucine rich repeat containing 39	-2,2087404	-1,14322387	0,00040559	0,03373901
A_66_P105032	NM_001145034	ENSMUST00000148314	620695	*Gm13889*	predicted gene 13889	-2,20911989	-1,14347172	0,00205912	0,04655586
A_66_P131851	NM_031169	ENSMUST00000020362	16533	*Kcnmb1*	potassium large conductance calcium-activated channel, subfamily	-2,24544248	-1,16699976	0,00088625	0,03654939
A_55_P2121408	NM_001277875	ENSMUST00000133355	22004	*Tpm2*	tropomyosin 2, beta	-2,2459772	-1,16734328	0,00049247	0,03476444
A_51_P194273	NM_011892	ENSMUST00000121148	24053	*Sgcg*	sarcoglycan, gamma (dystrophin-associated glycoprotein)	-2,24773257	-1,1684704	0,00163244	0,04294518
A_51_P116755	NM_026056	ENSMUST00000021802	67252	*Cap2*	CAP, adenylate cyclase-associated protein, 2 (yeast)	-2,25395493	-1,17245867	0,00033155	0,03315398
A_51_P221510	NM_029784	ENSMUST00000034749	76886	*Fam81a*	family with sequence similarity 81, member A	-2,26079819	-1,17683222	0,00162421	0,04294518
A_51_P240253	NM_019662	ENSMUST00000034351	56437	*Rrad*	Ras-related associated with diabetes	-2,26342557	-1,17850787	2,66E-05	0,03291643
A_55_P2025038	NM_013494	ENSMUST00000048967	12876	*Cpe*	carboxypeptidase E	-2,2881368	-1,19417331	0,00077506	0,03629498
A_51_P161308	NM_013667	ENSMUST00000046959	20518	*Slc22a2*	solute carrier family 22 (organic cation transporter), member 2	-2,28822563	-1,19422932	0,00013057	0,03291643
A_55_P2001920	NM_001290421	ENSMUST00000101454	192176	*Flna*	filamin, alpha	-2,28998249	-1,19533657	0,00040288	0,03373901
A_55_P2221236	AK085976		102242	*AU024180*	expressed sequence AU024180	-2,29745213	-1,2000348	0,00017815	0,03291643
A_55_P1963154	NM_016770	ENSMUST00000001824	53320	*Folh1*	folate hydrolase 1	-2,30257737	-1,20324963	0,00014786	0,03291643
A_55_P2043734	NM_001024624	ENSMUST00000087104	382253	*Cdkl5*	cyclin-dependent kinase-like 5	-2,30485432	-1,20467557	3,50E-05	0,03291643
A_55_P2028837	NM_027533	ENSMUST00000029451	70747	*Tspan2*	tetraspanin 2	-2,31258021	-1,2095034	0,00188411	0,04514203
A_55_P2030578	NM_027884	ENSMUST00000169786	21961	*Tns1*	tensin 1	-2,32206206	-1,21540653	0,00017446	0,03291643
A_51_P301998	NM_018881	ENSMUST00000111510	55990	*Fmo2*	flavin containing monooxygenase 2	-2,32766819	-1,21888542	0,00044591	0,03404162
A_55_P1974421	NM_013565	ENSMUST00000001548	16400	*Itga3*	integrin alpha 3	-2,3315527	-1,22129104	0,00028078	0,03315398
A_51_P101460	NM_023842	ENSMUST00000124830	109620	*Dsp*	desmoplakin	-2,33257258	-1,22192197	0,00172072	0,04371333
A_55_P1961736	NM_001286653	ENSMUST00000044895	53901	*Rcan2*	regulator of calcineurin 2	-2,33449722	-1,22311187	0,00067462	0,03555961
A_52_P440709	NM_023868	ENSMUST00000021750	20191	*Ryr2*	ryanodine receptor 2, cardiac	-2,33839977	-1,22552159	0,000229	0,03291643
A_55_P1967677	NM_001081351	ENSMUST00000115383	214642	*Cped1*	cadherin-like and PC-esterase domain containing 1	-2,35088074	-1,23320135	0,00036439	0,03369759
A_55_P2262593	AK142388		74633	*4930429F24Rik*	RIKEN cDNA 4930429F24 gene	-2,35165816	-1,23367837	0,00015072	0,03291643
A_55_P2116744	NM_011724	ENSMUST00000111635	22437	*Xirp1*	xin actin-binding repeat containing 1	-2,35759241	-1,23731432	0,00020201	0,03291643
A_55_P2217831	AK013682		73049	*2900054C01Rik*	RIKEN cDNA 2900054C01 gene	-2,35947991	-1,23846889	0,0005752	0,03507191
A_51_P358722	NM_173414	ENSMUST00000069763	236285	*Lancl3*	LanC lantibiotic synthetase component C-like 3 (bacterial)	-2,35981814	-1,23867568	0,00187806	0,04514203
A_65_P11603	NM_011918	ENSMUST00000022327	24131	*Ldb3*	LIM domain binding 3	-2,36262463	-1,24039044	0,00059669	0,03507191
A_51_P459350	NM_019771	ENSMUST00000103172	56431	*Dstn*	destrin	-2,36265793	-1,24041077	0,00067627	0,03555961
A_52_P409769	NM_194464	ENSMUST00000125758	17540	*Mrvi1*	MRV integration site 1	-2,36859685	-1,24403267	0,00220524	0,04740503
A_55_P2106645	NM_001012765	ENSMUST00000114913	224129	*Adcy5*	adenylate cyclase 5	-2,37242566	-1,24636288	0,0004085	0,03376519
A_55_P2095663	NM_008829	ENSMUST00000070463	18667	*Pgr*	progesterone receptor	-2,39687603	-1,26115529	0,0001645	0,03291643
A_55_P2035167	NM_001122758	ENSMUST00000191837	54216	*Pcdh7*	protocadherin 7	-2,4093835	-1,26866405	0,00104065	0,03812918
A_51_P173601	NM_020486	ENSMUST00000135632	57278	*Bcam*	basal cell adhesion molecule	-2,41318965	-1,2709413	0,00048507	0,0346996
A_51_P308298	NM_172118	ENSMUST00000088552	98932	*Myl9*	myosin, light polypeptide 9, regulatory	-2,43758115	-1,28545025	0,00101474	0,03808028
A_55_P2253607	NR_040353	ENSMUST00000148089	338535	*E030013I19Rik*	RIKEN cDNA E030013I19 gene	-2,43801183	-1,28570513	0,0003397	0,03315398
A_51_P302520	NM_010867	ENSMUST00000024847	17929	*Myom1*	myomesin 1	-2,46258137	-1,30017139	0,0004529	0,03423628
A_52_P567200	NM_011147	ENSMUST00000071204	237178	*Ppef1*	protein phosphatase with EF hand calcium-binding domain 1	-2,46833	-1,30353528	0,00055589	0,03476444
A_55_P2044653	NM_009999	ENSMUST00000072438	13088	*Cyp2b10*	cytochrome P450, family 2, subfamily b, polypeptide 10	-2,49695903	-1,32017215	0,00030568	0,03315398
A_55_P2033849	NM_172430	ENSMUST00000160953	77629	*Sphkap*	SPHK1 interactor, AKAP domain containing	-2,52171645	-1,33440606	2,18E-05	0,03291643
A_51_P450527	NM_011526	ENSMUST00000034590	21345	*Tagln*	transgelin	-2,53071852	-1,33954705	6,74E-05	0,03291643
A_55_P2021810	NM_018790	ENSMUST00000023268	11838	*Arc*	activity regulated cytoskeletal-associated protein	-2,5488258	-1,34983278	0,00176076	0,04380084
A_55_P2023727	NM_001001980	ENSMUST00000038188	77569	*Limch1*	LIM and calponin homology domains 1	-2,56153853	-1,35701059	0,00021573	0,03291643

A_51_P307082	NM_013904	ENSMUST00000019924	15214	*Hey2*	hairy/enhancer-of-split related with YRPW motif 2	-2,15044093	-1,10463251	0,0005527	0,03476444
A_51_P466685	NM_175206	ENSMUST00000056890	74165	*Fbxl22*	F-box and leucine-rich repeat protein 22	-2,15105147	-1,10504204	0,00066923	0,03555961
A_55_P2055031	NM_182808	ENSMUST00000122120	320265	*Tafa1*	TAFA chemokine like family member 1	-2,15123121	-1,10516259	0,00055266	0,03476444
A_51_P333518	NM_172966	ENSMUST00000074679	269016	*Sh3rf2*	SH3 domain containing ring finger 2	-2,15341971	-1,10662954	0,00014445	0,03291643
A_52_P172014	NM_016894	ENSMUST00000097648	51801	*Ramp1*	receptor (calcitonin) activity modifying protein 1	-2,16515349	-1,1144693	0,00050983	0,03476444
A_51_P451052	NM_175013	ENSMUST00000047666	226041	*Pgm5*	phosphoglucomutase 5	-2,17460081	-1,12075059	0,00177673	0,04399008
A_55_P1983754	NM_025557	ENSMUST00000111332	66425	*Pcp4l1*	Purkinje cell protein 4-like 1	-2,17517562	-1,12113188	0,00093074	0,03697411
A_51_P425798	NM_029920	ENSMUST00000085554	77521	*Mtus2*	microtubule associated tumor suppressor candidate 2	-2,17552958	-1,12136663	0,00053299	0,03476444
A_51_P283300	NM_023116	ENSMUST00000114723	12296	*Cacnb2*	calcium channel, voltage-dependent, beta 2 subunit	-2,17600534	-1,1216821	0,00032864	0,03315398
A_51_P105927	NM_001033158	ENSMUST00000085453	70784	*Rasl12*	RAS-like, family 12	-2,17995417	-1,1242978	0,00087417	0,03654939
A_52_P380301	NM_009472	ENSMUST00000106236	22253	*Unc5c*	unc-5 netrin receptor C	-2,18534913	-1,12786378	0,00036215	0,03369759
A_55_P2414619	XM_006520017	ENSMUST00000036439	12563	*Cdh6*	cadherin 6	-2,19739528	-1,13579441	0,00071583	0,03592056
A_55_P2107667	NM_010135	ENSMUST00000078719	13800	*Enah*	ENAH actin regulator	-2,20186473	-1,13872584	0,00158097	0,04250601
A_52_P419373	NM_175413	ENSMUST00000029573	109245	*Lrrc39*	leucine rich repeat containing 39	-2,2087404	-1,14322387	0,00040559	0,03373901
A_66_P105032	NM_001145034	ENSMUST00000148314	620695	*Gm13889*	predicted gene 13889	-2,20911989	-1,14347172	0,00205912	0,04655586
A_66_P131851	NM_031169	ENSMUST00000020362	16533	*Kcnmb1*	potassium large conductance calcium-activated channel, subfamily	-2,24544248	-1,16699976	0,00088625	0,03654939
A_55_P2121408	NM_001277875	ENSMUST00000133355	22004	*Tpm2*	tropomyosin 2, beta	-2,2459772	-1,16734328	0,00049247	0,03476444
A_51_P194273	NM_011892	ENSMUST00000121148	24053	*Sgcg*	sarcoglycan, gamma (dystrophin-associated glycoprotein)	-2,24773257	-1,1684704	0,00163244	0,04294518
A_51_P116755	NM_026056	ENSMUST00000021802	67252	*Cap2*	CAP, adenylate cyclase-associated protein, 2 (yeast)	-2,25395493	-1,17245867	0,00033155	0,03315398
A_51_P221510	NM_029784	ENSMUST00000034749	76886	*Fam81a*	family with sequence similarity 81, member A	-2,26079819	-1,17683222	0,00162421	0,04294518
A_51_P240253	NM_019662	ENSMUST00000034351	56437	*Rrad*	Ras-related associated with diabetes	-2,26342557	-1,17850787	2,66E-05	0,03291643
A_55_P2025038	NM_013494	ENSMUST00000048967	12876	*Cpe*	carboxypeptidase E	-2,2881368	-1,19417331	0,00077506	0,03629498
A_51_P161308	NM_013667	ENSMUST00000046959	20518	*Slc22a2*	solute carrier family 22 (organic cation transporter), member 2	-2,28822563	-1,19422932	0,00013057	0,03291643
A_55_P2001920	NM_001290421	ENSMUST00000101454	192176	*Flna*	filamin, alpha	-2,28998249	-1,19533657	0,00040288	0,03373901
A_55_P2221236	AK085976		102242	*AU024180*	expressed sequence AU024180	-2,29745213	-1,2000348	0,00017815	0,03291643
A_55_P1963154	NM_016770	ENSMUST00000001824	53320	*Folh1*	folate hydrolase 1	-2,30257737	-1,20324963	0,00014786	0,03291643
A_55_P2043734	NM_001024624	ENSMUST00000087104	382253	*Cdkl5*	cyclin-dependent kinase-like 5	-2,30485432	-1,20467557	3,50E-05	0,03291643
A_55_P2028837	NM_027533	ENSMUST00000029451	70747	*Tspan2*	tetraspanin 2	-2,31258021	-1,2095034	0,00188411	0,04514203
A_55_P2030578	NM_027884	ENSMUST00000169786	21961	*Tns1*	tensin 1	-2,32206206	-1,21540653	0,00017446	0,03291643
A_51_P301998	NM_018881	ENSMUST00000111510	55990	*Fmo2*	flavin containing monooxygenase 2	-2,32766819	-1,21888542	0,00044591	0,03404162
A_55_P1974421	NM_013565	ENSMUST00000001548	16400	*Itga3*	integrin alpha 3	-2,3315527	-1,22129104	0,00028078	0,03315398
A_51_P101460	NM_023842	ENSMUST00000124830	109620	*Dsp*	desmoplakin	-2,33257258	-1,22192197	0,00172072	0,04371333
A_55_P1961736	NM_001286653	ENSMUST00000044895	53901	*Rcan2*	regulator of calcineurin 2	-2,33449722	-1,22311187	0,00067462	0,03555961
A_52_P440709	NM_023868	ENSMUST00000021750	20191	*Ryr2*	ryanodine receptor 2, cardiac	-2,33839977	-1,22552159	0,000229	0,03291643
A_55_P1967677	NM_001081351	ENSMUST00000115383	214642	*Cped1*	cadherin-like and PC-esterase domain containing 1	-2,35088074	-1,23320135	0,00036439	0,03369759
A_55_P2262593	AK142388		74633	*4930429F24Rik*	RIKEN cDNA 4930429F24 gene	-2,35165816	-1,23367837	0,00015072	0,03291643
A_55_P2116744	NM_011724	ENSMUST00000111635	22437	*Xirp1*	xin actin-binding repeat containing 1	-2,35759241	-1,23731432	0,00020201	0,03291643
A_55_P2217831	AK013682		73049	*2900054C01Rik*	RIKEN cDNA 2900054C01 gene	-2,35947991	-1,23846889	0,0005752	0,03507191
A_51_P358722	NM_173414	ENSMUST00000069763	236285	*Lancl3*	LanC lantibiotic synthetase component C-like 3 (bacterial)	-2,35981814	-1,23867568	0,00187806	0,04514203
A_65_P11603	NM_011918	ENSMUST00000022327	24131	*Ldb3*	LIM domain binding 3	-2,36262463	-1,24039044	0,00059669	0,03507191
A_51_P459350	NM_019771	ENSMUST00000103172	56431	*Dstn*	destrin	-2,36265793	-1,24041077	0,00067627	0,03555961
A_52_P409769	NM_194464	ENSMUST00000125758	17540	*Mrvi1*	MRV integration site 1	-2,36859685	-1,24403267	0,00220524	0,04740503
A_55_P2106645	NM_001012765	ENSMUST00000114913	224129	*Adcy5*	adenylate cyclase 5	-2,37242566	-1,24636288	0,0004085	0,03376519
A_55_P2095663	NM_008829	ENSMUST00000070463	18667	*Pgr*	progesterone receptor	-2,39687603	-1,26115529	0,0001645	0,03291643
A_55_P2035167	NM_001122758	ENSMUST00000191837	54216	*Pcdh7*	protocadherin 7	-2,4093835	-1,26866405	0,00104065	0,03812918
A_51_P173601	NM_020486	ENSMUST00000135632	57278	*Bcam*	basal cell adhesion molecule	-2,41318965	-1,2709413	0,00048507	0,0346996
A_51_P308298	NM_172118	ENSMUST00000088552	98932	*Myl9*	myosin, light polypeptide 9, regulatory	-2,43758115	-1,28545025	0,00101474	0,03808028
A_55_P2253607	NR_040353	ENSMUST00000148089	338535	*E030013I19Rik*	RIKEN cDNA E030013I19 gene	-2,43801183	-1,28570513	0,0003397	0,03315398
A_51_P302520	NM_010867	ENSMUST00000024847	17929	*Myom1*	myomesin 1	-2,46258137	-1,30017139	0,0004529	0,03423628
A_52_P567200	NM_011147	ENSMUST00000071204	237178	*Ppef1*	protein phosphatase with EF hand calcium-binding domain 1	-2,46833	-1,30353528	0,00055589	0,03476444
A_55_P2044653	NM_009999	ENSMUST00000072438	13088	*Cyp2b10*	cytochrome P450, family 2, subfamily b, polypeptide 10	-2,49695903	-1,32017215	0,00030568	0,03315398
A_55_P2033849	NM_172430	ENSMUST00000160953	77629	*Sphkap*	SPHK1 interactor, AKAP domain containing	-2,52171645	-1,33440606	2,18E-05	0,03291643
A_51_P450527	NM_011526	ENSMUST00000034590	21345	*Tagln*	transgelin	-2,53071852	-1,33954705	6,74E-05	0,03291643
A_55_P2021810	NM_018790	ENSMUST00000023268	11838	*Arc*	activity regulated cytoskeletal-associated protein	-2,5488258	-1,34983278	0,00176076	0,04380084
A_55_P2023727	NM_001001980	ENSMUST00000038188	77569	*Limch1*	LIM and calponin homology domains 1	-2,56153853	-1,35701059	0,00021573	0,03291643

A_52_P420504	NM_007392	ENSMUST00000039631	11475	*Acta2*	actin, alpha 2, smooth muscle, aorta	-2,56407937	-1,35844092	6,14E-05	0,03291643
A_55_P2021540	NM_145136	ENSMUST00000101042	214384	*Myocd*	myocardin	-2,57092103	-1,3622853	0,0005661	0,03481832
A_55_P2290443	ENSMUST000001834	ENSMUST00000183482	15551	*Htr1b*	5-hydroxytryptamine (serotonin) receptor 1B	-2,58969527	-1,37278235	0,00053349	0,03476444
A_55_P2119287	NM_001159507	ENSMUST00000162293	243547	*Grip2*	glutamate receptor interacting protein 2	-2,60836739	-1,38314709	0,00023023	0,03291643
A_66_P123824	ENSMUST000000609	ENSMUST00000060989	20660	*Sorl1*	sortilin-related receptor, LDLR class A repeats-containing	-2,61619087	-1,3874678	0,00094442	0,03704536
A_55_P1952915	NM_015825	ENSMUST00000048770	50795	*Sh3bgr*	SH3-binding domain glutamic acid-rich protein	-2,62786212	-1,39388958	0,00094265	0,03703145
A_66_P122219	NM_001039347	ENSMUST00000098761	56543	*Kcnd3*	potassium voltage-gated channel, Shal-related family, member 3	-2,63043301	-1,39530031	0,00218001	0,04740503
A_51_P115715	NM_023049	ENSMUST00000127447	65256	*Asb2*	ankyrin repeat and SOCS box-containing 2	-2,64983751	-1,4059039	0,00076988	0,03619952
A_51_P350817	NM_009922	ENSMUST00000001384	12797	*Cnn1*	calponin 1	-2,66152804	-1,41225476	0,00054057	0,03476444
A_55_P2021565	NM_001164034	ENSMUST00000112244	18205	*Ntf3*	neurotrophin 3	-2,66721402	-1,41533359	0,00041319	0,03386016
A_55_P2130129	NM_010597	ENSMUST00000049230	16497	*Kcnab1*	potassium voltage-gated channel, shaker-related subfamily, beta n	-2,68642341	-1,4256867	0,00063943	0,03546117
A_51_P289889	NM_033525	ENSMUST00000042729	114249	*Npnt*	nephronectin	-2,68820158	-1,42664133	0,00119203	0,03904427
A_52_P579531	NM_016798	ENSMUST00000034053	53318	*Pdlim3*	PDZ and LIM domain 3	-2,70671513	-1,43654306	0,00037738	0,03373901
A_55_P2167922	NM_007868	ENSMUST00000141778	13405	*Dmd*	dystrophin, muscular dystrophy	-2,72831047	-1,44800783	0,00237553	0,04844509
A_66_P123617	NM_053106	ENSMUST00000059352	93689	*Lmod1*	leiomodin 1 (smooth muscle)	-2,73019552	-1,44900427	0,00089227	0,03656038
A_51_P269404	NM_008030	ENSMUST00000028010	14262	*Fmo3*	flavin containing monooxygenase 3	-2,80502545	-1,48801386	0,00030904	0,03315398
A_51_P433000	AK008733	ENSMUST00000029049	66371	*Chmp4c*	charged multivesicular body protein 4C	-2,83398522	-1,50283223	0,0003777	0,03373901
A_52_P6828	NM_023500	ENSMUST00000015486	22439	*Xk*	X-linked Kx blood group	-2,83413436	-1,50290816	0,00103195	0,03812918
A_55_P2133706	NM_001101510	ENSMUST00000135338	382111	*Susd5*	sushi domain containing 5	-2,87665717	-1,52439329	0,00082702	0,03629498
A_51_P449233	NM_172444	ENSMUST00000034829	207596	*Thsd4*	thrombospondin, type I, domain containing 4	-2,88547419	-1,52880843	0,00049557	0,03476444
A_55_P2167530	ENSMUST000000435	ENSMUST00000043503	268935	*Scube3*	signal peptide, CUB domain, EGF-like 3	-2,89692049	-1,53452009	0,00135222	0,04041885
A_55_P2117119	NM_028889	ENSMUST00000118687	98363	*Efhd1*	EF hand domain containing 1	-2,90243963	-1,53726606	0,00051847	0,03476444
A_51_P317941	NM_022032	ENSMUST00000019998	64058	*Perp*	PERP, TP53 apoptosis effector	-2,97279791	-1,57182139	0,00052064	0,03476444
A_55_P1988531	NM_001161775	ENSMUST00000090287	17880	*Myh11*	myosin, heavy polypeptide 11, smooth muscle	-2,9830869	-1,576806	0,00090689	0,03681551
A_51_P277431	NM_028804	ENSMUST00000027988	74186	*Ccdc3*	coiled-coil domain containing 3	-2,9975271	-1,5837728	0,00094101	0,03703145
A_55_P2095133	NM_080451	ENSMUST00000106427	118449	*Synpo2*	synaptopodin 2	-3,09790394	-1,63129241	0,0008161	0,03629498
A_55_P2103452	NM_010934	ENSMUST00000039303	18166	*Npy1r*	neuropeptide Y receptor Y1	-3,15820205	-1,65910347	6,08E-05	0,03291643
A_51_P162162	NM_009349	ENSMUST00000003569	21743	*Inmt*	indolethylamine N-methyltransferase	-3,19864074	-1,67745896	0,00123806	0,0393138
A_51_P309920	NM_001001309	ENSMUST00000028106	241226	*Itga8*	integrin alpha 8	-3,23643909	-1,69440735	0,00118369	0,03904427
A_52_P229972	NM_009202	ENSMUST00000024596	20517	*Slc22a1*	solute carrier family 22 (organic cation transporter), member 1	-3,35872631	-1,74791424	0,00028289	0,03315398

Table S4. GSEA analysis: enriched gene sets for DEGs

GO_BP significantly enriched gene sets in AngII-infused Tg-NOR-1^{VSMC} mice	
Gene set	**FDR q-value**
GO_CELL_CYCLE_PROCESS	<1E-4
GO_CELLULAR_RESPONSE_TO_DNA_DAMAGE_STIMULUS	<1E-4
GO_MITOTIC_NUCLEAR_DIVISION	<1E-4
GO_MITOTIC_CELL_CYCLE	<1E-4
GO_SYNAPTIC_SIGNALING	<1E-4
GO_VESICLE_MEDIATED_TRANSPORT_IN_SYNAPSE	<1E-4
GO_CHROMOSOME_SEGREGATION	1.301E-4
GO_CELL_CYCLE	2.456E-4
GO_NUCLEAR_CHROMOSOME_SEGREGATION	2.661E-4
GO_NEUROTRANSMITTER_TRANSPORT	2.902E-4
GO_MITOTIC_NUCLEAR_DIVISION	3.193E-4
GO_SISTER_CHROMATID_SEGREGATION	3.548E-4
GO_REGULATION_OF_CHROMOSOME_SEGREGATION	3.740E-4
GO_REGULATION_OF_NEUROTRANSMITTER_LEVELS	6.234E-4
GO_REGULATION_OF_IMMUNE_RESPONSE	6.723E-4
GO_NEUROTRANSMITTER_SECRETION	6.941E-4
GO_DNA_METABOLIC_PROCESS	7.143E-4
GO_REGULATION_OF_NUCLEAR_DIVISION	7.797E-4
GO_CELL_DIVISION	8.208E-4
GO_DNA_REPAIR	0.0011
GO_EXOCYTIC_PROCESS	0.0011
GO_AMINE_TRANSPORT	0.0011
GO_REGULATION_OF_MITOTIC_CELL_CYCLE	0.0013
GO_REGULATION_OF_CELL_CYCLE_PROCESS	0.0014
GO_REGULATION_OF_SECRETION	0.0014
GO_MONOAMINE_TRANSPORT	0.0015
GO_MULTICELLULAR_ORGANISMAL_RESPONSE_TO_STRESS	0.0023
GO_SYNAPTIC_VESICLE_EXOCYTOSIS	0.0036
GO_REGULATION_OF_IMMUNE_SYSTEM_PROCESS	0.0037
GO_REGULATION_OF_CELL_CYCLE_PHASE_TRANSITION	0.0040
GO_FEMALE_GAMETE_GENERATION	0.0040
GO_SYNAPSE_ORGANIZATION	0.0048
GO_CELL_CYCLE_CHECKPOINT	0.0048
GO_ATTACHMENT_OF_SPINDLE_MICROTUBULES_TO_KINETOCHORE	0.0048
GO_ORGANELLE_LOCALIZATION	0.0048
GO_POSITIVE_REGULATION_OF_CELL_CYCLE	0.0048
GO_MYELOID_LEUKOCYTE_MIGRATION	0.0049

GO_MEIOTIC_CELL_CYCLE_PROCESS	0.0053
GO_CELL_CELL_SIGNALING	0.0056
GO_DNA_PACKAGING	0.0061
GO_METAPHASE_ANAPHASE_TRANSITION_OF_CELL_CYCLE	0.0062
GO_NEUROTRANSMITTER_REUPTAKE	0.0063
GO_POSITIVE_REGULATION_OF_CELL_ACTIVATION	0.0063
GO_REGULATION_OF_CELL_CYCLE	0.0063
GO_SECRETION	0.0063
GO_ANTIGEN_PROCESSING_AND_PRESENTATION	0.0064
GO_MEIOTIC_CELL_CYCLE	0.0064
GO_CELL_CYCLE_PHASE_TRANSITION	0.0064
GO_ANTIGEN_PROCESSING_AND_PRESENTATION_OF_PEPTIDE_ ANTIGEN	0.0066
GO_POSITIVE_REGULATION_OF_CELL_CYCLE_PROCESS	0.0074
GO_POSITIVE_REGULATION_OF_IMMUNE_SYSTEM_PROCESS	0.0074
GO_SIGNAL_RELEASE	0.0074
GO_REGULATION_OF_SISTER_CHROMATID_SEGREGATION	0.0075
GO_SPINDLE_ORGANIZATION	0.0076
GO_CHROMOSOME_SEPARATION	0.0077
GO_CHROMOSOME_ORGANIZATION	0.0084
GO_ANTIGEN_PROCESSING_AND_PRESENTATION_OF_PEPTIDE_OR_PO LYSACCHARIDE_ANTIGEN_VIA_MHC_CLASS_II	0.0091
GO_DNA_CONFORMATION_CHANGE	0.0108
GO_DOPAMINE_TRANSPORT	0.011
GO_ADAPTIVE_IMMUNE_RESPONSE	0.010
GO_REGULATION_OF_CELL_ACTIVATION	0.0102
GO_GRANULOCYTE_MIGRATION	0.0106
GO_MITOTIC_CELL_CYCLE_CHECKPOINT	0.0109
GO_CELL_ACTIVATION	0.011
GO_NEGATIVE_REGULATION_OF_CELL_CYCLE_PROCESS	0.0114
GO_PEPTIDE_SECRETION	0.0114
GO_VESICLE_DOCKING	0.0121
GO_REGULATION_OF_REGULATED_SECRETORY_PATHWAY	0.0129
GO_DNA_REPLICATION	0.014
GO_BP significantly downregulated gene sets in AngII-infused Tg-NOR-1^{VSMC} mice	
Gene set	**FDR q-value**
GO_MUSCLE_CELL_DIFFERENTIATION	<1E-5
GO_MUSCLE_CONTRACTION	<1E-5
GO_MUSCLE_STRUCTURE_DEVELOPMENT	<1E-5
GO_MUSCLE_SYSTEM_PROCESS	<1E-5

GO_REGULATION_OF_MUSCLE_SYSTEM_PROCESS	<1E-5
GO_CIRCULATORY_SYSTEM_PROCESS	<1E-5
GO_ACTIN_FILAMENT_BASED_MOVEMENT	<1E-5
GO_ACTIN_FILAMENT_BASED_PROCESS	<1E-5
GO_ACTIN_MEDIATED_CELL_CONTRACTION	<1E-5
GO_STRIATED_MUSCLE_CONTRACTION	<1E-5
GO_HEART_PROCESS	<1E-5
GO_ORGANELLE_FISSION	<1E-5
GO_MUSCLE_TISSUE_DEVELOPMENT	7,219E-5
GO_CARDIAC_MUSCLE_CONTRACTION	7.821E-5
GO_CARDIAC_MUSCLE_CELL_CONTRACTION	2,392E-4
GO_THIOESTER_BIOSYNTHETIC_PROCESS	2.831E-4
GO_CELLULAR_AMIDE_METABOLIC_PROCESS	5.508E-4
GO_REGULATION_OF_BLOOD_CIRCULATION	5.784E-4
GO_MYOFIBRIL_ASSEMBLY	6.088E-4
GO_REGULATION_OF_ACTIN_FILAMENT_BASED_MOVEMENT	6.553E-4
GO_REGULATION_OF_MUSCLE_CONTRACTION	6.704E-4
GO_ACTION_POTENTIAL	5.901E-4
GO_REGULATION_OF_CARDIAC_MUSCLE_CELL_ACTION_POTENTIAL	0.0010
GO_REGULATION_OF_ACTION_POTENTIAL	0.0010
GO_REGULATION_OF_SYSTEM_PROCESS	0.0010
GO_CARDIAC_CONDUCTION	0.0011
GO_REGULATION_OF_HEART_RATE	0.0012
GO_MUSCLE_ORGAN_DEVELOPMENT	0.0012
GO_ACTIN_FILAMENT_ORGANIZATION	0.0012
GO_STRIATED_MUSCLE_CELL_DIFFERENTIATION	0.0012
GO_HEART_DEVELOPMENT	0.0012
GO_ACETYL_COA_METABOLIC_PROCESS	0.0012
GO_COENZYME_METABOLIC_PROCESS	0.0012
GO_FATTY_ACID_METABOLIC_PROCESS	0.0015
GO_LIPID_METABOLIC_PROCESS	0.0016
GO_MUSCLE_CELL_DEVELOPMENT	0.0018
GO_CARDIAC_MUSCLE_CELL_ACTION_POTENTIAL_INVOLVED_IN_CONT	0.0030
GO_REGULATION_OF_STRIATED_MUSCLE_CONTRACTION	0.0032
GO_COFACTOR_METABOLIC_PROCESS	0.0033
GO_COENZYME_BIOSYNTHETIC_PROCESS	0.0033
GO_THIOESTER_METABOLIC_PROCESS	0.0033
GO_MUSCLE_FILAMENT_SLIDING	0.0041
GO_REGULATION_OF_CARDIAC_MUSCLE_CONTRACTION	0.0045
GO_REGULATION_OF_SODIUM_ION_TRANSMEMBRANE_TRANSPORT	0.0045
GO_AMIDE_BIOSYNTHETIC_PROCESS	0.0046

GO_MULTICELLULAR_ORGANISMAL_MOVEMENT	0.0056
GO_REGULATION_OF_SODIUM_ION_TRANSPORT	0.0056
GO_REGULATION_OF_CARDIAC_CONDUCTION	0.0059
GO_ORGANIC_ACID_BIOSYNTHETIC_PROCESS	0.0075
GO_REGULATION_OF_MYOTUBE_DIFFERENTIATION	0.0086
GO_CARDIAC_MUSCLE_TISSUE_DEVELOPMENT	0.0087
GO_STEROL_BIOSYNTHETIC_PROCESS	0.0093
GO_REGULATION_OF_ACTIN_FILAMENT_BASED_PROCESS	0.0094
GO_ALCOHOL_METABOLIC_PROCESS	0.0097
GO_FATTY_ACID_BIOSYNTHETIC_PROCESS	0.0101
GO_COFACTOR_BIOSYNTHETIC_PROCESS	0.0105
GO_NUCLEOSIDE_BISPHOSPHATE_BIOSYNTHETIC_PROCESS	0.0105
GO_OXIDATION_REDUCTION_PROCESS	0.0109
GO_SULFUR_COMPOUND_BIOSYNTHETIC_PROCESS	0.0109
GO_REGULATION_OF_METAL_ION_TRANSPORT	0.0111
GO_REGULATION_OF_SODIUM_ION_TRANSMEMBRANE_TRANSPORTER	0.0112
GO_CIRCULATORY_SYSTEM_DEVELOPMENT	0.0112
GO_MULTICELLULAR_ORGANISMAL_SIGNALING	0.0113
GO_REGULATION_OF_TRANSMEMBRANE_RECEPTOR_PROTEIN_SERINE_THREONINE_KINASE_SIGNALING_PATHWAY	0.0110
GO_MONOCARBOXYLIC_ACID_METABOLIC_PROCESS	0.0114
GO_SMOOTH_MUSCLE_CELL_DIFFERENTIATION	0.0140
GO_STEROID_BIOSYNTHETIC_PROCESS	0.0144
GO_REGULATION_OF_LIPID_METABOLIC_PROCESS	0.0144
GO_HEART_PROCESS	0.0152
GO_CC significantly enriched gene sets in AngII-infused Tg-NOR-1^{VSMC} mice	
Gene set	**FDR q-value**
GO_SYNAPSE	<1E-4
GO_PRESYNAPSE	<1E-4
GO_TRANSPORT_VESICLE	<1E-4
GO_AXON	<1E-4
GO_SPINDLE	<1E-4
GO_EXOCYTIC_VESICLE	1.317E-4
GO_CONDENSED_CHROMOSOME	1.505E-4
GO_CHROMOSOMAL_REGION	1.756E-4
GO_CHROMOSOME_CENTROMERIC_REGION	2.426E-4
GO_SYNAPTIC_VESICLE_MEMBRANE	4.062E-4
GO_SCHAFFER_COLLATERAL_CA1_SYNAPSE	4.468E-4
GO_CONDENSED_CHROMOSOME_CENTROMERIC_REGION	5.600E-4
GO_KINETOCHORE	6.992E-4

GO_CHROMOSOMAL_REGION	8.101E-4
GO_SPINDLE_POLE	9.172E-4
GO_DENSE_CORE_GRANULE	0.0013
GO_NEURON_PROJECTION	0.0017
GO_GLUTAMATERGIC_SYNAPSE	0.0019
GO_COLLAGEN_TRIMER	0.0021
GO_CELL_BODY	0.0029
GO_MITOTIC_SPINDLE	0.0031
GO_VESICLE_MEMBRANE	0.0048
GO_CONDENSED_NUCLEAR_CHROMOSOME	0.0049
GO_SPINDLE_MICROTUBULE	0.0049
GO_SECRETORY_VESICLE	0.0055
GO_FIBRILLAR_COLLAGEN_TRIMER	0.0074
GO_NEURON_TO_NEURON_SYNAPSE	0.0076
GO_INTRINSIC_COMPONENT_OF_SYNAPTIC_VESICLE_MEMBRANE	0.0077
GO_NUCLEAR_CHROMOSOME	0.0111
GO_MICROTUBULE	0.0111
GO_TRANSPORT_VESICLE_MEMBRANE	0.0020
GO_TRANSFERASE_COMPLEX_TRANSFERRING_PHOSPHORUS_ CONTAINING_GROUPS	0.0295
GO_COMPLEX_OF_COLLAGEN_TRIMERS	0.0119
GO_DISTAL_AXON	0.0121
GO_NUCLEAR_CHROMOSOME	0.0122
GO_TERMINAL_BOUTON	0.0170
GO_PROTEIN_KINASE_COMPLEX	0.0199
GO_SOMATODENDRITIC_COMPARTMENT	0.0214
GO_GABA_ERGIC_SYNAPSE	0.0218
GO_INTRINSIC_COMPONENT_OF_PLASMA_MEMBRANE	0.0263
GO_PRESYNAPTIC_MEMBRANE	0.0288
GO_CONDENSED_NUCLEAR_CHROMOSOME_CENTROMERIC_REGION	0.0305
GO_KINESIN_COMPLEX	0.0380
GO_SERINE_THREONINE_PROTEIN_KINASE_COMPLEX	0.0308
GO_HIPPOCAMPAL_MOSSY_FIBER_TO_CA3_SYNAPSE	0.0413
GO_CELL_CORTEX_REGION	0.0422
GO_MICROTUBULE_ASSOCIATED_COMPLEX	0.0427
GO_PRESYNAPTIC_ACTIVE_ZONE	0.0462
GO_SYNAPTIC_MEMBRANE	0.0470
GO_CC significantly downregulated gene sets in AngII-infused Tg-NOR-1^{VSMC} mice	
Gene set	**FDR q-value**
GO_ACTIN_CYTOSKELETON	<1E-4

GO_CONTRACTILE_FIBER	<1E-4
GO_ANCHORING_JUNCTION	<1E-4
GO_CELL_SUBSTRATE_JUNCTION	<1E-4
GO_SARCOLEMMA	<1E-4
GO_I_BAND	<1E-4
GO_ACTOMYOSIN	1.319E-4
GO_SARCOLEMMA	2.195E-4
GO_ACTIN_FILAMENT_BUNDLE	1.951E-4
GO_GLYCOPROTEIN_COMPLEX	0.0044
GO_FILAMENTOUS_ACTIN	0.0059
GO_ACTIN_FILAMENT	0.0089
GO_SARCOPLASMIC_RETICULUM_MEMBRANE	0.0094
GO_CELL_CELL_JUNCTION	0.0094
GO_T_TUBULE	0.0096
GO_SUPRAMOLECULAR_POLYMER	0.0176
GO_INTERCALATED_DISC	0.0211
GO_MYOSIN_COMPLEX	0.0446
GO_CELL_CELL_CONTACT_ZONE	0.0465
GO_SUPRAMOLECULAR_COMPLEX	0.0480
Reactome significantly enriched gene sets in AngII-infused Tg-NOR-1^{VSMC} mice	
Gene set	**FDR q-value**
REACTOME_IMMUNOREGULATORY_INTERACTIONS_BETWEEN_A_LYMPHOID_AND_A_NON_LYMPHOID_CELL	<1E-4
REACTOME_CELL_CYCLE	<1E-4
REACTOME_MITOTIC_METAPHASE_AND_ANAPHASE	<1E-4
REACTOME_MITOTIC_PROMETAPHASE	<1E-4
REACTOME_CELL_CYCLE_CHECKPOINTS	<1E-4
REACTOME_MITOTIC_SPINDLE_CHECKPOINT	<1E-4
REACTOME_CELL_CYCLE_MITOTIC	<1E-4
REACTOME_M_PHASE	<1E-4
REACTOME_SEPARATION_OF_SISTER_CHROMATIDS	<1E-4
REACTOME_RESOLUTION_OF_SISTER_CHROMATID_COHESION	<1E-4
REACTOME_COPI_DEPENDENT_GOLGI_TO_ER_RETROGRADE_TRAFFIC	0.0011
REACTOME_RHO_GTPASES_ACTIVATE_FORMINS	0.0011
REACTOME_KINESINS	0.0012
REACTOME_GOLGI_TO_ER_RETROGRADE_TRANSPORT	0.0012
REACTOME_COLLAGEN_DEGRADATION	0.0013
REACTOME_NEURONAL_SYSTEM	0.0038
REACTOME_INTRA_GOLGI_AND_RETROGRADE_GOLGI_TO_ER_TRAFFIC	0.0040
REACTOME_COLLAGEN_CHAIN_TRIMERIZATION	0.0046

REACTOME_THE_ROLE_OF_GTSE1_IN_G2_M_PROGRESSION_AFTER_G2_CHECKPOINT	0.0058
REACTOME_TRANSMISSION_ACROSS_CHEMICAL_SYNAPSES	0.0059
REACTOME_MHC_CLASS_II_ANTIGEN_PRESENTATION	0.0135
REACTOME_NEUROTRANSMITTER_RECEPTORS_AND_POSTSYNAPTIC_SIGNAL_TRANSMISSION	0.0217
REACTOME_GPCR_LIGAND_BINDING	0.0248
REACTOME_DNA_REPAIR	0.0273
REACTOME_ADAPTIVE_IMMUNE_SYSTEM	0.0442
REACTOME_SEROTONIN_NEUROTRANSMITTER_RELEASE_CYCLE	0.0452
REACTOME_DOPAMINE_NEUROTRANSMITTER_RELEASE_CYCLE	0.0477
REACTOME_CLASS_A_1_RHODOPSIN_LIKE_RECEPTORS	0.0494
Reactome significantly downregulated gene sets in AngII-infused Tg-NOR-1^{VSMC} mice	
Gene set	**FDR q-value**
REACTOME_MUSCLE_CONTRACTION	<1E-4
REACTOME_SMOOTH_MUSCLE_CONTRACTION	<1E-4
REACTOME_METABOLISM_OF_LIPIDS	0.0015
REACTOME_BIOLOGICAL_OXIDATIONS	0.0016
REACTOME_CARDIAC_CONDUCTION	0.0059
REACTOME_RHO_GTPASES_ACTIVATE_CIT	0.0119
REACTOME_FATTY_ACID_METABOLISM	0.0125
REACTOME_PHASE_I_FUNCTIONALIZATION_OF_COMPOUNDS	0.0135
REACTOME_EPHA_MEDIATED_GROWTH_CONE_COLLAPSE	0.0140
REACTOME_RHO_GTPASES_ACTIVATE_PAKS	0.0143
REACTOME_REGULATION_OF_CHOLESTEROL_BIOSYNTHESIS_BY_SREBP_SREBF	0.0313
REACTOME_ION_HOMEOSTASIS	0.0328
REACTOME_HSF1_DEPENDENT_TRANSACTIVATION	0.0335
REACTOME_FATTY_ACYL_COA_BIOSYNTHESIS	0.0336
REACTOME_RHO_GTPASES_ACTIVATE_ROCKS	0.0340
REACTOME_ACTIVATION_OF_GENE_EXPRESSION_BY_SREBF_SREBP	0.0352
REACTOME_CELLULAR_RESPONSE_TO_HEAT_STRESS	0.0355
REACTOME_SEMA4D_INDUCED_CELL_MIGRATION_AND_GROWTH_CON	0.0355
REACTOME_INOSITOL_PHOSPHATE_METABOLISM	0.0367
REACTOME_SEMA4D_IN_SEMAPHORIN_SIGNALING	0.0380
REACTOME_CELL_EXTRACELLULAR_MATRIX_INTERACTIONS	0.0402

Table S5. Enriched Gene set members for selected pathways and cellular components

Upregulated DEGs		
Pathway term	**Genes**	**FDR q-value**
GO_MITOTIC_CELL_CYCLE	*Tubb3, Phox2b, Ppp2r2c, Ppp2r2b, Plagl1, Cdkn2a, Birc5, Tubb2b, Plk2, Sapcd2, Mki67, Cenpe, Stmn1,* ***Ccnb1****, Spag5, Ccna2, Rrm2, Fap, E2f8, Cdca5, Cdk1, Spc25, Kif22,* ***Kif20a****, Trip13, Plk1, Ska1, Aurka, Top2a, Ncaph, Cdca8, Ccnb2, Bub1, Ube2c, Prkcb, Kif11, Kif20b,* ***Cdc20****, Knstrn, Melk, Sox4, Cdkn3, Racgap1, Aif1, Nuf2, SgoL1, Kntc1, Kif4a, Igf1, Ckap2, Bub1b, Cdk14, Ccnf, Kifc1, Ect2, Pole, Nsl1, Rad51, Ndc80, Tpx2, Cdt1, Ccne1, Kif23, Nusap1, Ticrr, Kif15, Dlgap5, Iqgap3, Tacc3, Dscc1, Mybl2, Pbk, Bcat1, Nek2, Kif2c, Espl1, Haus4, Ezh2, Mcm5, Incenp, Cenpa, Odf2, Dsn1, Nek6, Dbf4, Lgmn, Mcm3, Ncapd2, Mcm2, Ska3, E2f1, Mad2l1, Gins1, Egfr, Brca2, Cks2, Bid, Mrnip, Ccnjl, Zwilch, Clspn, Rad51b, Cenpk, Tube1, Mastl, Zwint, Foxm1, Plk3, Rbbp8, Rrm1, Gadd45a*	<1E-4
GO_CELLULAR_RESPONSE_TO_ DNA_ DAMAGE_STIMULUS	*Plagl1, Plk2, Pmaip1,* ***Ccnb1****, E2f8,* ***Uhrf1****, Cdca5, Cdk1, Kif22, Exo1, Trip13, Plk1, Pclaf, Aurka, Top2a, Chaf1b, Fanca, Sox4, Aunip, Fignl1, Fen1, Pole, Rad51, Fanci, Ticrr, Neil3, Pycard, Mapt, Rad51ap1, Pak1, Bok, Mcm5, Gins2, Chaf1a, Mcm3, Mcm2, E2f1, Egfr, Snai2, Brca2, Bid, Mrnip, Rad54b, Clspn, Ankle1, Rad51b, Brip1, Mastl, Foxm1, Plk3, Rbbp8, Gadd45a, Spred3, Hmgb2, Esco2, Mpg, Chek2, Zdhhc16, Polr2i, Pms1, Usp51, Casp3, Stn1, Smyd2, Rfc3, Phf1*	<1E-4
GO_SYNAPTIC_SIGNALING	*Syt1, Slc6a2, Rit2, Ntrk1,* ***Npy****, Rab3b, Cplx1, Dbh, Th, Kcnmb4,* ***Syt4****, Cadps, Amph, Slc18a2, Asic2, Kif5a, Hcrtr1, Syt5, Syn2, Omp, Erc2, Rims3, Kcnq2, Ptn, Mapk8ip2, Syngr1, Celf4, Lrrc4c, Ache, Slc5a7, Nrxn1, Snph, Chrnb4, Tubb2b, Slc1a6, Cdh11, Plk2, Prkar1b, Kcnj10, Nrg1, Grm7, Ror2, Ppfia3, Gpr176, Glrb, Ly6h, Cspg5, Chrna3, P2rx2, Cdh2, Syt9, Penk, Clstn2, Prkcb,* ***Cdc20****, Syn1, Apba2*	<1E-4
GO_COLLAGEN_TRIMER	***Col10a1****, Col11a1,* ***Cthrc1****, Col9a1, Col12a1, Col8a1, Col8a2, Col5a3, Col1a1, Col16a1, C1ql3, Col3a1, Col5a2, Col5a1, Col1a2*	0.00206
GO_REGULATION_OF_IMMUNE_ SYSTEM_PROCESS	*Gnas,* ***Cd5l****, Ptn,* ***Adam8, Cd300c2,*** *Trem2,* ***Mmp12****, Col1a1, Pilra, Ror2, Lilrb4, Cyfip2, Susd4, Camk4, Clec7a, Thbs1, Tox, Mzb1, Lat2, Cd84, Ripk3, Gal, Ebi3, Runx1,* ***Sh2d1b1****, Fanca, Prkcb, Cd200r1, Hcst, Spn, Slit2, Col3a1, Mdk, C5ar1, Aif1, Ahr, Igf1, Raet1e, Plscr1, Cd276, Ubash3b, Gper1, Adora2b, Fcgr2b, Nckap1l, Col1a2, Slc11a1, Ccl3, Plcl2, Cd300ld, Prkcz, Pycard, Cmtm3, Slc7a11, Il18,Cadm1, Pak1, Sox9, Hes5, Pf4, Sox11, H2-Ob, Tspan6 Lgmn, Hist1h3g*	0.00375
GO_MYELOID_LEUKOCYTE_ MIGRATION	***Scg2****, Chga,* ***Adam8****, Trem2, Mcoln2, Ror2, Thbs1, Cd200r1, Slit2, Mdk, C5ar1, Aif1, Nckap1l, Ccl3, Ccl17, Pf4, Lgmn, Ptger4, Cxcl2, Cx3cl1*	0.00494
GO_ANTIGEN_PROCESSING_AND _ PRESENTATION	*Rab3c,* ***Dync1i1****, Rab3b, Kif5a, Trem2, Cenpe, Thbs1, Kif22, Kif11, Racgap1, Kif4a, Fcgr2b, Kif23, Kif15, Slc11a1, Pycard, Kif2c, H2-Ob, Lgmn*	0.00642
Downregulated DEGs		
Pathway term	**Genes**	**FDR-value**

GO_MUSCLE_STRUCTURE_ DEVELOPMENT	***Itga8***, ***Myh11***, *Xk, Lmod1, Dmd, Pdlim3, Npnt, Kcnab1, Asb2, Myocd, Tagln, Myom1, Ldb3, Ryr2, Dsp, Sgcg, Pgm5, Hey2, Myh14, Mylk, Csrp1, Mylk2, Dmpk, Sorbs2, Fbxo40, Sgca, Rbm24, Tpm1, Hdac9, Rbpms2, Nox4, Myl6, Cav3, Sgcd, Smarcd3, Speg, Atp2a2, Prdm6, Fzd7, Ccn3, Myo18b, Nkd1, Smtn, Igfbp5, Unc45a, Foxc1, Bnip2, Srf, Cfl2, Syne1, Pdlim7, Mbnl1, Bmp2, Ilk, Pdlim1, Epas1, Cryab, Rgs4, Creb1*	<1E-4
GO_ACTIN_CYTOSKELETON	*Synpo2,* ***Myh11****, Lmod1, Pdlim3,* ***Acta2****, Limch1, Arc, Myom1, Myl9, Dstn, Ldb3, Xirp1, Flna, Cap2, Tpm2, Pgm5, Myh14, Pawr, Abra, Mylk, Sorbs2, Nexn, Tpm1, Nox4, Filip1, Myl6, Cdc42ep3, Myo18b, Actn1, Smtn, Acaca, Pls3, Gsn, Ddr2, Actn4, Cfl2, Clic4, Dctn6, Pdlim7, Auts2, Hip1, Ilk, Pdlim1, Cryab, Myo1c, Vasp, Mical3, Msrb1, Jup*	<1E-4

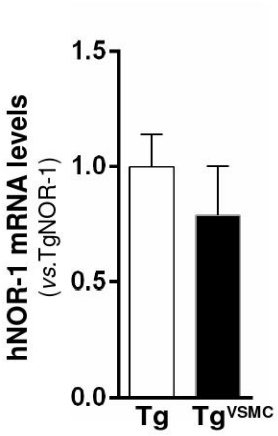

Figure S1. Transgene expression in NOR-1 transgenic mice. Human NOR-1 (hNOR-1) mRNA levels analyzed by real-time PCR in the medial aorta from both TgNOR-1 and TgNOR-1^{VSMC} (Tg^{VSMC}) mice. Data are mean ± SEM (n=8).

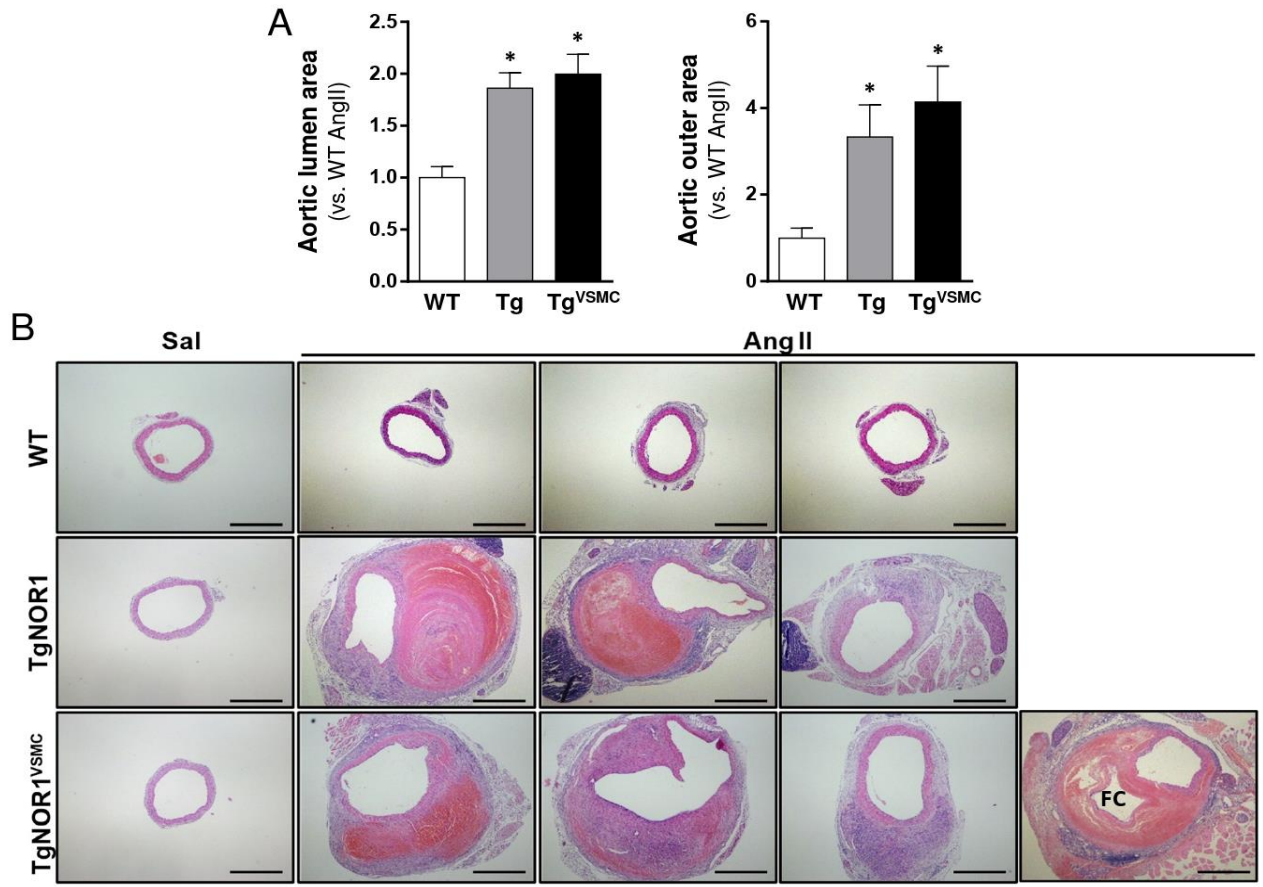

Figure S2: **Characteristics of abdominal aortic aneurysms promoted by NOR-1 transgenesis in response to AngII. A)** Luminal and outer areas of abdominal aortas from AngII infused mice quantified by image analysis in aortic sections from each experimental group (WT: wild-type; Tg: TgNOR-1 mice; Tg^{VSMC}: TgNOR-1^{VSMC} animals). Data represent mean ± SEM (n=10). * $p< 0.05$ *vs.* AngII-infused WT mice. One-way ANOVA. **B)** Representative images of abdominal aortas from WT and NOR- 1 transgenic mice after AngII infusion (Bar: 500 µm). The presence of a false channel (FC) into the hematoma could be observed in some aneurysms.

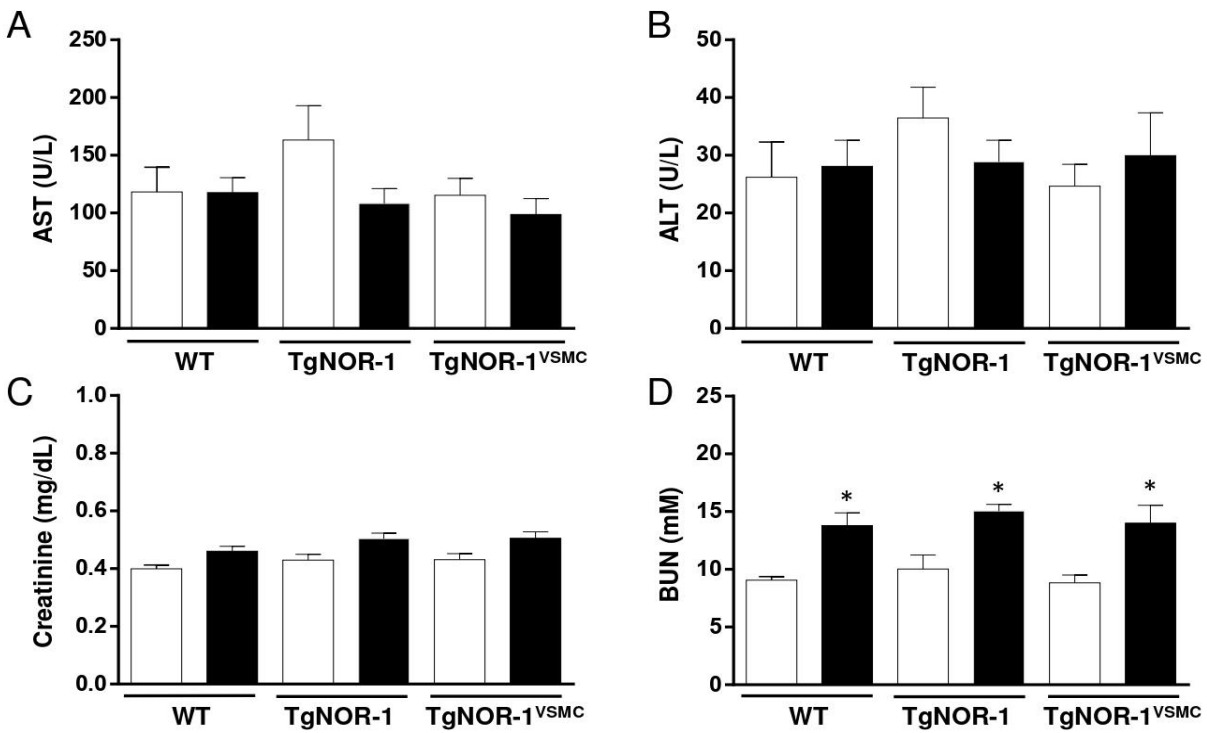

Figure S3: **NOR-1 transgenesis did not alter renal and hepatic function.** Biochemical parameters of renal and hepatic function were assessed in plasma samples from wild-type (WT), TgNOR-1 and TgNOR-1^{VSMC} mice infused with saline (white bars) or AngII (black bars). Levels of aspartate transaminase (AST; A) alanine transaminase (ALT; B), creatinine (C) and blood urea nitrogen (BUN; D) are shown. Data represent mean ± SEM (saline, n=8; AngII, n=10). * $p< 0.05$ *vs.* the same mice infused with saline. Two-way ANOVA.

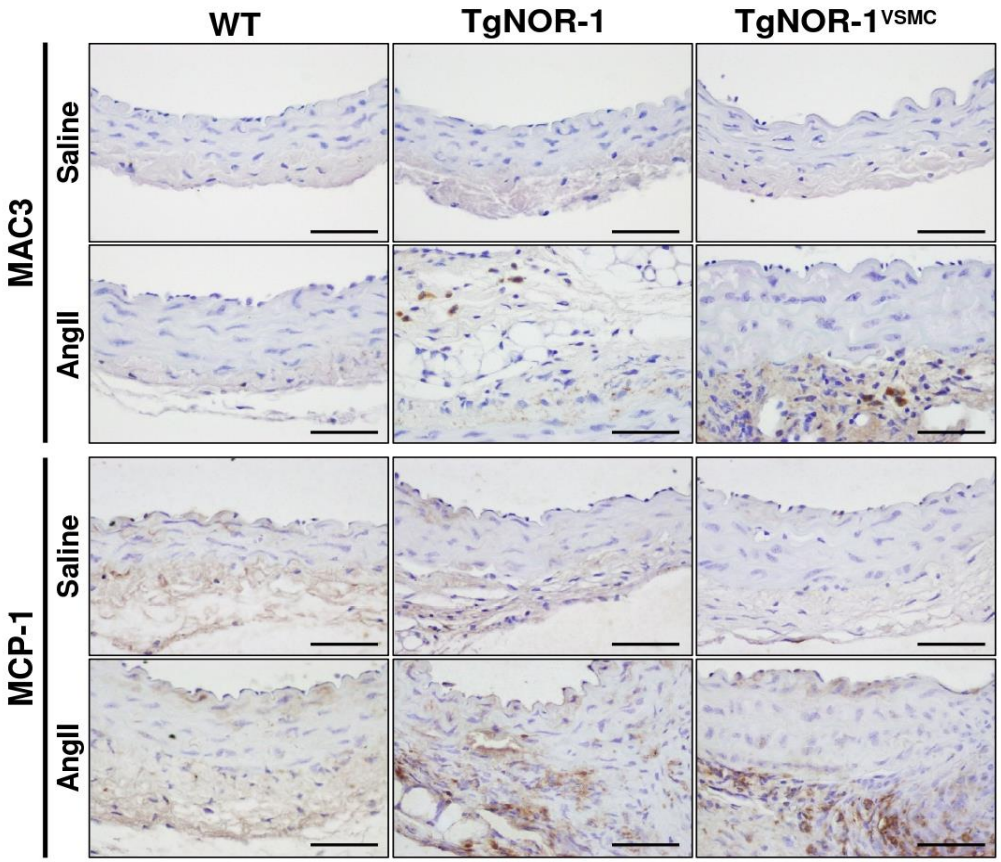

Figure S4. AngII-induced macrophage infiltration and MCP-1 expression are enhanced in NOR-1 transgenic mice. Wild-type (WT), TgNOR-1 and TgNOR-1^{VSMC} mice were infused with AngII (1000 ng/kg/min) or saline solution for 28 days. Representative images showing the infiltration of macrophages (MAC3+ cells) and MCP-1 immunostaining in aortic sections from each experimental group counterstained with haematoxilin. Bars: 50 μm.

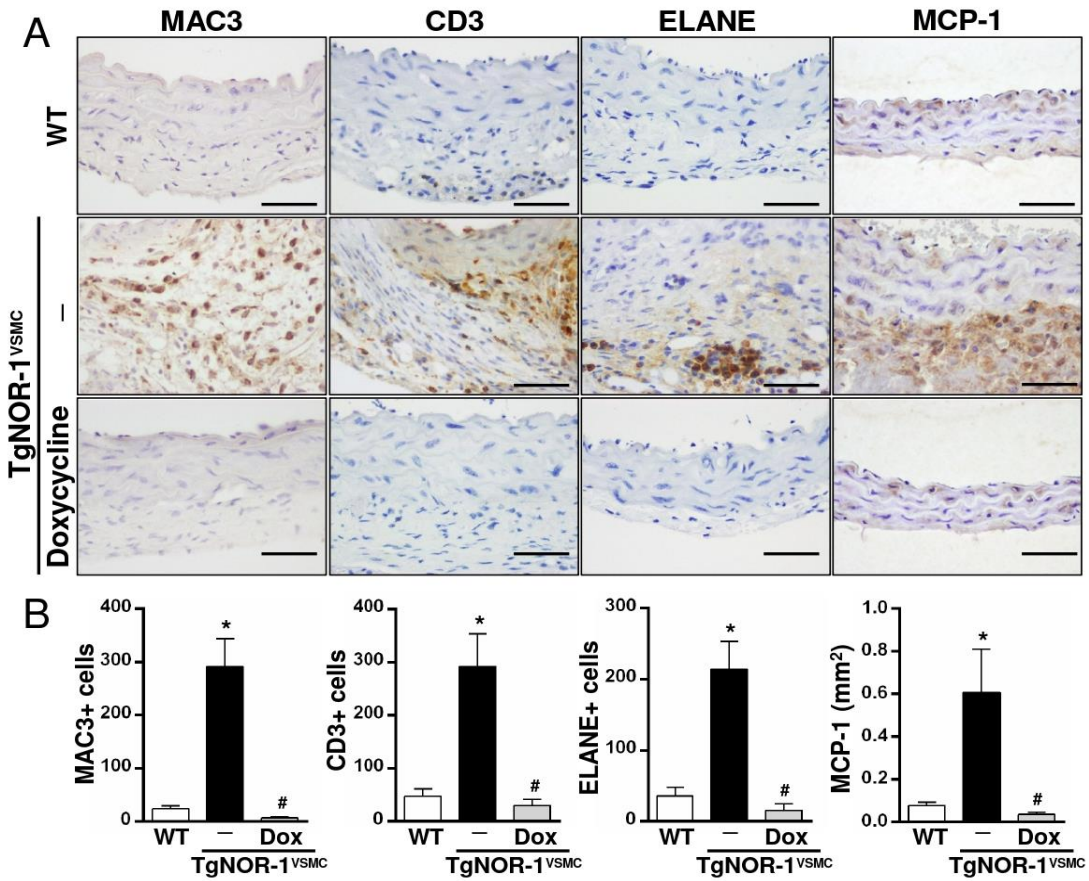

Figure S5. Doxycycline reduced inflammatory cell infiltration in the abdominal aorta from Ang-II-infused TgNOR-1^{VSMC} mice. AngII (1000 ng/kg/min) was infused into wild-type (WT) and TgNOR-1^{VSMC} mice for 28 days. TgNOR-1^{VSMC} mice were treated or not with Doxycycline (Dox; 30 mg/kg body weight/day). **A)** Aortic infiltration of macrophages (MAC3), lymphocytes (CD3) and neutrophils (elastase, neutrophil expressed, ELANE) and MCP-1 immunolabeling in AngII-infused mice (Bars: 50 µm). **B)** Quantitative analysis of positive cells per aortic section (MAC3, CD3 and ELANE) and area in mm^2 *per* aortic section (MCP-1). Data are expressed as mean ± SEM (WT, n=7; TgNOR-1^{VSMC}, n=8). $P< 0.05$; *, *vs*. AngII-infused WT mice; #, *vs*. AngII-infused TgNOR-1^{VSMC} mice. Kruskal–Wallis test for **B**.

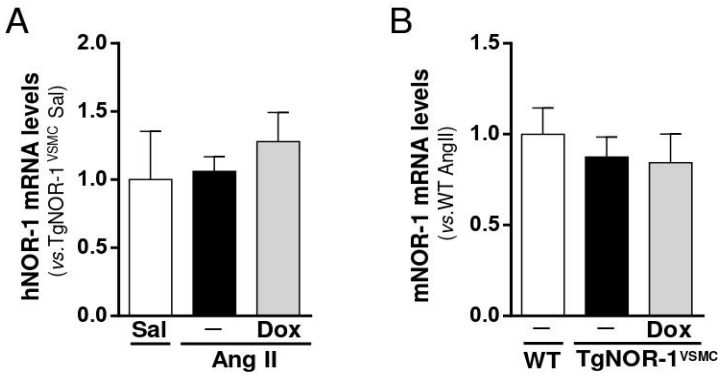

Figure S6: **Doxycycline did not alter the aortic expression of either hNOR-1 transgene or endogenous NOR-1 in TgNOR-1^{VSMC} mice. A)** Human NOR-1 (hNOR-1) mRNA levels assessed in aorta from TgNOR-1^{VSMC} mice infused with saline (Sal; white bars) or AngII (black bars) and treated or not with doxycycline (Dox; grey bars) (Sal-infused transgenic mice, n=10; AngII-infused transgenic mice, n=15; AngII-infused transgenic mice treated with doxycycline, n=10. **B)** Endogenous mRNA levels of NOR-1 (mNOR-1) assessed after AngII infusion in aorta from WT and TgNOR-1^{VSMC} mice treated or not with doxycyline (AngII-infused WT mice, n=15; AngII-infused transgenic mice, n=15; AngII-infused transgenic mice treated with doxycycline, n=10). Data represent mean ± SEM.

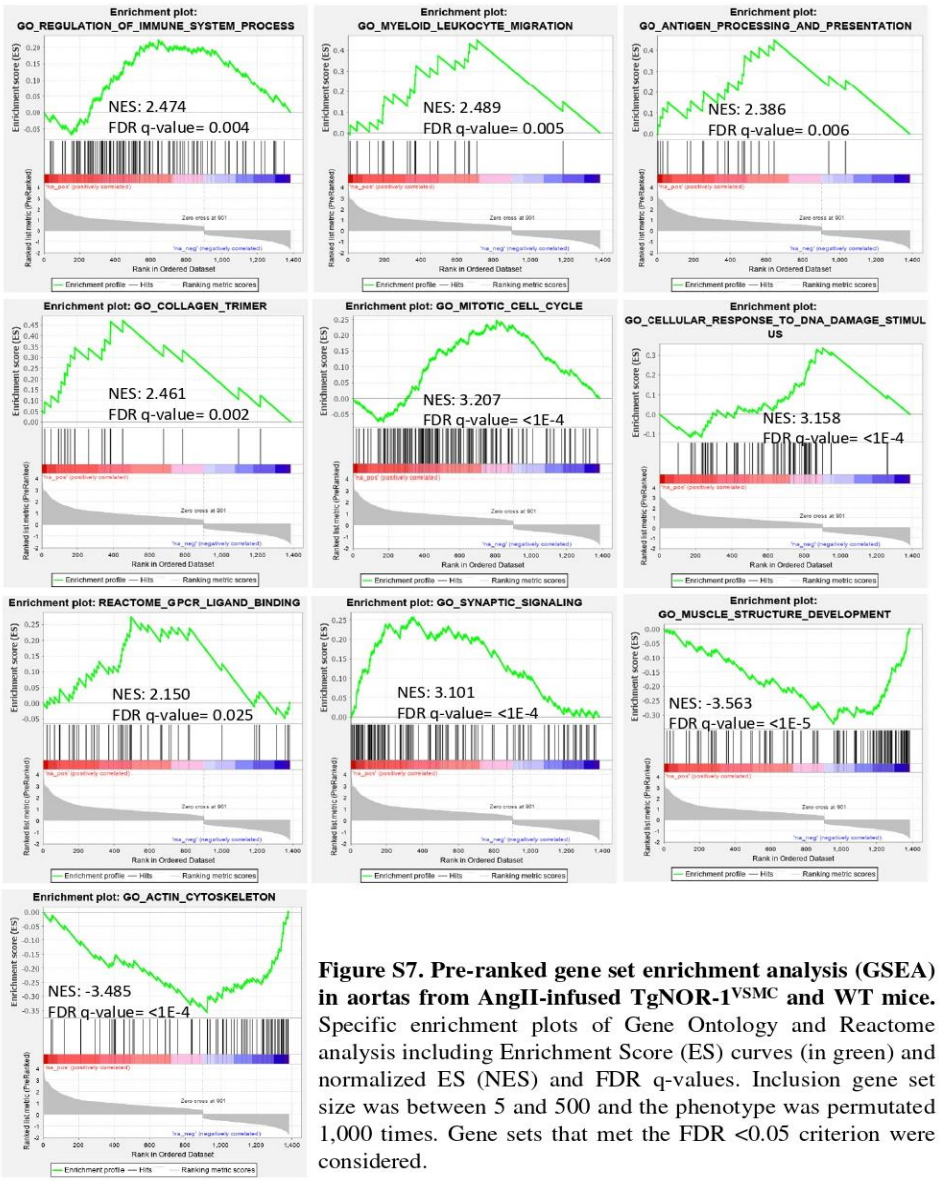

Figure S7. Pre-ranked gene set enrichment analysis (GSEA) in aortas from AngII-infused TgNOR-1^{VSMC} and WT mice. Specific enrichment plots of Gene Ontology and Reactome analysis including Enrichment Score (ES) curves (in green) and normalized ES (NES) and FDR q-values. Inclusion gene set size was between 5 and 500 and the phenotype was permutated 1,000 times. Gene sets that met the FDR <0.05 criterion were considered.

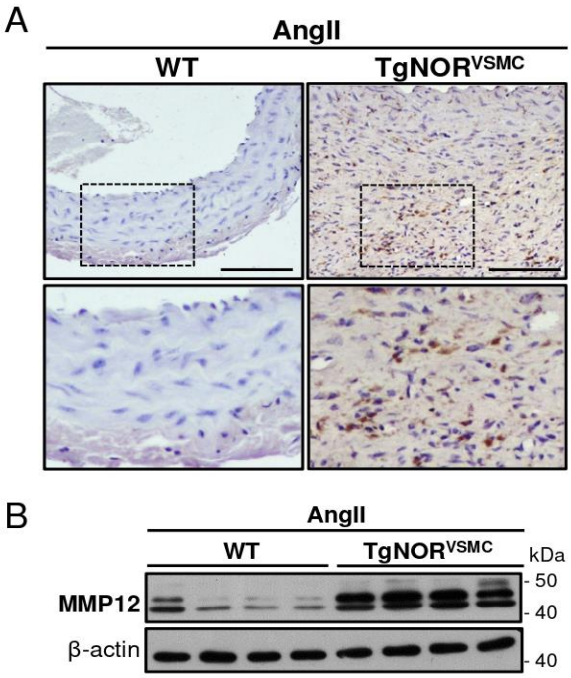

Figure S8. MMP12 protein level is enhanced by AngII infusion in the abdominal aorta from NOR-1 transgenic mice. Wild-type (WT) and TgNOR-1^{VSMC} mice were infused with AngII (1000 ng/kg/min) for 28 days. **A)** Immunohistochemical analysis of MMP-12 expression in abdominal aorta sections from these animals. Sections were counterstained with hematoxylin. The boxes indicate the magnified area shown in the lower panel (Bar: 100 μm). **B)** MMP12 protein levels were assessed by Western blot in aortic lysates from AngII-infused mice. Levels of β-actin are shown as a loading control. Protein size was estimated by the indicated position of molecular weight markers.

ANEXO-2

Resultados: Figura A1 y A2.

En ratones TgNOR-1^{CMLV} la expresión del trangen hNOR-1 controlada por el promotor SM22α se dirige principalmente a CMLV. Los análisis por PCR a tiempo real mostraron una elevada expresión del hNOR-1 en CMLV de la media de animales TgNOR-1^{CMLV}, en cambio la expresión de hNOR-1 en fibroblastos de la adventicia fue indetectable es estas condiciones experimentales (Figura A1).

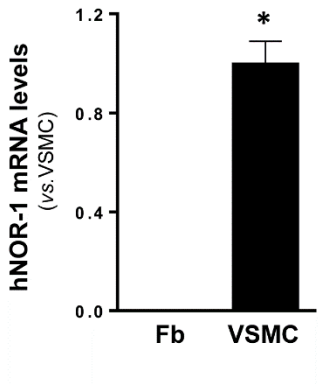

Figura A1. El promotor SM22α dirige la expresión del transgen a células musculares lisas vasculares (VSMC) de ratones TgNOR-1^{CMLV} pero no a fibroblastos de la adventicia. Niveles de mRNA del NOR-1 humano (hNOR-1) en VSMC y fibroblastos en cultivo aislados de la capa media y la adventicia respectivamente, se analizaron mediante PCR a tiempo real. Fibroblastos (Fb) de ratones TgNOR-1^{CMLV} y VSMC. Los valores se expresan como media ± SEM (n= 5). *P<0.0001; *vs*. VSMC.

En la patología aneurismática humana los niveles proteicos de NOR-1 incrementan alrededor de 10 veces en comparación con muestras de aorta sanas. Los niveles de proteína de NOR-1 en el ratón transgénico TgNOR-1^{CMLV} aumentan en ese rango respecto a ratones WT (Figura A2).

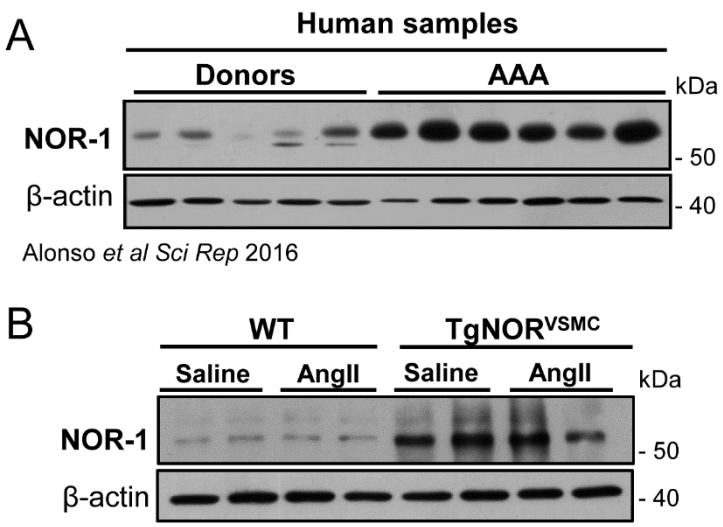

Figura A2. Niveles de proteína NOR-1 en AAA humanos y en la aorta abdominal de ratones TgNOR-1^{CMLV}. A) Los niveles de proteínas se analizaron mediante *Western blot* en muestras vasculares de pacientes con AAA y en aortas abdominales de individuos sanos (*donors*) (Alonso *et al*., 2016). **B)** Imagen representativa del análisis por *Western blot* para NOR-1 en aortas abdominales de animales WT y TgNOR-1^{CMLV} infundidos con solución salina (*Saline*) o AngII (100 ng/kg/min; 28 días). El tamaño de las proteínas se estimó mediante la posición del marcador de peso molecular (en kDa). La β-actina se empleó como control de carga.

PUBLICACIÓN 3

Targeting tyrosine hydroxylase for abdominal aortic aneurysm: impact on inflammation, oxidative stress and vascular remodeling

Laia Cañes, Judith Alonso, Carme Ballester-Servera, Saray Varona, José R. Escudero, Vicente Andrés, Cristina Rodríguez and José Martínez-González

Manuscrito en revisión

Introducción y objetivos: El AAA es una patología degenerativa que afecta aproximadamente entre un 4% y un 8% de los hombres de más de 65 años (Nordon *et al*., 2011). Esta enfermedad se caracteriza por una dilatación permanente de la aorta abdominal, cuyo diámetro crece progresivamente pudiendo producirse la ruptura aortica, responsable de más de 16.000 muertes al año en Estados Unidos (Mozaffarian *et al*., 2015). La pared arterial sufre un profundo remodelado destructivo debido a una respuesta inflamatoria crónica asociada con un aumento de la expresión de proteasas y la consecuente destrucción de las proteínas estructurales de matriz, además de una pérdida de CMLV por apoptosis. Actualmente, no existen fármacos para reducir la progresión del AAA, y el único tratamiento efectivo en aneurismas graves es la cirugía de reparación. Por ello, es necesario identificar nuevas estrategias terapéuticas que limiten el crecimiento del aneurisma y su eventual ruptura.

El sistema nervioso simpático controla la presión sanguínea y el tono vascular, y aunque se desconoce la posible contribución de este sistema al desarrollo de enfermedades vasculares como el AAA, recientemente se ha postulado la vinculación de la actividad simpática con la progresión y ruptura del aneurisma. Concretamente, los pacientes con disección aórtica presentan un aumento de la actividad simpática (Zhipeng *et al*., 2014), mientras que la denervación local del sistema nervioso simpático disminuye la dilatación de la aorta inducida en rata por la combinación de AngII y β-aminopropionitrilo (Hu *et al*., 2020). En un estudio reciente nuestro grupo ha descrito la inducción de vías relacionadas con la actividad simpática en un nuevo modelo de ratón que mimetiza gran parte de los aspectos de la patología aneurismática humana (Cañes *et al*., 2021). En este contexto, nuestro objetivo es estudiar la relación de las enzimas implicadas en la ruta de biosíntesis de catecolaminas con el AAA humano y analizar si la inhibición de la enzima tirosina hidroxilasa (TH), enzima limitante en la síntesis de catecolaminas, mejora el desarrollo del AAA en dos modelos experimentales de esta patología.

Resultados: Aunque la contribución del sistema simpático a la fisiopatología vascular es incierta, se ha sugerido que la actividad simpática podría contribuir al remodelado destructivo de la pared vascular durante la progresión del aneurisma. Resultados recientes mediante estudios de *microarray* en un modelo preclínico de AAA sugieren la inducción de genes relacionados con la vía de la tirosina hidroxilasa (TH), enzima limitante en la síntesis de catecolaminas, en tejidos aneurismáticos (Cañes *et al*., 2021). Por ello, se caracterizó la expresión de los componentes de la vía de síntesis y transporte de catecolaminas en la enfermedad aneurismática humana. En la aorta de pacientes con AAA se observó un incremento de los niveles de mRNA de *TH*, *DBH* (dopamina β-hidroxilasa) y del transportador de norepinefrina (*SLC6A2;* del inglés *solute carrier family 6 member 2*) en comparación con donantes sanos. La expresión de TH, se incrementó drásticamente en el tejido aneurismático humano, lo que

se asoció con un aumento significativo de los niveles proteicos de esta enzima. Los análisis inmuhistoquímicos detectaron la expresión de TH en zonas de inervación periférica, células inflamatorias y en algunas CMLV de la media.

En dos modelos experimentales susceptibles al desarrollo de AAA por infusión de AngII, los ratones ApoE$^{-/-}$ y TgNOR-1^{CMLV} detectamos niveles elevados en RNA de *Th*, *Dbh*, *Ddc* y *Slc6a2*. También se observó un incremento en los niveles de proteína TH en las aortas aneurismáticas de ambos modelos. Los análisis inmunohistoquímicos para esta enzima revelaron un patrón de expresión similar al descrito en los AAA humanos, con una marcada tinción en nervios periféricos, células inflamatorias y en menor medida en CMLV. Estos resultados, indican que la inducción de la TH es una característica común a la patología aneurismática humana y de modelos animales.

En estudios previos, nuestro grupo demostró la eficacia de la doxiciclina para prevenir la prevención de la formación de AAA inducidos por AngII en el ratón TgNOR-1^{CMLV} (Cañes *et al*., 2021). Destacar que, tras la infusión de AngII el tratamiento con doxiciclina normalizó la expresión de la *Th* en la aorta de estos ratones. En este contexto, nos planteamos determinar si el incremento de la expresión de la TH juega un papel relevante en la patología aneurismática. Con este objetivo ratones ApoE$^{-/-}$ infundidos con AngII se trataron con α-metil-*p*-tirosina (AMPT), un inhibidor específico de la TH. La progresión del aneurisma se monitorizó mediante ultrasonografía durante todo el periodo experimental. El AMPT previno la formación de AAA en el ratón ApoE$^{-/-}$ limitando el aumento del diámetro aórtico tras la infusión de AngII. En los animales ApoE$^{-/-}$ la incidencia de aneurisma en respuesta a AngII fue de un 80%, porcentaje que se redujo sustancialmente a un 10% por el tratamiento con AMPT, fármaco que además evitó el desarrollo de las formas más graves de aneurisma. También, se observó una ligera mejora en la tasa de supervivencia en el grupo de ratones tratados con AMPT, aunque no llegó a ser significativa. La eficacia del AMPT fue independiente del efecto hemodinámico ejercido por la AngII, ya que la presión sanguínea no se vio afectada por el tratamiento farmacológico. En cuanto al fenotipo vascular, tras la infusión de AngII el ratón ApoE$^{-/-}$ tratado con AMPT mostró características similares a las de los animales control, ya que este fármaco preservó la integridad de las fibras elásticas asociado a una normalización de la expresión de la MMP-2, así como de la actividad MMP. Además, en los animales infundidos con AngII, el AMPT disminuyó la expresión vascular de marcadores inflamatorios como EMR-1 y MCP1, y el reclutamiento de macrófagos, linfocitos y neutrófilos en la pared del vaso. Asimismo, el AMPT atenuó el aumento del estrés oxidativo inducido por la AngII. Estos efectos ejercidos por el AMPT se asociaron con la normalización de la expresión de la *Th*.

El AMPT también previno la formación de AAA en el ratón TgNOR-1^{VSMC} infundido con AngII, con una disminución del diámetro que fue significativa

desde el día 14. Este fármaco redujo la incidencia de aneurismas en el ratón TgNOR-1^{VSMC} y la gravedad de los mismos en respuesta a la AngII. Como previamente habíamos descrito (Cañes *et al*., 2021), la infusión de AngII en animales TgNOR-1^{VSMC} conllevó un 20% de muertes tempranas. El tratamiento con AMPT atenuó ligeramente este efecto, si bien no significativamente. También el AMPT limitó el remodelado vascular y el número de roturas de las fibras de elastina. En este grupo de animales, la expresión de *Mmp-2* y la actividad MMP, analizada por zimografía *in situ*, fue comparable a la encontrada en los animales control. Asimismo, el AMPT previno el incremento de la expresión de marcadores inflamatorios (EMR1, MCP-1, IL-1β, IL-6 y CXCL2) y del infiltrado inflamatorio (macrófagos, linfocitos y neutrófilos) inducidos por la AngII. La inhibición de la TH también redujo la mayor generación de ROS en la pared vascular detectada en el ratón transgénico infundido con AngII. Al igual que ocurría en el modelo ApoE^{-}, los efectos vasculares observados se asociaron con la normalización de la expresión de la *Th* en los animales tratados con AMPT.

Cabe destacar que en aneurismas humanos detectamos la existencia de una correlación significativa entre la expresión de *NOR-1* y la de la *TH*, la *DBH* y el *SLC6A2*, por lo que quisimos estudiar en profundidad los mecanismos moleculares que subyacen a la regulación de la TH y el papel del factor de transcripción NOR-1 en dicho proceso. De hecho, se ha demostrado la regulación de la TH por NURR1 en células no vasculares (Sakurada *et al*., 1999, Kim *et al*., 2003 C). Por lo tanto, se analizó si NOR-1 podría modular de forma directa la expresión de esta enzima. El análisis *in silico* del promotor proximal de la *TH* humana, identificó dos elementos consenso de tipo NBRE. Para verificar si NOR-1 regula la actividad transcripcional de la TH, se clonó el promotor proximal de esta enzima en el vector reportero de luciferasa pGL3. Los ensayos de actividad transcripcional en CMLV co-transfectadas con dichas construcciones y un vector de expresión de NOR-1 (pCMV5/hNOR-1) mostraron un incremento de la actividad transcripcional de la TH. Además, la mutagénesis de los elementos NBRE, reveló que el elemento más distal contribuye principalmente a la regulación de la TH por NOR-1 en CMLV.

Conclusión: Nuestro estudio demuestra la inducción de la vía de la TH en la patología aneurismática, sugiere el interés de esta enzima como diana terapéutica en esta enfermedad y señala al factor de transcripción NOR-1 como regulador de la expresión de la TH en CMLV

Targeting tyrosine hydroxylase for abdominal aortic aneurysm: impact on inflammation, oxidative stress and vascular remodeling

Laia Cañes[1,2,3], Judith Alonso[1,2,3], Carme Ballester-Servera[1,3], Saray Varona[1,2,3], José R Escudero[2,3,4], Vicente Andrés[2,6], Cristina Rodríguez[2,3,4,*] and José Martínez-González[1,2,3,*]

[1]Instituto de Investigaciones Biomédicas de Barcelona (IIBB-CSIC), Barcelona, Spain.

[2]CIBER de Enfermedades Cardiovasculares, ISCIII, Madrid, Spain.

[3]Instituto de Investigación Biomédica Sant Pau, Barcelona, Spain.

[4] Servicios Mancomunados de Angiología, Cirugía Vascular y Endovascular, Hospitales de la Santa Creu i Sant Pau/Dos de Mayo, Barcelona, Spain.

[5]Institut de Recerca Hospital de la Santa Creu i Sant Pau (IRHSCSP), Barcelona, Spain.

[6]Centro Nacional de Investigaciones Cardiovasculares Carlos III (CNIC), Madrid, Spain.

Short title:TH in abdominal aortic aneurysm.

[*]These authors contributed equally to this work. Correspondence should be addressed to C.R. IRHSCSP, C/Antoni Mª Claret, 08025 Barcelona, Spain (email: crodriguezs@santpau.cat) or J.M.-G. IIBB, Rosselló, 161, 08036 Barcelona, Spain (email: jose.martinez@iibb.csic.es)

Abstract

Pharmacological treatments for preventing abdominal aortic aneurysm (AAA) rupture or slowing aneurysm progression remains a challenge. It is increasingly recognized that sympathetic activity might play a role in the pathogenesis of AAA. Here, we show that in abdominal aorta samples from AAA patients, the expression of genes encoding for key enzymes involved in the catecholamine biosynthetic pathway (tyrosine hydroxylase [TH] and dopamine β-hydroxylase [DBH]) or the norepinephrine transporter SLC6A2 are upregulated. Similarly, the vascular expression of *Th*, *Dbh* and *Slc6a2* was increased in the aneurysmal aorta of two animals models susceptible to angiotensin II (AngII)-induced AAA: the apolipoprotein E-deficient ($ApoE^{-/-}$) model and a transgenic mouse that over-expresses the human nuclear receptor NOR-1 (Neuron-derived orphan receptor-1) in the vascular wall ($TgNOR\text{-}1^{VSMC}$). As a marker of sympathetic activity TH localizes to peripheral innervations, but also to inflammatory cells, and scattered vascular smooth muscle cells in human and mouse AAA. Interestingly, the preventive effect of doxycycline on AAA formation in AngII-treated $TgNOR\text{-}1^{VSMC}$ mice was associated to the normalization of the vascular expression of *Th*. Strikingly, the administration of the specific TH inhibitor α-methyl-*p*-tyrosine (AMPT) protected against the formation of AAA induced by AngII in both ApoE knockout and NOR-1 transgenic mice, limiting the progressive increase in aortic diameter without affecting blood pressure. The drug normalized vascular MMP-2 expression and MMP activity, preserving elastin integrity, attenuated the rise in vascular oxidative stress induced by AngII, and decreased the expression of inflammatory markers as well as the recruitment of macrophages, lymphocytes and neutrophils into the vessel wall. Finally, the nuclear receptor NOR-1 drove *TH* transcription though a NBRE located in the proximal region of the human *TH* promoter. Altogether, our results support the potential of pharmacological strategies targeting TH for the clinical management of AAA.

Key words: abdominal aortic aneurysm, tyrosine hydroxylase, animal models,

Introduction

Abdominal aortic aneurysm (AAA) is a common and life-threatening disorder affecting approximately 4% to 8% of men over 65 years of age.[1] It is characterized by a focal and permanent dilation of the abdominal aorta, whose diameter progressively grows increasing the risk of aortic rupture, a devastating condition responsible for more than 16,000 deaths each year in the United States alone.[2] In this disease the arterial wall suffers a chronic inflammatory stage with upregulation of proteinases that degrade structural matrix proteins and loss of vascular smooth muscle cells (VSMC), which leads to a destructive remodeling of the arterial wall. Despite the high prevalence of AAA, surgical repair of those more severe is currently the only effective way to treat the disease. Nowadays, pharmacological treatments for preventing aortic rupture or slowing aneurysm progression remains a challenge.[3] Therefore, it is mandatory to identify novel therapeutic strategies for the medical management of this disease.

The sympathetic nervous system is key in cardiovascular homeostasis by regulating cardiac output, systemic vascular resistance, heart rate and blood pressure. Alterations in sympathetic function impacts on cardiovascular diseases such as hypertension, heart failure and myocardial infarction;[4] however, little is known about its role on AAA. In the last years, it is increasingly recognized that sympathetic activity might actively contribute to aneurysm progression and rupture. In fact, human aortic dissection is frequently associated with an increase in sympathetic activity,[5] while local sympathetic denervation ameliorates experimental aneurysms.[6] Recently, using a new mouse model that overexpresses the neuron-derived orphan receptor-1 (NOR-1) in the vascular wall[7] and recapitulates key aspects of the human AAA, we suggested the upregulation of genes associated to sympathetic activity in aneurysmal aorta.[8] They include key components of the tyrosine hydroxylase (TH) pathway involved in the biosynthesis of catecholamines, important hormones and neurotransmitters in both the central and peripheral nervous systems.[9] The biological functions of the TH pathway, however, are far from being limited to those derived from the well-known effects of catecholamines on their main target tissues. Early studies showed that the inactivation of both TH alleles results in mid-gestational lethality, apparently due to cardiovascular failure.[10] More recently, it has been shown that the expression of TH during heart development is required to drive cells to a sino-atrial fate, the hallmark of cardiac chamber formation.[11] TH pathway also appears to be critical modulating the pancreatic endocrine precursor and insulin producing cell neogenesis,[12] as well as lymphocyte differentiation and function, thereby controlling immune homeostasis.[13,14] This multiplicity of functions would explain the reason

for the intricate mechanisms that regulate TH,[15,16] the first and rate-limiting step of the pathway, and the interest in this enzyme as a therapeutic target for human disease.[17] Here, we have addressed whether TH could actively contribute to AAA progression. Our data uncover the striking upregulation of the TH pathway in human AAA, and provide evidence that the inhibition of TH ameliorates AAA development in two experimental models of this disease. Altogether, these data support the interest of pharmacological strategies targeting TH for the clinical management of AAA.

Materials and methods

Aneurysm and donor sampling and preservation

Human aneurysmal samples were collected from patients undergoing open repair for AAA at the Hospital de la Santa Creu i Sant Pau (HSCSP; Barcelona, Spain), while healthy aortas were obtained from multi-organ donors as previously described.[18,19] The study was approved by the HSCSP Ethics Committee (12/031/1316) and was conducted according to the Declaration of Helsinki. Participation in the study of patients and control subjects was based upon informed consent of patients or legal representatives. Abdominal aorta segments were obtained from all patients and control subjects, following strict standard operating procedures and ethical guidelines. Samples of control subjects had no post-mortem evidence of abdominal aorta aneurysm, atherosclerotic plaques or other medical conditions that affect the study. Samples were rapidly collected and stored at −80°C for subsequent RNA or protein extraction.

Animal handling

Two animal models were used: apolipoprotein E-deficient ($ApoE^{-/-}$) mice (Charles River Ltd; Kent, UK) and a mouse model that specifically over-expresses the human nuclear receptor NOR-1 in the vascular wall ($TgNOR\text{-}1^{VSMC}$).[7,20] Transgenic mice and control littermates (wild-type; WT) on a C57BL/6J genetic background were bred in the Animal Experimentation Unit (Institut de Recerca de l'Hospital de la Santa Creu i Sant Pau, Barcelona, Spain). Animal handling and disposal were performed in accordance with the principles and guidelines established by the Spanish Policy for Animal Protection RD53/2013 and the European Union Directive 2010/63/UE. All procedures were approved by the local ethical committee (Law 5/June 21, 1995; Generalitat de Catalunya).

Three-month-old male mice were subjected to AngII [1000 ng/kg body weight (BW)/min; Sigma-Aldrich, St Louis, MO, USA] infusion via osmotic minipumps (model

1002, Alzet; Durect Corporation, Cupertino, CA, USA) for 28 days.[8] For the implantation of osmotic minipumps, mice were anaesthetised by isofluorane inhalation (1.5%). Anaesthetic depth was confirmed by loss of blink reflex and/or lack of response to tail pinch. The procedure takes about 15 min/mouse. Recovery after surgical procedures was carried out using aseptic techniques in a dedicated approved surgical area. The animals were kept warm in a heating pad until awake after surgery, and observed carefully by the investigators throughout the post-surgery period. AngII-infused mice were pretreated or not with doxycycline (Sigma-Aldrich; 30 mg/kg/day in the drinking water)[8] or with a tyrosine hydroxylase inhibitor (α-methyl-*p*-tyrosine [AMPT; Sigma-Aldrich]; 100 mg/Kg twice daily, i.p) throughout the 28 days experimental period. All treatments started 24 h before AngII infusion. ApoE$^{-/-}$ and transgenic mice infused with saline solution and AngII-challenged WT animals were used as controls.

Non-invasive measurement of systolic blood pressure

Systolic blood pressure (SBP) was non-invasively measured in conscious mice prior to and following treatment using the tail-cuff plethysmography method (CODA® tail-cuff blood pressure system; Kent Scientific Corporation; Torrington, CT, USA). Mice were trained for tail-cuff measurements over a period of 1 week. Blood pressure measurements were performed at the same time (between 9 a.m. and 11 a.m.) in order to avoid the influence of the circadian cycle.[8,21]

Basic measurements of ultrasound recording for abdominal aortas

Mice were anaesthetised with 1.5% isofluorane inhalation as indicated above and were lightly secured in the supine position to a warming platform. After shaving the precordium, an abdominal echography was performed to record abdominal aorta diameter using a Vevo 2100 ultrasound with a 30 MHz transducer (VisualSonics, Toronto, ON, Canada).[8,18,21] Abdominal aortas with diameters ≥1.5 mm were considered as aneurysms. All primary measurements were made from images captured on cine loops of 100 frames at the time of the study using the software provided by the echography machine.

Echocardiographic data was recorded at baseline and weekly throughout the experimental period. At the end of the experimental procedures, mice were euthanized via isofluorane overdose. The severity of the aneurysm was based on a 4-point grading scale previously described in detail:[22] type 0, no aneurysm; type I, dilated lumen in the suprarenal region of the aorta with no thrombus; type II, remodelled tissue in the suprarenal region that

frequently contained thrombus; type III, a pronounced bulbous form of type II that contained thrombus, and type IV, a form in which there are multiple AAAs containing thrombus.

Determination of the lipid profile and hepatic and renal function markers in plasma

Lipids were quantified with a colorimetric assay in plasma from ApoE$^{-/-}$ mice by using specific reagents for the assessment of triglycerides (Gernon, GN90125; RAL Técnica para el Laboratorio S.A., Barcelona, Spain) and total cholesterol levels (Gernon, GN20125) and a multicuvette rack reader (Clima MC-15, RAL Técnica para el Laboratorio S.A.) following the manufacturers' instructions. Aspartate transaminase (AST), alanine transaminase (ALT), creatinine and blood urea nitrogen (BUN) plasma levels were measured in a Cobas 6000/c501 autoanalyzer with specific reagents (Roche Diagnostics International Ltd, Basel, Switzerland)[8].

Analysis of mRNA levels

Total RNA was isolated using TRIsure™ reagent (Bioline) and reverse transcribed into cDNA using the High Capacity cDNA Reverse Transcription Kit (Applied Biosystems). Quantification of mRNA levels was performed by real-time PCR using the ABI PRISM 7900HT sequence detection system (Applied Biosystems). Specific primers and probes (provided by Applied Biosystems or Integrated DNA Technologies Inc, Coralville, IA, USA.) were used for the quantification of human mRNA levels for *TH* (HS.PT.58.369742), Dopamine β-Hydroxylase (*DBH*; Hs.PT.58.39251730), and β-actin (*ACTB*, Hs99999903_m1; used as reference gene). To assess mRNA levels in mouse tissues the following primers and probes were used for *Th* (Mm.PT.58.33106180), interleukin-6 (*Il6*; Mm00446191_m1), *Il1β* (Mm00434228_m1), C-C motif chemokine ligand 2 (*Ccl2 or Mcp1* (Mm00441242_m1), metalloproteinase-2 (*Mmp2;* MmPT.58.9606100), EGF-like module-containing mucin-like hormone receptor-like 1 (*Emr1*;MmPT.56a.11087779) and C-X-C Motif Chemokine Ligand 2 (*Cxcl2*; Mm00436450_m1). Further, specific primers for SYBR Green real-time PCR analysis were used for the assessment of solute carrier family 6 member 2 (*Slc6a2*; 5'-CTGGCTCTGGGGCAATACAAG-3' and 5'- GCCGACATAGAGGGCAATGA-3'), *Dbh* (5'-CGAGGAGAGATGGAGAACGC-3' and 5'-ATCTCGAGTCCTCTGTGCCT-3') and dopa decarboxylase (*Ddc*, 5'-GCCTTTTTGGCTGGAAGAGC-3' and 5'-GCTTGTGTGAACTCTGGGGA-3'). Glyceraldehyde-3-phosphate dehydrogenase (*Gadph*; Mm.PT.58.39a.1) expression was used as a reference gene for mouse tissues.

In situ detection of vascular O_2^- production

The oxidative fluorescent dye dihydroethidium (DHE, Sigma-Aldrich Co.) was used to evaluate the *in situ* production of O_2^-. Arterial segments were placed in phosphate-buffered saline (PBS) containing 30% sucrose for 20–50 min, transferred to a cryomold-containing Tissue Tek OCT embedding medium (Sakura Finetek Europe B.V., Alphen aan den Rijn, The Netherlands), and frozen in liquid nitrogen. Arterial sections were equilibrated for 30 min at 37 °C in Krebs-HEPES buffer (in mM: 130 NaCl, 5.6 KCl, 2 $CaCl_2$, 0.24 $MgCl_2$, 8.3 HEPES, 11 glucose, pH = 7.4). DHE (2 μM) was topically applied onto each section, cover-slipped and incubated for 30 min in a light-protected humidified chamber at 37°C. Fluorescence was visualized with a fluorescent laser scanning confocal microscope (Leica TCS SP2 equipped with a krypton/argon laser, × 40 objective; Leica Microsistemas S.L.U.). Fluorescence was detected with a 568 nm long-pass filter by using the same imaging settings for all experimental conditions. To minimize laser fluctuations from one day to another, data were expressed as % of signal in control arteries.[23]

Immunoblotting

Protein extracts were separated on SDS-polyacrylamide gels and transferred to polyvinylidene diflouride membranes (Immobilon, Merck-Millipore; IPVH00010). Blots were incubated with antibodies directed against TH (ab75875, Abcam, Cambridge, UK) and β-actin (A5441, Sigma-Aldrich). Bound antibodies were detected after incubation with appropriate HRP-conjugated secondary antibodies (Dako Products, Agilent, Santa Clara, CA, USA) and using the SuperSignal West Dura Extended Duration Substrate (Thermo Fisher Scientific). The size of detected proteins was estimated using protein molecular-mass standards (Hyperpage Prestained Protein Marker; Bioline, Paris, France). Equal loading of protein in each lane was verified by Ponceau staining and by β-actin signal.

Histological, immunohistochemical and immunocytochemical analysis

Tissues were fixed in 4% paraformaldehyde/0.1 M PBS (pH 7.4) for 24 hours and embedded in paraffin. Tissue sections (5-μm) were deparaffinised in xylene and rehydrated in graded ethanol solutions. Slides were then rinsed in distilled water and treated with 3% hydrogen peroxide in methanol for 30 min to remove endogenous peroxidase activity. Sections were then blocked with 10% normal serum and incubated overnight at 4 °C with antibodies against MAC-3 (sc-19991, Santa Cruz Biotechnology), CD3 (A0452, Dako, Agilent Technologies Co., Hamburg, Germany), MCP1 (sc-1785, 1:100, Santa Cruz Biotechnology Inc.), elastase,

neutrophil expressed (ELANE; M0752, Dako, Agilent Technologies Co., Hamburg, Germany) or MMP2 (ab51125; Abcam). After washing, samples were incubated for 1 h with a biotinylated secondary antibody (Vector Laboratories, Burlingame, CA, USA). After rinsing three times in PBS, standard Vectastain (ABC) avidin-biotin peroxidase complex (Vector Laboratories) was applied, and the slides were incubated for 30 min. Colour was developed using 3,3'-diaminobenzidine (DAB) and sections were counterstained with haematoxylin before dehydration, clearing, and mounting. Negative controls in which the primary antibody was omitted were included to test for non-specific binding. The histological characterization of aortic samples was performed by haematoxylin-eosin staining. To assess elastic fibre integrity, arterial sections were stained with orcein using a commercial kit (Casa Álvarez, Madrid, Spain).

***In situ* Zymography**

Gelatinolytic activity was assessed in OCT-embedded unfixed frozen tissue sections (8 μm) using Quenched Fluorogenic DQ™ gelatin (D-12054, Thermo Fisher Scientific) as a fluorogenic substrate.[8] Briefly, DQ-gelatin was dissolved in water at 1 mg/mL and then diluted 1:10 in 1% (w/v) low gelling temperature agarose (A9414, Sigma). The mixture was applied onto each section and cover-slipped. Samples were incubated at 4 ºC for 30 min, to allow gelatin gelling, and then maintained at room temperature for 24 h protected from light. FITC fluorescence was visualized using a Leica TCS SP5 confocal microscopy (excitation wavelength: 495 nm; emission wavelength: 515 nm) and the Leica LAS AF Lite software. Negative controls in which samples were pre-incubated with 20 mM EDTA before the addition of the labelled substrate were included.

Generation of promoter constructs and luciferase reporter assays

The human *TH* promoter (positions -3639 to -163 relative to the Transcription Start Site [TSS]; ENSG00000180176) was amplified by PCR from genomic DNA. The primers used were: 5´- TATACTCGAGCCCCTGGTCACCTGTTTTGT -3' (forward; XhoI site is underlined) and 5'- TATAAGATCTGGCTCGTCCGTGGAATCTAA -3' (reverse; BglII site is underlined). The PCR product was cloned into the pGL3 vector (Promega, Madison, WI, USA) (pGL3/pTH–3639). Two putative NBRE (-1480/-1472; -2353/-2345) sites located in *TH* promoter were mutated using the QuikChange™ Site-Directed Mutagenesis Kit (Agilent Technologies, Santa Clara, CA, USA) and primers (Supplementary Table S1). These constructs were used in transient transfection assays in rat VSMC as previously described.[24]

Briefly, transfections were performed in 12-well plates using 0.5 µg of the luciferase reporter plasmid together with the pCMV5/NOR-1 expression vector or the pCMV5 empty vector (0.05 µg), 0.5 µl PLUS™ Reagent and 1.25 µl of Lipofectamine™ LTX Reagent (ThermoFisher Scientific, Waltham, MA, USA) per well. The pRL-SV40 (25 ng) was included as an internal control (Promega). Firefly and renilla luciferase activities were measured using the Dual-Luciferase™ Reporter Assay System (Promega) and a luminometer (Orion I; Berthold Detection Systems, Pforzheim, Germany). Results were expressed as the ratio of Firefly to Renilla activity.

Statistical Analyses

Results are shown as mean±standard error of the mean (SEM). Significant differences were analysed using one-way ANOVA, two-way ANOVA with repeated measures or two-way ANOVA and the Tukey's tests. When normality failed, the Mann–Whitney rank sum test or the Kruskal–Wallis test were applied. Differences in AAA incidence were analyzed by the Chi square test ($\chi 2$). To determine association between variables, data were Log_{10} transformed and the Pearson Product Moment Correlation method (if variables are normally distributed) or the Spearman's rank-order correlation (as a non parametric test) were then used. Data were analysed with the GraphPad Prism version 6.01. Differences were considered significant at $p<0.05$.

Results

The catecholamine biosynthetic pathway is upregulated in human AAA

Although the role of the sympathetic system in vascular pathophysiology is unclear, it has been suggested that sympathetic activity could contribute to the destructive vascular remodeling underlying AAA progression.[5,6] Recent results from high-throughput microarray expression studies in a preclinical model suggest the upregulation of genes related to sympathetic activity in aneurysmal tissues.[8] As shown in Figure 1A-C, the expression of genes encoding for enzymes of the TH pathway such as *TH* and *DBH,* and the norepinephrine transporter *SLC6A2* was increased in abdominal aorta samples from AAA patients compared with healthy donors. In particular, the expression of TH, the rate-limiting enzyme in this pathway, was strongly up-regulated in human aneurysmal tissue. Likewise, protein levels corresponding to TH were consistently increased in these samples (Figure 1D). Further, immunohistochemical analysis detected the expression of TH in areas of peripheral

innervations and in inflammatory cells, whereas scattered TH-positive VSMC could be found in media (Figure 1E). Clinical data from patients and donors are shown in Supplemental Table S2.

Increased TH expression in mouse models of AAA

Next, we addressed whether the upregulation of the catecholamine biosynthetic pathway is also observed in the aneurysmal aorta from two experimental models of this disease. Quantitative analysis by real-time PCR revealed increased expression of *Th*, *Dbh, Ddc,* and *Scl6a2* in AAA from AngII-infused ApoE$^{-/-}$ (Figure 2A). Higher expression of these genes was also detected in AAA from a second model of this disease, the AngII-infused TgNOR-1^{VSMC} mouse[8] which overexpresses the nuclear receptor NOR-1 in the vascular wall (Figure 2B). Notably, a concomitant increase of TH protein levels was manifest in diseased aortas from both animal models (Figure 2C and D). Interestingly, the upregulation of aortic TH expression by AngII was more evident in the mouse strain sensitive to AAA than in WT animals (Supplemental Figure S1). Further, the immunohistochemical expression pattern uncovered in human AAA was similarly recapitulated in aneurysmal aortas from both mouse models, namely a pronounced staining in peripheral nerves and inflammatory cells and, to a lesser extent, in VSMC (Figure 2E). Collectively, these data indicate that the vascular upregulation of TH is a common feature of the aneurysmal disease in both humans and animal models.

The increase in TH activity contributes to AAA development in the AngII-infused ApoE$^{-/-}$ model.

We have previously shown the effectiveness of doxycycline to prevent the formation of AAA induced by AngII in TgNOR-1^{VSMC} mice.[8] Interestingly, as shown in Supplemental Figure S2, this effect is associated with the normalization of *Th* expression to values similar to those of control animals. In view of these data, we sought to determine whether the up-regulation of vascular TH might play an active role in AAA pathophysiology. For this purpose, α-methyl-*p*-tyrosine (AMPT), a specific inhibitor of TH, was administered to AngII-infused ApoE$^{-/-}$ mice and aneurysm progression was monitored by ultrasonography thorough the experimental period. Interestingly, AMPT protected against AAA formation in this model, limiting the progressive increase in aortic diameter evoked by the challenge with AngII (Figure 3A-C). While 80% of ApoE$^{-/-}$ mice infused with AngII developed aneurysms, AMPT substantially reduced this percentage to less than 10%, (Figure 3D) and avoided the

development of the most severe and complicated forms of AAA (Figure 3E). A slight improvement in the survival rate was detected in AMPT-treated mice although it did not reach statistical significance (Supplemental Figure S3A). The impact of AMPT was independent of hemodynamic effects, since this drug did not significantly affected the AngII-induced increase in blood pressure (Figure 3F). Neither body weight nor plasma lipid profile were modified by this intervention (Supplemental Table S3). Likewise, AMPT did not alter circulating levels of aspartate and alanine transaminases or those of creatinine in AngII-infused ApoE$^{-/-}$ mice, while significantly normalized blood urea nitrogen levels to values similar to those of control animals (Supplemental Figure S4A). Concerning vascular phenotype, AngII-infused ApoE$^{-/-}$ mice subjected to AMPT treatment recapitulated most features of saline-infused animals (Figure 3G), preserving elastin integrity associated with normalized vascular MMP-2 expression and MMP activity (Figure 4A-C and Supplementary Figure S5). Further, in AngII-challenged mice, AMPT decreased the vascular expression of inflammatory markers such as EMR-1 and MCP-1 (Figure 4D-E), and the recruitment of macrophages, lymphocytes and neutrophils into the vessel wall (Supplementary Figure S5). Likewise, AMPT attenuated the rise in vascular oxidative stress induced by AngII (Figure 4F). These vascular effects were associated to the downregulation of *Th* in AMPT treated animals (Supplementary Figure S6A).

The increase in TH activity contributes to the enhanced susceptibility of TgNOR-1^{VSMC} mice to AAA

AMPT also protected against AAA formation in the AngII-infused TgNOR-1^{VSMC} mouse model, an effect that reached statistical significance at day 14 (Figure 5A-C). This drug reduced the AngII-mediated increase in aneurysm incidence in transgenic mice (Figure 5D) and led to the development of less severe forms of aneurysms (Figure 5E) without affecting blood pressure levels (Figure 4F) or body weight (not shown). As previously reported,[8] Ang-II infusion in TgNOR-1^{VSMC} mice led to the early death of about 20% of animals, while a slight although not significant attenuation of this response was found in AMPT-treated mice (Supplemental Figure 3B). Further, AMPT attenuated vascular remodeling (Figure 5G) and the disruption of elastin fibers found in challenged NOR-1 transgenic mice (Figure 6A). Concomitantly, in AMPT-treated animals, both MMP-2 expression and MMP activity (examined by *in situ* zymography) were comparable to that of control animals infused with AngII (Figure 6B-C). Similarly, AMPT completely prevented the increase in the vascular

expression of inflammatory markers (EMR1, MCP-1, IL-1β, IL-6 and CXCL2) (Figure 6D-H) and the infiltration of inflammatory cells (macrophages, lymphocytes and neutrophils) induced by AngII (Supplementary Figure S7). The TH inhibitor also avoided the enhanced vascular generation of O_2^- (Figure 5I) detected in AngII-infused mice. These vascular effects were associated to the downregulation of TH in AMPT treated animals (Supplementary Figure S6B).

NOR-1 modulates human *TH* expression in VSMC

Interestingly, in human aneurysms we found a significant correlation between NOR-1 expression and that of *TH, DBH,* and *SLC6A2* (Supplementary Figure S8). These results prompted us to investigate the underlying molecular mechanisms and the role played by NOR-1. Since *TH* has been shown to be regulated by Nurr1 (NR4A2) in non-vascular cells,[25,26] we addressed whether NOR-1 could directly modulate *TH* expression. *In silico* analysis of human *TH* proximal promoter identified two putative NBRE sites (Supplementary Figure S9A). Transient cotransfection of VSMC with a *TH* promoter-driven luciferase reporter construct and a NOR-1 expression vector evidenced that NOR-1 overexpression significantly increased *TH* transcriptional activity (Supplementary Figure S9B). Further, site-directed mutagenesis revealed the major contribution of the distal NBRE site (located at -2353 bp) to the NR4A-dependent T*H* regulation (Supplementary Figure S9B). Therefore, these data are consistent with a potential NOR-1-dependent regulation of TH in VSMC.

Discussion

The lack of pharmacological approaches to treat or prevent AAA is a great handicap for the management of this disease. AAA patients live for years under the sword of Damocles, fearing a fatal rupture. Here we uncover an instrumental role of the TH pathway on the pathophysiology of this disease, and suggest the rate-limiting enzyme TH as a potential pharmacological target.

Our data evidence that genes encoding for proteins involved in the TH pathway and the transport of norepinephrine are upregulated in human aneurysmal samples. Previous expression microarray studies suggested that gene pathways related to neuronal activity are enriched in human AAA samples.[27] In that study, however, the regulation of genes of the TH pathway did not reach statistical significance. Recently, data from a whole genome-expression profiling analysis of aortic tissues from AngII-infused TgNOR-1^{VSMC} mice evidenced that AAA are enriched in gene sets related to sympathetic activation.[8] Here, we

confirm (by real-time PCR) and expand these observations in two mouse models prone to develop AngII-induced aortic aneurysm, the ApoE knockout mouse and a NOR-1 transgenic mouse. In particular, we ascertain that the expression of TH is strongly induced in aneurysmal lesions from both humans and animal models. Noteworthy, the increase in TH vascular expression triggered by AngII in both mouse models is in line with previous data reporting the upregulation of TH by this peptide hormone in other tissues, both *in vivo* and *in vitro*.[28,29] These data suggested that TH activity could play an active role in AAA development and in the ability of AngII to promote aneurysm formation.

Different evidences suggest that catecholamines critically influence vascular remodeling. Indeed, recent data sustain that sympathetic hyperactivity underlies the pathophysiology of aortopathies such thoracic aortic dissection (TAD),[5,30] and both sympathetic hyperactivity and aortic sympathetic nerve sprouting have been documented in patients with TAD.[5] Further, AngII, the major effector of the renin-angiotensin system and a key player in AAA development,[31] increases sympathetic activity leading to the upregulation of aortic MMP2, which plays a critical role in the onset and progression of several aortopathies including AAA.[32] Moreover, Hu *et al.*[6] showed that catecholamines regulate TGFβ signaling in aortic aneurysms, limiting VSMC proliferation and fostering apoptosis, thereby modulating vascular remodeling. Interestingly, the TH pathway has been previously documented in the vascular wall, and TH expression has been demonstrated in VSMC, endothelial cells and regulatory T cells.[14,33-35] In lymphocytes, endogenous catecholamines act in an autocrine/paracrine manner regulating their own activity,[13,14,35] while catecholamines released from endothelial cells could contribute to neovascularization.[34] In agreement, our studies in human and mouse aneurysms detected TH immunostaining localized to peripheral innervations but also to inflammatory cells and VSMC. Interestingly, we observe that the effectiveness of doxycycline to prevent the formation of AAA induced by AngII in TgNOR-1^{VSMC} mice[8] is associated with the normalization of vascular *Th* expression. Doxycycline is a MMP inhibitor which prevents the formation of experimental AAA in animal models,[36] and reduced vascular inflammation in clinical trials.[37] Therefore, the upregulation of the TH pathway could contribute to the destructive remodeling in AAA. However, the impact of this pathway on AAA formation remains unclear, and its potential as a therapeutic target for this disease has not been explored.

In ligth of these data, we tested the efficacy of TH blockade limiting AAA growth. AngII-infused ApoE$^{-/-}$ and TgNOR-1^{VSMC} mice were treated with AMPT, an orally available and well-tolerated competitive inhibitor of TH, which blocks catecholamine biosynthesis.[38,39]

This drug was administered at a dosage regimen that assured an effective inhibition of the enzyme.[40] Notably, under these conditions, AMPT largely protected from AngII-induced AAA in both experimental models. In the clinical setting, AMPT has only been approved for the control of hypertension and other symptoms associated with the excess of catecholamines produced by pheochromocytoma. In particular, AMPT is indicated for the preoperative preparation of patients referred for tumor surgery, thereby reducing its high perioperative mortality, for the management of those patients for whom surgery is contraindicated, and for the chronic treatment of malignant pheochromocytomas.[41] Further, this drug has also been proposed for the management of movement disorders and some neuropsychiatric diseases.[42] In patients with pheochromocytoma, AMPT limits the hypertensive response evoked by the catecholamine-producing tumor; however, no beneficial effect has been recognized for this drug on essential hypertension.[42] Similarly, in our hands AMPT did not affect blood pressure. Thus, targeting TH, this drug prevents AngII-induced AAA by impairing the vascular activity of AngII that promotes AAA formation, which has previously been shown to be largely independent of the AngII vasopressor function.[43] AMPT not only limited aortic diameter expansion, but also inflammation and vascular oxidative stress and preserved vascular wall integrity. TH activity has been associated with the generation of ROS and oxidative stress,[44,45] and inflammation.[46] Accordingly, in experimental models of AAA, we found that AMPT significantly attenuated vascular oxidative stress, reduced the immune infiltrate and improved the expression profile of proinflammatory cytokines, thus suggesting that TH upregulation could account, at least in part, to the pathophysiology of AAA. Consistently, previous reports have suggested that AMPT ameliorates oxidative stress and inflammation in other pathological settings.[47-49] Noteworthy, these vascular effects were associated to the downregulation of TH in AMPT treated animals. Therefore, our data indicate that TH upregulation negatively impact on AAA formation and support the potential of targeting this enzyme in AAA.

The regulation of TH expression is complex and cell type-specific.[25] Previous studies in non-vascular tissues identified *TH* as a target gene for the nuclear receptor Nurr1 (NR4A2). Surprisingly, Nurr1 transactivates or represses *TH* transcription (depending on cell-type).[26,50,51] Whether other members of the NR4A family, and specifically NOR-1 (NR4A3), that is upregulated in human AAA and contributes to vascular remodeling,[52,53] could also target *TH* is uncertain. We show that, in human AAA, NOR-1 expression significantly correlates with that of genes involved in the control of sympathetic activity including *TH*. Further, by transient transfection assays we identified two NBRE sites, in

particular one located at -2353 bp, responsible for the transcriptional regulation of human *TH* by NOR-1. Interestingly, despite the human *TH* promoter show low homology with *TH* promoters from other species this NBRE site is conserved among species (Supplementary Figure S10).[54]

Finally, interestingly enough, several case reports have described the coexistence of pheochromocytoma and other neuroendocrine tumors with aortic dissections and aneurysm rupture supporting that TH pathway hyperactivity might contribute to aneurysm development and eventually aortic rupture in these patients.[55-57] Further, high TH and both overall and regional aortic sympathetic nervous system activities have been documented in patients with TAD.[5] Our study evidences for the first time, that the upregulation oh the TH pathway could be critical in the pathophysiology of AAA, both in humans and animal experimental models, and supports the therapeutic potential of approaches based on targeting this pathway for the medical management of AAA.

Acknowledgements

We thank Silvia Aguiló for her technical assistance.

Sources of funding

This work was supported by the Spanish Ministerio de Ciencia e Innovación - Instituto de Salud Carlos III (ISCIII) [RTI2018-094727-B-100, PI18/0919], the Agència de Gestió d'Ajuts Universitaris i de Recerca (AGAUR) (2017-SGR-00333), and Sociedad Española de Arteriosclerosis (SEA-2019). The study was co-founded by Fondo Europeo de Desarrollo Regional (FEDER), a way to make Europe. L.C. and C.B-S were supported by a FI (AGAUR) and a FPU fellowship (Ministerio de Universidades), respectively.

Disclosures

None

References

1. Nordon IM, Hinchliffe RJ, Loftus IM, Thompson MM. Pathophysiology and epidemiology of abdominal aortic aneurysms. *Nat. Rev. Cardiol.* 2011;8:92-102.
2. Mozaffarian D, Benjamin EJ, Go AS, Arnett DK, Blaha MJ, Cushman M, de Ferranti S, Després JP, Fullerton HJ, Howard VJ, Huffman MD, Judd SE, Kissela BM, Lackland DT, Lichtman JH, Lisabeth LD, Liu S, Mackey RH, Matchar DB, McGuire DK, Mohler ER 3rd,

Moy CS, Muntner P, Mussolino ME, Nasir K, Neumar RW, Nichol G, Palaniappan L, Pandey DK, Reeves MJ, Rodriguez CJ, Sorlie PD, Stein J, Towfighi A, Turan TN, Virani SS, Willey JZ, Woo D, Yeh RW, Turner MB; American Heart Association Statistics Committee and Stroke Statistics Subcommittee. Heart disease and stroke statistics–2015 update: a report from the American Heart Association. *Circulation*. 2015;131:e29–322.

3. Golledge J. Abdominal aortic aneurysm: update on pathogenesis and medical treatments. *Nat. Rev. Cardiol*. 2019;16:225-242.
4. Grassi G, Seravalle G, Mancia G. Sympathetic activation in cardiovascular disease: evidence, clinical impact and therapeutic implications. *Eur. J. Clin. Invest*. 2015;45:1367-1375.
5. Zhipeng H, Zhiwei W, Lilei Y, Hao Z, Hongbing W, Zongli R, Hao C, Xiaoping H. Sympathetic hyperactivity and aortic sympathetic nerve sprouting in patients with thoracic aortic dissection. *Ann. Vasc. Surg*. 2014;28:1243-8.
6. Hu Z, Li B, Wang Z, Hu X, Zhang M, Chen R, Wu Q, Jia F. The sympathetic transmitter norepinephrine inhibits VSMC proliferation induced by TGFβ by suppressing the expression of the TGFβ receptor ALK5 in aorta remodeling. *Mol. Med. Rep*. 2020;22:387-397.
7. Rodríguez-Calvo R, Guadall A, Calvayrac O, Navarro MA, Alonso J, Ferrán B, de Diego A, Muniesa P, Osada J, Rodríguez C, Martínez-González J. Over-expression of neuron-derived orphan receptor-1 (NOR-1) exacerbates neointimal hyperplasia after vascular injury. *Hum. Mol. Genet*. 2013;22:1949-1959.
8. Cañes L, Martí-Pàmies I, Ballester-Servera C, Alonso J, Serrano E, Briones AM, Rodríguez C, Martínez-González J. High neuron derived orphan receptor-1 (NOR-1) expression strengthens the vascular wall response to angiotensin II leading to aneurysm formation in mice. *Hypertension* 2021 (*In press*).
9. Tank AW, Lee Wong D. Peripheral and central effects of circulating catecholamines. *Compr. Physiol*. 2015;5:1-15.
10. Zhou QY, Quaife CJ, Palmiter RD. Targeted disruption of the tyrosine hydroxylase gene reveals that catecholamines are required for mouse fetal development. *Nature*. 1995;374:640-643.
11. López-Sánchez C, Bártulos O, Martínez-Campos E, Gañán C, Valenciano AI, García-Martínez V, De Pablo F, Hernández-Sánchez C. Tyrosine hydroxylase is expressed during early heart development and is required for cardiac chamber formation. *Cardiovasc. Res*. 2010;88:111-120.

12. Vázquez P, Robles AM, de Pablo F, Hernández-Sánchez C. Non-neural tyrosine hydroxylase, via modulation of endocrine pancreatic precursors, is required for normal development of beta cells in the mouse pancreas. *Diabetologia*. 2014;57:2339-2347.
13. Bergquist J, Tarkowski A, Ekman R, Ewing A. Discovery of endogenous catecholamines in lymphocytes and evidence for catecholamine regulation of lymphocyte function via an autocrine loop. *Proc. Natl. Acad. Sci. USA*. 1994;91:12912-12916.
14. Cosentino M1, Fietta AM, Ferrari M, Rasini E, Bombelli R, Carcano E, Saporiti F, Meloni F, Marino F, Lecchini S. Human CD4+CD25+ regulatory T cells selectively express tyrosine hydroxylase and contain endogenous catecholamines subserving an autocrine/paracrine inhibitory functional loop. *Blood*. 2007;109:632-642.
15. Lenartowski R, Goc A. Epigenetic, transcriptional and posttranscriptional regulation of the tyrosine hydroxylase gene. *Int. J. Dev. Neurosci*. 2011;29:873-883.
16. Tekin I, Roskoski R Jr, Carkaci-Salli N, Vrana KE. Complex molecular regulation of tyrosine hydroxylase. *J. Neural. Transm. (Vienna)*. 2014;121:1451-1481.
17. Waløen K, Kleppe R, Martinez A, Haavik J. Tyrosine and tryptophan hydroxylases as therapeutic targets in human disease. *Expert. Opin. Ther. Targets*. 2017;21:167-180.
18. Orriols M, Varona S, Martí-Pàmies I, Galán M, Guadall A, Escudero JR, Martín-Ventura JL, Camacho M, Vila L, Martínez-González J, Rodríguez C. Down-regulation of Fibulin-5 is associated with aortic dilation: role of inflammation and epigenetics. *Cardiovasc. Res*. 2016;110:431-442.
19. Alonso J, Galán M, Martí-Pàmies I, Romero JM, Camacho M, Rodríguez C, Martínez-González J. NOR-1/NR4A3 regulates the cellular inhibitor of apoptosis 2 (cIAP2) in vascular cells: role in the survival response to hypoxic stress. *Sci. Rep*. 2016;6:34056.
20. Cañes L, Martí-Pàmies I, Ballester-Servera C, Herraiz-Martínez A, Alonso J, Galán M, Nistal JF, Muniesa P, Osada J, Hove-Madsen L, Rodríguez C, Martínez-González J. Neuron-derived orphan receptor-1 modulates cardiac gene expression and exacerbates angiotensin II-induced cardiac hypertrophy. *Clin Sci (Lond)*. 2020;134:359-377.
21. Galán M, Varona S, Orriols M, Rodríguez JA, Aguiló S, Dilmé J, Camacho M, Martínez-González J, Rodriguez C. Induction of histone deacetylases (HDACs) in human abdominal aortic aneurysm: therapeutic potential of HDAC inhibitors. *Dis. Model. Mech*. 2016;9:541-552.
22. Manning MW, Cassis LA, Daugherty A. Differential effects of doxycycline, a broad-spectrum matrix metalloproteinase inhibitor, on angiotensin II-induced atherosclerosis and abdominal aortic aneurysms. *Arterioscler. Thromb. Vasc. Biol*. 2003;23:483-488.

23. Martínez-Revelles S, García-Redondo AB, Avendaño MS, Varona S, Palao T, Orriols M, Roque FR, Fortuño A, Touyz RM, Martínez-González J, Salaices M, Rodríguez C, Briones AM. Lysyl oxidase induces vascular oxidative stress and contributes to arterial stiffness and abnormal elastin structure in hypertension: role of p38MAPK. *Antioxid. Redox Signal*. 2017;27:379-397.

24. Alonso J, Cañes L, García-Redondo AB, de Frutos PG, Rodríguez C, Martínez-González J. The nuclear receptor NOR-1 modulates redox homeostasis in human vascular smooth muscle cells. *J. Mol. Cell. Cardiol*. 2018;122:23-33.

25. Kim TE, Park MJ, Choi EJ, Lee HS, Lee SH, Yoon SH, Oh CK, Lee BJ, Kim SU, Lee YS, Lee MA. Cloning and cell type-specific regulation of the human tyrosine hydroxylase gene promoter. *Biochem. Biophys. Res. Commun*. 2003;312:1123-1131.

26. Sakurada K, Ohshima-Sakurada M, Palmer TD, Gage FH. Nurr1, an orphan nuclear receptor, is a transcriptional activator of endogenous tyrosine hydroxylase in neural progenitor cells derived from the adult brain. *Development*. 1999;126:4017-4026.

27. Lenk GM, Tromp G, Weinsheimer S, Gatalica Z, Berguer R, Kuivaniemi H. Whole genome expression profiling reveals a significant role for immune function in human abdominal aortic aneurysms. *BMC Genomics*. 2007;8:237.

28. Dogan MD1, Sumners C, Broxson CS, Clark N, Tümer N. Central angiotensin II increases biosynthesis of tyrosine hydroxylase in the rat adrenal medulla. *Biochem. Biophys. Res. Commun*. 2004;313:623-626.

29. Ma FY, Grattan DR, Bobrovskaya L, Dunkley PR, Bunn SJ. Angiotensin II regulates tyrosine hydroxylase activity and mRNA expression in rat mediobasal hypothalamic cultures: the role of specific protein kinases. *J. Neurochem*. 2004;90:431-441.

30. Hu R, Wang Z, Ren Z, Liu M. Autonomic remodeling may be responsible for decreased incidence of aortic dissection in STZ-induced diabetic rats via down-regulation of matrix metalloprotease 2. *BMC Cardiovasc. Disord*. 2016;16:200.

31. Hackam DG, Thiruchelvam D, Redelmeier DA. Angiotensin-converting enzyme inhibitors and aortic rupture: a population-based case-control study. *Lancet*. 2006; 368:659-665.

32. Hu Z, Wang Z, Wu H, Yang Z, Jiang W, Li L, Hu X. Ang II enhances noradrenaline release from sympathetic nerve endings thus contributing to the up-regulation of metalloprotease-2 in aortic dissection patients' aorta wall. *PLoS On*e. 2013;8:e76922.

33. Pfeil U, Kuncova J, Brüggmann D, Paddenberg R, Rafiq A, Henrich M, Weigand MA, Schlüter KD, Mewe M, Middendorff R, Slavikova J, Kummer W. Intrinsic vascular

dopamine - a key modulator of hypoxia-induced vasodilatation in splanchnic vessels. *J. Physiol*. 2014;592:1745-1756.

34. Sorriento D, Santulli G, Del Giudice C, Anastasio A, Trimarco B, Iaccarino G. Endothelial cells are able to synthesize and release catecholamines both in vitro and in vivo. *Hypertension*. 2012;60:129-136.
35. Huang HW, Zuo C, Chen X, Peng YP, Qiu YH. Effect of tyrosine hydroxylase overexpression in lymphocytes on the differentiation and function of T helper cells. *Int. J. Mol. Med*. 2016;38:635-642.
36. Dodd BR, Spence RA. Doxycycline inhibition of abdominal aortic aneurysm growth – a systematic review of the literature. *Curr. Vasc. Pharmacol*. 2011;9:471-478.
37. Baxter BT, Matsumura J, Curci JA, McBride R, Larson L, Blackwelder W, Lam D, Wijesinha M, Terrin M; N-TA3CT Investigators. Effect of doxycycline on aneurysm growth among patients with small infrarenal abdominal aortic aneurysms: a randomized clinical trial. *JAMA*. 2020;323:2029-2038.
38. Brogden RN, Heel RC, Speight TM, Avery GS. α-Methyl-*p*-tyrosine: A review of its pharmacology and clinical use. *Drugs*. 1981;21:81-89.
39. Naruse M, Satoh F, Tanabe A, Okamoto T, Ichihara A, Tsuiki M, Katabami T, Nomura M, Tanaka T, Matsuda T, Imai T, Yamada M, Harada T, Kawata N, Takekoshi K. Efficacy and safety of metyrosine in pheochromocytoma/paraganglioma: a multi-center trial in Japan. *Endocr. J*. 2018;65:359-371.
40. Meltzer HY, Fessler RG, Simonovic M, Doherty J, Fang VS. Effect of d- and l-amphetamine on rat plasma prolactin levels. *Psychopharmacology (Berl)*. 1979;61:63-69.
41. DEMSER (metyrosine) capsule. FDA prescribing information. https://www.drugs.com/pro/demser.html. Accessed October 31 2016.
42. Bloemen OJ, de Koning MB, E. Boot E, Booij J, van Amelsvoort TA. Challenge and therapeutic studies using alpha-methyl-para-tyrosine (AMPT) in neuropsychiatric disorders: a review. *Cent. Nerv. Syst. Agents Med. Chem*. 2008;8:249-256.
43. Cassis LA, Gupte M, Thayer S, Zhang X, Charnigo R, Howatt DA, Rateri DL, Daugherty A. ANG II infusion promotes abdominal aortic aneurysms independent of increased blood pressure in hypercholesterolemic mice. *Am. J. Physiol. Heart Circ. Physiol*. 2009;296:H1660-H1665.
44. Haavik J, Almås B, Flatmark T. Generation of reactive oxygen species by tyrosine hydroxylase: a possible contribution to the degeneration of dopaminergic neurons? *J. Neurochem*. 1997;68:328-332.

45. Meiser, J., Weindl, D. & Hiller, K. Complexity of dopamine metabolism. *Cell. Commun. Signal*. 2013;11:34.

46. Tolleson C, Claassen D. The function of tyrosine hydroxylase in the normal and Parkinsonian brain. *CNS Neurol. Disord. Drug Targets*. 2012;11:381-386.

47. Çimen O, Çimen FK, Gülaboğlu M, Bilgin AÖ, Çekiç AB, Eken H, Süleyman Z, Bilgin Y, Altuner D. The effect of metyrosine on oxidative gastric damage induced by ischemia/reperfusion in rats. Biochemical and histopathological evaluation. *Acta Cir. Bras*. 33:259-267.

48. Ahiskalioglu A, Ince I, Aksoy M, Ahiskalioglu EO, Comez M, Dostbil A, Celik M, Alp HH, Coskun R, Taghizadehghalehjoughi A, Suleyman B. Comparative investigation of protective effects of metyrosine and metoprolol against ketamine cardiotoxicity in rats. *Cardiovasc. Toxicol*. 2015;15:336-344.

49. Albayrak A, Polat B, Cadirci E, Hacimuftuoglu A, Halici Z, Gulapoglu M, Albayrak F, Suleyman H. Gastric anti-ulcerative and anti-inflammatory activity of metyrosine in rats. *Pharmacol. Rep*. 2010;62:113-119.

50. Kim KS, Kim CH, Hwang DY, Seo H, Chung S, Hong SJ, Lim JK, Anderson T, Isacson O. Orphan nuclear receptor Nurr1 directly transactivates the promoter activity of the tyrosine hydroxylase gene in a cell-specific manner. *J. Neurochem*. 2003;85:622-634.

51. Kim TE, Seo JS, Yang JW, Kim MW, Kausar R, Joe E, Kim BY, Lee MA. Nurr1 represses tyrosine hydroxylase expression via SIRT1 in human neural stem cells. *PLoS One*. 2013;8:e71469.

52. Martínez-González J, Rius J, Castelló A, Cases-Langhoff C, Badimon L. Neuron-derived orphan receptor-1 (NOR-1) modulates vascular smooth muscle cell proliferation. *Circ. Res*. 2003;92:96-103.

53. Martínez-González J, Badimon L. The NR4A subfamily of nuclear receptors: new early genes regulated by growth factors in vascular cells. *Cardiovasc. Res*. 2005;65:609-618.

54. Kessler MA, Yang M, Gollomp KL, Jin H, Iacovitti L. The human tyrosine hydroxylase gene promoter. *Brain Res. Mol. Brain Res*. 2003;112:8-23.

55. Ehata T, Karasawa F, Watanabe K, Satoh T. Unsuspected pheochromocytoma with abdominal aortic aneurysm--a case report. *Acta Anaesthesiol. Sin*. 1999;37:27-28.

56. Kota SK, Meher LK, Jammula S, Mohapatra S, Modi KD. Coexistence of pheochromocytoma with abdominal aortic aneurysm: an untold association. *Ann. Med. Health Sci. Res*. 2013; 3: 258-261.

57. Arıkan AA. Ruptured abdominal aortic aneurysm with a suprarenal tumor. *Braz. J. Cardiovasc. Surg*. 2018;33:522-524.

FIGURE LEGENDS

Figure 1. TH is upregulated in human AAA. A-C) *TH* (A), *DBH* (B) and *SLC6A2* (C) mRNA levels were analyzed in abdominal aorta from patients with AAA (n= 84) and healthy donors (Do; n= 16) by real time-PCR. Data are mean ± SEM. $P< 0.01$; *, *vs*. Donors. **D)** TH protein levels were evaluated by Western blot in aortic lysates from these samples. The immunoblot densitometric analysis is shown on right. Data are mean ± SEM (Donors, n= 10; AAA, n= 14). $P< 0.0001$; *, *vs*. Donors. **E)** Immunohistochemical analysis of TH expression in abdominal aorta sections from patients with AAA and donors. The indicated areas are magnified in lower panels (Bars: 100 µm [upper panels] and 50 µm [lower panels]). Arrowheads indicate TH positive cells (black: inflammatory cells; red: VSMC). Red arrows show positive staining in peripheral nerve endings. Mann-Whitney (A-C) and t-test (D).

Figure 2. TH is up-regulated in the aneurysmal abdominal aorta from experimental models of AAA. A) *Th*, *Dbh*, *Ddc* and *Slc6a2* mRNA levels analyzed by real-time PCR in abdominal aorta samples from ApoE$^{-/-}$ mice infused with Saline (white bars) or AngII (black bars; 1000 ng/kg/min) for 28 days. Data, normalized to GADPH expression, are expressed as mean ± SEM (Saline-infused ApoE$^{-/-}$ mice, n= 14; AngII-infused ApoE$^{-/-}$ mice, n= 15). $P< 0.05$; *, *vs*. Saline-infused mice. **B)** Wild-type (WT; white bars) and TgNOR-1^{VSMC} (Tg^{VSMC}; black bars) mice were infused with AngII for 28 days. *Th*, *Dbh, Ddc* and *Slc6a2* mRNA levels in abdominal aortas from each experimental group are shown. Data are mean ± SEM (WT mice, n= 10; TgNOR-1^{VSMC} mice, n= 15). $P< 0.001$; *, *vs*. WT mice. **C** and **D)** TH protein levels assessed by Western blot in aortic lysates from ApoE$^{-/-}$ mice infused with Saline or AngII (C) or in AngII-infused WT and TgNOR-1^{VSMC} (D). Data are expressed as mean ± SEM (Saline-infused ApoE$^{-/-}$ mice, n= 9; AngII-infused ApoE$^{-/-}$ animals, n= 15; AngII-infused WT and TgNOR-1^{VSMC}mice, n= 7). $P< 0.05$; *, *vs*. Saline-infused ApoE$^{-/-}$ or AngII-infused WT mice. Levels of β-actin are shown as a loading control. Protein size was

estimated by the indicated position of molecular weight markers. **E)** Representative immunohistochemical analysis for TH in abdominal aortas from each experimental group. Black and red arrowheads indicate TH positive cells in inflammatory cells and VSMC, respectively, while red arrows marks the positive staining of peripheral nerve endings. The indicated areas are magnified in righ panels (Bars: 50 μm). Mann-Whitney test.

Figure 3. AMPT prevents aneurysm development in the abdominal aorta from AngII-infused ApoE$^{-/-}$ mice. ApoE$^{-/-}$ mice were infused with Saline or AngII (1000 ng/kg/min) for 28 days. AngII-infused mice were treated or not with α-methyl-*p*-tyrosine (AMPT; 100 mg/Kg twice daily, i.p). **A)** Representative images of excised aortas from each experimental group. **B)** Abdominal aortic diameter assessed by ultrasonography. Data are mean ± SEM (Saline, n= 9; AngII-infused groups, n= 15). $P< 0.05$; *, *vs*. t0 for each experimental condition; #, *vs*. Saline-infused mice; $, *vs*. AngII-infused ApoE$^{-/-}$ mice non-treated with AMPT. **C)** Representative images of the ultrasonographic analysis. Transversal and longitudinal images are shown and the aortic diameter is traced with a yellow line. **D** and **E)** Incidence (D) and severity (E; based on Manning scale) of AAA in AngII-infused ApoE$^{-/-}$ mice treated or not with AMPT. $P< 0.05$; $, *vs*. AngII-infused ApoE$^{-/-}$ mice non-treated with AMPT (n as indicated in B). **F)** Blood pressure levels. Data are mean ± SEM (n as indicated in B). $P< 0.05$; *, *vs*. t0 for each experimental condition; #, *vs*. Saline-infused mice **G)** Representative hematoxylin-eosin staining of abdominal aortic sections from AngII-infused mice (Bars: 500 μm). Two-way ANOVA with repeated measures (**B** and **F**) and chi-square (**D**).

Figure 4. AMPT preserves elastin integrity and ameliorates vascular inflammation and oxidative stress induced by AngII in aorta from ApoE$^{-/-}$ mice. ApoE$^{-/-}$ mice were infused

with Saline or AngII (1000 ng/kg/min) for 28 days. AngII-infused mice were treated or not with α-methyl-*p*-tyrosine (AMPT; 100 mg/Kg twice daily, i.p). **A)** Orcein staining of abdominal aortas from Saline and AngII-infused ApoE$^{-/-}$ mice. Arrowheads mark elastin fibers ruptures. The indicated areas are magnified in lower panels (Bars: 100 μm). Quantification of the number of ruptures in elastin fibers *per* aortic section for each group. Data are mean ± SEM (Saline, n= 5; AngII-infused groups, n= 8). $P< 0.05$; *, *vs*. Saline-infused animals; # *vs*. AngII-infused ApoE$^{-/-}$ mice non-treated with AMPT. **B)** MMP activity *per* aortic section assessed by *in situ* zymography. Representative images are shown (Bars: 50 μm). Data are mean ± SEM (n= 8). $P< 0.05$; *, *vs*. AngII-infused ApoE$^{-/-}$ mice; #, *vs*. AngII-infused ApoE$^{-/-}$ animals non-treated with AMPT. **C-E)** mRNA levels of *Mmp2* (C), *Emr1* (D), *Mcp1* (E), analyzed by real-time PCR in abdominal aortas from AngII-treated mice. Data, normalized to *Gapdh* expression, are expressed as mean ± SEM (Saline, n= 9; AngII-infused groups, n= 10). $P< 0.05$; *, *vs*. Saline-infused ApoE$^{-/-}$ mice; #, *vs*. AngII-infused ApoE$^{-/-}$ mice non-treated with AMPT. **F)** Vascular superoxide anion production visualized by DHE staining in aortic sections from each group. Representative images are shown (Bars: 50 μm). Data are represented as mean ± SEM (n= 8). $P< 0.05$; *, *vs*. Saline-infused ApoE$^{-/-}$ mice; #, *vs*. AngII-infused ApoE$^{-/-}$ mice non-treated with AMPT. One-way ANOVA or Kruskal–Wallis test.

Figure 5. AMPT prevents aneurysm formation in AngII-infused TgNOR-1^{VSMC} mice. Wild-type (WT) and TgNOR-1^{VSMC} mice were infused with AngII (1000 ng/kg/min) for 28 days). TgNOR-1^{VSMC} mice were treated or not with α-methyl-*p*-tyrosine (AMPT; 100 mg/Kg twice daily, i.p). **A)** Representative images of excised aortas from each experimental group. **B)** Assessment of abdominal aortic diameter by ultrasonography. Data are mean ± SEM (WT mice, n= 10; TgNOR-1^{VSMC} groups, n= 15). $P< 0.05$; *, *vs*. t0 for each experimental

condition; $, *vs*. WT mice; #, *vs*. TgNOR-1^{VSMC} mice non-treated with AMPT. **C)** Representative images of the ultrasonographic analysis in AngII-challenged mice at 28 days. Transversal and longitudinal images are shown and the aortic diameter is traced with a yellow line. **D** and **E)** Incidence (D) and severity (E; based on Manning scale) of AAA in challenged mice. $P< 0.05$; $, *vs*. WT mice; # *vs*. TgNOR-1^{VSMC} mice non-treated with AMPT (n as indicated in B). **F)** Blood pressure levels. Data are mean ± SEM (WT mice, n= 7; TgNOR-1^{VSMC} groups, n= 12). $P< 0.05$; *, *vs*. t=0 for each experimental condition. **G)** Representative hematoxylin-eosin staining of abdominal aortic sections from AngII-infused mice (Bars: 500 µm). Two-way ANOVA with repeated measures (**B** and **F**) and chi-square (**D**).

Figure 6. AMPT limits elastin fiber rupture and ameliorates the increased expression of inflammatory markers and oxidative stress induced by AngII in TgNOR-1^{VSMC} mice. Wild-type (WT) and TgNOR-1^{VSMC} mice were infused with AngII (1000 ng/kg/min) for 28 days. TgNOR-1^{VSMC} mice were treated or not with α-methyl-*p*-tyrosine (AMPT; 100 mg/Kg twice daily, i.p). **A)** Orcein staining of abdominal aortas from each experimental group. Arrowheads mark elastin fibers ruptures. The indicated areas are magnified in lower panels. Bars: 100 µm. Quantification of the number of ruptures in elastin fibers *per* aortic section for each group. Data are mean ± SEM (n= 7). $P< 0.05$; *, *vs*. WT mice; # *vs*. TgNOR-1^{VSMC} mice non-treated with AMPT. **B)** MMP activity *per* aortic section assessed by *in situ* zymography. Representative images are shown (Bars: 50 µm). Data are mean ± SEM (n= 6). $P< 0.05$; *, *vs*. WT mice; #, *vs*. TgNOR-1^{VSMC} mice non-treated with AMPT. **C-H)** mRNA levels of *Mmp2* (C), *Emr1* (D), *Mcp1* (E), *Il6* (F), *Il1β* (G) and *Cxcl2* (H) analyzed by real-time PCR in abdominal aortas from each experimental group. Data, normalized to *Gapdh* expression, are expressed as mean ± SEM (WT mice, n=10; TgNOR-1^{VSMC} groups, n= 15). $P< 0.01$; *, *vs*. WT mice; #, *vs*. TgNOR-1^{VSMC} mice non-treated with AMPT. **I)** Vascular superoxide

anion production visualized by DHE staining in aortic sections from each group. Representative images are shown (Bars: 50 μm). Data are represented as mean ± SEM (n= 6). $P< 0.05$; *, *vs*. WT mice; #, *vs*. TgNOR-1^{VSMC} mice non-treated with AMPT. One-way ANOVA (C-I) or Kruskal–Wallis test (A and B).

Figure 1

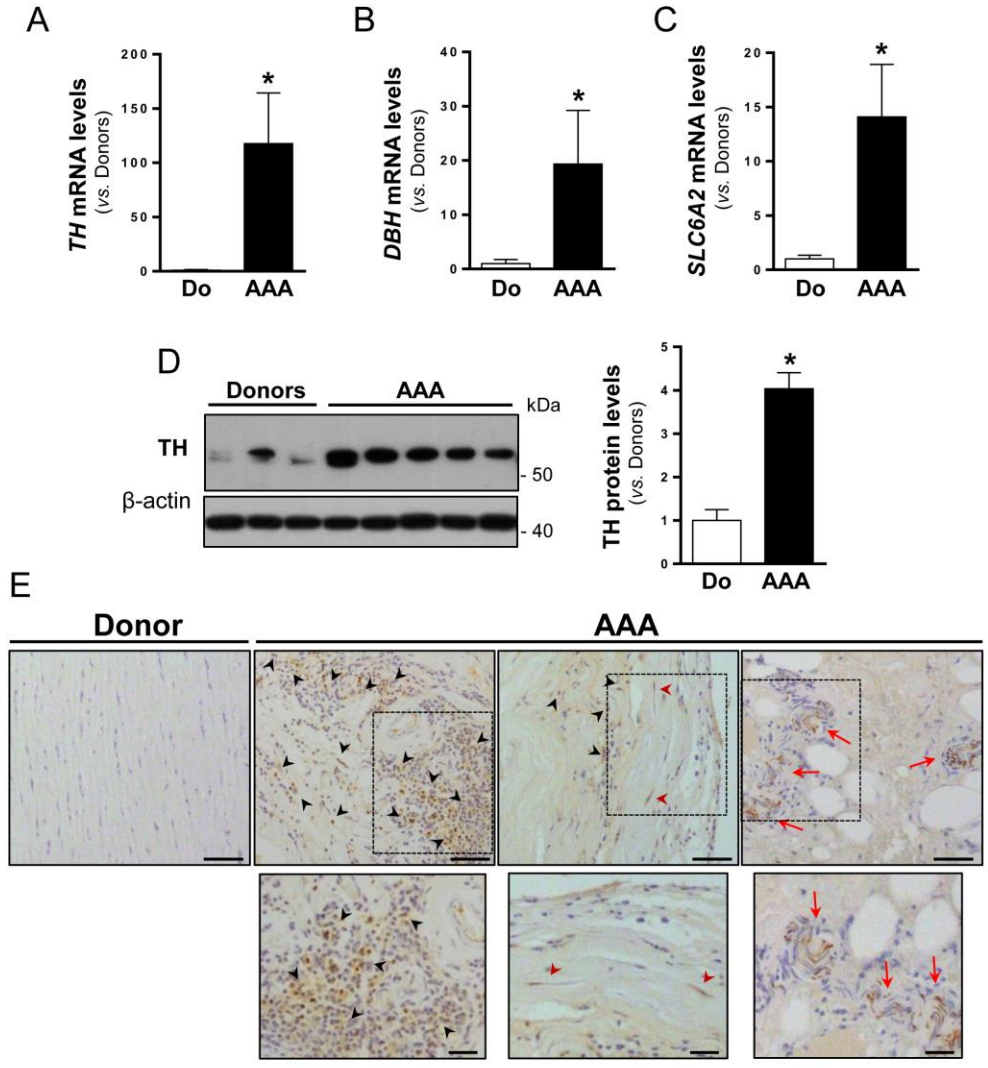
A
TH mRNA levels
(vs. Donors)
200
150
100
50
0
*
Do
AAA
B
DBH mRNA levels
(vs. Donors)
40
30
20
10
0
*
Do
AAA
C
SLC6A2 mRNA levels
(vs. Donors)
20
15
10
5
0
*
Do
AAA
D
Donors
AAA
kDa
TH
β-actin
50
40
TH protein levels
(vs. Donors)
5
4
3
2
1
0
*
Do
AAA
E
Donor
AAA

Figure 2

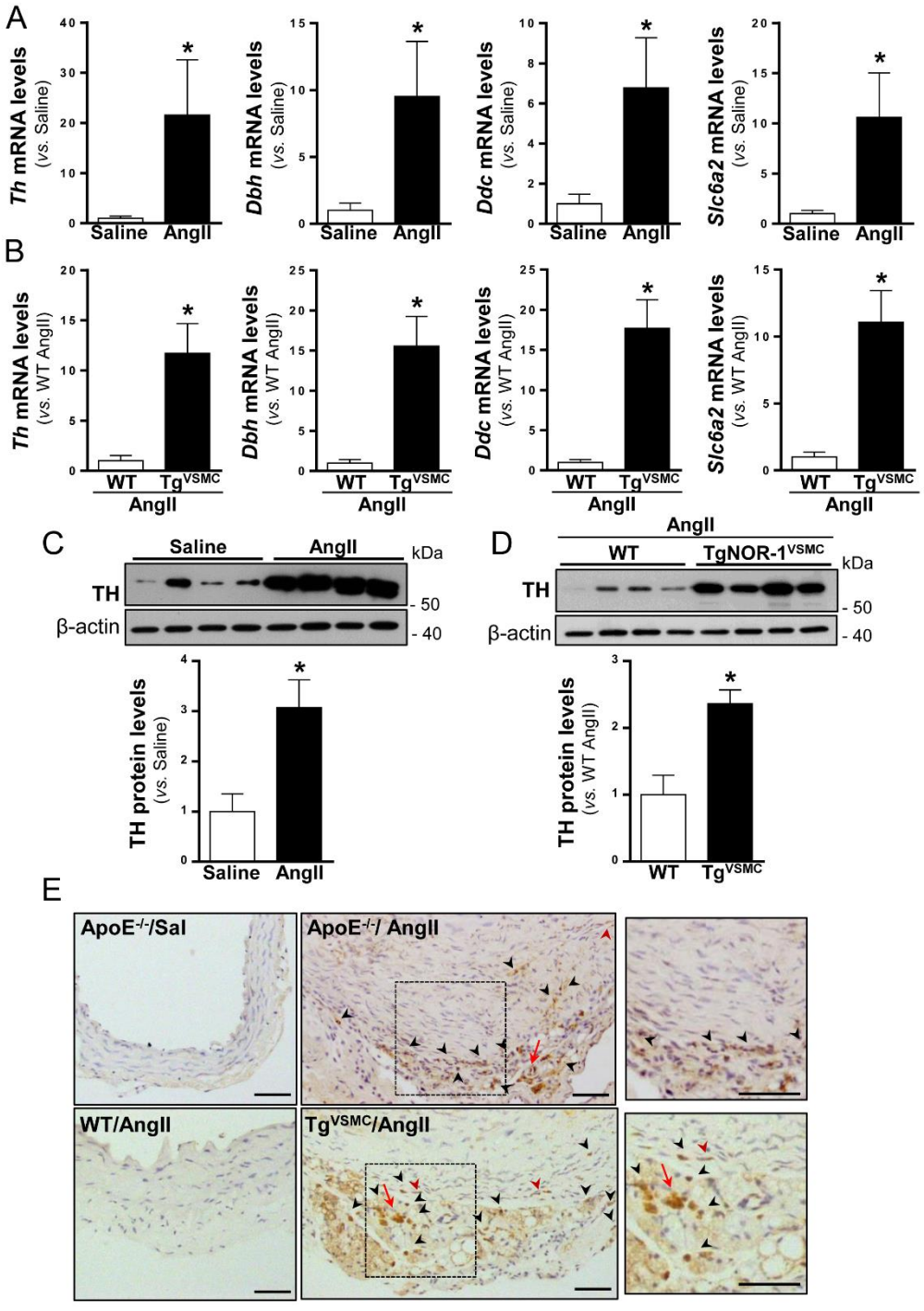
A
Th mRNA levels (vs. Saline)
Dbh mRNA levels (vs. Saline)
Ddc mRNA levels (vs. Saline)
Slc6a2 mRNA levels (vs. Saline)
Saline
AngII
B
Th mRNA levels (vs. WT AngII)
Dbh mRNA levels (vs. WT AngII)
Ddc mRNA levels (vs. WT AngII)
Slc6a2 mRNA levels (vs. WT AngII)
WT
TgVSMC
AngII
C
Saline
AngII
kDa
TH
β-actin
- 50
- 40
TH protein levels (vs. Saline)
D
AngII
WT
TgNOR-1VSMC
TH protein levels (vs. WT AngII)
E
ApoE-/-/Sal
ApoE-/-/ AngII
WT/AngII
TgVSMC/AngII

Figure 3

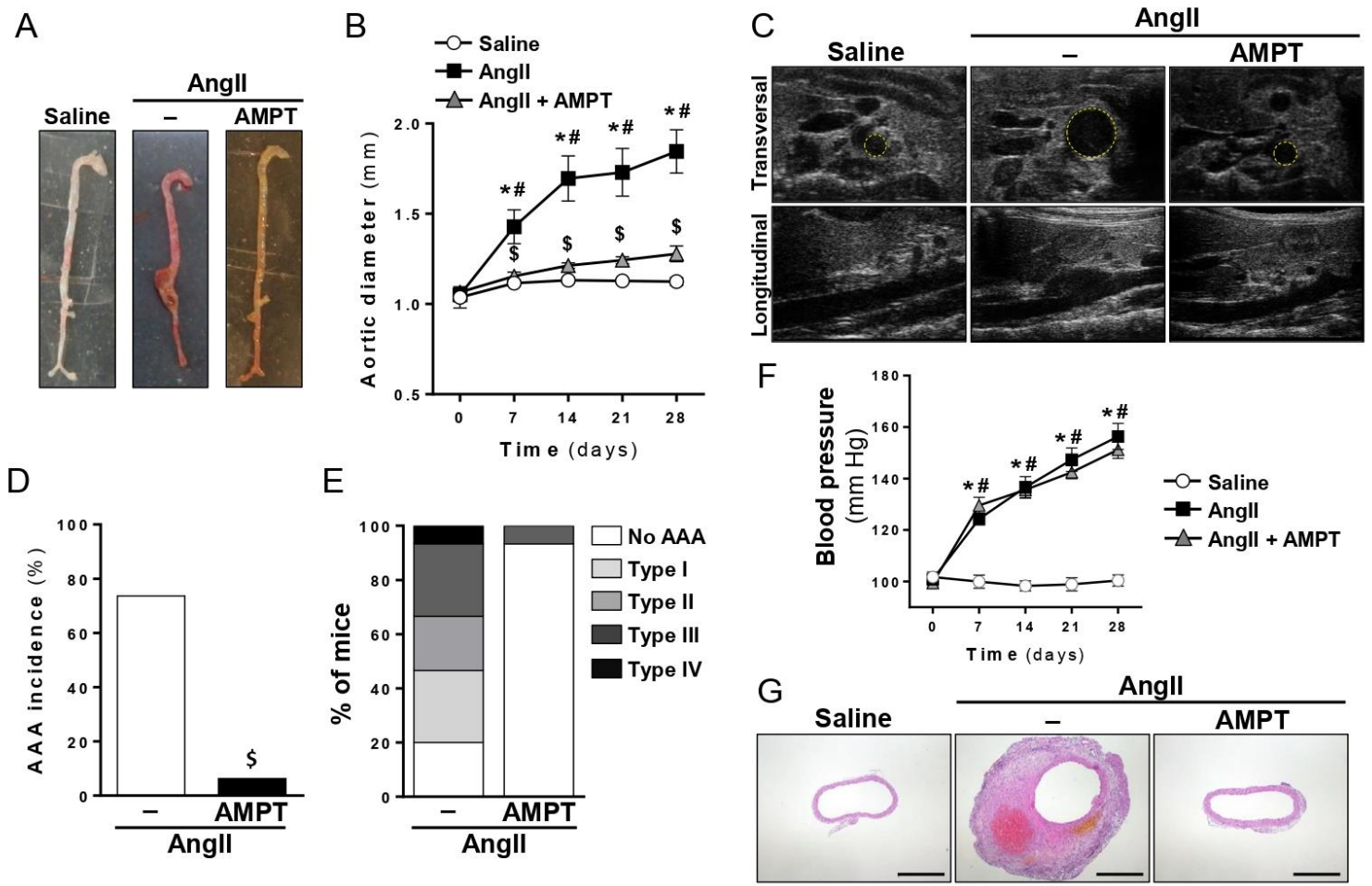
A
AngII
Saline
–
AMPT
B
Saline
AngII
AngII + AMPT
Aortic diameter (mm)
2.0
1.5
1.0
0.5
0
7
14
21
28
Time (days)
*#
$
C
AngII
Saline
–
AMPT
Transversal
Longitudinal
D
AAA incidence (%)
100
80
60
40
20
0
$
–
AMPT
AngII
E
% of mice
No AAA
Type I
Type II
Type III
Type IV
F
Blood pressure (mm Hg)
180
160
140
120
100
Saline
AngII
AngII + AMPT
G
AngII
Saline
–
AMPT

Figure 4

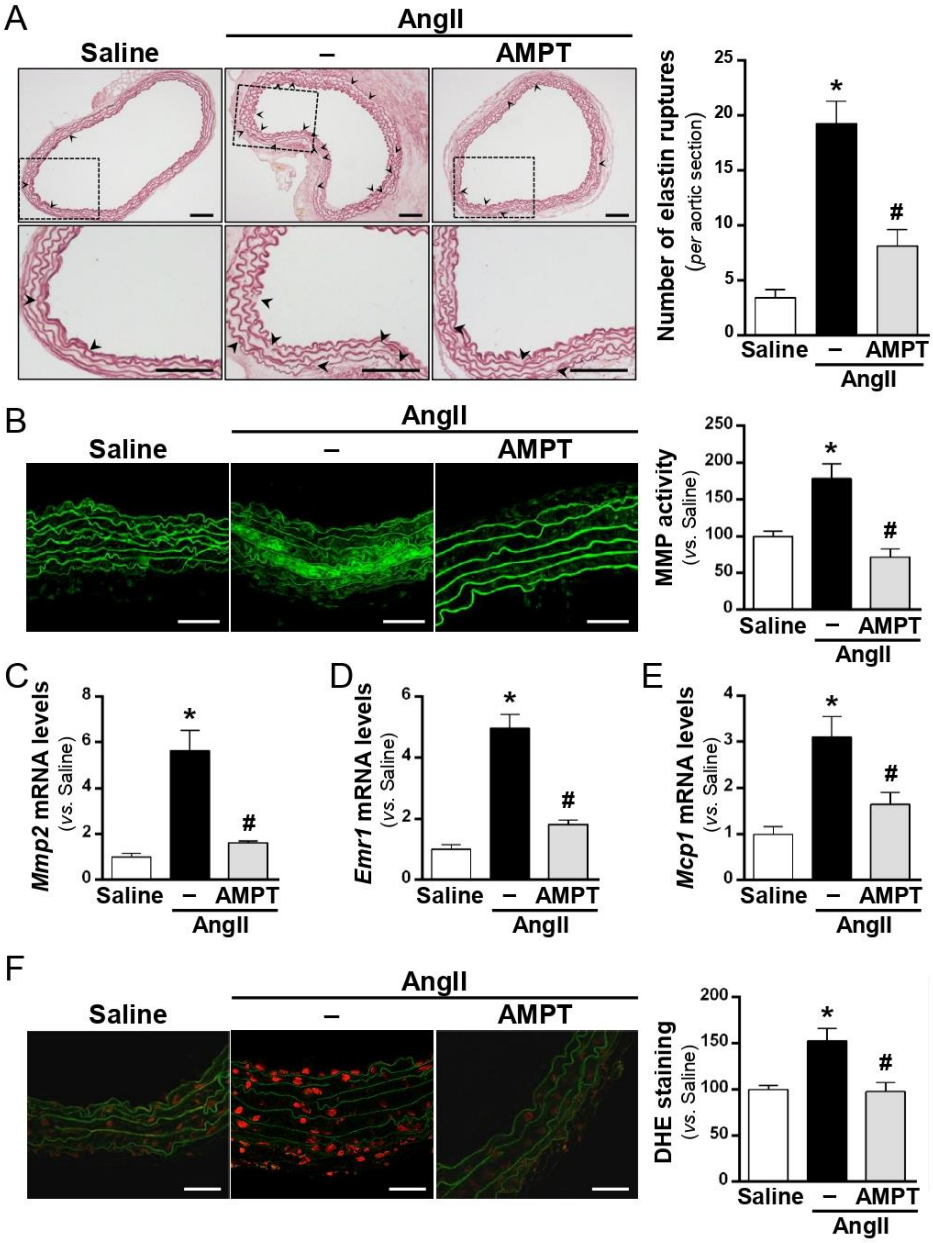
A
AngII
Saline
–
AMPT
Number of elastin ruptures
(per aortic section)
25
20
15
10
5
0
*
#
Saline
–
AMPT
AngII
B
AngII
Saline
–
AMPT
MMP activity
(vs. Saline)
250
200
150
100
50
0
*
#
Saline
–
AMPT
AngII
C
Mmp2 mRNA levels
(vs. Saline)
8
6
4
2
0
*
#
Saline
–
AMPT
AngII
D
Emr1 mRNA levels
(vs. Saline)
6
4
2
0
*
#
Saline
–
AMPT
AngII
E
Mcp1 mRNA levels
(vs. Saline)
4
3
2
1
0
*
#
Saline
–
AMPT
AngII
F
AngII
Saline
–
AMPT
DHE staining
(vs. Saline)
200
150
100
50
0
*
#
Saline
–
AMPT
AngII

Figure 5

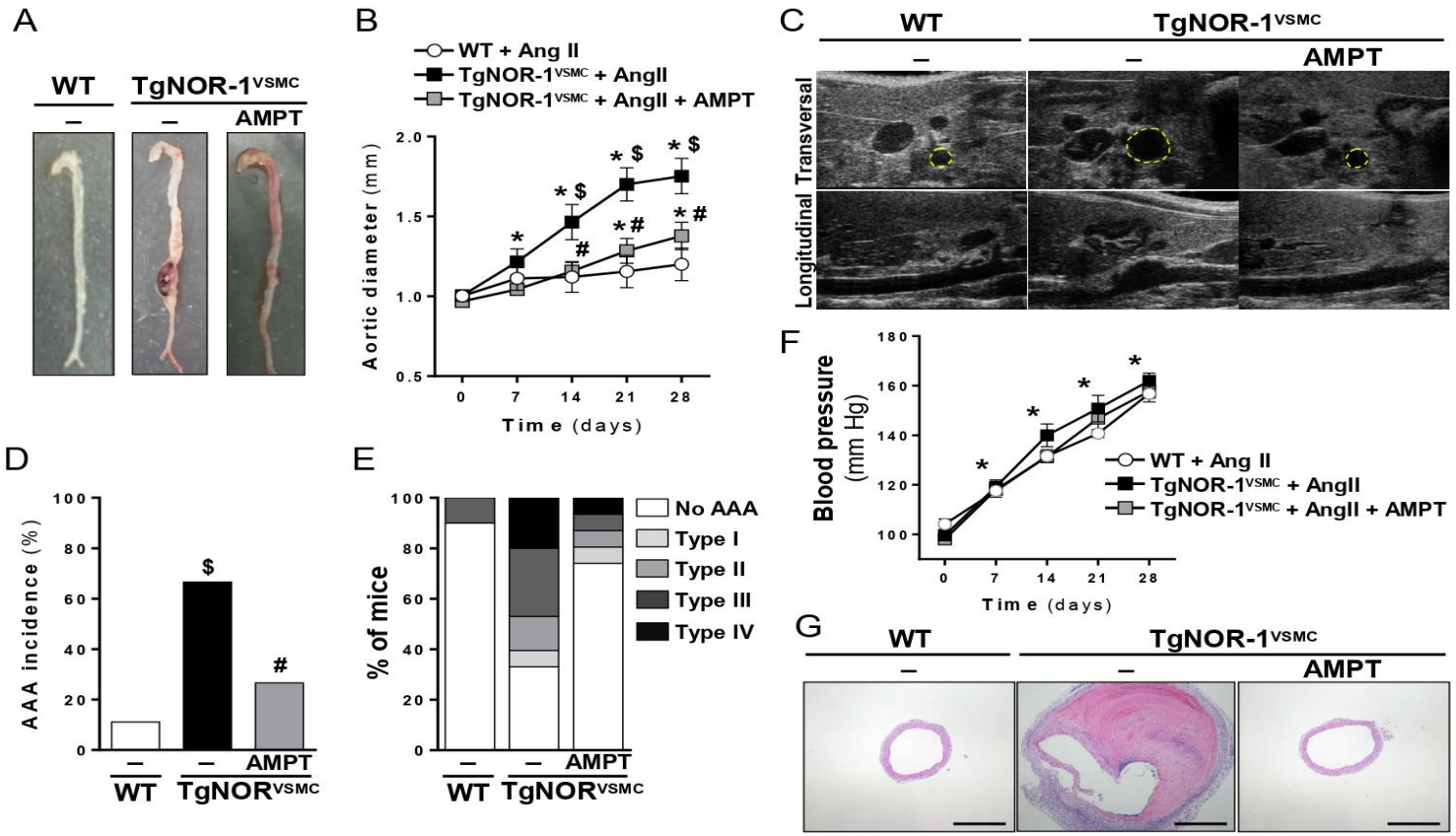
A
WT
TgNOR-1VSMC
–
–
AMPT
B
WT + Ang II
TgNOR-1VSMC + AngII
TgNOR-1VSMC + AngII + AMPT
Aortic diameter (mm)
2.0
1.5
1.0
0.5
0
7
14
21
28
Time (days)
C
WT
TgNOR-1VSMC
–
–
AMPT
Transversal
Longitudinal
D
AAA incidence (%)
100
80
60
40
20
0
$
#
–
–
AMPT
WT
TgNORVSMC
E
% of mice
100
80
60
40
20
0
No AAA
Type I
Type II
Type III
Type IV
–
–
AMPT
WT
TgNORVSMC
F
Blood pressure (mm Hg)
180
160
140
120
100
0
7
14
21
28
Time (days)
WT + Ang II
TgNOR-1VSMC + AngII
TgNOR-1VSMC + AngII + AMPT
G
WT
TgNOR-1VSMC
–
–
AMPT

Figure 6

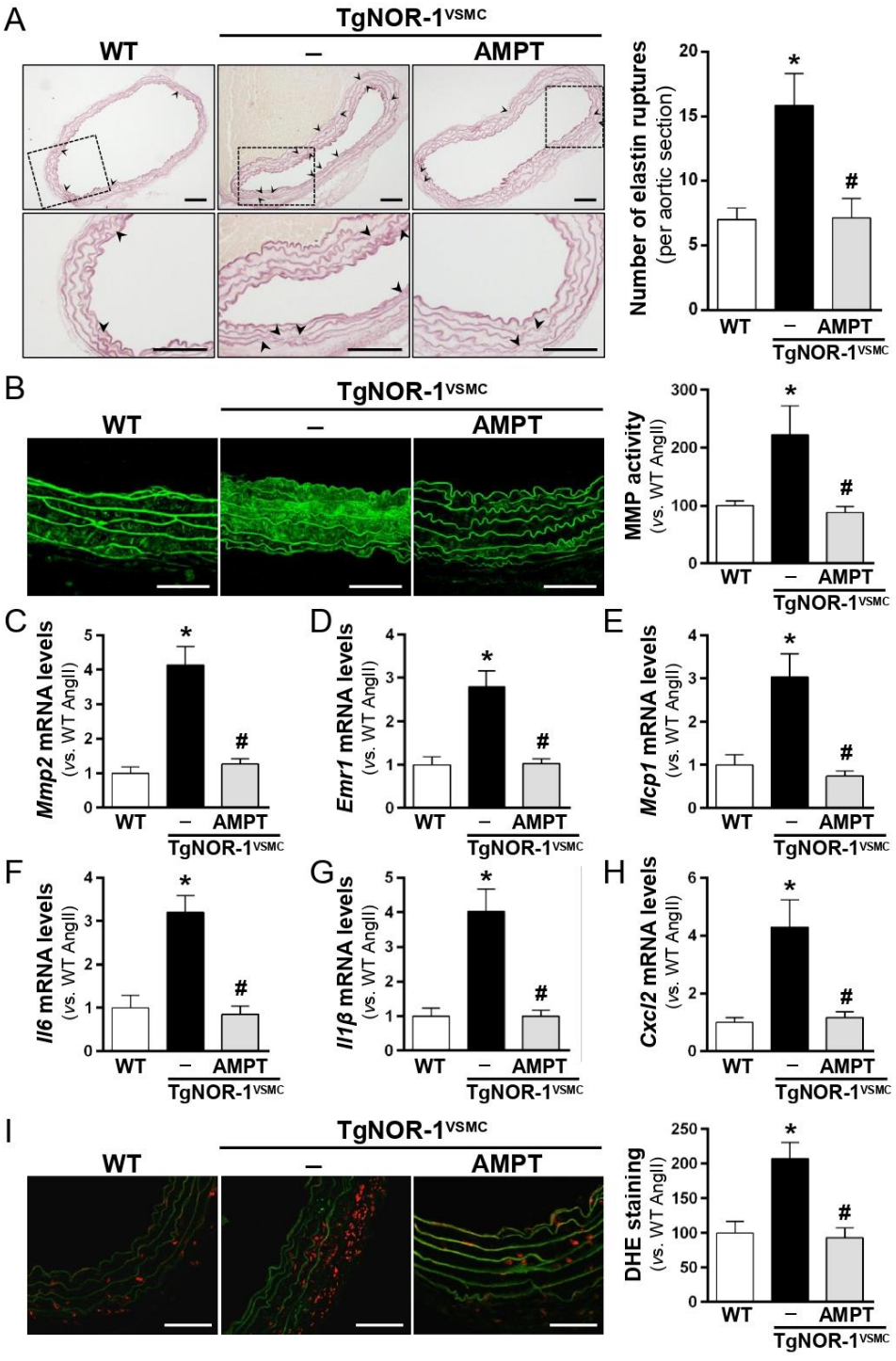
A
TgNOR-1VSMC
WT
–
AMPT
Number of elastin ruptures
(per aortic section)
B
MMP activity
(vs. WT AngII)
C
Mmp2 mRNA levels
(vs. WT AngII)
D
Emr1 mRNA levels
(vs. WT AngII)
E
Mcp1 mRNA levels
(vs. WT AngII)
F
Il6 mRNA levels
(vs. WT AngII)
G
Il1β mRNA levels
(vs. WT AngII)
H
Cxcl2 mRNA levels
(vs. WT AngII)
I
DHE staining
(vs. WT AngII)

SUPLEMENTARY INFORMATION

Targeting tyrosine hydroxylase for abdominal aortic aneurysm: impact on inflammation, oxidative stress and vascular remodeling

Laia Cañes, Judith Alonso, Carme Ballester-Servera, Saray Varona, José R. Escudero, Vicente Andrés, Cristina Rodríguez and José Martínez-González

On-line Data Supplement

Targeting tyrosine hydroxylase for abdominal aortic aneurysm: impact on inflammation, oxidative stress and vascular remodeling

Laia Cañes[1,2,3], Judith Alonso[1,2,3], Carme Ballester-Servera[1,3], Saray Varona[1,2,3], José R Escudero[2,3,4], Vicente Andrés[2,6], Cristina Rodríguez[2,3,4,*] and José Martínez-González[1,2,3,*]

[1]Instituto de Investigaciones Biomédicas de Barcelona (IIBB-CSIC), Barcelona, Spain.

[2]CIBER de Enfermedades Cardiovasculares, ISCIII, Madrid, Spain.

[3]Instituto de Investigación Biomédica Sant Pau, Barcelona, Spain.

[4] Servicios Mancomunados de Angiología, Cirugía Vascular y Endovascular, Hospitales de la Santa Creu i Sant Pau/Dos de Mayo, Barcelona, Spain.

[5]Institut de Recerca Hospital de la Santa Creu i Sant Pau (IRHSCSP), Barcelona, Spain.

[6]Centro Nacional de Investigaciones Cardiovasculares Carlos III (CNIC), Madrid, Spain.

Short title:TH in abdominal aortic aneurysm.

Address for correspondence:

José Martínez-González
Instituto de Investigaciones Biomédicas de Barcelona (IIBB-CSIC)
Rosselló, 161,
08036 Barcelona, Spain
Tel: +34935565896. Email: jose.martinez@iibb.csic.es or
Cristina Rodríguez Sinovas
Institut de recerca Hospital de la Santa creu i Sant Pau (IRHSCSP)
C/Antoni Mª Claret,
08025 Barcelona, Spain
Tel: +34965565897. Email: crodriguezs@santpau.cat

Supplemental Table S1. Oligonucleotides used for mutagenesis studies

NBRE site	Forward primer	Reverse primer
-1480	5'-TCAACAATAGCCCCTGGGACaaTTCCTAAAACTGCTTCAGC-3'	5'-GCTGAAGCAGTTTTAGGAAttGTCCCAGGGGCTATTGTTGA-3'
-2353	5'-CACTGCCGGATGTGGATTTaaCAATTCAGCAAATGTCTTCCAC-3'	5'-GTGGAAGACATTTGCTGAAttGTTAAATCCACATCCGGCAGTG-3'

NBRE sites are underlined and changes are indicated in lower case.

Supplemental Table S2. Patients and donors clinical features

Clinical parameters	Donors (n = 16)	AAA (n = 86)
Age (years ± SD)	63.5 ± 15.7	71.3 ± 6.1
Males (%)	81	100
Smoking (%)*	43.8	79.1
Hypertension (%)	50	69.8
Diabetes (%)	37.5	11.6
Hyperlipidemia (%)	18.8	65.1
Ischemic cardiomyopathy(%)	0	16.3

* Current and ex-smokers. AAA, abdominal aortic aneurysm; SD, standard deviation.

Supplemental Table S3. Impact of AMPT on body weight and plasma lipids in AngII-infused ApoE$^{-/-}$ mice

	ApoE$^{-/-}$/Saline	ApoE$^{-/-}$/AngII	ApoE$^{-/-}$ / AngII/ AMPT
BW (g)	28.0 ± 1.85	27.9 ± 1.6	29.5 ± 2.6
Total Chol (mg/dL)	466.8 ± 36.7	464.4 ± 35.8	492.2 ± 10.3
TG (mg/dL)	127.7 ± 39.8	158.5 ± 40.1	137.4 ± 34.01
n	9	10	11

BW: body weight; Chol: cholesterol; TG: triglycerides.

Supplemental Figure S1

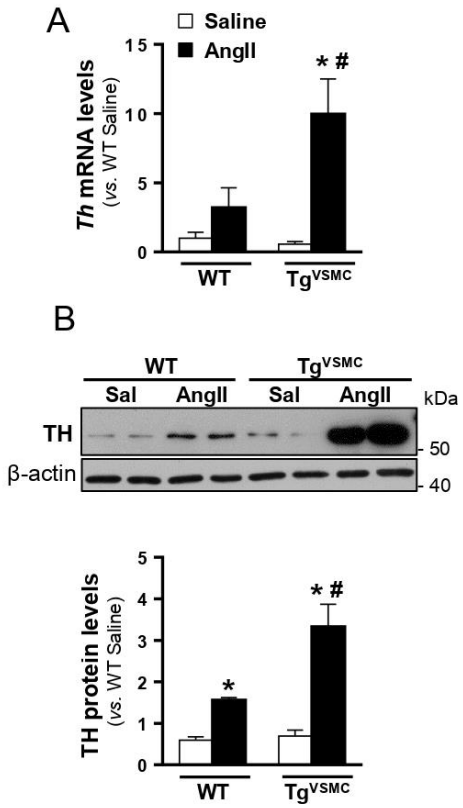

Supplemental Figure S1: **AngII increases aortic *Th* expression in TgNOR-1^{VSMC} mice. A)** *Th* mRNA levels were assessed by real-time PCR in abdominal aorta samples from WT and TgNOR-1^{VSMC} (Tg^{VSMC}) mice infused with saline (Sal; white bars) or AngII (1000 ng/kg/min for 28 days; black bars). Data normalized to GAPDH expression represent mean ± SEM (n= 15). **B)** TH protein levels were assessed in these samples by Western-blot. Levels of β-actin are shown as a loading control. Protein size was estimated by the indicated position of molecular weight markers.The immunoblot densitometric analysis is shown in the lower panel. Data are mean ± SEM (n= 7). *P*< 0.05; *, *vs*. saline-infused mice; # *vs*. AngII-infused WT mice. Two-way ANOVA

Supplemental Figure S2

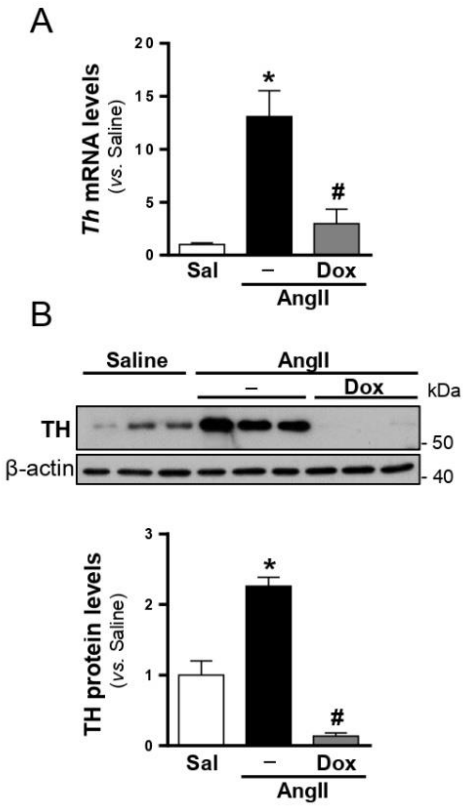

Supplemental Figure S2: **Doxycycline prevents the increase in aortic *Th* expression induced by AngII-infusion in TgNOR-1^{VSMC} mice. A)** *Th* mRNA levels analyzed by real-time PCR in abdominal aorta samples from TgNOR-1^{VSMC} mice infused with saline (Sal; white bars) or AngII (1000 ng/kg/min for 28 days; black bars), in the presence or in the absence of doxycycline (30 mg/kg/day; grey bars). Data normalized to GAPDH expression represent mean ± SEM (saline-infused TgNOR-1^{VSMC}, n=10; AngII-infused TgNOR-1^{VSMC}, n= 15; AngII-infused TgNOR-1^{VSMC} + doxycycline, n= 10). **B)** TH protein levels analyzed by Western-blot in the same experimental groups. Levels of β-actin are shown as a loading control. Protein size was estimated by the indicated position of molecular weight markers. The immunoblot densitometric analysis is shown in the lower panel. Data are mean ± SEM (n= 7). $P< 0.05$; *, *vs.* saline infused mice; # *vs.* untreated AngII-infused TgNOR-1^{VSMC} mice. Kruskal-Wallis.

Supplemental Figure S3

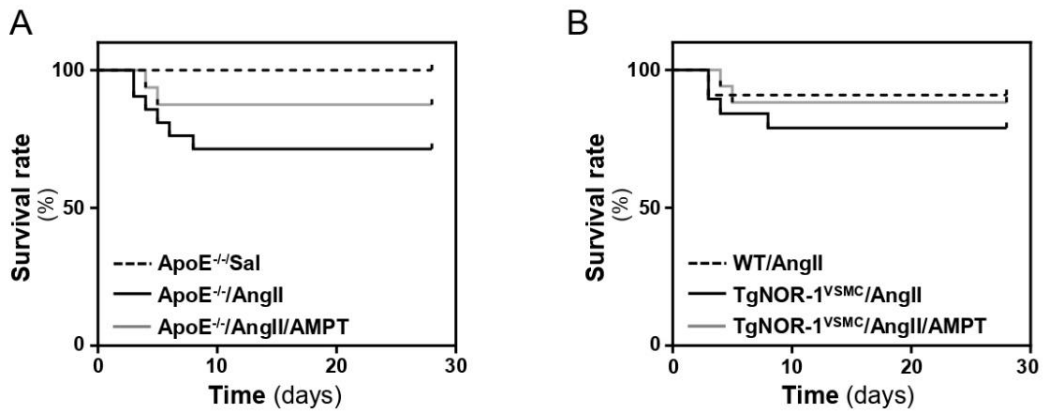

Supplemental Figure S3. AMPT attenuates the AngII-induced mortality in two mouse models of AAA. A) ApoE$^{-/-}$ mice were infused with Saline (Sal) or AngII (1000 ng/kg/min) for 28 days. AngII-infused ApoE$^{-/-}$ mice were treated or not with α-methyl-p-tyrosine (AMPT; 100 mg/Kg twice daily, i.p). The graph shows the survival rate of each experimental group (Saline-infused ApoE$^{-/-}$ mice, n= 9; AngII-infused ApoE$^{-/-}$ mice, n= 21; AngII-infused ApoE$^{-/-}$ mice treated with AMPT, n= 17). **B)** Graph showing the survival rate of Wild-type (WT) and TgNOR-1^{VSMC} mice both infused with AngII (1000 ng/kg/min) for 28 days. TgNOR-1^{VSMC} mice were treated or not with AMPT (WT, n= 11; TgNOR-1^{VSMC} non-treated with AMPT, n= 19; TgNOR-1^{VSMC} treated with AMPT, n= 17). There were no deaths in saline-infused groups (not shown).

Supplemental Figure S4

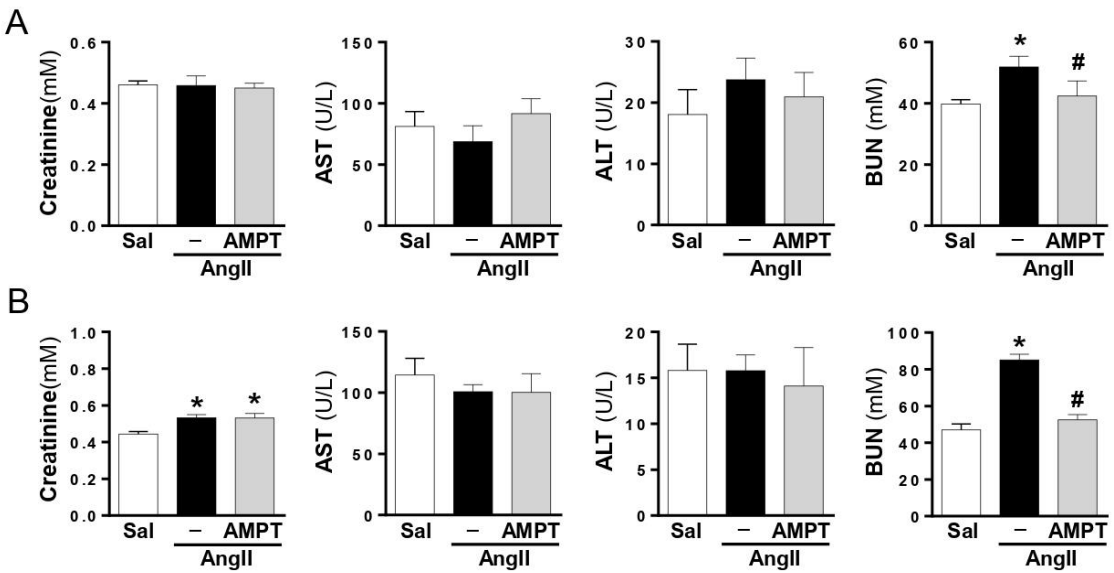

Supplemental Figure S4: **Impact of AMPT on renal and hepatic function in AngII-infused ApoE$^{-/-}$ and TgNOR-1^{VSMC} mice.** Biochemical parameters of renal and hepatic function were assessed in plasma samples from ApoE$^{-/-}$ (**A**) and TgNOR-1^{VSMC} (**B**) mice infused with saline (white bars) or AngII (black bars) in the presence or in the absence of AMPT (grey bars). Levels of aspartate transaminase (AST) alanine transaminase (ALT), creatinine and blood urea nitrogen (BUN) are shown. Data represent mean ± SEM (ApoE$^{-/-}$ saline, n=10; ApoE$^{-/-}$ AngII, n=11; ApoE$^{-/-}$ AngII + AMPT, n=10; TgNOR-1^{VSMC} saline, n=9; AngII-infused TgNOR-1^{VSMC} treated or not with AMPT, n=11). $p< 0.05$; *, *vs*. saline-infused mice; #, *vs*. untreated AngII-infused mice. Kruskal-Wallis.

Supplemental Figure S5

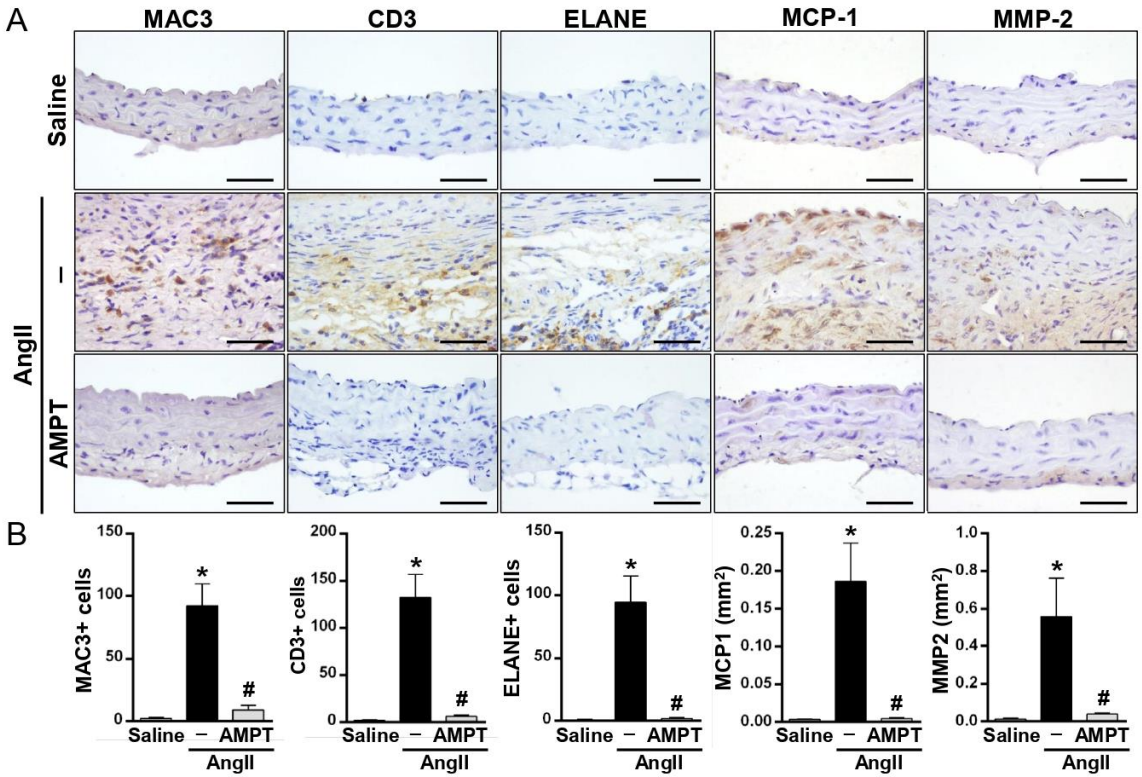

Supplemental Figure S5. Inflammation and MMP2 expression were attenuated by AMPT in AAA from AngII-infused ApoE$^{-/-}$ mice. ApoE$^{-/-}$ mice were infused with Saline or AngII (1000 ng/kg/min) for 28 days. AngII-infused mice were left untreated or treated with α-methyl-*p*-tyrosine (AMPT; 100 mg/Kg twice daily, i.p). **A)** Aortic infiltration of macrophages (MAC3), lymphocytes (CD3) and neutrophils (elastase, neutrophil expressed, ELANE) and staining for MCP1 and MMP2 in each group (Bars: 50 µm). **B)** Quantitative analysis of positive cells *per* aortic section (MAC3, CD3 and ELANE) and area in mm2 *per* aortic section (MCP1 and MMP2). Data are expressed as mean ± SEM (Saline, n= 6; AngII-infused groups, n=9). $P< 0.05$; *, *vs*. Saline-infused ApoE$^{-/-}$ mice; #, *vs*. AngII-infused ApoE$^{-/-}$ mice non-treated with AMPT. Kruskal–Wallis test.

Supplemental Figure S6

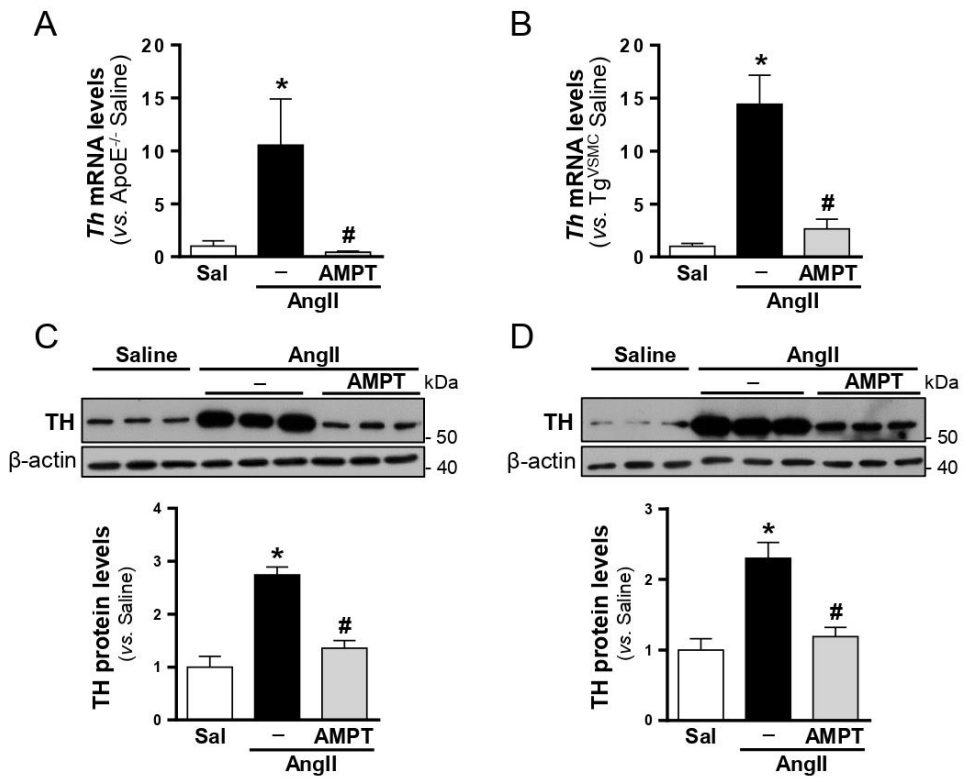

Supplemental Figure S6: **AMPT prevents the increase in aortic *Th* expression induced by AngII-infusion in experimental mouse models of AAA. A and B)** *Th* mRNA levels were analyzed by real-time PCR in abdominal aorta samples from ApoE$^{-/-}$ (**A**) or TgNOR-1^{VSMC} mice (**B**) infused with saline (Sal; white bars) or AngII (1000 ng/kg/min for 28 days; black bars), in the presence or in the absence of α-methyl-p-tyrosine (AMPT; 100 mg/Kg twice daily, i.p; grey bars). Data normalized to GAPDH expression represent mean ± SEM (saline-infused ApoE$^{-/-}$ mice, n= 9; AngII-infused ApoE$^{-/-}$ mice treated or not with AMPT, n= 10; saline-infused TgNOR-1^{VSMC}, n= 10; AngII-infused TgNOR-1^{VSMC} treated or not with AMPT, n= 15). **C** and **D**) Aortic TH protein levels were assessed by Western-blot in samples from ApoE$^{-/-}$ (C) and TgNOR-1^{VSMC} (D) mice treated as described above. Levels of β-actin are shown as a loading control. Protein size was estimated by the indicated position of molecular weight markers. Immunoblots densitometric analysis are shown in the lower panels. Data are mean ± SEM (n= 7). $P< 0.05$; *, *vs.* saline infused mice; # *vs.* untreated AngII-infused mice. Kruskal-Wallis

Supplemental Figure S7

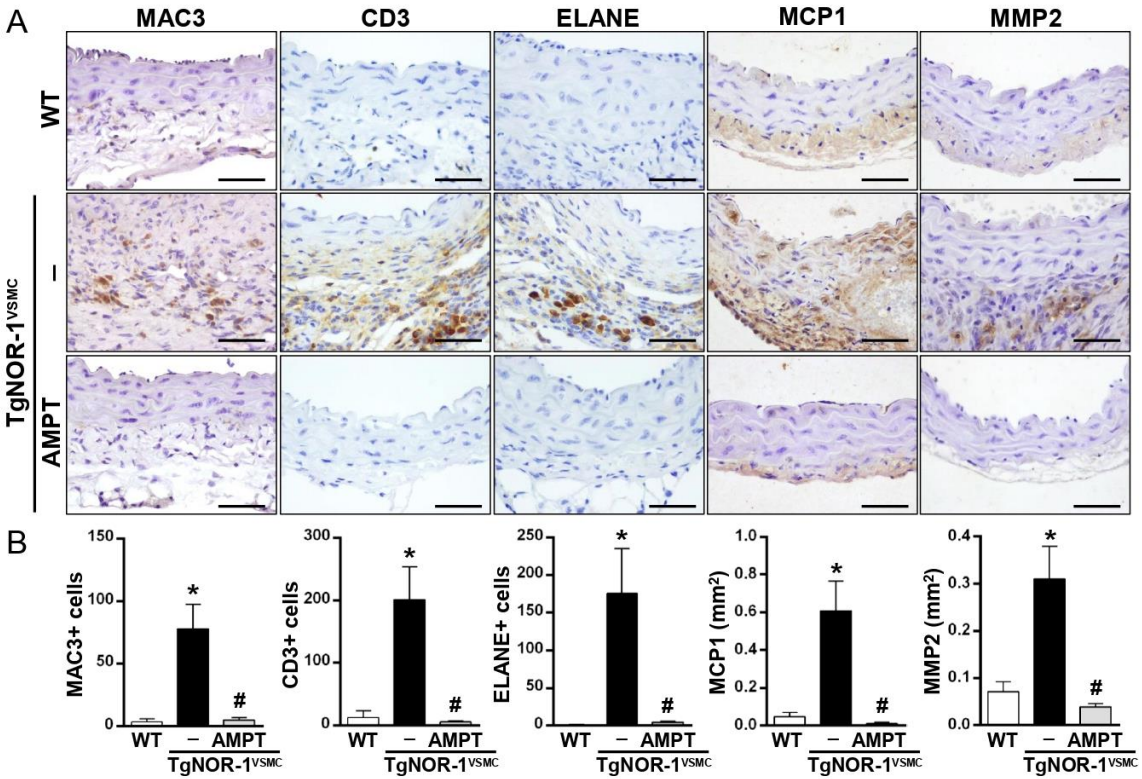

Supplemental Figure S7. AMPT attenuates inflammation and MMP2 expression in the abdominal aorta from AngII-infused TgNOR-1^{VSMC} mice. Wild-type (WT) and TgNOR-1^{VSMC} mice were infused with AngII (1000 ng/kg/min; 28 days). TgNOR-1^{VSMC} mice were treated or not with α-methyl-*p*-tyrosine (AMPT; 100 mg/Kg twice daily, i.p). **A)** Infiltration of macrophages (MAC3), lymphocytes (CD3) and neutrophils (elastase, neutrophil expressed, ELANE) and staining for MCP1 and MMP2 (Bars: 50 μm). **B)** Positive cells *per* aortic section (MAC3, CD3 and ELANE) and area in mm2 *per* aortic section (MCP1 and MMP2). Data are mean ± SEM (WT, n= 6; TgNOR-1^{VSMC}, n=8; TgNOR-1^{VSMC} + AMPT, n=10). $P< 0.05$; *, *vs*. WT; #, *vs*. TgNOR-1^{VSMC} non-treated with AMPT. Kruskal–Wallis test .

Supplemental Figure S9

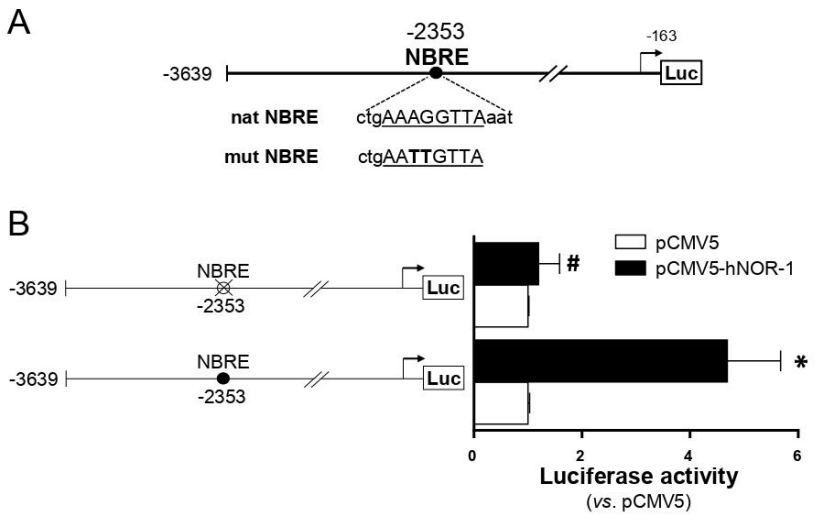

Supplemental Figure S9. NOR-1 regulates tyrosine hydroxylase (*TH*) transcriptional activity. A) Scheme depicting the structure of the proximal region of the human *TH* promoter and the location and sequence of the putative NBRE identified *in silico*. The native NBRE (nat NBRE) and the corresponding mutated sequence (mut NBRE) are underlined. Changes introduced by mutagenesis are highlighted in bold. **B)** Luciferase activity evaluated in rat vascular smooth muscle cells co-transfected with the luciferase reporter construct pGL3/pTH–3639 (or the form mutated in the putative NBRE located at -2353 bp) and a NOR-1 expression vector (pCMV5-NOR-1; black bars) or the corresponding empty plasmid (pCMV5; white bars). Data were normalized by Renilla luciferase activity and expressed as mean ± SEM (n= 8). $P<$ 0·0001; *, *vs*. cells cotransfected with pCMV5; # *vs*. cells cotransfected with the native pGL3/pTH–3639 and pCMV5-NOR-1 plasmids. Two-way ANOVA.

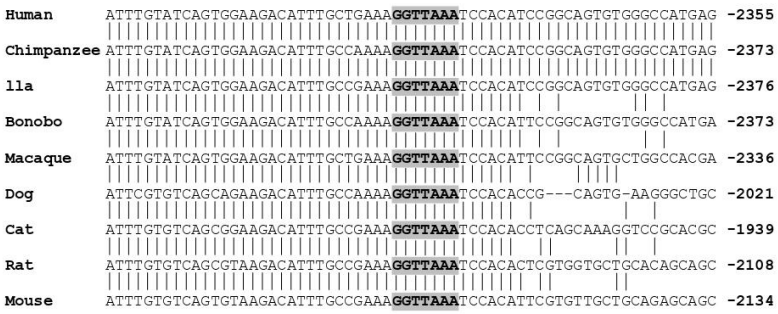

Supplemental Figure S10: **The NBRE site in *TH* promoter is conserved among species.** *TH* distal promoter sequences from different species were aligned with that corresponding to the human *TH* gene (ENSG00000180176) using Blast program. The conserved bases are indicated and the NBRE site in each sequence is highlighted in grey.

DISCUSIÓN

NOR-1 modula la expresión génica cardíaca y exacerba la hipertrofia cardíaca inducida por angiotensina II

Estudios previos desarrollados por nuestro grupo y otros autores han puesto en evidencia la expresión de NOR-1 en corazones sanos de cerdos, ratones y humanos (Ohkura *et al*., 1996 B, Martínez-González *et al*., 2003, Myers *et al*., 2009). A nivel patológico, se ha relacionado NOR-1 con la hipertrofia generada por estímulos beta adrenérgicos como el tratamiento con isoproterenol (Myers *et al*., 2009, Feng *et al*., 2015, Medzikovic *et al*., 2015). Sin embargo, no existen estudios en modelos específicos que analicen el papel de NOR-1 en la hipertrofia hipertensiva, pese a que la hipertensión es uno de los factores de riesgo más importantes para el desarrollo de la patología hipertrófica (Yildiz *et al*., 2020). La hipertrofia hipertensiva es el resultado de la hipertrofia de los cardiomiocitos, y de una mayor inflamación y fibrosis del miocardio. Estos cambios estructurales y funcionales en el corazón tienen como última consecuencia la insuficiencia cardíaca. Una elevación crónica de los niveles circulantes de AngII, péptido principal en la activación del sistema renina-angiotensina, juega un papel clave en la patogénesis de la hipertrófica cardíaca hipertensiva. Sin embargo, no se conocen todos los mecanismos por los que la AngII actúa en esta patología.

En este contexto, nuestro grupo ha estudiado la relación del factor de transcripción NOR-1, cuya expresión se regula por AngII en miocardio, con la regulación de genes implicados en la función cardíaca y el remodelado ventricular en respuesta a sobrecarga de presión. Para ello, se ha desarrollado un modelo de ratón transgénico que presenta una fuerte sobreexpresión de NOR-1 en el miocardio (TgNOR-1). El modelo TgNOR-1 fue generado usando el promotor CAG para dirigir la expresión del transgén. Este promotor contiene elementos de respuesta claves para el control de la expresión cardíaca y se ha utilizado previamente para expresar el transgén preferentemente en el corazón (Orbán *et al*., 2009, Galán *et al*., 2017). Con esta estrategia, se generó una construcción que fue validada mediante transfecciones transitorias *in vitro*, y posteriormente se empleó para generar los ratones transgénicos mediante procedimientos estándar. La sobreexpresión de hNOR-1 no alteró el desarrollo embrionario ni la viabilidad, los ratones TgNOR-1 no revelaron diferencias fenotípicas en comparación con sus hermanos de camada. Los análisis de inserción del transgen demostraron su integración en el área Chr7:33723172 que corresponde a una región no codificante Orbán et al., 2009. Además, los análisis de RNA y proteínas mostraron un patrón de expresión del hNOR-1, principalmente en tejidos cardiovasculares, sobre todo en corazón y en menor medida en aorta (Figura A1. Anexo 1, pag.97), como cabía esperar en base al promotor usado (Orbán *et al*., 2009, Galán *et al*., 2017).

Con el objetivo de analizar las consecuencias funcionales de la transgénesis de NOR-1 en el corazón, se analizó la sobreexpresión del transgen en las células mayoritarias del miocardio: cardiomiocitos y cardiofibroblastos. Los animales TgNOR-1 presentaron una expresión de hNOR-1 en los cardiomiocitos 100 veces mayor que en los cardiofibroblastos, que concordaba con resultados previos que afirmaban que el promotor CAG dirige la expresión principalmente a cardiomiocitos (Orbán et al., 2009). Los cardiomiocitos ventriculares representan un tercio del número total de células, pero contribuyen entre un 70-80% a la masa del corazón (Bernardo *et al*., 2010). Durante la hipertrofia cardíaca se produce una reducción del número de cardiomiocitos pero a la vez, éstos aumentan su tamaño, hipertrofiándose como respuesta compensatoria (Cohn *et al*., 2000). Los cardiomiocitos aislados del ratón TgNOR-1 poseen mayor tamaño (evaluado en secciones transversales) que los cardiomiocitos de los animales WT. En cuanto al fenotipo contráctil, los cardiomiocitos transgénicos presentaron una mayor expresión de *Myh7*, con una ratio *Myh7/Myh6* incrementada. Las isoformas α-MHC y β-MHC (codificadas por *MYH6* y *MHY7*, respectivamente) son mecanoenzimas que transforman la energía de la hidrólisis de ATP en fuerza mecánica produciendo la contracción del músculo. La α-MHC es más eficiente en este proceso, por lo que los corazones que expresan preferentemente esta isoforma tienen una mayor velocidad contráctil que aquellos que expresan la β-MHC (Sugiura *et al*., 1998). Concretamente, en el corazón de roedores, prevalece en más de un 90% la isoforma α; en cambio en humanos es la β-MHC la forma predominante en más de un 90% (Miyata *et al*., 2000). En ratones con cardiopatía se altera la ratio *Myh7/Myh6*, ya que disminuye la expresión de *Myh6* y a su vez aumenta la de *Myh7*, que es la predominante en la hipertrofia (Swynghedauw, 1986). Además, mutaciones en la β-MHC se han asociado con problemas de contracción celular (Spudich *et al*., 2016). En vista de la alteración del ratio *Myh7*/*Myh6* en los ratones TgNOR-1, evaluamos si la función contráctil podría estar alterada en los cardiomiocitos transgénicos. Para abordar este objetivo, medimos el acortamiento celular de los cardiomiocitos sometidos a estimulación eléctrica. De hecho, la sobreexpresión de NOR-1 aumentó el acortamiento celular fraccional, que es un índice de contractibilidad. Estos resultados sugieren que la transgénesis de NOR-1 afecta al comportamiento fisiológico de los cardiomiocitos y los predispone a un funcionamiento anómalo ante estímulos patológicos.

A su vez la funcionalidad y proliferación de los cardiofibroblastos juega un papel clave en la fibrosis cardíaca (Bernardo *et al*., 2010). Observamos que los cardiofibroblastos de los ratones transgénicos para NOR-1 fueron más activos en los experimentos de reparación de herida, en concordancia con resultados previos que demuestran la implicación de NOR-1 en la migración celular (Martínez-González *et al*., 2003, Rius *et al*., 2006, Martorell *et al*., 2007).

Además, nuestros resultados señalan que NOR-1 sería un nuevo regulador de la reprogramación de los fibroblastos, debido a que la sobreexpresión de este factor de transcripción incrementó los niveles de marcadores de transición fenotípica a miofibroblastos, como la α-actina y la transgelina, así como la síntesis de colágeno y PAI-1 que se han relacionado con la cicatrización de heridas y el remodelado cardíaco (Ghosh & Vaughan, 2012). A pesar de la baja expresión de NOR-1 en los cardiofibroblastos respecto a los cardiomiocitos, estos datos sugieren una importante implicación de NOR-1 en la fibrosis cardíaca.

La ecografía Doppler de los ratones TgNOR-1 jóvenes no mostró alteraciones en la función cardíaca respecto a animales WT de la misma edad. Sin embargo, se observó un incremento de la masa del corazón en ratones TgNOR-1 de 12 meses de edad en comparación con la de los ratones WT hermanos de camada. Esto sugiere que la transgénesis de NOR-1 predispondría a la hipertrofia. En el corazón de ratones WT y TgNOR-1 ambos infundidos con AngII, se observó un aumento de la expresión de *Nor-1*, pero no de *Nurr1* ni de *Nur77*. Estos resultados coinciden con estudios previos dónde muestran que la expresión de NOR-1 se induce en el corazón de ratones infundidos con AngII (Sawaki *et al*., 2015) y en cultivos celulares tratados con estímulos pro-hipertróficos (Amirak *et al*., 2013, Feng *et al*., 2015, Sadhan *et al*., 2018). Sin embargo, en cardiofibroblastos en cultivo tratados con AngII no se detectó un incremento en la expresión de *Nor-1*, lo que sugiere una interacción más compleja *in vivo* entre los diferentes elementos de las vías implicadas en la inducción del receptor nuclear observada en el corazón de los animales tratados con AngII. En vista de estos resultados, NOR-1 podría estar implicado en los efectos hipertróficos sobre el corazón producidos por la AngII. Con el fin de establecer la contribución de NOR-1 a la fisiopatología cardíaca, los ratones TgNOR-1 fueron infundidos con AngII, un inductor del remodelado cardíaco. Esta estrategia se había utilizado previamente por otros autores para analizar el papel de determinadas proteínas en la función y el remodelado cardíaco (Matsumoto *et al*., 2013, Galán *et al*., 2017). Nuestros resultados muestran que tras la infusión de AngII los ratones TgNOR-1 son más susceptibles a desarrollar hipertrofia cardiaca y fibrosis que los ratones WT. Estos animales presentan un aumento del grosor del septo intraventricular y un aumento del grosor de la pared posterior del ventrículo izquierdo respecto a los ratones control. Además, en presencia de AngII la transgénesis de NOR-1 promovió un incremento de la masa cardíaca del ventrículo izquierdo, de la ratio del peso del corazón frente al peso corporal y del área de los cardiomiocitos en comparación con ratones control, indicando todo ello un agravamiento de la hipertrofia cardíaca.

Los mecanismos que determinan la progresión de una hipertrofia adaptativa a la insuficiencia cardíaca aún están poco caracterizados. La respuesta

adaptativa inicial ejercida por la AngII en animales de exprimentación es variable y puede ir desde la ausencia de cambios funcionales (Murdoch *et al*., 2014, Toshihiro *et al*., 2016), a producirse un aumento de la función cardíaca debido a una respuesta compensatoria (Frank *et al*., 2007). Nuestros datos sugieren que NOR-1 podría desencadenar mecanismos clave inicialmente beneficiosos como respuesta compensatoria, pero la prolongación del estímulo patológico deriva en una hipertrofia patológica. En nuestro estudio, la sobrecarga de presión no afectó a la función cardíaca de los animales WT, que presentaron una leve hipertrofia y fibrosis. En cambio, los animales TgNOR-1 exhibieron una remodelación cardíaca exacerbada y un aumento de la fracción de eyección y de acortamiento como respuesta compensatoria. La infusión de AngII incrementó de forma similar la presión cardíaca en ratones transgénicos y WT, por lo que los efectos diferenciales entre estos grupos parecen ser independientes de los cambios hemodinámicos. En los ratones TgNOR-1 infundidos con AngII observamos una mayor expresión de genes como el *BNP*, cuya expresión es muy baja en adultos (Tham *et al*., 2015) o la *β-MHC*, cuya inducción es un mecanismo compensatorio en el desarrollo de la hipertrofia (Bernardo *et al*., 2010). Además, en este grupo también aumentó la expresión de marcadores fibróticos (*Col1a1, Col1a3, Ctgf, Pai-1 y Loxl2*). Por otro lado, en condiciones basales, los animales TgNOR-1 presentaron un incremento significativo en la expresión de genes clave en la función cardíaca (*Myh7*) y el remodelado (*Loxl2*), respecto al grupo WT, lo que podría sugerir una regulación directa por NOR-1 de estos genes.

El *MYH7* fue el primer gen relacionado con la cardiomiopatía hipertrófica familiar, además se ha descrito que mutaciones en el gen *MYH7* son causantes de un 40% de los casos en esta patología, que es la enfermedad cardiovascular hereditaria más común (Sabater-Molina *et al*., 2018). En modelos experimentales, la expresión cardíaca del *Myh7* se incrementa en respuesta a estímulos hipertróficos como la AngII (Martín-Sánchez *et al*., 2018). Nosotros observamos que la transgénesis de NOR-1 aumentó la expresión de *Myh7* en animales infundidos con AngII, y lo más relevante, que los animales TgNOR-1 infundidos con solución salina presentaron una mayor expresión de *Myh7* que los animales WT. De hecho, demostramos que NOR-1 regula la actividad transcripcional de *MYH7* a través de la interacción directa con un elemento NBRE en su promotor. La sobreexpresión de NOR-1 a niveles por encima del su rango fisiológico, mediante un sistema lentiviral en CMLV humanas, incrementó la expresión de genes que codifican proteínas expresadas típicamente en el músculo esquelético, incluyendo el *MYH7* (Ferrán *et al*., 2016). Debido a la importancia de la β-MHC en la función cardíaca y en la hipertrofia, estos resultados sugieren que la regulación del MYH7 por NOR-1 puede ser uno de los factores que predisponga a los ratones TgNOR-1 al desarrollo de hipertrofia cardíaca tanto espontánea como inducida por AngII.

Asimismo, en los ratones TgNOR-1 infundidos con AngII observamos una exacerbada respuesta fibrótica con una mayor deposición de colágeno tanto en áreas perivasculares como intersticiales. El aumento de la expresión de *Lox* y *Loxl2* se asoció, como cabría esperar, con un incremento en el grado de entrecruzamiento de las fibras de colágeno en el miocardio, acompañado de una mayor expresión de *Col1a1* y de *Pai-1*. El entrecruzamiento del colágeno determina la rigidez y función ventricular del corazón sometido a sobrecarga de presión (López *et al*., 2009, 2012, Kasner *et al*., 2011). De hecho, en pacientes con insuficiencia cardíaca hipertensiva el excesivo entrecruzamiento de colágeno se ha asociado con una peor prognosis (Ravassa *et al*., 2017). Los diferentes miembros de la familia de LOX catalizan la desaminación oxidativa de residuos de lisina e hidroxilisina de las fibras de colágeno y elastina, y son responsables del ensamblaje de las fibras de colágeno (Kasner *et al*., 2011). El incremento de LOX y LOXL2 se ha asociado con el desarrollo de fibrosis miocárdica en pacientes con insuficiencia cardíaca (López *et al*., 2009, 2012, Kasner *et al*., 2011) y también en modelos de daño cardíaco (González-Santamaría *et al*., 2015, Yang *et al*., 2016). Diversos estudios, describen un incremento de LOX y LOXL2 en la hipertrofia cardíaca y en el consecuente infarto de miocardio (Stefanon *et al*., 2013, González-Santamaría *et al*., 2015), además su inhibición mejora el remodelado cardiovascular y la función cardíaca (Martínez-Martínez *et al*., 2016, Yang *et al*., 2016). Al igual que LOX (Galán *et al*., 2017), la LOXL2 contribuye a la fibrosis, la disfunción cardíaca y la reprogramación fenotípica del fibroblasto a miofibroblasto, y por tanto juega un papel crucial en el remodelado cardíaco (Yang *et al*., 2016). Por todo ello, LOXL2 se ha propuesto como una posible diana terapéutica para la fibrosis cardíaca y el infarto de miocardio (Yang *et al*., 2016). A pesar del importante papel de LOXL2 en el remodelado cardíaco, se dispone de poca información sobre su regulación transcripcional. El promotor de *LOXL2* contiene elementos de unión para Smad, Sp1 y SMYD3. Sin embargo, se requiere de estudios específicos que analicen los elementos de respuesta en el promotor de *LOXL2* y sobre el mecanismo implicado en la regulación de LOXL2 durante el desarrollo de la hipertrofia cardíaca. Como se indicó anteriormente en condiciones basales la expresión cardíaca de LOXL2 es significativamente mayor en los ratones transgénicos que en los WT y demostramos que NOR-1 regula directamente la actividad transcripcional de *LOXL2* que presenta elementos NBRE en su promotor. Por tanto, la regulación de *LOXL2* por NOR-1 podría estar implicada en la respuesta hipertrófica de los ratones TgNOR-1.

El hecho de que en el ratón TgNOR-1 la sobrecarga de presión induzca un aumento en la fracción de eyección y de acortamiento como respuesta adaptativa podría constituir una limitación de nuestro estudio, ya que nuestro modelo no llega a desarrollar disfunción cardíaca. Por tanto, se necesitarían

nuevos estudios para determinar el papel de NOR-1 sobre la disfunción cardíaca a largo plazo.

En resumen, estos resultados indican que la sobreexpresión de NOR-1 predispone a padecer hipertrofia cardíaca, y proponen a este factor de transcripción como un importante regulador de genes implicados en la función y el remodelado cardíaco. Por lo tanto, el ratón TgNOR-1 podría ser una herramienta útil para esclarecer los mecanismos moleculares de la hipertrofia cardíaca y evaluar la efectividad de nuevas terapias farmacológicas en estudios pre-clínicos.

Actualmente, nuestro grupo está estudiando con más detalle el modelo TgNOR-1 en ausencia de estímulo hipertrófico para esclarecer que mecanismos son los responsables de la predisposición de estos ratones a la hipertrofia. Analizamos la expresión de genes codificantes para proteínas implicadas en la homeostasis del calcio. Para ello, se han analizado los genes implicados en la homeostasis del calcio (Figura A2. Anexo 1, pag.98). Concretamente se detectó un aumento significativo de la expresión de *Serca2a* y *Casq2* en los ratones transgénicos de NOR-1. La CASQ2 es la principal proteína de unión al calcio dentro del retículo sarcoplásmico, con lo que una mayor expresión de *Casq2* y de *Serca2a* que es el encargado de introducir el calcio a este orgánulo, se asocia con un mayor almacenaje de calcio en el retículo sarcoplásmico. Esto puede ocasionar liberaciones espontáneas de calcio (en inglés *sparks*), proceso adaptativo del miocardio previo al infarto de miocardio (Roderick *et al*., 2007). Además, observamos mayor estrés oxidativo tanto en el miocardio ratones TgNOR-1, como en cardiofibroblastos transgénicos en cultivo, lo que se asoció con un mayor nivel de oxidación proteica. Concretamente, se detectó un mayor nivel de oxidación de la CaMKII (Figura A3. Anexo 1, pag.99). La oxidación de la CaMKII produce su activación prolongada de forma independiente de los niveles de calcio, y en consecuencia incrementa la fosforilación de proteínas clave en la homeostasis del calcio como el RyR2 y PLN, lo que promueve entre otros efectos la hipertrofia de los cardiomiocito (Erickson et al., 2011). Además en modelos de hipertensión espontánea y de sobrecarga de presión se observó el incremento de la expresión de esta quinasa (Colomer *et al*., 2003).

Por último, hemos analizado la respuesta de los animales transgénicos a la hipertrofia inducida por el agonista β-adrenérgico isoproterenol. Esta aproximación es un modelo clásico de inducción de hipertrofia a través de la activación de la proteína quinasa A, responsable de la fosforilación de múltiples proteínas implicadas en la contracción cardíaca, entre ellos PLN o RyR2 (Barry *et al*., 2008). La infusión de isoproterenol en ratones WT y TgNOR-1 reveló un mayor incremento del grosor de la cavidades cardíacas, concretamente de la pared anterior y posterior de los ratones transgénicos. Aunque no mostró diferencias en la función cardíaca entre WT y TgNOR-1 (Tabla A1. Anexo 1, pag.100). Esto puede deberse a que el estímulo con isoproterenol es tan potente

que no se aprecia modulación por la transgénesis de NOR-1. Por todo ello, se requiere seguir investigando en los mecanismos por los que NOR-1 predispone a la hipertrofia cardíaca.

La sobreexpresión de NOR-1 en la pared vascular conduce a la formación de aneurismas de aorta abdominal en ratones en respuesta a angiotensina II

Estudios previos han implicado al factor de transcripción NOR-1 en la regulación de la inflamación (Zhao *et al*., 2010, Calvayrac *et al*., 2015, Tsilingiri *et al*., 2019), el remodelado de la MEC (Martí-Pàmies *et al*., 2017), el estrés oxidativo (Alonso *et al*., 2018) y la supervivencia/apoptosis celular (Alonso *et al*., 2016), procesos clave en la patología aneurismática. De hecho, hemos demostrado que la expresión de NOR-1 aumenta en la aorta de pacientes con AAA (Alonso *et al*., 2016). Sin embargo, se desconoce el papel concreto de NOR-1 en el desarrollo del AAA. Nuestro grupo ha desarrollado dos modelos transgénicos que sobreexpresan hNOR-1 en la vasculatura con el objetivo de estudiar si la función del receptor NOR-1 afecta al desarrollo del aneurisma inducido por AngII. También, se ha analizado la utilidad del modelo animal transgénico para hNOR-1 en la investigación de los mecanismos implicados en la patología aneurismática y en estudios preclínicos.

En los últimos 20 años, la infusión de AngII en ratones hipercolesterolémicos ($ApoE^{-/-}$) (Daugherty *et al*., 2000) ha constituido el modelo de experimentación animal más popular en el estudio del AAA. A pesar de reproducir distintas características de la patología aneurismática humana como la degradación de elastina, la inflamación, y la formación del trombo, los modelos animales actuales no son totalmente representativos de la enfermedad humana (Trachet *et al*., 2017). Durante las últimas tres décadas ha crecido el interés en el estudio de los receptores nucleares en el AAA, ya que éstos han demostrado una gran importancia en la biología vascular. Así la activación de los receptores de tipo PPARs (*peroxisome proliferator-activates receptors*) reduce el desarrollo del AAA, ya que disminuye el infiltrado de macrófagos, el remodelado de la MEC y la expresión de la osteopontina, una proteína implicada en la formación de AAA (Golledge, *et al*., 2010 B, Krishna *et al*., 2012). Nuestro grupo, se ha centrado en el estudio del receptor nuclear NOR-1 en esta enfermedad, debido a su papel en el control de la inflamación, la neovascularización, el estrés oxidativo y la apoptosis (Pei *et al*., 2006, Zhao *et al*., 2010, Alonso *et al*., 2016, 2018, Martí-Pàmies *et al*., 2017,). Pese a estos indicios, la supresión de la expresión de NOR-1 en células madre hematopoyéticas en el ratón deficiente para el receptor de LDL infundido con AngII, no disminuye el desarrollo de AAA (Qing *et al*., 2017). Otros autores han sugerido que la ausencia de efecto en este modelo podría deberse a diferentes razones, entre ellas destacar que podría ser que los genes regulados

por NOR-1 en los macrófagos casualmente no estén involucrados en el AAA, o que los cambios de expresión de estos genes no sean suficientes para afectar al desarrollo de la patología (Neels *et al*., 2020). Aunque este estudio descartaría la contribución de NOR-1 a la enfermedad, el aumento de la expresión de NOR-1 en CMLV de pacientes con AAA descrito por nuestro grupo ha motivado que realicemos estudios adicionales para esclarecer la función de NOR-1 en el AAA.

Nuestro estudio se ha centrado en el análisis del papel de NOR-1 sobre la susceptibilidad a la formación de AAA inducidos por AngII en un modelo no hiperlipémico y resistente a la formación de AAA como es la cepa C57BL/6J. En ratones que sobreexpresan NOR-1 a nivel cardiovascular (TgNOR-1) observamos que la transgénesis de NOR-1 promueve la formación de aneurismas inducidos por AngII. Para establecer qué tipo celular estaba implicado en este efecto, realizamos el mismo experimento con ratones TgNOR-1^{VSMC}, en los cuales se empleó el promotor SM22α para dirigir la expresión del hNOR-1 específicamente a CML (Rodríguez-Calvo *et al*., 2013). Los ratones TgNOR-1^{VSMC} presentan una elevada expresión de hNOR-1 en las CMLV de la aorta, mientras que el transgen no se detectó en otras células vasculares como los fibroblastos de la adventicia (Figura A1. Anexo 2, pag.177). Los dos modelos presentaron una incidencia y gravedad del AAA similar. Destacar que los aneurismas generados por la infusión de AngII en ambos modelos presentan características similares al modelo ApoE$^{-/-}$ infundido con AngII, localización suprarrenal, incremento de marcadores proinflamatorios y proteolíticos, mayor número de roturas en las fibras elásticas, producción de ROS y formación de un trombo intramural. Por tanto, la inducción de la expresión de NOR-1 en CMLV es suficiente para agravar la respuesta vascular a la AngII y por ello potenciar la inflamación, favorecer la dilatación aórtica y promover el AAA, así que los siguientes estudios se realizaron exclusivamente en el modelo TgNOR-1^{CMLV}. Además, en dicho modelo la transgénesis produce un incremento de la expresión vascular de NOR-1 similar al observado en pacientes con AAA (Figura A2. Anexo 2, pag.178). A pesar de la localización suprarrenal del aneurisma y la presencia de trombo intramural, características que difieren de las de la patología aneurismática humana, nuestro modelo parece recapitular aspectos clave de la enfermedad humana.

Estos resultados nos alentaron a validar la utilidad del ratón transgénico de NOR-1 infundido con AngII como modelo animal de utilidad preclínica en el ensayo de potenciales terapias contra el AAA. Con este objetivo, los animales transgénicos se trataron con doxiciclina, un inhibidor de MMP que ha demostrado su eficacia previniendo la formación de AAA en diferentes modelos animales como el modelo de elastasa en rata (Curci *et al*., 1998, Sho *et al*., 2004) y ratón (Bartoli *et al*., 2006), el modelo de ratón ApoE$^{-/-}$ con

infusión de AngII (Turner *et al*., 2008) y el de combinación de AngII con dieta rica en grasas (Manning *et al*., 2003). En nuestro modelo transgénico infundido con AngII el tratamiento con doxiciclina disminuyó el infiltrado inflamatorio, así como la actividad MMPs y el estrés oxidativo en la pared vascular, disminuyendo la incidencia de aneurismas. Estos resultados concuerdan con estudios previos realizados en modelos animales y confirman la utilidad pre-clínica de nuestro ratón TgNOR-1^{CMLV}. Por otra parte, en ensayos clínicos la doxiciclina redujo la inflamación y la actividad MMP en pacientes con AAA. Pese a esto los resultados en pacientes han sido en cierto modo descorazonadores ya que estos efectos no se tradujeron en la reducción del diámetro aórtico (Mosorin *et al*., 2001, Baxter *et al*., 2002, Abdul-Hussien *et al*., 2009). Recientemente, un estudio clínico en fase II realizado en un mayor número de pacientes con dos años de seguimiento concluyó que la doxiciclina no reduce el crecimiento del diámetro de los AAA de pequeño tamaño (Baxter *et al*, 2020). Sin embargo, la tasa de crecimiento del AAA descrita en este estudio fue menor que en ensayos anteriores. Esto sugiere que el seguimiento de 2 años podría ser demasiado corto para evidenciar el efecto de la doxiciclina. Además, se observó que la doxiciclina redujo los niveles de la proteína C reactiva, lo que sugiere un efecto antiinflamatorio de la doxiciclina en estos pacientes. Por tanto, no se puede descartar el posible beneficio de la inhibición de la actividad MMP sobre la estabilización del AAA en humanos y se requiere de una mayor investigación.

En la pared aneurismática de nuestro modelo animal transgénico, evidenciamos una elevada expresión de quimioquinas, citoquinas y enzimas proteolíticos (IL-6, IL-1β, CXCL2, MCP-1 y MMP2) características del desarrollo del AAA. Además, quisimos definir que grupos de genes o vías podrían contribuir a explicar la mayor susceptibilidad de los ratones transgénicos de NOR-1infundidos con AngII. Los análisis comparativos a gran escala de los perfiles de expresión de ratones WT y TgNOR-1^{VSMC} ambos infundidos con AngII, identificaron 1500 genes diferencialmente expresados. La magnitud de las diferencias fue moderada ya que ambos grupos se expusieron a AngII. Sin embargo, parte de los genes identificados, concretamente 167 genes se habían descritos previamente entre los más diferencialmente expresados en el modelo ApoE$^{-/-}$ infundido con AngII (Rush *et al*., 2009). El análisis GSEA identificó genes agrupados por procesos biológicos o componentes celulares significativamente enriquecidos en el ratón TgNOR-1^{VSMC} infundido con AngII. A través del GSEA, se establecieron comparativas con las bases de datos del proyecto de ontología génica (GO, del inglés *gene ontology*) y del *Reactome*. En la aorta de los ratones TgNOR-1^{VSMC} infundidos con AngII, se observó un enriquecimiento en grupos de genes implicados en procesos biológicos relacionados con inflamación, ciclo celular y activación simpática. Además, teniendo en cuenta los términos GO de tipo

componente celular, se identificaron grupos de genes asociados al remodelado de la MEC. A su vez, los genes inhibidos están relacionados con procesos biológicos como la contracción del músculo, el citoesqueleto de actina y la respuesta de estrés térmico. El análisis con la base de datos de *Reactome* confirmó los resultados obtenidos y evidencio la regulación de procesos biológicos y vías de transducción de señales similares a las citadas anteriormente.

Según la información obtenida través del GSEA, se seleccionaron genes concretos para su validación por PCR, atendiendo a dos criterios: aquellos que estuvieran más diferencialmente expresados en las vías de interés y/o que se hubiera vinculado con la enfermedad aneurismática. Entre ellos se incluyen genes diferencialmente regulados que representan procesos biológicos como los relacionados con el remodelado de la matriz extracelular (*Col10a1*, *Cthrc1*, *Mmp12* y *Loxl2*), la respuesta inmune (*Cd5l, Adam8, Dync1i1, Cd300c2, Sh2d1b* y *Scg2*), la actividad simpática (*Scg2*, *Npy* y *Syt4*), el ciclo celular, respuesta a daño al DNA (*Uhrf1*, *Ccnb1*, *Kif20a*, y *Cdc20*), la función y diferenciación de las células musculares y la organización del citoesqueleto (*Acta2*, *Myh11* e *Itga8*). La expresión diferencial de todos estos genes se confirmó por PCR a tiempo real. En concreto, estudios de expresión a gran escala con muestras de pacientes con aneurismas abdominales, torácicos e intracraneales se demostró la inducción de *COL10A1*, *MMP12* y *CTHRC1* (Courtois *et al*., 2014, Kleinloog *et al*., 2016, Sulkava *et al*., 2017). También, se incrementó la expresión de estos genes en estudios de *microarrays* en el modelo de infusión de AngII en ratones ApoE$^{-/-}$ (Rush *et al*., 2009, Spin *et al*., 2011) e incluso en el modelo de elastasa en conejos (Holcomb *et al*., 2015). Destacar, la expresión diferencial de *Loxl2* tanto en nuestro modelo, como en el ratón ApoE$^{-/-}$ infundido con AngII (Spin *et al*., 2011). Los miembros de la familia LOX son enzimas modificadoras de la MEC, y los análisis de expresión génica han demostrado que en humanos *LOX* aumenta su expresión en AAA (Courtois *et al*., 2014). También, se han descrito diversos polimorfismos en el gen *LOXL2* que se asocian con una mayor predisposición a padecer aneurismas intracraneales (Akagawa *et al*., 2007). En cuanto a los genes identificados por su mayor expresión en el ratón TgNOR-1^{VSMC} infundido con AngII, e implicados en la respuesta inmune, destacar el gen *Cd5l.* Su incremento no se ha detectado en otros modelos como el del ratón ApoE$^{-/-}$, pero sí en la patología aneurismática humana, dónde su expresión se asocia con el crecimiento del aneurisma (Andersen *et al*., 2018). Este estudio identifica a la proteína CD5L, entre otras, como posible diana farmacológica. En diferentes enfermedades aneurismáticas humanas como el AAA, la dilatación de la aorta torácica, el aneurisma intracraneal, y también en modelos experimentales se ha observado un aumento de la expresión de otros genes implicados en la respuesta inmune como *ADAM8* (Levula *et al*., 2011), *CD300C* (Kleinloog *et al*., 2016) y

SH2D1B (Hinterseher *et al*., 2015). Curiosamente, una de las vías más significativamente aumentados en el aneurisma de los ratones transgénicos para NOR-1 es la vía de actividad simpática. Concretamente, confirmamos la inducción de la SCG2 es una proteína involucrada en la migración transendotelial de las células inflamatorias que se considera un marcador de actividad simpática, se ha relacionado con hipertensión y cuya expresión aumenta en aneurismas humanos tanto intracraneales (Jiang *et al*., 2013) como de aorta torácica (Sulkava *et al.*, 2017). La SCG2 se almacena en los gránulos cromafines conjuntamente con el NPY cuya expresión también aumenta en nuestro modelo. El NPY es un neurotrasmisor simpático también expresado en CMLV e implicado en patologías caracterizadas por hiperactividad simpática como la hipertensión y el remodelado vascular. De hecho sus receptores,Y1R, Y2R y Y5R se han relacionado con enfermedades cardiovasculares como la hipertensión, aterosclerosis, diabetes, cardiomiopatías hipertróficas e infarto de miocardio (Tan *et al*., 2018). Por su parte, la SYT4 se expresa tanto en neuronas como en VSMC (Barnes *et al*., 2017) y es considerada un mediador clave en la progresión del aneurisma en la aorta ascendente (Tobin *et al*., 2019). De entre los genes implicados en ciclo celular y daño al DNA modulados diferencialmente, el UHRF1 se ha asociado a AAA tanto en modelos experimentales como humanos (Elia *et al*., 2018). CDC20, CCNB1 y KIF20A se han asociado con aterosclerosis y disecciones aorticas en humanos (Schwill *et al*., 2013, Jiang & Si, 2019). Además estos dos últimos, están fuertemente expresados tanto en modelos experimentales de aneurismas aórticos inducidos por AngII como en modelos de aorta ascendente del síndrome de Marfan (Wang *et al*., 2019).

Curiosamente, en estudios de expresión a gran escala, se observó que los genes *NOR-1*, *NUR77* y *NURR1* están entre los genes más diferencialmente expresados en zonas de ruptura del aneurisma en humanos (Choke *et al*., 2009). Destacar, que los grupos de genes enriquecidos en la aorta aneurismática de los ratones TgNOR-1^{VSMC} coinciden con genes identificados mediante análisis bioinformático en muestras de disección aórtica humana (*CDC20*, *CCNB1*, *KIF20A*, *CDK1*, *PBK*, *RACGAP*, *TOP2A*, *CCNB2*, *MAD2L1* y *AURKA*) (Schwill *et al*., 2013, Jiang & Si, 2019). Por último, de los genes inhibidos en nuestro modelo transgénico se confirmó la inhibición de *Acta2*, *Myh11* e *Itga8*, que habían sido descrito previamente en la patología aneurismática humana y se asocian con una mayor predisposición al aneurisma (Armstrong *et al*., 2002). Por todo ello, la AngII promueve la formación de aneurismas en el ratón TgNOR-1^{VSMC} a través de la regulación de diferentes vías que recapitulan mecanismos clave en la patología aneurismática. Sin embargo, diversos genes regulados en el ratón transgénico de NOR-1 no están regulados de forma similar en el ratón $ApoE^{-/-}$ infundido con AngII, que es el modelo murino más estudiado y experimentalmente más parecido al nuestro (Rush *et al.*, 2009, Spin *et al*.,

2011). En concreto, nuestro modelo y no el modelo de ratón deficiente en ApoE$^{-/-}$, mimetiza el incremento de la expresión de *Cd5l*, descrito previamente en humanos y asociado al crecimiento del aneurisma (Andersen *et al*., 2018), y otros genes que codifican para proteínas relacionadas en respuesta inmune/inflamatoria como *Cd300c2* (ortólogo de *CD300C*) (Kleinloog *et al*., 2016), *Sh2d1b1* (ortólogo de *SH2D1B*) (Hinterseher *et al*., 2015) y *Scg2* (Shi *et al*., 2009, Sulkava *et al*., 2017), como también la inhibición de genes implicados en la regulación del citoesqueleto de actina (Modrego *et al*., 2012). Enfatizar, que el incremento de la expresión vascular de NOR-1 en la patología aneurismática humana (Choke *et al*., 2009, Alonso *et al*., 2016;) no la reproduce el modelo ApoE$^{-/-}$ con infusión con AngII, lo cual podría explicar que ciertos genes, regulados directamente o indirectamente por NOR-1, no se modulen de la misma forma en el modelo clásico.

En resumen, mediante el uso de dos modelos animales generados por nuestro grupo hemos demostrado que la inducción de NOR-1 en la pared vascular potencia la expresión de una serie de genes inducidos por AngII, lo que incrementa la capacidad de la AngII para promover la formación de aneurismas. Nuestros resultados indican que los ratones transgénicos para NOR-1 podrían ser nuevos modelos experimentales pre-clínicos. Futuros estudios, deberían esclarecer qué genes concretos regulados por NOR-1 directa o indirectamente, lo convierten en un factor clave que facilita el proceso aneurismático.

La tirosina hidroxilasa como diana farmacológica en el aneurisma de aorta abdominal: impacto sobre la inflamación, el estrés oxidativo y el remodelado vascular

La escasez de tratamientos farmacológicos para limitar o prevenir el AAA es un gran obstáculo en el manejo de esta enfermedad, ya que la ruptura aneurismática es impredecible. Este estudio ha desvelado la relevante función de la TH en la patofisiología de esta enfermedad, y sugiere que esta enzima podría constituir una posible diana farmacológica.

En muestras aneurismáticas humanas hemos detectado una mayor expresión de genes implicados en la biosíntesis y transporte de catecolaminas. Estudios de expresión en aneurimas humanas mediante *microarray* habían sugerido sugirieron un enriquecimiento génico en vías relacionadas con actividad neuronal (Lenk *et al*., 2007). Sin embargo, en este estudio no se detectó una regulación significativa de genes implicados en la vía de la TH. Recientemente, en estudios de expresión a gran escala, nuestro grupo detectó la inducción de genes relacionados con la actividad simpática en el tejido aneurismático de un modelo experimental de la enfermedad, el ratón TgNOR-1^{VSMC} infundido con AngII (Cañes *et al*., 2021). En este trabajo, hemos confirmado estas

observaciones en dos modelos animales susceptibles a desarrollar AAA inducido por AngII, el ratón ApoE$^{-/-}$ y el ratón TgNOR-1^{VSMC}. En concreto, hemos detectado una fuerte inducción de la expresión de la TH, la enzima limitante en la síntesis de catecolaminas, en lesiones aneurismáticas humanas y de modelos animales. En la aorta humana, observamos un incremento de dos de las principales isoformas de la TH (Haycock, 2002), mientras que en muestras de ratón se incrementó el nivel proteico de la única isoforma de esta enzima descrita en esta especie previamente (Haycock, 2002). Destacar, que la mayor expresión vascular de la TH en respuesta a la AngII en ambos modelos, concuerda con datos previos que demuestran la inducción de esta enzima por la AngII en otros tejidos, tanto *in vivo* como *in vitro* (Dogan *et al*., 2004, Ma *et al.*, 2004). Estos resultados sugieren que la actividad TH podría jugar un papel relevante en el desarrollo del AAA y en la capacidad de la AngII para promover la formación de aneurismas.

Distintas evidencias sugieren que las catecolaminas podrían influir de manera relevante en el remodelado vascular. Concretamente se ha descrito que la hiperactividad simpática subyace la fisiopatología de aortopatías como la TAD (Zhipeng *et al*., 2014, Hu *et al*., 2016), y tanto la hiperactividad simpática como el desarrollo de ramificaciones nerviosas se han detectado en la aorta de pacientes con TAD (Zhipeng *et al*., 2014). Además, la AngII, el principal inductor del sistema renina angiotensina, mediador clave en el desarrollo del AAA en humanos y modelos animales (Hackam *et al*., 2006), incrementa la actividad simpática. Este efecto aumenta la expresión aórtica de la MMP2, que desempeña un papel fundamental en el desarrollo de distintas aortopatías, entre ellas el AAA (Hu *et al*., 2013). Estos autores demostraron que las catecolaminas regulan la señalización TGF-β en aneurismas aórticos, lo que limita la proliferación de las CMLV y favorece su apoptosis, modulando así el remodelado vascular. Destacar que ya se había descrito la expresión de componentes de la vía de la TH en la pared vascular. La expresión de esta enzima se ha demostrado en CMLV, células endoteliales y en linfocitos T (Sorriento *et al*., 2012, Pfeil *et al*., 2014, Huang *et al*., 2016). En los linfocitos, las catecolaminas endógenas actúan de manera autocrina/paracrina regulando la actividad de estas células (Bergquist *et al*., 1994, Cosentino *et al*., 2007, Huang *et al*., 2016), mientras que las catecolaminas liberadas por las células endoteliales podrían contribuir a la neovascularización (Sorriento *et al*., 2012). En concordancia, nuestros estudios en aneurismas humanos y de ratón mostraron tinción para TH de forma localizada en zonas de inervación periférica, pero también en células inflamatorias y en CMLV. Destacar que la doxiciclina que previene la formación de AAA inducidos por AngII en ratones TgNOR-1^{VSMC}, es capaz de normalizar la expresión vascular de la *Th* (Cañes *et al*., 2021). Por lo tanto, la inducción de esta enzima podría contribuir al remodelado destructivo en el AAA. Sin embargo hasta la realización de

nuestros resultados, el impacto de esta vía en la formación del AAA era incierto, y no se había estudiado su capacidad como diana terapéutica para esta enfermedad.

En este contexto, analizamos la eficacia del bloqueo de la TH para limitar el crecimiento del AAA. Para ello se trataron ratones ApoE$^{-/-}$ y TgNOR-1^{VSMC} infundidos con AngII con AMPT, un inhibidor competitivo de TH biodisponible por vía oral y bien tolerado, que bloquea la biosíntesis de catecolaminas (Brogden *et al*., 1981, Naruse *et al*., 2018). La dosis administrada de este fármaco aseguraba una inhibición eficaz de la enzima tal y como se había descrito (Meltzer *et al*., 1979). En particular, bajo estas condiciones, el AMPT protegió frente al AAA inducido por AngII en ambos modelos experimentales. En el ámbito clínico, el AMPT se aprobó para el control de la hipertensión y otros síntomas asociados con el exceso de catecolaminas producidas por el feocromocitoma. Concretamente, el AMPT está indicado en el tratamiento preoperatorio de aquellos pacientes que tienen que ser intervenidos quirúrgicamente de este tumor lo que reduce la elevada mortalidad perioperatoria de esta intervención. También está indicado para el manejo de los pacientes en los que la cirugía está contraindicada y para el tratamiento crónico de los feocromocitomas malignos (DEMSER). Además, se ha propuesto el uso de este fármaco para el tratamiento de trastornos del movimiento y algunas enfermedades neuropsiquiatrías (Bloemen *et al*., 2008). En los pacientes con feocromocitoma, el AMPT bloquea la respuesta hipertensiva producida por las catecolaminas liberadas por el tumor, sin embargo, no se ha observado un efecto beneficioso de este fármaco sobre la hipertensión esencial (Bloemen *et al*., 2008). En consonancia, en nuestros experimentos, el AMPT no afectó a la presión sanguínea. Por lo tanto, el bloqueo de la TH previno la formación de AAA inducidas por AngII, lo cual promueve la formación de aneurismas de manera independiente de su función vasopresora (Cassis *et al*., 2009). El AMPT no sólo limitó el incremento del diámetro aórtico en respuesta a AngII, sino que también redujo la inflamación y el estrés oxidativo vascular, y preservó la integridad de la pared vascular. Otros autores ya habían asociado la actividad de la TH con la generación de ROS y la inflamación (Haavik *et al*., 1997, Tolleson & Claassen, 2012, Meiser *et al*., 2013). De acuerdo con estas observaciones en los modelos experimentales de AAA que hemos estudiado la inhibición de la TH con AMPT atenuó significativamente el estrés oxidativo vascular, redujo el infiltrado inflamatorio y mejoro el perfil de citoquinas pro-inflamatorias, lo que sugiere que la inducción de la TH podría contribuir al menos, en parte, a la fisiopatología del AAA. Destacar que estudios previos también habían sugerido que el AMPT podría mejorar el estrés oxidativo y la inflamación en otros contextos patológicos (Albayrak *et al*., 2010, Ahiskalioglu *et al*., 2015, Çimen *et al*., 2018). Y lo que es más importante, todos estos efectos vasculares del

AMPT se asociaron con una disminución de la expresión aórtica de la *Th*. Por lo tanto, nuestros resultados indican que la inducción de la TH tiene un impacto negativo en la formación del AAA y señala a la TH como enzima diana en la patología aneurismática.

La regulación de la expresión de la TH es compleja y específica del tipo celular (Kim *et al*., 2003 D). Análisis previos en tejidos no vasculares identificaron a la TH como gen diana de NURR1. Concretamente, NURR1 activa la expresión de la TH mediante su unión a un elemento situado a 1 kb del inicio de transcripción (Sakurada *et al*., 1999, Kim *et al*., 2003 C). Sorprendentemente, y dependiendo del tipo celular, NURR1 también puede actuar como represor de la transcripción de la TH (Kim *et al*., 2013), lo que sugiere la existencia de una compleja red implicada en la regulación de su expresión. Actualmente, se desconoce si otros miembros de la familia NR4A, y más concretamente NOR-1, podrían también regular la transcripción de la TH. En aneurismas humanos hemos detectado la existencia de una correlación significativa entre la expresión de *NOR-1* y la de genes implicados en la biosíntesis y transporte de catecolaminas, entre ellos la *TH*. Los ensayos de actividad transcripcional identificaron dos elementos putativos NBRE y determinamos que particularmente uno de ellos, situado a -2353 pb, es el responsable de la regulación transcripcional de la TH por NOR-1 en CMLV. El promotor humano de la TH presenta una baja homología con los promotores de otras especies, como la rata y el ratón, sin embargo, este NBRE se sitúa en una región conservada entre especies (Kessler *et al*., 2003).

Finalmente, destacar que diversos casos clínicos han descrito la coexistencia de feocromocitomas y de otros tumores neuroendocrinos con disecciones aorticas y rupturas aneurismáticas, lo que respalda que la hiperactividad de la vía de la TH podría contribuir al desarrollo del aneurisma y con la eventual ruptura aortica en algunos pacientes (Ehata *et al*., 1999, Kota *et al*., 2013, Arıkan 2018). Además, se ha descrito que en pacientes con TAD se produce un incremento de la TH y de la actividad simpática tanto general como aórtica (Zhipeng *et al*., 2014). Nuestro estudio demuestra por primera vez que la inducción de la vía de la TH puede ser relevante en la fisiopatología del AAA, tanto en humanos como en modelos experimentales, y sugiere el interés de la TH como diana terapéutica en la patología aneurismática.

CONCLUSIONES

En relación al primer objetivo se concluye:

1. En los ratones transgénicos que sobreexpresan NOR-1 en la pared vascular, la infusión de AngII desencadena un incremento del infiltrado inflamatorio, del remodelado de la MEC, del estrés oxidativo, así como una desestructuración de las láminas elásticas que predispone al desarrollo de AAA.
2. Los análisis de expresión diferencial nos han permitido identificar genes relacionados con procesos biológicos relevantes en la patología aneurismática relacionados con inflamación, citoesqueleto, diferenciación de la célula muscular y activación simpática.
3. En la aorta aneurismática de pacientes y del modelo animal transgénico de NOR-1 se induce la expresión de genes relacionados con la actividad simpática como *TH*, *DBH* y *DDC*.

En cuanto al segundo objetivo se concluye:

1. Los cardiomiocitos de los ratones TgNOR-1 son de mayor tamaño y presentan alteraciones en la contractibilidad, factores que predispondrían a la hipertrofia celular.
2. Los cardiofibroblastos de ratones transgénicos de NOR-1 sobreexpresan genes como *Acta1* y transgrelina, marcadores de transdiferenciación a miofibroblasto.
3. La transgénesis de NOR-1 en el miocardio promueve el remodelado cardíaco en ratones de mediana edad.
4. La transgénesis de NOR-1 en el miocardio agrava la hipertrofía cardíaca inducida por sobrecarga de presión.
5. NOR-1 regula la actividad transcripcional de *Loxl2* que codifica para un enzima implicado en la maduración de la MEC, clave en el remodelado cardíaco.

En relación al tercer objetivo se concluye:

1. El tratamiento con la doxiciclina disminuye el infiltrado inflamatorio, la actividad metaloproteinasa y el estrés oxidativo en la pared vascular en los ratones TgNOR-1^{CMLV} infundidos con AngII, disminuyendo la incidencia de AAA.
2. La inhibición de la actividad TH mediante AMPT previene la formación del AAA inducido por AngII, tanto en el ratón TgNOR-1^{CMLV} como en el $ApoE^{-/-}$.
3. El tratamiento con AMPT atenúa el remodelado vascular, la desestructuración y ruptura de las láminas elásticas, el infiltrado inflamatorio y el estrés oxidativo, en el modelo animal $ApoE^{-/-}$ y en el ratón transgénico de NOR-1.

BIBLIOGRAFÍA

Abdul-Hussien, H., Hanemaaijer, R., Verheijen, J. H., van Bockel, J. H., Geelkerken, R. H., & Lindeman, J. H. N. (2009). Doxycycline therapy for abdominal aneurysm: Improved proteolytic balance through reduced neutrophil content. *Journal of Vascular Surgery*, *49*(3), 741–749. https://doi.org/10.1016/j.jvs.2008.09.055

Aggarwal, S., Qamar, A., Sharma, V., & Sharma, A. (2011). Abdominal aortic aneurysm: A comprehensive review. *Experimental and Clinical Cardiology*, *16*(1), 11–15.

Aherne, C. M., McMorrow, J., Kane, D., FitzGerald, O., Mix, K. S., & Murphy, E. P. (2009). Identification of NR4A2 as a transcriptional activator of IL-8 expression in human inflammatory arthritis. *Molecular Immunology*, *46*(16), 3345–3357. https://doi.org/10.1016/j.molimm.2009.07.019

Ahiskalioglu, A., Ince, I., Aksoy, M., Ahiskalioglu, E. O., Comez, M., Dostbil, A., Celik, M., Alp, H. H., Coskun, R., Taghizadehghalehjoughi, A., & Suleyman, B. (2015). Comparative Investigation of Protective Effects of Metyrosine and Metoprolol Against Ketamine Cardiotoxicity in Rats. *Cardiovascular Toxicology*, *15*(4), 336–344. https://doi.org/10.1007/s12012-014-9301-z

Akagawa, H., Narita, A., Yamada, H., Tajima, A., Krischek, B., Kasuya, H., Hori, T., Kubota, M., Saeki, N., Hata, A., Mizutani, T., & Inoue, I. (2007). Systematic screening of lysyl oxidase-like (LOXL) family genes demonstrates that LOXL2 is a susceptibility gene to intracranial aneurysms. *Human Genetics*, *121*(3–4), 377–387. https://doi.org/10.1007/s00439-007-0333-3

Albayrak, A., Polat, B., Cadirci, E., Hacimuftuoglu, A., Halici, Z., Gulapoglu, M., Albayrak, F., & Suleyman, H. (2010). Gastric anti-ulcerative and anti-inflammatory activity of metyrosine in rats. *Pharmacological Reports : PR*, *62*(1), 113–119. https://doi.org/10.1016/s1734-1140(10)70248-6

Alonso, J., Cañes, L., García-Redondo, A. B., de Frutos, P. G., Rodríguez, C., & Martínez-González, J. (2018). The nuclear receptor NOR-1 modulates redox homeostasis in human vascular smooth muscle cells. *Journal of Molecular and Cellular Cardiology*, *122*(August 2018), 23–33. https://doi.org/10.1016/j.yjmcc.2018.08.002

Alonso, J., Galán, M., Martí-Pàmies, I., Romero, J. M., Camacho, M., Rodríguez, C., & Martínez-González, J. (2016). NOR-1/NR4A3 regulates the cellular inhibitor of apoptosis 2 (cIAP2) in vascular cells: role in the survival response to hypoxic stress. *Scientific Reports*, *6*, 34056. https://doi.org/10.1038/srep34056

Amirak, E., Fuller, S. J., Sugden, P. H., & Clerk, A. (2013). p90 ribosomal S6 kinases play a significant role in early gene regulation in the cardiomyocyte response to G(q)-protein-coupled receptor stimuli,

endothelin-1 and α(1)-adrenergic receptor agonists. *The Biochemical Journal*, *450*(2), 351–363. https://doi.org/10.1042/BJ20121371

Andersen, C. B., Lindholt, J. S., Urbonavicius, S., Halekoh, U., Jensen, P. S., Stubbe, J., Rasmussen, L. M., & Beck, H. C. (2018). Abdominal aortic aneurysms growth is associated with high concentrations of plasma proteins in the intraluminal thrombus and diseased arterial tissue. *Arteriosclerosis, Thrombosis, and Vascular Biology*, *38*(9), 2254–2267. https://doi.org/10.1161/ATVBAHA.117.310126

Arai, M., Alpert, N. R., MacLennan, D. H., Barton, P., & Periasamy, M. (1993). Alterations in sarcoplasmic reticulum gene expression in human heart failure: A possible mechanism for alterations in systolic and diastolic properties of the failing myocardium. *Circulation Research*, *72*(2), 463–469. https://doi.org/10.1161/01.RES.72.2.463

Aranda, A., & Pascual, A. (2001). Nuclear hormone receptors and gene expression. *Physiological Reviews*, *81*(3), 1269–1304. https://doi.org/10.1152/physrev.2001.81.3.1269

Arıkan, A. A. (2018). Ruptured abdominal aortic aneurysm with a suprarenal tumor. *Brazilian Journal of Cardiovascular Surgery*, *33*(5), 522–524. https://doi.org/10.21470/1678-9741-2017-0166

Armstrong, P. J., Johanning, J. M., Calton, W. C., Delatore, J. R., Franklin, D. P., Han, D. C., Carey, D. J., & Elmore, J. R. (2002). Differential gene expression in human abdominal aorta: aneurysmal versus occlusive disease. *Journal of Vascular Surgery*, *35*(2), 346–355. https://doi.org/10.1067/mva.2002.121071

Arnsten, A. F. T. (1997). Catecholamine regulation of the prefrontal cortex. *Journal of Psychopharmacology*, *11*(2), 151–162. https://doi.org/10.1177/026988119701100208

Arredondo, C., Orellana, M., Vecchiola, A., Pereira, L. A., Galdames, L., & Andrés, M. E. (2013). PIASγ Enhanced SUMO-2 Modification of Nurr1 Activation-Function-1 Domain Limits Nurr1 Transcriptional Synergy. *PLOS ONE*, *8*(1), e55035. https://doi.org/10.1371/journal.pone.0055035

Baicu, C. F., Stroud, J. D., Livesay, V. A., Hapke, E., Holder, J., Spinale, F. G., & Zile, M. R. (2003). Changes in extracellular collagen matrix alter myocardial systolic performance. *American Journal of Physiology - Heart and Circulatory Physiology*, *284*(1 53-1), 122–132. https://doi.org/10.1152/ajpheart.00233.2002

Baker, K. D., Shewchuk, L. M., Kozlova, T., Makishima, M., Hassell, A., Wisely, B., Caravella, J. A., Lambert, M. H., Reinking, J. L., Krause, H., Thummel, C. S., Willson, T. M., & Mangelsdorf, D. J. (2003). The Drosophila Orphan Nuclear Receptor DHR38 Mediates an

Atypical Ecdysteroid Signaling Pathway. *Cell*, *113*(6), 731–742. https://doi.org/10.1016/S0092-8674(03)00420-3

Barish, G. D., Downes, M., Alaynick, W. A., Yu, R. T., Ocampo, C. B., Bookout, A. L., Mangelsdorf, D. J., & Evans, R. M. (2005). A Nuclear Receptor Atlas: Macrophage Activation. *Molecular Endocrinology*, *19*(10), 2466–2477. https://doi.org/10.1210/me.2004-0529

Barnes, R. H., Akama, T., Öhman, M. K., Woo, M. S., Bahr, J., Weiss, S. J., Eitzman, D. T., & Chun, T. H. (2017). Membrane-tethered metalloproteinase expressed by vascular smooth muscle cells limits the progression of proliferative atherosclerotic lesions. *Journal of the American Heart Association*, *6*(7). https://doi.org/10.1161/JAHA.116.003693

Barry, S. P., Davidson, S. M., & Townsend, P. A. (2008). Molecular regulation of cardiac hypertrophy. *The International Journal of Biochemistry & Cell Biology*, *40*(10), 2023–2039. https://doi.org/10.1016/J.BIOCEL.2008.02.020

Bartoli, M. A., Parodi, F. E., Chu, J., Pagano, M. B., Mao, D., Baxter, B. T., Buckley, C., Ennis, T. L., & Thompson, R. W. (2006). Localized Administration of Doxycycline Suppresses Aortic Dilatation in an Experimental Mouse Model of Abdominal Aortic Aneurysm. *Annals of Vascular Surgery*, *20*(2), 228–236. https://doi.org/10.1007/s10016-006-9017-z

Baudino, T. A., Carver, W., Giles, W., & Borg, T. K. (2006). Cardiac fibroblasts: Friend or foe? *American Journal of Physiology - Heart and Circulatory Physiology*, *291*(3). https://doi.org/10.1152/ajpheart.00023.2006

Baxter, B. T., Matsumura, J., Curci, J. A., McBride, R., Larson, L., Blackwelder, W., Lam, D., Wijesinha, M., Terrin, M., & N-TA3CT Investigators (2020). Effect of Doxycycline on Aneurysm Growth Among Patients With Small Infrarenal Abdominal Aortic Aneurysms: A Randomized Clinical Trial. *JAMA*, *323*(20), 2029–2038. https://doi.org/10.1001/jama.2020.5230

Baxter, B. T., Pearce, W. H., Waltke, E. A., Littooy, F. N., Hallett, J. W., Kent, K. C., Upchurch, G. R., Chaikof, E. L., Mills, J. L., Fleckten, B., Longo, G. M., Lee, J. K., & Thompson, R. W. (2002). Prolonged administration of doxycycline in patients with small asymptomatic abdominal aortic aneurysms: Report of a prospective (Phase II) multicenter study. *Journal of Vascular Surgery*, *36*(1), 1–12. https://doi.org/10.1067/mva.2002.125018

Bei, Y., Yuan-Ying, J., Shaoping, C., Guijun, Y., & Jianxin, S. (2009). The Orphan Nuclear Receptor Nur77 Suppresses Endothelial Cell Activation

Through Induction of IκBα Expression. *Circulation Research*, *104*(6), 742–749. https://doi.org/10.1161/CIRCRESAHA.108.192286

Benoit, G., Cooney, A., Giguere, V., Ingraham, H., Lazar, M., Muscat, G., Perlmann, T., Renaud, J. P., Schwabe, J., Sladek, F., Tsai, M. J., & Laudet, V. (2006). International union of pharmacology. LXVI. Orphan nuclear receptors. *Pharmacological Reviews*, *58*(4), 798–836. https://doi.org/10.1124/pr.58.4.10

Bergquist, J., Tarkowski, A., Ekman, R., & Ewing, A. (1994). Discovery of endogenous catecholamines in lymphocytes and evidence for catecholamine regulation of lymphocyte function via an autocrine loop. *Proceedings of the National Academy of Sciences*, *91*(26), 12912 LP – 12916. https://doi.org/10.1073/pnas.91.26.12912

Bernardo, B. C., Weeks, K. L., Pretorius, L., & McMullen, J. R. (2010). Molecular distinction between physiological and pathological cardiac hypertrophy: Experimental findings and therapeutic strategies. *Pharmacology and Therapeutics*, *128*(1), 191–227. https://doi.org/10.1016/j.pharmthera.2010.04.005

Bers, D. M. (2006). Altered cardiac myocyte Ca regulation in heart failure. *Physiology*, *21*(6), 380–387. https://doi.org/10.1152/physiol.00019.2006

Bers, D. M. (2014). Cardiac Sarcoplasmic Reticulum Calcium Leak: Basis and Roles in Cardiac Dysfunction. *Annual Review of Physiology*, *76*(1), 107–127. https://doi.org/10.1146/annurev-physiol-020911-153308

Bloemen, O., de Koning, M., Boot, E., Booij, J., & van Amelsvoort, T. A. (2012). Challenge and Therapeutic Studies Using Alpha-Methyl-para-Tyrosine (AMPT) in Neuropsychiatric Disorders: A Review. *Central Nervous System Agents in Medicinal Chemistry*, *8*(4), 249–256. https://doi.org/10.2174/187152408786848102

Bonta, P. I., Pols, T. W., van Tiel, C. M., Vos, M., Arkenbout, E. K., Rohlena, J., Koch, K. T., de Maat, M. P., Tanck, M. W., de Winter, R. J., Pannekoek, H., Biessen, E. A., Bot, I., & de Vries, C. J. (2010). Nuclear receptor Nurr1 is expressed in and is associated with human restenosis and inhibits vascular lesion formation in mice involving inhibition of smooth muscle cell proliferation and inflammation. *Circulation*, *121*(18), 2023–2032. https://doi.org/10.1161/CIRCULATIONAHA.109.885673

Bonta, P. I., van Tiel, C. M., Vos, M., Pols, T. W., van Thienen, J. V., Ferreira, V., Arkenbout, E. K., Seppen, J., Spek, C. A., van der Poll, T., Pannekoek, H., & de Vries, C. J. (2006). Nuclear receptors Nur77, Nurr1, and NOR-1 expressed in atherosclerotic lesion macrophages reduce lipid loading and inflammatory responses. *Arteriosclerosis, thrombosis, and vascular biology*, *26*(10), 2288–2294. https://doi.org/10.1161/01.ATV.0000238346.84458.5d

Brady, A. R., Thompson, S. G., Fowkes, F. G. R., Greenhalgh, R. M., & Powell, J. T. (2004). Abdominal aortic aneurysm expansion: Risk factors and time intervals for surveillance. *Circulation*, *110*(1), 16–21. https://doi.org/10.1161/01.CIR.0000133279.07468.9F

Brogden, R. N., Heel, R. C., Speight, T. M., & Avery, G. S. (1981). α-Methyl-p-Tyrosine: A Review of its Pharmacology and Clinical Use. *Drugs*, *21*(2), 81–89. https://doi.org/10.2165/00003495-198121020-00001

Brouwers, F. P., De Boer, R. A., Van Der Harst, P., Voors, A. A., Gansevoort, R. T., Bakker, S. J., Hillege, H. L., Van Veldhuisen, D. J., & Van Gilst, W. H. (2013). Incidence and epidemiology of new onset heart failure with preserved vs. reduced ejection fraction in a community-based cohort: 11-year follow-up of PREVEND. *European Heart Journal*, *34*(19), 1424–1431. https://doi.org/10.1093/eurheartj/eht066

Brown, R. D., Ambler, S. K., Mitchell, M. D., & Long, C. S. (2005). THE CARDIAC FIBROBLAST: Therapeutic Target in Myocardial Remodeling and Failure. *Annual Review of Pharmacology and Toxicology*, *45*(1), 657–687. https://doi.org/10.1146/annurev.pharmtox.45.120403.095802

Burillo, E., Lindholt, J., Molina-sanchez, P., Jorge, I., Martinez-Pinna, R., Blanco-Colio, L., Tarín, C., Torres-Fonseca, M., Esteban, M., Laustsen, J., Ramos-Mozo, P., Calvo, E., Lopez, J., de Ceniga, M., Michel, J.-B., Egido, J., Andrés, V., Vázquez, J., Meilhac, O., & Martín-Ventura, J. (2015). ApoA-I/HDL-C levels are inversely associated with abdominal aortic aneurysm progression. *Thrombosis and Haemostasis*, *113*. https://doi.org/10.1160/TH14-10-0874

Busuttil, R. W., Rinderbriecht, H., Flesher, A., & Carmack, C. (1982). Elastase activity: The role of elastase in aortic aneurysm formation. *Journal of Surgical Research*, *32*(3), 214–217. https://doi.org/10.1016/0022-4804(82)90093-2

Calvayrac, O., Rodríguez-Calvo, R., Martí-Pamies, I., Alonso, J., Ferrán, B., Aguiló, S., Crespo, J., Rodríguez-Sinovas, A., Rodríguez, C., & Martínez-González, J. (2015). NOR-1 modulates the inflammatory response of vascular smooth muscle cells by preventing NFκB activation. *Journal of Molecular and Cellular Cardiology*, *80*, 34–44. https://doi.org/10.1016/j.yjmcc.2014.12.015

Cassis, L. A., Gupte, M., Thayer, S., Zhang, X., Charnigo, R., Howatt, D. A., Rateri, D. L., & Daugherty, A. (2009). ANG II infusion promotes abdominal aortic aneurysms independent of increased blood pressure in hypercholesterolemic mice. *American Journal of Physiology. Heart and Circulatory Physiology*, *296*(5), H1660-5. https://doi.org/10.1152/ajpheart.00028.2009

Cañes, L., Martí-Pàmies, I., Ballester-Servera, C., Herraiz-Martínez, A., Alonso, J., Galán, M., Nistal, J. F., Muniesa, P., Osada, J., Hove-Madsen, L., Rodríguez, C., & Martínez-González, J. (2020). Neuron-derived orphan receptor-1 modulates cardiac gene expression and exacerbates angiotensin II-induced cardiac hypertrophy. Clinical science (London, England : 1979), 134(3), 359–377. https://doi.org/10.1042/CS20191014

Cañes, L., Martí-Pàmies, I., Ballester-Servera, C., Alonso, J., Serrano, E., Rodríguez, C. and Martínez-González, J. (2021) High neuron derived orphan receptor-1 (NOR-1) expression strengthens the vascular wall response to angiotensin II leading to aneurysm formation in mice. *Hypertension, in press*.

Chen, J. D., & Evans, R. M. (1995). A transcriptional co-repressor that interacts with nuclear hormone receptors. *Nature*, *377*(6548), 454–457. https://doi.org/10.1038/377454a0

Cheng, L. E., Chan, F. K., Cado, D., & Winoto, A. (1997). Functional redundancy of the Nur77 and Nor-1 orphan steroid receptors in T-cell apoptosis. *The EMBO Journal*, *16*(8), 1865–1875. https://doi.org/10.1093/emboj/16.8.1865

Cheng, Z., Völkers, M., Din, S., Avitabile, D., Khan, M., Gude, N., Mohsin, S., Bo, T., Truffa, S., Alvarez, R., Mason, M., Fischer, K. M., Konstandin, M. H., Zhang, X., Heller Brown, J., & Sussman, M. A. (2011). Mitochondrial translocation of Nur77 mediates cardiomyocyte apoptosis. *European Heart Journal*, *32*(17), 2179–2188. https://doi.org/10.1093/eurheartj/ehq496

Choke, E., Cockerill, G. W., Dawson, J., Wilson, R. W., Jones, A., Loftus, I. A. N. M., & Thompson, M. M. (2006). Increased Angiogenesis at the Site of Abdominal Aortic Aneurysm Rupture. *Annals of the New York Academy of Sciences*, *1085*(1), 315–319. https://doi.org/10.1196/annals.1383.007

Choke, E., Cockerill, G. W., Laing, K., Dawson, J., Wilson, W. R. W., Loftus, I. M., & Thompson, M. M. (2009). Whole Genome-expression Profiling Reveals a Role for Immune and Inflammatory Response in Abdominal Aortic Aneurysm Rupture. *European Journal of Vascular and Endovascular Surgery*, *37*(3), 305–310. https://doi.org/10.1016/j.ejvs.2008.11.017

Chung, S., Sonntag, K.-C., Andersson, T., Bjorklund, L. M., Park, J.-J., Kim, D.-W., Kang, U. J., Isacson, O., & Kim, K.-S. (2002). Genetic engineering of mouse embryonic stem cells by Nurr1 enhances differentiation and maturation into dopaminergic neurons. *The European Journal of Neuroscience*, *16*(10), 1829–1838. https://doi.org/10.1046/j.1460-9568.2002.02255.x

Çimen, O., Çimen, F. K., Gülapoğlu, M., Bilgin, A. Ö., Çekiç, A. B., Eken, H., Süleyman, Z., Bilgin, Y., & Altuner, D. (2018). The effect of metyrosine on oxidative gastric damage induced by ischemia/reperfusion in rats. Biochemical and histopathological evaluation. *Acta Cirurgica Brasileira*, *33*(3), 259–267. https://doi.org/10.1590/s0102-865020180030000008

Codina, A., Benoit, G., Gooch, J. T., Neuhaus, D., Perlmann, T., & Schwabe, J. W. R. (2004). Identification of a novel co-regulator interaction surface on the ligand binding domain of Nurr1 using NMR footprinting. *Journal of Biological Chemistry*, *279*(51), 53338–53345. https://doi.org/10.1074/jbc.M409096200

Cohn, J. N., Ferrari, R., & Sharpe, N. (2000). Cardiac remodeling-concepts and clinical implications: A consensus paper from an International Forum on Cardiac Remodeling. *Journal of the American College of Cardiology*, *35*(3), 569–582. https://doi.org/10.1016/S0735-1097(99)00630-0

Colomer, J. M., Mao, L., Rockman, H. A., & Means, A. R. (2003). Pressure Overload Selectively Up-Regulates Ca2+/Calmodulin-Dependent Protein Kinase II in Vivo. *Molecular Endocrinology*, *17*(2), 183–192. https://doi.org/10.1210/me.2002-0350

Cornuz, J., Pinto, C. S., Tevaearai, H., & Egger, M. (2004). Risk factors for asymptomatic abdominal aortic aneurysm: Sytematic review and meta-analysis of population-based screening studies. *European Journal of Public Health*, *14*(4), 343–349. https://doi.org/10.1093/eurpub/14.4.343

Cosentino, M., Fietta, A. M., Ferrari, M., Rasini, E., Bombelli, R., Carcano, E., Saporiti, F., Meloni, F., Marino, F., & Lecchini, S. (2007). Human CD4+CD25+ regulatory T cells selectively express tyrosine hydroxylase and contain endogenous catecholamines subserving an autocrine/paracrine inhibitory functional loop. *Blood*, *109*(2), 632–642. https://doi.org/10.1182/blood-2006-01-028423

Couchonnal, L. F., & Anderson, M. E. (2008). The role of calmodulin kinase II in myocardial physiology and disease. *Physiology (Bethesda, Md.)*, *23*, 151–159. https://doi.org/10.1152/physiol.00043.2007

Courtois, A., Nusgens, B. V., Hustinx, R., Namur, G., Gomez, P., Kuivaniemi, H., Defraigne, J. O., Colige, A. C., & Sakalihasan, N. (2014). Gene expression study in positron emission tomography-positive abdominal aortic aneurysms identifies CCL18 as a potential biomarker for rupture risk. *Molecular Medicine (Cambridge, Mass.)*, *20*, 697–706. https://doi.org/10.2119/molmed.2014.00065

Curci, J. A., Mao, D., Bohner, D. G., Allen, B. T., Rubin, B. G., Reilly, J. M., Sicard, G. A., & Thompson, R. W. (2000). Preoperative treatment with doxycycline reduces aortic wall expression and activation of matrix metalloproteinases in patients with abdominal aortic aneurysms. *Journal*

of Vascular Surgery, *31*(2), 325–342. https://doi.org/10.1016/S0741-5214(00)90163-0

Curci, J. A., Petrinec, D., Liao, S., Golub, L. M., & Thompson, R. W. (1998). Pharmacologic suppression of experimental abdominal aortic aneurysms: A comparison of doxycycline and four chemically modified tetracyclines. *Journal of Vascular Surgery*, *28*(6), 1082–1093. https://doi.org/10.1016/S0741-5214(98)70035-7

Dale, M. A., Ruhlman, M. K., & Baxter, B. T. (2015). Inflammatory cell phenotypes in AAAs: their role and potential as targets for therapy. *Arteriosclerosis, Thrombosis, and Vascular Biology*, *35*(8), 1746–1755. https://doi.org/10.1161/ATVBAHA.115.305269

Daubner, S. C., Le, T., & Wang, S. (2011). Tyrosine hydroxylase and regulation of dopamine synthesis. *Archives of Biochemistry and Biophysics*, *508*(1), 1–12. https://doi.org/10.1016/j.abb.2010.12.017

Daugherty, A., Manning, M. W., & Cassis, L. A. (2000). Angiotensin II promotes atherosclerotic lesions and aneurysms in apolipoprotein E-deficient mice. *The Journal of Clinical Investigation*, *105*(11), 1605–1612. https://doi.org/10.1172/JCI7818

Defawe, O., Colige, A., Lambert, C., Delvenne, P., Lapière, C., Limet, R., Nusgens, B., & Sakalihasan, N. (2004). Gradient of proteolytic enzymes, their inhibitors and matrix proteins expression in a ruptured abdominal aortic aneurysm. *European Journal of Clinical Investigation*, *34*, 513–514. https://doi.org/10.1111/j.1365-2362.2004.01371.x

DEMSER (metyrosine) capsule. FDA prescribing information. https://www.drugs.com/pro/demser.html. Accessed October 31 2016.

Derk, F., Christian, K., Martin, van E., Doris, G., Christiane, H., Stefanie, L., Rainer, W., A., K. H., & Norbert, F. (2007). Calsarcin-1 Protects Against Angiotensin-II–Induced Cardiac Hypertrophy. *Circulation*, *116*(22), 2587–2596. https://doi.org/10.1161/CIRCULATIONAHA.107.711317

Dobrin, P. B., Baker, W. H., & Gley, W. C. (1984). Elastolytic and Collagenolytic Studies of Arteries: Implications for the Mechanical Properties of Aneurysms. *Archives of Surgery*, *119*(4), 405–409. https://doi.org/10.1001/archsurg.1984.01390160041009

Dogan, M. D., Sumners, C., Broxson, C. S., Clark, N., & Tümer, N. (2004). Central angiotensin II increases biosynthesis of tyrosine hydroxylase in the rat adrenal medulla. *Biochemical and Biophysical Research Communications*, *313*(3), 623–626. https://doi.org/10.1016/j.bbrc.2003.11.161

Dubick, M. A., Keen, C. L., DiSilvestro, R. A., Eskelson, C. D., Ireton, J., &

Hunter, G. C. (1999). Antioxidant Enzyme Activity in Human Abdominal Aortic Aneurysmal and Occlusive Disease. *Proceedings of the Society for Experimental Biology and Medicine*, *220*(1), 39–45. https://doi.org/10.3181/00379727-220-44342

Eghbali, M., Deva, R., Alioua, A., Minosyan, T. Y., Ruan, H., Wang, Y., Toro, L., & Stefani, E. (2005). Molecular and functional signature of heart hypertrophy during pregnancy. *Circulation Research*, *96*(11), 1208–1216. https://doi.org/10.1161/01.RES.0000170652.71414.16

Ehata, T., Karasawa, F., Watanabe, K., & Satoh, T. (1999). Unsuspected pheochromocytoma with abdominal aortic aneurysm--a case report. *Acta Anaesthesiologica Sinica*, *37*(1), 27–28.

Elia, L., Kunderfranco, P., Carullo, P., Vacchiano, M., Farina, F. M., Hall, I. F., Mantero, S., Panico, C., Papait, R., Condorelli, G., & Quintavalle, M. (2018). UHRF1 epigenetically orchestrates smooth muscle cell plasticity in arterial disease. *The Journal of Clinical Investigation*, *128*(6), 2473–2486. https://doi.org/10.1172/JCI96121

Emil, K. K., Christian, T.-P., Hilmar, G. G., Martin, E., Berg, R. H., & Riis, H. P. (2015). Angiotensin-Converting Enzyme Inhibitors and Angiotensin II Receptor Blockers in Patients With Abdominal Aortic Aneurysms. *Arteriosclerosis, Thrombosis, and Vascular Biology*, *35*(3), 733–740. https://doi.org/10.1161/ATVBAHA.114.304428

Erickson, J. R., Joiner, M. A., Guan, X., Kutschke, W., Yang, J., Oddis, C. V, Bartlett, R. K., Lowe, J. S., O'Donnell, S. E., Aykin-Burns, N., Zimmerman, M. C., Zimmerman, K., Ham, A.-J. L., Weiss, R. M., Spitz, D. R., Shea, M. A., Colbran, R. J., Mohler, P. J., & Anderson, M. E. (2008). A dynamic pathway for calcium-independent activation of CaMKII by methionine oxidation. *Cell*, *133*(3), 462–474. https://doi.org/10.1016/j.cell.2008.02.048

Erickson, J. R., Julie He, B., Grumbach, I. M., & Anderson, M. E. (2011). CaMKII in the cardiovascular system: Sensing redox states. *Physiological Reviews*, *91*(3), 889–915. https://doi.org/10.1152/physrev.00018.2010

Erten, Y., Tulmac, M., Derici, U., Pasaoglu, H., Reis, K. A., Bali, M., Arinsoy, T., Cengel, A., & Sindel, S. (2005). An Association Between Inflammatory State and Left Ventricular Hypertrophy in Hemodialysis Patients. *Renal Failure*, *27*(5), 581–589. https://doi.org/10.1080/08860220500200072

Escriva, H., Bertrand, S., & Laudet, V. (2004). The evolution of the nuclear receptor superfamily. *Essays in Biochemistry*, *40*(February), 11–26. https://doi.org/10.1042/bse0400011

Fagard, R. H. (1997). IMPACT OF DIFFERENT SPORTS AND TRAINING

ON CARDIAC STRUCTURE AND FUNCTION. *Cardiology Clinics*, *15*(3), 397–412. https://doi.org/https://doi.org/10.1016/S0733-8651(05)70348-9

Fahrner, T. J., Carroll, S. L., & Milbrandt, J. (1990). The NGFI-B protein, an inducible member of the thyroid/steroid receptor family, is rapidly modified posttranslationally. *Molecular and Cellular Biology*, *10*(12), 6454–6459. https://doi.org/10.1128/mcb.10.12.6454

Feng, X.-J., Gao, H., Gao, S., Li, Z., Li, H., Lu, J., Wang, J.-J., Huang, X.-Y., Liu, M., Zou, J., Ye, J.-T., & Liu, P.-Q. (2015). The orphan receptor NOR1 participates in isoprenaline-induced cardiac hypertrophy by regulating PARP-1. *British Journal of Pharmacology*, *172*(11), 2852–2863. https://doi.org/10.1111/bph.13091

Ferrán, B., Martí-Pàmies, I., Alonso, J., Rodríguez-Calvo, R., Aguiló, S., Vidal, F., Rodríguez, C., & Martínez-González, J. (2016). The nuclear receptor NOR-1 regulates the small muscle protein, X-linked (SMPX) and myotube differentiation. *Scientific Reports*, *6*(March), 1–11. https://doi.org/10.1038/srep25944

Forsdahl, S. H., Singh, K., Solberg, S., & Jacobsen, B. K. (2009). Risk factors for abdominal aortic aneurysms: a 7-year prospective study: the tromsø study, 1994 2001. *Circulation*, *119*(16), 2202–2208. https://doi.org/10.1161/CIRCULATIONAHA.108.817619

Frey, N., Katus, H. A., Olson, E. N., & Hill, J. A. (2004). Hypertrophy of the Heart: A New Therapeutic Target? *Circulation*, *109*(13), 1580–1589. https://doi.org/10.1161/01.CIR.0000120390.68287.BB

Fu, Y., Luo, L., Luo, N., Zhu, X., & Garvey, W. T. (2007). NR4A orphan nuclear receptors modulate insulin action and the glucose transport system: Potential role in insulin resistance. *Journal of Biological Chemistry*, *282*(43), 31525–31533. https://doi.org/10.1074/jbc.M701132200

Galán, M., Varona, S., Guadall, A., Orriols, M., Navas, M., Aguiló, S., De Diego, A., Navarro, M. A., García-Dorado, D., Rodríguez-Sinovas, A., Martínez-González, J., & Rodriguez, C. (2017). Lysyl oxidase overexpression accelerates cardiac remodeling and aggravates angiotensin II–induced hypertrophy. *FASEB Journal*, *31*(9), 3787–3799. https://doi.org/10.1096/fj.201601157RR

Gary, P. H. . J. B. M. . S. C. T. et al. (1990). The New England Journal of Medicine Downloaded from nejm.org on April 1, 2015. For personal use only. No other uses without permission. Copyright © 1990 Massachusetts Medical Society. All rights reserved. *The New English Journal of Medicine*, *323*(16), 1120–1123.

Ghosh, A. K., & Vaughan, D. E. (2012). PAI-1 in tissue fibrosis. *Journal of Cellular Physiology*, *227*(2), 493–507. https://doi.org/10.1002/jcp.22783

Gizard, F., Zhao, Y., Findeisen, H. M., Qing, H., Cohn, D., Heywood, E. B., Jones, K. L., Nomiyama, T., & Bruemmer, D. (2011). Transcriptional regulation of S phase kinase-associated protein 2 by NR4A orphan nuclear receptor NOR1 in vascular smooth muscle cells. *The Journal of Biological Chemistry*, *286*(41), 35485–35493. https://doi.org/10.1074/jbc.M111.295840

Glass, C. K., & Ogawa, S. (2006). Combinatorial roles of nuclear receptors in inflammation and immunity. *Nature Reviews Immunology*, *6*(1), 44–55. https://doi.org/10.1038/nri1748

Glass, C. K., & Rosenfeld, M. G. (2000). The coregulator exchange in transcriptional functions of nuclear receptors. *Genes and Development*, *14*(2), 121–141. https://doi.org/10.1101/gad.14.2.121

Golledge, J., Cullen, B., Rush, C., Moran, C. S., Secomb, E., Wood, F., Daugherty, A., Campbell, J. H., & Norman, P. E. (2010 B). Peroxisome proliferator-activated receptor ligands reduce aortic dilatation in a mouse model of aortic aneurysm. *Atherosclerosis*, *210*(1), 51–56. https://doi.org/10.1016/j.atherosclerosis.2009.10.027

Golledge, J., & Norman, P. E. (2010). Atherosclerosis and abdominal aortic aneurysm: cause, response, or common risk factors?. A*rteriosclerosis, thrombosis, and vascular biology*, *30*(6), 1075–1077. https://doi.org/10.1161/ATVBAHA.110.206573

Golledge, J., Muller, J., Daugherty, A., & Norman, P. (2006). Abdominal aortic aneurysm: Pathogenesis and implications for management. *Arteriosclerosis, Thrombosis, and Vascular Biology*, *26*(12), 2605–2613. https://doi.org/10.1161/01.ATV.0000245819.32762.cb

Golledge, J., van Bockxmeer, F., Jamrozik, K., McCann, M., & Norman, P. E. (2010 A). Association Between Serum Lipoproteins and Abdominal Aortic Aneurysm. *American Journal of Cardiology*, *105*(10), 1480–1484. https://doi.org/10.1016/j.amjcard.2009.12.076

González-Santamaría, J., Villalba, M., Busnadiego, O., López-Olañeta, M. M., Sandoval, P., Snabel, J., López-Cabrera, M., Erler, J. T., Hanemaaijer, R., Lara-Pezzi, E., & Rodríguez-Pascual, F. (2015). Matrix cross-linking lysyl oxidases are induced in response to myocardial infarction and promote cardiac dysfunction. *Cardiovascular Research*, *109*(1), 67–78. https://doi.org/10.1093/cvr/cvv214

Gradman, A. H., & Alfayoumi, F. (2006). From Left Ventricular Hypertrophy to Congestive Heart Failure: Management of Hypertensive Heart Disease. *Progress in Cardiovascular Diseases*, *48*(5), 326–341.

https://doi.org/10.1016/j.pcad.2006.02.001

Grigoryants, V., Hannawa, K. K., Pearce, C. G., Sinha, I., Roelofs, K. J., Ailawadi, G., Deatrick, K. B., Woodrum, D. T., Cho, B. S., Henke, P. K., Stanley, J. C., Eagleton, M. J., & Upchurch Jr, G. R. (2005). Tamoxifen up-regulates catalase production, inhibits vessel wall neutrophil infiltration, and attenuates development of experimental abdominal aortic aneurysms. *Journal of Vascular Surgery*, *41*(1), 108–114. https://doi.org/10.1016/j.jvs.2004.09.033

Grossman, W., Jones, D., & McLaurin, L. P. (1975). Wall stress and patterns of hypertrophy in the human left ventricle. *Journal of Clinical Investigation*, *56*(1), 56–64. https://doi.org/10.1172/JCI108079

Gruber, F., Hufnagl, P., Hofer-Warbinek, R., Schmid, J. A., Breuss, J. M., Huber-Beckmann, R., Lucerna, M., Papac, N., Harant, H., Lindley, I., de Martin, R., & Binder, B. R. (2003). Direct binding of Nur77/NAK-1 to the plasminogen activator inhibitor 1 (PAI-1) promoter regulates TNFα-induced PAI-1 expression. *Blood*, *101*(8), 3042–3048. https://doi.org/10.1182/blood-2002-07-2331

Haavik, J., Almås, B., & Flatmark, T. (1997). Generation of reactive oxygen species by tyrosine hydroxylase: a possible contribution to the degeneration of dopaminergic neurons? *Journal of Neurochemistry*, *68*(1), 328–332. https://doi.org/10.1046/j.1471-4159.1997.68010328.x

Hackam, D. G., Thiruchelvam, D., & Redelmeier, D. A. (2006). Angiotensin-converting enzyme inhibitors and aortic rupture: a population-based case-control study. *Lancet (London, England)*, *368*(9536), 659–665. https://doi.org/10.1016/S0140-6736(06)69250-7

Hanna, R. N., Shaked, I., Hubbeling, H. G., Punt, J. A., Wu, R., Herrley, E., Zaugg, C., Pei, H., Geissmann, F., Ley, K., & Hedrick, C. C. (2012). NR4A1 (Nur77) deletion polarizes macrophages toward an inflammatory phenotype and increases atherosclerosis. *Circulation Research*, *110*(3), 416–427. https://doi.org/10.1161/CIRCRESAHA.111.253377

Hamers, A. A., Vos, M., Rassam, F., Marinković, G., Kurakula, K., van Gorp, P. J., de Winther, M. P., Gijbels, M. J., de Waard, V., & de Vries, C. J. (2012). Bone marrow-specific deficiency of nuclear receptor Nur77 enhances atherosclerosis. *Circulation research*, *110*(3), 428–438. https://doi.org/10.1161/CIRCRESAHA.111.260760

Haycock, J. W. (2002). Species differences in the expression of multiple tyrosine hydroxylase protein isoforms. *Journal of Neurochemistry*, *81*(5), 947–953. https://doi.org/10.1046/j.1471-4159.2002.00881.x

Haycock, J. W., George, R. J., & Waymire, J. C. (1985). In situ phosphorylation of tyrosine hydroxylase in chromaffin cells: Localization to soluble

compartments. *Neurochemistry International*, *7*(2), 301–308. https://doi.org/https://doi.org/10.1016/0197-0186(85)90119-6

Hazel, T. G., Nathans, D., & Lau, L. F. (1988). A gene inducible by serum growth factors encodes a member of the steroid and thyroid hormone receptor superfamily. *Proceedings of the National Academy of Sciences*, *85*(22), 8444 LP – 8448. https://doi.org/10.1073/pnas.85.22.8444

Hedvat, C. V, & Irving, S. G. (1995). The isolation and characterization of MINOR, a novel mitogen-inducible nuclear orphan receptor. *Molecular Endocrinology*, *9*(12), 1692–1700. https://doi.org/10.1210/mend.9.12.8614405

Hellenthal, F. A. M. V. I., Buurman, W. A., Wodzig, W. K. W. H., & Schurink, G. W. H. (2009). Biomarkers of abdominal aortic aneurysm progression. Part 2: inflammation. *Nature Reviews Cardiology*, *6*(8), 543–552. https://doi.org/10.1038/nrcardio.2009.102

Hinterseher, I., Schworer, C. M., Lillvis, J. H., Stahl, E., Erdman, R., Gatalica, Z., Tromp, G., & Kuivaniemi, H. (2015). Immunohistochemical analysis of the natural killer cell cytotoxicity pathway in human abdominal aortic aneurysms. *International Journal of Molecular Sciences*, *16*(5), 11196–11212. https://doi.org/10.3390/ijms160511196

Hirsch, A. T., Haskal, Z. J., Hertzer, N. R., Bakal, C. W., Creager, M. A., Halperin, J. L., Hiratzka, L. F., Murphy, W. R., Olin, J. W., Puschett, J. B., Rosenfield, K. A., Sacks, D., Stanley, J. C., Taylor, L. M., Jr, White, C. J., White, J., White, R. A., Antman, E. M., Smith, S. C., Jr, Adams, C. D., … Vascular Disease Foundation (2006). ACC/AHA 2005 Practice Guidelines for the management of patients with peripheral arterial disease (lower extremity, renal, mesenteric, and abdominal aortic): a collaborative report from the American Association for Vascular Surgery/Society for Vascular Surgery, Society for Cardiovascular Angiography and Interventions, Society for Vascular Medicine and Biology, Society of Interventional Radiology, and the ACC/AHA Task Force on Practice Guidelines (Writing Committee to Develop Guidelines for the Management of Patients With Peripheral Arterial Disease): endorsed by the American Association of Cardiovascular and Pulmonary Rehabilitation; National Heart, Lung, and Blood Institute; Society for Vascular Nursing; TransAtlantic Inter-Society Consensus; and Vascular Disease Foundation. *Circulation*, *113*(11), e463–e654. https://doi.org/10.1161/CIRCULATIONAHA.106.174526

Hoffmann, J. M., & Partridge, L. (2015). Nuclear hormone receptors: Roles of xenobiotic detoxification and sterol homeostasis in healthy aging. *Critical Reviews in Biochemistry and Molecular Biology*, *50*(5), 380–392. https://doi.org/10.3109/10409238.2015.1067186

Holcomb, M., Ding, Y. H., Dai, D., McDonald, R. J., McDonald, J. S., Kallmes, D. F., & Kadirvel, R. (2015). RNA-sequencing analysis of messenger RNA/MicroRNA in a rabbit aneurysm model identifies pathways and genes of interest. *American Journal of Neuroradiology*, *36*(9), 1710–1715. https://doi.org/10.3174/ajnr.A4390

Holla, V. R., Mann, J. R., Shi, Q., & DuBois, R. N. (2006). Prostaglandin E2 regulates the nuclear receptor NR4A2 in colorectal cancer. *The Journal of Biological Chemistry*, *281*(5), 2676–2682. https://doi.org/10.1074/jbc.M507752200

Hörlein, A. J., Näär, A. M., Heinzel, T., Torchia, J., Gloss, B., Kurokawa, R., Ryan, A., Kamei, Y., Söderström, M., Glass, C. K., & Rosenfeld, M. G. (1995). Ligand-independent repression by the thyroid hormone receptor mediated by a nuclear receptor co-repressor. *Nature*, *377*(6548), 397–404. https://doi.org/10.1038/377397a0

Houard, X., Ollivier, V., Louedec, L., Michel, J.-B., & Bäck, M. (2009). Differential inflammatory activity across human abdominal aortic aneurysms reveals neutrophil-derived leukotriene B4 as a major chemotactic factor released from the intraluminal thrombus. *The FASEB Journal*, *23*(5), 1376–1383. https://doi.org/10.1096/fj.08-116202

Hu, R., Wang, Z., Ren, Z., & Liu, M. (2016). Autonomic remodeling may be responsible for decreased incidence of aortic dissection in STZ-induced diabetic rats via down-regulation of matrix metalloprotease 2. *BMC Cardiovascular Disorders*, *16*(1), 200. https://doi.org/10.1186/s12872-016-0375-3

Hu, Z., Li, B., Wang, Z., Hu, X., Zhang, M., Chen, R., Wu, Q., & Jia, F. (2020). The sympathetic transmitter norepinephrine inhibits VSMC proliferation induced by TGFβ by suppressing the expression of the TGFβ receptor ALK5 in aorta remodeling. *Molecular Medicine Reports*, *22*(1), 387–397. https://doi.org/10.3892/mmr.2020.11088

Hu, Z., Wang, Z., Wu, H., Yang, Z., Jiang, W., Li, L., & Hu, X. (2013). Ang II enhances noradrenaline release from sympathetic nerve endings thus contributing to the up-regulation of metalloprotease-2 in aortic dissection patients' aorta wall. *PloS One*, *8*(10), e76922–e76922. https://doi.org/10.1371/journal.pone.0076922

Huang, H. W., Zuo, C., Chen, X., Peng, Y. P., & Qiu, Y. H. (2016). Effect of tyrosine hydroxylase overexpression in lymphocytes on the differentiation and function of T helper cells. *International Journal of Molecular Medicine*, *38*(2), 635–642. https://doi.org/10.3892/ijmm.2016.2639

Hunter, G. C., Dubick, M. A., Keen, C. L., & Eskelson, C. D. (1991). Effects of Hypertension on Aortic Antioxidant Status in Human Abdominal

Aneurysmal and Occlusive Disease. *Proceedings of the Society for Experimental Biology and Medicine*, *196*(3), 273–279. https://doi.org/10.3181/00379727-196-43188

Huo, Y., Yi, B., Chen, M., Wang, N., Chen, P., Guo, C., & Sun, J. (2014). Induction of Nur77 by hyperoside inhibits vascular smooth muscle cell proliferation and neointimal formation. *Biochemical Pharmacology*, *92*(4), 590–598. https://doi.org/10.1016/j.bcp.2014.09.021

Iemitsu, M., Miyauchi, T., Maeda, S., Sakai, S., Kobayashi, T., Fujii, N., Miyazaki, H., Matsuda, M., & Yamaguchi, I. (2001). Physiological and pathological cardiac hypertrophy induce different molecular phenotypes in the rat. *American Journal of Physiology - Regulatory Integrative and Comparative Physiology*, *281*(6 50-6), 2029–2036. https://doi.org/10.1152/ajpregu.2001.281.6.r2029

Jean-Baptiste, M. (2003). Anoïkis in the Cardiovascular System. *Arteriosclerosis, Thrombosis, and Vascular Biology*, *23*(12), 2146–2154. https://doi.org/10.1161/01.ATV.0000099882.52647.E4

Ji, L., Gong, C., Ge, L., Song, L., Chen, F., Jin, C., Zhu, H., & Zhou, G. (2017). Orphan nuclear receptor Nurr1 as a potential novel marker for progression in human pancreatic ductal adenocarcinoma. *Experimental and Therapeutic Medicine*, *13*(2), 551–559. https://doi.org/10.3892/etm.2016.3968

Jiang, T., & Si, L. (2019). Identification of the molecular mechanisms associated with acute type A aortic dissection through bioinformatics methods. *Brazilian Journal of Medical and Biological Research = Revista Brasileira de Pesquisas Medicas e Biologicas*, *52*(11), e8950–e8950. https://doi.org/10.1590/1414-431X20198950

Jiang, Y., Zhang, M., He, H., Chen, J., Zeng, H., Li, J., & Duan, R. (2013). MicroRNA/mRNA profiling and regulatory network of intracranial aneurysm. *BMC Medical Genomics*, *6*(1), 1. https://doi.org/10.1186/1755-8794-6-36

Jin, H., Romano, G., Marshall, C., Donaldson, A. E., Suon, S., & Iacovitti, L. (2006). Tyrosine hydroxylase gene regulation in human neuronal progenitor cells does not depend on Nurr1 as in the murine and rat systems. *Journal of Cellular Physiology*, *207*(1), 49–57. https://doi.org/10.1002/jcp.20534

Jin, J., Arif, B., Garcia-Fernandez, F., Ennis, T. L., Davis, E. C., Thompson, R. W., & Curci, J. A. (2012). Novel mechanism of aortic aneurysm development in mice associated with smoking and leukocytes. *Arteriosclerosis, Thrombosis, and Vascular Biology*, *32*(12), 2901–2909. https://doi.org/10.1161/ATVBAHA.112.300208

Jordi, R., José, M.-G., Javier, C., & Lina, B. (2004). Involvement of Neuron-Derived Orphan Receptor-1 (NOR-1) in LDL-Induced Mitogenic Stimulus in Vascular Smooth Muscle Cells: Role of CREB. *Arteriosclerosis, Thrombosis, and Vascular Biology*, *24*(4), 697–702. https://doi.org/10.1161/01.ATV.0000121570.00515.dc

José, M.-G., Jordi, R., Ana, C., Claudia, C.-L., & Lina, B. (2003). Neuron-Derived Orphan Receptor-1 (NOR-1) Modulates Vascular Smooth Muscle Cell Proliferation. *Circulation Research*, *92*(1), 96–103. https://doi.org/10.1161/01.RES.0000050921.53008.47

Kadmiel, M., & Cidlowski, J. A. (2013). Glucocorticoid receptor signaling in health and disease. *Trends in Pharmacological Sciences*, *34*(9), 518–530. https://doi.org/10.1016/j.tips.2013.07.003

Kakishita, M., Nakamura, K., Asanuma, M., Morita, H., Saito, H., Kusano, K., Nakamura, Y., Emori, T., Matsubara, H., Sugaya, T., Ogawa, N., & Ohe, T. (2003). Direct evidence for increased hydroxyl radicals in angiotensin II-induced cardiac hypertrophy through angiotensin II type 1a receptor. *Journal of Cardiovascular Pharmacology*, *42 Suppl 1*, S67—70. https://doi.org/10.1097/00005344-200312001-00015

Karin, A. E., Vivian, de W., Maaike, van B., A.E., van A. T., M., G. J., Bruno, P., Hans, P., & J.M., de V. C. (2002). Protective Function of Transcription Factor TR3 Orphan Receptor in Atherogenesis. *Circulation*, *106*(12), 1530–1535. https://doi.org/10.1161/01.CIR.0000028811.03056.BF

Kasner, M., Westermann, D., Lopez, B., Gaub, R., Escher, F., Kühl, U., Schultheiss, H.-P., & Tschöpe, C. (2011). Diastolic Tissue Doppler Indexes Correlate With the Degree of Collagen Expression and Cross-Linking in Heart Failure and Normal Ejection Fraction. *Journal of the American College of Cardiology*, *57*(8), 977–985. https://doi.org/https://doi.org/10.1016/j.jacc.2010.10.024

Katagiri, Y., Hirata, Y., Milbrandt, J., & Guroff, G. (1997). Differential regulation of the transcriptional activity of the orphan nuclear receptor NGFI-B by membrane depolarization and nerve growth factor. *Journal of Biological Chemistry*, *272*(50), 31278–31284. https://doi.org/10.1074/jbc.272.50.31278

Kaye, D. M., Lefkovits, J., Jennings, G. L., Bergin, P., Broughton, A., & Esler, M. D. (1995). Adverse consequences of high sympathetic nervous activity in the failing human heart. *Journal of the American College of Cardiology*, *26*(5), 1257–1263. https://doi.org/https://doi.org/10.1016/0735-1097(95)00332-0

Kessler, M. A., Yang, M., Gollomp, K. L., Jin, H., & Iacovitti, L. (2003). The human tyrosine hydroxylase gene promoter. *Molecular Brain Research*, *112*(1), 8–23. https://doi.org/https://doi.org/10.1016/S0169-

328X(02)00694-0

Kharlap, M. S., Timofeeva, A. V, Goryunova, L. E., Khaspekov, G. L., Dzemeshkevich, S. L., Ruskin, V. V, Akchurin, R. S., Golitsyn, S. P., & Beabealashvilli, R. S. H. (2006). Atrial Appendage Transcriptional Profile in Patients with Atrial Fibrillation with Structural Heart Diseases. *Annals of the New York Academy of Sciences*, *1091*(1), 205–217. https://doi.org/10.1196/annals.1378.067

Kim, K. S., Kim, C. H., Hwang, D. Y., Seo, H., Chung, S., Hong, S. J., Lim, J. K., Anderson, T., & Isacson, O. (2003 C). Orphan nuclear receptor Nurr1 directly transactivates the promoter activity of the tyrosine hydroxylase gene in a cell-specific manner. *Journal of Neurochemistry*, *85*(3), 622–634. https://doi.org/10.1046/j.1471-4159.2003.01671.x

Kim, S. O., Ono, K., Tobias, P. S., & Han, J. (2003 A). Orphan nuclear receptor Nur77 is involved in caspase-independent macrophage cell death. *The Journal of Experimental Medicine*, *197*(11), 1441–1452. https://doi.org/10.1084/jem.20021842

Kim, T. E., Lee, H. S., Lee, Y. B., Hong, S. H., Lee, Y. S., Ichinose, H., Kim, S. U., & Lee, M. A. (2003 D). Sonic hedgehog and FGF8 collaborate to induce dopaminergic phenotypes in the Nurr1-overexpressing neural stem cell. *Biochemical and Biophysical Research Communications*, *305*(4), 1040–1048. https://doi.org/https://doi.org/10.1016/S0006-291X(03)00879-9

Kim, T. E., Park, M. J., Choi, E. J., Lee, H. S., Lee, S.-H., Yoon, S. H., Oh, C.-K., Lee, B. J., Kim, S. U., Lee, Y. S., & Lee, M. A. (2003 B). Cloning and cell type-specific regulation of the human tyrosine hydroxylase gene promoter. *Biochemical and Biophysical Research Communications*, *312*(4), 1123–1131. https://doi.org/https://doi.org/10.1016/j.bbrc.2003.11.029

Kim, T. E., Seo, J. S., Yang, J. W., Kim, M. W., Kausar, R., Joe, E., Kim, B. Y., & Lee, M. A. (2013). Nurr1 Represses Tyrosine Hydroxylase Expression via SIRT1 in Human Neural Stem Cells. *PLOS ONE*, *8*(8), e71469. https://doi.org/10.1371/journal.pone.0071469

Kleinloog, R., Verweij, B. H., Van Der Vlies, P., Deelen, P., Swertz, M. A., De Muynck, L., Van Damme, P., Giuliani, F., Regli, L., Van Der Zwan, A., Van Der Sprenkel, J. W. B., Han, K. Sen, Gosselaar, P., Van Rijen, P. C., Korkmaz, E., Post, J. A., Rinkel, G. J. E., Veldink, J. H., & Ruigrok, Y. M. (2016). RNA Sequencing Analysis of Intracranial Aneurysm Walls Reveals Involvement of Lysosomes and Immunoglobulins in Rupture. *Stroke*, *47*(5), 1286–1293. https://doi.org/10.1161/STROKEAHA.116.012541

Knuutinen, A., Kokkonen, N., Risteli, J., Vähäkangas, K., Kallioinen, M., Salo,

T., Sorsa, T., & Oikarinen, A. (2002). Smoking affects collagen synthesis and extracellular matrix turnover in human skin. *British Journal of Dermatology*, *146*(4), 588–594. https://doi.org/10.1046/j.1365-2133.2002.04694.x

Koshy, S. K. G., Reddy, H. K., & Shukla, H. H. (2003). Collagen cross-linking: new dimension to cardiac remodeling. *Cardiovascular Research*, *57*(3), 594–598. https://doi.org/10.1016/S0008-6363(02)00877-5

Kota, S., Kota, S., Meher, L., Jammula, S., Mohapatra, S., & Modi, K. (2013). Coexistence of pheochromocytoma with abdominal aortic aneurysm: an untold association. *Annals of Medical and Health Sciences Research*, *3*(2), 258–261. https://doi.org/10.4103/2141-9248.113672

Krishna, S. M., Seto, S. W., Moxon, J. V, Rush, C., Walker, P. J., Norman, P. E., & Golledge, J. (2012). Fenofibrate increases high-density lipoprotein and sphingosine 1 phosphate concentrations limiting abdominal aortic aneurysm progression in a mouse model. *The American Journal of Pathology*, *181*(2), 706–718. https://doi.org/10.1016/j.ajpath.2012.04.015

Kuivaniemi, H., Ryer, E. J., Elmore, J. R., & Tromp, G. (2015). Understanding the pathogenesis of abdominal aortic aneurysms. *Expert Review of Cardiovascular Therapy*, *13*(9), 975–987. https://doi.org/10.1586/14779072.2015.1074861

Kuivaniemi, H., Shibamura, H., Arthur, C., Berguer, R., Cole, C. W., Juvonen, T., Kline, R. A., Limet, R., MacKean, G., Norrgård, Ö., Pals, G., Powell, J. T., Rainio, P., Sakalihasan, N., Van Vlijmen-van Keulen, C., Verloes, A., & Tromp, G. (2003). Familial abdominal aortic aneurysms: Collection of 233 multiplex families. *Journal of Vascular Surgery*, *37*(2), 340–345. https://doi.org/10.1067/mva.2003.71

Kuusisto, J., Kärjä, V., Sipola, P., Kholová, I., Peuhkurinen, K., Jääskeläinen, P., Naukkarinen, A., Ylä-Herttuala, S., Punnonen, K., & Laakso, M. (2012). Low-grade inflammation and the phenotypic expression of myocardial fibrosis in hypertrophic cardiomyopathy. *Heart (British Cardiac Society)*, *98*(13), 1007–1013. https://doi.org/10.1136/heartjnl-2011-300960

Lappas, M. (2014). The NR4A receptors Nurr1 and Nur77 are increased in human placenta from women with gestational diabetes. *Placenta*, *35*(11), 866–875. https://doi.org/https://doi.org/10.1016/j.placenta.2014.08.089

Larsson, E., Granath, F., Swedenborg, J., & Hultgren, R. (2009). A population-based case-control study of the familial risk of abdominal aortic aneurysm. *Journal of Vascular Surgery*, *49*(1), 47–51. https://doi.org/10.1016/j.jvs.2008.08.012

Laudet, V. (1997). Evolution of the nuclear receptor superfamily: early

diversification from an ancestral orphan receptor. *Journal of Molecular Endocrinology*, *19*(3), 207–226. https://doi.org/10.1677/jme.0.0190207

Law, S. W., Conneely, O. M., DeMayo, F. J., & O'Malley, B. W. (1992). Identification of a new brain-specific transcription factor, NURR1. *Molecular Endocrinology*, *6*(12), 2129–2135. https://doi.org/10.1210/mend.6.12.1491694

Lebel, M., Gauthier, Y., Moreau, A., & Drouin, J. (2001). Pitx3 activates mouse tyrosine hydroxylase promoter via a high-affinity binding site. *Journal of Neurochemistry*, *77*(2), 558–567. https://doi.org/10.1046/j.1471-4159.2001.00257.x

Lederle, F. A., Johnson, G. R., & Wilson, S. E. (2001). Abdominal aortic aneurysm in women. *Journal of Vascular Surgery*, *34*(1), 122–126. https://doi.org/10.1067/mva.2001.115275

LeFevre, M. L., & Force, on behalf of the U. S. P. S. T. (2014). Screening for Abdominal Aortic Aneurysm: U.S. Preventive Services Task Force Recommendation Statement. *Annals of Internal Medicine*, *161*(4), 281–290. https://doi.org/10.7326/M14-1204

Lenk, G. M., Tromp, G., Weinsheimer, S., Gatalica, Z., Berguer, R., & Kuivaniemi, H. (2007). Whole genome expression profiling reveals a significant role for immune function in human abdominal aortic aneurysms. *BMC Genomics*, *8*, 237. https://doi.org/10.1186/1471-2164-8-237

Leon, L., & Greisler, H. P. (2003). Vascular grafts. *Expert Review of Cardiovascular Therapy*, *1*(4), 581–594. https://doi.org/10.1586/14779072.1.4.581

Levula, M., Paavonen, T., Valo, T., Pelto-Huikko, M., Laaksonen, R., Kahonen, M., Huovila, A., Lehtimaki, T., Tarkka, M., & Mennander, A. A. (2011). A disintegrin and metalloprotease -8 and -15 and susceptibility for ascending aortic dissection. *Scandinavian Journal of Clinical and Laboratory Investigation*, *71*(6), 515–522. https://doi.org/10.3109/00365513.2011.591939

Levy, D., Garrison, R. J., Savage, D. D., Kannel, W. B., & Castelli, W. P. (1990). Prognostic Implications of Echocardiographically Determined Left Ventricular Mass in the Framingham Heart Study. *New England Journal of Medicine*, *322*(22), 1561–1566. https://doi.org/10.1056/NEJM199005313222203

Li, H., Kolluri, S. K., Gu, J., Dawson, M. I., Cao, X., Hobbs, P. D., Lin, B., Chen, G., Lu, J., Lin, F., Xie, Z., Fontana, J. A., Reed, J. C., & Zhang, X. (2000). Cytochrome c release and apoptosis induced by mitochondrial targeting of nuclear orphan receptor TR3. *Science (New York, N.Y.)*,

289(5482), 1159–1164. https://doi.org/10.1126/science.289.5482.1159

Li, P., Liu, Y., Yi, B., Wang, G., You, X., Zhao, X., Summer, R., Qin, Y., & Sun, J. (2013). MicroRNA-638 is highly expressed in human vascular smooth muscle cells and inhibits PDGF-BB-induced cell proliferation and migration through targeting orphan nuclear receptor NOR1. *Cardiovascular Research*, *99*(1), 185–193. https://doi.org/10.1093/cvr/cvt082

Li, Y., & Lau, L. F. (1997). Adrenocorticotropic Hormone Regulates the Activities of the Orphan Nuclear Receptor Nur77 through Modulation of Phosphorylation*. *Endocrinology*, *138*(10), 4138–4146. https://doi.org/10.1210/endo.138.10.5464

Libby, P., & Lee, R. T. (2000). Matrix matters. *Circulation*, *102*(16), 1874–1876. https://doi.org/10.1161/01.CIR.102.16.1874

Libby, P., Ridker, P. M., & Hansson, G. K. (2011). Progress and challenges in translating the biology of atherosclerosis. *Nature*, *473*(7347), 317–325. https://doi.org/10.1038/nature10146

Liberale, L., Carbone, F., Montecucco, F., & Sahebkar, A. (2020). Statins reduce vascular inflammation in atherogenesis: A review of underlying molecular mechanisms. *International Journal of Biochemistry and Cell Biology*, *122*(February). https://doi.org/10.1016/j.biocel.2020.105735

Lindholt, J. S., Sørensen, J., Søgaard, R., & Henneberg, E. W. (2010). Long-term benefit and cost-effectiveness analysis of screening for abdominal aortic aneurysms from a randomized controlled trial. *BJS (British Journal of Surgery)*, *97*(6), 826–834. https://doi.org/10.1002/bjs.7001

Liu, J., Merlie, J. P., Todd, R. D., & O'Malley, K. L. (1997). Identification of cell type-specific promoter elements associated with the rat tyrosine hydroxylase gene using transgenic founder analysis. *Molecular Brain Research*, *50*(1), 33–42. https://doi.org/https://doi.org/10.1016/S0169-328X(97)00163-0

Liu, Y., Zhang, J., Yi, B., Chen, M., Qi, J., Yin, Y., Lu, X., Jasmin, J.-F., & Sun, J. (2014). Nur77 suppresses pulmonary artery smooth muscle cell proliferation through inhibition of the STAT3/Pim-1/NFAT pathway. *American Journal of Respiratory Cell and Molecular Biology*, *50*(2), 379–388. https://doi.org/10.1165/rcmb.2013-0198OC

Liu, Z.-G., Smith, S. W., McLaughlin, K. A., Schwartz, L. M., & Osborne, B. A. (1994). Apoptotic signals delivered through the T-cell receptor of a T-cell hybrid require the immediate–early gene nur77. *Nature*, *367*(6460), 281–284. https://doi.org/10.1038/367281a0

Lloyd-Jones, D., Adams, R., Carnethon, M., De Simone, G., Ferguson, T. B., Flegal, K., Ford, E., Furie, K., Go, A., Greenlund, K., Haase, N., Hailpern,

S., Ho, M., Howard, V., Kissela, B., Kittner, S., Lackland, D., Lisabeth, L., Marelli, A., … Hong, Y. (2009). Heart Disease and Stroke Statistics—2009 Update. *Circulation*, *119*(3). https://doi.org/10.1161/circulationaha.108.191261

López, B., Querejeta, R., González, A., Beaumont, J., Larman, M., & Díez, J. (2009). Impact of treatment on myocardial lysyl oxidase expression and collagen cross-linking in patients with heart failure. *Hypertension*, *53*(2), 236–242. https://doi.org/10.1161/HYPERTENSIONAHA.108.125278

López, B., Querejeta, R., González, A., Larman, M., & Díez, J. (2012). Collagen cross-linking but not collagen amount associates with elevated filling pressures in hypertensive patients with stage C heart failure: potential role of lysyl oxidase. *Hypertension*, *60*(3), 677–683. https://doi.org/10.1161/HYPERTENSIONAHA.112.196113

Louwrens, H. D., Adamson, J., Powell, J. T., & Greenhalgh, R. M. (1993). Risk factors for atherosclerosis in men with stenosing or aneurysmal disease of the abdominal aorta. *International Angiology : A Journal of the International Union of Angiology*, *12*(1), 21–24. http://europepmc.org/abstract/MED/8376906

Lu, B., Yu, H., Zwartbol, M., Ruifrok, W. P., van Gilst, W. H., de Boer, R. A., & Silljé, H. H. W. (2012). Identification of hypertrophy- and heart failure-associated genes by combining in vitro and in vivo models. *Physiological Genomics*, *44*(8), 443–454. https://doi.org/10.1152/physiolgenomics.00148.2011

Lusis, A. J. (2010). Atherosclerosis Aldons. *Nature*, *407*(6801), 233–241. https://doi.org/10.1038/35025203.Atherosclerosis

Lynne, H. E., Yong-Jian, G., K., S. G., D., W. A., James, K., & Peter, L. (1999). Death of Smooth Muscle Cells and Expression of Mediators of Apoptosis by T Lymphocytes in Human Abdominal Aortic Aneurysms. *Circulation*, *99*(1), 96–104. https://doi.org/10.1161/01.CIR.99.1.96

Ma, F. Y., Grattan, D. R., Bobrovskaya, L., Dunkley, P. R., & Bunn, S. J. (2004). Angiotensin II regulates tyrosine hydroxylase activity and mRNA expression in rat mediobasal hypothalamic cultures: the role of specific protein kinases. *Journal of Neurochemistry*, *90*(2), 431–441. https://doi.org/10.1111/j.1471-4159.2004.02492.x

Maier, L. S., Zhang, T., Chen, L., DeSantiago, J., Brown, J. H., & Bers, D. M. (2003). Transgenic CaMKIIdeltaC overexpression uniquely alters cardiac myocyte Ca2+ handling: reduced SR Ca2+ load and activated SR Ca2+ release. *Circulation Research*, *92*(8), 904–911. https://doi.org/10.1161/01.RES.0000069685.20258.F1

Maira, M., Martens, C., Philips, A., & Drouin, J. (1999). Heterodimerization

between members of the Nur subfamily of orphan nuclear receptors as a novel mechanism for gene activation. *Molecular and Cellular Biology*, *19*(11), 7549–7557. https://doi.org/10.1128/mcb.19.11.7549

Mangelsdorf, D. J., Thummel, C., Beato, M., Herrlich, P., Schütz, G., Umesono, K., Blumberg, B., Kastner, P., Mark, M., Chambon, P., & Evans, R. M. (1995). The nuclear receptor superfamily: The second decade. *Cell*, *83*(6), 835–839. https://doi.org/10.1016/0092-8674(95)90199-X

Manning, M. W., Cassis, L. A., & Daugherty, A. (2003). Differential effects of doxycycline, a broad-spectrum matrix metalloproteinase inhibitor, on angiotensin II-induced atherosclerosis and abdominal aortic aneurysms. *Arteriosclerosis, thrombosis, and vascular biology*, *23*(3), 483–488. https://doi.org/10.1161/01.ATV.0000058404.92759.32

Martí-Pàmies, I., Cañes, L., Alonso, J., Rodríguez, C., & Martínez-González, J. (2017). The nuclear receptor NOR-1/NR4A3 regulates the multifunctional glycoprotein vitronectin in human vascular smooth muscle cells. *FASEB Journal*, *31*(10), 4588–4599. https://doi.org/10.1096/fj.201700136RR

Martín-Sánchez, P., Luengo, A., Griera, M., Orea, M. J., López-Olañeta, M., Chiloeches, A., Lara-Pezzi, E., de Frutos, S., Rodríguez–Puyol, M., Calleros, L., & Rodríguez–Puyol, D. (2018). H-ras deletion protects against angiotensin II–induced arterial hypertension and cardiac remodeling through protein kinase G-Iβ pathway activation. *The FASEB Journal*, *32*(2), 920–934. https://doi.org/https://doi.org/10.1096/fj.201700134RRRR

Martínez-González, J., & Badimon, L. (2005). The NR4A subfamily of nuclear receptors: new early genes regulated by growth factors in vascular cells. *Cardiovascular Research*, *65*(3), 609–618. https://doi.org/10.1016/j.cardiores.2004.10.002

Martínez-González, J., Varona, S., Cañes, L., Galán, M., Briones, A. M., Cachofeiro, V., & Rodríguez, C. (2019). Emerging roles of lysyl oxidases in the cardiovascular system: New concepts and therapeutic challenges. *Biomolecules*, *9*(10). https://doi.org/10.3390/biom9100610

Martínez-Gonzélez, J., Llorente-Cortés, V., & Badimon, L. (2001). Biología celular y molecular de las lesiones ateroscleróticas. *Revista Espanola de Cardiologia*, *54*(2), 218–231. https://doi.org/10.1016/s0300-8932(01)76294-x

Martínez-López, D., Camafeita, E., Cedó, L., Roldan-Montero, R., Jorge, I., García-Marqués, F., Gómez-Serrano, M., Bonzon-Kulichenko, E., Blanco-Vaca, F., Blanco-Colio, L. M., Michel, J. B., Escola-Gil, J. C., Vázquez, J., & Martin-Ventura, J. L. (2019). APOA1 oxidation is

associated to dysfunctional high-density lipoproteins in human abdominal aortic aneurysm. *EBioMedicine*, *43*, 43–53. https://doi.org/10.1016/j.ebiom.2019.04.012

Martínez-López, D., Cedó, L., Metso, J., Burillo, E., García-León, A., Canyelles, M., Lindholt, J. S., Torres-Fonseca, M., Blanco-Colio, L. M., Vázquez, J., Blanco-Vaca, F., Jauhiainen, M., Martín-Ventura, J. L., & Escolà-Gil, J. C. (2018). Impaired HDL (high-density lipoprotein)-mediated macrophage cholesterol efflux in patients with abdominal aortic aneurysm-brief report. *Arteriosclerosis, Thrombosis, and Vascular Biology*, *38*(11), 2750–2754. https://doi.org/10.1161/ATVBAHA.118.311704

Martínez-Martínez, E., Rodríguez, C., Galán, M., Miana, M., Jurado-López, R., Bartolomé, M. V., Luaces, M., Islas, F., Martínez-González, J., López-Andrés, N., & Cachofeiro, V. (2016). The lysyl oxidase inhibitor (β-aminopropionitrile) reduces leptin profibrotic effects and ameliorates cardiovascular remodeling in diet-induced obesity in rats. *Journal of Molecular and Cellular Cardiology*, *92*, 96–104. https://doi.org/10.1016/j.yjmcc.2016.01.012

Martinez-Pinna, R., Lindholt, J. S., Blanco-Colio, L. M., Dejouvencel, T., Madrigal-Matute, J., Ramos-Mozo, P., Vega de Ceniga, M., Michel, J. B., Egido, J., Meilhac, O., & Martin-Ventura, J. L. (2010). Increased levels of thioredoxin in patients with abdominal aortic aneurysms (AAAs). A potential link of oxidative stress with AAA evolution. *Atherosclerosis*, *212*(1), 333–338. https://doi.org/10.1016/j.atherosclerosis.2010.05.031

Martorell, L., Gentile, M., Rius, J., Rodríguez, C., Crespo, J., Badimon, L., & Martínez-González, J. (2009). The hypoxia-inducible factor 1/NOR-1 axis regulates the survival response of endothelial cells to hypoxia. *Molecular and Cellular Biology*, *29*(21), 5828–5842. https://doi.org/10.1128/MCB.00945-09

MartorelL, L., Martínez-González, J., Crespo, J., Calvayrac, O., & Badimon, L. (2007). Neuron-derived orphan receptor-1 (NOR-1) is induced by thrombin and mediates vascular endothelial cell growth. *Journal of Thrombosis and Haemostasis*, *5*(8), 1766–1773. https://doi.org/10.1111/j.1538-7836.2007.02627.x

Maruyama, K., Tsukada, T., Ohkura, N., Bandoh, S., Hosono, T., & Yamaguchi, K. (1998). The NGFI-B subfamily of the nuclear receptor superfamily (Review). *International Journal of Oncology*, *12*, 1237–1243. https://doi.org/10.3892/ijo.12.6.1237

Matsumoto, E., Sasaki, S., Kinoshita, H., Kito, T., Ohta, H., Konishi, M., Kuwahara, K., Nakao, K., & Itoh, N. (2013). Angiotensin II-induced cardiac hypertrophy and fibrosis are promoted in mice lacking Fgf16.

Genes to Cells : Devoted to Molecular & Cellular Mechanisms, *18*(7), 544–553. https://doi.org/10.1111/gtc.12055

Maxwell, M. A., & Muscat, G. E. O. (2006). The NR4A subgroup: immediate early response genes with pleiotropic physiological roles. *Nuclear Receptor Signaling*, *4*, e002–e002. https://doi.org/10.1621/nrs.04002

McGill, J., McMahan, C. A., Herderick, E. E., Malcom, G. T., Tracy, R. E., & Jack, P. (2000). Origin of atherosclerosis in childhood and adolescence. *American Journal of Clinical Nutrition*, *72*(5 SUPPL.). https://doi.org/10.1093/ajcn/72.5.1307s

Medzikovic, L., de Vries, C. J. M., & de Waard, V. (2019). NR4A nuclear receptors in cardiac remodeling and neurohormonal regulation. *Trends in Cardiovascular Medicine*, *29*(8), 429–437. https://doi.org/10.1016/j.tcm.2018.11.015

Medzikovic, L., Schumacher, C. A., Verkerk, A. O., van Deel, E. D., Wolswinkel, R., van der Made, I., Bleeker, N., Cakici, D., van den Hoogenhof, M. M. G., Meggouh, F., Creemers, E. E., Remme, C. A., Baartscheer, A., de Winter, R. J., de Vries, C. J. M., Arkenbout, E. K., & de Waard, V. (2015). Orphan nuclear receptor Nur77 affects cardiomyocyte calcium homeostasis and adverse cardiac remodelling. *Scientific Reports*, *5*(1), 15404. https://doi.org/10.1038/srep15404

Medzikovic, L., van Roomen, C., Baartscheer, A., van Loenen, P. B., de Vos, J., Bakker, E. N. T. P., Koenis, D. S., Damanafshan, A., Creemers, E. E., Arkenbout, E. K., de Vries, C. J. M., & de Waard, V. (2018). Nur77 protects against adverse cardiac remodelling by limiting neuropeptide Y signalling in the sympathoadrenal-cardiac axis. *Cardiovascular Research*, *114*(12), 1617–1628. https://doi.org/10.1093/cvr/cvy125

Meiser, J., Weindl, D., & Hiller, K. (2013). Complexity of dopamine metabolism. *Cell Communication and Signaling*, *11*(1), 34. https://doi.org/10.1186/1478-811X-11-34

Meltzer, H. Y., Fessler, R. G., Simonovic, M., Doherty, J., & Fang, V. S. (1979). Effect of d- and l-amphetamine on rat plasma prolactin levels. *Psychopharmacology*, *61*(1), 63–69. https://doi.org/10.1007/BF00426812

Michel, J.-B., Martin-Ventura, J. L., Nicoletti, A., & Ho-Tin-Noé, B. (2014). Pathology of human plaque vulnerability: Mechanisms and consequences of intraplaque haemorrhages. *Atherosclerosis*, *234*(2), 311–319. https://doi.org/10.1016/j.atherosclerosis.2014.03.020

Michel, J. B., Martin-Ventura, J. L., Egido, J., Sakalihasan, N., Treska, V., Lindholt, J., Allaire, E., Thorsteinsdottir, U., Cockerill, G., & Swedenborg, J. (2011). Novel aspects of the pathogenesis of aneurysms

of the abdominal aorta in humans. *Cardiovascular Research*, *90*(1), 18–27. https://doi.org/10.1093/cvr/cvq337

Mickael, D., Volakakis, N., Björklund, A., & Perlmann, T. (2013). NURR1 in Parkinson disease - From pathogenesis to therapeutic potential. *Nature Reviews. Neurology*, *9*. https://doi.org/10.1038/nrneurol.2013.209

Milbrandt, J. (1988). Nerve growth factor induces a gene homologous to the glucocorticoid receptor gene. *Neuron*, *1*(3), 183–188. https://doi.org/10.1016/0896-6273(88)90138-9

Miyata, S., Minobe, W., Bristow, M. R., & Leinwand, L. A. (2000). Myosin heavy chain isoform expression in the failing and nonfailing human heart. *Circulation Research*, *86*(4), 386–390. https://doi.org/10.1161/01.RES.86.4.386

Modrego, J., López-Farré, A. J., Martínez-López, I., Muela, M., Macaya, C., Serrano, J., & Moñux, G. (2012). Expression of cytoskeleton and energetic metabolism-related proteins at human abdominal aortic aneurysm sites. *Journal of Vascular Surgery*, *55*(4), 1124–1133. https://doi.org/https://doi.org/10.1016/j.jvs.2011.10.033

Molinoff, P. B., & Axelrod, J. (1971). Biochemistry of Catecholamines. *Annual Review of Biochemistry*, *40*(1), 465–500. https://doi.org/10.1146/annurev.bi.40.070171.002341

Moll, F. L., Powell, J. T., Fraedrich, G., Verzini, F., Haulon, S., Waltham, M., van Herwaarden, J. A., Holt, P. J. E., van Keulen, J. W., Rantner, B., Schlösser, F. J. V, Setacci, F., & Ricco, J.-B. (2011). Management of Abdominal Aortic Aneurysms Clinical Practice Guidelines of the European Society for Vascular Surgery. *European Journal of Vascular and Endovascular Surgery*, *41*, S1–S58. https://doi.org/10.1016/j.ejvs.2010.09.011

Moras, D., & Gronemeyer, H. (1998). The nuclear receptor ligand-binding domain: Structure and function. *Current Opinion in Cell Biology*, *10*(3), 384–391. https://doi.org/10.1016/S0955-0674(98)80015-X

Mosorin, M., Juvonen, J., Biancari, F., Satta, J., Surcel, H.-M., Leinonen, M., Saikku, P., & Juvonen, T. (2001). Use of doxycycline to decrease the growth rate of abdominal aortic aneurysms: A randomized, double-blind, placebo-controlled pilot study. *Journal of Vascular Surgery*, *34*(4), 606–610. https://doi.org/10.1067/mva.2001.117891

Mosser, D. M., & Edwards, J. P. (2008). Exploring the full spectrum of macrophage activation. *Nature Reviews. Immunology*, *8*(12), 958–969. https://doi.org/10.1038/nri2448

Murdoch, C. E., Chaubey, S., Zeng, L., Yu, B., Ivetic, A., Walker, S. J., Vanhoutte, D., Heymans, S., Grieve, D. J., Cave, A. C., Brewer, A. C.,

Zhang, M., & Shah, A. M. (2014). Endothelial NADPH Oxidase-2 Promotes Interstitial Cardiac Fibrosis and Diastolic Dysfunction Through Proinflammatory Effects and Endothelial-Mesenchymal Transition. *Journal of the American College of Cardiology*, *63*(24), 2734–2741. https://doi.org/https://doi.org/10.1016/j.jacc.2014.02.572

Murphy, E. P., McEvoy, A., Conneely, O. M., Bresnihan, B., & FitzGerald, O. (2001). Involvement of the nuclear orphan receptor NURR1 in the regulation of corticotropin-releasing hormone expression and actions in human inflammatory arthritis. *Arthritis and Rheumatism*, *44*(4), 782–793. https://doi.org/10.1002/1529-0131(200104)44:4<782::AID-ANR134>3.0.CO;2-H

Myers, S. A., Eriksson, N., Burow, R., Wang, S.-C. M., & Muscat, G. E. O. (2009). β-Adrenergic signaling regulates NR4A nuclear receptor and metabolic gene expression in multiple tissues. *Molecular and Cellular Endocrinology*, *309*(1), 101–108. https://doi.org/https://doi.org/10.1016/j.mce.2009.05.006

Nadal-Ginard, B., Kajstura, J., Leri, A., & Anversa, P. (2003). Myocyte death, growth, and regeneration in cardiac hypertrophy and failure. *Circulation Research*, *92*(2), 139–150. https://doi.org/10.1161/01.RES.0000053618.86362.DF

Nagashima, H., Aoka, Y., Sakomura, Y., Sakuta, A., Aomi, S., Ishizuka, N., Hagiwara, N., Kawana, M., & Kasanuki, H. (2002). A 3-hydroxy-3-methylglutaryl coenzyme A reductase inhibitor, cerivastatin, suppresses production of matrix metalloproteinase-9 in human abdominal aortic aneurysm wall. *Journal of Vascular Surgery*, *36*(1), 158–163. https://doi.org/10.1067/mva.2002.123680

Naruse, M., Satoh, F., Tanabe, A., Okamoto, T., Ichihara, A., Tsuiki, M., Katabami, T., Nomura, M., Tanaka, T., Matsuda, T., Imai, T., Yamada, M., Harada, T., Kawata, N., & Takekoshi, K. (2018). Efficacy and safety of metyrosine in pheochromocytoma/paraganglioma: A multi-center trial in Japan. *Endocrine Journal*, *65*(3), 359–371. https://doi.org/10.1507/endocrj.EJ17-0276

Navas-Madroñal, M., Rodriguez, C., Kassan, M., Fité, J., Escudero, J. R., Cañes, L., Martínez-González, J., Camacho, M., & Galán, M. (2019). Enhanced endoplasmic reticulum and mitochondrial stress in abdominal aortic aneurysm. *Clinical Science*, *133*(13), 1421–1438. https://doi.org/10.1042/CS20190399

Neels, J. G., Hassen-Khodja, R., & Chinetti, G. (2020). Nuclear receptors in abdominal aortic aneurysms. *Atherosclerosis*, *297*(February), 87–95. https://doi.org/10.1016/j.atherosclerosis.2020.02.009

Neubauer, S. (2007). The Failing Heart — An Engine Out of Fuel. *New*

England Journal of Medicine, *356*(11), 1140–1151. https://doi.org/10.1056/NEJMra063052

Newby, A. C. (2012). Matrix metalloproteinase inhibition therapy for vascular diseases. *Vascular Pharmacology*, *56*(5), 232–244. https://doi.org/https://doi.org/10.1016/j.vph.2012.01.007

Newman, K. M., Jean-Claude, J., Li, H., Ramey, W. G., & Tilson, M. D. (1994). Cytokines that activate proteolysis are increased in abdominal aortic aneurysms. *Circulation*, *90*(5 Pt 2), II224-7. http://europepmc.org/abstract/MED/7955258

Nomiyama, T., Nakamachi, T., Gizard, F., Heywood, E. B., Jones, K. L., Ohkura, N., Kawamori, R., Conneely, O. M., & Bruemmer, D. (2006). The NR4A orphan nuclear receptor NOR1 is induced by platelet-derived growth factor and mediates vascular smooth muscle cell proliferation. *The Journal of Biological Chemistry*, *281*(44), 33467–33476. https://doi.org/10.1074/jbc.M603436200

Nomiyama, T., Zhao, Y., Gizard, F., Findeisen, H. M., Heywood, E. B., Jones, K. L., Conneely, O. M., & Bruemmer, D. (2009). Deficiency of the NR4A neuron-derived orphan receptor-1 attenuates neointima formation after vascular injury. *Circulation*, *119*(4), 577–586. https://doi.org/10.1161/CIRCULATIONAHA.108.822056

Nordon, I. M., Hinchliffe, R. J., Loftus, I. M., & Thompson, M. M. (2011). Pathophysiology and epidemiology of abdominal aortic aneurysms. *Nature Reviews Cardiology*, *8*(2), 92–102. https://doi.org/10.1038/nrcardio.2010.180

Ogata, T., MacKean, G. L., Cole, C. W., Arthur, C., Andreou, P., Tromp, G., & Kuivaniemi, H. (2005). The lifetime prevalence of abdominal aortic aneurysms among siblings of aneurysm patients is eightfold higher than among siblings of spouses: an analysis of 187 aneurysm families in Nova Scotia, Canada. *Journal of Vascular Surgery*, *42*(5), 891–897. https://doi.org/10.1016/j.jvs.2005.08.002

Ohkura, N., Hijikuro, M., & Miki, K. (1996). Antisense oligonucleotide to NOR-1, a novel orphan nuclear receptor, induces migration and neurite extension of cultured forebrain cells. *Molecular Brain Research*, *35*(1), 309–313. https://doi.org/https://doi.org/10.1016/0169-328X(95)00210-J

Ohkura, N., Ito, M., Tsukada, T., Sasaki, K., Yamaguchi, K., & Miki, K. (1996). Structure, mapping and expression of a human NOR-1 gene, the third member of the Nur77/NGFI-B family. *Biochimica et Biophysica Acta (BBA) - Gene Structure and Expression*, *1308*(3), 205–214. https://doi.org/https://doi.org/10.1016/0167-4781(96)00101-7

Orbán, T. I., Apáti, Á., Németh, A., Varga, N., Krizsik, V., Schamberger, A.,

Szebényi, K., Erdei, Z., Várady, G., Karászi, É., Homolya, L., Német, K., Gócza, E., Miskey, C., Mátés, L., Ivics, Z., Izsvák, Z., & Sarkadi, B. (2009). Applying a "double-feature" promoter to identify cardiomyocytes differentiated from human embryonic stem cells following transposon-based gene delivery. *Stem Cells*, *27*(5), 1077–1087. https://doi.org/10.1002/stem.45

Ouriel, K., Green, R. M., Donayre, C., Shortell, C. K., Elliott, J., & DeWeese, J. A. (1992). An evaluation of new methods of expressing aortic aneurysm size: Relationship to rupture. *Journal of Vascular Surgery*, *15*(1), 12–20. https://doi.org/https://doi.org/10.1016/0741-5214(92)70008-9

Owens 3rd, A. P., Edwards, T. L., Antoniak, S., Geddings, J. E., Jahangir, E., Wei, W.-Q., Denny, J. C., Boulaftali, Y., Bergmeier, W., Daugherty, A., Sampson, U. K. A., & Mackman, N. (2015). Platelet Inhibitors Reduce Rupture in a Mouse Model of Established Abdominal Aortic Aneurysm. *Arteriosclerosis, Thrombosis, and Vascular Biology*, *35*(9), 2032–2041. https://doi.org/10.1161/ATVBAHA.115.305537

Oyekan, A. (2011). PPARs and their Effects on the Cardiovascular System. *Clinical and Experimental Hypertension*, *33*(5), 287–293. https://doi.org/10.3109/10641963.2010.531845

Parks, W. C., Wilson, C. L., & López-Boado, Y. S. (2004). Matrix metalloproteinases as modulators of inflammation and innate immunity. *Nature Reviews Immunology*, *4*(8), 617–629. https://doi.org/10.1038/nri1418

Parodi, J. C., Palmaz, J. C., & Barone, H. D. (1991). Transfemoral Intraluminal Graft Implantation for Abdominal Aortic Aneurysms. *Annals of Vascular Surgery*, *5*(6), 491–499. https://doi.org/10.1007/BF02015271

Pei, L., Castrillo, A., Chen, M., Hoffmann, A., & Tontonoz, P. (2005). Induction of NR4A orphan nuclear receptor expression in macrophages in response to inflammatory stimuli. *Journal of Biological Chemistry*, *280*(32), 29256–29262. https://doi.org/10.1074/jbc.M502606200

Pei, L., Castrillo, A., & Tontonoz, P. (2006). Regulation of macrophage inflammatory gene expression by the orphan nuclear receptor Nur77. *Molecular Endocrinology (Baltimore, Md.)*, *20*(4), 786–794. https://doi.org/10.1210/me.2005-0331

Perlmann, T., & Jansson, L. (1995). A novel pathway for vitamin A signaling mediated by RXR heterodimerization with NGFI-B and NURR1. *Genes and Development*, *9*(7), 769–782. https://doi.org/10.1101/gad.9.7.769

Pfeil, U., Kuncova, J., Brüggmann, D., Paddenberg, R., Rafiq, A., Henrich, M., Weigand, M. A., Schlüter, K. D., Mewe, M., Middendorff, R., Slavikova, J., & Kummer, W. (2014). Intrinsic vascular dopamine - a key modulator

of hypoxia-induced vasodilatation in splanchnic vessels. *Journal of Physiology*, *592*(8), 1745–1756. https://doi.org/10.1113/jphysiol.2013.262626

Philips, A., Lesage, S., Gingras, R., Maira, M. H., Gauthier, Y., Hugo, P., & Drouin, J. (1997). Novel dimeric Nur77 signaling mechanism in endocrine and lymphoid cells. *Molecular and Cellular Biology*, *17*(10), 5946–5951. https://doi.org/10.1128/mcb.17.10.5946

Piechota-Polanczyk, A, Goraca, A., Demyanets, S., Mittlboeck, M., Domenig, C., Neumayer, C., Wojta, J., Nanobachvili, J., Huk, I., & Klinger, M. (2012). Simvastatin Decreases Free Radicals Formation in the Human Abdominal Aortic Aneurysm Wall via NF-κB. *European Journal of Vascular and Endovascular Surgery*, *44*(2), 133–137. https://doi.org/10.1016/j.ejvs.2012.04.020

Piechota-Polanczyk, Aleksandra, Jozkowicz, A., Nowak, W., Eilenberg, W., Neumayer, C., Malinski, T., Huk, I., & Brostjan, C. (2015). The Abdominal Aortic Aneurysm and Intraluminal Thrombus: Current Concepts of Development and Treatment. *Frontiers in Cardiovascular Medicine*, *2*(May), 1–14. https://doi.org/10.3389/fcvm.2015.00019

Pluim, B. M., Zwinderman, A. H., Van Der Laarse, A., & Van Der Wall, E. E. (2000). The athlete's heart: A meta-analysis of cardiac structure and function. *Circulation*, *101*(3), 336–344. https://doi.org/10.1161/01.CIR.101.3.336

Prall, A. K., Longo, G. M., Mayhan, W. G., Waltke, E. A., Fleckten, B., Thompson, R. W., & Baxter, B. T. (2002). Doxycycline in patients with abdominal aortic aneurysms and in mice: Comparison of serum levels and effect on aneurysm growth in mice. *Journal of Vascular Surgery*, *35*(5), 923–929. https://doi.org/10.1067/mva.2002.123757

Qing, H., Jones, K. L., Heywood, E. B., Lu, H., Daugherty, A., & Bruemmer, D. (2017). Deletion of the NR4A nuclear receptor NOR1 in hematopoietic stem cells reduces inflammation but not abdominal aortic aneurysm formation. *BMC Cardiovascular Disorders*, *17*(1), 271. https://doi.org/10.1186/s12872-017-0701-4

Qing, H., Liu, Y., Zhao, Y., Aono, J., Jones, K. L., Heywood, E. B., Howatt, D., Binkley, C. M., Daugherty, A., Liang, Y., & Bruemmer, D. (2014). Deficiency of the NR4A orphan nuclear receptor NOR1 in hematopoietic stem cells accelerates atherosclerosis. *Stem Cells (Dayton, Ohio)*, *32*(9), 2419–2429. https://doi.org/10.1002/stem.1747

R. Dodd, B., & A. Spence, R. (2011). Doxycycline Inhibition of Abdominal Aortic Aneurysm Growth - A Systematic Review of the Literature. *Current Vascular Pharmacology*, *9*(4), 471–478. https://doi.org/10.2174/157016111796197288

Raffort, J., Lareyre, F., Clément, M., Hassen-Khodja, R., Chinetti, G., & Mallat, Z. (2017). Monocytes and macrophages in abdominal aortic aneurysm. *Nature Reviews Cardiology*, *14*(8), 457–471. https://doi.org/10.1038/nrcardio.2017.52

Raffort, J., Lareyre, F., Clément, M., Hassen-Khodja, R., Chinetti, G., & Mallat, Z. (2018). Diabetes and aortic aneurysm: current state of the art. *Cardiovascular Research*, *114*(13), 1702–1713. https://doi.org/10.1093/cvr/cvy174

Railton, C. J., Wolpin, J., Lam-McCulloch, J., & Belo, S. E. (2010). Renin-angiotensin blockade is associated with increased mortality after vascular surgery. *Canadian Journal of Anesthesia*, *57*(8), 736–744. https://doi.org/10.1007/s12630-010-9330-4

Ranhotra, H. (2014). The NR4A orphan nuclear receptors: Mediators in metabolism and diseases. *Journal of Receptor and Signal Transduction Research*, *35*, 1–5. https://doi.org/10.3109/10799893.2014.948555

Ranhotra, H. S. (2013). The orphan nuclear receptors in cancer and diabetes. *Journal of Receptors and Signal Transduction*, *33*(4), 207–212. https://doi.org/10.3109/10799893.2013.781624

Rao, F., Zhang, K., Zhang, L., Rana, B. K., Wessel, J., Fung, M. M., Rodriguez-Flores, J. L., Taupenot, L., Ziegler, M. G., & O'Connor, D. T. (2010). Human tyrosine hydroxylase natural allelic variation: Influence on autonomic function and hypertension. *Cellular and Molecular Neurobiology*, *30*(8), 1391–1394. https://doi.org/10.1007/s10571-010-9535-7

Ravassa, S., López, B., Querejeta, R., Echegaray, K., San José, G., Moreno, M. U., Beaumont, F. J., González, A., & Díez, J. (2017). Phenotyping of myocardial fibrosis in hypertensive patients with heart failure. Influence on clinical outcome. *Journal of Hypertension*, *35*(4). https://journals.lww.com/jhypertension/Fulltext/2017/04000/Phenotyping_of_myocardial_fibrosis_in_hypertensive.27.aspx

Rius, J., Martínez-González, J., Crespo, J., & Badimon, L. (2006). NOR-1 is involved in VEGF-induced endothelial cell growth. *Atherosclerosis*, *184*(2), 276–282. https://doi.org/10.1016/j.atherosclerosis.2005.04.008

Rizzo, M., Krayenbühl, P.-A., Pernice, V., Frasheri, A., Battista Rini, G., & Berneis, K. (2009). LDL size and subclasses in patients with abdominal aortic aneurysm. *International Journal of Cardiology*, *134*(3), 406–408. https://doi.org/https://doi.org/10.1016/j.ijcard.2007.12.082

Roderick, H. L., Higazi, D. R., Smyrnias, I., Fearnley, C., Harzheim, D., & Bootman, M. D. (2007). *Calcium in the heart : when it ' s good , it ' s very very good , but when it ' s bad , it ' s horrid*. 957–961.

Rodríguez-Calvo, R., Guadall, A., Calvayrac, O., Navarro, M. A., Alonso, J., Ferrán, B., de Diego, A., Muniesa, P., Osada, J., Rodríguez, C., & Martínez-González, J. (2013). Over-expression of Neuron-derived Orphan Receptor-1 (NOR-1) exacerbates neointimal hyperplasia after vascular injury. *Human Molecular Genetics*, *22*(10), 1949–1959. https://doi.org/10.1093/hmg/ddt042

Rosenkranz, A. C., Hood, S. G., Woods, R. L., Dusting, G. J., & Ritchie, R. H. (2003). B-type natriuretic peptide prevents acute hypertrophic responses in the diabetic rat heart: Importance of cyclic GMP. *Diabetes*, *52*(9), 2389–2395. https://doi.org/10.2337/diabetes.52.9.2389

Roth, G. A., Huffman, M. D., Moran, A. E., Feigin, V., Mensah, G. A., Naghavi, M., & Murray, C. J. L. (2015). Global and regional patterns in cardiovascular mortality from 1990 to 2013. *Circulation*, *132*(17), 1667–1678. https://doi.org/10.1161/CIRCULATIONAHA.114.008720

Rubartelli, A., Bajetto, A., Allavena, G., Wollman, E., & Sitia, R. (1992). Secretion of thioredoxin by normal and neoplastic cells through a leaderless secretory pathway. *Journal of Biological Chemistry*, *267*(34), 24161–24164.

Rush, C., Nyara, M., Moxon, J. V., Trollope, A., Cullen, B., & Golledge, J. (2009). Whole genome expression analysis within the angiotensin II-apolipoprotein E deficient mouse model of abdominal aortic aneurysm. *BMC Genomics*, *10*, 1–20. https://doi.org/10.1186/1471-2164-10-298

Sabater-Molina, M., Pérez-Sánchez, I., Hernández del Rincón, J. P., & Gimeno, J. R. (2018). Genetics of hypertrophic cardiomyopathy: A review of current state. *Clinical Genetics*, *93*(1), 3–14. https://doi.org/10.1111/cge.13027

Sadhan, D., Erli, Z., Parijat, S., Vishnu, A., A., R. M., Kenneth, S., Amy, L., Linda, L., Mei, W., Zhuo, C., Mitsuo, K., Jung, O. H., Qianyun, G., Xinyue, Z., Bin, Z., Haitong, Z., Qinghao, Z., Wei, W., Yongjian, W., & Rama, N. (2018). A Novel Angiotensin II–Induced Long Noncoding RNA Giver Regulates Oxidative Stress, Inflammation, and Proliferation in Vascular Smooth Muscle Cells. *Circulation Research*, *123*(12), 1298–1312. https://doi.org/10.1161/CIRCRESAHA.118.313207

Sakalihasan, N, Limet, R., & Defawe, O. D. (2005). Abdominal aortic aneurysm. *The Lancet*, *365*(9470), 1577–1589. https://doi.org/10.1016/S0140-6736(05)66459-8

Sakalihasan, Natzi, Delvenne, P., Nusgens, B. V, Limet, R., & Lapière, C. M. (1996). Activated forms of MMP_2 and MMP_9 in abdominal aortic aneurysms. *Journal of Vascular Surgery*, *24*(1), 127–133. https://doi.org/10.1016/S0741-5214(96)70153-2

Sakalihasan, Natzi, Michel, J. B., Katsargyris, A., Kuivaniemi, H., Defraigne, J. O., Nchimi, A., Powell, J. T., Yoshimura, K., & Hultgren, R. (2018). Abdominal aortic aneurysms. *Nature Reviews Disease Primers*, *4*(1). https://doi.org/10.1038/s41572-018-0030-7

Sakurada, K., Ohshima-Sakurada, M., Palmer, T. D., & Gage, F. H. (1999). Nurr1, an orphan nuclear receptor, is a transcriptional activator of endogenous tyrosine hydroxylase in neural progenitor cells derived from the adult brain. *Development*, *126*(18), 4017–4026.

Salata, K., Syed, M., Hussain, M. A., de Mestral, C., Greco, E., Mamdani, M., Tu, J. V., Forbes, T. L., Bhatt, D. L., Verma, S., & Al-Omran, M. (2018). Statins Reduce Abdominal Aortic Aneurysm Growth, Rupture, and Perioperative Mortality: A Systematic Review and Meta-Analysis. *Journal of the American Heart Association*, *7*(19). https://doi.org/10.1161/jaha.118.008657

Samak, M., Fatullayev, J., Sabashnikov, A., Zeriouh, M., Schmack, B., Farag, M., Popov, A. F., Dohmen, P. M., Choi, Y. H., Wahlers, T., & Weymann, A. (2016). Cardiac Hypertrophy: An Introduction to Molecular and Cellular Basis. *Medical Science Monitor Basic Research*, *22*, 75–79. https://doi.org/10.12659/MSMBR.900437

Sambri, I., Crespo, J., Aguiló, S., Ingrosso, D., Rodríguez, C., & González, J. M. (2015). MiR-17 and -20a target the neuron-derived orphan receptor-1 (NOR-1) in vascular endothelial cells. *PLoS ONE*, *10*(11), 1–13. https://doi.org/10.1371/journal.pone.0141932

Satriano, J. A., Shuldiner, M., Hora, K., Xing, Y., Shan, Z., & Schlondorff, D. (1993). Oxygen radicals as second messengers for expression of the monocyte chemoattractant protein, JE/MCP-1, and the monocyte colony-stimulating factor, CSF-1, in response to tumor necrosis factor-alpha and immunoglobulin G. Evidence for involvement of reduced . *The Journal of Clinical Investigation*, *92*(3), 1564–1571. https://doi.org/10.1172/JCI116737

Sawaki, D., Hou, L., Tomida, S., Sun, J., Zhan, H., Aizawa, K., Son, B.-K., Kariya, T., Takimoto, E., Otsu, K., Conway, S. J., Manabe, I., Komuro, I., Friedman, S. L., Nagai, R., & Suzuki, T. (2015). Modulation of cardiac fibrosis by Krüppel-like factor 6 through transcriptional control of thrombospondin 4 in cardiomyocytes. *Cardiovascular Research*, *107*(4), 420–430. https://doi.org/10.1093/cvr/cvv155

Scheuer, J., Malhotra, A., Hirsch, C., Capasso, J., & Schaible, T. F. (1982). Physiologic cardiac hypertrophy corrects contractile protein abnormalities associated with pathologic hypertrophy in rats. *Journal of Clinical Investigation*, *70*(6), 1300–1305. https://doi.org/10.1172/JCI110729

Schiffrin, E. L. (2012). Vascular remodeling in hypertension: Mechanisms and treatment. *Hypertension*, *59*(2 SUPPL. 1), 367–374. https://doi.org/10.1161/HYPERTENSIONAHA.111.187021

Schweitzer, M., Mitmaker, B., Obrand, D., Sheiner, N., Abraham, C., Dostanic, S., Meilleur, M., Sugahara, T., & Chalifour, L. E. (2009). Atorvastatin Modulates Matrix Metalloproteinase Expression, Activity, and Signaling in Abdominal Aortic Aneurysms. *Vascular and Endovascular Surgery*, *44*(2), 116–122. https://doi.org/10.1177/1538574409348352

Schwill, S., Seppelt, P., Grünhagen, J., Ott, C.-E., Jugold, M., Ruhparwar, A., Robinson, P. N., Karck, M., & Kallenbach, K. (2013). The fibrillin-1 hypomorphic mgR/mgR murine model of Marfan syndrome shows severe elastolysis in all segments of the aorta. *Journal of Vascular Surgery*, *57*(6), 1628-1636.e3. https://doi.org/https://doi.org/10.1016/j.jvs.2012.10.007

Scrogin, K. E., Samarel, A., & Koshman, Y. (2013). Tyrosine hydroxylase expression is elevated in the intermediolateral cell column of upper, but not lower thoracic spinal segments of rats with ischemic heart failure. *The FASEB Journal*, *27*(1_supplement), 699.19-699.19. https://doi.org/10.1096/fasebj.27.1_supplement.699.19

Shao, Q., Shen, L.-H., Hu, L.-H., Pu, J., Qi, M.-Y., Li, W.-Q., Tian, F.-J., Jing, Q., & He, B. (2010). Nuclear receptor Nur77 suppresses inflammatory response dependent on COX-2 in macrophages induced by oxLDL. *Journal of Molecular and Cellular Cardiology*, *49*(2), 304–311. https://doi.org/10.1016/j.yjmcc.2010.03.023

Sherman, F. T. (2008). Screening for abdominal aortic aneurysms in the elderly. *Geriatrics*, *63*(3), 15–16.

Shi, C., Awad, I. A., Jafari, N., Lin, S., Du, P., Hage, Z. A., Shenkar, R., Getch, C. C., Bredel, M., Batjer, H. H., & Bendok, B. R. (2009). Genomics of human intracranial aneurysm wall. *Stroke*, *40*(4), 1252–1261. https://doi.org/10.1161/STROKEAHA.108.532036

Sho, E., Chu, J., Sho, M., Fernandes, B., Judd, D., Ganesan, P., Kimura, H., & Dalman, R. L. (2004). Continuous periaortic infusion improves doxycycline efficacy in experimental aortic aneurysms. *Journal of Vascular Surgery*, *39*(6), 1312–1321. https://doi.org/10.1016/j.jvs.2004.01.036

Sladek, F. M., Ruse Jr, M. D., Nepomuceno, L., Huang, S. M., & Stallcup, M. R. (1999). Modulation of transcriptional activation and coactivator interaction by a splicing variation in the F domain of nuclear receptor hepatocyte nuclear factor 4alpha1. *Molecular and Cellular Biology*, *19*(10), 6509–6522. https://doi.org/10.1128/mcb.19.10.6509

Solaro, R. J. (2010). Sarcomere Control Mechanisms and the Dynamics of the Cardiac Cycle. *Journal of Biomedicine and Biotechnology*, *2010*, 105648. https://doi.org/10.1155/2010/105648

Sorriento, D., Santulli, G., Del Giudice, C., Anastasio, A., Trimarco, B., & Iaccarino, G. (2012). Endothelial cells are able to synthesize and release catecholamines both in vitro and in vivo. *Hypertension (Dallas, Tex. : 1979)*, *60*(1), 129–136. https://doi.org/10.1161/HYPERTENSIONAHA.111.189605

Spin, J. M., Hsu, M., Azuma, J., Tedesco, M. M., Deng, A., Dyer, J. S., Maegdefessel, L., Dalman, R. L., & Tsao, P. S. (2011). Transcriptional profiling and network analysis of the murine angiotensin II-induced abdominal aortic aneurysm. *Physiological Genomics*, *43*(17), 993–1003. https://doi.org/10.1152/physiolgenomics.00044.2011

Spudich, J. A., Aksel, T., Bartholomew, S. R., Nag, S., Kawana, M., Yu, E. C., Sarkar, S. S., Sung, J., Sommese, R. F., Sutton, S., Cho, C., Adhikari, A. S., Taylor, R., Liu, C., Trivedi, D., & Ruppel, K. M. (2016). Effects of hypertrophic and dilated cardiomyopathy mutations on power output by human β-cardiac myosin. *The Journal of Experimental Biology*, *219*(Pt 2), 161–167. https://doi.org/10.1242/jeb.125930

Stanley, W. C., & Chandler, M. P. (2002). Energy metabolism in the normal and failing heart: Potential for therapeutic interventions. *Heart Failure Reviews*, *7*(2), 115–130. https://doi.org/10.1023/A:1015320423577

Stanley, W. C., Recchia, F. A., & Lopaschuk, G. D. (2005). Myocardial substrate metabolism in the normal and failing heart. *Physiological Reviews*, *85*(3), 1093–1129. https://doi.org/10.1152/physrev.00006.2004

Stefanon, I., Valero-Muñoz, M., Fernandes, A. A., Ribeiro Jr, R. F., Rodríguez, C., Miana, M., Martínez-González, J., Spalenza, J. S., Lahera, V., Vassallo, P. F., & Cachofeiro, V. (2013). Left and right ventricle late remodeling following myocardial infarction in rats. *PloS One*, *8*(5), e64986–e64986. https://doi.org/10.1371/journal.pone.0064986

Steuer, J., Lachat, M., Veith, F. J., & Wanhainen, A. (2015). Endovascular grafts for abdominal aortic aneurysm. *European Heart Journal*, *37*(2), 145–151. https://doi.org/10.1093/eurheartj/ehv593

Sugiura, S., Kobayakawa, N., Fujita, H., Yamashita, H., Momomura, S., Chaen, S., Omata, M., & Sugi, H. (1998). Comparison of unitary displacements and forces between 2 cardiac myosin isoforms by the optical trap technique: molecular basis for cardiac adaptation. *Circulation research*, *82*(10), 1029–1034. https://doi.org/10.1161/01.res.82.10.1029

Sulkava, M., Raitoharju, E., Mennander, A., Levula, M., Seppälä, I., Lyytikäinen, L. P., Järvinen, O., Illig, T., Klopp, N., Mononen, N.,

Laaksonen, R., Kähönen, M., Oksala, N., & Lehtimäki, T. (2017). Differentially expressed genes and canonical pathways in the ascending thoracic aortic aneurysm - The Tampere Vascular Study. *Scientific Reports*, *7*(1), 1–8. https://doi.org/10.1038/s41598-017-12421-4

Sweeting, M. J., Thompson, S. G., Brown, L. C., Greenhalgh, R. M., & Powell, J. T. (2010). Use of angiotensin converting enzyme inhibitors is associated with increased growth rate of abdominal aortic aneurysms. *Journal of Vascular Surgery*, *52*(1), 1–4. https://doi.org/10.1016/j.jvs.2010.02.264

Swynghedauw, B. (1986). Developmental and functional adaptation of contractile proteins in cardiac and skeletal muscles. *Physiological Reviews*, *66*(3), 710–771. https://doi.org/10.1152/physrev.1986.66.3.710

Takeda, N., & Manabe, I. (2011). Cellular Interplay between Cardiomyocytes and Nonmyocytes in Cardiac Remodeling. *International Journal of Inflammation*, *2011*, 535241. https://doi.org/10.4061/2011/535241

Takeshi, M., B., S.-K. V., Beate, F., & Rudi, B. (1997). Platelet-Derived Growth Factor–Stimulated Superoxide Anion Production Modulates Activation of Transcription Factor NF-κB and Expression of Monocyte Chemoattractant Protein 1 in Human Aortic Smooth Muscle Cells. *Circulation*, *96*(7), 2361–2367. https://doi.org/10.1161/01.CIR.96.7.2361

Tan, C. M. J., Green, P., Tapoulal, N., Lewandowski, A. J., Leeson, P., & Herring, N. (2018). The role of neuropeptide Y in cardiovascular health and disease. *Frontiers in Physiology*, *9*(SEP), 1–13. https://doi.org/10.3389/fphys.2018.01281

Tank, A. W., & Wong, D. L. (2015). Peripheral and central effects of circulating catecholamines. *Comprehensive Physiology*, *5*(1), 1–15. https://doi.org/10.1002/cphy.c140007

Thakar, R. G., Cheng, Q., Patel, S., Chu, J., Nasir, M., Liepmann, D., Komvopoulos, K., & Li, S. (2009). Cell-shape regulation of smooth muscle cell proliferation. *Biophysical Journal*, *96*(8), 3423–3432. https://doi.org/10.1016/j.bpj.2008.11.074

Tham, Y. K., Bernardo, B. C., Ooi, J. Y. Y., Weeks, K. L., & McMullen, J. R. (2015). Pathophysiology of cardiac hypertrophy and heart failure: signaling pathways and novel therapeutic targets. *Archives of Toxicology*, *89*(9), 1401–1438. https://doi.org/10.1007/s00204-015-1477-x

Tim, F., J., T. R., Andrew, C., J., H. D., M., G. R., & T., P. J. (1995). Inflammation and Matrix Metalloproteinases in the Enlarging Abdominal Aortic Aneurysm. *Arteriosclerosis, Thrombosis, and Vascular Biology*, *15*(8), 1145–1151. https://doi.org/10.1161/01.ATV.15.8.1145

Tobin, S. W., Alibhai, F. J., Lee, M. M., Yeganeh, A., Wu, J., Li, S. H., Guo,

J., Tsang, K., Tumiati, L., Rocha, R., Butany, J., Yau, T. M., Ouzounian, M., David, T. E., Weisel, R. D., & Li, R. K. (2019). Novel mediators of aneurysm progression in bicuspid aortic valve disease. *Journal of Molecular and Cellular Cardiology*, *132*(December 2018), 71–83. https://doi.org/10.1016/j.yjmcc.2019.04.022

Toghill, B. J., Saratzis, A., & Bown, M. J. (2017). Abdominal aortic aneurysm—an independent disease to atherosclerosis? *Cardiovascular Pathology*, *27*, 71–75. https://doi.org/10.1016/j.carpath.2017.01.008

Tolleson, C., & Claassen, D. (2012). The function of tyrosine hydroxylase in the normal and Parkinsonian brain. *CNS & neurological disorders drug targets*, *11*(4), 381–386. https://doi.org/10.2174/187152712800792794

Tomasek, J. J., Gabbiani, G., Hinz, B., Chaponnier, C., & Brown, R. A. (2002). Myofibroblasts and mechano: Regulation of connective tissue remodelling. *Nature Reviews Molecular Cell Biology*, *3*(5), 349–363. https://doi.org/10.1038/nrm809

Tomita, N., Yamasaki, K., Izawa, K., Kunugiza, Y., Osako, M. K., Ogihara, T., & Morishita, R. (2008). Inhibition of experimental abdominal aortic aneurysm progression by nifedipine. *International Journal of Molecular Medicine*, *21*(2), 239–244. https://doi.org/10.3892/ijmm.21.2.239

Torres-Fonseca, M., Galan, M., Martinez-Lopez, D., Cañes, L., Roldan-Montero, R., Alonso, J., Reyero-Postigo, T., Orriols, M., Mendez-Barbero, N., Sirvent, M., Blanco-Colio, L. M., Martínez, J., Martin-Ventura, J. L., & Rodríguez, C. (2019). Pathophisiology of abdominal aortic aneurysm: biomarkers and novel therapeutic targets. *Clinica e Investigacion En Arteriosclerosis*, *31*(4), 166–177. https://doi.org/10.1016/j.arteri.2018.10.002

Toshihiro, T., Yoko, S.-H., Yilin, H., Sumiharu, S., Syuji, K., Midori, N., Nobuyuki, U., Taro, F., Tomohisa, S., Kinta, H., Etsuo, C., Johji, K., Yujiro, A., & Kazuo, K. (2016). Angiotensin II Stimulation of Cardiac Hypertrophy and Functional Decompensation in Osteoprotegerin-Deficient Mice. *Hypertension*, *67*(5), 848–856. https://doi.org/10.1161/HYPERTENSIONAHA.115.06689

Trachet, B., Aslanidou, L., Piersigilli, A., Fraga-Silva, R. A., Sordet-Dessimoz, J., Villanueva-Perez, P., Stampanoni, M. F. M., Stergiopulos, N., & Segers, P. (2017). Angiotensin II infusion into ApoE-/- mice: A model for aortic dissection rather than abdominal aortic aneurysm? *Cardiovascular Research*, *113*(10), 1230–1242. https://doi.org/10.1093/cvr/cvx128

Tsilingiri, K., De La Fuente, H., Relaño, M., Sánchez-Díaz, R., Rodríguez, C., Crespo, J., Sánchez-Cabo, F., Dopazo, A., Alonso-Lebrero, J. L., Vara, A., Vázquez, J., Casasnovas, J. M., Alfonso, F., Ibáñez, B., Fuster, V., Martínez-González, J., Martín, P., & Sánchez-Madrid, F. (2019).

Oxidized Low-Density Lipoprotein Receptor in Lymphocytes Prevents Atherosclerosis and Predicts Subclinical Disease. *Circulation*, *139*(2), 243–255. https://doi.org/10.1161/CIRCULATIONAHA.118.034326

Turner, G. H., Olzinski, A. R., Bernard, R. E., Aravindhan, K., Karr, H. W., Mirabile, R. C., Willette, R. N., Gough, P. J., & Jucker, B. M. (2008). In vivo serial assessment of aortic aneurysm formation in apolipoprotein E-deficient mice via MRI. *Circulation. Cardiovascular imaging*, *1*(3), 220–226. https://doi.org/10.1161/CIRCIMAGING.108.787358

Umebayashi, R., Uchida, H. A., Kakio, Y., Subramanian, V., Daugherty, A., & Wada, J. (2018). Cilostazol Attenuates Angiotensin II-Induced Abdominal Aortic Aneurysms but Not Atherosclerosis in Apolipoprotein E-Deficient Mice. *Arteriosclerosis, Thrombosis, and Vascular Biology*, *38*(4), 903–912. https://doi.org/10.1161/ATVBAHA.117.309707

van den Akker, F., de Jager, S. C. A., & Sluijter, J. P. G. (2013). Mesenchymal stem cell therapy for cardiac inflammation: immunomodulatory properties and the influence of toll-like receptors. *Mediators of Inflammation*, *2013*, 181020. https://doi.org/10.1155/2013/181020

Vardulaki, K. A., Walker, N. M., Day, N. E., Duffy, S. W., Ashton, H. A., & Scott, R. A. P. (2000). Quantifying the risks of hypertension, age, sex and smoking in patients with abdominal aortic aneurysm. *British Journal of Surgery*, *87*(2), 195–200. https://doi.org/10.1046/j.1365-2168.2000.01353.x

Vinayavekhin, N., & Saghatelian, A. (2011). Discovery of a protein-metabolite interaction between unsaturated fatty acids and the nuclear receptor Nur77 Using a metabolomics approach. *Journal of the American Chemical Society*, *133*(43), 17168–17171. https://doi.org/10.1021/ja208199h

Virani, S. S., Alonso, A., Benjamin, E. J., Bittencourt, M. S., Callaway, C. W., Carson, A. P., Chamberlain, A. M., Chang, A. R., Cheng, S., Delling, F. N., Djousse, L., Elkind, M. S. V., Ferguson, J. F., Fornage, M., Khan, S. S., Kissela, B. M., Knutson, K. L., Kwan, T. W., Lackland, D. T., … Tsao, C. W. (2020). Heart Disease and Stroke Statistics—2020 Update. In *Circulation*. https://doi.org/10.1161/cir.0000000000000757

Wagner, J., Åkerud, P., Castro, D. S., Holm, P. C., Canals, J. M., Snyder, E. Y., Perlmann, T., & Arenas, E. (1999). Induction of a midbrain dopaminergic phenotype in Nurr1-overexpressing neural stem cells by type 1 astrocytes. *Nature Biotechnology*, *17*(7), 653–659. https://doi.org/10.1038/10862

Walton, L. J., Franklin, I. J., Bayston, T., Brown, L. C., Greenhalgh, R. M., Taylor, G. W., & Powell, J. T. (1999). Inhibition of prostaglandin E2 synthesis in abdominal aortic aneurysms: implications for smooth muscle cell viability, inflammatory processes, and the expansion of abdominal aortic aneurysms. *Circulation*, *100*(1), 48–54.

https://doi.org/10.1161/01.cir.100.1.48

Wang, L., Dong, X., Zhou, W., Zeng, Q., & Mao, Y. (2011). PDGF-induced proliferation of smooth muscular cells is related to the regulation of CREB phosphorylation and Nur77 expression. *Journal of Huazhong University of Science and Technology [Medical Sciences]*, *31*(2), 169–173. https://doi.org/10.1007/s11596-011-0245-2

Wang, L., Gong, F., Dong, X., Zhou, W., & Zeng, Q. (2010). Regulation of vascular smooth muscle cell proliferation by nuclear orphan receptor Nur77. *Molecular and Cellular Biochemistry*, *341*(1), 159–166. https://doi.org/10.1007/s11010-010-0447-0

Wang, Q., Liu, Z., Ren, J., Morgan, S., Assa, C., & Liu, B. (2015). Receptor-interacting protein kinase 3 contributes to abdominal aortic aneurysms via smooth muscle cell necrosis and inflammation. *Circulation Research*, *116*(4), 600–611. https://doi.org/10.1161/CIRCRESAHA.116.304899

Wang, R.-H., He, J.-P., Su, M.-L., Luo, J., Xu, M., Du, X.-D., Chen, H.-Z., Wang, W.-J., Wang, Y., Zhang, N., Zhao, B.-X., Zhao, W.-X., Shan, Z.-G., Han, J., Chang, C., & Wu, Q. (2013). The orphan receptor TR3 participates in angiotensin II-induced cardiac hypertrophy by controlling mTOR signalling. *EMBO Molecular Medicine*, *5*(1), 137–148. https://doi.org/10.1002/emmm.201201369

Wang, W., Liu, Q., Wang, Y., Piao, H., Li, B., Zhu, Z., Li, D., Wang, T., Xu, R., & Liu, K. (2019). Verification of hub genes in the expression profile of aortic dissection. *PLOS ONE*, *14*(11), e0224922. https://doi.org/10.1371/journal.pone.0224922

Wang, X. Q., Liu, Y., Cai, H. H., Peng, Y. P., & Qiu, Y. H. (2016). Expression of tyrosine hydroxylase in CD4+ T cells contributes to alleviation of Th17/Treg imbalance in collagen-induced arthritis. *Experimental Biology and Medicine*, *241*(18), 2094–2103. https://doi.org/10.1177/1535370216660635

Wang, Z., Benoit, G., Liu, J., Prasad, S., Aarnisalo, P., Liu, X., Xu, H., Walker, N. P. C., & Perlmann, T. (2003). Structure and function of Nurr1 identifies a class of ligand-independent nuclear receptors. *Nature*, *423*(6939), 555–560. https://doi.org/10.1038/nature01645

Wärnmark, A., Treuter, E., Wright, A. P. H., & Gustafsson, J. Å. (2003). Activation Functions 1 and 2 of Nuclear Receptors: Molecular Strategies for Transcriptional Activation. *Molecular Endocrinology*, *17*(10), 1901–1909. https://doi.org/10.1210/me.2002-0384

Weber, K. T. (1989). Cardiac interstitium in health and disease: The fibrillar collagen network. *Journal of the American College of Cardiology*, *13*(7), 1637–1652. https://doi.org/10.1016/0735-1097(89)90360-4

Weber, K. T., Brilla, C. G., & Janicki, J. S. (1993). Myocardial fibrosis: functional significance and regulatory factors. *Cardiovascular Research*, *27*(3), 341–348. https://doi.org/10.1093/cvr/27.3.341

Weintraub, N. L. (2009). Understanding abdominal aortic aneurysm. *New England Journal of Medicine*, *361*(11), 1114. https://doi.org/10.1056/NEJMcibr0905244

Wemmelund, H., Jørgensen, T. M. M., Høgh, A., Behr-Rasmussen, C., Johnsen, S. P., & Lindholt, J. S. (2017). Low-dose aspirin and rupture of abdominal aortic aneurysm. *Journal of Vascular Surgery*, *65*(3), 616-625.e4. https://doi.org/10.1016/j.jvs.2016.04.061

Wilmink, T. B. M., Quick, C. R. G., & Day, N. E. (1999). The association between cigarette smoking and abdominal aortic aneurysms. *Journal of Vascular Surgery*, *30*(6), 1099–1105. https://doi.org/10.1016/S0741-5214(99)70049-2

Wilson, J. S., Virag, L., Di Achille, P., Karšaj, I., & Humphrey, J. D. (2013). Biochemomechanics of intraluminal thrombus in abdominal aortic aneurysms. *Journal of Biomechanical Engineering*, *135*(2), 1–14. https://doi.org/10.1115/1.4023437

Wilson, T. E., Fahrner, T. J., Johnston, M., & Milbrandt, J. (1991). Identification of the DNA binding site for NGFI-B by genetic selection in yeast. *Science*, *252*(5010), 1296 LP – 1300. https://doi.org/10.1126/science.1925541

Witta, J., Baffi, J. S., Palkovits, M., Mezey, É., Castillo, S. O., & Nikodem, V. M. (2000). Nigrostriatal innervation is preserved in Nurr1-null mice, although dopaminergic neuron precursors are arrested from terminal differentiation. *Molecular Brain Research*, *84*(1), 67–78. https://doi.org/https://doi.org/10.1016/S0169-328X(00)00211-4

Wong, D. R., Willett, W. C., & Rimm, E. B. (2007). Smoking, Hypertension, Alcohol Consumption, and Risk of Abdominal Aortic Aneurysm in Men. *American Journal of Epidemiology*, *165*(7), 838–845. https://doi.org/10.1093/aje/kwk063

Woods, R. L. (2004). Cardioprotective functions of atrial natriuretic peptide and B-type natriuretic peptide: A brief review. *Clinical and Experimental Pharmacology and Physiology*, *31*(11), 791–794. https://doi.org/10.1111/j.0305-1870.2004.04073.x

Woronicz, J. D., Calnan, B., Ngo, V., & Winoto, A. (1994). Requirement for the orphan steroid receptor Nur77 in apoptosis of T-cell hybridomas. *Nature*, *367*(6460), 277–281. https://doi.org/10.1038/367277a0

Yan, G., Zhu, N., Huang, S., Yi, B., Shang, X., Chen, M., Wang, N., Zhang, G., Talarico, J. A., Tilley, D. G., Gao, E., & Sun, J. (2015). Orphan

Nuclear Receptor Nur77 Inhibits Cardiac Hypertrophic Response to Beta-Adrenergic Stimulation. *Molecular and Cellular Biology*, *35*(19), 3312 LP – 3323. https://doi.org/10.1128/MCB.00229-15

Yang, F., Dong, A., Mueller, P., Caicedo, J., Sutton, A. M., Odetunde, J., Barrick, C. J., Klyachkin, Y. M., Abdel-Latif, A., & Smyth, S. S. (2012). Coronary artery remodeling in a model of left ventricular pressure overload is influenced by platelets and inflammatory cells. *PloS One*, *7*(8), e40196–e40196. https://doi.org/10.1371/journal.pone.0040196

Yang, J., Savvatis, K., Kang, J. S., Fan, P., Zhong, H., Schwartz, K., Barry, V., Mikels-Vigdal, A., Karpinski, S., Kornyeyev, D., Adamkewicz, J., Feng, X., Zhou, Q., Shang, C., Kumar, P., Phan, D., Kasner, M., López, B., Diez, J., … Chang, C.-P. (2016). Targeting LOXL2 for cardiac interstitial fibrosis and heart failure treatment. *Nature Communications*, *7*, 13710. https://doi.org/10.1038/ncomms13710

Yang, Y., Zhu, W.-Z., Joiner, M., Zhang, R., Oddis, C. V, Hou, Y., Yang, J., Price, E. E., Gleaves, L., Eren, M., Ni, G., Vaughan, D. E., Xiao, R.-P., & Anderson, M. E. (2006). Calmodulin kinase II inhibition protects against myocardial cell apoptosis in vivo. *American Journal of Physiology. Heart and Circulatory Physiology*, *291*(6), H3065—75. https://doi.org/10.1152/ajpheart.00353.2006

Yildiz, M., Oktay, A. A., Stewart, M. H., Milani, R. V., Ventura, H. O., & Lavie, C. J. (2020). Left ventricular hypertrophy and hypertension. *Progress in Cardiovascular Diseases*, *63*(1), 10–21. https://doi.org/10.1016/j.pcad.2019.11.009

Yokokura, H., Hiromatsu, S., Akashi, H., Kato, S., & Aoyagi, S. (2007). Effects of Calcium Channel Blocker Azelnidipine on Experimental Abdominal Aortic Aneurysms. *Surgery Today*, *37*(6), 468–473. https://doi.org/10.1007/s00595-006-3367-6

Yoshimura, K., Nagasawa, A., Kudo, J., Onoda, M., Morikage, N., Furutani, A., Aoki, H., & Hamano, K. (2015). Inhibitory effect of statins on inflammation-related pathways in human abdominal aortic aneurysm tissue. *International Journal of Molecular Sciences*, *16*(5), 11213–11228. https://doi.org/10.3390/ijms160511213

Zeng, H., Qin, L., Zhao, D., Tan, X., Manseau, E. J., Mien, V. H., Senger, D. R., Brown, L. F., Nagy, J. A., & Dvorak, H. F. (2006). Orphan nuclear receptor TR3/Nur77 regulates VEGF-A-induced angiogenesis through its transcriptional activity. *Journal of Experimental Medicine*, *203*(3), 719–729. https://doi.org/10.1084/jem.20051523

Zetterström, R H, Solomin, L., Mitsiadis, T., Olson, L., & Perlmann, T. (1996). Retinoid X receptor heterodimerization and developmental expression distinguish the orphan nuclear receptors NGFI-B, Nurr1, and Nor1.

Molecular Endocrinology, *10*(12), 1656–1666. https://doi.org/10.1210/mend.10.12.8961274

Zetterström, Rolf H, Solomin, L., Jansson, L., Hoffer, B. J., Olson, L., & Perlmann, T. (1997). Dopamine Neuron Agenesis in Nurr1-Deficient Mice. *Science*, *276*(5310), 248 LP – 250. https://doi.org/10.1126/science.276.5310.248

Zhan, Y., Du, X., Chen, H., Liu, J., Zhao, B., Huang, D., Li, G., Xu, Q., Zhang, M., Weimer, B. C., Chen, D., Cheng, Z., Zhang, L., Li, Q., Li, S., Zheng, Z., Song, S., Huang, Y., Ye, Z., … Wu, Q. (2008). Cytosporone B is an agonist for nuclear orphan receptor Nur77. *Nature Chemical Biology*, *4*(9), 548–556. https://doi.org/10.1038/nchembio.106

Zhang, C., van der Voort, D., Shi, H., Zhang, R., Qing, Y., Hiraoka, S., Takemoto, M., Yokote, K., Moxon, J. V, Norman, P., Rittié, L., Kuivaniemi, H., Atkins, G. B., Gerson, S. L., Shi, G.-P., Golledge, J., Dong, N., Perbal, B., Prosdocimo, D. A., & Lin, Z. (2016). Matricellular protein CCN3 mitigates abdominal aortic aneurysm. *The Journal of Clinical Investigation*, *126*(4), 1282–1299. https://doi.org/10.1172/JCI82337

Zhang, S., Du, X., Chen, Y., Tan, Y., & Liu, L. (2018). Potential Medication Treatment According to Pathological Mechanisms in Abdominal Aortic Aneurysm. *Journal of Cardiovascular Pharmacology*, *71*(1). https://journals.lww.com/cardiovascularpharm/Fulltext/2018/01000/Potential_Medication_Treatment_According_to.7.aspx

Zhang, T., Maier, L. S., Dalton, N. D., Miyamoto, S., Ross, J. J., Bers, D. M., & Brown, J. H. (2003). The deltaC isoform of CaMKII is activated in cardiac hypertrophy and induces dilated cardiomyopathy and heart failure. *Circulation Research*, *92*(8), 912–919. https://doi.org/10.1161/01.RES.0000069686.31472.C5

Zhao, X. Y., Cui, S. W., Wang, X. Q., Peng, Y. P., & Qiu, Y. H. (2013). Tyrosine hydroxylase expression in CD4+ T cells is associated with joint inflammatory alleviation in collagen type II-induced arthritis. *Rheumatology International*, *33*(10), 2597–2605. https://doi.org/10.1007/s00296-013-2788-y

Zhao, Y., Howatt, D. A., Gizard, F., Nomiyama, T., Findeisen, H. M., Heywood, E. B., Jones, K. L., Conneely, O. M., Daugherty, A., & Bruemmer, D. (2010). Deficiency of the NR4A orphan nuclear receptor NOR1 decreases monocyte adhesion and atherosclerosis. *Circulation Research*, *107*(4), 501–511. https://doi.org/10.1161/CIRCRESAHA.110.222083

Zheng, J., Wei, C.-C., Hase, N., Shi, K., Killingsworth, C. R., Litovsky, S. H., Powell, P. C., Kobayashi, T., Ferrario, C. M., Rab, A., Aban, I., Collawn,

J. F., & Dell'Italia, L. J. (2014). Chymase mediates injury and mitochondrial damage in cardiomyocytes during acute ischemia/reperfusion in the dog. *PloS One*, *9*(4), e94732–e94732. https://doi.org/10.1371/journal.pone.0094732

Zhipeng, H., Zhiwei, W., Lilei, Y., Hao, Z., Hongbing, W., Zongli, R., Hao, C., & Xiaoping, H. (2014). Sympathetic hyperactivity and aortic sympathetic nerve sprouting in patients with thoracic aortic dissection. *Annals of Vascular Surgery*, *28*(5), 1243–1248. https://doi.org/10.1016/j.avsg.2013.11.016

Zhou, H., Wang, J., Zhu, P., Zhu, H., Toan, S., Hu, S., Ren, J., & Chen, Y. (2018). NR4A1 aggravates the cardiac microvascular ischemia reperfusion injury through suppressing FUNDC1-mediated mitophagy and promoting Mff-required mitochondrial fission by CK2α. *Basic Research in Cardiology*, *113*(4), 23. https://doi.org/10.1007/s00395-018-0682-1

Zhu, W.-Z., Wang, S.-Q., Chakir, K., Yang, D., Zhang, T., Brown, J. H., Devic, E., Kobilka, B. K., Cheng, H., & Xiao, R.-P. (2003). Linkage of beta1-adrenergic stimulation to apoptotic heart cell death through protein kinase A-independent activation of Ca2+/calmodulin kinase II. *The Journal of Clinical Investigation*, *111*(5), 617–625. https://doi.org/10.1172/JCI16326